UNIVERSIDAD DE EXTREMADURA

TESIS DOCTORAL

MECANISMOS MOLECULARES DE LOS EFECTOS NOCIVOS DE LA INGESTA DE AMINOÁCIDOS OXIDADOS Y NITROSADOS MEDIANTE ENSAYOS *IN VITRO* E *IN VIVO*

SILVIA DÍAZ-VELASCO CASTELA

Programa de Doctorado en Ciencia de los Alimentos

Conformidad del Director Mario Estévez García

Esta tesis cuenta con la autorización del director de la misma y de la Comisión Académica del programa. Dichas autorizaciones constan en el Servicio de la Escuela Internacional de Doctorado de la Universidad de Extremadura (modelo 1).

2024

AGRADECIMIENTOS

Me gustaría mostrar mi agradecimiento tanto a las personas como a los organismos, que, de una u otra manera, han contribuido a la consecución de esta Tesis Doctoral.

En primer lugar, a las entidades que han permitido que se desarrolle esta Tesis, al Ministerio de Economía y Competitividad dentro del Proyecto AGL2017-84586R "Oxidación de proteínas en alimentos: desde la química fundamental hasta el impacto sobre la nutrición y la salud" y al Ministerio de Ciencia, Innovación y Universidades por la concesión del contrato predoctoral de 4 años (grant number PRE2018-084001) que he disfrutado y me ha permitido desarrollar esta Tesis.

A mi director de Tesis, Mario Estévez García, en breve futuro Catedrático del Área de Tecnología de los Alimentos de la Facultad de Veterinaria de Cáceres, por depositar en mí su confianza desde el principio de este proyecto, ya que sin su ayuda esto no hubiera sido posible. Agradecerle la excelente formación que he recibido por su parte para poder enfrentarme a este mundo científico tan competitivo y transmitirme todos los conocimientos sobre el tema que ha versado la Tesis Doctoral.

A Antonio González, Profesor Titular del Departamento de Fisiología, por su inestimable ayuda a la hora de enseñarme a realizar cultivos celulares en mi primera etapa de formación. A Fernando Peña, Catedrático del Departamento de Reproducción Animal, por posibilitar los análisis de citometría de flujo. A Josué Delgado, en breve futuro Profesor Titular del Área de Higiene y Seguridad Alimentaria, por sus enseñanzas sobre el mundo de la proteómica y en la última etapa a Remigio Martínez, Doctor en Patologías Infecciosas y a María Panadero, directora del Animalario de la Facultad de Veterinaria de Cáceres, por adentrarme en la experimentación animal.

También quería agradecerles a mis compañeros de trabajo por tantos momentos compartidos, de risas y cotilleos en el café, por hacerme la vida más amena y alegre. En especial, quería mostrar mi cariño a mis compañeros de despacho, Guadalupe Sánchez, Juan Carlos Solomando y David Morcuende, por

hacerme la vida más feliz con vuestras risas, comentarios, locuras, cotilleos y nuestros festines a base de bombones, chaskis y lo que se nos ponga por delante, gracias por ser como sois y no cambiéis nunca vuestra esencia.

Por último, dar las gracias a mis padres por haberme inculcado a lo largo de mi vida los valores de esfuerzo, responsabilidad, tesón y lucha, no sólo para los estudios sino para la vida en general, porque la vida es para los fuertes, y no es fuerte el que nunca se cae, sino el que se cae y luego se levanta como el Ave Fénix para resurgir de sus cenizas. A Loli, a Jacinto y a María, porque, aunque sean mi familia política, siempre han estado ahí apoyándome, tanto en los buenos como en los momentos más malos, siempre se lo agradeceré.

Y por último a Javi, el pilar de mi vida, porque sin él y sin su apoyo tal vez esta Tesis no hubiera sido posible, por su capacidad de levantarme cada vez que me siento derrotada y por sacarme una sonrisa todos los días de mi vida. Por nuestro futuro.

“Todo hombre, si se lo propone,

puede ser escultor de su propio cerebro”

Santiago Ramón y Cajal

Premio Nobel de Medicina en 1906

GLOSARIO

- 3NT: 3-nitrotirosina
- 4-HNE: 4-hidroxi-2-nonenal
- α-AA: ácido α-aminoadípico
- α-AS: semialdehído α-aminoadípico o alisina (en inglés, *α-aminoadipic semialdehyde*)
- γ-GS: semialdehído γ-glutámico (en inglés, *glutamic semialdehyde*)
- AGEs: productos finales de glicación avanzada (en inglés, *advanced glycation end products*)
- AOPPs: productos avanzados de oxidación proteica (en inglés, *advanced oxidation protein products*)
- CAT: catalasa
- EA: ácido elágico (en inglés, *ellagic acid*)
- GPx: glutation peroxidasa
- GSH: glutation reducido
- GSSH: glutation oxidado
- IBD: enfermedad inflamatoria intestinal (en inglés, *inflammatory bowel disease*)
- MDA: malondialdehído
- NO: óxido nítrico
- ROS: especies reactivas del oxígeno (en inglés, *reactive oxygen species*)
- RNS: especies reactivas del nitrógeno (en inglés, *reactive nitrogen species*)
- SOD: superóxido dismutasa

INDICE

RESUMEN

El estrés oxidativo está asociado con múltiples enfermedades de diferente índole, tales como enfermedades de origen gastrointestinal, trastornos neurológicos, síndromes metabólicos y, ciertamente, con el envejecimiento. El consumo de alimentos procesados y ultraprocesados con alto contenido en proteínas y lípidos oxidados puede estar involucrado de este tipo de trastornos. En particular, las proteínas oxidadas, han sido menos estudiadas hasta ahora en comparación con los productos de oxidación lipídica. Por este hecho, el estudio de los aminoácidos oxidados y nitrosados provenientes de la oxidación proteica producida a causa del estrés oxidativo es una cuestión importante relacionada directamente con la salud. En el año 2015, la Agencia Internacional de Investigación del Cáncer (IARC), determinó incluir en el grupo 1 (su consumo causa cáncer) a los productos cárnicos procesados, y a la carne roja en el grupo 2A (su consumo probablemente causa cáncer), en base a estudios epidemiológicos que indicaban la conexión entre la ingesta de estos alimentos con la mayor probabilidad de padecer cáncer colorrectal, entre otras neoplasias, aunque los mecanismos moleculares implicados en esta correlación eran desconocidos. La acumulación de aminoácidos oxidados y nitrosados presentes en alimentos procesados, tales como en los productos cárnicos, entre otros alimentos, puede estar implicada en la instauración de condiciones de estrés oxidativo en el organismo, provocando daños celulares en biomoléculas importantes tales como proteínas, lípidos y ADN. Para revertir estos efectos, el empleo de estrategias antioxidantes puede ser una buena alternativa para reducir la oxidación proteica sufrida en este tipo de productos. En la presente Tesis Doctoral, un aminoácido oxidado denominado ácido α-aminoadípico (α-AA), y el aminoácido nitrosado 3-nitrotirosina (3NT), han sido estudiados mediante su exposición a modelos *in vitro* e *in vivo* a dosis encontradas en alimentos, combinándolos además con el compuesto fenólico ácido elágico (EA). Los estudios llevados a cabo en esta Tesis Doctoral mediante técnicas moleculares avanzadas como la proteómica han permitido determinar que estos aminoácidos oxidados/nitrosados provocan estrés oxidativo tanto en cultivos celulares como en animales, incrementándose además las condiciones pro-oxidantes en combinación con el compuesto fenólico. Por lo tanto, queda demostrado que el estudio de los mecanismos moleculares subyacentes de este tipo de compuestos, presentes en alimentos, es de suma importancia a causa de las consecuencias perjudiciales para la salud.

Palabras Clave: estrés oxidativo; ácido α-aminoadípico; 3-nitrotirosina; ácido elágico; proteómica; citometría flujo.

ABSTRACT

Oxidative stress is associated with multiple disorders, such as gastrointestinal diseases, neurological disorders, metabolic syndromes and, certainly, with aging. Consumption of processed and ultra-processed foods with high content of oxidized proteins and lipids may be involved in these disorders. In particular, oxidized proteins have been less studied in comparison to lipid oxidation products. In this sense, the study of oxidized and nitrosated amino acids, as a consequence of protein oxidation produced by oxidative stress, has a crucial role directly related to health. In 2015, the International Cancer Research Agency (IARC) determined to include processed meat products in group 1 (consumption causes cancer) and red meat in group 2A (consumption probably causes cancer), based on epidemiological studies that indicated the connection between the intake of these foods with the highest probability of suffering from colorectal cancer, among other neoplasias, although the molecular mechanisms involved in this correlation were unknown. The accumulation of oxidized and nitrosated amino acids present in processed foods, such as meat products, among other foods, may be involved in the establishment of oxidative stress conditions, impacting in major biomolecules such as proteins, lipids and DNA. To reverse these effects, the use of antioxidant strategies can be a great alternative to reduce protein oxidation suffered in these products. In the present PhD Thesis, an oxidized amino acid named α-aminoadipic acid (α-AA), and the nitrosated amino acid 3-nitrotyrosine (3NT), have been studied by their exposure to *in vitro* and *in vivo* models at food-compatible doses, in combination with the phenolic compound ellagic acid (EA). The studies performed in this PhD Thesis by means of advanced molecular techniques such as proteomics have allowed to determine that these oxidized/nitrosated amino acids cause oxidative stress in both cell cultures and animals, further increasing pro-oxidant conditions in combination with the phenolic compound. Therefore, is evidence that the study of the underlying molecular mechanisms of these compounds, present in food, has a crucial importance due to the harmful consequences for health.

Keywords: oxidative stress; α-aminoadipic acid; 3-nitrotyrosine; ellagic acid; proteomics; flow cytometry.

1. INTRODUCCIÓN

1. 1. Concepto de oxidación y estrés oxidativo

1.1.1. Oxidación

La oxidación es un proceso natural que tiene lugar en todos los sistemas vivos aerobios debido a que durante el catabolismo de biomoléculas que usamos como biocombustible celular, el oxígeno, el cual es esencial para la supervivencia, actúa como aceptor final de electrones en la fosforilación oxidativa. Este proceso permite una degradación eficiente de biomoléculas para la obtención de energía que finaliza con la "respiración celular" en las mitocondrias. Durante el proceso de respiración mitocondrial, tienen lugar reacciones de óxido-reducción (redox), en las cuales se producen ganancias y pérdidas de electrones, mecanismo por el que se obtiene la energía celular. Alrededor del 1-3% del oxígeno molecular (O_2) empleado en este proceso se transforma en las llamadas especies reactivas del oxígeno (en inglés, *reactive oxygen species*, ROS) (Tauffenberger & Magistretti, 2021), que a su vez pueden reaccionar con compuestos nitrogenados dando lugar a las especies reactivas del nitrógeno (en inglés, *reactive nitrogen species*, RNS) (Beckman, 1996). Estas especies reactivas son las que comúnmente se denominan como radicales libres.

Estos radicales libres presentan en su estructura una capa de electrones de valencia no apareada, lo que les confiere una alta inestabilidad y reactividad, tendiendo a abstraer electrones de otras moléculas próximas para estabilizarse. Este fenómeno de abstracción de electrones por parte de un radical libre a una molécula susceptible inicia el fenómeno de oxidación de la molécula atacada por el radical mientras que éste último se reduce. A partir del O_2, a causa de la adición sucesiva de electrones, se forman las diferentes especies reactivas, como son el radical superóxido ($O_2^{\bullet -}$), el peróxido de hidrógeno (H_2O_2), y el radical hidroxilo ($OH^{\bullet}$) (Tauffenberger & Magistretti, 2021) (Figura 1.1). Es importante matizar que el radical superóxido y el hidroxilo sí son radicales de por sí, al tener en su estructura electrones desapareados, mientras que el H_2O_2 no es considerado un radical como tal, pero sí promueve igualmente la oxidación. De esta manera, todas estas especies reactivas son consideradas como ROS.

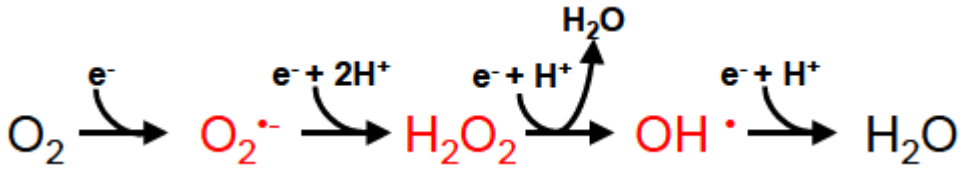

Figura 1.1. Generación de las distintas especies reactivas del oxígeno. Fuente: Elaboración propia

Asimismo, como se ha mencionado anteriormente, también se producen las especies reactivas del nitrógeno (RNS), a partir de la reacción del radical $O_2^{\bullet-}$ con la molécula óxido nítrico (NO) presente en los tejidos, generando radicales como el dióxido de nitrógeno ($NO_2^{\bullet}$) y compuestos no radicales como el ácido nitroso (HNO_2) y el peroxinitrito ($ONOO^-$) (Hellwig, 2019), siendo este último altamente reactivo y dañino para las moléculas adyacentes (Pacher *et al*., 2007). Por este motivo, la generación de ROS va íntimamente relacionada con la producción de RNS, siendo además una reacción irreversible (Estévez *et al*., 2017).

Otro mecanismo importante en la formación de ROS es la reacción de Fenton. El hierro que se encuentra en los alimentos, sobre todo en la carne roja, es extraordinariamente efectivo a la hora de promover la formación de radicales libres. Al entrar en contacto con ROS, como por ejemplo el H_2O_2, el hierro en estado ferroso (Fe^{2+}) se oxida a férrico (Fe^{3+}) (Wiseman & Halliwell, 1996), formándose además en esta reacción el radical hidroxilo ($OH^{\bullet}$), que se considera el radical libre más reactivo y peligroso en seres vivos (Valko *et al*., 2007).

$$Fe^{2+} + H_2O_2 \rightarrow Fe^{3+} + OH^- + OH^{\bullet}$$

Afortunadamente, para neutralizar estos radicales libres, los organismos poseen mecanismos de defensas antioxidantes, formado por enzimas tales como las enzimas glutatión peroxidasa (GPx), catalasa (CAT) y superóxido dismutasa (SOD), además de otras moléculas con capacidad antioxidante como glutatión, tocoferol (vitamina E), ácido ascórbico (vitamina C) y carotenoides (Pamplona & Costantini, 2011), entre otros muchos.

1.1.2. Estrés oxidativo

Cuando se produce un desequilibrio entre la generación de ROS/RNS y las defensas antioxidantes en la célula, se produce la condición de estrés oxidativo. Esta situación tiene lugar cuando existe una sobreproducción de ROS/RNS y/o cuando se produce un descenso de las defensas antioxidantes y la consecuencia directa de este desequilibrio es la oxidación de biomoléculas valiosas como proteínas, lípidos estructurales (fosfolípidos, colesterol) y el ADN, entre otras (Estévez *et al*., 2017).

Dentro del organismo, debe existir un equilibrio entre sustancias pro-oxidantes y defensas antioxidantes que las neutralicen protegiendo al organismo de sus efectos nocivos. Cuando la generación de compuestos pro-oxidantes (por ejem. radicales libres) se incrementa y sobrepasa la capacidad de las defensas antioxidantes existentes se produce el estrés oxidativo. Esta circunstancia tiene lugar a causa de multitud de factores, entre los cuales se encuentran factores endógenos

(procesos inflamatorios, enfermedades metabólicas…) y factores exógenos como la ingesta de alimentos con alta cantidad de sustancias pro-oxidantes (alimentos ultra procesados) y/o fácilmente oxidables (ácidos grasos poliinsaturados), inhalación de aire contaminado (contaminación ambiental, tabaquismo), situaciones de estrés físico/psicológico así como hábitos tóxicos (alcoholismo) (Sharifi-Rad *et al*., 2020). Del mismo modo, una depleción de las defensas antioxidantes conduce igualmente a una situación de desequilibrio aun cuando no haya una sobreproducción de radicales libres. Esto puede ocurrir en personas con dietas deficientes de alimentos ricos en antioxidantes y vitaminas/minerales (frutas, verduras), sedentarismo o personas de edad avanzada donde las defensas antioxidantes comienzan un inevitable declive (Sharifi-Rad *et al*., 2020).

Como ya se ha comentado, existe una relación directa entre los alimentos, la dieta, y el estrés oxidativo en seres humanos. Las reacciones de oxidación y el estrés oxidativo son inherentes a los sistemas biológicos y, en la cadena alimentaria, dichas reacciones tienen lugar desde la cría y sacrificio del animal hasta el consumidor final, pasando por todos los procesos de almacenamiento y transformación de la carne (y otras materias primas) en productos elaborados (Soladoye *et al*., 2015). La adición de aditivos, forma de presentación y envasado, conservación y condiciones de cocinado promueven que se produzcan reacciones de oxidación que hacen que se acumulen ROS/RNS en los alimentos a lo largo de esta cadena (Estévez, 2015). Las ROS/RNS son moléculas altamente reactivas (Liochev, 2013) y debido a su corta vida media (aproximadamente 10^{-9}s), reaccionan muy cerca de su sitio de formación (Valko *et al*., 2007), siendo potencialmente peligrosas para las moléculas adyacentes que son susceptibles de sufrir reacciones de degradación oxidativa. Entre todos los alimentos, hay algunos que son particularmente susceptibles a la oxidación entre los que se encuentran la carne y los productos cárnicos (particularmente por su elevado nivel de hierro hemínico, pro-oxidante) y alimentos con elevado nivel de ácidos grasos poliinsaturados como productos del pescado y aceites vegetales (Christi & Harwoo, 2020).

Una exposición continua a radicales libres y su efecto pro-oxidante sobre proteínas, lípidos y ADN, puede provocar a lo largo del tiempo un efecto bioacumulativo de daños oxidativos en dichas moléculas que puede, a su vez, conducir, a la aparición de enfermedades relacionadas con el estrés oxidativo (Figura 1.2).

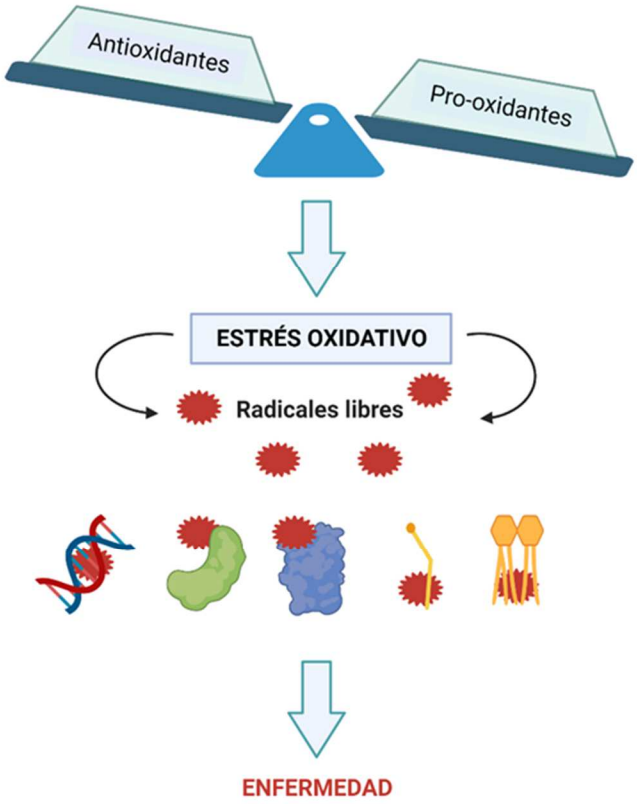

Figura 1.2. Mecanismo de aparición de estrés oxidativo. Fuente: Elaboración propia

En la literatura científica hay una profusa cantidad de estudios que relacionan directamente el estrés oxidativo con diversas patologías, tanto de origen gastrointestinal, como neurológico, metabólico, además de relacionarse con la aparición de diversos tipos de cáncer, y evidentemente, con el envejecimiento (Forman & Zhang, 2021; Klran *et al*., 2023; Sharifi-Rad *et al*., 2020), entre otras muchas.

Las enfermedades atribuidas al estrés oxidativo, relacionadas con el tracto gastrointestinal, suelen ser de tipo inflamatorio, como la enfermedad inflamatoria del intestino (en inglés, *inflammatory bowel disease*, IBD), dentro de la cual se incluyen enfermedades como la colitis ulcerosa y la enfermedad de Crohn (D'Haens *et al*., 2022). El cáncer colorrectal, como una alta incidencia en todo el mundo, también tiene relación directa con la aparición de estrés oxidativo. Referente a las patologías neurológicas, la enfermedad de Parkinson (Puspita *et al*., 2017), la enfermedad de Alzheimer (Bai *et al*., 2022) y la depresión (Correia *et al*., 2023) se encuentran también asociadas al estrés oxidativo, existiendo además interconexión entre la diabetes (Dewanjee *et al*., 2022) y otros síndromes metabólicos (Oguntibeju, 2019). El envejecimiento y las enfermedades relacionadas con la edad (Liguori *et al*., 2018; Maldonado *et al*., 2023), y el cáncer (Arfin *et al*., 2021; Hayes *et al*., 2020; Moloney & Cotter, 2018; Sosa *et al*., 2013), tienen todas ellas también una conexión con la aparición del estrés oxidativo.

Debido a la implicación del estrés oxidativo en la aparición y progreso de gran cantidad de patologías, es importante tomar estrategias en el mundo de la tecnología de los alimentos para evitar, o en todo caso disminuir, la producción de ROS/RNS en los productos alimenticios, y particularmente en alimentos ultra procesados derivados de alimentos susceptibles (por ejem. carne y productos cárnicos) a lo largo de la cadena alimentaria.

1.1.3. Nutrición and estrés oxidativo postprandial y luminal

El daño oxidativo producido por ROS/RNS tiene un efecto acumulativo en moléculas como proteínas, lípidos y ADN, como se ha comentado previamente. Uno de los principales factores que influyen en la aparición de estrés oxidativo en el organismo es la composición de la dieta (*Qiao et al*., 2013; Tomasello *et al*., 2016). El consumo de proteínas oxidadas es la principal fuente de estrés oxidativo a través de la dieta, siendo la carne y procesados cárnicos los productos que mayor contenido presentan (Estévez & Xiong, 2019). La influencia de estas proteínas oxidadas, junto con otros componentes de la dieta también oxidados, como por ejemplo los lípidos, se ve reflejada en el organismo con la aparición de dos condiciones directamente relacionadas con el consumo de sustancias pro-oxidantes, tales como el estrés oxidativo postprandial y el estrés oxidativo luminal, conceptos que se definen a continuación.

Independientemente de la oxidación que los alimentos hayan sufrido durante la ya mencionada cadena de procesado, los alimentos ingeridos, una vez dentro del organismo, se siguen oxidando durante las diversas fases de la digestión (Estévez & Xiong, 2019). La fase de la digestión gástrica es una en las que estas reacciones se potencian particularmente debido al bajo pH y la limitada presencia de defensas antioxidantes endógenas (Van Hecke *et al*., 2015). La oxidación que se produce en la luz del intestino se denomina estrés oxidativo luminal, pudiendo provocar a lo largo del tiempo daños tisulares (Figura 1.3) dando lugar a la aparición de diversas patologías como enfermedades inflamatorias del intestino, tanto benignas, como malignas (Estévez & Luna, 2017). Los productos de oxidación presentes en la luz del intestino (generados ya sea durante el procesado de los alimentos o durante la digestión) se absorben a través del epitelio intestinal y se distribuyen por el torrente sanguíneo. La elevación, en sangre y otros tejidos internos, de marcadores de oxidación consecuencia de una dieta pro-oxidante, se denomina estrés oxidativo postprandial (Kanner e*t a*l., 2017).

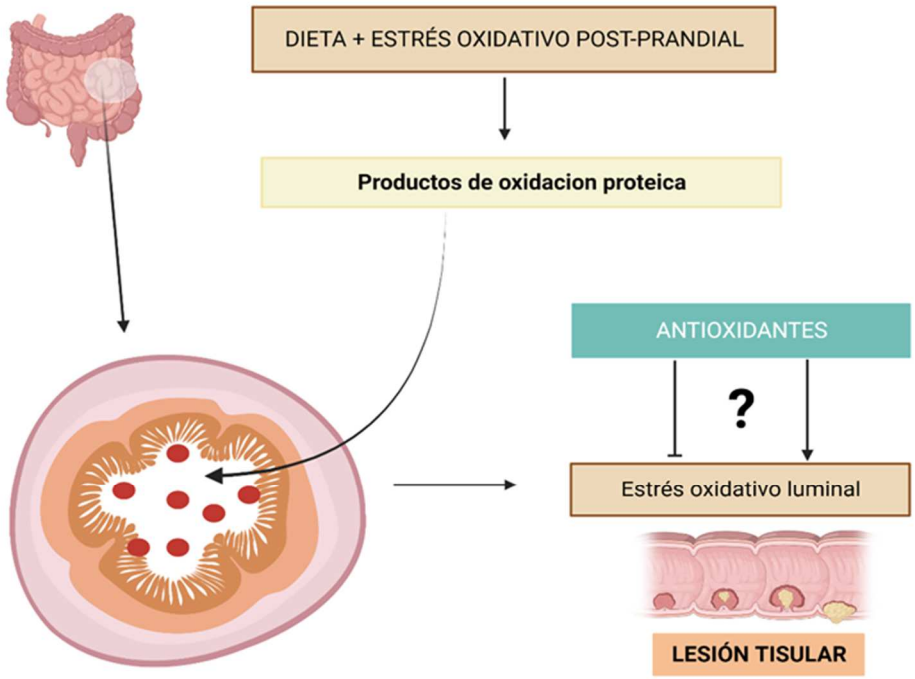

Figura 1.3. Estrés oxidativo luminal y postprandial. Fuente: Elaboración propia

Tanto los aminoácidos oxidados como los aminoácidos nitrosados están involucrados en la aparición de estrés oxidativo luminal (Circu and Aw, 2012; Estévez & Xiong, 2019) y postprandial (Ceriello, 2002; Papuc *et al*., 2017). El estrés oxidativo postprandial se puede medir a través de marcadores de oxidación presentes en plasma tanto de animales como de humanos, donde un aumento está relacionado con el consumo excesivo de carne roja y procesada (Van Hecke *et al*., 2016, Van Hecke et al., 2015). Esta consecuencia podría estar relacionada con la cantidad elevada de productos de oxidación presentes en estos alimentos, como proteínas y lípidos oxidados, y también debido a su alto contenido en hierro, que como ya se comentó previamente. A todo ello se une también la falta de componentes antioxidantes en la carne roja. Por su parte, el estrés oxidativo luminal se relaciona fundamentalmente con un desequilibrio del estado redox en la luz o lumen del intestino (Estévez & Luna, 2017), la cual se encuentra expuesta permanentemente a sustancias pro-oxidantes ingeridas en la dieta, que provocan la inflamación de la mucosa derivando en enfermedades inflamatorias intestinales, entre muchas otras.

1.2. Oxidación proteica: concepto y mecanismos

La oxidación de las proteínas es la modificación que se produce en la estructura proteica (cadena hidrocarbonada o cadena lateral de aminoácidos) en un ambiente pro-oxidante a través de la mediación de radicales libres u otras sustancias reactivas (por ejem. dicarbonilos). La cadena hidrocarbonada y los grupos funcionales asociados a la cadena lateral de los aminoácidos son, en general, donde se producen las principales modificaciones, como son la rotura de dicha cadena (enlaces peptídicos), la unión de dos aminoácidos que provoca el entrecruzamiento y formación de agregados proteicos y la formación de aminoácidos oxidados (Stadtman & Levine, 2003). Las estructuras con enlaces dobles, estructuras aromáticas y aminoácidos azufrados son las más susceptibles al fenómeno de abstracción de un átomo de hidrógeno por parte de las ROS (Estévez, 2015). Estas estructuras son ricas en electrones, lo que las convierte en dianas potenciales de captación de los mismos por un aceptor fuerte de electrones, como en este caso serían las ROS.

Los mecanismos de oxidación proteica más importantes, tales como carbonilación y carboxilación de proteínas, oxidación de tioles y aminoácidos aromáticos y nitrosación de proteínas se describen a continuación.

1.2.1. Carbonilación y carboxilación

La carbonilación y la carboxilación son unas de las modificaciones post-traduccionales más relevantes que tienen lugar en las proteínas. Por una parte, la carbonilación consiste en la desaminación oxidativa de aminoácidos alcalinos como lisina, prolina y arginina mediada por radicales libres (Davies, 2016), siendo además un proceso irreversible. En concreto, el aminoácido lisina, al sufrir el ataque de los radicales hidroxilo, pasa a ser un producto intermediario inestable que rápidamente se hidroliza dando lugar al semialdehído α-aminoadípico o alisina (α-AS) (Figura 1.4), siendo uno de los carbonilos más abundantes en células y alimentos (Stadtman & Levine, 2003; Estévez *et al*., 2021).

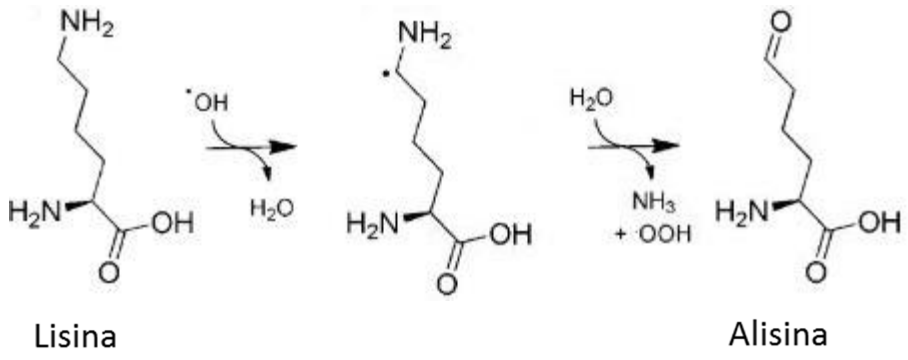

Figura 1.4. Desaminación oxidativa del aminoácido lisina mediada por radicales hidroxilos convirtiéndose en el carbonilo semialdehído α-aminoadípico o alisina (α-AS). Fuente: Hellwig (2019)

Por otro lado, la carboxilación es una reacción química en la que un grupo aldehído o cetona pasa a convertirse en un grupo carboxílico a través de un proceso de oxidación. De esta manera, α-AS se transforma en ácido α-aminoadípico (α-AA), producto final del proceso de oxidación de la lisina (Figura 1.5) (Sell *et al*., 2007).

Por su parte, los aminoácidos arginina y prolina, al encontrarse en un ambiente pro-oxidante, sufren una desaminación oxidativa mediada por ROS, convirtiéndose en semialdehído γ-glutámico (γ-GS) (Stadtman & Levine, 2003), el considerado como el segundo carbonilo más abundante en alimentos y seres vivos sometidos a mecanismos de estrés oxidativo.

Figura 1.5. Oxidación de semialdehído α-aminoadípico (α-AS) a ácido α- aminoadípico (α-AA). Fuente: Adaptado de Pena *et al*. (2017)

1.2.2. Oxidación de tioles y aminoácidos aromáticos

Existen aminoácidos que contienen en su estructura un grupo funcional formado por un átomo de azufre y un átomo de hidrógeno (-SH), denominándose este grupo funcional tiol o grupo sulfhidrilo. Los aminoácidos cisteína y metionina, contienen un grupo tiol en su estructura, lo que les hace muy susceptibles a la oxidación.

En el caso del aminoácido cisteína, cuando se encuentra en un ambiente pro-oxidante, se oxida dando lugar a enlaces disulfuro entre dos cisteínas provocando su unión y formando agregados de proteínas denominados cistinas (Yruela & Sebastián, 2014) (Figura 1.6.).

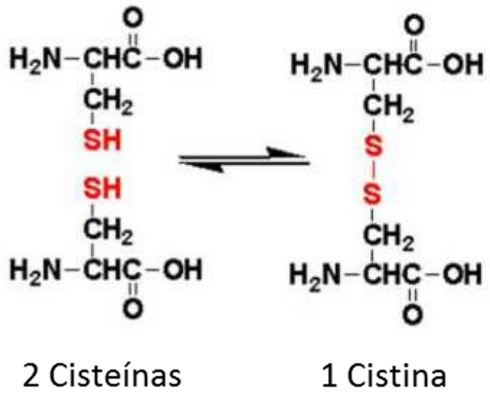

Figura 1.6. Oxidación de dos cisteínas dando lugar a una cistina. Fuente: Yruela & Sebastián (2014)

Por su parte, el aminoácido metionina da lugar, como consecuencia de su oxidación, a un nuevo compuesto denominado metionina sulfóxido, por la introducción de un átomo de oxígeno en su estructura (Figura 1.7), producto que también se encuentra relacionado con el estrés oxidativo (dos Santos *et al*., 2017).

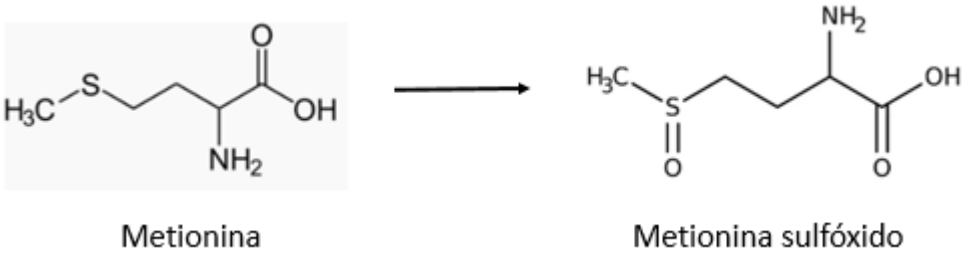

Figura 1.7. Conversión de metionina en metionina sulfóxido mediante oxidación. Fuente: Adaptado de Peskin *et al*. (2009)

Otro grupo de aminoácidos susceptibles de oxidarse en un ambiente redox son los aminoácidos aromáticos, entre los que se encuentran la tirosina y el triptófano.

El aminoácido tirosina se oxida en presencia de radicales hidroxilo, produciéndose una agregación proteica (Figura 1.8) que consiste en la unión de dos tirosinas dando como resultado a una ditirosina (Maina *et al*., 2022).

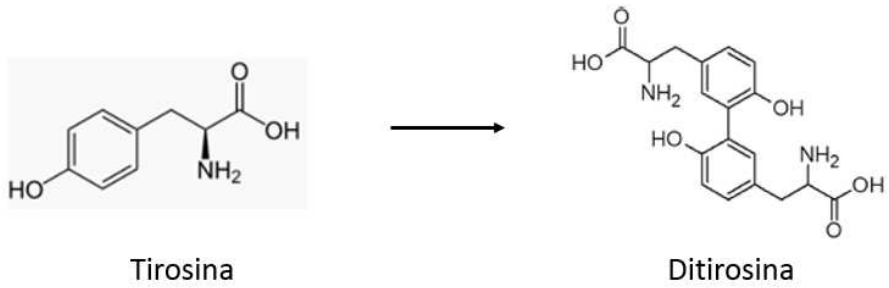

Figura 1.8. Agregación de dos tirosinas formando una ditirosina. Fuente: Adaptado de Skaff *et al*. (2005)

Por otro lado, a partir de la oxidación del aminoácido triptófano, se obtienen los compuestos denominados quinureninas. En primer lugar, el triptófano se oxida convirtiéndose en L-quinurenina y a partir de ella, de nuevo por oxidación, se obtiene el ácido quinurénico (Figura 1.9). Estos aminoácidos se forman a partir del triptófano dentro de la ruta de las quinureninas, ruta que si se ve afectada por un ambiente pro-oxidante da lugar a un desequilibrio en la formación de estos aminoácidos oxidados, relacionándose con enfermedades, sobre todo de tipo neurológico (Tsuji *et al*., 2023).

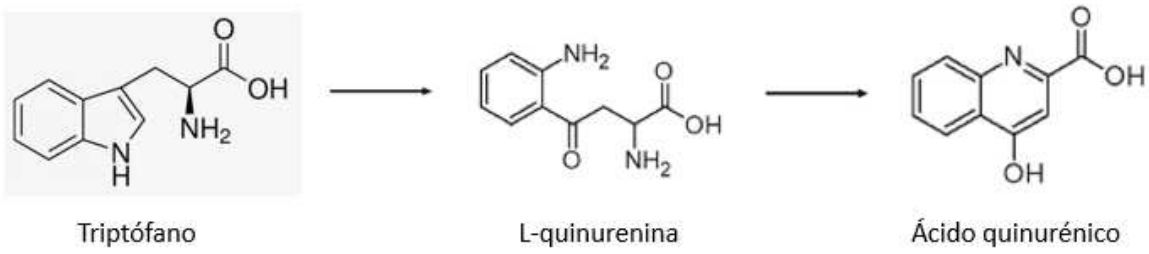

Figura 1.9. Conversión de triptófano en L-quinurenina y ácido quinurénico. Fuente: Adaptado de Biernacki *et al*. (2020)

1.2.3. Nitrosación de proteínas: formación de RNS y 3-nitrotirosina

Además del proceso de oxidación de proteínas producida por ROS, existe también el fenómeno de nitrosación de proteínas a través de RNS. Los radicales libres, sobre todo el $O_2^{\bullet-}$, reaccionan con compuestos derivados del nitrógeno, como el NO, una importante molécula de señalización celular, dando lugar a un agente oxidante mucho más potente denominado peroxinitrito ($ONOO^-$) *(Pacher et al*., 2007). La reacción entre $O_2^{\bullet-}$ y NO es extremadamente rápida y totalmente espontánea, con lo cual la formación de peroxinitrito en los sistemas celulares es inevitable. Al igual que la carbonilación, la nitrosación de proteínas es un proceso irreversible y está ligado irremediablemente con la formación previa de ROS, como ya se ha razonado previamente.

El peroxinitrito puede provocar una oxidación directa de las moléculas adyacentes, o reaccionar con dióxido de carbono (CO_2) o protones (H^+) dando lugar a nitrosoperoxicarbonato ($ONOOCO_2^-$) y ácido peroxinitroso (ONOOH) respectivamente, todas ellas RNS. Por otro lado, el trióxido de dinitrógeno (N_2O_3) formado a partir de la reacción entre NO y NO_2, da lugar a reacciones de nitrosación en aminoácidos (Figura 1.10).

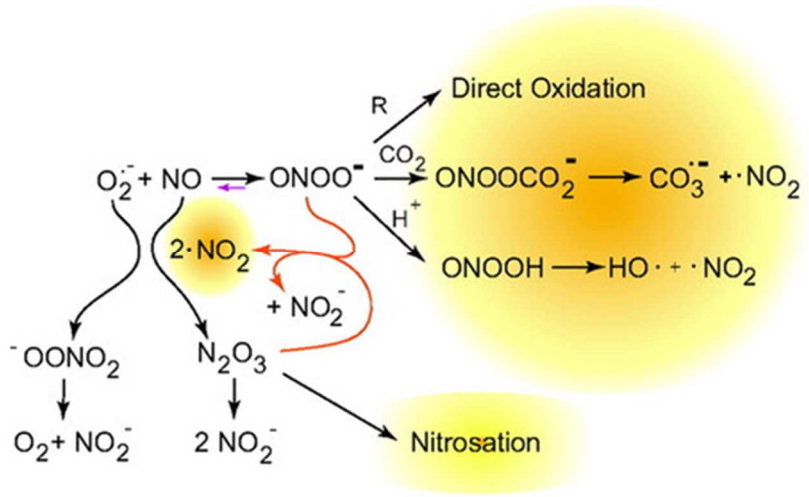

Figura 1.10. Formación de RNS. Fuente: Pacher *et al*. (2007)

Tanto las RNS radicales como no radicales provocan la nitrosación de aminoácidos como la tirosina, conduciendo así a la formación de 3-nitrotirosina (3NT) (Ceriello, 2002; Pacher *et al*., 2007) (Figura 1.11).

Figura 1.11. Nitrosación de tirosina en 3-nitrotirosina (3NT). Fuente: Adaptado de Ahsan (2013)

Se ha demostrado que la 3NT se forma durante el procesado de alimentos curados por la adición de nitritos, como en el caso de los embutidos (Villaverde *et al*., 2014a, 2014b). El peligro de la nitrosación de las proteínas radica en su irreversibilidad, al igual que la carbonilación, pudiendo afectar a la actividad de enzimas metabólicas y a la regulación de la señalización celular (Griswold-Prenner *et al*., 2023; Mallozzi *et al*., 1997). El 3NT es un prometedor biomarcador de estrés oxidativo, no solo por su implicación en enfermedades como el Parkinson, Alzheimer, Huntington, y otras menos conocidas como la enfermedad de Lou Gehrig y la enfermedad priónica (Bandookwala & Sengupta, 2020), sino también porque la alteración en el perfil de 3-nitrotirosina ocurre mucho antes de que aparezca cualquier síntoma de la enfermedad, siendo realmente importante en el diagnóstico precoz de este tipo de enfermedades (Bandookwala & Sengupta, 2020).

1.3. Relevancia de la oxidación proteica en ciencia de los alimentos, nutrición y medicina

El proceso de oxidación y las reacciones redox tienen lugar en los sistemas biológicos y se van generando a lo largo de la cadena alimentaria, desde la granja con la cría, el manejo y sacrificio de los animales, pasando por el procesado de la carne y derivados cárnicos hasta llegar al consumidor, donde los nutrientes (y productos de oxidación de los mismos) son absorbidos por parte del intestino y distribuidos a través de la sangre por todo el cuerpo (Estévez *et al*., 2017).

Los animales seleccionados para el crecimiento rápido y la producción de carne son especialmente susceptibles a las reacciones de oxidación, ya que su metabolismo energético acelerado exacerba la transformación de energía y proteínas de la dieta en músculo esquelético. Actualmente, este tipo de cría genera animales con episodios de estrés oxidativo agudos y/o crónicos, desembocando en

problemas para su salud, afectando a la calidad de los productos cárnicos que se obtienen de ellos (Estévez, 2015). A esto se suma que, tras su sacrificio, el músculo esquelético va a sufrir una serie de eventos, como el colapso de los mecanismos antioxidantes que tenían lugar en vivo, la disminución del pH de la carne y aumento de la oxidación por la exposición de la canal del animal al oxígeno ambiental, que favorecen, entre todos, la formación de ROS y la aparición de reacciones de oxidación (Soladoye *et al*., 2015).

A pesar de las diferencias entre un animal vivo y la carne y productos cárnicos, los mecanismos de oxidación son similares, teniendo las reacciones redox, en este caso, consecuencias directas sobre su calidad (Soladoye *et al*., 2015). Las proteínas, al ser los componentes principales del músculo, juegan un papel crucial desde el punto de vista nutricional, tecnológico y sensorial en la carne y en los productos cárnicos (Domínguez *et al*., 2022; Luna & Estévez, 2019), siendo por ello un motivo importante de estudio en el campo de las ciencias de los alimentos. La oxidación de proteínas, al tratarse de una modificación covalente de las mismas, puede causar daños irreversibles en su estructura, lo que desemboca en resultados indeseables en su calidad tanto a nivel sensorial como nutricional y tecnológico (Domínguez *et al*., 2022), dando lugar a cambios en el color, el sabor, el aroma o la textura, entre otros, debido a procesos de proteólisis, desnaturalización y oxidación de los aminoácidos (Falowo *et al*., 2014).

La oxidación de proteínas en los alimentos depende de factores endógenos y exógenos. De manera endógena, la oxidación de proteínas en carne y productos cárnicos se debe a la alta concentración de proteínas y, en concreto, de aminoácidos diana para las ROS/RNS tales como la lisina, triptófano y tirosina (Utrera & Estévez, 2013), entre otros, a causa de su estructura química. Por otra parte, la carne roja es especialmente sensible a la oxidación proteica debido a su alta concentración en hierro hemo. El hierro de la carne se encuentra unido al grupo hemo de la mioglobina, proteína encargada de suministrar oxígeno al músculo (Vanek & Kohli, 2023). A cada molécula de mioglobina se encuentra unido un átomo de hierro, por este motivo, la carne roja es una excelente diana para los radicales libres por medio de la reacción de Fenton (Estévez, 2011)

Los factores exógenos de la oxidación proteica están relacionados con el tratamiento de la carne a lo largo de la cadena de procesado del producto. Una vez los animales son sacrificados, el procesamiento de la carne puede pasar por diferentes tratamientos tales como adición de aditivos, salado, curado, madurado, picado, loncheado, congelado, cocinado, altas presiones, empaquetado, entre otros (Soladoye *et al*., 2015). Todos estos procesos influyen, en un grado u otro, en la integridad y estado redox de las proteínas.

La calidad de una proteína alimentaria tanto desde el punto de vista nutricional como tecnológico depende, en gran medida de que su estructura sea la adecuada para cumplir con sus propiedades funcionales (emulsificantes, gelificantes etc.). Por esta razón, conservar su estructura inicial lo más intacta posible es primordial, situación que se pierde cuando estos aminoácidos son atacados por las ROS/RNS, además de cuando son sometidos a los procesos tecnológicos mencionados, modificando su estructura.

Con respecto a la adición de aditivos, la tendencia actual de las empresas alimentarias es disminuir la cantidad de aditivos que añaden a los productos, tales como nitratos, sulfatos, glutamato, entre otros, ante la relación que existe en la literatura científica entre estas sustancias y trastornos asociados con ellos (Samuels, 2020; Van Hecke *et al*., 2017). En el proceso de madurado, se ha comprobado que la concentración de carbonilos es mayor es una carne madurada (en inglés, *aging*), que en una carne no sometida a este tratamiento (Santé-Lhoutellier *et al*., 2008). Con respecto al salado, se han hallado efectos pro-oxidantes de la sal y su afectación a la digestibilidad de los productos cárnicos (Choi & Chin, 2021), mientras que en el proceso de curado se ha observado un incremento de carbonilos en la carne curada (Ventanas *et al*., 2007).

En el picado y loncheado la oxidación de la carne es mayor a causa del incremento de la superficie del producto en contacto con el oxígeno (Estévez, 2011), y en la carne congelada también existe un aumento de la cantidad de proteínas oxidadas (Utrera & Estévez, 2013). En relación con el cocinado, existen multitud de manera de cocinar la carne, en estofado (al vapor, cocida), a la plancha, frita, ahumada, en el microondas, entre otros, tanto en la industria como en casa. Estos procesos de cocinado tienen en común el aumento de la concentración de ROS en la carne y los productos cárnicos y en consecuencia la oxidación proteica (Traore *et al*., 2012). La carne sometida a altas presiones entre 100 y 900 Megapascales (MPa) (en inglés *high-pressure processing*, HHP) también han sido estudiadas. Se sabe que las HHP afectan a la estructura de la carne en mayor o menor medida, en función de la temperatura y la presión empleadas (Soladoye *et al*., 2015), desnaturalizando de esta manera las proteínas y haciéndolas más accesibles a las ROS/RNS, promoviendo su oxidación. Por otra parte, el material y los gases empleados en el empaquetado influyen en la aparición de carbonilos en la carne envasada (De Palo *et al*., 2013).

Desde el punto de vista nutricional, todos estos procesos afectan al valor biológico de la proteína de la carne y productos cárnicos. La alteración de la estructura de los aminoácidos afecta a la digestibilidad de las proteínas y la biodisponibilidad de los aminoácidos, siendo menos susceptibles a ser digeridas provocando la pérdida de valor nutricional (Boye *et al*., 2012). Por su parte, Luna & Estévez (2019)

también corroboraron la conexión entre la severidad de la carbonilación en proteínas de carne y productos lácteos y la disminución de su digestibilidad.

La influencia de la nutrición en la modulación del equilibrio redox del organismo es un tema candente de actualidad, catalogándose a la carne roja y a los productos cárnicos procesados como sustancias pro-oxidantes. En 2015, el informe publicado por la Agencia Internacional de Investigación del Cáncer (IARC, 2015), organismo perteneciente a la Organización Mundial de la Salud, estableció incluir a los productos cárnicos procesados en el grupo 1 (su consumo causa cáncer) y a la carne roja en el grupo 2A (su consumo probablemente causa cáncer). Esta decisión se tomó en base a estudios epidemiológicos que indicaban la conexión entre la ingesta de dichos alimentos con la aparición de cáncer colorrectal, entre otras neoplasias (Aune *et al*., 2013; Chan *et al*., 2011; Micha *et al*., 2012, 2010; Pan *et al*., 2011; Xu *et al*., 2013).

Los estudios epidemiológicos prospectivos realizados por Chan *et al*. (2011) revelaron que el riesgo de padecer cáncer colorrectal aumentaba linealmente con el aumento de la ingesta de carnes rojas y procesadas hasta aproximadamente 140 g/día. Los análisis mostraron un aumento del riesgo de aparición de cáncer colorrectal en un 17% por el aumento de la ingesta de carne roja en 100 g/día, mientras que este riesgo aumentaba en un 18% por cada 50 g/día de aumento de ingesta de productos cárnicos procesados. Los metaanálisis realizados por Micha *et al*. (2012, 2010) asociaron el consumo de carne roja y procesada con enfermedades cardiovasculares y también con la aparición de diabetes tipo 2 (Micha *et al*., 2010; Pan *et al*., 2011). Por otro lado, otros estudios epidemiológicos encontraron una interrelación entre el cáncer colorrectal y las enfermedades cardiovasculares (Lee *et al*., 2013; Yang *et al*., 2010) y también entre la diabetes tipo 2 y el cáncer colorrectal (De Bruijn *et al*., 2013; Deng *et al*., 2012). Estudios realizados a posteriori han comenzado a revelar cuales son las sustancias y mecanismos que se encuentran implicados en la relación entre el consumo de carne roja y productos cárnicos procesados y diversas patologías. En 2017, se demostró por primera vez la existencia de tres compuestos discriminantes que aparecían en la carne roja en mayor cantidad que en la carne blanca, como son los aminoácidos oxidados ditirosina, L-quinurenina y ácido quinurénico (Rombouts *et al*., 2017).

Otros estudios han relacionado el aumento de las reacciones oxidativas y la nitrosación de proteínas durante la digestión con el consumo de carne roja bien cocinada y el cáncer colorrectal *(Van Hecke et al*., 2015). Además, el consumo de carne a corto plazo promueve el estrés oxidativo sistémico y la inflamación en ratas. La oxidación de la carne durante la digestión puede no solo dar lugar a la formación de productos de oxidación causando estrés oxidativo sistémico, sino afectar también a las

mucosas gastrointestinales, el corazón y el riñón (Van Hecke *et al*., 2016). Este hecho podría estar conectado con las enfermedades del tracto gastrointestinal, como la IBD, colitis ulcerosa y enfermedad de Crohn. En otros estudios se ha descubierto que, el consumo combinado de carne de vacuno cocida picada y sacarosa estimula el estrés oxidativo y la hipertrofia cardíaca en ratas (Van Hecke *et al*., 2019). Este trabajo determinó que el consumo de carne roja junto con sacarosa aumentaba los parámetros de estrés oxidativo estudiados en la sangre de los animales, tales como malondialdehído (MDA), 4-hidroxi-2-nonenal (4-HNE), hexanal (HEX), glutation (GSH), glutation oxidado (GSSG), y actividad de GPx. Por lo tanto, estas investigaciones podrían demostrar cuales son las bases de la asociación epidemiológica del consumo de carne roja y procesada con enfermedades cardiovasculares y también con la aparición de diabetes. En experimentos de expresión génica llevados a cabo en ratas con una alimentación basada en piensos de pollo y ternera durante dos semanas (Jakobsen *et al*., 2017), no se encontraron marcadores genéticos que relacionaran el cáncer colorrectal con el consumo de ninguno de los dos tipos de carne en este plazo de tiempo. Estos resultados sugieren que los mecanismos implicados en la aparición de cáncer colorrectal necesitan más tiempo para causar un daño de tipo neoplásico al intestino, mientras que en otros trabajos sí se produce a este tiempo un aumento de marcadores de oxidación sistémica e inflamación en el mismo, que podría ser la antesala de la aparición de cáncer.

Además del cáncer colorrectal, en el tracto gastrointestinal aparecen patologías que tienen como base un desequilibrio redox, como es el caso de la IBD (Estévez & Luna, 2017). La IBD incluye a un grupo heterogéneo de enfermedades como la colitis ulcerosa, síndrome de colon irritable y la enfermedad de Crohn (D'Haens *et al*., 2022; Wehkamp *et al*., 2016). La sintomatología de estas enfermedades suele ser dolor abdominal y diarrea recurrente, privando de calidad de vida a las personas que lo padecen. La susceptibilidad a la IBD está determinada por una combinación de factores genéticos y ambientales (McGovern *et al*., 2015). En el ambiente donde se producen las lesiones de IBD hay una fuerte actividad redox, en el que las ROS y las RNS desempeñan un papel importante, tanto en la señalización inflamatoria como en el daño al tejido circundante (Biasi *et al*., 2013). Teniendo en cuenta que la oxidación de la carne causa estrés oxidativo sistémico e inflamación en la mucosa intestinal (Van Hecke *et al*., 2016), ésta podría ser la correlación entre los trastornos asociados a IBD y la ingesta de carne roja y/o productos cárnicos procesados.

En trabajos previos al informe publicado por la IARC en 2015, se relacionaba a las proteínas oxidadas, y en concreto al α-AA, con la aparición de efectos adversos con su ingesta en animales (Akagawa *et al*., 2002; Sell *et al*., 2007; Wang *et al*., 2013). El α-AA, y otros aminoácidos oxidados provenientes de la tirosina y el triptófano, como la ditirosina y las quinureninas, expuestos inicialmente a la mucosa

intestinal, se absorben a través de las microvellosidades y se distribuyen por el torrente sanguíneo a los órganos del cuerpo, como el páncreas (Ding *et al*., 2017; Wang *et al*., 2013), riñón e hígado (Yang *et al.*, 2017), provocando daños en ellos. Los marcadores de estrés oxidativo más utilizados actualmente en investigación son los carbonilos, AGEs (productos finales de glicación avanzada, en inglés*, advanced glycation end products*) y GSH/GSSG para la oxidación proteica; 4-HNE y MDA para oxidación lipídica; y 8-oxoguanina (8-oxodG) para la oxidación de DNA/RNA (Frijhoff *et al*., 2015).

Existen estudios que ponen de manifiesto que la ingesta de PUFAs (ácidos grasos poliinsaturados, en inglés, *Poly Unsaturated Fatty Acids*), los cuales son ácidos grasos altamente oxidables debido a la presencia de varios enlaces dobles en su estructura, inducen estrés oxidativo e inflamación *(Awada et al*., 2012). Otras investigaciones afirman que el grupo hemo favorece las reacciones de oxidación en el organismo, y demuestran su potencial pro-oxidante en la asociación entre el consumo de carne roja y el cáncer colorrectal (Bastide *et al*., 2015). Tan es así, que los productos finales de la oxidación lipídica provenientes de los PUFAs (4-HNE and MDA), son empleados como biomarcadores de estrés oxidativo y junto con el hierro hemo inducen un ambiente colónico que promueve el cáncer en ratas (Guéraud *et al*., 2015).

Algunos estudios clínicos enfatizan en emplear la carbonilación de proteínas plasmáticas como un marcador fiable para evaluar el riesgo de sufrir cáncer colorrectal (Chang *et al*., 2008; Yeh *et al*., 2010). En otros trabajos, Šebeková *et al*. (2012) destacaron que los AOPPs (productos avanzados de oxidación proteica, en inglés, *advanced oxidation protein products*) pueden utilizarse como marcadores proteicos de daño oxidativo, ya que en pacientes con enfermedad renal crónica aumentaron las concentraciones de AOPPs en sangre/orina, cuya estructura está compuesta principalmente por ditirosina y carbonilos. Asimismo, existen estudios que afirman que los tioles (su depleción) pueden ser empleados como marcadores de IBD (Passos *et al*., 2023), y que el 3NT puede ser reconocido como un indicador de nitrosación de proteínas en alimentos (Ozyurt & Otles, 2020).

En la Tabla 1.1 se muestra distintos productos de oxidación proteica relacionados con enfermedades encontrados en la bibliografía científica.

Tabla 1.1. Distintos productos de oxidación proteica y las enfermedades con las que se relacionan.

PRODUCTO DE OXIDACIÓN	PATOLOGÍA	MODELO EXPERIMENTAL	ROL DEL PRODUCTO DE OXIDACIÓN	REFERENCIAS
α-AA	Diabetes	Humanos	Marcador	Wang *et al*. (2013)
α-AA	Resistencia a la insulina en obesidad	Humanos	Marcador	Lee *et al*. (2019)
α-AA	Depresión	Ratas	Marcador	Ni *et al*. (2014)
α-AA	Daño astrocítico	Cultivo celular	Inductor del daño	Voronkov *et al*. (2021)
α-AA	Aumento de estrés y depresión	Ratas y ratones	Inductor del trastorno	David *et al*. (2019)
3NT	Enfermedad de Alzheimer y Parkinson	Humanos	Marcador	Bandookwala & Sengupta (2020)
Tioles	IBD	Humanos	Marcador	Passos *et al*. (2023)
3NT, ditirosina, AOPPs, AGEs	Deterioro del aprendizaje espacial y de la memoria	Ratones	Inductor del trastorno	Li *et al*. (2019a)
Ditirosina	Disfunción de la secreción de insulina	Ratones	Inductor del trastorno	Ding *et al*. (2017)
Ditirosina	Deterioro del aprendizaje espacial y de la memoria	Ratas	Inductor del trastorno	Li *et al*. (2019b)
AOPPs	Insuficiencia renal crónica	Humanos	Marcador	Šebeková *et al*. (2012)

Carbonilos, ditirosina, AOPPs	Fibrosis hepática y renal	Ratones	Inductores del daño	Li *et al*. (2014)
Disminución ratio GSH/GSSH	Enfermedad de Alzheimer y Parkinson	Humanos	Marcador	Owen & Butterfiel (2010)

Se han analizado gran cantidad de tipos de carnes y productos cárnicos que tienen contenidos significativos de proteínas oxidadas, en concreto carbonilos, como son el bacon (Soladoye *et al*., 2017), cecina de pollo (Silva *et al*., 2016), sangre cocinada (Frame *et al*., 2020), hamburguesas de pollo (Neto *et al*., 2021), jamón cocido (Armenteros *et al*., 2016), entre otros. En el pescado y productos procesados del mismo también se han encontrado carbonilos en una abundancia significativa, tales como la trucha arco iris picada (Bitalebi *et al*., 2019) y surimi de pescado (Zhao *et al*., 2019). Es importante destacar que todos los productos nombrados previamente, como se puede observar, han sido sometidos a tratamientos como el ahumado, curado, cocido, picado, o se les han añadido aditivos como en el caso del surimi. Aunque, por otro lado, también se han encontrado carbonilos en productos frescos como la carne de conejo (Wang *et al*., 2018), carne de cerdo (Hernández-López *et al*., 2016) y gambas crudas (Ruvalcaba-Márquez *et al*., 2021). No solamente en la carne y productos cárnicos se han encontrado cantidades significativas de carbonilos, sino también en productos lácteos, habiendo mayor cantidad en el queso feta, seguido de la leche y el yogur (Kalaitsidis *et al*., 2021). Curiosamente, también en leche en polvo para lactantes (Chen *et al*., 2019), pero afortunadamente en menor cantidad. Los productos vegetales, como la proteína de soja, también contienen cantidades significativas de carbonilos (Yu *et al*., 2018; Zhang *et al*., 2017).

Mientras que la relación entre el consumo de productos de la oxidación proteica (carbonilos y otros aminoácidos oxidados) y la aparición de graves enfermedades neurológicas asociadas al estrés oxidativo como la enfermedad de Alzheimer, la enfermedad de Parkinson y la depresión, están aún bajo estudio (Estévez & Xiong, 2019), el consumo de alimentos ultraprocesados sí parecen estar contribuyendo a la aparición de éstas y otras enfermedades crónicas. En 2021, se realizó un estudio por parte del Centro Nacional de Salud y Nutrición de Estados Unidos, en el que se evaluó la relación entre el consumo de alimentos ultraprocesados y el rendimiento cognitivo en adultos (Cardoso *et al*., 2022). Este trabajo determinó que el consumo de alimentos ultraprocesados derivaba en un peor desarrollo de pruebas que evaluaban el lenguaje y la función cognitiva en personas adultas que no sufrían ni diabetes ni enfermedades cardiovasculares.

Las ROS están vinculadas con este tipo de enfermedades neurológicas, en las cuales se producen lesiones de las proteínas y el ADN, provocando inflamación, daño tisular y una posterior apoptosis celular (Uttara *et al*., 2009). Con respecto a la enfermedad de Alzheimer, se ha demostrado que el estrés oxidativo afecta al aprendizaje y a la memoria de los pacientes que la padecen (Kamat *et al*., 2014). Baraibar *et al*. (2012) descubrieron que las células sometidas a un estrés oxidativo severo se mantenían en un estado de detención del ciclo celular, asociado a la formación de agregados de proteínas oxidadas. Estos agregados proteicos no son capaces de ser eliminados de manera equilibrada entre su formación y su eliminación por parte del proteasoma, el sistema empleado por las células para degradar las proteínas no deseadas. Esta condición fue corroborada posteriormente por *Höhn et al*. (2017), donde se asociaba el detención del ciclo celular con el envejecimiento y la enfermedad de Alzheimer. Curiosamente, el tipo de proteasoma que se encarga de la degradación de las proteínas carboniladas, denominado proteasoma 20s (Lefaki *et al*., 2017), no es capaz de degradar proteínas extremadamente carboniladas y agregadas (Estévez & Xiong, 2019), lo que concuerda con los cúmulos de agregados proteicos encontrados en la enfermedad de Alzheimer.

Otro factor a tener en cuenta en las enfermedades neurológicas son la ruta de las quinureninas, resultado de la oxidación del triptófano. Trabajos relacionados con el estudio de esta ruta, relacionan enfermedades como la depresión, la epilepsia, el autismo, la enfermedad de Alzheimer, la esquizofrenia y la mayor susceptibilidad al suicidio con un exceso de estrés oxidativo en la ruta de las quinureninas (Braidy & Grant, 2017; González Esquivel *et al*., 2017). Asimismo, la influencia de los carbonilos se ve reflejada en la enfermedad de Alzheimer y la enfermedad de Parkinson por sexos. Los hombres con enfermedad de Alzheimer mostraron valores significativamente más altos de carbonilos en sangre en comparación con los hombres del grupo control y hombres con enfermedad de Parkinson, mientras que el grupo de las mujeres con enfermedad de Alzheimer presentó valores más bajos (Sharma *et al*., 2020). También se observaron diferencias específicas por sexo para otros marcadores relevantes como la 3NT y el MDA (Sharma *et al*., 2020).

Productos de oxidación como carbonilos, quinureninas, aminoácidos nitrosados como la 3NT, etc., están presentes en muchos alimentos y las ingerimos a través de la dieta, y particularmente vehiculados por alimentos ultraprocesados, que contienen elevados niveles de estos compuestos. El hecho de que la ingesta de estos productos de oxidación proteica (estrés oxidativo post-prandial) puedan contribuir al estrés oxidativo orgánico en seres humanos requiere de nuevos y más ambiciosos experimentos puesto que es un tema poco estudiado. Parece razonable considerar que la ingesta sostenida de estos compuestos, particularmente a través de la ingesta de alimentos ultraprocesados, podría estar contribuyendo a la aparición o agravamiento de enfermedades crónicas donde estos

mismos compuestos se saben están presentes y juegan un importante papel en la fisiopatología de la enfermedad. Sin embargo, el impacto sobre la salud de la ingesta de proteínas y/o aminoácidos oxidados es un tema del que se sabe aún muy poco.

1.4 Compuestos antioxidantes y uso terapéutico

Los antioxidantes son moléculas que son capaces de donar un electrón a un radical libre y neutralizarlo. Son donadores de electrones que tras ceder un electrón a un radical libre, la molécula resultante con un número impar de electrones en su capa de valencia continúa siendo químicamente estable. De esta manera, contribuye a detener la propagación de las reacciones de oxidación producidas por los radicales libres (Kotha *et al*., 2022).

En todos los organismos existen diferentes tipos de defensas antioxidantes para luchar contra las ROS/RNS, que se pueden catalogar en enzimas antioxidantes, compuestos no enzimáticos con capacidad antioxidante y proteínas quelantes de metales de transición. Las enzimas antioxidantes paralizan la propagación radicalaria y neutralizan los radicales libres ya formados. Dentro de este conjunto, las enzimas más importantes son CAT, SOD y GPx. Los sistemas no enzimáticos son moléculas con capacidad antioxidante donando electrones a las ROS/RNS, y, de ese modo, neutralizándolas. El glutatión, ácido ascórbico, (vitamina C), α-tocoferol (vitamina E), ácido úrico, bilirrubina, polifenoles y carotenoides son las moléculas antioxidantes más representativas del sistema endógeno de defensa antioxidante. Por último, las proteínas quelantes de metales de transición atrapan átomos de hierro y cobre libres, evitando así que la reacción de Fenton tenga lugar. La albúmina, transferrina y ceruloplasmina son las proteínas más relevantes (Condello & Meschini, 2021).

En la naturaleza existen gran multitud de compuestos antioxidantes, sobre todo provenientes de plantas, denominados fitoquímicos. En los últimos tiempos, ha habido un sumo interés en el impacto de los fitoquímicos naturales en los alimentos que pueden funcionar como antioxidantes en el cuerpo humano. Este interés ha surgido a partir de la creencia popular que define a los oxidantes como nocivos y a los antioxidantes como totalmente saludables (Kotha *et al*., 2022). Es importante destacar que la bioaccesibilidad, biodisponibilidad y metabolismo de los antioxidantes son factores importantes a tener en cuenta. Existen fitoquímicos, como los flavonoides, dentro del grupo de los polifenoles, que se alteran estructuralmente *in vivo* por lo que su administración debería ser con el uso de sistemas adecuados como liposomas y nanopartículas, entre otros (Panche *et al*., 2016), para que puedan surtir sus efectos en el organismo.

En el campo de las ciencias de los alimentos, el uso de compuestos antioxidantes puede ser una buena alternativa para reducir la oxidación proteica sufrida en la carne y productos cárnicos procesados, como por ejemplo en hamburguesas, salchichas, albóndigas, entre otros (Estévez, 2021). Pero, además, hay evidencias que demuestran que la incorporación de antioxidantes en los alimentos no solo puede estar motivado para proteger al alimento de la oxidación, sino también para llegar hasta el consumidor final y proteger a éste del estrés oxidativo. En la literatura científica, se pueden encontrar multitud de trabajos que emplean compuestos con capacidad antioxidante en el estudio de la posible mejora de los síntomas de muchas enfermedades. En el caso de la IBD, se ha comprobado que el empleo de flavonoides mitiga la gravedad del estrés oxidativo y la inflamación intestinal en etapas tempranas de este trastorno. En concreto, las quercetinas, las catequinas y la silimarina funcionan como moduladores celulares eficaces de las vías de señalización de la proteína quinasa y quinasas lipídicas que impulsan la IBD (Sahoo *et al*., 2023). Con respecto al cáncer colorrectal, compuestos como β-carotenos, ascorbato, licopeno, curcumina, epigalocatequinas y resveratrol, aportan una mejora de la biología tumoral, efecto antiinflamatorio y quelación del hierro tanto en modelos *in vitro*, animales y humanos (Condello & Meschini, 2021). En las enfermedades de origen neurológico, la investigación de sustancias antioxidantes también es un gran campo de actuación, encontrándose gran cantidad de compuestos, no solo fitoquímicos, que tienen propiedades beneficiosas antiinflamatorias, antioxidantes, antidepresivas, neuroprotectoras, entre otras, en el tratamiento de este tipo de trastornos (Morén *et al*., 2022).

Uno de los compuestos con efectos antioxidantes documentalmente más destacados y con efectos variados es el ácido elágico (en inglés, *ellagic acid*, EA). El EA se encuentra dentro de la familia de los polifenoles y está presente en diversas especies vegetales, como *Larrea tridentata, Euphorbia antisyphilitica, Fluorencia cernua, Jatropha dioica* y *Punica granatum L.*, entre otros (Alfei *et al*., 2020; Ascacio-Valdés *et al*., 2013). Estructuralmente, el EA es un derivado dimérico del ácido gálico (Figura 1.12), producido principalmente por la hidrólisis de elagitaninos y posee propiedades antiinflamatorias, antiproliferativas, antioxidantes y antimutagénicas, tanto *in vitro* como *in vivo* (Sharifi-Rad *et al*., 2022). *Punica granatum L*. cuyo fruto es la granada, contiene particularmente grandes concentraciones de EA, alrededor de 811 mg/L (García-Villalba *et al*., 2015).

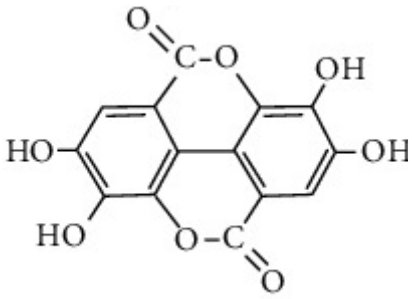

Figura 1.12. Estructura del ácido elágico (EA). Fuente: Ascacio-Valdés *et al*. (2013)

Numerosos estudios indican que el EA puede estar involucrado en la regulación de un amplio espectro de vías de señalización celular para prevenir, mitigar o ralentizar la progresión de enfermedades cardiovasculares, neurodegenerativas, diabetes y cáncer (Sharifi-Rad *et al*., 2022).

1.5. Metodologías avanzadas en ciencias de los alimentos y la nutrición

Para el estudio de la oxidación de las proteínas y sus repercusiones tanto en sistemas *in vitro* como *in vivo*, es necesario la utilización de técnicas avanzadas para el estudio en profundidad de estas consecuencias. En primer lugar, la elección del sistema modelo a emplear en la investigación es un aspecto fundamental, comenzando por modelos más fáciles de manejar y sin implicaciones éticas, como el caso de los cultivos celulares, y más adelante, la utilización de modelos animales, que proporcionan más información global sobre lo que sucede en un organismo con todas sus interacciones, pero con implicaciones éticas cuestionables.

El estudio de la repercusión de la oxidación proteica en modelos animales y modelos *in vitro,* se deben realizar con las técnicas actualmente más avanzadas para conseguir los resultados más acordes a la realidad sobre lo que está sucediendo dentro de ese modelo. Las consecuencias dentro de las células o en el proteoma tanto en tejidos como en células son estudiadas en esta tesis, con las técnicas de citometría de flujo, análisis de carbonilos y proteómica, siendo todas pioneras en el campo de ciencias de los alimentos.

A continuación, se describen las técnicas mencionadas con la finalidad de conocer los mecanismos moleculares implicados en la oxidación de proteínas.

1.5.1. Experimentación animal y cultivo celular

La experimentación animal es toda acción de carácter científico, experimental o docente que pueda llegar a suponer un ataque al estado de bienestar del animal, susceptible de causarle dolor,

sufrimiento, angustia o agravio (Real Decreto 53/2013). El inicio de la conciencia de la utilización de modelos alternativos a la experimentación animal surgió por primera vez en la Segunda Guerra Mundial, donde el régimen nazi, sorprendentemente, ya que promovió una limpieza étnica en seres humanos, proclamó los derechos de los animales. En años sucesivos, esta conciencia fue incrementándose y tomando cabida en el mundo científico, hasta que el 1959, Russell y Burch desarrollaron el concepto de la triple R, que se basa en la reducción, reemplazo y refinamiento (3Rs) del uso de animales y su sustitución por otros métodos y mejora de estos.

La reducción consiste en la utilización de un diseño experimental y análisis estadístico apropiado, evitando al máximo los experimentos innecesarios y el número de animales empleados en ellos. El refinamiento involucra la adopción de normas y parámetros internacionales del manejo animal y la optimización de su ambiente, modificando los protocolos de experimentación de tal manera que causen el menor dolor, sufrimiento, angustia o agravia al animal. Por último, el reemplazo consiste en la utilización de métodos alternativos al uso de animales, tanto en experimentación científica como en actividades de docencia (Real Decreto 53/2013).

De la necesidad del reemplazo de los animales en el campo de la experimentación, surgió el empleo del cultivo celular como una técnica empleada para la sustitución del uso masivo de animales en experimentos científicos (Vallejo *et al*., 2017). Estos cultivos celulares provienen de líneas celulares inmortales, con una serie de características que las hacen apropiadas para poder llevar a cabo experimentos científicos reproducibles. Los cultivos celulares son capaces de dar lugar a monocapas celulares con gran capacidad de resistencia y adaptación al medio donde se están cultivando, además de tener una reproducción ilimitada (Pinto *et al*., 1983).

Las líneas de cultivos celulares puras (formadas por un solo tipo de célula dividiéndose en clones) más utilizadas en el estudio de permeabilidad de sustancias simulando un modelo de intestino son las células de la línea CACO-2 (Figura 1.13). Estas células provienen de adenocarcinoma de colon humano y tienen la gran ventaja de diferenciarse a lo largo del tiempo (exactamente 21 días), adquiriendo características morfológicas y bioquímicas similares a los enterocitos (Ding *et al*., 2021; Pinto *et al*., 1983).

En el campo de las ciencias de los alimentos, son muchos los trabajos que utilizan como modelo experimental el cultivo celular formado por células CACO-2. Estas células se emplean tanto para estudiar sustancias potencialmente dañinas, como contaminantes presentes en los alimentos o sustancias del metabolismo de los ácidos grasos en el intestino (Guibourdenche *et al*., 2021; Peng *et*

al., 2007; Qiu *et al*., 2023; Rodríguez-Viso *et al*., 2022), como para elucidar la posible capacidad antioxidante de moléculas presentes en plantas u otros organismos (Ahmed *et al*., 2020; Andrade *et al*., 2017; Duda-Chodak *et al*., 2009; Gómez *et al*., 2019).

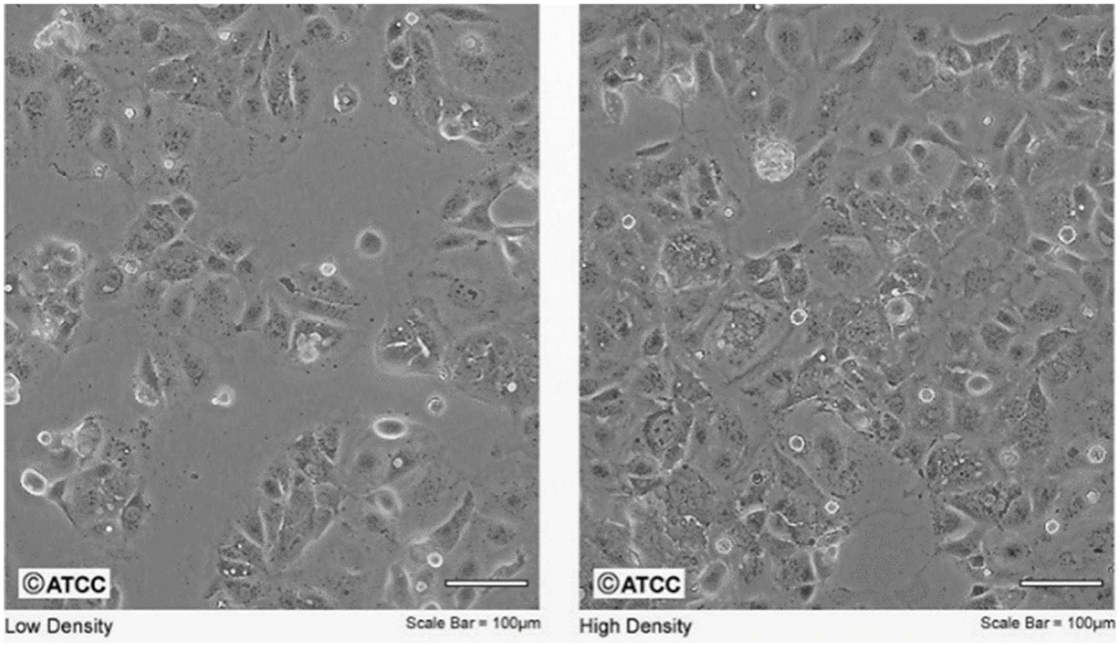

Figura 1.13. Cultivo celular de células CACO-2 en baja y alta densidad. Fuente: ATCC (American Type Culture Collection)

Para estudios relacionados con enfermedades neurológicas, un modelo empleado para la aproximación a lo que sería en vivo en un animal, son comúnmente empleadas las células SH-SY5Y (Figura 1.14). Estas células derivan de neuroblastoma humano y se pueden diferenciar durante 7 días por la adición de ácido retinoico, adquiriendo propiedades neuronales como el crecimiento de neuritas y cambios morfológicos para imitar la respuesta neuronal (Nicolini *et al*., 1998; Påhlman *et al*., 1984). Gran cantidad de experimentos emplean el uso de esta línea celular para la evaluación de compuestos con posibles aplicaciones terapéuticas en enfermedades neurológicas (Johnson *et al*., 2020; Unno *et al*., 2017) y también para el estudio de sustancias potencialmente neurotóxicas implicadas en la aparición de estas enfermedades (Donzelli *et al*., 2004; Faria *et al*., 2016; Lopez-Suarez *et al*., 2022).

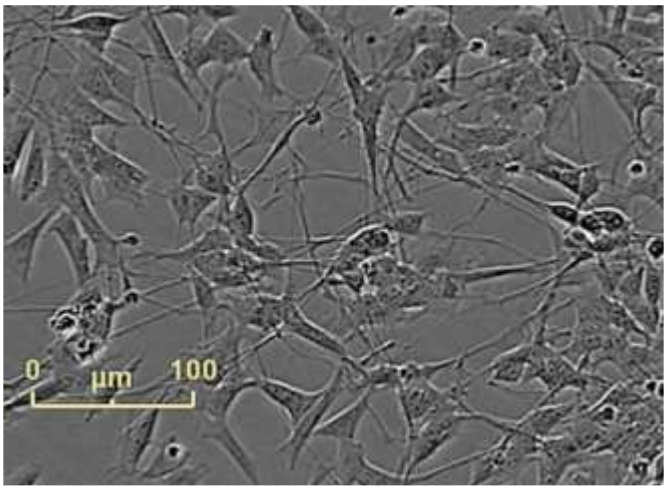

Figura 1.14. Cultivo celular de células SH-SY5Y. Fuente: ECCAC (European Collection of Authenticated Cell Cultures)

Entre las desventajas de las líneas celulares se encuentran su sensibilidad a la contaminación bacteriana y fúngica, aunque mucho menor que en el caso de cultivos celulares provenientes de animales. Asimismo, un cultivo celular da menor información sobre lo que realmente está sucediendo con respecto a un proceso biológico, ya que es un sistema aislado y no se encuentra en contacto con todos los mecanismos del organismo que pueden inferir en un proceso. Por lo tanto, la utilización de cultivos celulares puede suministrar una información aproximada de lo que está sucediendo en un grupo de células, pero en muchas ocasiones estos resultados no pueden ser extrapolables a modelos animales o humanos por la falta de información que proporciona este modelo con respecto al organismo en su conjunto.

De aquí surge la necesidad de seguir empleado la experimentación animal, para verificar o refutar los resultados que se obtienen empleando el cultivo celular y además estudiar los posibles efectos adversos que se producen en animales antes de llevar a cabo los estudios científicos en humanos. El Real Decreto 53/2013 establece que sólo se podrán utilizar animales cuando su uso esté justificado por la finalidad que se persigue, valorando su oportunidad siempre en términos de sus potenciales beneficiosos. Las especies de animales mamíferos autorizadas para poder utilizarlas en experimentación son ratón (*Mus musculus*), rata (*Rattus norvegicus*), cobaya (*Cavia porcellus*), hámsters, perros, gatos, bovinos, ovinos, caprinos, porcinos y todas las especies de primates no humanos, éste último caso restringido a casos muy especiales. Por otro lado, las especies de animales

no mamíferos incluidas son aves de granja, ranas, pez cebra, hurones, anfibios, reptiles, entre otros (RD 53/2013, Capítulo IV, Artículo 19).

En la presente tesis doctoral se emplearon las especies *Mus musculus* (cepa C57BL/6) y *Rattus norvegicus* (cepa Wistar) para el estudio de los posibles efectos toxicológicos de los aminoácidos oxidados estudiados y el posible beneficio del uso de un compuesto fenólico. El manejo, sacrificio y protocolos experimentales fueron aprobados por el Comité Institucional de Bioética (referencia 57/2016).

1.5.2. Citometría de flujo

La citometría de flujo es una herramienta para el análisis de múltiples parámetros celulares individuales de poblaciones heterogéneas. Un citómetro de flujo implica un instrumento que ilumina las células a medida que fluyen individualmente frente a una fuente de luz y posteriormente detecta y correlaciona las señales de esas células emiten. Los citómetros a menudo pueden medir objetos que no son células, como por ejemplo partículas. Por lo tanto, es más adecuado emplear el término "evento" para indicar la materia que es interpretada por el citómetro de flujo como una sola partícula (Juan-García *et al*., 2013).

Los eventos, células o partículas dispersan la luz y esta luz dispersada es la que detecta el aparato, pero parte de esa luz emitida no es luz dispersada, sino fluorescencia. Muchas partículas tienen autofluorescencia natural y esto puede ser detectado por el citómetro de flujo, situación que debe tenerse en cuenta. Las células o eventos de interés deben ser teñidos con un fluorocromo o sonda fluorescente antes de que puedan ser analizados por el citómetro. Una sonda fluorescente absorbe la luz de ciertos colores específicos y luego emite luz de un color diferente (generalmente de una longitud de onda más larga).

Las células provenientes del cultivo celular deben ser estudiadas empleando técnicas no destructivas, como es el caso de la citometría de flujo. La característica *sine qua non* de esta técnica es la necesidad de que las células a analizar se encuentren intactas. Por lo tanto, es una buena elección, rápida y fiable para estudiar el estrés oxidativo y otros parámetros celulares conservando la integridad celular (Juan-García *et al*., 2013; McKinnon, 2018; Picot *et al*., 2012). Junto con la citometría de flujo, existen otras técnicas, como HPLC (Cromatografía líquida de Alta Resolución, en inglés, *High Performance Liquid Cromatography*), método TBARs (Sustancias Reactivas al Ácido Tiobarbitúrico, en inglés, *Thiobarbituric Acid Reactive Substances*) o el ensayo Comet (en inglés, *Comet assay*) que son empleadas en estudios para la búsqueda de sustancias procedentes del estrés oxidativo como el α-AS, el MDA o el 8-oxodG

(Chang *et al*., 2008; Collins, 2014). Pero a diferencia de la citometría de flujo, estas técnicas sí son destructivas.

Una de las ventajas más destacadas de la citometría de flujo es la capacidad de enumerar, correlacionar y resumir un gran número de células o eventos individuales a una velocidad entre 500 y 5.000/s. Para conseguir resultados fiables, se deben analizar como mínimo unos 10.000 eventos (Givan, 2011). Las mediciones con esta técnica se realizan dentro de una suspensión, pasando miles de células por segundo a través de uno o varios tipos de láser, capturando la luz que emerge de cada célula a su paso (Juan-García *et al*., 2013). En general, los eventos deben medir entre 1-30 mm de diámetro aproximadamente. Si los eventos son muy pequeños, el citómetro podría no detectarlos, mientras que, si por el contrario los eventos son demasiado voluminosos, podrían obstruir el aparato. Las partículas para la citometría de flujo deben estar suspendidas en un tampón a una concentración de $5x10^5$ a $5x10^6$/ml. La luz emitida por cada evento es detectada y almacenada en un archivo de datos para su posterior análisis.

Las sondas fluorescentes se pueden conjugar con anticuerpos y, en este caso, la fluorescencia de una célula o evento será una lectura de la cantidad de fluorescencia emitida por la proteína/antígeno (en el citoplasma, núcleo o superficie de la célula) unida al anticuerpo. Una cuestión importante es conocer qué sondas son las adecuadas para el citómetro de flujo. Dependiendo de que en longitud de onda se quiere medir, qué tipo de parámetro se quiere analizar y en qué tipo de partículas se quieren realizar esas mediciones, se elegirán unas sondas u otras. Esto requiere no solo el conocimiento de la longitud de onda a emplear, sino también las especificidades de longitud de onda de los filtros frente a los fotodetectores del instrumento, y las características de absorción y emisión de las sondas.

Los fluorocromos utilizados para teñir las células deben ser capaces de absorber una longitud de onda en concreto del espectro de luz y los detectores deben tener filtros apropiados para detectar la fluorescencia emitida (Givan, 2011). Actualmente, se utilizan hasta siete láseres con longitudes de onda de emisión entre 325 y 808 nm para lograr una alta flexibilidad en la elección de las sondas fluorescentes (Cossarizza *et al*., 2019), pero los más utilizados son el ion argón, el ion kriptón, los láseres de helio-neón, el láser azul en estado sólido, láser de diodo rojo o verde, láser de diodo violeta o muy cerca del ultravioleta y láser de fibra naranja. El láser más comúnmente utilizado es el láser azul en estado sólido, siendo su longitud de onda de emisión de 488 nm (Givan, 2011)

La luz emitida por cada evento es representada mediante gráficos de puntos, figuras tridimensionales, histogramas, entre otros. En estos gráficos se representan normalmente la intensidad de fluorescencia

de cada sonda que se correlaciona con la intensidad del parámetro estudiado. Otra ventaja de este método radica en la posibilidad de determinar una amplia gama de parámetros celulares, como, por ejemplo, como la viabilidad celular, el estado redox, o el nivel de apoptosis y necrosis donde la citometría de flujo ofrece la posibilidad de separar físicamente las subpoblaciones (Picot *et al*., 2012). Muchas de estas mediciones se pueden hacer simultáneamente en las mismas células, empleando sondas que no se solapen unas con otras (Perfetto *et al*., 2004) suponiendo un gran ahorro de tiempo.

La citometría de flujo tiene una amplia gama de aplicaciones en investigación que incluyen, inmunofenotipado, análisis de ADN multiparamétrico, estudios de proliferación, conteo celular, entre otras muchas (Picot *et al*., 2012). Esta técnica es una herramienta útil en estudios redox para el análisis rápido de células individuales en una mezcla de un cultivo celular, pero no es una técnica ampliamente utilizada en cultivos celulares, y menos aún en el análisis de procesos redox donde se estudian sustancias oxidantes de los alimentos, siendo más bien una técnica complementaria. A pesar de ello, esta tendencia está cambiando en el campo de los cultivos celulares y las ciencias de los alimentos, donde cada vez más estudios emplean la citometría de flujo como unas de sus principales herramientas (Bouaziz *et al*., 2008; Cilla *et al*., 2018; He *et al*., 2019; Hu *et al*., 2019; Xie *et al*., 2014).

1.5.3. Técnicas ÓMICAS

Las técnicas ÓMICAS son un conjunto de técnicas de última generación que evalúan la información contenida en las principales moléculas de los organismos vivos, como son el ADN, ARNm, proteínas y metabolitos. Las técnicas existentes hoy en día, dependiendo de las moléculas que se quieran estudiar, se clasifican en genómica, transcriptómica, proteómica y metabolómica (Patti *et al*., 2012). La genómica está enfocada al estudio del genoma (conjunto de genes que forman el ADN), a su caracterización y cuantificación. Una de las aplicaciones de la genómica es la identificación de las mutaciones que se producen en genes asociados a enfermedades.

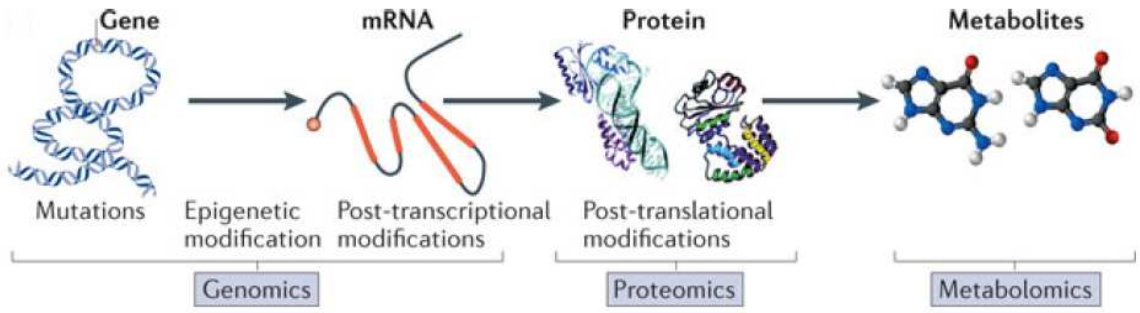

Figura 1.15. Genómica, proteómica y metabolómica. Fuente: Adaptado de Patti *et al*. (2012)

La transcriptómica se dedica al estudio de los cambios post-transcripcionales, es decir, las modificaciones epigenéticas que se producen en la transcripción de ADN a ARNm. La proteómica, por su parte, trata el estudio del proteoma de los organismos, es decir, el conjunto de proteínas que forman un individuo, estudiando las modificaciones post-traduccionales que tienen lugar en ese proteoma. Por último, la metabolómica consiste en el estudio de moléculas que se encuentran en el organismo, tales como azúcares, nucleótidos, lípidos, entre otros (Figura 1.15).

La proteómica es el estudio de la composición, estructura, funciones e interacciones de las proteínas y sus actividades celulares (Wilkins *et al*., 1996). La proteómica proporciona una mejor comprensión de la estructura y función del organismo que la genómica, sin embargo, es mucho más complicado que ésta porque la expresión de proteínas se altera según el tiempo y las condiciones ambientales (Holman *et al*., 2013).

Existe una variedad de técnicas proteómicas que incluyen electroforesis en gel unidimensional (1D) y bidimensional (2D) (Vercauteren *et al*., 2004). En el gel bidimensional, la separación de proteínas tiene lugar en dos dimensiones: la primera según su punto isoeléctrico y la segunda según su peso molecular (Ranjbar *et al*., 2017). Asimismo, también existen técnicas proteómicas de alto rendimiento sin gel, como la técnica de identificación de proteínas multidimensional (Washburn *et al*., 2001), o la tecnología shotgun (Wolters *et al*., 2001), entre otras muchas. La cuantificación no dirigida de cromatografía líquida de alta resolución-espectrometría de masas (LC-MS) en tándem se utilizan comúnmente para el procesamiento de alto rendimiento, la cual permite separar e identificar mezclas de péptidos complejas (Al-Amrani *et al*., 2021).

La técnica de proteómica está conformada por varios pasos, en la que cada paso debe estar muy bien controlado para evitar que factores no biológicos interfieran con la expresión y la interacción de las proteínas. La preparación de la muestra es un paso crucial en esta técnica, ya que solubiliza todas las proteínas de la muestra y elimina todos los compuestos inhibidores que pueda interferir en ella, como por ejemplo los lípidos (Rabilloud & Lelong, 2011). El método SDS-PAGE (sodium dodecyl sulfate polyacrylamide gel electrophoresis) para la separación y aislamiento de proteínas por electroforesis (Graves & Haystead, 2002) es comúnmente el más utilizado.

Entre las aplicaciones de la proteómica se encuentran la generación de conocimiento profundo, complejo y preciso sobre los mecanismos moleculares implicados en la aparición y progresión de enfermedades, las funciones celulares y también el descubrimiento de biomarcadores. Esta tecnología puede identificar y monitorear biomarcadores mediante el análisis de las proteínas en los fluidos corporales, como la orina, el suero, el líquido cefalorraquídeo e incluso el aliento exhalado. La proteómica también puede facilitar el desarrollo de fármacos al proporcionar un mapa completo de las interacciones de las proteínas asociadas con las vías de la enfermedad, pudiendo comparar grupos de pacientes con respecto a grupos controles sanos (Al-Amrani *et al*., 2021).

En el campo de las ciencias de los alimentos, la proteómica se emplea para analizar muy diversos productos alimenticios, como por ejemplo especies de cultivos económicamente importantes como el garbanzo (Pandey *et al*., 2018), o el estudio de compuestos antioxidantes de interés como el extracto de romero enriquecido con polifenoles (Valdés *et al*., 2016). Relacionado con la carne y productos cárnicos, se pueden encontrar trabajos que analizan la Influencia del daño oxidativo a las proteínas en la terneza de la carne (Malheiros *et al*., 2019), el estudio de modificaciones oxidativas de las proteínas de la carne de cerdo bajo la influencia de tratamientos térmicos variados en tiempo y temperatura (Mitra *et al*., 2018), o perturbaciones oxidativas y deterioro de la calidad de la pechuga de pollo en piezas con miopatías (Carvalho *et al*., 2023). Asimismo, los análisis de aminoácidos discriminantes entre carne roja y carne blanca (Rombouts *et al*., 2017) han empleado la técnica de proteómica, aportando mucha información en el conocimiento de los aminoácidos oxidados presentes en la carne y productos cárnicos.

2. PLANTEAMIENTO Y OBJETIVOS

2. PLANTEAMIENTO Y OBJETIVOS

Teniendo en cuenta i) el desconocimiento de los mecanismos moleculares de los posibles efectos nocivos para la salud causados por la ingesta de aminoácidos oxidados y nitrosados presentes en los alimentos y ii) que el posible empleo de compuestos antioxidantes para intentar paliar los efectos nocivos causados por estos compuestos es desconocido, el **principal objetivo** de esta Tesis Doctoral es identificar los mecanismos moleculares implicados en la respuesta a la ingesta de aminoácidos oxidados y nitrosados frente a la amenaza de estrés oxidativo y otros efectos nocivos mediante el empleo de técnicas moleculares avanzadas, como la proteómica.

Para cumplir con este objetivo general se plantearon los siguiente objetivos parciales:

- Estudiar la posible citotoxicidad de diferentes aminoácidos nitrosados y oxidados sobre células intestinales humanas cultivadas *in vitro*.

- Dilucidar los mecanismos moleculares subyacentes de los efectos toxicológicos del aminoácido oxidado, α-AA, tanto *in vitro* como *in vivo*.

- Conocer los efectos nocivos del aminoácido nitrosado, 3NT, mediante el estudio de los mecanismos moleculares afectados tanto en cultivos celulares como en animales.

- Mitigar el posible efecto perjudicial de la ingesta del aminoácido oxidado α-AA y el aminoácido nitrosado 3NT con el empleo de compuestos fenólicos como posible uso terapéutico frente al estrés oxidativo *in vitro* e *in vivo*.

3. DISEÑO EXPERIMENTAL

La presente Tesis Doctoral está dividida en seis capítulos bien diferenciados. En el primer capítulo se quiso realizar una primera evaluación de los aminoácidos oxidados/nitrosados más citados en la bibliografía científica, en base a su posible implicación en la generación de estrés oxidativo. Los aminoácidos estudiados fueron α-AA, ditirosina, 3NT, quinurenina y ácido quinurénico, a una dosis de 200µM, concentración compatible con las encontradas en alimentos. Todos estos compuestos y demás reactivos utilizados en el estudio fueron comprados en Panreac (Panreac Química, S. A., Barcelona, España), Merck (Merck, Darmstadt, Alemania) y Sigma Chemicals (Sigma-Aldrich, Steinheim, Alemania). Para analizar el efecto de cada compuesto se utilizó un modelo *in vitro* de cultivo celular, en este caso de adenocarcinoma de colon humano denominado CACO-2, obtenido de la Colección Europea de Cultivos Celulares Autenticados (ECACC, Salisbury, Reino Unido) (Figura 3.1).

Previamente al experimento, las células se diferenciaron de manera espontánea durante 21 días, para así permitir que adquirieran características morfológicas y bioquímicas similares a los enterocitos (Ding *et al*., 2021; Pinto *et al*., 1983). Posteriormente, un lote de células fue incubado durante 4 horas y otro lote durante 72 horas con los distintos aminoácidos oxidados/nitrosados, analizándose, por triplicado, su efecto en el cultivo celular mediante citometría de flujo, concentración de GSH por UHPLC-MS/MS mediante el método de Ortega Ferrusola *et al*. (2017) y concentración de productos de oxidación proteica primarios y avanzados mediante el protocolo descrito por Utrera *et al*. (2011) (Capítulo 4.1). En los ensayos de citometría de flujo se utilizó la sonda Hoechst 33342 para medir viabilidad celular, la sonda CellROX® para evaluar la concentración del anión $O_2^{\bullet -}$, y las sondas CellEvent Caspase-3/7 Green Detection Reagent y homodímero de etidio para medir apoptosis y necrosis, respectivamente.

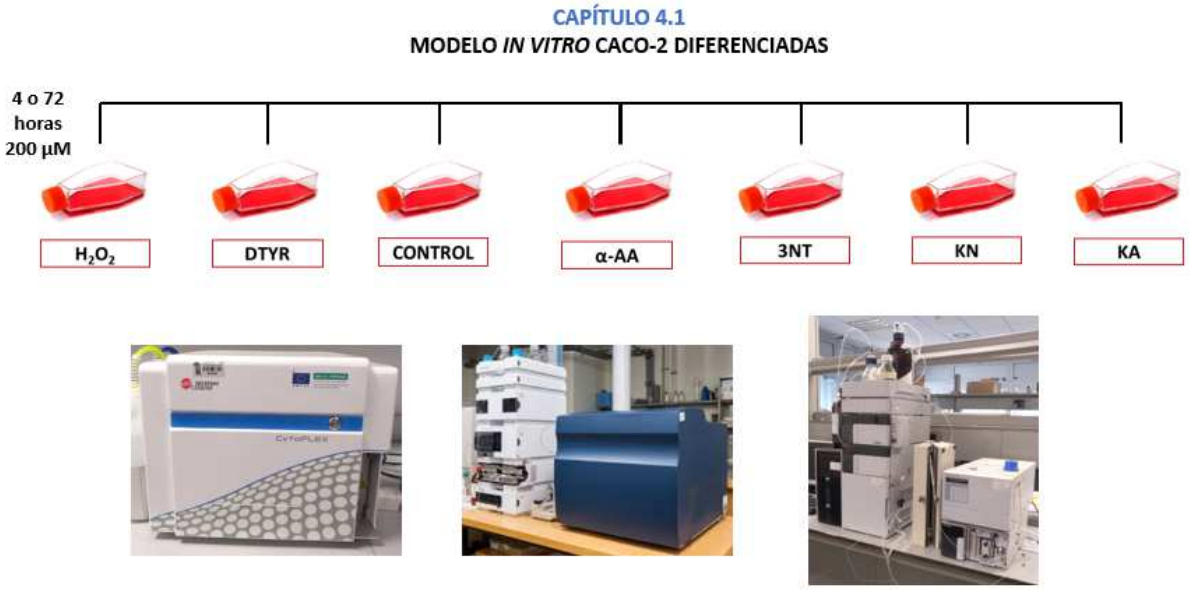

Figura 3.1. Diseño experimental *in vitro* del Capítulo 4.1

En base a los resultados obtenidos de este primer trabajo y la literatura científica existente, se decidió continuar la tesis con el estudio más en profundidad del α-AA mediante proteómica (Capítulo 4.2), técnica molecular avanzada. Se empleó de nuevo el modelo *in vitro* de células diferenciadas CACO-2 utilizando la misma dosis que en el Capítulo 4.1, durante 72 horas. Para el ensayo de proteómica, las muestras fueron tratadas y analizadas siguiendo el protocolo descrito por (Delgado *et al*., 2019), analizándose las muestras por quintuplicado. En este segundo trabajo, para complementar el estudio se empleó también la técnica de citometría de flujo y el protocolo de oxidación proteica descrito por Utrera *et al*. (2011). (Figura 3.2).

Posteriormente, se decidió realizar un tercer estudio con el mismo modelo experimental *in vitro* diferenciado, utilizando la misma dosis que en los Capítulos 4.1 y 4.2, el mismo tiempo de exposición y las mismas técnicas, pero aplicado al aminoácido nitrosado 3NT (Capítulo 4.3). Adicionalmente, se expuso el cultivo celular diferenciado a una combinación de 3NT y EA (Capítulo 4.3) (Figura 3.2), compuesto fenólico con propiedades antioxidantes bien descritas en la bibliografía.

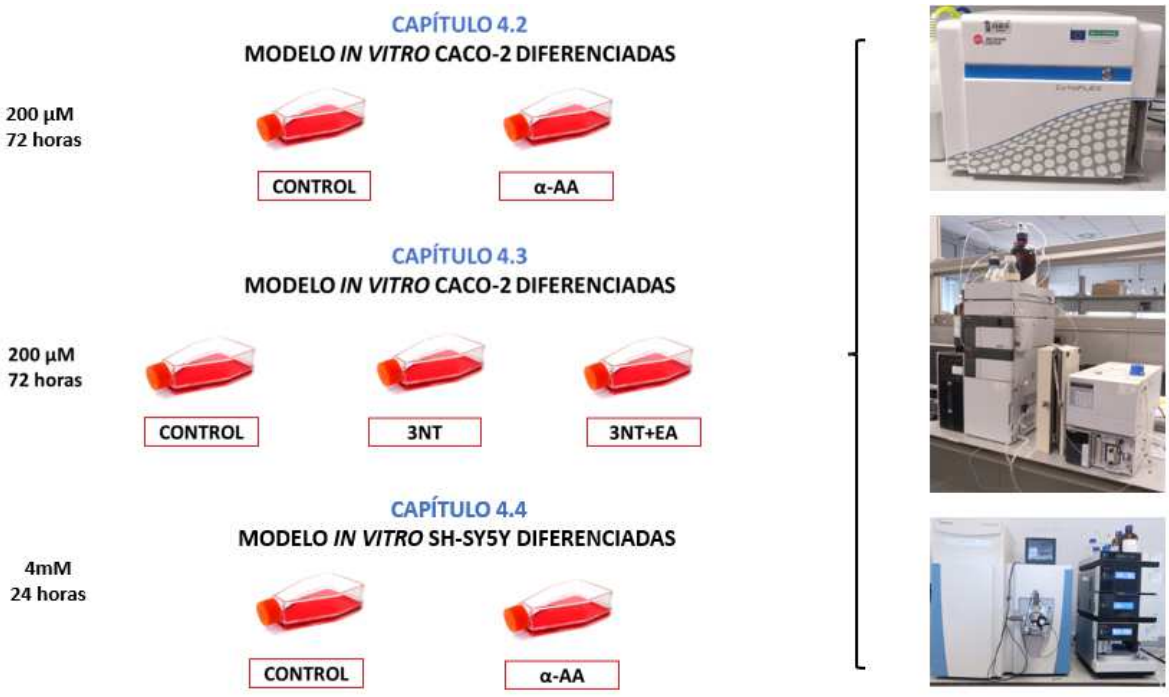

Figura 3.2. Diseño experimental *in vitro* de los Capítulos 4.2, 4.2 y 4.4

Tras este tercer estudio, se determinó utilizar otro modelo *in vitro* de cultivo celular, en este caso células provenientes de neuroblastoma humano denominadas SH-SY5Y (Capítulo 4.4). Este modelo experimental fue expuesto a una dosis de 4mM, dosis utilizada en otros trabajos donde encontraron generación de estrés oxidativo en cortes de cerebro de ratas adolescentes (da Silva *et al*., 2017). Antes de la exposición a este compuesto durante 24 horas, las células fueron diferenciadas mediante la adición de ácido retinoico durante 7 días, para la adquisición de características neuronales como el crecimiento de neuritas y cambios morfológicos para imitar la respuesta neuronal (Nicolini *et al*., 1998; Påhlman *et al*., 1984). Las técnicas fueron las mismas que las empleadas en los Capítulos previos (4.1, 4.2, 4.3) (Figura 3.2).

Para poder corroborar los resultados obtenidos hasta ese momento *in vitro*, se decidió exponer los aminoácidos y el compuesto antioxidante a modelos *in vivo*, en concreto, a la cepa de ratón C57BL/6, comúnmente utilizada como modelo experimental. En esta ocasión, para llevar a cabo el estudio, se disolvieron en agua de bebida los aminoácidos y el compuesto fenólico, dividiéndose los grupos de animales en α-AA, α-AA+EA (Capítulo 4.5), 3NT, 3NT +EA (Capítulo 4.6) y su respectivo grupo control, tal y como se muestra en la Figura 3.3. Los animales tenían acceso *ad libitum* tanto al agua de bebida como al pienso. Cada condición se replicó por duplicado en jaulas separadas, conteniendo cada jaula 2-3 animales.

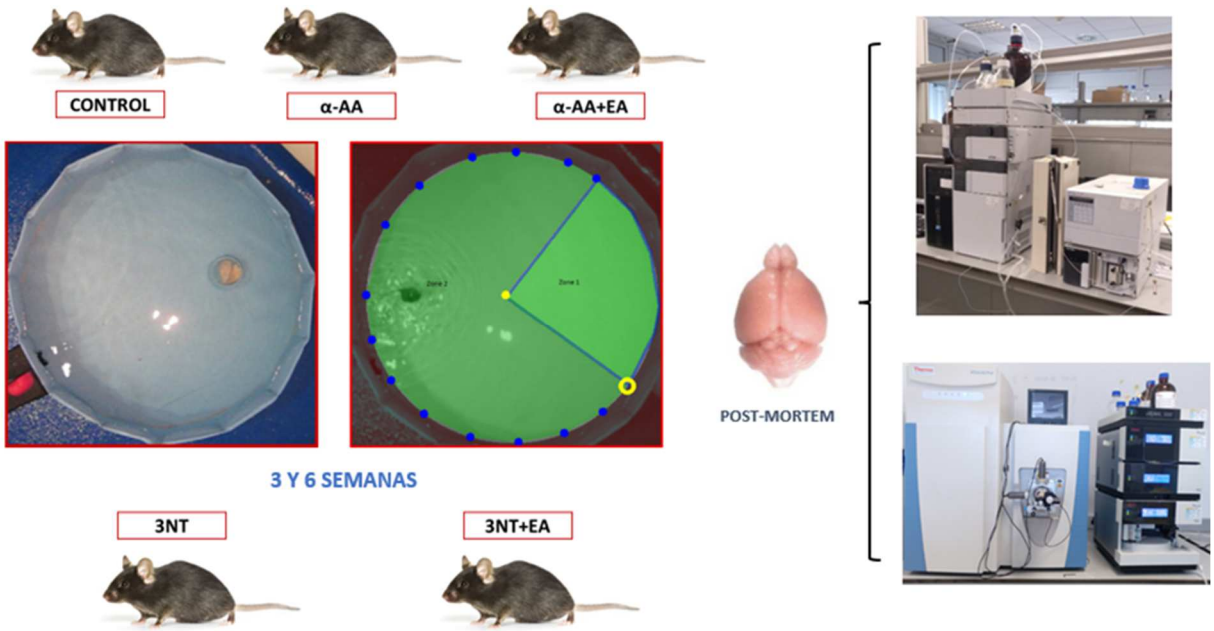

Figura 3.3. Diseño experimental *in vivo* de los Capítulos 4.5 y 4.6

Para estudiar la posible pérdida de memoria espacial en los ratones a causa de la exposición a estos compuestos, se realizó la prueba del laberinto de Morris, que consiste en una piscina dividida en dos áreas, en una de las cuales se coloca una plataforma no visible para los animales, que tienen que encontrar a mitad (3 semanas) y al final (6 semanas) del experimento. Previamente, los ratones fueron entrenados para encontrar la plataforma, teniendo como única referencia una señal colocada en sentido contrario a donde estaba situada la plataforma bajo el agua, siguiendo las indicaciones descritas por Patil *et al*. (2009) (Figura 3.3).

El experimento tuvo lugar durante 6 semanas, tras las cuales los ratones fueron eutanasiados y todos los órganos fueron recogidos y congelados a -80ºC para su posterior análisis. Finalmente, se analizó el cerebro de cada uno de los integrantes de cada grupo de estudio mediante ensayos de proteómica y mediciones de productos de oxidación proteica (Figura 3.3) de igual manera que en los capítulos anteriores.

4. RESULTADOS

4. RESULTADOS

Capítulo 4.1. Noxious effects of selected food-occurring oxidized amino acids on differentiated CACO-2 intestinal human cells.

Capítulo 4.2. Protein oxidation marker, α-amino adipic acid, impairs proteome of differentiated human enterocytes: Underlying toxicological mechanism.

Capítulo 4.3. Ellagic acid triggers the necrosis of differentiated human enterocytes exposed to 3-nitro-tyrosine: An MS-based proteomic study.

Capítulo 4.4. α-Amino adipic acid, marker of protein oxidation and analogue of neurotransmitter glutamic acid, causes mitochondrial disturbance, oxidative stress and apoptosis on differentiated human neuronal SH-SY5Y cells.

Capítulo 4.5. The intake of ellagic acid decreases the oxidative stress caused by α-amino adipic acid in the brain of C57BL/6 mice: underlying molecular mechanisms via proteomic approach

Capítulo 4.6. Food-compatible doses of 3-nitrotyrosine causes loss of spatial memory in C57BL/6 mice: investigation of molecular mechanisms by brain proteomics

Capítulo 4.1. Noxious effects of selected food-occurring oxidized amino acids on differentiated CACO-2 intestinal human cells.

Efectos nocivos de aminoácidos oxidados presentes en alimentos seleccionados sobre células humanas intestinales diferenciadas CACO-2.

DOI: https://doi.org/10.1016/j.fct.2020.111650

Autores: Silvia Díaz-Velasco, Antonio González, Fernando J. Peña, Mario Estévez

Año de publicación: 2020

Revista: Food and Chemical Toxicology

Indice de Impacto JCR (2020): 6.023

Food and Chemical Toxicology 144 (2020) 111650

Contents lists available at ScienceDirect

Food and Chemical Toxicology

journal homepage: www.elsevier.com/locate/foodchemtox

Noxious effects of selected food-occurring oxidized amino acids on differentiated CACO-2 intestinal human cells

S. Díaz-Velasco [a], A. González [b], F.J. Peña [c], Mario Estévez [a,*]

[a] IPROCAR Research Institute, TECAL Research Group, University of Extremadura, 10003, Cáceres, Spain
[b] Institute of Molecular Pathology Biomarkers, University of Extremadura, 10003, Cáceres, Spain
[c] Spermatology Laboratory, University of Extremadura, 10003, Cáceres, Spain

ARTICLE INFO

Keywords:
Dityrosine
3-Nitrotyrosine
Kynurenine
Aminoadipic acid
ROS generation
Glutathione

ABSTRACT

The harmful effects of food-occurring oxidized amino acids, namely, aminoadipic acid (AAA), dityrosine (DTYR), L-kynurenine (KN), kynurenic acid (KA) and 3-nitrotyrosine (3NT), were studied on differentiated CACO-2 cells by flow cytometry and quantification of glutathione (GSH), and allysine. Cells were exposed to food-relevant doses (200 μM) of each compound for 4 or 72h and compared to a control (no stimulated cells). All oxidized amino acids induced apoptosis and results indicated that underlying mechanisms depended on the chemical nature of the species. AAA, KN and KA caused ROS generation and severe oxidative stress in 96%, 98% and 89% of exposed cells (77% in control cells), leading to significant GSH depletion and allysine accretion (1.5, 1.5 and 1.6 nmol allysine/mg protein, respectively at 4h; control: 0.22 nmol/mg protein; $p < 0.05$). DTYR and 3NT induced significant apoptosis to 29% and 25% of cells (control: 16%; $p < 0.05$) and necrosis to 28% and 26% of cells (control: 23%) at 72h by ROS-independent mechanisms. KN and KA were found to induce a cycle arrest effect on CACO-2 cells. These findings emphasize the potential harmful effects of the intake of oxidized proteins and amino acids and urge the necessity of carrying out further molecular studies.

1. Introduction

Oxidative reactions are inherent to biological systems and occur throughout the food chain, from the farm to the table. In living tissues, the formation of reactive oxygen species (ROS) in mitochondria is a consequence of the energetic metabolism (Davies, 2005). Under physiological conditions, ROS, such as free radicals and hydrogen peroxide (H_2O_2), are counteracted by the endogenous antioxidant defenses. Yet, the imbalance between the generation of the pro-oxidant species and such defenses (i.e. glutathione, catalase, superoxide dismutase, among others) leads to oxidative stress (Davies, 2005). Under these pro-oxidative conditions, proteins are oxidized and the amino acid side chains are degraded into various oxidation products. Lysine is oxidized, in a first stage, into allysine, to subsequently yield a carboxylic acid, the α-aminoadipic acid (AAA) (Hellwig, 2019). The oxidative damage to tyrosine leads to the formation of protein crosslinks, namely, dityrosine (DTYR). Tryptophan is oxidized by ROS to form a variety of compounds with kynurenine (KN) and kynurenic acid (KA) being two of the most abundant (Hellwig, 2019). In the course of oxidative stress, the conversion between ROS and reactive nitrogen species (RNS) occurs straightforwardly and, as a result, proteins may be oxidized and nitrosated simultaneously (Skibsted, 2011). The attack of RNS on tyrosine leads to the formation of 3-nitrotyrosine (3NT). Under severe oxidative stress, the oxidative damage to proteins leads to serious biological consequences including loss of protein functionality, impaired physiological processes and pathological conditions. The aforementioned oxidized amino acids have been recognized as reliable indicators of protein oxidation, aging and disease (Davies, 2005). (see Fig. 1)

Protein oxidation also occurs in food systems and the severity and consequences of this reaction depend on endogenous (composition) and external factors (storage and processing conditions) (Soladoye et al., 2015). Muscle foods, and particularly red meats, are highly sensitive to protein oxidation owing to their high concentration in protein, susceptible amino acids (lysine, tyrosine, sulfur-containing…) and reactive heme iron (Soladoye et al., 2015; Utrera and Estévez, 2013). Some technological processes (size reduction, high temperatures, long storage, microwaving…) promotes protein oxidation and their effects on food quality are more evident in severely processed foods (Estévez, 2011; Soladoye et al., 2015). This topic has concentrated considerable attention among food scientists given the negative impact of protein

* Corresponding author. IPROCAR Research Institute, TECAL research group, University of Extremadura, 10003, Spain.
E-mail address: mariovet@unex.es (M. Estévez).

https://doi.org/10.1016/j.fct.2020.111650
Received 23 May 2020; Received in revised form 21 July 2020; Accepted 23 July 2020
Available online 1 August 2020
0278-6915/© 2020 Elsevier Ltd. All rights reserved.

oxidation on food protein functionality and food quality (Hellwig, 2019). Oxidized proteins display altered functional properties and decreased susceptibility to be digested, causing the loss of nutritional value (Soladoye et al., 2015). Recent evidences show the potential noxious effects of the intake of oxidized proteins and amino acids. Dietary oxidized proteins contribute to inducing oxidative stress in the gastrointestinal tract (also known as *luminal oxidative stress*) and in internal organs upon intestinal uptake (Estévez and Xiong, 2019). The contribution of diet and protein oxidation on specific gut disorders has been documented for ulcerative gastritis (Van-Hecke et al., 2018), inflammatory bowel disease (Tian et al., 2017), and gastric and colonic neoplasias (Perše, 2013). Yet, the implication of particular oxidized amino acids as well as their precise molecular basis of their pathogenesis is poorly understood. In regards to the role of diet in serious gut diseases, red and processed meats are the only foods identified as carcinogens by the World Health Organization (WHO). The report by the International Agency for Research on Cancer (IARC, 2015) is based on epidemiological studies and indicates the connection between the intake of such foods with the onset of colorectal cancer, among other neoplasias. However, the underlying mechanisms of the carcinogenic effects of red and processed meats are still far from being fully understood. Interestingly, Rombouts et al. (2017) identified two protein oxidation products, namely, dityrosine and kynurenine, as discriminating compounds in red meat digests vs. white meat digests. According to these authors, this finding incriminates these chemical species in pathological processes promoted by red meat consumption. Yet, such implication requires to be proven by scientific evidence and the underlying molecular mechanisms of the toxic effects of these and other oxidized amino acids are unknown.

In this scenario, this study was designed to assess the cytotoxic effects of particular oxidized amino acids on human intestinal cells. These species were selected based on i) their occurrence and significance in foods and ii) on the previous evidence of potential toxicological concerns. To fulfill this objective, differentiated CACO-2 cells were exposed to protein oxidation products commonly found in processed muscle foods and analyzed for i) the onset of oxidative stress, apoptosis, necrosis by flow-cytometry; ii) the depletion of endogenous glutathione and iii) the oxidative damage to proteins.

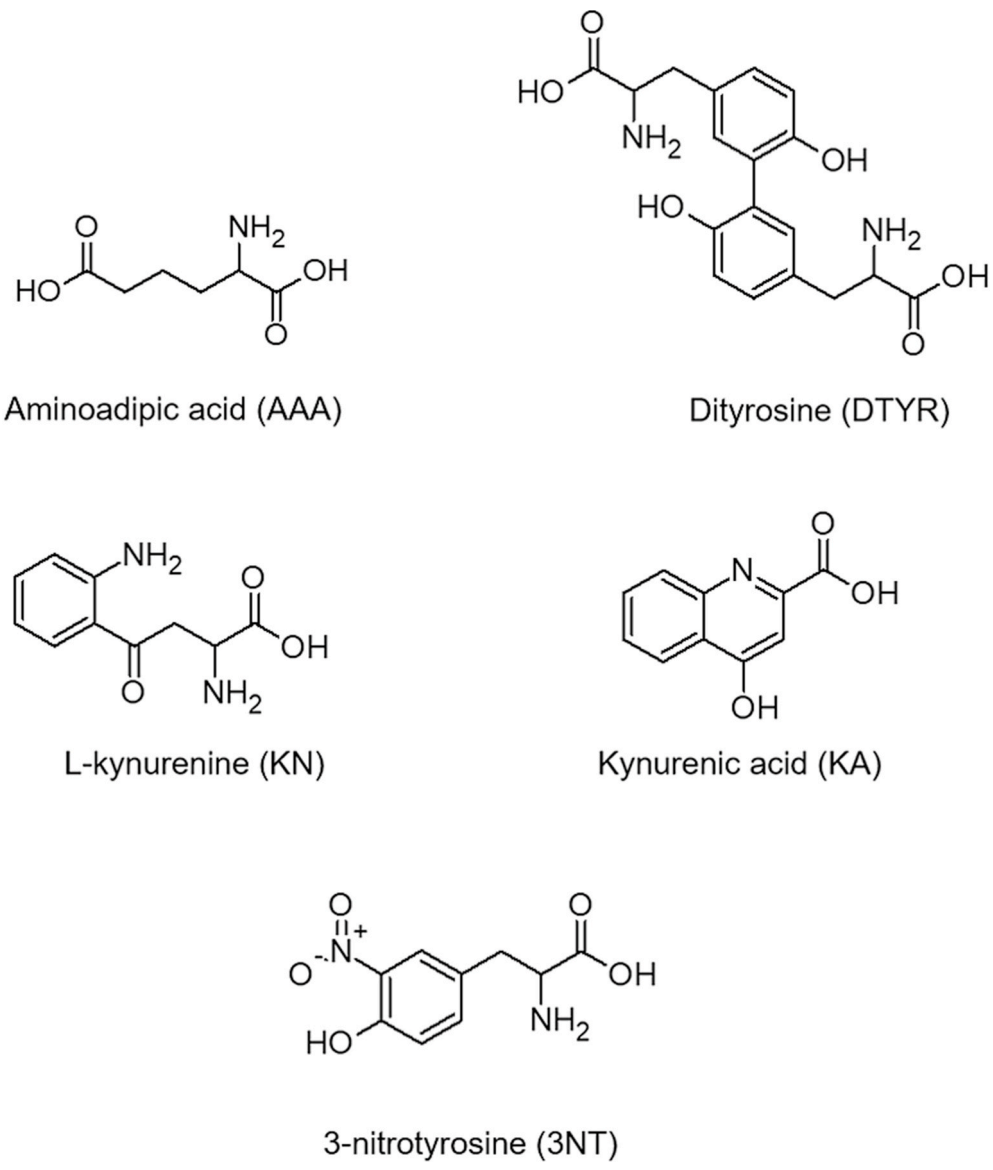

Fig. 1. Chemical structures of the food-occuring amino acids under investigation in the present study.

2. Material and methods

2.1. Chemicals and cells

All chemicals, reagents and proteins used for the present work were purchased from Panreac (Panreac Química, S. A., Barcelona, Spain), Merck (Merk, Darmstadt, Germany) and Sigma Chemicals (Sigma-Aldrich, Steinheim, Germany). Water used was purified by passage through a Milli-Q system (Millipore Corp., Bedford, MA). The molarities of all reactants are referring to the final concentration in the reaction mixture. Cells were purchased from the ECACC (European Collection of Authenticated Cell Cultures, Salisbury, UK).

2.2. Cell culture

The human adenocarcinoma cell line CACO-2 was obtained from ECACC and passages between 40 and 46 were used for cell culture studies. Cells were cultured in T-75 flasks at 37 °C in a humidified incubator 5%CO_2/95% air in Eagle's Minimum Essential Medium (EMEM) supplemented with fetal bovine serum (FBS) (10% v/v), non-essential amino acids (1% v/v) and L-glutamine (1% v/v). Cells were harvested at 90% confluence using 0.25% trypsin in 1 mM EDTA solution and seeded onto new culture flasks.

2.3. Experimental setting

Oxidized amino acids, AAA, DTYR, KN, KA and 3NT, were used at 200 μM and dissolved in 10 mL of supplemented EMEM. Upon reaching 90% confluence, cells were allowed to differentiate for 21 days and then exposed individually to each of the aforementioned species for 4 or 72h in T-75 flasks at 37 °C in a humidified incubator 5%CO_2/95% air. For comparison purposes, cells incubated in standard EMEM (CONTROL) and others incubated with 200 μM H_2O_2 (Positive CONTROL) under the aforementioned conditions, were also considered, totaling 7 experimental groups. Concentration of H_2O_2 and of selected oxidized amino acids was set based on the data available in the literature (Utrera and Estévez, 2013; Wijeratne et al., 2005; Ozyurt and Otles, 2020). At sampling times (4 and 74h), cells were removed using 0.25% trypsin in 1 mM EDTA, centrifuged at 68 g for 5 min and suspended in 1 mL of phosphate-buffered saline (PBS) solution for further analyses.

2.4. Flow cytometry analysis

Flow cytometry analyses were conducted using a Cytoflex® flow cytometer (Beckman Coulter) equipped with violet, blue and red lasers. The instrument was calibrated daily using specific calibration beads provided by the manufacturer. A compensation overlap was performed before each experiment. Files were exported as FCS files and analyzed using FlowJoV 10.4.1 Software (Ashland, OR, USA). Samples (4 and 72h) were diluted in PBS to a final concentration 5×10^6 cells/mL. The cells were stained with 1 μL of Hoechst 33342 (16.2 mM stock solution), 1 μL of CellROX (2.5 mM stock solution) and 1 μL CellEvent Caspase-3/7 Green Detection Reagent (2 mM stock solution). After thorough mixing, the cell suspension was incubated at room temperature in the dark for 20 min; then were loaded with 1 μL ethidium homodimer (1.167 mM in DMSO) and incubated for further 10 min. Finally, the samples were filtered through MACS® smartStrainer 30 μm filters and immediately run on the flow cytometer. The controls consisted of unstained and single stained controls to properly set gates and compensations.

2.5. Quantification of glutathione

The reduced (GSH) form of glutathione was analyzed in cells (4 and 72h) by UHPLC-MS/MS according to the method reported by Ortega Ferrusola et al. (2017). Analytes were extracted from lysed cells upon sonication (1 min) and ultracentrifugation (4000 g/5 min). The supernatant was filtered through 0.22 μL nylon filters and diluted for LC analysis. Chromatographic and spectrometer conditions were published elsewhere (Ortega Ferrusola et al., 2017). Quantification was performed injecting standard curves of the original compounds in the same conditions. Results were expressed as nmol GSH/mg protein.

2.6. Assessment of protein oxidation

Both early (allysine) and advanced oxidation protein products (AOPP) were assessed in CACO-2 cells at 4 and 72h. The procedure described by Utrera et al. (2011) was followed for the quantification of allysine and using HPLC-FLD with minor modifications. One hundred μL of the cell lysates were dispensed in 2 mL screw-capped Eppendorf tubes and treated with 1 ml of cold 10% trichloroacetic acid solution. Each Eppendorf was vortexed and then proteins were precipitated with centrifugation at 2240*g* for 5 min at 4 °C. The supernatant was removed, and the resulting pellet was treated again with 1 mL of cold 5% TCA solution. A new centrifugation was performed at 2240 g for 5 min at 4 °C for protein precipitation. The supernatant was removed, and then the pellets were derivatized with p-amino-benzoic acid (ABA), purified and hydrolyzed following the procedure described elsewhere (Utrera et al., 2011). The hydrolysates were evaporated at 40 °C *in vacuo* to dryness using a centrifuge concentrator (Eppendorf, Hamburg, Germany). Finally, the generated residue was reconstituted with 200 μL of Milli-Q water and then filtered through hydrophilic polypropylene GH Polypro (GHP) syringe filters (0.45 μm pore size, Pall Corporation, NJ, USA) for HPLC analysis. Details on the chromatograph apparatus as well as on the separation, elution and identification of the compounds of interest were published elsewhere (Utrera et al., 2011). Allysine-ABA was synthesized and purified following the procedure reported by Akagawa et al., (2002), and injected in the same conditions than samples. Allysine-ABA in the samples was identified by comparing the retention time with that of the reference pure compound. Standard solutions of ABA (ranging from 0.1 to 0.5 mM) were also injected in the same chromatographic conditions to create a standard curve. The peak corresponding to allysine-ABA was manually integrated and the resulting areas plotted against the aforementioned standard curve. Results are expressed as nmol of allysine per mg of protein.

AOPP were assessed using fluorescence spectroscopy in accordance to the method described by Luna and Estévez (2019). AOPP was excited at 350 nm, and the emitted fluorescence was recorded from 400 to 500 nm. The excitation and emission slits were both set to 10 nm and scanning speed was 500 nm/min. Results are expressed as fluorescence intensity (Area units).

2.7. Statistical analysis

All experiments were performed in triplicate and each individual sample at each sampling time was analyzed twice for each measurement. Data was analyzed for normality and homoscedasticity. The effect of the exposure to the oxidized/nitrosated amino acids was assessed at each sampling time by Analysis of Variance (ANOVA). The Tukey's test was used for multiple comparisons of the means. The effect of the incubation time on the same measurements was assessed by Student's t-test. The significance level was set at $p < 0.05$. SPSS (version 15.0) was used for statistical analysis of the data .

3. Results and discussion

3.1. Oxidative stress in CACO-2 cells. Effect of hydrogen peroxide

The evolution of viability (Table 1), ROS (Table 2) and apoptosis/necrosis (Table 3 and 4, respectively) in CACO-2 control cells were as expected. The increase in ROS throughout the assay, as a likely consequence of energy metabolism, contributes to increasing levels of apoptotic and necrotic cells. Apoptosis is a controlled mechanism of cell

destruction different to necrosis. Apoptosis is associated with the activation of certain specific proteases named caspases, not causing inflammation, while necrosis can cause an inflammatory response. ROS trigger apoptosis that leads to cell death and it is clearly established that oxidative stress is the cause of apoptosis, and not backwards (Matés, 1999). H_2O_2 was used in the experiments as a positive control of oxidative stress generation due to its oxidizing capacity. Both, in live tissues and in cells grown *in vitro*, H_2O_2 is decomposed through the Fenton reaction in the presence of transition metals leading to the formation of the hydroxyl radical ($HO^{\bullet}$), the most powerful and harmful free radical in biological systems (Davies, 2005). The incorporation of H_2O_2 into a biological system ensures the formation of free radicals and, therefore, the induction of oxidative reactions and oxidative stress. Preliminary tests showed that the H_2O_2 included in our samples was fully depleted after 72 h of incubation, which suggests the expected degradation of H_2O_2 into radical species. Consistently, CACO-2 cells treated with H_2O_2 had a higher subpopulation of cells with ROS than that in the control counterparts at 72h (Table 2). However, the generation of ROS had no consequences on apoptotic or necrotic events. In fact, CACO-2 cells treated with H_2O_2 had a lower proportion of apoptotic and necrotic cells than the control counterparts (Tables 3 and 4).

Despite of the recognized pro-oxidant actions of H_2O_2, the effects of this compound on CACO-2 cells are variable according to the literature. Németh et al. (2007) reported the generation of ROS and the occurrence of oxidative stress in CACO-2 cells treated with H_2O_2. Wijeratne et al. (2005) showed that this effect largely depends on the concentration of H_2O_2 used. On this regard, the harmful effects of H_2O_2 on CACO-2 cells observed by Németh et al. (2007), occurred at a concentration between 5 and 20 times higher than the one used in the present study. Using a concentration (250 μM), similar to that used in this study, Wijeratne et al. (2005) observed negligible negative effects. Furthermore, these authors observed that incubation with these H_2O_2 levels caused a CACO-2 cells antioxidant response, which consisted in a GPx increase activity. This effect, also described by Olivera et al. (2018), would explain that an isolated and mild oxidative stress event (low H_2O_2 concentration) is interpreted by the cell as a pro-oxidant threat, which responds by strengthening the antioxidant defenses. It is reasonable to consider that similar circumstances took place in our study. H_2O_2-generated radicals would explain the increase in ROS cells at 72h, and such oxidative threat, probably increased the levels of antioxidant defenses in CACO-2 cells, which would explain that apoptotic and necrotic cell levels were lower than control. The analysis of the concentration of GSH (Table 5) illustrates the effect of H_2O_2 exposure on the antioxidant response of CACO-2 cells. While the concentration of GSH was lower in H_2O_2- treated cells as compared to the control at 4 h, the concentration of this antioxidant tripeptide increased 4-fold at the end of the assay (72 h) in the former cells, with this concentration being significantly higher than in the other treatments. It is generally known that complex redox-regulation systems occur in human cells and that chemical species may not be considered antioxidant or pro-oxidant but redox-active species (Valko et al., 2007). The global effect (positive/antioxidant or negative/pro-oxidant) depends on numerous factors including the dose of the species and the physiological state of the cell (Dröge, 2002). On this line, a pro-oxidant threat may induce an antioxidant response from the cell aimed to unbalance the redox stage towards a reductive condition that protects the cell against oxidative stress. GSH is considered a major intracellular antioxidant compound but the underlying antioxidant mechanisms as well as its role as inhibitor of oxidative stress are complex and matters of enduring research (Desideri et al., 2019). The extent of protein oxidative damage in cells exposed to H_2O_2 is consistent with the results already reported. The concentration of allysine and

Table 1
Percentages of viable (Hoechst +) CACO-2 cells (means ± standard deviation) upon exposure to hydrogen peroxide and oxidized amino acids (200 μM) for 4 and 72 h.

	4 h	72 h	p^A
CONTROL	$65.70^{c} \pm 4.33$	$68.80^{b} \pm 7.22$	ns
H_2O_2	$74.54^{b} \pm 2.40$	$68.20^{b} \pm 0.89$	*
AAA	$69.57^{c} \pm 1.19$	$62.48^{c} \pm 3.73$	*
3NT	$59.75^{d} \pm 1.07$	$54.77^{c} \pm 6.86$	ns
DTYR	$53.81^{e} \pm 1.39$	$58.05^{c} \pm 0.78$	**
KN	$92.88^{a} \pm 1.14$	$91.25^{a} \pm 1.05$	ns
KA	$94.23^{a} \pm 1.21$	$92.35^{a} \pm 1.58$	ns

[A]Significance in student T-test for comparison between means from the two sampling days within one treatment: *p < 0.05; **: p < 0.01; ns: no significant.
[a-e] Means within the same sampling time bearing different superscripts are significantly different from each other in ANOVA (p < 0.001).

Table 2
Percentages of CACO-2 cells under oxidative stress (Cell Rox +) (means ± standard deviation) upon exposure to hydrogen peroxide and oxidized amino acids (200 μM) for 4 and 72 h.

	4 h	72 h	p^A
CONTROL	$77.16^{b} \pm 5.05$	$88.25^{b} \pm 4.88$	*
H_2O_2	$74.50^{bc} \pm 7.24$	$95.95^{a} \pm 1.20$	***
AAA	$76.64^{b} \pm 6.38$	$95.53^{a} \pm 4.70$	***
3NT	$72.85^{c} \pm 3.36$	$85.57^{b} \pm 5.08$	***
DTYR	$74.87^{bc} \pm 2.23$	$64.88^{c} \pm 0.16$	***
KN	$95.04^{a} \pm 1.21$	$98.29^{a} \pm 1.62$	ns
KA	$96.94^{a} \pm 1.36$	$88.81^{b} \pm 2.78$	**

[A] Significance in student T-test for comparison between means from the two sampling days within one treatment: *p < 0.05; **: p < 0.01; ***: p < 0.001; ns: no significant.
[a-c] Means within the same sampling time bearing different superscripts are significantly different from each other in ANOVA (p < 0.001).

Table 3
Percentages of apoptotic CACO-2 cells (Caspase 3 +) (means ± standard deviation) upon exposure to hydrogen peroxide and oxidized amino acids (200 μM) for 4 and 72 h.

	4 h	72 h	p^A
CONTROL	$11.22^{c} \pm 2.58$	$16.46^{e} \pm 1.13$	*
H_2O_2	$7.75^{d} \pm 0.71$	$14.52^{f} \pm 0.11$	***
AAA	$16.25^{b} \pm 1.83$	$20.48^{d} \pm 1.48$	*
3NT	$16.09^{b} \pm 1.28$	$29.45^{b} \pm 2.55$	***
DTYR	$20.35^{a} \pm 1.56$	$24.69^{c} \pm 1.49$	**
KN	$21.15^{a} \pm 1.24$	$35.29^{a} \pm 1.08$	***
KA	$15.27^{b} \pm 1.20$	$27.28^{b} \pm 1.02$	***

[A] Significance in student T-test for comparison between means from the two sampling days within one treatment: *p < 0.05; **: p < 0.01; ***: p < 0.001; ns: no significant.
[a-f] Means within the same sampling time bearing different superscripts are significantly different from each other in ANOVA (p < 0.001).

Table 4
Percentages of necrotic CACO-2 cells (Ethidium homodimer +) (means ± standard deviation) upon exposure to hydrogen peroxide and oxidized amino acids (200 μM) for 4 and 72 h.

	4 h	72 h	p^A
CONTROL	$15.88^{bc} \pm 2.86$	$22.82^{b} \pm 3.38$	*
H_2O_2	$7.95^{e} \pm 0.26$	$7.80^{c} \pm 1.19$	ns
AAA	$14.79^{c} \pm 1.58$	$20.59^{b} \pm 1.43$	*
3NT	$19.98^{a} \pm 1.64$	$28.06^{a} \pm 1.91$	***
DTYR	$11.63^{d} \pm 0.10$	$26.34^{a} \pm 1.27$	***
KN	$11.28^{d} \pm 0.98$	$19.60^{b} \pm 1.87$	***
KA	$3.25^{f} \pm 0.76$	$2.20^{d} \pm 0.30$	*

[A] Significance in student T-test for comparison between means from the two sampling days within one treatment: *p < 0.05; **: p < 0.01; ***: p < 0.001; ns: no significant.
[a-f] Means within the same sampling time bearing different superscripts are significantly different from each other in ANOVA (p < 0.001).

Table 5
GSH (nmol/mg protein) in CACO-2 cells (means ± standard deviation) upon exposure to hydrogen peroxide and oxidized amino acids (200 μM) for 4 and 72 h.

	4 h	72 h	p[A]
CONTROL	0.39[a]±0.08	0.28[c]±0.04	***
H_2O_2	0.20[b] ± 0.06	0.81[a]±0.12	***
AAA	0.22[b] ± 0.05	0.26[c]±0.03	ns
3NT	0.30[a]±0.05	0.44[b] ± 0.06	*
DTYR	0.30[a]±0.04	0.23[c]±0.02	*
KN	0.15[c]±0.02	0.22[c]±0.04	ns
KA	0.24[b] ± 0.02	0.24[c]±0.05	ns

[A] Significance in student T-test for comparison between means from the two sampling days within one treatment: *p < 0.05; ***: p < 0.001; ns: no significant.
[a-c] Means within the same sampling time bearing different superscripts are significantly different from each other in ANOVA (p < 0.001).

AOPP in H_2O_2-treated cells was higher than in the control counterparts at 4 h (Table 6). Yet, the protein oxidation markers were found at lower concentrations in the cells challenged with H_2O_2 at 72 h than in control cells, which is in line with the hypothesis of the antioxidant response. GSH is known to protect proteins and other biomolecules through mechanisms such as the S-glutathionylation mechanism by which GSH is bound to protein thiols to protect the latter against oxidative degradation (Métayer et al., 2008). Therefore, the stimulation of GSH synthesis in CACO-2 cells by the exposure to H_2O_2 could be, at least, partly responsible for the protection of cellular proteins against oxidative damage, which would be reflected in the limited impact of H_2O_2 on apoptosis and necrosis.

3.2. Effect of AAA

The main protein carbonyl α-aminoadipic semialdehyde (AAS) and its end-product, the α-aminoadipic acid (AAA), have been used as markers of protein oxidation and disease in humans and experimental animals (Wang et al., 2013; Lee et al., 2019). It is a well-known intermediate in the biosynthesis and degradation of lysine and it is also formed under glyco-oxidative and radical-mediated oxidative stress (Wang et al., 2013; Lee et al., 2019). Beyond its role as marker of oxidative stress and disease, recent studies proposed the involvement of AAA in the physiology of pancreatic cells, processes of insulin resistance and onset of diabetes in humans and experimental animals (Wang et al., 2013; Lee et al., 2019). Both AAS and AAA are formed in processed muscle foods and have also been used as indicator of the oxidative damage to food proteins (Timm-Heinrich et al., 2013; Utrera et al., 2013).

Table 6
Early (nmol allysine/mg protein; A) and advanced oxidation protein products (AOPP; fluorescence intensity, B) in CACO-2 cells (means ± standard deviation) upon exposure to hydrogen peroxide and oxidized amino acids (200 μM) for 4 and 72 h.

(A)

	4 h	72 h	p[A]
CONTROL	0.22[d] ± 0.05	2.04[a]±0.50	***
H_2O_2	0.35[c]±0.08	1.28[b] ± 0.23	***
AAA	1.52[a]±0.26	1.14[b] ± 0.35	*
3NT	0.20[d] ± 0.06	1.25[b] ± 0.35	***
DTYR	0.61[b] ± 0.18	1.06[c]±0.22	***
KN	1.53[a]±0.23	0.35[e]±0.11	***
KA	1.61[a]±0.24	0.49[d] ± 0.16	***

(B)

	4 h	72 h	p[A]
CONTROL	196[c]±15	305[d] ± 20	***
H_2O_2	204[c]±11	275[d] ± 23	*
AAA	295[b] ± 12	490[b] ± 72	***
3NT	202[c]±27	288[d] ± 29	*
DTYR	199[c]±18	324[c]±38	**
KN	345[a]±22	610[a]±108	***
KA	349[a]±28	595[a]±85	***

[A] Significance in student T-test for comparison between means from the two sampling days within one treatment: *p < 0.05; **: p < 0.01; ***: p < 0.001; ns: no significant.
[a-e] Means within the same sampling time bearing different superscripts are significantly different from each other in ANOVA (p < 0.001).

Our results originally indicate that exposure to 200 μM AAA leads to remarkable physiological changes in human intestinal CACO-2 cells. At long-term exposure (72h) a significant decrease in cell viability occurred along with a concomitant increase in ROS levels. Comparing the results with positive control, both at 4 and 72h, cell viability is lower in the treatment with AAA, with this result being highly significant (p < 0.001). In relation to ROS formation, AAA promotes the formation of ROS at an intensity comparable to positive control at 72h, but unlike H_2O_2, the pro-oxidative disturbance caused by AAA leads to reduction in the viability of CACO-2 cells. The noxious effects of AAA included ability to induce apoptosis in CACO-2 cells. No significant effects of AAA were observed in regard to necrotic events. Therefore, the results obtained confirm that AAA is capable of generating oxidative stress with an intensity similar to that displayed by H_2O_2 (both at the same concentration) while, AAA, unlike H_2O_2, has pro-apoptotic effects. Although the results are quantitatively similar to H_2O_2 in relation to the generation of ROS, the mechanisms involved are reasonably different. AAA is, itself, a final oxidation product from lysine and unlike H_2O_2, may not be directly implicated in the generation of ROS. The underlying fundamentals of ROS generation by AAA may likely involve cellular signaling mechanisms and/or alteration of the energy metabolism at the mitochondria. Fiermonte et al. (2001) described the transport of AAA into mitochondria and the subsequent transformation into oxoadipate and L-glutamate in the presence of oxoglutarate and 2-aminoadipate transaminase. da Silva et al. (2017), established a direct relationship between AAA and oxidative stress, which connects with the results obtained in the present study. These authors observed how AAA is capable of causing oxidative stress in rat neuronal cells, which led to pathophysiological alterations in nervous tissue. According to their findings, the AAA acts as an analogue of glutamate and competitively blocks enzymes that play an important role in neuronal physiology. This observation is consistent with the recent review by Estévez and Xiong (2019) who reported that dietary oxidized amino acids exert noxious effects by acting as analogs of the original amino acids or other biomolecules, blocking certain physiological pathways. It is worth highlighting that AAA may not only act as analogue of glutamate, the interconversion between both species is carried out in mitochondria (Fiermonte et al., 2001). Therefore, the oxidative stress observed in AAA-exposed CACO-2 cells may have been caused by either AAA directly or glutamate as the latter is well known for inducing mitochondrial dynamic imbalance and oxidative stress in human cells (Kumari et al., 2012). The disturbance of the cellular function could have caused an impairment of the cell imbalance redox, which eventually leads to oxidative stress.

The pro-oxidative threat caused by AAA induced a significant depletion of intracellular GSH at 4 h. Unlike H_2O_2, the exposure to 200 μM AAA had no apparent response in terms of GSH provision at long term (72 h). da Silva et al. (2017) observed an increase in ROS and RNS together with a depletion of antioxidant defenses (specifically GSH) in brain tissue of rats exposed to 4 mM AAA. It is hence, plausible that AAA noxious effects are dose-dependent as 8 fold-times higher concentration of this carboxylic acid considerably worsened the biological effects described in the present study. The induction of oxidative stress caused by AAA and the apparent lack of effective antioxidant response by the cell led to a significant accretion of protein carbonyls at 4 h (Table 6A). Allysine and other protein carbonyls may react with protein-bound amines via Schiff base formation to yield AOPP, typically fluorescent protein aggregates (Verrastro et al., 2015). Consistently, the

concentration of allysine decreased as the concentration of AOPP increased over time in AAA-exposed cells. The pro-oxidative environment promoted by this oxidized amino acid also led to a remarkable formation of AOPP, as compared to control cells. The accumulation of protein carbonyls and AOPP has been directly related to health disorders, including several inflammatory and neoplasic disorders in the gastrointestinal tract (Estıvez and Luna, 2017). According to the present results, the potentially harmful effect of AAA in intestinal cells could take place at food-occurring concentrations.

3.3. Effect of tyrosine oxidation and nitrosation products

The exposure of CACO-2 cells to DTYR (200 μM) caused a significant decrease in viable cells at 4 and 72h, and like AAA, the percentage of apoptotic cells consequently increased over time as compared to the control group. Furthermore, DTYR caused a significant increase of necrotic events in CACO-2 cells at 72 h. Surprisingly, this oxidized form of tyrosine did not cause toxic effects on CACO-2 cells through the generation of free radicals, as of the percentage of cells with ROS is lower than the control group. The lack of impact in terms of ROS generation is also reflected in a negligible impact on the concentration of intracellular GSH and on the extent of protein oxidation. This shows that the routes and mechanisms affected by this oxidized amino acid are different to those previously described for AAA, indicating that the chemical nature, plays, as expected, an important role in the response of the intestinal cell to the oxidized amino acids. The toxicity of dietary DTYR is documented in the scientific literature and involves the onset of numerous physiological processes in experimental animals such as hepatic injury, renal and brain dysfunction (Li et al., 2019; Yang et al., 2017). It is worth highlighting that doses applied in the aforementioned studies (up to 420 μg/kg body weight) are much higher than those used in the present study. Therefore, the present results indicate that low dietary DTYR concentrations (200 μM) may already induce apoptosis and necrosis in intestinal cells. In regard to the mechanisms, scientific evidences emphasize the role of the chemical structure of the DTYR and its ability to act as analogs of other bioactive species in their pathological effects. Several revealing studies carried out by Ding et al. (2017) reported that DTYR act as an analogue of the T3 hormone, owing to their similar chemical structure, causing physiological alterations in pancreas.

The process of protein nitrosation is irreversible and, therefore, can seriously affect the regulation of cell signaling and metabolic enzymes activity. Exposure to 3NT caused reduced cell viability as compared to control and positive control, with this result being highly significant ($P < 0.001$). The present results indicate that the potential cytotoxic effects of 3NT are independent of the exposure time as the harmful effects were observed at 4 and 72 h. As for DTYR, the effect of 3NT on cell viability does not seem to be related to the generation of ROS. The results of apoptosis and necrosis levels are in this case consistent with the negative effects on cell viability: the exposure of CACO-2 cells to 3NT increases the occurrence of apoptotic and necrotic events. Among all tested species, 3NT was the only being capable of increasing the levels of necrosis significantly both, in the short, and in the long term. The intracellular concentration of GSH was not depleted in cells exposed to 3NT, which supports the hypothesis that the effect of this species on the present cells did not involve a redox imbalance. Consistently, no impact was observed on the oxidative damage to cellular proteins. Blanchard-Fillion (2006) reported that 3-NT caused neuronal cell apoptosis through inhibition of caspase inhibitors and Zhang and Wei (2013) found that this compound caused apoptosis in rat cardiomyocytes. The nitrosation of food proteins is a topic of growing interest due to the formation of this compound in cured (nitrite-added) muscles foods both during processing and during digestion of processed meat. While 3NT is known to be formed during processing of cured muscle foods (Villaverde et al., 2014), the potential implication of dietary 3NT on particular physiological disorders is indefinite. This study originally supports that the exposure of CACO-2 cells to 3NT has noxious effects that leads to apoptosis and necrosis. The underlying molecular mechanisms required a more profound study.

3.4. Effect of tryptophan oxidation products

KN and KA are naturally present in cells as intermediates of tryptophan metabolism. Beyond their role as building blocks, tryptophan and the several metabolites from the "kynurenine pathway", including KN and KA, have been reported to display bioactivity in the brain-gut axis (Kennedy et al., 2017). However, they may also be formed as a result of oxidative stress and tryptophan oxidation also takes place in processed foods such as dairy and processed meats (Soladoye et al., 2015). In fact, KN, specifically, was found to occur in greater quantity in digests from red meat than in those from white meat (Rombouts et al., 2017). This finding incriminates KN as a compound that could play a relevant role in the potentially negative health effects attributed to red meat.

Exposure to KN and KA (200 μM each) induced severe oxidative stress in human intestinal cells as more than 95% of the cells exposed to these species suffered from such condition. The significant depletion of intracellular GSH already at 4 h is consistent with the occurrence of intense pro-oxidative conditions. As well as AAA, the cellular metabolism of KA and KN is targeted in mitochondria and their involvement in NAD + synthesis, mitochondrial function and metabolic disturbances are well documented (Castro-Portuguez and Sutphin, 2020). In the present study, KA and KN were found to induce intense oxidative stress as a likely result of a mitochondrial redox imbalance. Furthermore, apoptosis was promoted in CACO-2 cells with percentages of apoptotic cells doubling control at 72 h. Yet, the onset of apoptotic changes was not followed by a subsequent process of necrosis. The percentage of necrotic cells upon exposure to KN was similar to that of control cells while KA significantly reduced the occurrence of such events in CACO-2 cells. In fact, KN and KA enhanced CACO-2 cells viability, as the percentages of viable cells among those exposed to KN and KS is higher than those found among cells from the control and positive control groups. In view of the results, the cells, affected by a severe oxidative stress, seemed to have entered into apoptosis and remained in a state at which biological processes are suspended. The process in which apoptosis is interrupted and cells are kept in a state of *cycle arrest* has been reported to occur in cells subjected to chronic oxidative stress (Baraibar and Friguet, 2012). According to scientific literature, a massive oxidation of cellular proteins under severe pro-oxidative conditions cause a failure of the proteasome system that executes cellular autolysis by degrading cellular proteins (Nyström, 2005). Severely oxidized proteins in cells may not be recognized by cellular proteases and accumulate in cells causing the cycle arrest (Nyström, 2005; Höhn et al., 2017). Among all other treatments, cells exposed to tryptophan oxidation products were found to have the highest levels of allysine (together with AAA), a specific marker of protein oxidation. The concentration of allysine decreased dramatically at 72 h confirming its involvement in advanced oxidative reactions such as those leading to the formation of AOPP. The occurrence of the latter in CACO-2 cells exposed to KA and KN was significantly higher than in the other cells, emphasizing the severe oxidative stress caused by these species. This finding supports the role of KN and KA in inducing pro-oxidative conditions leading to severe oxidative damage to proteins, which is, in turn, a required condition for an impaired autolysis and the occurrence of cycle arrest. This cellular condition has been reported in a number of diseases associated with chronic oxidative stress, protein oxidation and aging such as Alzheimer's (Nyström, 2005; Höhn et al., 2017). These results are scientifically relevant given the occurrence of KN and other tryptophan oxidation products in foods (i.e. red meats; Rombouts et al., 2017) and the recognized role of these species in the gut-brain axis (Kennedy et al., 2017). Studies aimed to study the effect of KN and KA in CACO-2 cells are scarce. Walczak et al. (2011), reported KA inhibited the proliferation of several cancer cells lines, including CACO-2 cells. However, Szalardy et al. (2012) linked high levels of KA with cognitive impairment

association showing that the abundance of this metabolite determines its biological effect. Both compounds should be evaluated in detail to determine the underlying mechanisms behind their ability to induce such severe pro-oxidative conditions, confirm the subsequent effect on the cycle arrest of intestinal cells and assess the overall biological impact of such mechanisms.

4. Conclusion

This study provides original evidence on the potential noxious effects of various oxidized and nitrosated amino acids generally present in foods. The effects on ROS generation, oxidative stress, apoptosis and necrosis are specific for each amino acid, which indicates structure-specific mechanisms of action. Further studies on each of these species will be aimed to study dose effects and unveil the molecular mechanisms by using proteomic approaches. Given that these harmful effects could be reproduced in *in vivo* conditions, the necessity of applying food and dietary antioxidant strategies seem to be required. On the other hand, the toxic effects of these oxidized amino acids may be studied for their potential use in therapeutic treatments, alone or in combination with other cytotoxic molecules.

CRediT authorship contribution statement

S. Díaz-Velasco: Data curation, Methodology, Formal analysis, Writing - original draft. **A. González:** Data curation, Methodology, Funding acquisition, Supervision, Formal analysis, Validation, Writing - review & editing. **F.J. Peña:** Data curation, Methodology, Funding acquisition, Supervision, Formal analysis, Validation, Writing - review & editing. **Mario Estévez:** Conceptualization, Funding acquisition, Project administration, Resources, Supervision, Validation, Writing - review & editing.

Declaration of competing interest

The authors declare that they have no known competing financial interests or personal relationships that could have appeared to influence the work reported in this paper.

Acknowledgement

M.E., A.G. and F.J.P. acknowledge the Spanish Ministry of Economics and Competitiveness (SMEC) for funding this study through the projects AGL2017-84586-R, BFU2016-79259-R and AGL2017-83149-R, respectively. The “Gobierno de Extremadura” is also acknowledged for financial support (GR108104, GR18070 and GR18008).

References

Akagawa, M, Sasaki, T, Suyama, K, 2002. Oxidative deamination of lysine residue in plasma protein of diabetic rats: Novel mechanism via the Maillard reaction. Eur J Biochem 69 (22), 5451–5458. https://doi.org/10.1046/j.1432-1033.2002.03243.x.

Baraibar, M.A., Liu, L., Ahmed, E.K., Friguet, B., 2012. Protein oxidative damage at the crossroads of cellular senescence, aging, and age-related diseases. Oxidative Medicine and Cellular Longevity. https://doi.org/10.1155/2012/919832.

Blanchard-Fillion, B., Prou, D., Polydoro, M. y col, 2006. Metabolism of 3-nitrotyrosine induces apoptotic death in dopaminergic cells. J. Neurosci. 26 (23), 6124–6130. https://doi.org/10.1523/jneurosci.1038-06.2006. https://search.crossref.org/?q=Metabolism+of+3-nitrotyrosine+induces+apoptotic+death+in+dopaminergic+cells.

Castro-Portuguez, R., Sutphin, G.L., 2020. Kynurenine pathway, NAD+ synthesis, and mitochondrial function: targeting tryptophan metabolism to promote longevity and healthspan. Exp. Gerontol. 132 https://doi.org/10.1016/j.exger.2020.110841.

da Silva, J.C., Amaral, A.U., Cecatto, C., Wajner, A., dos Santos Godoy, K., Ribeiro, R.T., Wajner, M., 2017. α-Ketoadipic acid and α-aminoadipic acid cause disturbance of glutamatergic neurotransmission and induction of oxidative stress in vitro in brain of adolescent rats. Neurotox. Res. 32 (2), 276–290. https://doi.org/10.1007/s12640-017-9735-8.

Davies, M.J., 2005. The oxidative environment and protein damage. Biochim. Biophys. Acta Protein Proteonomics 1703, 93–109. https://doi.org/10.1016/j.bbapap.2004.08.007.

Desideri, E., Ciccarone, F., Ciriolo, M.R., 2019. Targeting glutathione metabolism: partner in crime in anticancer therapy. Nutrients 11. https://doi.org/10.3390/nu11081926.

Ding, Y.Y., Li, Z.Q., Cheng, X.R., Ran, Y.M., Wu, S.J., Shi, Y., Le, G., 2017. Dityrosine administration induces dysfunction of insulin secretion accompanied by diminished thyroid hormones T3 function in pancreas of mice. Amino Acids 49 (8), 1401–1414. https://doi.org/10.1007/s00726-017-2442-1.

Dröge, W., 2002. Free radicals in the physiological control of cell function. Physiol. Rev. 82, 47–95. https://doi.org/10.1152/physrev.00018.2001. https://search.crossref.org/?q=Free+radicals+in+the+physiological+control+of+cell+function.

Estévez, M., 2011. Protein carbonyls in meat systems: a review. Meat Sci. 89 (3), 259–279. https://doi.org/10.1016/j.meatsci.2011.04.025.

Estévez, M., Luna, C., 2017. Dietary protein oxidation: a silent threat to human health? Crit. Rev. Food Sci. Nutr. 57 (17), 3781–3793. https://doi.org/10.1111/1750-3841.14460.

Estévez, M., Xiong, Y., 2019. Intake of oxidized proteins and amino acids and causative oxidative stress and disease: recent scientific evidences and hypotheses. J. Food Sci. 84 (3), 387–396. https://doi.org/10.1111/1750-3841.14460.

Fiermonte, G., Dolce, V., Palmieri, L., Ventura, M., Runswick, M.J., Palmieri, F., Walker, J.E., 2001. Identification of the human mitochondrial oxodicarboxylate carrier. Bacterial expression, reconstitution, functional characterization, tissue distribution, and chromosomal location. J. Biol. Chem. 276 (11), 8225–8230. https://doi.org/10.1074/jbc.M009607200.

Hellwig, M., 2019. The chemistry of protein oxidation in food. Angew. Chem. Int. Ed. 58, 16742–16763. https://doi.org/10.1002/anie.201814144.

Höhn, A., Weber, D., Jung, T., Ott, C., Hugo, M., Kochlik, B., Castro, J.P., 2017. Happily (n)ever after: aging in the context of oxidative stress, proteostasis loss and cellular senescence. Redox Biol. 11, 482–501. https://doi.org/10.1016/j.redox.2016.12.001.

IARC, 2015. Red Meat and Processed Meat. In: In IARC Monographs, 2015, p. 114.

Kennedy, P.J., Cryan, J.F., Dinan, T.G., Clarke, G., 2017. Kynurenine pathway metabolism and the microbiota-gut-brain axis. Neuropharmacology 112, 399–412. https://doi.org/10.1016/j.neuropharm.2016.07.002.

Kumari, S., Mehta, S.L., Li, P.A., 2012. Glutamate induces mitochondrial dynamic imbalance and autophagy activation: preventive effects of selenium. PloS One 7 (6), e39382.

Lee, H.J., Jang, H.B., Kim, W.H., Park, K.J., Kim, K.Y., Park, S.I., Lee, H.J., 2019. 2-Aminoadipic acid (2-AAA) as a potential biomarker for insulin resistance in childhood obesity. Sci. Rep. 9 (1), 1–10. https://doi.org/10.1038/s41598-019-49578-z.

Li, B., Ge, Y., Xu, Y., Lu, Y., Yang, Y., Han, L., Le, G., 2019. Spatial learning and memory impairment in growing mice induced by major oxidized tyrosine product dityrosine. J. Agric. Food Chem. 67 (32), 9039–9049. https://doi.org/10.1021/acs.jafc.9b04253.

Luna, C, Estévez, M, 2019. Formation of allysine in β-lactoglobulin and myofibrillar proteins by glyoxal and methylglyoxal: Impact on water-holding capacity and in vitro digestibility. Food Chem 271, 87–93. https://doi.org/10.1016/j.foodchem.2018.07.167.

Matés, J.M., Pérez-Gómez, C., De Castro, I.N., 1999. Antioxidant enzymes and human diseases. Clin. Biochem. 32, 595–603. https://doi.org/10.1016/S0009-9120(99)00075-2.

Métayer, S., Seiliez, I., Collin, A., Duchêne, S., Mercier, Y., Geraert, P.A., Tesseraud, S., 2008. Mechanisms through which sulfur amino acids control protein metabolism and oxidative status. JNB (J. Nutr. Biochem.) 19, 207–215. https://doi.org/10.1016/j.jnutbio.2007.05.006.

Németh, E., Halász, A., Baráth, Á., Gálfi, P., 2007. Influence of lactic acid bacteria and their spent culture supernatant on hydrogen peroxide-induced interleukin-8 synthesis and necrosis of Caco-2 cells. Food Agric. Immunol. 18 (2), 95–105. https://doi.org/10.1080/09540100701464303.

Nyström, T., 2005. Role of oxidative carbonylation in protein quality control and senescence. EMBO J. 24 (7), 1311–1317. https://doi.org/10.1038/sj.emboj.7600599.

Oliveira, M.F., Geihs, M.A., França, T.F.A., Moreira, D.C., Hermes-Lima, M., 2018. Is “preparation for oxidative stress” a case of physiological conditioning hormesis? Front. Physiol. 1–6 https://doi.org/10.3389/fphys.2018.00945.

Ortega Ferrusola, C., Anel-López, L., Ortiz-Rodriguez, J.M., et al., 2017. Stallion spermatozoa surviving freezing and thawing experience membrane depolarization and increased intracellular Na^+. Andrology 5 (6), 1174–1182. https://doi.org/10.1111/andr.12419.

Ozyurt, V H, Otles, S, 2020. Investigation of the effect of sodium nitrite on protein oxidation markers in food protein suspensions. J Food Biochem 44 (3), e13152. https://doi.org/10.1111/jfbc.13152.

Perše, M., 2013. Oxidative stress in the pathogenesis of colorectal cancer: cause or consequence? BioMed Res. Int. 2013 https://doi.org/10.1155/2013/725710.

Rombouts, C., Hemeryck, L.Y., Van Hecke, T., De Smet, S., De Vos, W.H., Vanhaecke, L., 2017. Untargeted metabolomics of colonic digests reveals kynurenine pathway metabolites, dityrosine and 3-dehydroxycarnitine as red versus white meat discriminating metabolites. Sci. Rep. 7, 1–13. https://doi.org/10.1038/srep42514.

Skibsted, L.H., 2011. Nitric oxide and quality and safety of muscle based foods. Nitric Oxide Biol. Chem. 24, 176–183. https://doi.org/10.1016/j.niox.2011.03.307.

Soladoye, O.P., Juárez, M.L., Aalhus, J.L., Shand, P., Estévez, M., 2015. Protein oxidation in processed meat: mechanisms and potential implications on human health. Compr. Rev. Food Sci. Food Saf. 14 (2), 106–122. https://doi.org/10.1111/1541-4337.12127.

Szalardy, L., Zadori, D., Toldi, J., Fulop, F., Klivenyi, P., Vecsei, L., 2012. Manipulating kynurenic acid levels in the brain – on the edge between neuroprotection and

cognitive dysfunction. Curr. Top. Med. Chem. 12 (16), 1797–1806. https://doi.org/10.2174/156802612803989264.

Tian, T., Wang, Z., Zhang, J., 2017. Pathomechanisms of oxidative stress in inflammatory bowel disease and potential antioxidant therapies. Oxid. Med. Cell. Longev. 2017 https://doi.org/10.1155/2017/4535194.

Timm-Heinrich, M., Eymard, S., Baron, C.P., Nielsen, H.H., Jacobsen, C., 2013. Oxidative changes during ice storage of rainbow trout (Oncorhynchus mykiss) fed different ratios of marine and vegetable feed ingredients. Food Chem. 136 (3–4), 1220–1230. https://doi.org/10.1016/j.foodchem.2012.09.019.

Utrera, M., Morcuende, D., Rodríguez-Carpena, J.G., Estévez, M., 2011. Fluorescent HPLC for the detection of specific protein oxidation carbonyls - α-aminoadipic and γ-glutamic semialdehydes - in meat systems. Meat Sci. 89 (4), 500–506. https://doi.org/10.1016/j.meatsci.2011.05.017.

Utrera, M., Estévez, M., 2013. Oxidative damage to poultry, pork, and beef during frozen storage through the analysis of novel protein oxidation markers. J. Agric. Food Chem. 61 (33), 7987–7993. https://doi.org/10.1021/jf402220q.

Valko, M., Leibfritz, D., Moncol, J., Cronin, M.T.D., Mazur, M., Telser, J., 2007. Free radicals and antioxidants in normal physiological functions and human disease. Int. J. Biochem. Cell Biol. 39 (1), 44–84. https://doi.org/10.1016/j.biocel.2006.07.001.

Van Hecke, T., Basso, V., De Smet, S., 2018. Lipid and protein oxidation during in vitro gastrointestinal digestion of pork under Helicobacter pylori gastritis conditions. J. Agric. Food Chem. 66 (49), 13000–13010. https://doi.org/10.1021/acs.jafc.8b04335.

Verrastro, I., Pasha, S., Jensen, K.T., Pitt, A.R., Spickett, C.M., 2015. Mass spectrometry-based methods for identifying oxidized proteins in disease: advances and challenges. Biomolecules 5 (2), 378–411. https://doi.org/10.3390/biom5020378.

Villaverde, A., Ventanas, J., Estévez, M., 2014. Nitrite promotes protein carbonylation and Strecker aldehyde formation in experimental fermented sausages: are both events connected? Meat Sci. 98 (4), 665–672. https://doi.org/10.1016/j.meatsci.2014.06.017.

Walczak, K., Dąbrowski, W., Langner, E., Zgrajka, W., Piłat, J., Kocki, T., Turski, W.A., 2011. Kynurenic acid synthesis and kynurenine aminotransferases expression in colon derived normal and cancer cells. Scand. J. Gastroenterol. 46 (7–8), 903–912. https://doi.org/10.3109/00365521.2011.579159.

Wang, T.J., Ngo, D., Psychogios, N., Dejam, A., Larson, M.G., Vasan, R.S., Gerszten, R.E., 2013. 2-Aminoadipic acid is a biomarker for diabetes risk. J. Clin. Invest. 123 (10), 4309–4317. https://doi.org/10.1172/JCI64801.

Wijeratne, S.S.K., Cuppett, S.L., Schlegel, V., 2005. Hydrogen peroxide induced oxidative stress damage and antioxidant enzyme response in Caco-2 human colon cells. J. Agric. Food Chem. 53 (22), 8768–8774. https://doi.org/10.1021/jf0512003.

Yang, Y., Zhang, H., Yan, B., Zhang, T., Gao, Y., Shi, Y., Le, G., 2017. Health effects of dietary oxidized tyrosine and dityrosine administration in mice with nutrimetabolomic strategies. J. Agric. Food Chem. 65 (32), 6957–6971. https://doi.org/10.1021/acs.jafc.7b02003.

Zhang, Y.-L., Wei, J.-R., 2013. 3-Nitrotyrosine, a biomarker for cardiomyocyte apoptosis induced by diabetic cardiomyopathy in a rat model. Mol. Med. Rep. 8 (4), 989–994. https://doi.org/10.3892/mmr.2013.1644.

Capítulo 4.2. Protein oxidation marker, a-amino adipic acid, impairs proteome of differentiated human enterocytes: Underlying toxicological mechanisms

El marcador de oxidación de proteínas, ácido a-amino adípico, afecta al proteoma de enterocitos humanos diferenciados: mecanismos toxicológicos subyacentes

DOI: https://doi.org/10.1016/j.bbapap.2022.140797

Autores: Silvia Díaz-Velasco, Josué Delgado, Fernando J. Peña, Mario Estévez

Año de publicación: 2022

Revista: Biochimica et Biophysica Acta (BBA) - Proteins and Proteomics

Indice de Impacto JCR (2022): 4.125

BBA - Proteins and Proteomics 1870 (2022) 140797

Contents lists available at ScienceDirect

BBA - Proteins and Proteomics

journal homepage: www.elsevier.com/locate/bbapap

Research paper

Protein oxidation marker, α-amino adipic acid, impairs proteome of differentiated human enterocytes: Underlying toxicological mechanisms

S. Díaz-Velasco [a], J. Delgado [b], F.J. Peña [c], Mario Estévez [a,*]

[a] Food Technology and Quality (TECAL), Institute of Meat and Meat Products (IPROCAR), Universidad de Extremadura, Cáceres, Spain
[b] Food Hygiene and Safety (HISEALI), Institute of Meat and Meat Products (IPROCAR), Universidad de Extremadura, Cáceres, Spain
[c] Spermatology Laboratory, Universidad de Extremadura, Cáceres, Spain

ARTICLE INFO

Keywords:
α-Amino Adipic acid
Mitochondria
Na^+/K^+-ATPase
Tricarboxylic acid cycle
Proteomics
Flow cytometry

ABSTRACT

Protein oxidation and oxidative stress are involved in a variety of health disorders such as colorectal adenomas, inflammatory bowel's disease, neurological disorders and aging, among others. In particular, the specific final oxidation product from lysine, the α-amino adipic acid (α-AA), has been found in processed meat products and emphasized as a reliable marker of type II diabetes and obesity. Currently, the underlying mechanisms of the biological impairments caused by α-AA are unknown. To elucidate the molecular basis of the toxicological effect of α-AA, differentiated human enterocytes were exposed to dietary concentrations of α-AA (200 μM) and analyzed by flow cytometry, protein oxidation and proteomics using a Nanoliquid Chromatography-Orbitrap MS/MS. Cell viability was significantly affected by α-AA ($p < 0.05$). The proteomic study revealed that α-AA was able to alter cell homeostasis through impairment of the Na^+/K^+-ATPase pump, energetic metabolism, and antioxidant response, among other biological processes. These results show the importance of dietary oxidized amino acids in intestinal cell physiology and open the door to further studies to reveal the impact of protein oxidation products in pathological conditions.

1. Introduction

Oxidative stress and protein oxidation are involved in assorted health disorders such as cardiovascular disease, neurological disorders, diabetes, aging, rheumatoid arthritis, muscular dystrophy, Parkinson's syndrome and Alzheimer's disease [1,2]. Other pathological conditions such as inflammatory bowel's disease (IBD) [3] and colorectal adenomas [4] are closely related to oxidative stress and chronic inflammation. The accretion of oxidized proteins as a result of enduring oxidative stress impairs cellular homeostasis and leads to physiological impairments [1]. Furthermore, oxidized proteins and amino acids are markers of several of the aforementioned diseases. In particular, the α-amino adipic acid (α-AA), the specific final oxidation product of lysine, has been emphasized as a reliable marker of cataractogenesis, renal failure and aging [5], and more recently as an early indicator of type II diabetes and obesity [6,7]. Even though the ability of α-AA to impair both endocrine and exocrine pancreas physiology has been documented, the underlying molecular mechanisms of the toxic effects of specific oxidized amino acids, such as α-AA, in human cells, is mostly unknown. Estaras et al. [8] reported that α-AA has deleterious actions on mouse pancreatic acinar cells. Moreover, α-AA is associated with disorders in brain and pancreatic tissues [9]. According to da Silva et al. [10] α-AA caused oxidative stress in neuronal cells of rats, which led to pathophysiological alterations in nervous tissue. In a previous in vitro study on differentiated human colon CACO-2 cell line [11], we reported that α-AA caused a ROS-mediated cytotoxic effect, leading to apoptotic events. These results are relevant since dietary oxidized proteins and α-AA have been found to contribute to in vivo oxidative stress and cause toxicological effects on intestinal cells and on internal organs, upon intestinal uptake [6,12]. α-AA has been found in concentrations up to 200 μM in severely processed meat products such as ready-to-eat beef patties [13]. Interestingly, processed meat and red meat were included in 2015 by the International Agency for Research on Cancer [14] in groups 1 and 2A of carcinogenic substances, based on epidemiological studies. Yet again, the potential implication of dietary oxidized amino acids on this and many other pathological conditions linked to oxidative stress, is unknown.

The present study aims to decipher the molecular basis of the toxicological effect of α-AA on differentiated human colon CACO-2 cells. To fulfil this objective, these intestinal cells were exposed to dietary

* Corresponding author at: Institute of Meat and Meat Products (IPROCAR), University of Extremadura, Avd. Universidad, sn. 10003 Cáceres, Spain.
E-mail address: mariovet@unex.es (M. Estévez).

https://doi.org/10.1016/j.bbapap.2022.140797
Received 5 April 2022; Received in revised form 28 May 2022; Accepted 6 June 2022
Available online 9 June 2022
1570-9639/© 2022 The Authors. Published by Elsevier B.V. This is an open access article under the CC BY-NC-ND license (http://creativecommons.org/licenses/by-nc-nd/4.0/).

concentrations of α-AA (200 μM) and subsequently analyzed by means of a high-resolution mass spectrometry-based proteomics using a Nanoliquid Chromatography-Orbitrap MS/MS. CACO-2 cells are used as an experimental model since their spontaneous differentiation for 21 days allows them to achieve morphological and biochemical characteristics similar to enterocytes [15]. Supportive flow cytometry studies and protein oxidation measurements were applied.

2. Material and methods

2.1. Chemicals

All reagents, chemicals and α-AA standard compound (CAS Number 542–32-5) were obtained from Sigma Chemicals (Sigma-Aldrich, Steinheim, Germany), Fisher (Fisher Scientific S.L., Madrid, Spain) and Panreac (Panreac Química, S. A., Barcelona, Spain). Ultrapure water was prepared by Milli-Q water purification system (Millipore Corp, Bedford, MA).

2.2. Cell culture

Human colon adenocarcinoma CACO-2 cell line was purchased from ECACC (European Collection of Authenticated Cell Cultures, Salisbury, UK). Passages between 40 and 46 were used for cell culture studies. Cells were grown in T-75 flasks in EMEM (Eagle's Minimum Essential Medium) supplemented with fetal bovine serum (FBS) (10% *v*/v), L-glutamine (1% v/v) and non-essential amino acids (1% v/v) at 37 °C in humidified atmosphere and 5% CO_2. When cells reached 90% confluence, they were allowed to differentiate into enterocytes for 21 days. Such differentiation was confirmed by visualization by phase-contrast microscopy. After that, they were harvested using 0.25% trypsin in 1 mM EDTA solution.

2.3. Experimental setting

α-AA was used at 200 μM and dissolved in 10 mL of supplemented EMEM. Concentrations of α-AA are food-compatible according to the data available in the literature [13,16–18]. α-AA was then added and exposed to enterocytes for 72 h in T-75 flasks at 37 °C in a humidified incubator 5%CO_2/95% air. For comparison purposes, CONTROL cells were incubated in standard EMEM in the same conditions. The whole experiment was replicated five times independent flasks for both treated and CONTROL cells. At 72 h, cells were harvested using 0.25% trypsin in 1 mM EDTA, centrifuged at 126*g* for 5 min and suspended in 1 mL of phosphate-buffered saline (PBS) solution for further analysis.

2.4. Flow cytometry analysis

Samples were diluted in PBS to a final concentration 5×10^6 cells/mL and analyses were carried out using a Cytoflex® LX flow cytometer (Beckman Coulter, Brea, CA, USA) equipped with blue, red, violet, ultraviolet, yellow and infrared lasers. The instrument was calibrated daily employing specific calibration beads provided by the manufacturer. A compensation overlap was performed before each experiment. Files were exported as FCS files and loaded and analyzed using Cytobank Software (Beckman Coulter, Brea, CA, USA). Cells were stained with 1 μL of Hoechst 33342 (16.2 mM stock solution), 1 μL of CellROX Deep Red ® (2.5 mM stock solution), and 0.3 μL of JC-1 (1 μM) to measure cell viability, ROS occurrence and mitochondrial activity, respectively. After thorough mixing, the cell suspension was incubated at room temperature in the dark for 20 min; then 10 μM of MCB-1 were added to the samples and incubated for a further 10 min to measure the reduced form of glutathione (GSH) concentration. Dead cells were excluded after staining the cells with ViaKrome 808 Fixable Viability Dye (Beckman Brea, CA, USA) following the instructions of the manufacturer. Lastly, the samples were filtered through MACS® smart trainer 30 μm filters and immediately run on the flow cytometer. Hoechst 33342 was excited with the violet laser (355 nm) and fluorescence recorded at 450/50 nm band pass filter; MCB was excited with the violet laser (405 nm) and fluorescence recorded at 405/30 bandpass filter, JC-1 was excited with the yellow laser (561 nm) the aggregates and blue laser (488 nm) the monomers and fluorescence collected at 525/50 and 610/20 nm bandpass filters respectively; CellROX® deep red was excited with the red laser 638 nm and fluorescence collected at 660/10 nm bandpass, finally, Viakrome 808 was excited with the infrared laser (808 nm) and fluorescence collected at 885/40 nm bandpass filter. The controls consisted of unstained and single-stained controls to properly set gates and compensations. Positive controls for high mitochondrial membrane potential (JC-1) consisted in high-quality stallion spermatozoa, these cells present a high mitochondrial activity [19]. Positive controls for reactive oxygen species (ROS) consisted of cells treated with menadione as indicated in Muñoz et al. [20].

2.5. Analysis of protein oxidation markers

Two main protein carbonyls, the α-aminoadipic and γ-glutamic semialdehydes (α-AS and γ-GS, respectively) were quantified in the enterocytes from the present study. The procedure described by Utrera et al. was followed with minor modifications [21]. One hundred μL of the cell lysates were dispensed in 2 mL screw-capped Eppendorf tubes and treated with 1 mL of cold 10% trichloroacetic acid (TCA) solution. Each Eppendorf was vortexed and then proteins were precipitated with centrifugation at 2240*g* for 5 min at 4 °C. The supernatant was removed, and the resulting pellet was treated again with 1 mL of cold 5% TCA solution. A new centrifugation was performed at 2240*g* for 5 min at 4 °C for protein precipitation. The supernatant was removed, and then the pellets were derivatized with p-amino-benzoic acid (ABA), purified and hydrolyzed following the procedure described elsewhere [21]. The hydrolysates were evaporated at 40 °C in vacuo to dryness using a centrifuge concentrator (Eppendorf, Hamburg, Germany). Finally, the generated residue was reconstituted with 200 μL of Milli-Q water and then filtered through hydrophilic polypropylene GH Polypro (GHP) syringe filters (0.45 μm pore size, Pall Corporation, NJ, USA) for HPLC analysis. Details on the chromatograph apparatus as well as on the separation, elution and identification of the compounds of interest were published elsewhere [21]. α-AS-ABA and γ-GS-ABA were synthesized and purified following the procedure reported by Akagawa et al. [22] and injected in the same conditions than samples. Both semialdehydes were identified in samples by comparing their retention times with those of the reference pure compounds. Standard solutions of ABA (ranging from 0.1 to 0.5 mM) were also injected in the same chromatographic conditions to create a standard curve. The peaks corresponding to both semialdehydes were manually integrated and the resulting areas plotted against the aforementioned standard curve. Results are expressed as nmol of protein carbonyl per mg of protein.

2.6. Sample preparation for LC-MS/MS based proteomics

Samples were added 0.5 mL of lysis buffer pH 7,5 (100 mM Tris-HCl, 50 mM NaCl, 10% glycerol, 0.5 M EDTA pH 8,5). Immediately before use, lysis buffer was added 100 mM PMSF (Phenylmethansulfonylfluorid) and 100 μg/mL Pepstatin in a 1:100 proportion. Samples were shaken for a minute in an agitator adding to each screw-capped Eppendorf tube 3–4 magnetized metal balls at 30 1/s (Retsch, Haan, Germany). Then, they were sonicated 3 times in batches of 10 pulses (Branson Ultrasonics, Danbury, USA). Lysates were incubated on ice for 1 h and were centrifuged in a 5427 R (Eppendorf, Hamburg, Germany) at 18064*g* for 10 min at 4 °C. All the supernatant was passed into new screw-capped Eppendorf tubes. Protein concentration was measured with a Coomasie Protein Assay Reagent Ready to Use employing a Nanodrop 2000c Spectophotometer and a Nanodrop 2000 software (USA). Protein concentration must be ≥1 μg/μL. Aliquots

containing 50 μg of proteins were partially run in SDS-PAGE (4% stacking and 12% separating), just stopped when they reached the separating part of the gel to be in gel digested according to Shevchenko et al. [23], with some modifications. The gel was stained with Coomassie blue R250. Each lane was cut into 1 mm^3 pieces and then were subjected to in-gel digestion. Milli-Q water was added to each sample to wash them and were unstained with 100% methanol and 50 mM ammonium bicarbonate. After, samples were dehydrated for 5 min with 100% acetonitrile and 50 mM ammonium bicarbonate. Supernatant was removed and 100% acetonitrile was added. Then, supernatant was discarded and was dried at room temperature in vacuo using a centrifugal vacuum concentrator (Gyrozen, Daejeon, Korea). Samples were incubated with 0.5 M DTT in 50 mM ammonium bicarbonate for 20 min at 56 °C for protein reduction. The resulting free thiol (-SH) groups were alkylated by incubating the samples with 0.55 M iodoacetamide in 50 mM ammonium bicarbonate for 15 min at room temperature in the dark. Supernatant was removed and milli-Q water was added twice to wash samples and then were dehydrated for 5 min with 100% acetonitrile and 50 mM ammonium bicarbonate. Supernatant was removed and 100% acetonitrile was added, then it was discarded and dried in a vacuum concentrator. Samples were rehydrated with a mix of 50 mM ammonium bicarbonate, 1 μL of ProteaseMAX (Promega, USA) and 1.8 μg of trypsin (Promega). After, they were incubated for 1 h at 50 °C and added 1 μL of 100% formic acid to stop the proteolysis and were sonicated in a water bath for 5 min. Supernatant was removed of each sample and placed it into new screw-capped Eppendorf tubes for drying in a vacuum concentrator. Before analyzing the samples on the Orbitrap LC-MS/MS, loading buffer was added (98% milli-Q water, 2% acetonitrile, 0.05% trifluoroacetic acid), and sonicated in a water bath for 5 min and centrifuged at 18064*g* for 15 min at room temperature and put them into vials of Orbitrap LC-MS/MS.

2.7. Label-free quantitative proteomic analyses

A Q-Exactive Plus mass spectrometer coupled to a Dionex Ultimate 3000 RSLCnano (Thermo Scientific) analyzed 5 μg from each digest. Data was collected using a Top15 method for MS/MS scans [24]. Comparative proteome abundance and data analysis were carried out using MaxQuant software (version 1.6.0.15.0; https://www.maxquant.org/download_asset/maxquant/latest)) and Perseus (v 1.6.14.0) to organize the data and perform statistical analysis. Carbamidomethylation of cysteines was set as a fixed modification; oxidation of methionines and acetylation of N-terminals were set as variable modifications. Database searching was performed against *Homo sapiens* protein database (www.uniprot.org). The maximum peptide / protein false discovery rates (FDR) were set to 1% based on comparison to a reverse database. The LFQ algorithm was used to generate normalized spectral intensities and infer relative protein abundance. Proteins were identified with at least two peptides, and those proteins that matched to a contaminant database or the reverse database were removed, and proteins were only retained in final analysis if they were detected in at least two replicates from at least one treatment. Quantitative analysis was performed using a *t*-test to compare treatments with the control. The qualitative analysis was also performed to detect proteins that were found in at least three replicates of a given treated group but were undetectable in the comparison control group. All proteins satisfying one of these two aforementioned criteria were identified as discriminating proteins, and their corresponding genes were grouped by biological processes and molecular functions through ClueGO (v. 2.5.6) [25]. To define term-term interrelations and functional groups based on shared genes between the terms, the Kappa score was stablished at 0.4. Three GO terms and 4% of genes covered were set as the minimum required to be retained in the final result. The *p*-value was corrected by Bonferroni step down and set as $p \leq 0.05$.

2.8. Statistical analysis

All experiments were performed five times and each individual sample was analyzed twice for flow cytometry. Data was analyzed for normality and homoscedasticity. The effect of the exposure to α-AA was assessed by Analysis of Variance (ANOVA). The Tukey's test was used for multiple comparisons of the means. The effect of the incubation time on the same measurements was assessed by Student's *t*-test. The significance level was set at $p < 0.05$. SPSS (version 15.0) was used for statistical analysis of the data.

3. Results

3.1. Flow cytometry and protein oxidation markers

Parameters analyzed by flow cytometry were cell viability, mitochondrial activity, ROS occurrence, and reduced form of glutathione (GSH) concentration. Cells were processed and analyzed as described in material and methods. Fig. 1A-E show representative cytograms of the 6-colors experiment conducted as well as positive control for mitochondrial membrane potential and ROS production (Fig. 1F and G, respectively). Results show a significant decrease in viability among enterocytes exposed to α-AA compared to control cells ($p < 0.05$) (Fig. 1H). Cells exposed to α-AA showed a reduction in mitochondrial activity and an increase in ROS (Fig. 1I and J), though, in this case, not to a significant extent ($p > 0.05$). No significant differences were found between treatments for the concentration of GSH when considering live cells (data not shown). Yet, among the population of dead cells, a significant increase in GSH concentration was observed as compared to control counterparts (Fig. 1K).

The analysis of protein oxidation markers α-AS and γ-GS, revealed significantly higher concentrations of both protein carbonyls in cells exposed to α-AA (1.26 ± 0.31 nmol/mg protein; 0.49 ± 0.19 nmol/mg protein, respectively) than in the control cells (0.59 ± 0.11 nmol/mg protein; 0.21 ± 0.08 nmol/mg protein, respectively).

3.2. Proteomic analyses induced by α-AA

The LFQ analyses identified a total of 1695 proteins. Quantitative ($p < 0.05$) and qualitative (only detected in one condition) changes in protein abundance were identified (Table S1 Supplementary material). 234 proteins were significantly influenced by α-AA, among those, 91 were found in lower abundance in cells treated with α-AA while 45 were only found in control samples. Conversely, 97 proteins were detected in higher quantity by α-AA treatment and only one was found in α-AA-treated cells. For a rational and organized description and discussion of results, discriminating proteins and their corresponding genes were grouped by biological processes and molecular functions (Fig. 2A–D). Specific pathways for each of these processed and full details of identified proteins and associated genes are provided in Tables S2–S5 Supplementary material. Among all proteins identified in differentiated enterocytes, those which concentrations were more severely affected by the exposure to α-AA, are listed in Table 1. Only discriminating proteins having defined biological significance are presented in the following sections.

3.2.1. Proteins found in lower relative quantity in CACO-2 cells exposed to α-AA exposure

3.2.1.1. ATPase activity. The exposure to α-AA caused disturbance to a number of biological processes in enterocytes with Na^+/K^+-exchanging ATPase activity, being one the most affected among all biological processes (Fig. 2A and Supplementary Table S2) for the low abundance of the protein sodium/potassium-transporting ATPase subunit alpha-1 (ATP1A1; Fold change: 0.72) (Table 1 and Supplementary Table S1).

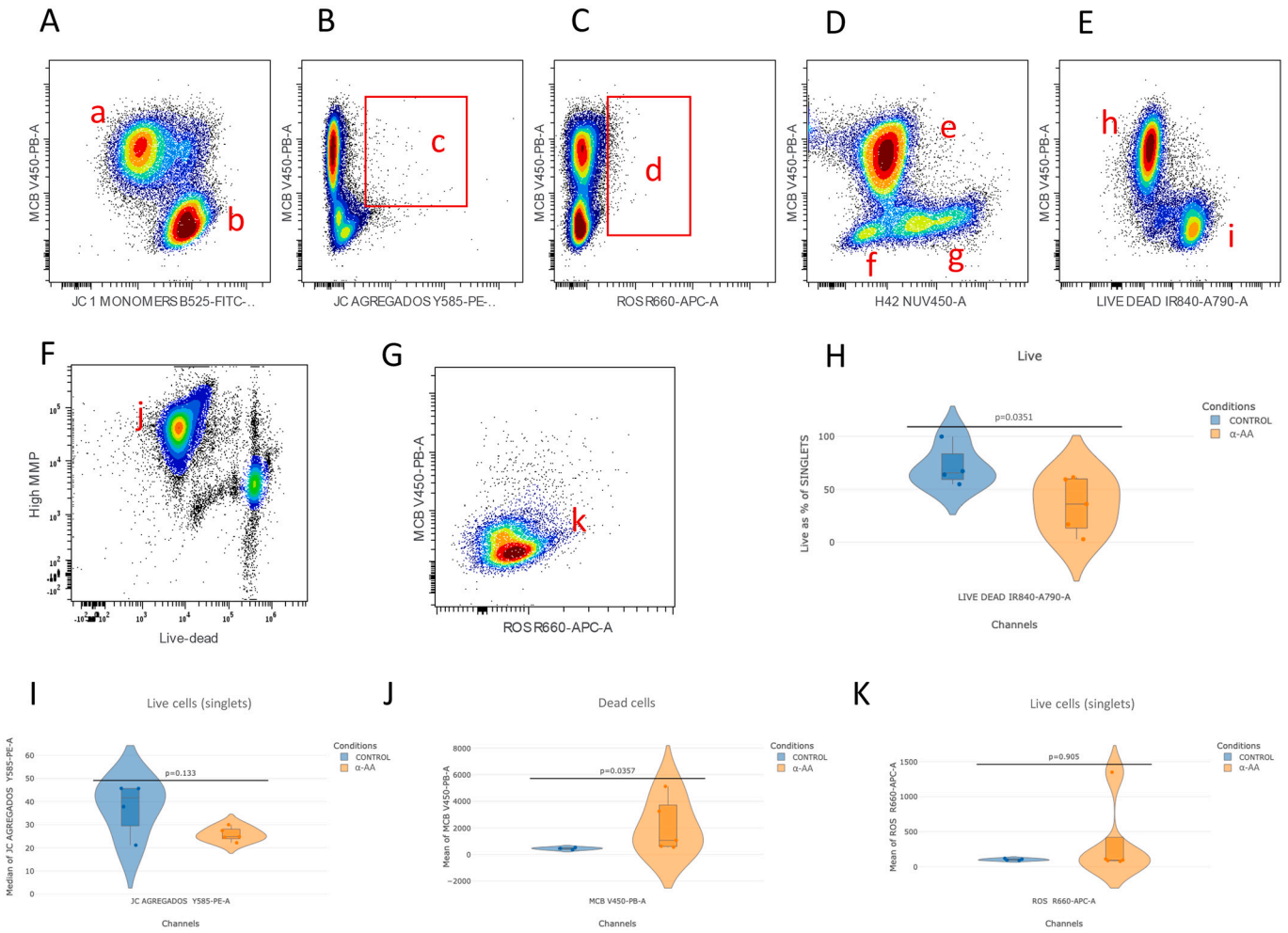

Fig. 1. Flow cytometry applied to the effect of α-AA exposure to differentiated human enterocytes. A) Cells showing significant amounts of GSH (a) and cells showing low mitochondrial activity (b); B) Dot plot showing in the Y-axis the MCB fluorescence corresponding to GSH, in the X-axis JC-1 aggregates fluorescence corresponding to highly active mitochondria (events in c); C) Dot plot showing in the Y-axis the MCB fluorescence corresponding to GSH, in the X-axis production of Reactive Oxygen Species (ROS) (events in d); D) Dot plot showing the GSH in cells (e) in relation to DNA positive events (f and g). Cells in g have increased membrane permeability; E) Dot plots showing live (h) and dead cells; F) Positive control for mitochondria showing high mitochondrial membrane potential (j) and positive controls for cells producing high amounts of ROS (k). H) Changes in viability; I) Changes in mitochondrial membrane potential in live cells; J) ROS in live cells; K) GSH content in dead cells.

The results from the molecular functions were consistent as the phosphorylative mechanism of sodium transmembrane transporter activity and the phosphorylate mechanism of potassium transmembrane transporter activity, reduced in quantity in protein ATP1A1 again (Fig. 2B and Supplementary Table S3). Together with protein kinase C alpha type (PRKCA), which appears only in control cells, protein ATP1A1 is implicated in cell communication by electrical coupling (Supplementary Table S2). The lower amount of ATP1A1 is also involved in glucocorticoid biosynthetic and metabolic processes, in steroid hormone binding and the cell responses to glycoside (Supplementary Tables S2 and S3). Phosphorylative mechanism of calcium transmembrane transporter activity was also affected by α-AA (Supplementary Table S3) In this case, the protein sarcoplasmic/endoplasmic reticulum calcium ATPase subunit alpha-2 (ATP2A2; Fold change: 0.73) (Table 1 and Supplementary Table S1), concerned with the ATPase sarcoplasmic/endoplasmic reticulum Ca^{2+} transporting, were found to be in lower abundance in α-AA treated cells. ADP binding (Supplementary Table S3) was found to be reduced in proteins such as ATP1A1, mitochondrial glutamate dehydrogenase 1 (GLUD1; Fold change: 0.79), mitochondrial glutamate dehydrogenase 2 (GLUD2; Fold change: 0.79), NADP-dependent malic enzyme, (ME1; Fold change: 0.62) and the regulatory gamma subunit of 5'-AMP-activated protein kinase (PRKAG1, which appears only in control) (Supplementary Table S1).

3.2.1.2. Nucleoside bisphosphate metabolic process. In this group, the exposure to α-AA led to a significant decrease of proteins involved in acetyl-CoA biosynthetic and metabolic processes in different pathways. Proteins acetyl-coenzyme A synthetase (ACSS2, only in control), lactate dehydrogenase (LDHD, Fold change: 0.73), liver carboxylesterase (CES1, Fold change: 0.67), mitochondrial malonyl-CoA decarboxylase (MLYCD, Fold change: 0.82), (Dihydrolipoyllysine-residue mitochondrial succinyltransferase component of 2-oxoglutarate dehydrogenase complex (DLST, Fold change: 0.81) and catalase (CAT, Fold change: 0.64) were found in lower quantity in cells exposed to α-AA (Table 1 and Supplementary Tables S1 and S2). Mitochondrial methylcrotonoyl-CoA carboxylase beta chain (MCCC2, Fold change: 0.72) and 3-hydroxyacyl-CoA dehydrogenase type-2 (HSD17B10, Fold change: 0.71), involved in branched-amino acid metabolic and catabolic processes (Table 1 and Supplementary Tables S1 and S2), were also diminished in α-AA treated cells.

3.2.1.3. Cellular amino acid metabolic process. Proteins involved in cellular amino acid metabolic process were found at lower concentrations in α-AA-treated cells compared to control cells ($p < 0.01$) (Fig. 2A).

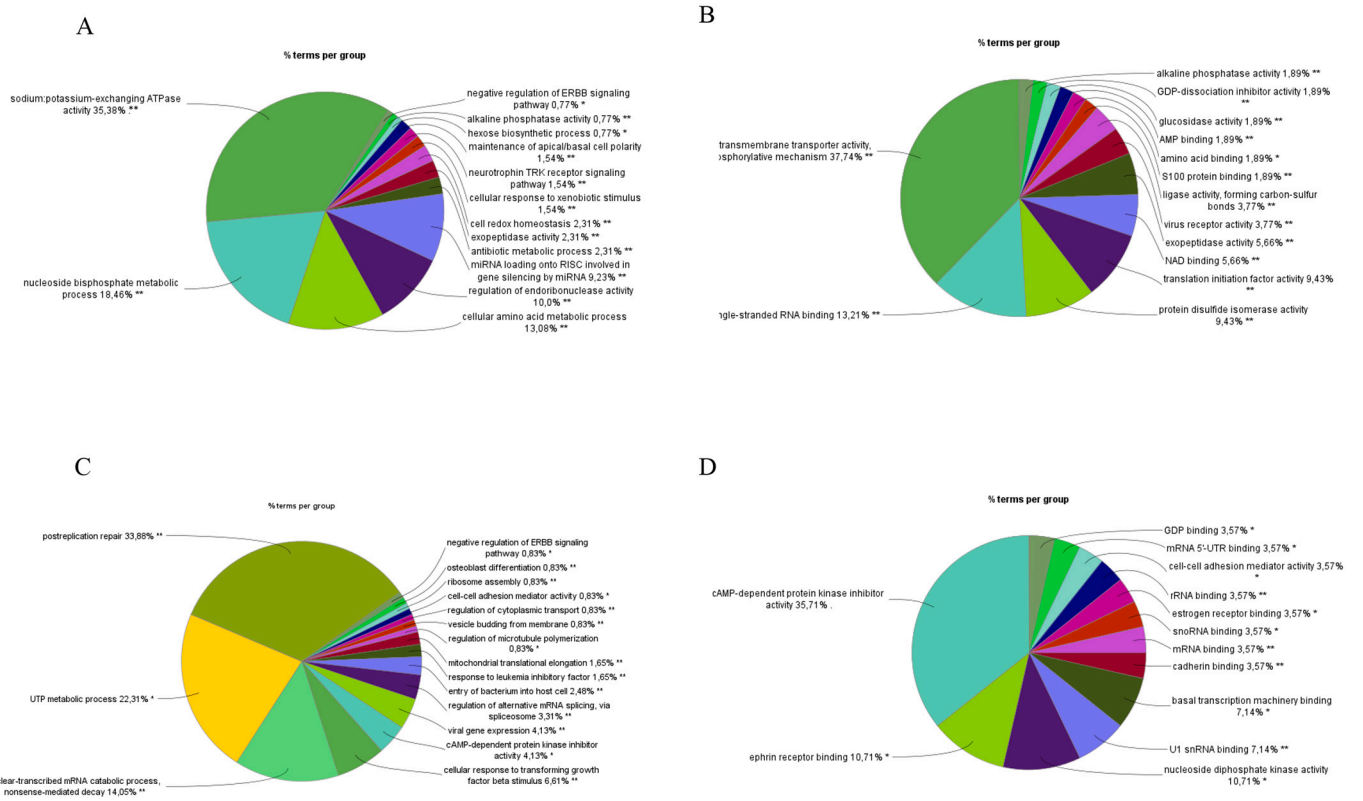

Fig. 2. Percentages of proteins annotated by Gene Ontology (* $p < 0.05$, ** $p < 0.01$) found in lower relative quantity in biological processes (A) and molecular functions (B), and percentages of proteins found in higher relative quantity in biological processes (C) and molecular functions (D) on differentiated human enterocytes as affected by exposure to 200 μM α-AA for 72 h.

Particularly, in the term tricarboxylic acid metabolic process, GLUD1 is lowered in abundance together with argininosuccinate synthase (ASS1, Fold change: 0.71), isocitrate dehydrogenase (IDH2, Fold change: 0.64) and iron-responsive element-binding protein 2 (IREB2, only in control) (Table 1 and Supplementary Tables S1 and S2). Glutamine family amino acid biosynthetic process is also found reduced, represented by proteins such as GLUD1, GLUD2 and ASS1 (Supplementary Table S1). On the other hand, certain proteins of the aspartate family amino acid metabolic process were found in lower quantity such as alkaline phosphatase placental type (ALPP, only in control), ASS1, DLST, procollagen-lysine, 2-oxoglutarate 5-dioxygenase 2 (PLOD2, only in control) and LDHD (Table 1 and Supplementary Tables S1 and S2). Within molecular functions, NAD-binding was found in lower quantity in proteins such as GLUD1 and IDH2 (Supplementary Table S3), where NAD is required as coenzyme. Furthermore, in amino acid binding, proteins GLUD1, GLUD2 and ASS1 were the only found in lower abundance in this process (Supplementary Table S3). On the other hand, proteins with oxidoreductase activity and NAD or NADP as proton acceptors, such as alcohol dehydrogenase 4 (ADH4, only in control), aldo-keto reductase family 1 member C2, (AKR1C2, Fold change: 0.50), aflatoxin B1 aldehyde reductase member 3 (AKR7A3, only in control) and dehydrogenase/reductase SDR family member 11 (DHRS11, Fold change: 0.69) (Table 1 and Supplementary Tables S1–S3), were found in decreased abundance in α-AA treated cells.

3.2.1.4. Protein disulfide isomerase activity. In both, biological processes and in molecular functions, proteins related with disulfide oxidoreductase activity (GSH activity) such as endoplasmic reticulum protein 44 (ERP44, Fold change: 0.81), protein disulfide isomerase A1 (P4HB, Fold change: 0.85), protein disulfide isomerase A3 (PDIA3, Fold change: 0.72), protein disulfide isomerase A4 (PDIA4, Fold change: 0.76) and glutathione S-transferase A2 (GSTA2, Fold change: 0.60) (Table 1 and Supplementary Tables S1–S3), were decreased in abundance in cells exposed to α-AA.

3.2.1.5. Regulation of endoribonuclease activity and miRNA loading onto RISC involved in gene silencing by miRNA. The exposure to α-AA caused a reduction in the abundance of chaperone related proteins such as the heat shock 70 kDa protein 1A (HSPA1A, Fold change: 0.76), heat shock 70 kDa protein 1B (HSPA1B, Fold change: 0.76), ATP-binding cassette, sub-family E, member 1, (ABCE1, Fold change: 0.57) and high mobility group protein B1, (HMGB1, Fold change: 0.74) (Table 1 and Supplementary Tables S1 and S2). Thus, within biological processes, proteins implicated in protein folding chaperone, protein folding in endoplasmic reticulum, endoribonuclease and ribonuclease activities were identified as the affected in proteins calreticulin (CALR, Fold change: 0.79), 78 kDa glucose-regulated protein (HSPA5, Fold change: 0.79) (Table 1 and Supplementary Table S1) and PDIA3 in addition to HSPA1A and HSPA1B (Supplementary Table S1).

Regarding miRNA (microRNA) loading onto RISC (miRNA-induce silencing complex), a number of AGO (argonaute) proteins were reduced in the presence of α-AA, namely AGO1, AGO2, AGO3 and AGO4 (all present only in control) (Table 1 and Supplementary Tables S1–S3).

3.2.1.6. Other proteins of biological significance found in lower relative quantity in α-AA-treated cells. Other significantly changed proteins found in lower quantity that have not been included in previous sections are tubulin beta-8 chain (TUBB8, Fold change: 0.15), intestinal sucrase-isomaltase, (SI, Fold change: 0.41), KDEL motif-containing protein 2 (KDELC2, Fold change: 0.47), 14–3-3 protein sigma (SFN, Fold change: 0.51) and glucosidase 2 subunit beta (PRKCSH, Fold change: 0.51) (Table 1 and Supplementary Table S1).

Proteins of biological significance only found in control samples are rootletin protein (CROCC), cilia- and flagella-associated protein 20

Table 1
Proteins from differentiated human enterocytes affected by the exposure to 200 μM α-AA for 72 h.

Protein name	Gene name	*p*-value	Fold-change[1]	Biological function	FASTA accession number
Protein kinase C alpha type	*PRKCA*	–	C	Cell communication by electrical coupling	J3KRN5
5'-AMP-activated protein kinase, regulatory gamma subunit	*PRKAG1*	–	C	ADP binding	F8VYY9
Acetyl-coenzyme A synthetase	*ACSS2*	–	C	Acetyl-CoA metabolic and biosynthetic processes	Q4G0E8
Alkaline phosphatase placental type	*ALPP*	–	C	Cellular amino acid metabolic process	B2R7C7
Iron-responsive element-binding protein 2	*IREB2*	–	C	Involved in tricarboxylic acid cycle	P48200
Procollagen-lysine,2-oxoglutarate 5-dioxygenase 2	*PLOD2*	–	C	Cellular amino acid metabolic process	E7ETU9
Alcohol dehydrogenase 4	*ADH4*	–	C	Oxidoreductase activity, acting on the CH-OH group of donors, NAD or NADP as acceptor	A0A024RDF8
Aflatoxin B1 aldehyde reductase member 3	*AKR7A3*	–	C	Oxidoreductase activity, acting on the CH-OH group of donors, NAD or NADP as acceptor	O95154
Protein argonaute-1, protein argonaute-2, protein argonaute-3, protein argonaute-4	*AGO1, AGO2, AGO3, AGO4*	–	C	miRNA loading onto RISC involved in gene silencing by miRNA	Q5TA58
Rootletin	*CROCC*	–	C	Internal structure of cilia and flagella	Q5TZA2
Cilia- and flagella-associated protein 20	*CFAP20*	–	C	Internal structure of cilia and flagella	Q9Y6A4
Ubiquitin carboxyl-terminal hydrolase isoenzyme L3	*UCHL3*	–	C	Deubiquitinating enzyme	P15374
Brain acid soluble protein 1	*BASP1*	–	C	Binding to protein kinase C alpha type	P80723
Endophilin-B2	*SH3GLB2*	–	C	Endosomal trafficking	Q9NR46
Cyclin-dependent kinase 2	*CDK2*	–	C	Entry in mitosis and DNA damage prevention	P24941
Caspase-3	*CASP3*	–	C	Apoptosis	P42574
Methionine aminopeptidase 1	*METAP1*	–	C	Normal progression through cell cycle	P53582
Cdc42-interacting protein 4	*STP*	–	C	Regulation of actin cytoskeleton	Q15642
Tubulin beta-8 chain	*TUBB8*	0.002	0.15	Structural constituent of cytoskeleton	Q3ZCM7
Sucrase-isomaltase, intestinal	*SI*	0.041	0.41	Hydrolyzing monosaccharides	P14410
KDEL motif-containing protein 2	*KDELC2*	0.039	0.47	Protein glycosidation	Q7Z4H8
Aldo-keto reductase family 1 member C2	*AKR1C2*	0.033	0.5	Oxidoreductase activity, acting on the CH-OH group of donors, NAD or NADP as acceptor	P52895
Glucosidase 2 subunit beta	*PRKCSH*	0.043	0.51	Glucosidase activity	K7ELL7
14–3-3 protein sigma	*SFN*	0.024	0.51	Cell cycle regulation and signal transduction	P31947
ATP-binding cassette sub-family E member 1	*ABCE1*	0.04	0.57	Regulation of *endo*- and ribonuclease activity	P61221
Glutathione S-transferase A2	*GSTA2*	0.0004	0.6	Protection against oxidative stress	P09210
NADP-dependent malic enzyme	*ME1*	0.0003	0.62	Oxidoreductase activity, acting on the CH-OH group of donors, NAD or NADP as acceptor	P48163
Isocitrate dehydrogenase	*IDH2*	0.002	0.64	Tricarboxylic acid metabolic process	P48735
Catalase	*CAT*	0.004	0.64	Cellular amino acid metabolic process/Protection against oxidative stress	P04040
Liver carboxylesterase	*CES1*	0.002	0.67	Acetyl-CoA metabolic and biosynthetic processes	P23141
Dehydrogenase/reductase SDR family member 11	*DHRS11*	0.001	0.69	Oxidoreductase activity, acting on the CH-OH group of donors, NAD or NADP as acceptor	Q6UWP2
3-hydroxyacyl-CoA dehydrogenase type-2	*HSD17B10*	0.026	0.71	Branched-amino acid metabolic and catabolic processes	Q99714
Argininosuccinate synthase	*ASS1*	0.019	0.71	Tricarboxylic acid metabolic process	Q5T6L4
Methylcrotonoyl-CoA carboxylase beta chain, mitochondrial	*MCCC2*	0.004	0.72	Branched-amino acid metabolic and catabolic processes	A0A140VK29
Sodium/potassium-transporting ATPase subunit alpha-1	*ATP1A1*	0.041	0.72	Establishment or maintenance of transmembrane electrochemical gradient	P05023
Protein disulfide isomerase A3	*PDIA3*	0.001	0.72	Protein disulfide isomerase activity	B3KQT9
Sarcoplasmic/endoplasmic reticulum calcium ATPase subunit alpha-2	*ATP2A2*	0.005	0.73	ATPase-coupled cation transmembrane transporter activity	A0A0S2Z3L2
Lactate dehydrogenase	*LDHD*	0.028	0.73	Acetyl-CoA metabolic and biosynthetic processes	Q86WU2
High mobility group protein B1	*HMGB1*	0.04	0.74	Interaction with nucleosomes, transcription factors, and histones	P09429
Protein disulfide isomerase A4	*PDIA4*	0.008	0.76	Protein disulfide isomerase activity	A0A090N8Y2
Heat shock 70 kDa protein 1A	*HSPA1A*	0.001	0.76	Regulation of endo- and ribonuclease activity; Protein folding chaperone	P0DMV8
Heat shock 70 kDa protein 1B	*HSPA1B*	0.001	0.76	Regulation of endo- and ribonuclease activity; Protein folding chaperone	A0A0G2JIW1
Glutamate dehydrogenase 1	*GLUD1*	0.002	0.79	Tricarboxylic acid cycle	P00367
Glutamate dehydrogenase 2	*GLUD2*	0.002	0.79	Tricarboxylic acid cycle	P49448
Calreticulin	*CALR*	0.002	0.79	Calcium-binding chaperone, protein folding chaperone in endoplasmic reticulum	P27797
78 kDa glucose-regulated protein	*HSPA5*	0.028	0.79	Protein folding in endoplasmic reticulum	P11021
Dihydrolipoyllysine-residue succinyltransferase	*DLST*	0.036	0.81	Tricarboxylic acid cycle	Q6IBS5
Endoplasmic reticulum protein 44	*ERP44*	0.035	0.81	Protein disulfide isomerase activity	Q9BS26
Malonyl-CoA decarboxylase, mitochondrial	*MLYCD*	0.037	0.82	Acetyl-CoA metabolic and biosynthetic processes	O95822
Protein disulfide isomerase A1	*P4HB*	0.019	0.85	Protein disulfide isomerase activity	B3KQT9
60S ribosomal protein L11	*RPL11*	0.027	1.25	Nuclear-transcribed mRNA catabolic process nonsense mediated decay	P62913
60S ribosomal protein L26	*RPL26*	0.004	1.33	Nuclear-transcribed mRNA catabolic process nonsense mediated decay	P61254
cAMP-dependent protein kinase type II-alpha regulatory subunit	*PRKAR2A*	0.045	1.35	cAMP-dependent protein kinase regulator activity	A0A0S2Z472

(*continued on next page*)

Table 1 (*continued*)

Protein name	Gene name	*p*-value	Fold-change[1]	Biological function	FASTA accession number
Microtubule-associated protein RP/EB family member 1	*MAPRE1*	0.005	1.4	Regulation of microtubule polymerization	Q15691
Ubiquitin carboxyl-terminal hydrolase 10	*USP10*	0.019	1.46	Postreplication repair	Q14694
Adenylate kinase 4	*AK4*	0.005	1.49	Synthesis of nucleotides and ribonucleotides triphosphate	P27144
60S ribosomal protein L12	*RPL12*	0.027	1.49	Nuclear-transcribed mRNA catabolic process nonsense mediated decay	P30050
Tubulin beta chain	*TUBB*	0.025	1.58	Structural constituent of cytoskeleton	P07437
Protein mago nashi homolog	*MAGOH*	0.009	1.6	Regulation of alternative mRNA splicing, via spliceosome	P61326
Proto-oncogene tyrosine-protein kinase Src	*SRC*	0.001	1.63	Regulation of actin cytoskeleton	P12931
Actin-related protein 2/3 complex subunit 4	*ARPC4*	0.043	1.67	Actin polymerization and DNA repair	P59998
U1 small nuclear ribonucleoprotein A	*SNRPA*	0.033	1.67	Regulation of alternative mRNA splicing, via spliceosome	P09012
Polyubiquitin B	*UBB*	0.002	1.68	Postreplication repair	B4DV12
Ubiquitin C	*UBC*	0.002	1.68	Postreplication repair	L8B196
Ubiquitin-60S ribosomal protein L40	*UBA52*	0.002	1.68	Postreplication repair	P62987
Ubiquitin- 40S ribosomal protein S27a	*RPS27A*	0.002	1.68	Postreplication repair	Q5RKT7
cAMP-dependent protein kinase type I-alpha regulatory subunit	*PRKAR1A*	0.022	1.71	cAMP-dependent protein kinase regulator activity	K7EPB2
Ras-related protein Rab-1B	*RAB1B*	0.026	1.75	Intracellular membrane trafficking	Q9H0U4
Replication factor C subunit 4	*RFC4*	0.018	1.77	Postreplication repair	P35249
RNA binding motif protein, X-linked-like-1	*RBMXL1*	0.02	1.78	Regulation of alternative mRNA splicing, via spliceosome	Q96E39
Serine/arginine-rich splicing factor 3	*SRSF3*	0.021	1.83	Regulation of alternative mRNA splicing, via spliceosome	P84103
40S ribosomal protein S25	*RPS25*	0.046	1.93	Nuclear-transcribed mRNA catabolic process nonsense mediated decay	P62851
Ubiquitin-conjugating enzyme E2 variant 1	*UBE2V1*	0.042	2.01	Postreplication repair	Q13404
Nucleoside-diphosphate kinase B	*NME2*	0.025	2.16	Synthesis of nucleotides and ribonucleotides triphosphate	P22392
Nucleoside-diphosphate kinase	*NME1-NME2*	0.025	2.16	Synthesis of nucleotides and ribonucleotides triphosphate	J3KPD9
Arfaptin-1	*ARFIP1*	0.009	2.35	Regulation of cytoplasmic transport	P53367
Serine/arginine-rich splicing factor 7	*SRSF7*	0.007	2.41	Regulation of alternative mRNA splicing, via spliceosome	Q16629
60S ribosomal protein L27a	*RPL27A*	0.006	2.72	Nuclear-transcribed mRNA catabolic process nonsense mediated decay	P46776
Profilin-1	*PFN1*	0.039	2.98	Regulation of cytoplasmic transport	P07737
40S ribosomal protein S10	*RPS10*	0.015	3.23	Nuclear-transcribed mRNA catabolic process nonsense mediated decay	P46783
40S ribosomal protein S18	*RPS18*	0.017	3.6	Nuclear-transcribed mRNA catabolic process nonsense mediated decay	P62269
28S ribosomal protein S27, mitochondrial	*MRPS27*	–	A	Mitochondrial translation and rRNA binding	Q8N6F2

[1] C: found only in control samples. A: found only in α-AA samples.

(CFAP20), ubiquitin carboxyl-terminal hydrolase isoenzyme L3 (UCHL3), brain acid soluble protein 1 (BASP1), endophilin-B2 (SH3GLB2), cyclin-dependent kinase 2 (CDK2), caspase-3 (CASP3), methionine aminopeptidase 1 (METAP1) and cdc42-interacting protein 4 (STP) (Table 1 and Supplementary Table S1).

3.2.2. *Proteins found in higher relative quantity in CACO-2 cells exposed to α-AA*

3.2.2.1. cAMP-dependent protein kinase inhibitor activity. Within molecular functions, the cAMP-dependent protein kinase (PKA) inhibitor activity was one of the most affected by the presence of α-AA (Fig. 2D). Namely, proteins such as alpha regulatory subunits of cAMP-dependent protein kinases type I (PRKAR1A, Fold change: 1.71), and type II (PRKAR2A, Fold change: 1.35) (Table 1 and Supplementary Tables S1–S5) were significantly increased in abundance in α-AA treated cells.

3.2.2.2. Post-replication repair. Within biological processes, proteins involved in post-replication repair increased in α-AA-treated cells as compared to control samples with this process being among the most affected in α-AA treated cells (Fig. 2C). Proteins such as the ubiquitin-conjugating enzyme E2 variant 1 (UBE2V1, Fold change: 2.01), the subunit 4 of replication factor C (RFC4, Fold change: 1.77), the ubiquitin-40S ribosomal protein S27a (RPS27A, Fold change: 1.68), the ubiquitin-60S ribosomal protein L40 (UBA52, Fold change: 1.68), the polyubiquitin B (UBB, Fold change: 1.68), the ubiquitin C (UBC, Fold change: 1.68), and the ubiquitin carboxyl-terminal hydrolase 10 (USP10, Fold change: 1,46) (Table 1 and Supplementary Tables S1–S4) were particularly affected. All these proteins are part of the ubiquitin system.

3.2.2.3. UTP metabolic process. Processes related to UTP metabolic process and the metabolism and synthesis of triphosphate nucleotides and ribonucleotides were also significantly affected by the exposure to α-AA (Fig. 2C and D). A number of proteins belonging to these processes were found in higher abundance in α-AA-treated cells compared to the control counterparts ($p < 0.05$), including nucleoside-diphosphate kinase (NME1-NME2, Fold change: 2.16) and nucleoside-diphosphate kinase B (NME2, Fold change: 2.16) and adenylate kinase 4 (AK4, Fold change: 1.49) (Table 1 and Supplementary Tables S1–S4).

3.2.2.4. Nuclear-transcribed mRNA catabolic process nonsense mediated decay. Proteins involved in nuclear-transcribed mRNA catabolic process nonsense mediated decay were in higher abundance in α-AA-treated cells compared to control samples ($p < 0.01$) (Fig. 2C). All the proteins

that appear in this process are implicated in 60s ribosomal proteins and 40s ribosomal proteins such as 40S ribosomal protein S18 (RPS18, Fold change: 3.60), 40S ribosomal protein S10 (RPS10, Fold change: 3.23), 60S ribosomal protein L27a (RPL27A, Fold change: 2.72), 40S ribosomal protein S25 (RPS25, Fold change: 1.93), 60S ribosomal protein L12 (RPL12, Fold change: 1.49), 60S ribosomal protein L26 (RPL26, Fold change: 1.33) and 60S ribosomal protein L11 (RPL11, Fold change: 1.25) (Table 1 and Supplementary Tables S1–S4) among others.

3.2.2.5. U1 snRNA binding and regulation of alternative mRNA splicing. In both, molecular functions and biological processes, proteins implicated in U1 snRNA (small nuclear RNA) binding, were found in higher quantity in α-AA treated cells. Proteins such as serine/arginine-rich splicing factor 7 (SRSF7, Fold change: 2.41), serine/arginine-rich splicing factor 3 (SRSF3, Fold change: 1.83), x-linked-like-1 RNA binding motif protein, (RBMXL1, Fold change: 1.78), U1 small nuclear ribonucleoprotein A (SNRPA, Fold change: 1.67) and protein mago nashi homolog (MAGOH, Fold change: 1.60) are involved in U1 snRNA binding and regulation of alternative mRNA splicing, via spliceosome (Table 1 and Supplementary Tables S1–S5).

3.2.2.6. Other proteins of biological significance found in higher relative quantity in α-AA-treated cells. The concentrations of several proteins implicated in these processes, such as profilin-1 (PFN1, Fold change: 2.98), arfaptin-1 (ARFIP1, Fold change: 2.35), ras-related protein Rab-1B (RAB1B, Fold change: 1.75), subunit 4 of actin-related protein 2/3 complex (ARPC4, Fold change: 1.67), proto-oncogene tyrosine-protein kinase Src (SRC, Fold change: 1.63), tubulin beta chain (TUBB, Fold change: 1.58) and microtubule-associated protein RP/EB family member 1 (MAPRE1, Fold change: 1.40) (Table 1 and Supplementary Tables S1–S5), were significantly increased in α-AA treated cells as compared to the control counterparts. The mitochondrial 28S ribosomal protein S27 (MRPS27) (Table 1 and Supplementary Table S1) was only found in the proteome of enterocytes exposed to α-AA.

4. Discussion

Oxidative stress is a condition that has been studied for years and is associated with multiple health disorders. Dietary oxidized lipids and proteins are known to impair the redox status in humans and contribute to such pathological conditions [12]. Yet, the underlying molecular pathways implicated in the toxicological effects of individual oxidized amino acids are poorly understood. While the pathophysiological effects of lipid oxidation products such as malondialdehyde (MDA) and 4-hydroxy nonenal (4-HNE) have been studied at a molecular level [26] the mechanisms by which oxidized proteins and amino acids could impair cell homeostasis is wholly unknown. This is of scientific relevance since oxidized amino acids such as α-AA, are commonly found in processed and red meat products that are, in turn, involved in the occurrence of postprandial, oxidative stress in the gastrointestinal tract and chronic inflammation processes [27,28]. As follows, the most relevant biological impairments caused by α-AA in differentiated human enterocytes are discussed. Fig. 3 illustrates the biological processes and metabolic pathways affected in these cells by the exposure to α-AA.

4.1. Impact of α-AA on electrical homeostasis and transepithelial function

α-Catalytic subunits proteins of the different ATPases in the cell, such as α subunits of Na^+/K^+-ATPase and Ca^{2+}-ATPase were significantly reduced in abundance in the presence of α-AA. Therefore, the results

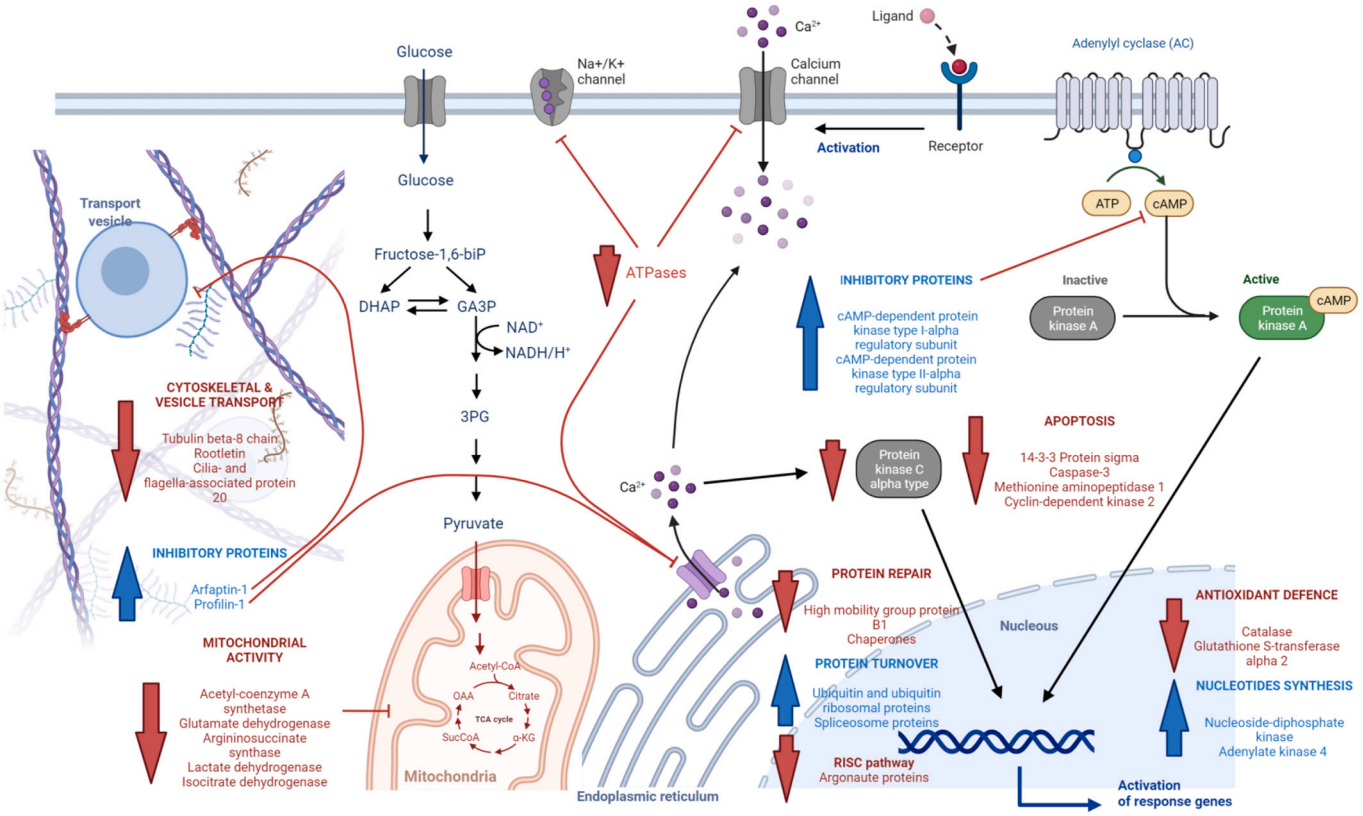

Fig. 3. Proposal of mechanisms underlying the cell toxicological effects of α-AA on differentiated human enterocytes. Upstream head blue arrows indicate higher concentration of proteins in α-AA treated cells. Downstream head red arrows indicate lower concentration of proteins in α-AA treated cells. Blunt head red arrows indicate an inhibited biological process or metabolic pathway. (For interpretation of the references to colour in this figure legend, the reader is referred to the web version of this article.)

suggest that these essential processes are partially suppressed in the presence of α-AA. The energy used in Na^+/K^+ exchange, maintains a physiological electrochemical gradient and disturbances in this fundamental cell function, may lead to health disorders [29]. The proteins involved in biological processes requiring glycosative reactions, were found to be in lower abundance or suppressed upon α-AA. For instance, glucocorticoid biosynthesis and related metabolic processes were diminished in the presence of α-AA, where glucocorticoids are steroid hormones synthesized in the intestinal mucosa by steroidogenic enzymes [30]. The response to glycosides was also impaired by the exposure to α-AA. Glycosides are secondary metabolites where a sugar moiety is linked to an aglycone molecule by an N-, S-, O- or C-glycosidic bond [31]. Glucose uptake, required for the synthesis of both glucocorticoids and glycosides, could have been affected by the disturbance of α-AA to the membrane Na^+/K^+ ATPase activity, as above mentioned. Therefore, an intracellular depletion of glucose caused by perturbation of Na^+/glucose cotransporters could explain an impairment of the biosynthesis of glucose-dependent molecules. The impairment of glucocorticoid metabolism could lead to physiological consequences as these hormones display anti-inflammatory local effects [32]. Thus, these results would be in line with other previous studies where α-AA was identified as a potential modulator of glucose homeostasis [6] and was associated with insulin resistance [7].

4.2. Cytoskeletal dynamics and vesicle transport

Tubulin is a structural constituent of cytoskeleton and forms microtubules in the cell, which have different functions such as maintenance of cell structure, protein trafficking and mitosis [33]. In this study, the occurrence of the protein tubulin beta-8 chain was significantly lower (Table 1 and Supplementary Table S1) in α-AA-treated cells, as compared to the control. Gilbert et al. [34] reported that the depolymerization of tubulin in enterocytes interfered in the displacement of apical proteins such as intestinal sucrase-isomaltase and the placental type alkaline phosphatase, which normally reaches a highly polarized apical distribution. A similar behavior was observed in sodium/potassium-transporting ATPase subunit alpha-1 in MCDK cells [35]. These results support the hypothesis that α-AA could act as an inhibitor of tubulin, which would in turn explain the lower concentration of intestinal sucrase-isomaltase and sodium/potassium-transporting ATPase subunit alpha-1, and the lack of placental type alkaline phosphatase, in cells treated with α-AA. Thus, α-AA affects the transport of these proteins within the cell, plausibly rendering them incapable of exerting their function in their cellular location.

Actin is another component of the cytoskeleton responsible for the transport of vesicles throughout the cytoplasm, among other functions [36]. The occurrence of proteins involved in the regulation of actin polymerization and vesicle transport, such as arfaptin-1, profilin-1, ras-related protein Rab-1B and proto-oncogene tyrosine-protein kinase Src, was significantly higher in α-AA-treated cells compared to the control. Huang et al. [37] reported that overexpression of arfaptin-1 inhibits vesicle transport while Shao et al. [38] found that profilin-1 inhibits actin polymerization. Furthermore, α-AA treated cells lacked several proteins such as endophilin-B2, which alters endosomal trafficking in vitro [39], Cdc42-interacting protein 4, involved in regulation of actin cytoskeleton [40] and the quantity of the protein glucosidase 2 subunit beta, an enzyme that cleaves glucose residues from nascent glycoproteins [41] was lowered. Thus, in this way, both actin polymerization and vesicle transport were inhibited processes, preventing the aforementioned proteins from correctly performing their function, as in the case of tubulin. Furthermore, profilin-1 inhibits the formation of IP3 (inositol trisphosphate) by binding to PIP2 (phosphatidylinositol 4,5-bisphosphate) [42], which is responsible for the release of calcium into the intracellular space activating protein kinase C alpha type. This is coherent with the present results as protein kinase C alpha type and brain acid soluble protein 1, were not found in α-AA treated cells. The results are also consistent with the lower abundance of sarcoplasmic/endoplasmic reticulum calcium ATPase subunit alpha-2 protein in α-AA treated cells compared to the control counterparts.

4.3. Impact of α-AA on energy metabolism and mitochondrial function

The disturbance of the energy metabolism caused by α-AA in intestinal cells may be caused by the impairment that such oxidized amino acid is able to induce at the mitochondrial level. Glutamate dehydrogenase (GDH) is a mitochondrial enzyme that catalyzes glutamate into 2-oxoglutarate (2-OG) [43], and it plays a major role in mitochondrial TCA cycle and energetic cell homeostasis. The exposure to α-AA significantly reduced the quantity of the two GDH isozymes. As mentioned in due course, other enzymes involved in acetyl-CoA biosynthesis and TCA cycle are also affected in cells exposed to α-AA, which corroborates the noxious effect of this oxidized amino acid in the energetic metabolism of the intestinal cell. Studies in pigs have shown that approximately 90% of dietary glutamate is metabolized in the intestine and 50% of it is oxidized to CO_2 [44]. This metabolic behavior not only fulfils intestinal cell energy demand, it is also necessary to keep the Na^+/K^+ ATPase pump active [45]. TCA cycle and Na^+/K^+ ATPases are interconnected processes because the energy obtained in TCA cycle is fundamental to keep the Na^+/K^+ ATPase pump active, and a direct and immediate consequence of Na+/K+ ATPase inhibition is the disruption of central carbon metabolism [46]. The mitochondrial disturbance of α-AA was already suggested by flow cytometry results, where a decrease in mitochondrial activity was revealed in cells exposed to α-AA, though not to a significant extent (Fig. 1I). The lower abundance of proteins such as glutamate dehydrogenase, NADP-dependent malic enzyme, 5'-AMP-activated protein kinase regulatory gamma subunit, isocitrate dehydrogenase and argininosuccinate synthase, is consistent with a decreased mitochondrial activity.

As anticipated, different proteins related to acetyl-CoA biosynthesis and TCA cycle such as glutamate dehydrogenase, isocitrate dehydrogenase and argininosuccinate synthase [47] were found in lower abundance in the presence of α-AA. This fact could have contributed to the significant decrease in mitochondrial activity through the impairment of the TCA cycle and other related pathways. Glutamine family amino acid biosynthetic process and aspartate family amino acid metabolic process were found to comprise proteins with lowered abundance such as glutamate dehydrogenase, argininosuccinate synthase and alkaline phosphatase placental type, argininosuccinate synthase, dihydrolipoyllysine-residue mitochondrial succinyltransferase, procollagen-lysine,2-oxoglutarate 5-dioxygenase 2 and lactate dehydrogenase, respectively. Proteins dihydrolipoyllysine-residue mitochondrial succinyltransferase and procollagen-lysine,2-oxoglutarate 5-dioxygenase 2, are particularly implicated in lysine degradation. Thus, as these proteins are found in lower abundance in the presence of α-AA, they can affect lysine degradation process and may be involved in accumulation of lysine in cell, which may lead to physiological impairments [48]. With α-AA being an oxidation product of lysine, the suppression of molecular mechanisms involved in lysine degradation seems reasonable.

4.4. Oxidative stress and antioxidant defenses

A decreased and inefficient mitochondrial activity is typically linked to ROS generation and the onset of oxidative stress [49]. In fact, da Silva et al. [10] reported a significant increase in ROS in rat neuronal cells as induced by α-AA. Consistently, in a previous study, the exposure of differentiated enterocytes to α-AA for 72 h led to ROS generation with respect to the control cells [11]. In our present study, such condition was not confirmed by the flow cytometry analysis. Yet, other analyses indicate the depletion of antioxidant defenses and the accretion of protein carbonyls in α-AA treated cells, with both conditions typically occurring under oxidative stress. The concentration of catalase, known to

counteract peroxides [50], was significantly lower in α-AA treated cells compared to the control counterparts. Other relevant oxidoreductases that could be involved in detoxifying dietary oxidation products such as alcohol dehydrogenase 4 and aflatoxin B1 aldehyde reductase member 3 [51] were not found in α-AA treated cells. These results indicate that certain antioxidant defenses were whether depleted in cells exposed to α-AA or that the antioxidant response in these cells failed to be appropriately activated.

On the other hand, glutathione (GSH) is a tetrapeptide with remarkable antioxidant activity in cells. While no apparent effect of α-AA was found in relation to GSH content in live cells (data not shown), da Silva et al. [10] found a significant depletion of GSH in the cerebral cortex of rats exposed to 4 mM of α-AA. In our previous study [11], the long-term exposure (72 h) of differentiated CACO-2 cells to 200 μM of α-AA had no effect on the occurrence of GSH. Interestingly in the population of dead cells, a significant increase in GSH concentration was observed, probably due to a compensatory increase in GSH after an oxidative insult (Fig. 1K), compared with control cells. Yet, this event is a reflection of a failed antioxidant response as the concentration of glutathione S-transferase alpha 2 (encoded by *GSTA2* gene) was lower in cells exposed to α-AA compared to the control cells. This enzyme detoxifies pro-oxidative substances by catalyzing the nucleophilic attack by GSH on electrophilic atoms of such reactive substrates [52]. Therefore, the synthesis and accretion of GSH in α-AA-exposed cells seemed inoperable without the timely involvement of the appropriate enzymes, with these cells eventually dying, still holding high concentrations of GSH. Additionally, Falkner et al. [53] reported that glucocorticoids regulate *GSTA2* gene in cultured rat hepatocytes, repressing its expression at low concentrations (10 to 100 nM) but promoting its expression at high concentrations (>1 μM). Hence, it is reasonable that the lower concentration of glutathione S-transferase A2 observed in this study, would reflect the lower quantity of proteins involved in glucocorticoid biosynthetic and metabolic processes.

4.5. Impact of α-AA on protein conformation, functionality and repair

Chaperone proteins are implicated in preventing aberrant protein folding and aggregations [54]. Proteins such as ATP-binding cassette sub-family E member 1, implicated in ribosome biogenesis, and chaperone proteins heat shock 70 kDa protein 1A and heat shock 70 kDa protein 1B [54], were found in lower quantity in cells exposed to α-AA. Moreover, the concentration of high mobility group protein B1 HMGB1, one of the most important chromatin proteins that interacts with nucleosomes, transcription factors and histones [55], was significantly lower in α-AA-treated cells compared to the control. Thus, α-AA may be contributing to the occurrence of aberrant protein conformations and impaired functionalities as denoted by the higher extent of protein carbonylation in α-AA-treated cells than in the control counterparts. The ubiquitin system plays a central role in protein homeostasis by regulating the turnover of proteins involved in processes such as signal transduction, DNA repair and apoptosis, among others [56]. In this study, the higher abundance of the ubiquitin-dependent degradation of proteins may respond to the disability of the chaperone system to repair aberrant proteins, which leads to increased occurrence of anomalous protein conformations. This result is consistent with the accretion of protein carbonyls and the lack of ubiquitin carboxyl-terminal hydrolase isozyme L3, a deubiquitinating enzyme [57].

Consistently, the nuclear-transcribed mRNA catabolic process nonsense mediated decay is found in higher quantity in α-AA-treated cells. The nonsense mediated decay pathway for nuclear-transcribed mRNAs prevents the translation of such mRNA into truncated and potentially harmful proteins [58]. The higher abundance of proteins involved in this pathway could prevents the formation of truncated and potentially harmful proteins while U1 snRNA binding protein (part of the spliceosome) is as well found increased in quantity, probably to remove misfolded or truncated proteins. The results from a previous study [11] are consistent with the present ones in regards to α-AA promoting the oxidative damage to cell proteins. The present results show an attempt of the cell to revert these modifications in proteins. Thus, all the processes in which proteins are in higher abundance are aimed to DNA repair, and others are associated with mechanisms to prevent truncated proteins. This is also linked to the lower abundance of proteins argonaute (AGO), that are responsible for repressing miRNA translation [59]. The lower abundance of these proteins in α-AA-treated cells in conjunction with the higher quantity of proteins involved in nucleoside and ribonucleoside biosynthetic and metabolic processes, support the hypothesis that the RISC complex is repressed. This would enable the expression of non-silencing genes and therefore, facilitate the synthesis of new non-truncated proteins.

4.6. Impact of α-AA on stress response, apoptosis and cell cycle

Intestinal cells display a number of biochemical mechanisms to maintain homeostasis and response against physical, biological and chemical threats. PKA plays an important role in the maintenance of cellular homeostatic processes, in cell metabolism and in the intracellular signal transduction process [60]. In this study, the regulatory subunits of PKA, which regulate the cAMP-PKA binding process, are upwardly inhibited in cells exposed to α-AA. Therefore, the effect of α-AA on inhibiting the multiple functions in which PKA is involved, may lead to various impaired physiological processes including a suitable cell response against this chemical threat. This may affect, among others, to the ability of the cell to shift their gene expression patterns and activate, as a result, defense mechanisms under stress conditions [61]. On this line, miRNA is assembled with AGO proteins to form the RNA-induced silencing complex (RISC), which pairs with target miRNAs and represses their expression [59]. α-AA significantly affected this regulation process by downregulating genes encoding argonaute proteins (AGO1, AGO2, AGO3 and AGO4).

Regarding cell cycle regulation and apoptosis, certain proteins involved in these processes were at significantly lower concentrations, or were not found, in α-AA treated cells. Among these, we may cite 14–3-3 protein sigma, caspase-3, methionine aminopeptidase 1 and cyclin-dependent kinase 2. These results, as well as those from flow cytometer, indicate that α-AA affects cell viability. Yet, this condition does not seem to be manifested in a high quantity of proteins implicated in apoptosis, but rather to a lower abundance of those involved in a suitable maintenance of cell cycle.

Finally, as aforementioned, one protein, 28S ribosomal protein S27 mitochondrial, was found only in α-AA-treated cells. This protein is a RNA-binding component that is involved in mitochondrial protein synthesis and in biogenesis and maintenance of organelles [62]. This is consistent with the hypothesis of the stimulation of protein synthesis α-AA-treated cells in order to maintain homeostasis and prevent apoptosis.

5. Conclusion

This paper described, for the first time, the underlying mechanisms of the biological impairments caused by the oxidized amino acid, α-AA, on differentiated human enterocytes. The analysis of the proteome suggests that lysine oxidation end-product alters cell homeostasis through a variety of mechanisms that include transepithelial transportation, energy supply and vesicle transportation of proteins. While certain antioxidant defenses and repair mechanisms are diminished by the α-AA, the cell activates protein turn-over mechanisms to avoid apoptosis. These results emphasize the role of dietary oxidized amino acids in intestinal cell physiology and provides grounds to unveil, in further studies, the impact of this and other protein oxidation products in intestinal pathological conditions.

Declaration of Competing Interest

The authors declare that they have no known competing financial interests or personal relationships that could have appeared to influence the work reported in this paper.

Acknowledgements

The financial support from the Spanish Ministry of Economics and Competitiveness (SMEC) is acknowledged (project number AGL2017-84586-R). The "Junta de Extremadura/FEDER" is also acknowledged for financial support (grant number GR108104). S. Díaz-Velasco is recipient of a fellowship from the Spanish Ministry of Science, Innovation and Universities (PRE2018-084001).

Appendix A. Supplementary data

Supplementary data to this article can be found online at https://doi.org/10.1016/j.bbapap.2022.140797.

References

[1] B.S. Berlett, E.R. Stadtman, Protein oxidation in aging, disease, and oxidative stress, J. Biol. Chem. 272 (1997) 20313–20316, https://doi.org/10.1074/jbc.272.33.20313.
[2] J.M. Dos Santos, S. Tewari, R.H. Mendes, The role of oxidative stress in the development of diabetes mellitus and its complications, J. Diabetes Res. 2019 (2019), https://doi.org/10.1155/2019/4189813.
[3] A.R. Bourgonje, M. Feelisch, K.N. Faber, A. Pasch, G. Dijkstra, H. van Goor, Oxidative stress and redox-modulating therapeutics in inflammatory bowel disease, Trends Mol. Med. 26 (2020) 1034–1046, https://doi.org/10.1016/j.molmed.2020.06.006.
[4] W.Q. Chen, W.S. Lian, Y.F. Yuan, M.Q. Li, The synergistic effects of oxaliplatin and piperlongumine on colorectal cancer are mediated by oxidative stress, Cell Death Dis. 10 (2019) 1–12, https://doi.org/10.1038/s41419-019-1824-6.
[5] D.R. Sell, C.M. Strauch, W. Shen, V.M. Monnier, 2-Aminoadipic acid is a marker of protein carbonyl oxidation in the aging human skin: effects of diabetes, renal failure and sepsis, Biochem. J. 404 (2007) 269–277, https://doi.org/10.1042/BJ20061645.
[6] T.J. Wang, D. Ngo, N. Psychogios, A. Dejam, M.G. Larson, R.S. Vasan, A. Ghorbani, J. O'Sullivan, S. Cheng, E.P. Rhee, S. Sinha, E. McCabe, C.S. Fox, C.J. O'Donnell, J. E. Ho, J.C. Florez, M. Magnusson, K.A. Pierce, A.L. Souza, Y. Yu, C. Carter, P. E. Light, O. Melander, C.B. Clish, R.E. Gerszten, 2-Aminoadipic acid is a biomarker for diabetes risk, J. Clin. Invest. 123 (2013) 4309–4317, https://doi.org/10.1172/JCI64801.
[7] H.J. Lee, H.B. Jang, W.H. Kim, K.J. Park, K.Y. Kim, S.I. Park, H.J. Lee, 2-Aminoadipic acid (2-AAA) as a potential biomarker for insulin resistance in childhood obesity, Sci. Rep. 9 (2019) 1–10, https://doi.org/10.1038/s41598-019-49578-z.
[8] M. Estaras, F.Z. Ameur, M. Estévez, S. Díaz-Velasco, A. Gonzalez, The lysine derivative aminoadipic acid, a biomarker of protein oxidation and diabetes-risk, induces production of reactive oxygen species and impairs trypsin secretion in mouse pancreatic acinar cells, Food Chem. Toxicol. 145 (2020), 111594, https://doi.org/10.1016/j.fct.2020.111594.
[9] D.R. Brown, H.A. Kretzschmar, The glio-toxic mechanism of α-aminoadipic acid on cultured astrocytes, J. Neurocytol. 27 (1998) 109–118, https://doi.org/10.1023/A:1006947322342.
[10] J.C. da Silva, A.U. Amaral, C. Cecatto, A. Wajner, K. dos Santos Godoy, R. T. Ribeiro, A. de Mello Gonçalves, Â. Zanatta, M.S. da Rosa, S.O. Loureiro, C. R. Vargas, G. Leipnitz, D.O.G. de Souza, M. Wajner, α-Ketoadipic acid and α-aminoadipic acid cause disturbance of glutamatergic neurotransmission and induction of oxidative stress in vitro in brain of adolescent rats, Neurotox. Res. 32 (2017) 276–290, https://doi.org/10.1007/s12640-017-9735-8.
[11] S. Díaz-Velasco, A. González, F.J. Peña, M. Estévez, Noxious effects of selected food-occurring oxidized amino acids on differentiated CACO-2 intestinal human cells, Food Chem. Toxicol. 144 (2020) 1–8, https://doi.org/10.1016/j.fct.2020.111650.
[12] M. Estévez, Y. Xiong, Intake of oxidized proteins and amino acids and causative oxidative stress and disease: recent scientific evidences and hypotheses, J. Food Sci. 84 (2019) 387–396, https://doi.org/10.1111/1750-3841.14460.
[13] M. Utrera, V. Parra, M. Estévez, Protein oxidation during frozen storage and subsequent processing of different beef muscles, Meat Sci. 96 (2014) 812–820, https://doi.org/10.1016/j.meatsci.2013.09.006.
[14] IARC, Carcinogenicity of consumption of red and processed meat, Lancet Oncol. 16 (2015) 1599–1600, https://doi.org/10.1016/S1470-2045(15)00444-1.
[15] M. Pinto, S. Robine Leon, M.D. Appay, Enterocyte-like differentiation and polarization of the human colon carcinoma cell line Caco-2 in culture, Biol. Cell. 47 (1983) 323–330.
[16] M. Utrera, M. Estévez, Oxidation of myofibrillar proteins and impaired functionality: underlying mechanisms of the carbonylation pathway, J. Agric. Food Chem. 60 (2012) 8002–8011, https://doi.org/10.1021/jf302111j.
[17] M. Timm-Heinrich, S. Eymard, C.P. Baron, H.H. Nielsen, C. Jacobsen, Oxidative changes during ice storage of rainbow trout (*Oncorhynchus mykiss*) fed different ratios of marine and vegetable feed ingredients, Food Chem. 136 (2013) 1220–1230, https://doi.org/10.1016/j.foodchem.2012.09.019.
[18] M. Utrera, M. Estévez, Oxidative damage to poultry, pork, and beef during frozen storage through the analysis of novel protein oxidation markers, J. Agric. Food Chem. 61 (2013) 7987–7993, https://doi.org/10.1021/jf402220q.
[19] J.M. Ortiz-Rodríguez, F.E. Martín-Cano, G.L. Gaitskell-Phillips, A. Silva, C. Ortega-Ferrusola, M.C. Gil, F.J. Peña, Low glucose and high pyruvate reduce the production of 2-oxoaldehydes, improving mitochondrial efficiency, redox regulation, and stallion sperm function†, Biol. Reprod. 105 (2021) 519–532, https://doi.org/10.1093/BIOLRE/IOAB073.
[20] P.M. Muñoz, C.O. Ferrusola, G. Vizuete, M.P. Dávila, H.R. Martinez, F.J. Peña, Depletion of intracellular thiols and increased production of 4-hydroxynonenal that occur during cryopreservation of stallion spermatozoa Lead to caspase activation, loss of motility, and cell death, Biol. Reprod. 93 (2015), https://doi.org/10.1095/BIOLREPROD.115.132878.
[21] M. Utrera, D. Morcuende, J.G. Rodríguez-Carpena, M. Estévez, Fluorescent HPLC for the detection of specific protein oxidation carbonyls - α-aminoadipic and γ-glutamic semialdehydes – in meat systems, Meat Sci. 89 (2011) 500–506, https://doi.org/10.1016/j.meatsci.2011.05.017.
[22] M. Akagawa, T. Sasaki, K. Suyama, Oxidative deamination of lysine residue in plasma protein of diabetic rats: novel mechanism via the Maillard reaction, Eur. J. Biochem. 269 (2002) 5451–5458, https://doi.org/10.1046/j.1432-1033.2002.03243.x.
[23] A. Shevchenko, H. Tomas, J. Havliš, J.V. Olsen, M. Mann, In-gel digestion for mass spectrometric characterization of proteins and proteomes, Nat. Protoc. 1 (2007) 2856–2860, https://doi.org/10.1038/nprot.2006.468.
[24] J. Delgado, F. Núñez, M.A. Asensio, R.A. Owens, Quantitative proteomic profiling of ochratoxin a repression in Penicillium nordicum by protective cultures, Int. J. Food Microbiol. 305 (2019), 108243, https://doi.org/10.1016/j.ijfoodmicro.2019.108243.
[25] G. Bindea, B. Mlecnik, H. Hackl, P. Charoentong, M. Tosolini, A. Kirilovsky, W.-H. Fridman, F. Pagès, Z. Trajanoski, J. Galon, ClueGO: a Cytoscape plug-in to decipher functionally grouped gene ontology and pathway annotation networks, Bioinformatics. 25 (2009) 1091–1093, https://doi.org/10.1093/bioinformatics/btp101.
[26] A. Ayala, M.F. Muñoz, S. Argüelles, Lipid peroxidation: production, metabolism, and signaling mechanisms of malondialdehyde and 4-hydroxy-2-nonenal, Oxidative Med. Cell. Longev. 2014 (2014), https://doi.org/10.1155/2014/360438.
[27] J. Kanner, J. Selhub, A. Shpaizer, B. Rabkin, I. Shacham, O. Tirosh, Redox homeostasis in stomach medium by foods: the postprandial oxidative stress index (POSI) for balancing nutrition and human health, Redox Biol. 12 (2017) 929–936, https://doi.org/10.1016/j.redox.2017.04.029.
[28] D. de La Pomélie, V. Santé-Lhoutellier, T. Sayd, P. Gatellier, Oxidation and nitrosation of meat proteins under gastro-intestinal conditions: consequences in terms of nutritional and health values of meat, Food Chem. 243 (2018) 295–304, https://doi.org/10.1016/j.foodchem.2017.09.135.
[29] A.N. Shrivastava, A. Triller, R. Melki, Cell biology and dynamics of neuronal Na+/K+-ATPase in health and diseases, Neuropharmacology. 169 (2020), 107461, https://doi.org/10.1016/j.neuropharm.2018.12.008.
[30] I. Cima, N. Corazza, B. Dick, A. Fuhrer, S. Herren, S. Jakob, E. Ayuni, C. Mueller, T. Brunner, Intestinal epithelial cells synthesize glucocorticoids and regulate T cell activation, J. Exp. Med. 200 (2004) 1635–1646, https://doi.org/10.1084/jem.20031958.
[31] K.B. Louie, S.M. Kosina, Y. Hu, H. Otani, M. de Raad, A.N. Kuftin, N.J. Mouncey, B. P. Bowen, T.R. Northen, Mass spectrometry for natural product discovery, in: Compr. Nat. Prod. III, Elsevier, 2020, pp. 263–306, https://doi.org/10.1016/b978-0-12-409547-2.14834-6.
[32] A.E. Coutinho, K.E. Chapman, The anti-inflammatory and immunosuppressive effects of glucocorticoids, recent developments and mechanistic insights, Mol. Cell. Endocrinol. 335 (2011) 2–13, https://doi.org/10.1016/j.mce.2010.04.005.
[33] R.A. Stanton, K.M. Gernert, J.H. Nettles, R. Aneja, Drugs that target dynamic microtubules: a new molecular perspective, Med. Res. Rev. 31 (2011) 443–481, https://doi.org/10.1002/med.20242.
[34] T. Gilbert, A. Le Bivic, A. Quaroni, E. Rodriguez-Boulan, Microtubular organization and its involvement in the biogenetic pathways of plasma membrane proteins in Caco-2 intestinal epithelial cells, J. Cell Biol. 113 (1991) 275–288, https://doi.org/10.1083/jcb.113.2.275.
[35] M.J. Caplan, H.C. Anderson, G.E. Palade, J.D. Jamieson, Intracellular sorting and polarized cell surface delivery of (Na+,K+)ATPase, an endogenous component of MDCK cell basolateral plasma membranes, Cell. 46 (1986) 623–631, https://doi.org/10.1016/0092-8674(86)90888-3.
[36] S.R. Goodman, W.E. Zimmer, Cytoskeleton, in: Med. Cell Biol., Third ed., Elsevier Inc., 2007, pp. 59–100, https://doi.org/10.1016/B978-0-12-370458-0.50008-6.
[37] L.H. Huang, W.C. Lee, S.T. You, C.C. Cheng, C.J. Yu, Arfaptin-1 negatively regulates Arl1- mediated retrograde transport, PLoS One 10 (2015), https://doi.org/10.1371/journal.pone.0118743.
[38] J. Shao, W.J. Welch, N.A. DiProspero, M.I. Diamond, Phosphorylation of profilin by ROCK1 regulates polyglutamine aggregation, Mol. Cell. Biol. 28 (2008) 5196–5208, https://doi.org/10.1128/mcb.00079-08.

[39] J.M. Serfass, Y. Takahashi, Z. Zhou, Y.I. Kawasawa, Y. Liu, N. Tsotakos, M. M. Young, Z. Tang, L. Yang, J.M. Atkinson, Z.C. Chroneos, H.G. Wang, Endophilin B2 facilitates endosome maturation in response to growth factor stimulation, autophagy induction, and influenza A virus infection, J. Biol. Chem. 292 (2017) 10097–10111, https://doi.org/10.1074/jbc.M117.792747.
[40] T. Itoh, K.S. Erdmann, A. Roux, B. Habermann, H. Werner, P. De Camilli, Dynamin and the actin cytoskeleton cooperatively regulate plasma membrane invagination by BAR and F-BAR proteins, Dev. Cell 9 (2005) 791–804, https://doi.org/10.1016/J.DEVCEL.2005.11.005.
[41] M.F. Pelletier, A. Marcil, G. Sevigny, C.A. Jakob, D.C. Tessier, E. Chevet, R. Menard, J.J.M. Bergeron, D.Y. Thomas, The heterodimeric structure of glucosidase II is required for its activity, solubility, and localization in vivo, Glycobiology. 10 (2000) 815–827, https://doi.org/10.1093/glycob/10.8.815.
[42] P.J. Goldschmidt-Clermont, L.M. Machesky, J.J. Baldassare, T.D. Pollard, The actin-binding protein profilin binds to PIP2 and inhibits its hydrolysis by phospholipase C, Science (80-.) 247 (1990) 1575–1578, https://doi.org/10.1126/science.2157283.
[43] M. Monné, A. Vozza, F.M. Lasorsa, V. Porcelli, F. Palmieri, Mitochondrial carriers for aspartate, glutamate and other amino acids: a review, Int. J. Mol. Sci. 20 (2019) 4456, https://doi.org/10.3390/ijms20184456.
[44] B. Stoll, D.G. Burrin, J. Henry, H. Yu, F. Jahoor, P.J. Reeds, Substrate oxidation by the portal drained viscera of fed piglets, Am. J. Physiol. Endocrinol. Metab. 277 (1999), https://doi.org/10.1152/ajpendo.1999.277.1.e168.
[45] P. Vaugelade, L. Posho, B. Darcy-Vrillon, F. Bernard, M.T. Morel, P.H. Duée, Intestinal oxygen uptake and glucose metabolism during nutrient absorption in the pig, Proc. Soc. Exp. Biol. Med. 207 (1994) 309–316, https://doi.org/10.3181/00379727-207-43821.
[46] S.M. Sanderson, Z. Xiao, A.J. Wisdom, S. Bose, M.V. Liberti, M.A. Reid, E. Hocke, S. G. Gregory, D.G. Kirsch, J.W. Locasale, The Na+/K+ ATPase regulates glycolysis and modifies immune metabolism in tumors, BioRxiv. (2020), https://doi.org/10.1101/2020.03.31.018739.
[47] P. Prasun, Disorders of pyruvate metabolism and tricarboxylic acid cycle, in: Mitochondrial Med., Elsevier, 2019, pp. 83–95, https://doi.org/10.1016/b978-0-12-817006-9.00015-0.
[48] J. Bouchereau, M. Schiff, Inherited disorders of lysine metabolism: a review, J. Nutr. 150 (2020) 2556S–2560S, https://doi.org/10.1093/jn/nxaa112.
[49] S. Kausar, F. Wang, H. Cui, The role of mitochondria in reactive oxygen species generation and its implications for neurodegenerative diseases, Cells. 7 (2018) 274, https://doi.org/10.3390/cells7120274.
[50] M. Schieber, N.S. Chandel, ROS function in redox signaling and oxidative stress, Curr. Biol. 24 (2014) R453–R462, https://doi.org/10.1016/j.cub.2014.03.034.
[51] K.M. Schaich, Toxicity of lipid oxidation products consumed in the diet, Bailey's Ind. Oil Fat. Prod. (2020) 1–88, https://doi.org/10.1002/047167849X.BIO116.
[52] K.W. Kang, S.H. Choi, S.G. Kim, Peroxynitrite activates nf-e2-related factor 2/antioxidant response element through the pathway of phosphatidylinositol 3-kinase: the role of nitric oxide synthase in rat glutathione S-transferase A2 induction, Nitric Oxide Biol. Chem. 7 (2002) 244–253, https://doi.org/10.1016/S1089-8603(02)00117-9.
[53] K.C. Falkner, J.A. Pinaire, G.-H. Xiao, T.E. Geoghegan, R.A. Prough, Regulation of the rat glutathione S-transferase A2 gene by glucocorticoids: involvement of both the glucocorticoid and Pregnane X receptors, Mol. Pharmacol. 60 (2001).
[54] H. Saibil, Chaperone machines for protein folding, unfolding and disaggregation, Nat. Rev. Mol. Cell Biol. 14 (2013) 630–642, https://doi.org/10.1038/nrm3658.
[55] M.E. Bianchi, A. Agresti, HMG proteins: dynamic players in gene regulation and differentiation, Curr. Opin. Genet. Dev. 15 (2005) 496–506, https://doi.org/10.1016/j.gde.2005.08.007.
[56] D. Buac, M. Shen, S. Schmitt, F. Rani Kona, R. Deshmukh, Z. Zhang, C. Neslund-Dudas, B. Mitra, Q.P. Dou, From Bortezomib to other inhibitors of the proteasome and beyond, Curr. Pharm. Des. 19 (2013) 4025–4038, https://doi.org/10.2174/1381612811319220012.
[57] C. Liao, R. Beveridge, J.J.R. Hudson, J.D. Parker, S.C. Chiang, S. Ray, M.E. Ashour, I. Sudbery, M.J. Dickman, S.F. El-Khamisy, UCHL3 regulates topoisomerase-induced chromosomal break repair by controlling TDP1 proteostasis, Cell Rep. 23 (2018) 3352–3365, https://doi.org/10.1016/j.celrep.2018.05.033.
[58] T. Kurosaki, L.E. Maquat, Nonsense-mediated mRNA decay in humans at a glance, J. Cell Sci. 129 (2016) 461–467, https://doi.org/10.1242/jcs.181008.
[59] V. Glorian, G. Maillot, S. Polès, J.S. Iacovoni, G. Favre, S. Vagner, HuR-dependent loading of miRNA RISC to the mRNA encoding the Ras-related small GTPase RhoB controls its translation during UV-induced apoptosis, Cell Death Differ. 18 (2011) 1692–1701, https://doi.org/10.1038/cdd.2011.35.
[60] E. London, M. Bloyd, C.A. Stratakis, PKA functions in metabolism and resistance to obesity: lessons from mouse and human studies, J. Endocrinol. 246 (2020) R51–R64, https://doi.org/10.1530/JOE-20-0035.
[61] K.A. Spriggs, M. Bushell, A.E. Willis, Translational regulation of gene expression during conditions of cell stress, Mol. Cell 40 (2010) 228–237, https://doi.org/10.1016/j.molcel.2010.09.028.
[62] S.M.K. Davies, M.I.G. Lopez Sanchez, R. Narsai, A.M.J. Shearwood, M.F.M. Razif, I. D. Small, J. Whelan, O. Rackham, A. Filipovska, MRPS27 is a pentatricopeptide repeat domain protein required for the translation of mitochondrially encoded proteins, FEBS Lett. 586 (2012) 3555–3561, https://doi.org/10.1016/j.febslet.2012.07.043.

Capítulo 4.3. Ellagic Acid Triggers the Necrosis of Differentiated Human Enterocytes Exposed to 3-Nitro-Tyrosine: An MS-Based Proteomic Study

El ácido elágico desencadena la necrosis de enterocitos humanos diferenciados expuestos a 3-nitro-tirosina: un estudio proteómico basado en MS

DOI: https://doi.org/10.3390/antiox11122485

Autores: Silvia Díaz-Velasco, Josué Delgado, Fernando J. Peña, Mario Estévez

Año de publicación: 2022

Revista: Antioxidants

Indice de Impacto JCR (2022): 7.0

antioxidants

Article

Ellagic Acid Triggers the Necrosis of Differentiated Human Enterocytes Exposed to 3-Nitro-Tyrosine: An MS-Based Proteomic Study

Silvia Díaz-Velasco [1], Josué Delgado [2], Fernando J. Peña [3] and Mario Estévez [1,*]

[1] Food Technology and Quality (TECAL), Institute of Meat and Meat Products (IPROCAR), Universidad de Extremadura, 10003 Cáceres, Spain
[2] Food Hygiene and Safety (HISEALI), Institute of Meat and Meat Products (IPROCAR), Universidad de Extremadura, 10003 Cáceres, Spain
[3] Spermatology Laboratory, Universidad de Extremadura, 10003 Cáceres, Spain
* Correspondence: mariovet@unex.es

Abstract: To study the molecular basis of the toxicological effect of a dietary nitrosated amino acid, namely, 3-nitrotyrosine (3-NT), differentiated human enterocytes were exposed to dietary concentrations of this species (200 μM) and analyzed for flow cytometry, protein oxidation markers and MS-based proteomics. The possible protective role of a dietary phytochemical, ellagic acid (EA) (200 μM), was also tested. The results revealed that cell viability was significantly affected by exposure to 3-NT, with a concomitant significant increase in necrosis ($p < 0.05$). 3-NT affected several biological processes, such as histocompatibility complex class II (MHC class II), and pathways related to type 3 metabotropic glutamate receptors binding. Addition of EA to 3-NT-treated cells stimulated the toxicological effects of the latter by reducing the abundance of proteins involved in mitochondrial conformation. These results emphasize the impact of dietary nitrosated amino acids in intestinal cell physiology and warn about the potential negative effects of ellagic acid when combined with noxious metabolites.

Keywords: 3-Nitro-L-tyrosine; ellagic acid; proteomics; flow cytometry; protein oxidation; MHC class II; mitochondria

check for updates

Citation: Díaz-Velasco, S.; Delgado, J.; Peña, F.J.; Estévez, M. Ellagic Acid Triggers the Necrosis of Differentiated Human Enterocytes Exposed to 3-Nitro-Tyrosine: An MS-Based Proteomic Study. *Antioxidants* **2022**, *11*, 2485. https://doi.org/10.3390/antiox11122485

Academic Editors: Giancarlo Aldini, Alessandra Altomare and Giovanna Baron

Received: 3 October 2022
Accepted: 9 December 2022
Published: 17 December 2022

Publisher's Note: MDPI stays neutral with regard to jurisdictional claims in published maps and institutional affiliations.

Copyright: © 2022 by the authors. Licensee MDPI, Basel, Switzerland. This article is an open access article distributed under the terms and conditions of the Creative Commons Attribution (CC BY) license (https://creativecommons.org/licenses/by/4.0/).

1. Introduction

Oxidative stress is related to assorted health disorders such as type 2 diabetes mellitus, hypertension, atherosclerosis, pulmonary diseases, systemic inflammatory response syndrome, aging, cancer and Alzheimer's disease, among others [1,2]. Reactive oxygen species (ROS) and reactive nitrogen species (RNS) are involved in oxidative stress through the imbalance between ROS/RNS and antioxidant defenses [2]. Specifically, 3-nitro-L-tyrosine (3-NT), a nitrosation product of tyrosine, is formed during processing of nitrite-added foods (cured foods) [3,4] and is recognized as an indicator of protein nitration in foods and other biological systems [5]. In addition, 3-NT has been used as a biomarker of acute and chronic inflammatory processes, which indicates the involvement of the nitrosation product in pathological conditions [6,7]. While the potential toxicity of 3-NT has been documented, the underlying molecular mechanisms are poorly understood. Blanchard-Fillion et al. [7] reported that 3-NT is transported into rat neuronal cells via the L-aromatic amino acid transporter and is mis-incorporated into proteins such as α-tubulin and decreases the synthesis of dopamine. In these cells, 3-NT is eventually able to induce caspase-3 mediated apoptosis which the authors associated with the onset of neurological disorders such as Parkinson's disease [7]. Consistently, Zhang and Wei [8] found that 3-NT induced apoptosis in cardiomyocytes in a type 2 diabetes rat model. Neutralization of 3-NT counteracted the apoptosis and diabetic myocardiopathy in rats, which reasonably incriminates the

chemical species in the pathogenesis [8]. In a previous in vitro study [9], we reported that 3-NT caused oxidative stress, accretion of oxidized proteins and necrotic events in human enterocytes, leading to a significant decrease in viability of these cells. 3-NT has been found in concentrations of up to 200 μM in food protein suspensions and in fermented sausages [5,10,11]. Interestingly, processed meats, including cured meats, were identified as group 1 carcinogens by the International Agency for Research on Cancer [12] based on epidemiological studies. It is wholly unknown whether nitrosated proteins and amino acids, such as 3-NT, are contributing or not to the potential health concerns of dietary cured meats on the gastrointestinal tract (GIT).

Ellagic acid (EA) is a polyphenolic compound that is widely found in plant materials such as pomegranate fruit [13]. The protective effect of EA against ROS and oxidative stress has been documented in both in vitro and in vivo studies [14]. Much less is known about the potential protection that EA and other phytochemicals may exert against RNS and nitrosative stress. We hypothesized whether EA could counteract the noxious effects of 3-NT in a biological system. Advanced methodologies, such as label-free quantitative MS-based proteomics, along with other techniques such as flow cytometry, have been recently found to provide original insight into the molecular mechanisms of the toxicological effects of oxidized amino acids [15].

Both chemical species under study (3-NT and EA) are common dietary components and both are firstly exposed to cells from the intestinal epithelium. The purpose of this study was to decipher the molecular basis of the potential toxicological effect of 3-NT and the hypothetical protective role of EA on differentiated human colon CACO-2 cells. These cells were used as an experimental model of human enterocytes upon spontaneous differentiation for 21 days [16]. To achieve the aforementioned objective, these human intestinal cells were treated with food-compatible doses of 3-NT and EA (200 μM) for 72 h, and subsequently analyzed by flow cytometry analyses, oxidative stress and high-resolution mass-spectrometry-based proteomics using a Q-Exactive Orbitrap MS/MS.

2. Materials and Methods

2.1. Cells and Chemicals

Human colon adenocarcinoma CACO-2 cell line was purchased from ECACC (European Collection of Authenticated Cell Cultures, Salisbury, UK). 3-NT (CAS Number 621-44-3) and EA (CAS Number 476-66-4) were acquired from Sigma-Aldrich (Sigma-Aldrich, Steinheim, Germany). The other reagents were obtained from Panreac (Panreac Química, S. A., Barcelona, Spain), Sigma-Aldrich (Sigma-Aldrich, Steinheim, Germany) and Fisher (Fisher Scientific S.L., Madrid, Spain). Water used was purified by passage through a Milli-Q system (Millipore Corp., Bedford, MA, USA).

2.2. Cell Culture

Passages between 40 and 46 of human colon adenocarcinoma CACO-2 cell line were used. Cells were cultured in T-75 flasks at 37 ºC in a humidified incubator 95% air/5% CO_2 in Eagle's Minimum Essential Medium (EMEM) supplemented with fetal bovine serum (FBS) (10% *v/v*), non-essential amino acids (1% *v/v*) and L-glutamine (1% *v/v*). Cells were allowed to differentiate into enterocytes for 21 days upon reaching 90% confluence. Finally, cells were collected using a combination of 0.25% trypsin and 1 mM EDTA.

2.3. Experimental Setting

Both 3-NT and EA were dissolved in 10 mL of the culture medium (supplemented EMEM) at a final concentration of 200 μM in. The concentration of 3-NT used in the present study is within the range found in processed foods and food digests [5,10]. The same concentration of EA was used to study the possible protective effect at equivalent concentration. 3-NT and 3-NT+EA were then added and exposed to differentiated CACO-2 cells in T-75 flasks at 37 °C in a humidified incubator 95%air/5%CO_2. For comparative purposes, CONTROL cells were incubated under equivalent conditions in standard EMEM.

The entire assay was repeated five times (true replicates) in independent flasks for 3-NT, 3-NT+EA and CONTROL cells. After 72 h, cells were harvested using 0.25% trypsin in 1 mM EDTA, centrifuged for 5 min at 126 g and suspended in 1 mL of phosphate-buffered saline (PBS) solution for further analysis. The sampling time was chosen in accordance with previous preliminary studies, aiming to set condition parameters to guarantee a clear visualization of proteome changes in response to exposure to the chemical species under study.

2.4. Flow Cytometry Analyses

Flow cytometry analyses were conducted using a Cytoflex®LX flow cytometer (Beckman Coulter, Brea, CA, USA) equipped with red, blue, violet, ultraviolet, yellow and infrared lasers. The instrument was calibrated daily using specific calibration beads provided by the manufacturer. A compensation overlap was performed before each experiment. Files were exported as FCS files and analyzed using FlowJoV 10.4.1 Software (Ashland, OR, USA). Samples were diluted in PBS to a final concentration 5×10^6 cells/mL and stained with 1 µL of Hoechst 33,342 (16.2 mM stock solution), 1 µL of CellROX (2.5 mM stock solution) and 1 µL CellEvent Caspase-3/7 Green Detection Reagent (2 mM stock solution) to measure cell viability, ROS occurrence and apoptosis events, respectively. After thorough mixing, the cell suspension was incubated at room temperature for 20 min in the dark, then was loaded with 1 µL ethidium homodimer (1.167 mM in DMSO) and incubated for a further 10 min to measure necrosis events. Finally, the samples were filtered through MACS®smartStrainer 30 µm filters and immediately run on the flow cytometer. The controls consisted of unstained and single-stained controls to properly set gates and compensations.

2.5. Quantification of Protein Carbonyls

Both α-aminoadipic semialdehyde (α-AS) and γ-glutamic semialdehyde (γ-GS), two main protein carbonyls, were quantified in differentiated human enterocytes. The procedure reported by Utrera et al. [17] was replicated with slight changes described as follows. Briefly, 100 µL of the cell lysates were treated with 1 mL of cold 10% trichloroacetic acid (TCA) solution, and then proteins were precipitated with centrifugation at 2240× *g* for 5 min at 4 °C. The supernatant was removed, and the resulting pellet was treated with 1 mL of cold 5% TCA. Proteins were then precipitated by applying cold 5% TCA and centrifugation at 2240× *g* for 5 min. Protein-bound carbonyls were then derivatized with p-amino-benzoic acid (ABA) followed by a subsequent acid hydrolysis in 6M HCl and 110 °C for 18 h. The hydrolysates were evaporated at 40 °C in a vacuum concentrator, and the generated residues were reconstituted with 200 µL of Milli-Q water and then filtered through hydrophilic polypropylene GH Polypro (GHP) syringe filters (0.45 µm pore size, Pall Corporation, NJ, USA) for HPLC analysis. Details on the chromatography apparatus, as well as on the separation, elution and identification of the compounds of interest, were published in Utrera et al. [17]. Standard α-AS-ABA and γ-GS-ABA were synthesized according to the protocol described by Akagawa et al. [18]. Identification of α-AS and γ-GS in samples was carried out by comparing their retention times with those of the synthesized standard compounds. A standard curve of ABA was prepared by injecting increasing known concentrations of this fluorescent species (0.1 to 0.5 mM). The peaks corresponding to both α-AS-ABA and γ-GS-ABA were manually integrated and the resulting areas plotted against the ABA standard curve. Results are expressed as nmol of protein carbonyl per mg of protein.

2.6. Endogenous Antioxidant Enzymes

The activity of two endogenous antioxidant enzymes, namely, catalase (CAT) and superoxide dismutase (SOD), was determined by spectrophotometric methods. One unit (U) of catalase was defined as the amount of protein from cell lysate needed to decompose

1 mmol of H_2O_2 per min. One unit of SOD was defined as the amount of protein from cell lysate required to inhibit pyrogallol autoxidation by 50%.

2.7. Sample Preparation for LC-MS/MS Based Proteomics

The procedure carried out for the preparation of tryptic peptides from cultured cells has already been described by Díaz-Velasco et al. [15]. Samples were treated with 0.5 mL of lysis buffer pH 7.5 (100 mM Tris-HCl, 50 mM NaCl, 10% glycerol, 0.5 M EDTA pH 8.5) containing 100 mM PMSF (Phenylmethansulfonylfluorid) and 100 µg/mL Pepstatin in a 1:100 proportion. Samples were stirred and sonicated (Branson Ultrasonics, Danbury, CT, USA). Lysates were incubated on ice for 1 h and centrifuged at 9032× *g* for 10 min at 4 °C. Supernatants were analyzed for protein concentration. Aliquots containing 50 µg of proteins were partially run in SDS-PAGE (4% stacking and 12% separating). Runs were stopped as soon as samples reached the separating part of the gel to be digested in-gel. The gel was stained with Coomassie blue R250 and each lane was cut into 1 mm^3 pieces and subjected to in-gel digestion. Samples were incubated with 0.5 M DTT in 50 mM ammonium bicarbonate for 20 min at 56 °C for protein reduction. The resulting free thiol (-SH) groups were alkylated by incubating the samples with 0.55 M iodoacetamide in 50 mM ammonium bicarbonate for 15 min in the dark at room temperature (22 °C). Afterwards, samples were treated with 50 mM ammonium bicarbonate, ProteaseMAX (Promega, Madison, WI, USA) and trypsin (Promega, USA) and incubated for 2 h at 37 °C. The proteolysis was stopped by adding formic acid. Supernatants were dried in vacuo and subsequently reconstituted with loading buffer (98% milli-Q water, 2% acetonitrile and 0.05% trifluoroacetic acid).

2.8. Label-Free Quantitative Proteomic Analyses

A Q-Exactive Plus mass spectrometer coupled to a Dionex Ultimate 3000 RSLCnano (Thermo Scientific, Waltham, MA, USA) analyzed 5 µg from each digest. Data was collected using a Top15 method for MS/MS scans following the procedure described by Delgado et al. [19], with some modifications as described in [15]. Comparative proteome abundance and data analysis were conducted using MaxQuant software (version 1.6.0.15.0) and Perseus (v 1.6.14.0) to organize the data and perform statistical analysis. Carbamidomethylation of cysteines was set as a fixed modification; oxidation of methionines and acetylation of N-terminals were set as variable modifications. Database searching was carried out against Homo sapiens UNIPROT protein database. The maximum peptide/protein false discovery rates (FDR) were set to 1% based on comparison to a reverse database. The MaxLFQ algorithm was used to generate normalized spectral intensities and infer relative protein abundance. Proteins were only retained in final analysis if they were detected in at least two replicates from at least one treatment, and the proteins that matched to a contaminant database or the reverse database were removed. Quantitative analysis was performed using a T-test to compare treatments with the control. Fold change (FC) is expressed as Log_2. This refers to the degree of quantity change for a particular protein between cells (control vs. treatment). If FC is <1, the change denotes a decrease in the concentration of protein in treated samples (vs. control) while fold change >1 indicates a significant increase in the concentration of that protein in the treated sample (vs. control). When a given protein is only present in one of the groups, fold change cannot be measured and such condition is denoted in tables as "C" (if protein is only present in C, in other words, exposure to whatever treatment leads to a complete depletion of the protein) or 3-NT (if protein is only present in 3-NT-exposed cells) or 3-NT+EA (if protein is only present in cells exposed to the combination of both species). A qualitative analysis was also performed to detect proteins that were found in at least three replicates of a given group of samples (i.e., treated) and were undetectable in the counterpart group (i.e., control). Proteins satisfying one of these two aforementioned criteria were identified as discriminating proteins, and their corresponding genes were grouped by biological processes and molecular functions using ClueGO (v. 2.5.6) [20]. To define term–term inter-relations and functional groups based on shared genes between the terms, the Kappa score was established at 0.4. Three GO terms

and 4% of genes covered were set as the minimum required to be retained in the final result. The *p*-value was corrected by Bonferroni step down and set as $p < 0.05$.

2.9. Statistical Analysis

All experiments were carried out five times and each individual sample was measured twice for flow cytometry. Data was analyzed for normality and homoscedasticity, and the effect of the exposure to 3-NT and 3-NT+EA was evaluated by Analysis of Variance (ANOVA). Tukey's test was used for multiple comparisons of the means. The effect of the incubation time on the same measurements was assessed by Student's t-test. SPSS (version 15.0) was used for statistical analysis of the data and the significance level was set at $p < 0.05$.

3. Results

3.1. Flow Cytometry and Protein Oxidation Markers

In this study, the parameters analyzed by flow cytometry were cell viability, ROS occurrence, apoptosis and necrosis. The results showed a significant decrease in the percentage of live cells among differentiated human enterocytes exposed to 3-NT compared to control cells ($p < 0.05$) (Figure 1A). The decreased viability of cells exposed to 3-NT was manifested in a significant increase of necrotic events ($p < 0.05$) (Figure 1A). Cells exposed to 3-NT showed a significant decrease in ROS occurrence ($p < 0.05$) (Figure 1B) and no significant effect was observed in the percentage of live cells for caspase-3-mediated apoptotic events (Figure 1A) as compared to control counterparts. Cells exposed to the combination of 3-NT+EA showed a significant decrease in the percentage of live cells ($p < 0.05$) (Figure 1C), a significant reduction in the percentage of live cells of apoptotic events ($p < 0.01$) and a significant and remarkable increase in necrotic events ($p < 0.01$), as compared to cells exposed only to 3-NT. No significant differences were found in ROS occurrence between non-treated cells and 3-NT+EA (Figure 1D). To elucidate whether the effects observed in the 3-NT+EA group were a result of the occurrence of EA or the interaction between both species, an additional assay was performed to assess the impact of EA alone. This phytochemical showed a mild (non-significant) positive effect on human enterocytes as compared with a control group, with a clear trend to an increased viability and decreased apoptotic and necrotic events (Figure 1E–G).

The analysis of protein oxidation markers α-AS and γ-GS was assessed by the detection of early (specific protein carbonyls, α-AS and γ-GS) and advanced oxidation protein products (AOPPs) (Figure 2). The results show that the exposure to 3-NT led to a significant accretion of protein carbonyls in enterocytes, while this increase was not significant for AOPPs. The addition of EA to 3-NT-treated cells caused another significant and highly remarkable increase in protein carbonyls and AOPPs as compared to both Control and 3-NT counterparts.

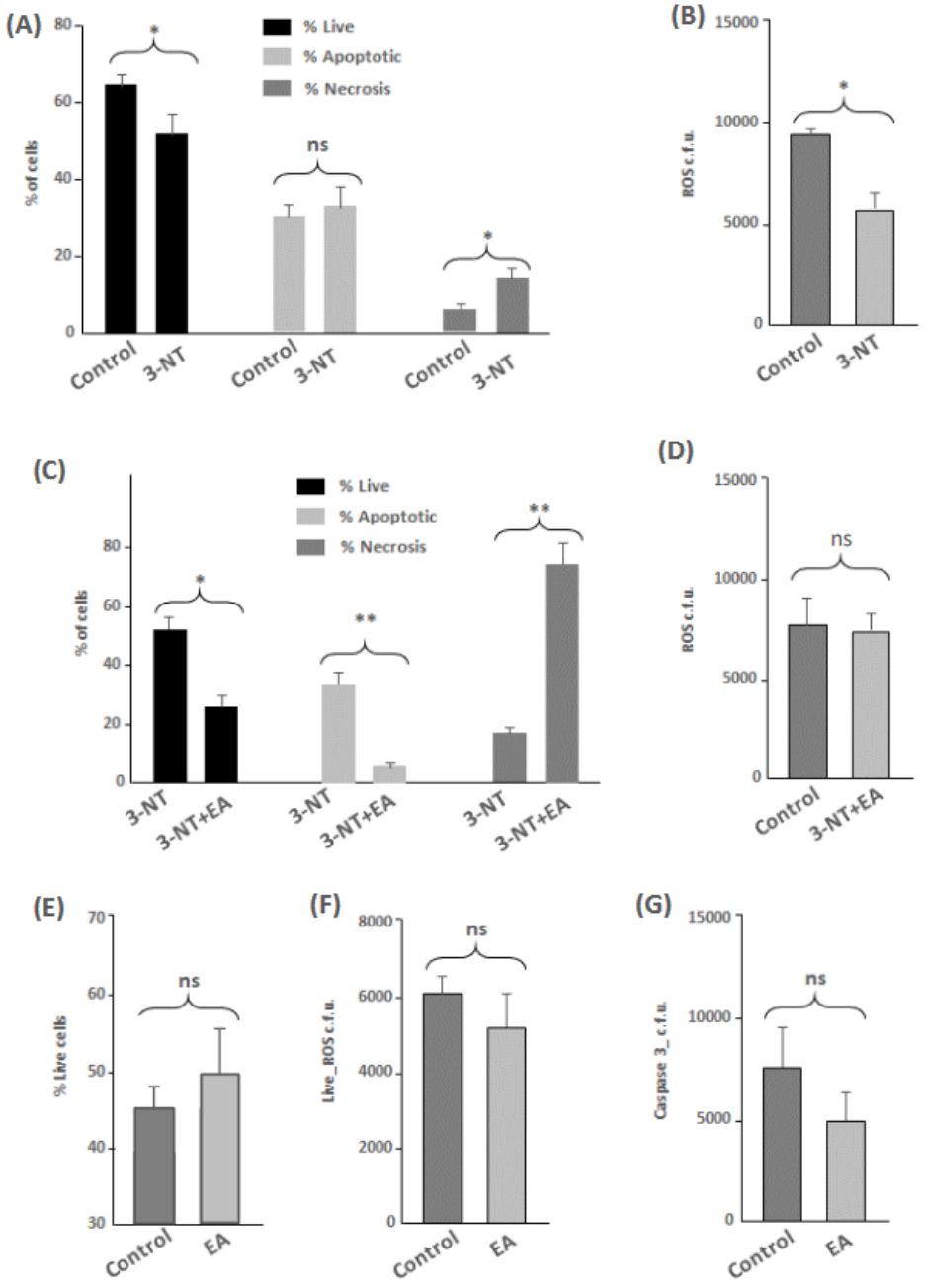

Figure 1. Percentages of live cells (Hoechst +), apoptotic cells (Caspase 3+) and necrotic cells (Ethidium homodimer +) on human enterocytes as affected by exposure to 200 μM 3-NT for 72 h compared to control counterparts (**A**). Relative fluorescence units (r.f.u.) of ROS occurrence (Cell Rox +) on human enterocytes as affected by exposure to 200 μM 3-NT for 72 h compared to control counterparts (**B**). Percentages of live cells (Hoechst +), apoptotic cells (Caspase 3+) and necrotic cells (Ethidium homodimer +) on differentiated human enterocytes as affected by exposure to 200 μM 3-NT+ 200 μM EA for 72 h compared to 200 μM 3-NT treated cells (**C**). Relative fluorescence units (r.f.u.) of ROS occurrence (Cell Rox +) on human enterocytes as affected by exposure to 200 μM 3-NT+ 200 μM EA for 72 h compared to control counterparts (**D**). Percentages of live cells (Hoechst +) (**E**), relative fluorescence units (r.f.u.) of ROS occurrence (Cell Rox +) (F) and relative fluorescence units (r.f.u.) of apoptotic events (Caspase 3+) (**G**) on human enterocytes as affected by exposure to 200 μM EA for 72 h compared to control counterparts. Results are expressed as means ± standard deviations. Asterisk on top of bars denote significant differences (* $p < 0.05$; ** $p < 0.01$) between paired group of samples (control vs. 3-NT; 3-NT vs. 3-NT). Ns: no significant differences.

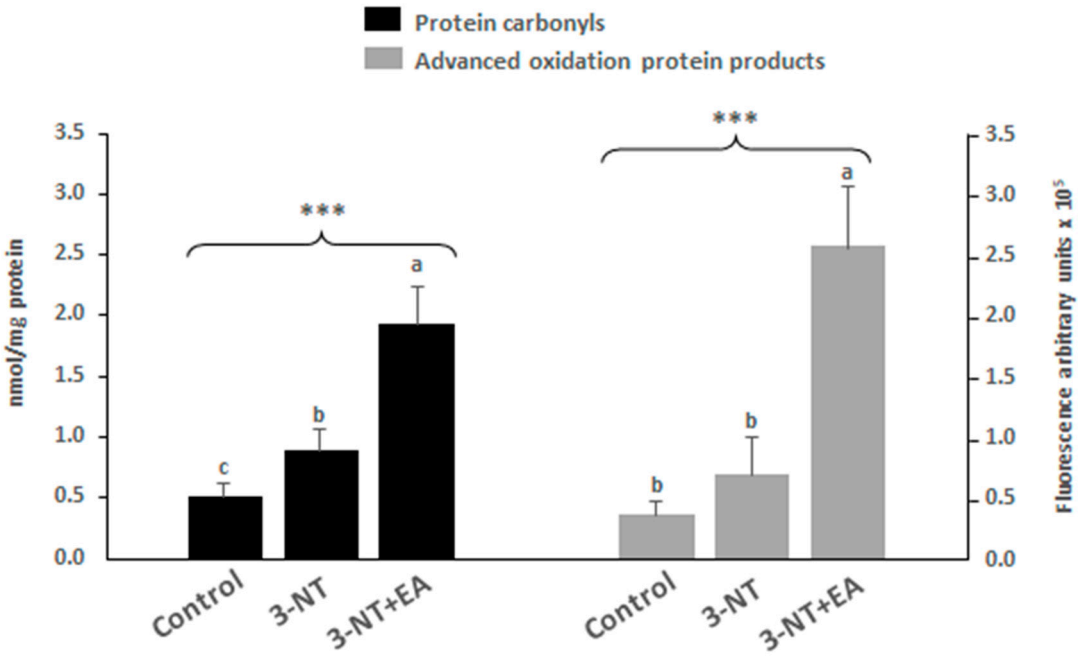

Figure 2. Protein carbonyls (nmol/mg protein of α-AS and γ-GS) (black bars) and advanced oxidation protein products (Pentosidine; fluorescence intensity) (grey bars) on differentiated human enterocytes upon exposure to 200 μM 3-NT and 200 μM 3-NT+200 μM EA for 72 h. Asterisks on top of bars denote significant differences between group of samples in ANOVA (*** $p < 0.001$). (a–c) Different letters on top of bars denote significant differences between means in post-hoc Tukey tests ($p < 0.05$).

3.2. Proteomic Analyses

The MS-based proteomic platform enabled the identification of 2398 proteins in total. All these proteins were identified with at least two peptides and a FDR <1%. Quantitative ($p < 0.05$) and qualitative (only detected in one condition) changes in protein abundance were studied (Tables S1 and S2). To analyze the possible harmful effects of 3-NT, a first comparison was made between the proteomes from non-treated control cells versus 3-NT-treated cells. In this case, 150 proteins were significantly influenced by 3-NT, with 56 among those being found in lower abundance in cells treated with 3-NT, and 15 being only found in non-treated control samples. On the other hand, 63 proteins were detected in higher quantity in cells exposed to 3-NT and 16 were only found in 3-NT-treated cells. To study the hypothetical protective role of EA against 3-NT, an additional comparison was made between the proteomes from 3-NT-treated cells versus 3-NT+EA-treated cells. In this case, 1214 proteins were significantly influenced by 3-NT+EA; among those, 481 were detected in lower abundance in cells exposed to 3-NT+EA, 365 were found in higher quantity in 3-NT+EA treated cells, 23 were only detected in the presence of 3-NT+EA and 345 were only found in 3-NT treated cells. For a systematized and comprehensible description and discussion of results, discriminating proteins were grouped by biological processes and molecular functions. The comparison between non-treated control cells versus 3-NT-treated cells (possible harmful effect of 3-NT) is shown in Graphs SG1A-SG1D in the Supplementary Material. The comparison between 3-NT-treated cells versus 3-NT+EA-treated cells (3-NT vs. hypothetical protective role of EA) is shown in Graphs SG2A-SG2D in the Supplementary Material. Specific terms for each of these processes and full details of discriminating proteins and associated genes are provided in Supplementary Material Tables S3–S10. Tables 1 and 2 show a selection of representative proteins from each relevant biological process and molecular function affected by the presence of 3-NT and 3-NT+EA. Only discriminating proteins having a defined biological significance are presented in the following sections.

Table 1. Proteins from differentiated human enterocytes affected by the exposure to 200 μM 3-nitrotyrosine for 72 h in comparison to the non-treated control (C).

Protein Name	Gene Name	*p*-Value	Fold-Change [1]	Biological Function	FASTA Accession Number
Rho-associated protein kinase 2	*ROCK2*	-	C	Involved in blebs formation	O75116
STAM-binding protein	*STAMBP*	-	C	Associated with intracellular accumulation of ubiquitinated protein	O95630
3 beta-hydroxysteroid dehydrogenase/Delta 5–>4-isomerase type 1	*HSD3B1*	-	C	Oxidation and isomerization in the biosynthesis of hormonal steroids	P14060
3 beta-hydroxysteroid dehydrogenase/Delta 5–>4-isomerase type 2	*HSD3B2*	-	C	Oxidation and isomerization in the biosynthesis of hormonal steroids	P26439
Glycogen synthase kinase-3 beta	*GSK3B*	-	C	Protein tau phosphorylation	P49841
Arf-GAP with Rho-GAP domain, ANK repeat and PH domain-containing protein 1	*ARAP1*	-	C	Reorganization of actin cytoskeleton	Q96P48
DNA-directed RNA polymerase II subunit RPB1	*POLR2A*	-	C	Transcription of DNA into RNA	P24928
Exocyst complex component 5	*EXOC5*	-	C	Involved in exocytosis	O00471
Alcohol dehydrogenase 4	*ADH4*	-	C	Oxidoreductase activity	A0A0D9SFB5
Developmentally regulated GTP-binding protein 2	*DRG2*	-	C	Maintenance of cell structure and protein trafficking	P55039
STAM-binding protein	*STAMBP*	-	C	Signal transduction for cell growth	O95630
Cirhin	*CIRH1A*	-	C	Pre-ribosomal RNA transcription	L0R599
F-actin-capping protein subunit beta	*CAPZB*	-	C	Cytoskeletal organization	P47756
Coronin-2A	*CORO2A*	-	C	Actin filament binding	Q92828
U6 snRNA-associated Sm-like protein LSm2	*LSM2*	-	C	Involved in RNA-binding proteins	Q9Y333
Cytoplasmic dynein 1 heavy chain 1	*DYNC1H1*	0.044	0.53	Motility of vesicles through microtubules	Q14204
Delta (24)-sterol reductase	*DHCR24*	0.037	0.55	Protection against oxidative stress and apoptosis	Q15392
Interferon regulatory factor 3	*IRF3*	0.020	0.63	Related to immunity	Q14653
Myosin-10	*MYH14*	0.036	0.68	Cytoskeleton reorganization	P35580
Lipopolysaccharide-responsive and beige-like anchor protein	*LRBA*	0.026	0.70	Vesicle trafficking of immune effector	P50851
AP-1 complex subunit sigma-1A	*AP1S1*	0.002	0.71	Related to clathrin	P61966
DNA-directed RNA polymerase II subunit RPB2	*POLR2B*	0.008	0.71	Component of RNA polymerase II	P30876
Histone H2B tipo 1-L	*H2BC13*	0.048	0.73	Histone related to nucleosome	Q99880
Histone H2B type 1-M	*H2BC14*	0.048	0.73	Histone related to nucleosome	Q99879
Histone H2B type 1-N	*H2BC15*	0.048	0.73	Histone related to nucleosome	Q99877
Histone H2B type 2-F	*H2BC18*	0.048	0.73	Histone related to nucleosome	Q5QNW6
Histone H2B type 1-D	*H2BC5*	0.048	0.73	Histone related to nucleosome	P58876
Histone H2B type 1-H	*H2BC9*	0.048	0.73	Histone related to nucleosome	Q93079
D-dopachrome decarboxylase	*DDT*	0.024	0.74	Tautomerization of D-dopachrome	P30046
D-dopachrome decarboxylase-like protein	*DDTL*	0.024	0.74	Lyase activity	A6NHG4
Eukaryotic translation initiation factor 3 subunit D	*EIF3D*	0.022	0.75	Early steps of protein synthesis	O15371
Sorting nexin-9	*SNX9*	0.009	0.75	Intracellular vesicle trafficking	O75116
SWI/SNF-related matrix-associated actin-dependent regulator of chromatin subfamily A member 5	*SMARCA5*	0.049	0.78	Helicase involved in nucleosome-remodeling activity	O60264
Ribosome-binding protein 1	*RRBP1*	0.017	0.78	Mediates interaction between ribosome and endoplasmic reticulum membrane	Q9P2E9
Coatomer subunit alpha	*COPA*	0.026	0.79	Formation of blebs in Golgi apparatus	P53621

Table 1. *Cont.*

Protein Name	Gene Name	*p*-Value	Fold-Change [1]	Biological Function	FASTA Accession Number
Dynactin subunit 1	*DCTN1*	0.046	0.82	Cofactor involved in microtubule motor cytoplasmic dynein	Q14203
Eukaryotic translation initiation factor 2 subunit 3	*EIF2S3*	0.045	0.86	Early steps of protein synthesis	P41091
Eukaryotic translation initiation factor 2 subunit 3B	*EIF2S3B*	0.045	0.86	Early steps of protein synthesis	Q2VIR3
Beta-centractin	*ACTR1B*	0.026	0.87	Motility of vesicles through microtubules	P42025
Leukocyte elastase inhibitor	*SERPINB1*	0.037	0.87	Inflammatory caspase activation	P30740
Thioredoxin reductase 1, cytoplasmic	*TXNRD1*	0.032	1.15	Regulation of cellular redox and reductase activity on H_2O_2	Q16881
Calmodulin-1; Calmodulin-2; Calmodulin-3	*CALM1, CALM2, CALM3*	0.009	1.29	Involved in nitric oxide synthase regulator activity, adenylate cyclase activator activity and positive, negative regulation of ryanodine-sensitive calcium-release channel activity, type 3 metabotropic glutamate receptor binding and N-terminal myristoylation domain binding	P0DP23; P0DP24; P0DP25
Mitochondrial glutamate carrier 1	*SLC25A22*	0.002	1.30	Mitochondrial carrier of glutamate	E9PJH7
60S ribosomal protein L11	*RPL11*	0.033	1.57	Component of the ribosome	P62913
Cadherin-17	*CDH17*	0.009	1.71	Calcium-dependent cell adhesion protein involved in intestinal peptide transport	Q12864
Tumor susceptibility gene 101 protein	*TSG101*	0.045	2.00	Regulator of vesicular trafficking process	Q99816
Serine/arginine repetitive matrix protein 1	*SRRM1*	0.042	2.13	Involved in numerous pre-mRNA processing elvents, part of pre- and post-splicing	Q8IYB3
Neutral amino acid transporter B (0)	*SLC1A5*	0.005	2.22	Sodium-dependent amino acids transporter including glutamine	Q15758
U1 small nuclear ribonucleoprotein C	*SNRPC*	-	3-NT	Component of the spliceosome	P09234
CD2 antigen cytoplasmic tail-binding protein 2	*CD2BP2*	-	3-NT	Involved in pre-mRNA splicing	O95400
Carcinoembryonic antigen-related cell adhesion molecule 1	*CEACAM1*	-	3-NT	Coinhibitory receptor in immune response	P13688
La-related protein 4B	*LARP4B*	-	3-NT	mRNA translation	Q92615
Lipid droplet regulating VLDL assembly factor AUP1	*AUP1*	-	3-NT	Translocation of misfolded proteins and degradation by the proteasome	Q9Y679
Non-homologous end-joining factor 1	*NHEJ1*	-	3-NT	DNA repair	Q9H9Q4
DNA-directed RNA polymerase II subunit RPB3	*POLR2C*	-	3-NT	Transcription of DNA into RNA	P19387

[1] Fold change (FC) indicates the degree of quantity change for a particular protein between cells (control vs. 3-NT); FC <1 denotes a decrease in the concentration of protein in the treated sample (vs. control); FC >1 indicates a significant increase in the concentration of the protein in treated sample (vs. control). When a given protein is only present in one of the groups, fold change cannot be measured and such condition is denoted as "C" (if protein is only present in C cells) or 3-NT (if protein is only present in 3-NT-exposed cells). 3-NT3-NT.

Table 2. Proteins from differentiated human enterocytes affected by the exposure to 200 μM 3-nitrotyrosine + 200 μM ellagic acid for 72 h in comparison to those exposed to 200 μM 3-nitrotyrosine for 72 h.

Protein Name	Gene Name	p-Value	Fold Change [1]	Biological Function	FASTA Accession Number
Translation initiation factor eIF-2B subunit alpha	*EIF2B1*	-	3-NT	Catalyzes the exchange of eukaryotic initiation factor 2-bound GDP for GTP	Q14232
Eukaryotic translation initiation factor 2 subunit 2	*EIF2S2*	-	3-NT	Involved in the early steps of protein synthesis along with GTP and tRNA	P20042
La-related protein 1	*LARP1*	-	3-NT	RNA-binding protein	Q6PKG0
ATP synthase subunit delta, mitochondrial	*ATP5F1D*	-	3-NT	Component of mitochondrial membrane ATP synthase	P30049

Table 2. *Cont.*

Protein Name	Gene Name	p-Value	Fold Change [1]	Biological Function	FASTA Accession Number
MICOS complex subunit MIC13	*MICOS13*	-	3-NT	Component of the MICOS complex, formation and maintenance of mitochondrial cristae	Q5XKP0
Mitochondrial inner membrane protein OXA1L	*OXA1L*	-	3-NT	Insertion of integral membrane proteins into the mitochondrial inner membrane	Q15070
ATP-binding cassette sub-family B member 10, mitochondrial	*ABCB10*	-	3-NT	Exporting from the mitochondrial matrix to the cytosol in an ATP-dependent manner	Q9NRK6
Ribosome-releasing factor 2, mitochondrial	*GFM2*	-	3-NT	Mitochondrial GTPase involved in mitochondrial protein biosynthesis	Q969S9
Phosphatidylinositol-binding clathrin assembly protein	*PICALM*	-	3-NT	Cytoplasmic adapter protein related to clathrin-mediated endocytosis	Q13492
Plasma membrane calcium-transporting ATPase 4	*ATP2B4*	-	3-NT	Calcium/calmodulin-regulated enzyme, catalyzes hydrolysis of ATP coupled with transport of calcium out of the cell	P23634
Epidermal growth factor receptor	*EGFR*	-	3-NT	Receptor tyrosine kinase binding	P00533
MICOS complex subunit MIC19	*CHCHD3*	1.41×10^{-5}	0.07	Component of the MICOS complex, maintenance of mitochondrial crista junctions	Q9NX63
Histone H1.4	*H1-4*	1.00×10^{-4}	0.08	Nucleosome assembly	P10412
ATP synthase subunit alpha, mitochondrial	*ATP5F1A*	0.010	0.17	Component of mitochondrial membrane ATP synthase	P25705
60S ribosomal protein L13	*RPL13*	0.011	0.22	Component of the ribosome	P26373
Dynamin-2	*DNM2*	0.014	0.26	Microtubule-associated protein, able to bind and hydrolyze GTP	P50570
60S ribosomal protein L23a	*RPL23A*	1.80×10^{-3}	0.26	Component of the ribosome	P62750
60S ribosomal protein L12	*RPL12*	1.86×10^{-6}	0.27	Component of the ribosome	P30050
ATP synthase subunit beta, mitochondrial	*ATP5F1B*	0.026	0.31	Component of mitochondrial membrane ATP synthase	P06576
40S ribosomal protein S7	*RPS7*	0.003	0.33	Component of the ribosome	P62081
DnaJ homolog subfamily C member 11	*DNAJC11*	0.004	0.33	Component of the MICOS complex, mitochondrial inner membrane organization	Q9NVH1
Dynamin-like 120 kDa protein, mitochondrial	*OPA1*	4.21×10^{-5}	0.34	Regulates the equilibrium between mitochondrial fusion and mitochondrial fission	O60313
Stomatin-like protein 2, mitochondrial	*STOML2*	2.00×10^{-4}	0.38	Mitochondrial protein involved in the activity of mitochondria	Q9UJZ1
Adenylate kinase 4, mitochondrial	*AK4*	3.07×10^{-6}	0.38	Interconversion of nucleoside phosphates	P27144
EF-hand domain-containing protein 1, mitochondrial	*LETM1*	1.60×10^{-4}	0.40	Mitochondrial proton/calcium antiporter, assembly of the supercomplexes of the respiratory chain	O95202
Monocarboxylate transporter 1	*SLC16A1*	9.00×10^{-4}	0.41	Proton-coupled monocarboxylate transporter	P53985
ATP synthase subunit O, mitochondrial	*ATP5PO*	2.39×10^{-5}	0.42	Component of mitochondrial membrane ATP synthase	P48047
Eukaryotic initiation factor 4A-II	*EIF4A2*	9.13×10^{-5}	0.43	Required for mRNA binding to ribosome	Q14240
Eukaryotic translation initiation factor 4E	*EIF4E*	0.026	0.46	Involved in protein synthesis and ribosome binding	P06730
ATP synthase subunit d, mitochondrial	*ATP5PD*	5.35×10^{-5}	0.46	Component of mitochondrial membrane ATP synthase	O75947
MICOS complex subunit MIC60	*IMMT*	4.74×10^{-6}	0.47	Component of the MICOS complex, maintenance of mitochondrial cristae morphology	Q16891
60S ribosomal protein L11	*RPL11*	0.035	0.49	Component of the ribosome	P62913

Table 2. *Cont.*

Protein Name	Gene Name	p-Value	Fold Change [1]	Biological Function	FASTA Accession Number
ATP synthase subunit gamma, mitochondrial	*ATP5F1C*	3.1×10^{-4}	0.50	Component of mitochondrial membrane ATP synthase	P36542
ATP synthase F (0) complex subunit B1, mitochondrial	*ATP5PB*	1.63×10^{-5}	0.50	Component of mitochondrial membrane ATP synthase	P24539
AFG3-like protein 2	*AFG3L2*	4.1×10^{-3}	0.50	Involved in the regulation of OPA1	Q9Y4W6
Sorting and assembly machinery component 50 homolog	*SAMM50*	0.003	0.60	Maintenance of the structure of mitochondrial cristae and the assembly of the mitochondrial respiratory chain complexes	Q9Y512
Cytochrome c oxidase subunit 5B, mitochondrial	*COX5B*	1.9×10^{-3}	0.61	Component of the cytochrome c oxidase	P10606
Calcium/calmodulin-dependent protein kinase type II subunit beta	*CAMK2B*	0.014	0.66	Calcium/calmodulin-dependent protein kinase	Q13554
Guanine nucleotide-binding protein G(s) subunit alpha isoforms XLas	GNAS	0.008	0.67	Transducer in pathways controlled by G protein-coupled receptors, activation of adenylate cyclase	Q5JWF2
Heat shock protein HSP 90-beta	*HSP90AB1*	3.13×10^{-6}	0.68	Chaperone involved in cell cycle control and signal transduction	P08238
Pyruvate kinase PKM	*PKM*	4.1×10^{-4}	0.7	Glycolytic enzyme generating ATP and translation regulator of endoplasmic reticulum-associated ribosomes	P14618
RNA-binding protein 4	*RBM4*	0.007	0.73	Splicing of pre-mRNA and translation regulation	Q9BWF3
Calmodulin-1; Calmodulin-2; Calmodulin-3	*CALM1; CALM2; CALM3*	0.022	0.73	Nucleotide binding, 3 metabotropic glutamate receptor binding, N-terminal myristoylation domain binding, adenylate cyclase activator activity and nitric oxide synthase regulator activity	P0DP23; P0DP24; P0DP25
Calcium-binding mitochondrial carrier protein Aralar2	*SLC25A13*	4.1×10^{-4}	0.74	Mitochondrial and calcium-binding carrier, exchange cytoplasmic glutamate with mitochondrial aspartate	Q9UJS0
Heat shock protein HSP 90-alpha	*HSP90AA1*	0.008	0.82	Chaperone involved in cell cycle control and signal transduction	P07900
Proteasome subunit alpha type 1	*PSMA1*	0.009	1.18	Component of proteasome complex involved in the proteolytic degradation of most intracellular proteins	P25786
Proteasome subunit beta type-5	*PSMB5*	0.002	1.19	Component of proteasome complex involved in the proteolytic degradation of most intracellular proteins	P28074
Protein disulfide-isomerase A4	*PDIA4*	0.017	1.21	Catalyzes the rearrangement of -S-S- bonds	P13667
Aldo-keto reductase family 1 member A1	*AKR1A1*	0.013	1.24	Catalyzes the NADPH-dependent reduction of carbonyl-containing compounds, detoxifying enzyme	P14550
Glutathione synthetase	*GSS*	0.039	1.25	Catalyzes the production of glutathione	P48637
Glutathione reductase, mitochondrial	*GSR*	0.007	1.25	Maintains high levels of reduced glutathione in the cytosol	P00390
Proteasome subunit beta type 4	*PSMB4*	0.015	1.32	Non-catalytic component of proteasome complex involved in the proteolytic degradation of most intracellular proteins	P28070
Glutaredoxin-related protein 5, mitochondrial	*GLRX5*	0.032	1.33	Involved in mitochondrial iron-sulfur cluster transfer	Q86SX6
Serine hydroxymethyltransferase, mitochondrial	*SHMT2*	0.003	1.34	Catalyzes the cleavage of serine to glycine	P34897
Aflatoxin B1 aldehyde reductase member 2	*AKR7A2*	0.002	1.35	NADPH-dependent aldehyde reductase activity	O43488
Proteasome subunit beta type 1	*PSMB1*	0.002	1.40	Non-catalytic component of proteasome complex involved in the proteolytic degradation of most intracellular proteins	P20618

Table 2. *Cont.*

Protein Name	Gene Name	p-Value	Fold Change [1]	Biological Function	FASTA Accession Number
3-hydroxyacyl-CoA dehydrogenase type-2	*HSD17B10*	0.007	1.42	Hydroxysteroid dehydrogenase activity in steroid hormones	Q99714
Thioredoxin-like protein 1	*TXNL1*	1.5×10^{-4}	1.44	Disulfide oxidoreductase activity	O43396
Replication protein A 70 kDa DNA-binding subunit	*RPA1*	1.4×10^{-4}	1.45	DNA replication and response to DNA damage	P27694
Sorbitol dehydrogenase	*SORD*	1.3×10^{-3}	1.46	Catalyzes the reversible NAD^+-dependent oxidation of sugar alcohols, a key enzyme in the polyol pathway	Q00796
Proteasome subunit beta type 3	*PSMB3*	0.008	1.55	Non-catalytic component of proteasome complex involved in the proteolytic degradation of most intracellular proteins	P49720
Proteasome subunit alpha type 6	*PSMA6*	9.00×10^{-4}	1.62	Component of proteasome complex involved in the proteolytic degradation of most intracellular proteins	P60900
Alpha-N-acetylgalactosaminidase	*NAGA*	0.004	1.64	Involved in the breakdown of glycolipids	P17050
Alcohol dehydrogenase class-3	*ADH5*	0.021	1.71	Catalyzes the oxidation of S-(hydroxymethyl) glutathione	P11766
Cathepsin B	*CTSB*	0.016	1.72	Catabolism of intracellular proteins	P07858
Thioredoxin	*TXN*	0.001	1.73	Involved in antioxidant reactions	P10599
Serine hydroxymethyltrans-ferase, cytosolic	*SHMT1*	2.3×10^{-4}	1.74	Interconversion of serine and glycine	P34896
Selenium-binding protein 1	*SELENBP1*	0.006	1.75	Catalyzes the oxidation of methanethiol	Q13228
Lysosomal Pro-X carboxypeptidase	*PRCP*	0.005	1.77	Cleavage of amino acids	P42785
Leukotriene A-4 hydrolase	*LTA4H*	6.06×10^{-5}	1.78	Aminopeptidase activity	P09960
Proteasome subunit beta type 2	*PSMB2*	0.008	1.79	Non-catalytic component of proteasome complex involved in the proteolytic degradation of most intracellular proteins	P49721
Succinate dehydrogenase [ubiquinone] iron–sulfur subunit, mitochondrial	*SDHB*	1.7×10^{-3}	1.87	Iron–sulfur protein subunit of succinate dehydrogenase, involved in complex II of the mitochondrial electron transport chain	P21912
N-acetylated-alpha-linked acidic dipeptidase 2	*NAALAD2*	0.022	1.87	Dipeptidase activity	Q9Y3Q0
Aspartyl aminopeptidase	*DNPEP*	6.67×10^{-6}	1.98	Protein metabolism	Q9ULA0
Replication protein A 14 kDa subunit	*RPA3*	0.003	2.02	Controls DNA repair and DNA damage checkpoint activation	P35244
Ubiquitin-40S ribosomal protein S27a	*RPS27A*	0.002	2.02	Postreplication repair	P62979
Ubiquitin-60S ribosomal protein L40	*UBA52*	0.002	2.02	Postreplication repair	P62987
Polyubiquitin-B	*UBB*	0.002	2.02	Postreplication repair	P0CG47
Polyubiquitin-C	*UBC*	0.002	2.02	Postreplication repair	P0CG48
Fatty aldehyde dehydrogenase	*ALDH3A2*	2.96×10^{-5}	2.08	Catalyzes the oxidation of aliphatic aldehydes to fatty acids	P51648
Thioredoxin domain-containing protein 17	*TXNDC17*	3.91×10^{-6}	2.19	Disulfide reductase with peroxidase activity	Q9BRA2
Glycine dehydrogenase (decarboxylating), mitochondrial	*GLDC*	2.17×10^{-5}	2.23	Catalyzes the degradation of glycine	P23378
Delta-1-pyrroline-5-carboxylate dehydrogenase, mitochondrial	*ALDH4A1*	0.009	2.42	Involved in the interconnexion between the urea and tricarboxylic acid cycles	P30038
Catalase	*CAT*	5.92×10^{-6}	2.66	Protection against oxidative stress	P04040
Proliferating cell nuclear antigen	*PCNA*	0.002	2.86	DNA replication and DNA repair	P12004
Tissue alpha-L-fucosidase	*FUCA1*	0.001	2.86	Related to glycoside metabolic process	P04066

Table 2. *Cont.*

Protein Name	Gene Name	p-Value	Fold Change [1]	Biological Function	FASTA Accession Number
Aldo-keto reductase family 1 member C3	*AKR1C3*	2.83×10^{-5}	3.21	Oxidoreductase activity	P42330
Dipeptidyl peptidase 2	*DPP7*	1.24×10^{-6}	3.40	Degradation of tripeptides	Q9UHL4
DNA ligase 3	*LIG3*	-	3-NT+EA	Correct defective DNA strand-break repair	P49916
Alcohol dehydrogenase 4	*ADH4*	-	3-NT+EA	Oxidoreductase activity	P08319
DNA-directed RNA polymerase II subunit RPB1	*POLR2A*	-	3-NT+EA	Transcription of DNA into RNA	P24928
Glutathione S-transferase Mu 3	*GSTM3*	-	3-NT+EA	Detoxification of endogenous compounds	P21266
Alcohol dehydrogenase 4	*ADH4*	-	3-NT+EA	Oxidoreductase activity, acting on the CH-OH group of donors, NAD or NADP as acceptor	A0A0D9SFB5

[1] Fold change (FC) indicates the degree of quantity change for a particular protein between cells (3-NT vs. 3-NT+EA). FC <1 denotes a decrease in the concentration of protein; FC >1 indicates a significant increase in the concentration of the protein. When a given protein is only present in one of the groups, fold change cannot be measured, and such condition is denoted as "3-NT" (if protein is only present in 3-NT-exposed cells) or 3-NT+EA (if protein is only present in cells exposed to both chemical species). 3-NT3-NT3-NT3-NT.

3.2.1. Proteins Found in Lower Relative Quantity in Cells Exposed to 3-NT Compared to Control Counterparts

Antigen Processing and Presentation of Exogenous Peptide Antigen via MHC Class II

Among all biological processes affected by the exposure of 3-NT, the proteins implicated in the antigen processing and presentation of exogenous peptide antigen via MHC class II (SG. 1A) were particularly targeted (63.64%, $p < 0.01$). The proteins involved in this process (Supplementary Table S3) were beta-centractin (ACTR1B; fold change: 0.87), AP-1 complex subunit sigma-1A (AP1S1, fold change: 0.71), cytoplasmic dynein 1 heavy chain 1 (DYNC1H1; fold change: 0.53), myosin-10 (MYH10; fold change: 0.68) and F-actin-capping protein subunit beta (CAPZB, only in control) (Tables 1 and S1–S3).

Cytoplasmic Translational Initiation

The exposure of 3-NT caused a significant decrease (18.18%, $p < 0.01$) (SG. 1A) in proteins involved in the cytoplasmic translational initiation. Namely, eukaryotic translation initiation factor 2 subunit 3 (EIF2S3; fold change: 0.86), eukaryotic translation initiation factor 2 subunit 3B (EIF2S3B; fold change: 0.86) and eukaryotic translation initiation factor 3 subunit D (EIF3D; fold change: 0.75) were particularly affected by 3-NT exposure (Tables 1 and S1–S3).

Nucleosome Assembly

Other biological processes affected by the exposure of 3-NT (9.09%, $p < 0.01$) (SG. 1A) were related to the nucleosome assembly. The histones H2B type 1-L (H2BC13), H2B type 1-M (H2BC14), H2B type 1-N (H2BC15), H2B type 2-F (H2BC18), H2B type 1-D (H2BC5) and H2B type 1-H (H2BC9), all with a fold change of 0.73, were found in lower quantities in 3-NT-treated cells as compared to the control counterparts. The member 5 of subfamily A of SWI/SNF-related matrix-associated actin-dependent regulator of chromatin (SMARCA5, fold change: 0.78) also appeared in this process in a lower amount along with the aforementioned histones (Tables 1 and S1–S3).

Mitotic Cytokinesis

Mitotic cytokinesis was also affected by 3-NT exposure (9.09%, $p < 0.01$) (SG. 1A). Related proteins found in lower quantities in 3-NT cells compared to control cells were MYH10, Rho-associated protein kinase 2 (ROCK2, only in control), sorting nexin-9 (SNX9, fold change 0.75) and the STAM-binding protein (STAMBP; only in control) (Tables 1 and S1–S3).

Intramolecular Oxidoreductase Activity, Transposing C=C bonds

Within molecular functions, the most affected process by the exposure of 3-NT was the intramolecular oxidoreductase activity, transposing C=C bonds (50.0%, $p < 0.01$) (SG. 1B). Among the most affected proteins, we identified the D-dopachrome decarboxylase (DDT; fold change: 0.74), D-dopachrome decarboxylase-like protein (DDTL; fold change: 0.74), 3 beta-hydroxysteroid dehydrogenase/Delta 5→4-isomerase type 1 (HSD3B1; only in control) and 3 beta-hydroxysteroid dehydrogenase/Delta 5→4-isomerase type 2 (HSD3B2; only in control) (Tables 1 and S1–S4).

Tau Protein Binding

Proteins involved in the tau protein binding activity were also diminished in cells exposed to 3-NT (25.0%, $p < 0.01$) (SG. 1B), such as the subunit 1 of dynactin (DCTN1; fold change: 0.82), glycogen synthase kinase-3 beta (GSK3B, only in control) and Rho-associated protein kinase 2 (ROCK2; only in control) (Tables 1 and S1–S4).

Other Proteins of Biological Significance Found in Lower Relative Quantity in 3-NT-Treated Cells

Other biologically relevant proteins found in lower quantities were delta (24)-sterol reductase (DHCR24, fold change: 0.55), interferon regulatory factor 3 (IRF3, fold change: 0.63), lipopolysaccharide-responsive and beige-like anchor protein (LRBA, fold change: 0.70), subunit RPB2 of DNA-directed RNA polymerase II (POLR2B, fold change: 0.71), protein 1 of ribosome-binding (RRBP1, fold change: 0.78), subunit alpha of coatomer (COPA, fold change: 0.79) and leukocyte elastase inhibitor (SERPINB1, fold change: 0.87) (Tables 1 and S1). Some other proteins were only found in control samples (completely suppressed in the presence of 3-NT). Among the latter, we emphasize Arf-GAP with Rho-GAP domain, ANK repeat and PH domain-containing protein 1 (ARAP1), subunit RPB1 of DNA-directed RNA polymerase II (POLR2A), component 5 of exocyst complex (EXOC5), alcohol dehydrogenase 4 (ADH4), protein 2 of developmentally regulated GTP-binding (DRG2), STAM-binding protein (STAMBP), Cirhin (CIRH1A), coronin-2A (CORO2A), U6 snRNA-associated Sm-like protein LSm2 (LSM2) and factor 1 of TRPM8 channel-associated (TCAF1) (Tables 1 and S1).

3.2.2. Proteins Found in Higher Relative Quantity in Cells Exposed to 3-NT Compared to Control Counterparts

Positive Regulation of Cyclic-Nucleotide Phosphodiesterase Activity

The biological process most widely affected by the exposure of 3-NT (87.01%, $p < 0.01$) was positive regulation of cyclic nucleotide phosphodiesterase activity (SG. 1C). Among the most affected pathways, we identified the nitric oxide synthase regulator activity, adenylate cyclase activator activity and positive and negative regulation of ryanodine-sensitive calcium-release channel activity (Supplementary Table S5). The proteins affected in all these processes were calmodulin-1, calmodulin-2 and calmodulin-3 (CALM1, CALM2 and CALM3; Fold change: 1.29) (Tables 1 and S1–S5).

Type 3 Metabotropic Glutamate Receptor Binding

The most affected molecular function in the presence of 3-NT was type 3 metabotropic glutamate receptor binding (86.36%, $p < 0.05$) (SG. 1D) in which the aforementioned calmodulin proteins, are implicated (CALM1, CALM2 and CALM3) (Supplementary Table S6). Other pathways affected were nitric oxide synthase regulator activity, adenylate cyclase activator activity and N-terminal myristoylation domain binding (Supplementary Table S6).

Other Proteins of Biological Significance Found in Higher Relative Quantity in 3-NT-Treated Cells

Other biologically relevant proteins found in significantly higher quantity in 3-NT-treated cells were: neutral amino acid transporter B(0) (SLC1A5, fold change: 2.22), ser-

ine/arginine repetitive matrix protein 1 (SRRM1, fold change: 2.13), tumor susceptibility gene 101 protein (TSG101, fold change: 2.00), Cadherin-17 (CDH17, fold change: 1.71), 60S ribosomal protein L11 (RPL11, fold change: 1.57) and mitochondrial glutamate carrier 1 (SLC25A22, fold change: 1.30) (Tables 1 and S1).

Proteins of biological significance only found in 3-NT-treated cells that have not been included previously but are complementary to previous results were: U1 small nuclear ribonucleoprotein C (SNRPC), CD2 antigen cytoplasmic tail-binding protein 2 (CD2BP2), carcinoembryonic antigen-related cell adhesion molecule 1 (CEACAM1), La-related protein 4B (LARP4B), lipid droplet-regulating VLDL assembly factor AUP1 (AUP1), non-homologous end-joining factor 1 (NHEJ1), subunit RPB3 of DNA-directed RNA polymerase II (POLR2C) and proton-coupled folate transporter (SLC46A1) (Tables 1 and S1).

3.2.3. Proteins Found in Lower Relative Quantity in Cells Exposed to 3-NT+EA Compared to 3-NT Counterparts

Intracellular Transport

The biological process most influenced by the exposure of 3-NT+EA (18.72%, $p<0.01$) was intracellular transport (SG. 2A). The cytoplasmic translational initiation process was one of the most affected in proteins such as subunit alpha of translation initiation factor eIF-2B (EIF2B1, only in 3-NT), subunit 2 of eukaryotic translation initiation factor 2(EIF2S2, only in 3-NT), eukaryotic initiation factor 4A-II (EIF4A2, fold change: 0.43), eukaryotic translation initiation factor 4E (EIF4E, fold change: 0.46), RNA-binding protein 4 (RBM4, fold change: 0.73) and monocarboxylate transporter 1 (SLC16A1, fold change: 0.40), among others (Tables 2 and S2–S7). These proteins are also implicated in other processes such as translational initiation, protein targeting to ER (endoplasmic reticulum) translation regulator activity and nucleic acid binding (Supplementary Table S7), which were, for this reason, also affected by 3-NT+AE exposure. Ribosomal proteins were also found in lower abundance such as La-related protein 1 (LARP1, only in 3-NT), 60S ribosomal protein L12 (RPL12, fold change: 0.27), 60S ribosomal protein L23a (RPL23A, fold change: 0.26), 60S ribosomal protein L13 (RPL13, fold change: 0.22), 40S ribosomal protein S7 (RPS7, fold change: 0.33) and 60S ribosomal protein L11 (RPL11, fold change: 0.49) (Tables 2 and S2–S7).

Purine Nucleotide Metabolic Process

Proteins involved in the metabolic process of purine nucleotides were found at lower quantity in 3-NT+EA treated cells compared to 3-NT samples (8.15%, $p < 0.01$) (SG. 2A). Specific routes such as the cristae formation, mitochondrial ATP synthesis coupled proton transport and energy coupled proton transport, down electrochemical gradient, were severely decreased. Some relevant proteins in the aforementioned processes are the subunits alpha (ATP5F1A), beta (ATP5F1B) and gamma (ATP5F1C) of the mitochondrial ATP synthase (fold changes: 0.17; 0.31 and 0.50, respectively). The subunit delta of the same mitochondrial ATP synthase, (ATP5F1D) was not found in enterocytes when EA was combined to 3-NT. Other relevant mitochondrial proteins were also found in lower abundance such as the subunit B1 of the mitochondrial ATP synthase F(0) complex (ATP5PB, fold change: 0.50), the subunit d of the mitochondrial ATP synthase, (ATP5PD, fold change: 0.46), the subunit O of the mitochondrial ATP synthase, (ATP5PO, fold change: 0.42), the subunit 5B of the mitochondrial cytochrome c oxidase, (COX5B, fold change: 0.61) and the mitochondrial stomatin-like protein 2 (STOML2, fold change: 0.38) (Tables 2 and S2–S7). Other remarkable proteins implicated in the ATP biosynthetic process, such as pyruvate kinase PKM (PKM, fold change: 0.70) and calcium-binding mitochondrial carrier protein Aralar2 (SLC25A13, fold change: 0.74), were in lower abundance in cells exposed to 3-NT+EA than in those exposed only to 3-NT. Interestingly, various relevant proteins involved in the mitochondrial membrane organization were also remarkably found in lower quantities when EA was combined with 3-NT. Among the latter, we may emphasize AFG3-like protein 2 (AFG3L2, fold change: 0.50), mitochondrial dynamin-like 120 kDa protein (OPA1, fold change, 0.34), the subunits MIC19 (CHCHD3), MIC60 (IMMT) and MIC13 (MICOS13) of

the mitochondrial MICOS complex, (fold changes: 0.07; 0.47, respectively, while the latter was only present in 3-NT-treated cells), DnaJ homolog protein (member 11, subfamily C) (DNAJC11, fold change: 0.33), the mitochondrial EF-hand domain-containing protein 1 (LETM1, fold change: 0.40), the mitochondrial inner membrane protein OXA1L (OXA1L, only in 3-NT) and sorting and assembly machinery component 50 homolog (SAMM50, fold change: 0.60) (Tables 2 and S2–S7).

Nucleotide Binding and Nitric Oxide Synthase Regulator Activity

Among molecular functions in human enterocytes, nucleotide binding was the most affected by 3-NT+EA exposure (26.83%, $p < 0.01$), along with nitric oxide synthase regulator activity (7.32%, $p < 0.01$) (SG. 2B). In nucleotide binding, terms related to this molecular function such as ATPase activity, GTP binding, nucleotide binding and ATP binding were influenced by the exposure of 3-NT+EA (Supplementary Table S8). Proteins in lower abundance were mitochondrial adenylate kinase 4 (AK4, fold change: 0.38), mitochondrial ATP-binding cassette (member 10, sub-family B), (ABCB10, only in 3-NT), dynamin-2 (DNM2, fold change: 0.26), mitochondrial ribosome-releasing factor 2 (GMF2, only in 3-NT), histone H1.4 (H1-4, fold change: 0.08), calmodulin-1 and calmodulin-3 (CALM1, CALM3 fold change: 0.73), among many others (Tables 2 and S2–S8).

Within the processes implicated in the regulating activity of nitric oxide synthase, the type 3 metabotropic glutamate receptor binding, the N-terminal myristoylation domain binding, the adenylate cyclase activator activity and the nitric oxide synthase regulator activity were some of the most affected in human enterocytes by exposure to 3-NT+EA. Proteins found in lower quantity were CALM1, CALM2, CALM3, subunit beta of calcium/calmodulin-dependent protein kinase type II (CAMK2B, fold change: 0.66), phosphatidylinositol-binding clathrin assembly protein (PICALM, only in 3-NT), subunit alpha of guanine nucleotide-binding protein G(s) isoforms XLas (GNAS, fold change: 0.67), ATPase 4 of plasma membrane calcium-transporting (ATP2B4, only in 3-NT), epidermal growth factor receptor (EGFR, only in 3-NT), heat shock protein HSP 90-alpha (HSP90AA1, fold change: 0.82) and heat shock protein HSP 90-beta (HSP90AB1, fold change: 0.68) (Tables 2 and S2–S8).

3.2.4. Proteins Found in Higher Relative Quantity in Cells Exposed to 3-NT+EA Compared to 3-NT Counterparts

Posttranscriptional Regulation of Gene Expression

The exposure to 3-NT+EA affected the post-transcriptional regulation of gene expression (19.28%, $p < 0.01$) in human enterocytes (SG. 2C). Within this biological process, the more affected functions were peptidase activity and proteasomal ubiquitin-independent protein catabolic process. In this regard, several subunits of the proteasome system were found in higher abundance, namely, alpha type-1 (PSMA1, fold change: 1.18), alpha type-6 (PSMA6, fold change: 1.62), beta type-1 (PSMB1, fold change: 1.40), beta type-2 (PSMB2, fold change: 1.79), beta type-3 (PSMB3, fold change: 1.55), beta type-4 (PSMB4, fold change: 1.32) and beta type-5 (PSMB5, fold change: 1.19) (Tables 2 and S2–S9).

Organic Substance Catabolic Process

The catabolism of organic substances was also upregulated (10.78%, $p < 0.01$) by the influence of 3-NT+EA (SG. 2C). Proteins found in higher quantity in the catabolic process of L-serine were the iron–sulfur subunit of the mitochondrial succinate dehydrogenase [ubiquinone], (SDHB, fold change: 1.87), both the cytosolic (SHMT1) and mitochondrial (SHMT2) serine hydroxymethyltransferases, (fold changes: 1.74 and 1.34, respectively) and sorbitol dehydrogenase (SORD, fold change: 1.46) (Tables 2 and S2–S9). Other relevant enzymes such as catalase (CAT, fold change: 2.66) and mitochondrial glycine dehydrogenase (decarboxylating) (GLDC, fold change: 2.23) were identified as some of the most affected by the exposure to 3-NT+EA (Tables 2 and S2–S9).

Protein-Containing Complex Assembly

The protein-containing complex assembly was also one of the most affected biological processes in human enterocytes exposed to 3-NT+EA (9.15%, $p < 0.01$) (SG. 2C). Within this group, the most affected were error-free translation synthesis, error-prone translation synthesis and nucleotide-excision repair (DNA gap filling). The proliferating cell nuclear antigen (PCNA, fold change: 2.86), 70 kDa DNA-binding subunit of replication protein A (RPA1, fold change: 1.45), 14 kDa subunit of replication protein A (RPA3, fold change: 2.02), ribosomal protein S27a of ubiquitin-40S (RPS27A, fold change: 2.02), ribosomal protein L40 of ubiquitin-60S (UBA52, fold change: 2.02), polyubiquitin-B (UBB, fold change: 2.02), polyubiquitin-C (UBC, fold change: 2.02) and DNA ligase 3 (LIG3, only in 3-NT+EA) were the proteins found in higher quantity in this case (Tables 2 and S2–S9)

Oxidoreductase Activity

The oxidoreductase activity of enterocytes was also upregulated in 3-NT+EA-treated cells (7.84%, $p < 0.01$) (SG. 2C). Several relevant processes were affected, including dihydrotestosterone 17-beta-dehydrogenase activity, carnitine biosynthetic process, glyceraldehyde-3-phosphate dehydrogenase (NAD+) (non-phosphorylating) activity, aldehyde dehydrogenase NAD+, NAD(P)+ activity and the glycoside metabolic process, among others (Supplementary Table S9). The analysis of the molecular functions also revealed an up-regulation of the oxidoreductase activity acting on the CH-OH group of donors (19.35%, $p < 0.01$) (SG. 2D). In this case, it is worth emphasizing the up-regulation of the dihydrotestosterone 17-beta-dehydrogenase activity, glyceraldehyde-3-phosphate dehydrogenase (NAD+) (non-phosphorylating) activity, aldehyde dehydrogenase NAD+ and NAD(P)+ activity, and alcohol dehydrogenase (NADP+) activity (Supplementary Table S10). Some relevant enzymes accounting for these effects were member C3 of the aldo-keto reductase family 1 (AKR1C3, fold change: 3.21), type-2 3-hydroxyacyl-CoA dehydrogenase (HSD17B10, fold change: 1.42), mitochondrial delta-1-pyrroline-5-carboxylate dehydrogenase (ALDH4A1 fold change: 2.42), SHMT1, class-3 alcohol dehydrogenase (ADH5 1.71), fatty aldehyde dehydrogenase (ALDH3A2, fold change: 2.08), alcohol dehydrogenase 4 (ADH4, only in 3-NT+EA), alcohol dehydrogenase [NADP (+)] (AKR1A1, fold change: 1.24), aflatoxin B1 aldehyde reductase (member 2) (AKR7A2, fold change: 1.35), tissue alpha-L-fucosidase (FUCA1, fold change: 2.86) and alpha-N-acetylgalactosaminidase (NAGA, fold change: 1.64), among others (Tables 2 and S2–S9)

Aminopeptidase Activity

The aminopeptidase activity was one of the most affected molecular functions (11.29%, $p < 0.01$) (SG. 2D). The proteins found in higher abundance from this group were cathepsin B (CTSB, fold change: 1.72), aspartyl aminopeptidase (DNPEP, fold change: 1.98), dipeptidyl peptidase 2 (DPP7, fold change: 3.40), leukotriene A-4 hydrolase (LTA4H, fold change: 1.78), N-acetylated-alpha-linked acidic dipeptidase 2 (NAALAD2, fold change: 1.87) and lysosomal Pro-X carboxypeptidase (PRCP, fold change: 1.77) (Tables 2 and S10).

Oxidoreductase Activity, Acting on a Sulfur Group of Donors

The analysis of the molecular functions also revealed up-regulation of oxidoreductases acting on the sulfur group of donors (6.45%, $p < 0.01$) (SG. 2D). Within this group, some relevant proteins which were significantly found in higher abundance were thioredoxin domain-containing protein 17 (TXNDC17, fold change: 2.19), thioredoxin (TXN, fold change: 1.73), mitochondrial glutaredoxin-related protein 5 (GLRX5, fold change: 1.33), mitochondrial glutathione reductase (GSR, fold change: 1.25), glutathione synthetase (GSS, fold change: 1.25), protein disulfide isomerase A4 (PDIA4, fold change: 1.21), selenium-binding protein 1 (SELENBP1, fold change: 1.75), and thioredoxin-like protein 1 (TXNL1, fold change: 1.44) (Tables 2 and S2–S10).

Other Proteins of Biological Significance Found in Higher Relative Quantity

Proteins of biological significance only found in 3-NT+EA treated cells that have not been included in the previous biological processes/molecular functions are alcohol dehydrogenase 4 (ADH4), glutathione S-transferase Mu 3 (GSTM3), ferroptosis suppressor protein 1 (AIFM2), heme oxygenase 1 (HMOX1) and subunit RPB1 of DNA-directed RNA polymerase II (POLR2A) (Tables 2 and S2).

3.3. Endogenous Antioxidant Enzyme Activity

Further to the full proteome of the cells under study, the activity of two major antioxidant enzymes, namely, catalase (CAT) and superoxide dismutase (SOD) was analyzed to gain further insight into the physiological response of the cell to the exposure to the tested dietary species (Figure 3). Consistent with the proteome results, the catalase activity in cells exposed to 3-NT-EA was significantly higher than in those treated with 3-NT alone, or in control. While superoxide dismutase was not identified as discriminating between treatments, the assessment of its activity revealed that enterocytes challenged with 3-NT+EA had significantly higher SOD activity than the other two counterparts.

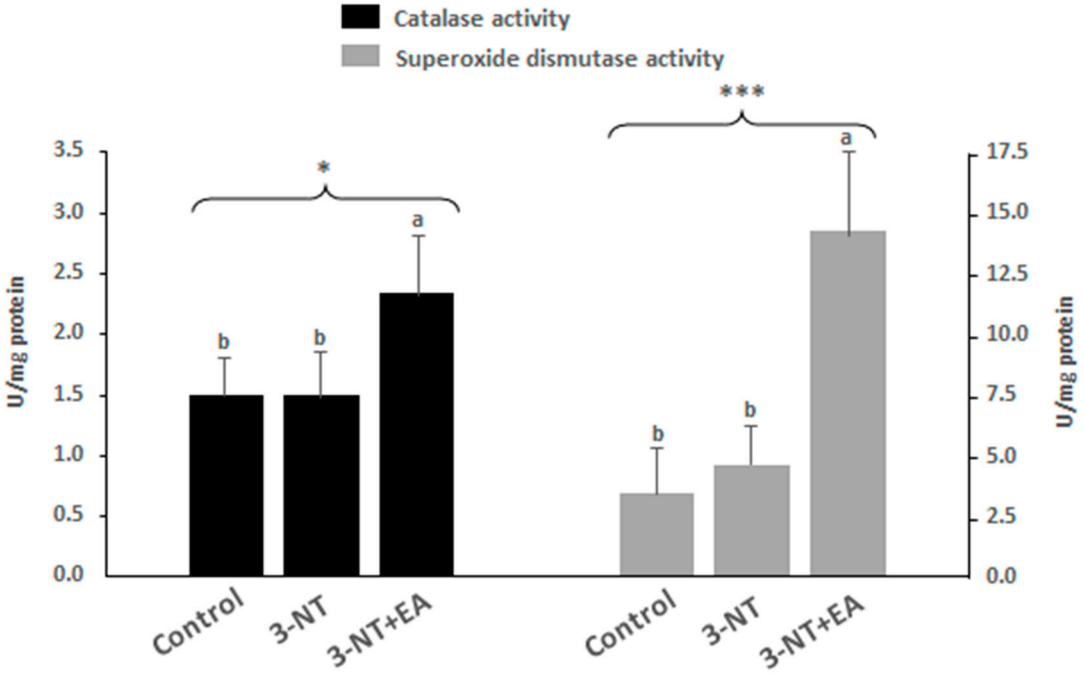

Figure 3. Antioxidant activity of catalase (black bars) and superoxide dismutase (grey bars) on differentiated human enterocytes upon exposure to 200 μM 3-NT and 200 μM 3-NT+200 μM EA for 72 h. Asterisks on top of bars denote significant differences between group of samples in ANOVA (* $p<0.05$; *** $p < 0.001$).(a–b) Different letters on top of bars denote significant differences between means in post-hoc Tukey tests ($p < 0.05$).

4. Discussion

Presently, the onset of oxidative and nitrosative stress is associated with multiple pathologies [1,2]. Dietary oxidized amino acids have been documented to induce redox imbalance and impairment of organic functions in human cells [15,21]. According to our hypotheses, 3-NT could be implicated in the assorted health disorders attributed to the intake of processed cured meat products, while the application of recognized antioxidants such as EA could contribute to counteract the redox-related biological impairments of 3-NT. The results from the present study revealed that 3-NT is certainly implicated in the impairment of specific biological functions in human enterocytes; however, the exposure to EA was not found to counteract such impairments. Contrary to our initial hypothesis, the combination of 3-NT and EA led to a severe impairment of the proteome of the enterocytes

with remarkable increase in necrosis. Such cell injure can be visualized in the Picture S1 (Available as Supplementary Material). The most relevant biological impairments caused by 3-NT and 3-NT+EA in differentiated human enterocytes are discussed as follows. Figure 4 illustrates the metabolic pathways affected in these cells by the exposure to 3-NT and 3-NT+EA.

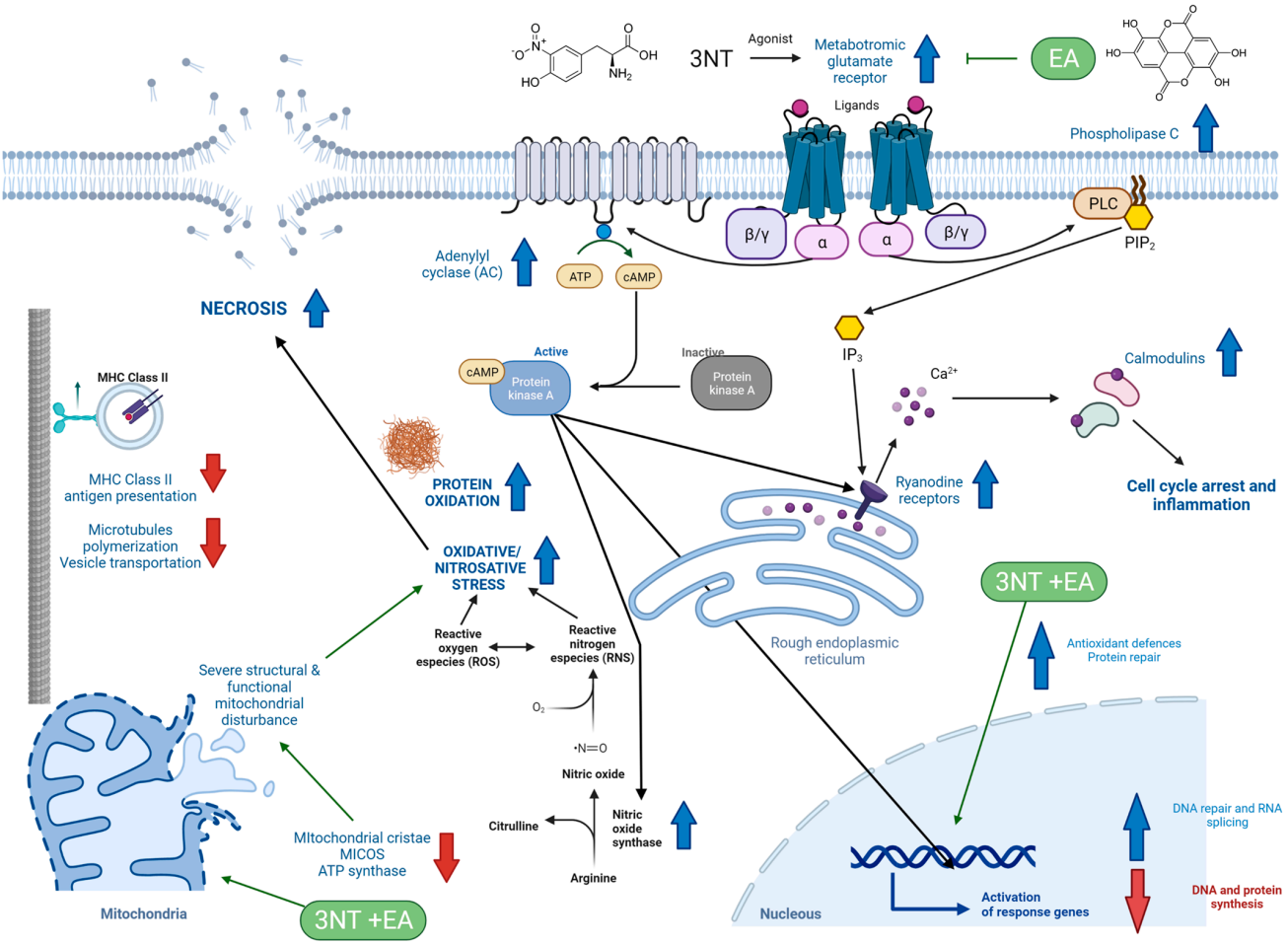

Figure 4. Proposal of underlying molecular mechanisms of the toxicological effects of 200 µM 3-NT and 200 µM 3-NT+200 µM EA for 72 h on differentiated human enterocytes. Upstream head blue arrows indicate higher concentration of proteins/upregulated biological processes in treated enterocytes. Downstream head red arrows indicate lower concentration of proteins/downregulated biological processes in treated enterocytes. Blunt head connectors indicate an inhibited biological process or metabolic pathway. Effect of EA is specifically denoted by green arrows. (For interpretation of the references to colour in this figure legend, the reader is referred to the web version of this article). The mechanisms and routes depicted in this Figure are proposed based on the interpretation of the data from cytometry, proteomics and accretion of protein oxidation (oxidative stress). Confirmation of the impairment of all these downstream paths and interconnections of complex cellular mechanisms requires further specific studies.

4.1. Impact of 3-NT and 3-NT+EA on Calmodulin-Dependent Intracellular Signaling Pathway

The calmodulin protein family is a group of biologically relevant proteins, which play a central role in Ca^{2+} cell sensing, ion channel regulation and molecular signaling pathways with multiple physiological implications [22]. The higher relative quantity of 3 calmodulin proteins suggests that 3-NT exposure would have, as a primary molecular mechanism, the impairment of downstream biological processes depending on such proteins. As identified by CLUEGO, 3-NT upregulated the cyclic nucleotide phosphodiesterase activity and type 3 metabotropic glutamate receptor binding activity, which directly affects the nitric

oxide synthase regulator activity, the adenylate cyclase activator activity, the regulation of ryanodine-sensitive calcium-release channel activity and the N-terminal myristoylation domain binding. These processes and functions accounted for around 87% of all proteomic upregulations caused by 3-NT exposure, which highlights the relevance of these molecular mechanisms in the potential toxicological effects of this nitrosated species.

Type 3 metabotropic glutamate receptors are constituted by seven transmembrane domains coupled to the G-protein signaling system [23]. The adenylate cyclase activator activity enables the formation of cAMP from ATP [24]. On the other hand, cyclic nucleotide phosphodiesterase activity is responsible for eliminating the excess of cAMP in the cell by converting it into 5′-AMP [24]. cAMP activates the catalytic subunits of protein kinase A (PKA), which goes to the nucleus, activating transcription factors [25]. PKA is also involved in the activation of ryanodine receptors (RYRs) [26], which can also be activated by IP3 through the phospholipase C pathway [27]. RYRs release calcium from rough endoplasmic reticulum (RER) to the cytosol, which, in turn, activates calmodulin proteins [26]. All these processes seemed to be increased by the effect of 3-NT exposure, and the consequences of such up-regulation have been described as harmful for enterocytes. In a recent study, Cunningham et al. [28] reported that activation of the calmodulin downstream molecular pathway in intestinal cells is initiated by an epithelial injury and leads to cell cycle arrest and inflammation processes. The inactivation of such molecular pathway protected against murine inflammatory bowel disease and colitis. It is, therefore, reasonable to consider that the higher abundance of calmodulin proteins found in enterocytes when treated with 3-NT may have harmful biological consequences. Consistently, proteins corresponding to DNA repair and RNA splicing were in higher quantities as compared to control counterparts. 3-NT-treated enterocytes showed impaired processes responsible for carrying out a normal synthesis of DNA and proteins (Table 1). These results are compatible with impaired cell cycle regulation. Consistently with our current study, Santulli et al. [27] observed the activation of RyRs by oxidative and nitrosative species and emphasized that these molecular mechanisms are implicated in the onset of various pathological conditions such as diabetes mellitus, hypertension and skeletal muscle disorders, among others.

3-NT is also involved in increasing nitric oxide synthase regulatory activity. Nitric oxide synthase (NOS) is an enzyme that catalyzes the conversion of L-arginine to L-citrulline producing nitric oxide (NO) [29], and has a binding domain to calmodulin. The cyclic-nucleotide phosphodiesterase activity, also increased in 3-NT-treated cells, is involved in the activation of inducible nitric oxide synthase (iNOS) via adenylate cyclase/protein kinase A dependent of stimulatory G-protein [29]. At high levels of NO, or in the presence of ROS, the formation of peroxynitrite and its potential cytotoxic effects are enhanced [30]. Peroxynitrite can damage a variety of molecules in cells, including DNA and proteins, leading to apoptosis and necrosis [30], a situation which, in fact, occurred in the present study. Peroxynitrite plays a crucial role in chronic inflammatory diseases, diabetes, cancer and neurodegenerative disorders, among others [30], affect T cells and negatively influence the immune response [31], corresponding with the aforementioned obtained results, where MHC class II-restricted antigen presentation for $CD4^+$ T cell-dependent was affected. Currently, 3-NT is recognized as a biomarker of up-regulated inducible NO synthase in inflammation [32]. Interestingly, 3-NT, a product of the nitrosative stress to proteins, would contribute to inducing further nitrosative stress by the activation of specific metabolic routes.

The molecular function of N-terminal myristoylation domain binding is affected by 3-NT exposure. N-myristylation of proteins is a co-translational lipidic modification of many eukaryotic proteins [33]. Myristoylation directly regulates the biological activity of endothelial nitric oxide synthase (eNOS), increasing calcium flows, and activating the calcium/calmodulin complex (calcium/CaM). This process is involved in the regulation of cell-signaling pathways in biological processes such as carcinogenesis and immune function [33]. Thus, for all of the above mentioned, 3-NT can be considered as an agonist of type 3 metabotropic glutamate receptors in cells, which stimulates different relevant pathways.

Acting as such, 3-NT promotes the deregulation of cAMP and calcium metabolism, which affects, in turn, the normal operation of the immune system through calmodulin.

The results obtained in EA-treated cells were coherent with those found in the literature, in which the ability of EA to enhance calcium metabolism, apoptosis and necrosis in tumor cells, is reported (revised by Mohammadinejad et al., [34]). However, enterocytes treated with EA led to an attempt to reverse some of the above-mentioned impaired biological functions (Supplementary Table S8). It was ignored whether a higher dose of EA would be necessary to compensate the effects of 3-NT on these pathways. Yet, the injurious effects of the combination of both species at these concentrations on enterocytes in terms of oxidative stress and necrosis, discussed in due course, suggest that, unlike our initial hypothesis, EA does not exert a protective effect against 3-NT-induced toxicity, but the opposite.

4.2. Impact of 3-NT and 3-NT+EA on Immune System and Steroid Hormones

The immune system is a network of cells and biological processes that protects an organism from internal and external hazardous substances. The major histocompatibility complex (MHC) is involved in the codification of proteins found on the surface of the cell recognizing potential antigens. Antigenic peptide-loaded MHC class II molecules (peptide–MHC class II) are expressed on the surface of professional antigen-presenting cells (APCs) such as macrophages, B cells, dendritic cells and thymic epithelial cells [35]. As the primary barrier between human organism and its environment, intestinal epithelial cells, as observed in the present study, express MHC class II in their surface, although the functional consequences of this expression are not fully understood [36]. All these cells present the antigen to antigen-specific $CD4^+$ T cells, a mechanism that is essential for a specific and effective immune response [35]. In this study, processes involved in the antigen processing and presentation of exogenous peptide antigen via MHC class II were affected by the exposure of 3-NT. Proteins implicated in the motility of vesicles through microtubules (MYH10) [37], blebs formation (ROCK2) [38], vesicle trafficking (SNX9) [39], reorganization of actin cytoskeleton, exocytosis and early steps of protein synthesis (EIF2S3, EIF2S3B and EIF3D) [40] (Table 1) were significantly reduced in abundance in the presence of 3-NT compared to control counterparts. The lower relative abundance of tau protein binding function in 3-NT-treated cells is consistent with the impairment of the MHC class II mediated process (Supplementary Table S4). The tau protein binding was decreased in DCTN1 protein, which is an essential cofactor involved in most cellular functions of the microtubule motor cytoplasmic dynein [41] and in GSK3B protein, an essential key in protein tau phosphorylation. It is, hence, reasonable to hypothesize that the decrease of microtubule polymerization prevents vesicles of antigenic peptide-loaded MHC class II molecules from reaching the cell surface. Other proteins related to immunity, such as IRF3 [42] or LRBA [43], were also found in lower quantities in the presence of dietary concentrations of 3-NT. These results suggest that 3-NT impairs the ability of enterocytes to act as APCs and effectively contribute to protection against biological hazards. This could be explained by i) an impaired synthesis of proteins related to immunity, and ii) an impaired transportation of such proteins to the cell surface. These results are consistent with those published by Birnboim et al. [32] and Ahsan [44], where 3-NT is linked to systemic autoimmunogenic conditions and is related to diseases associated with immunological reactions where formation of Tyr-nitrated proteins has a major role [45]. Thus, 3-NT has a toxicological effect in the immune system through its implication in the decrease of MHC class II-restricted antigen presentation for CD4+ T cell-dependent, which is, as aforementioned, necessary for a suitable immune response. In addition, the results obtained revealed that the incorporation of EA to enterocytes did not seem to have an impact on this biological impairment caused by 3-NT.

In relation to steroid hormones, the proteins HSD3B1 and HSD3B2, involved in oxidation and isomerization in the biosynthesis of hormonal steroids [46], were not found in 3-NT treated cells. Steroid hormones are involved in a number of processes such as immune

functions, inflammation, the control of metabolism and sexual development through sex steroids and corticosteroids [47]. Interestingly, protein HSD17B10 was found in terms dihydrotestosterone 17-beta-dehydrogenase activity and lipid oxidation (Supplementary Table S9) in higher abundance in 3-NT+EA-treated cells. This protein, with hydroxysteroid dehydrogenase activity in steroid hormones [48], may be positive to cells as it may counteract the drop in proteins HSD3B1 and HSD3B2 caused by 3-NT. Therefore, EA may enable physiological biosynthesis of hormonal steroids in enterocytes and counteract, at some extent, the impairment caused by 3-NT.

4.3. Impact of 3-NT and 3-NT+EA on Antioxidant Defenses and Oxidative Stress

The analysis of specific protein oxidation markers in enterocytes revealed that the combination of 3-NT and EA remarkably promoted the onset of oxidative stress in enterocytes. These indicators of the oxidative damage to proteins are formed as a result of the oxidative deamination of alkaline amino acids (i.e., lysine) in the presence of ROS [49]. It is known that decreased and inefficient mitochondrial activity is linked to ROS generation, and, consequently, to oxidative stress [50]. Enterocytes exposed to 3-NT+EA showed a significant decrease in mitochondrial cristae formation and a lower abundance in proteins related to mitochondrial ATP synthase. The proteins found in lower abundance in 3-NT+EA-treated cells were related to the MICOS complex (mitochondrial contact site and cristae organizing system) (Table 2). MICOS is a multi-subunit complex found in the inner mitochondrial membrane. Mitochondrial function and its architecture are closely related because an anomalous mitochondrial architecture leads to mitochondrial dysfunction [51]. MICOS is involved in human diseases such as amyotrophic lateral sclerosis, Alzheimer's and Parkinson's disease [51]. In agreement with the present results, several previous studies reported that EA inhibits mitochondrial respiration and had a negative impact on the restoration of both GSH and ATP, and on mitochondrial complex II function [52,53]. The remarkable impact of EA in promoting oxidative stress in 3-NT-treated enterocytes (as measured by protein oxidation) could be a plausible consequence of the disturbance effect of the phytochemical on mitochondrial activity. This could be one likely mechanism behind the profusely reported pro-oxidant activity of ellagic acid [54]. It is known that such pro-oxidant action depends on a number of factors, including the dose and occurrence of oxygen molecules and transition metals [54]. The present study reveals that 3-NT activates this pro-oxidant mechanism as exposure to EA alone, had, in general, protective effects on enterocytes against oxidative stress, apoptosis and necrosis (Figure 1E–G). The molecular mechanism by which the combination of both species leads to such severe oxidative stress and necrosis is yet to be elucidated.

The oxidative damage to proteins measured in 3-NT+EA cells apparently contrasts with the lack of differences in ROS as assessed by flow cytometry. The lack of correspondence between both measurements is consistent with a previous study performed in human enterocytes exposed to 3-NT [9]. It is reasonable to hypothesize that, at the point of cell harvesting, ROS were already depleted while the effects of their pro-oxidative effects (oxidative damage and necrosis) were noticeable. Furthermore, the probe employed for cytometric ROS measurement detects, specifically, superoxide radicals, concentration of which commonly reflects mitochondrial activity. An impaired mitochondrial respiration is, in fact, compatible with the present results, which would actually explain the creation of a cellular pro-oxidative environment with other ROS that would, in turn, lead to the remarkable accretion of oxidized proteins.

The effect of 3-NT+EA on promoting the occurrence of detoxifying enzymes such as GSS and GSR (both involved in glutathione metabolism), GSTM3 and CAT in enterocytes, supports the hypothesis of enterocytes reinforcing the endogenous antioxidant defenses in response to the pro-oxidative environment caused by the combination of both chemical species. These enzymes are known to increase in cells in response to oxidative stress [55,56]. Furthermore, ADH4, which is well known for playing a relevant role in detoxifying ROS in enterocytes as a primary barrier to dietary pro-oxidative species [57], was only found in cells

exposed to both 3-NT and EA. The proteomic results are consistent with additional analysis of the endogenous antioxidant activity of CAT and SOD. The activity of both enzymes was significantly higher in cells treated with 3-NT'+EA than in the other two groups of cells (3-NT, control). However, this attempt to strengthen the endogenous antioxidant defenses failed, as observed in the extent of oxidative damage to proteins and the severe necrosis found in enterocytes exposed to 3-NT+EA.

4.4. Impact of 3-NT and 3-NT+EA in Cell Viability, Apoptosis, Necrosis and Protein Repair

The flow cytometry assessment revealed that 3-NT caused a significant decrease in cell viability ($p < 0.05$) and a significant increase in necrosis ($p < 0.05$) (Figure 1A). As discussed above, the cytotoxicity exerted by 3-NT on enterocytes may be derived from the up-regulation of calcium-dependent biological functions that may have caused physiological impairments, including the onset of oxidative stress. While the increase of ROS was not detected by flow cytometry in 3-NT-treated cells, the accretion of oxidized proteins was significant as compared to CONTROL cells. The up-regulation of type 3 metabotropic glutamate receptors in the presence of 3-NT led to a higher abundance in a number of enzymes involved in important pathways of cellular metabolism, including nitric oxide synthase. This enzyme increases the amount of NO in cells, which makes the formation of RNS species possible, along with 3-NT, such as peroxynitrite. This species can damage DNA and proteins, increasing apoptosis and necrosis [30,31], with necrosis being the most characteristic mechanism induced by peroxinitrite [30]. In a previous study [9], a significant decrease of cell viability was accompanied by a significant increase in necrosis. Other studies have reported the same situation in cell cultures and animal models [8,58].

The significant decrease in cell viability ($p < 0.05$) in enterocytes exposed to 3-NT and EA, is reflected in a remarkable significant increase in necrosis compared to 3-NT treated cells ($p < 0.01$) (Figure 1C). Cells exposed to 3-NT and EA seemed to enter into necrosis, which shows the severe chemical insult caused by the combination of these two chemical species. On the other hand, the significant decrease in apoptosis ($p < 0.01$) may be caused by of the ability of EA to counteract the upregulation of type 3 metabotropic glutamate receptors caused by 3-NT. Yet, the most plausible means of cytotoxicity caused by 3-NT+EA, which would explain the remarkable increase in oxidized proteins and cell necrosis, would be the severe mitochondrial disturbance. Such physiological impairment was manifested in the proteome by downregulation of the MICOS complex and other proteins implicated in the mitochondrial respiratory chain (Table 2). As aforementioned, an abnormal mitochondrial conformation leads to mitochondrial dysfunction [51] and the onset of oxidative stress, which would explain, in turn, the significant and remarkable accretion of oxidized proteins and increased necrosis. Indeed, the protein CHCHD3, which plays an important role in maintaining the stability of the MICOS complex and the morphology of mitochondrial cristae [59], is remarkably diminished in 3-NT+EA-treated enterocytes along with other proteins related to this complex (Table 2).

Finally, the process of protein repair was also affected by the exposure to 3-NT+EA. Proteins related to the proteasome complex involved in the proteolytic degradation of most intracellular proteins [60] were found in higher abundance in the presence of 3-NT+EA-treated cells. Other proteins involved in post-replication repair and DNA damage checkpoint activation, such as RPA3 [61], were also increased in quantity as compared to 3-NT-treated cells. These results are coherent with the aforementioned attempt of the enterocytes to counteract the severe oxidative insult induced by the combination of 3-NT and EA. These efforts were, however, insufficient to avoid massive cell necrosis caused by these two chemical species.

5. Conclusions

We describe, for the first time, the underlying molecular mechanisms of the toxicological effects of 3-NT in human enterocytes. While this proteomics-based approach enables the study of these noxious effects from a comprehensive perspective, the confirmation

of the impairment of all these downstream paths and interconnections of complex cellular mechanisms requires further specific studies. According to the generated data, the nitrosated amino acid 3-NT impairs several calcium-dependent physiological processes and affects the ability of enterocytes to act as antigen-presenting cells, compromising the immune response against potential biological threats. While it could be thought that EA would revert some of these mechanisms, the combination of 3-NT and the phytochemical led to compromised cell viability through anomalous mitochondria conformation and functionality, leading to severe oxidative stress and massive cell necrosis. These results highlight the importance of the study of dietary nitrosated amino acids in intestinal cell physiology, as they commonly occur in processed meat/dairy products where nitrite is used. Furthermore, the toxicological effects of 3-NT+EA should be studied for potential therapeutic studies in which cell death is deliberately induced.

Supplementary Materials: The following supporting information can be downloaded at: https://www.mdpi.com/article/10.3390/antiox11122485/s1

Author Contributions: S.D.-V.: data curation, methodology, formal analysis, writing—original draft; J.D.: data curation, methodology, funding acquisition, supervision, formal analysis, validation, writing—review and editing; F.J.P.: data curation, methodology, funding acquisition, supervision, formal analysis, validation, writing—review and editing; M.E.: conceptualization, funding acquisition, project administration, resources, supervision, validation, writing—review and editing. All authors have read and agreed to the published version of the manuscript.

Funding: This research was funded by the Spanish Ministry of Economics and Competitiveness (SMEC) (project number AGL2017-84586-R) and "Junta de Extremadura/FEDER" (grant number GR18104). S. Díaz-Velasco is recipient of a fellowship from the Spanish Ministry of Science, Innovation and Universities (grant number PRE2018-084001). Q-Exactive Orbitrap equipment was acquired by a grant from the Spanish Ministry of Science and Innovation (MCIN/AEI/ 10.13039/501100011033) (grant number UNEX-AE-3394).

Institutional Review Board Statement: Not applicable.

Informed Consent Statement: Not applicable.

Data Availability Statement: All data is contained within the article or supplementary material, including raw data from Proteomics.

Conflicts of Interest: The authors declare no conflict of interest.

References

1. Forman, H.J.; Zhang, H. Targeting Oxidative Stress in Disease: Promise and Limitations of Antioxidant Therapy. *Nat. Rev. Drug Discov.* **2021**, *20*, 689–709. [CrossRef] [PubMed]
2. Liguori, I.; Russo, G.; Curcio, F.; Bulli, G.; Aran, L.; Della-Morte, D.; Gargiulo, G.; Testa, G.; Cacciatore, F.; Bonaduce, D.; et al. Oxidative Stress, Aging, and Diseases. *Clin. Interv. Aging* **2018**, *13*, 757. [CrossRef] [PubMed]
3. Estévez, M.; Li, Z.; Soladoye, O.P.; Van-Hecke, T. Health Risks of Food Oxidation. *Adv. Food Nutr. Res.* **2017**, *82*, 45–81. [CrossRef] [PubMed]
4. Villaverde, A.; Ventanas, J.; Estévez, M. Nitrite Promotes Protein Carbonylation and Strecker Aldehyde Formation in Experimental Fermented Sausages: Are Both Events Connected? *Meat Sci.* **2014**, *98*, 665–672. [CrossRef] [PubMed]
5. Ozyurt, V.H.; Otles, S. Investigation of the Effect of Sodium Nitrite on Protein Oxidation Markers in Food Protein Suspensions. *J. Food Biochem.* **2020**, *44*, e13152. [CrossRef]
6. Yang, H.; Zhang, Y.; Pöschl, U. Quantification of Nitrotyrosine in Nitrated Proteins. *Anal. Bioanal. Chem.* **2010**, *397*, 879–886. [CrossRef] [PubMed]
7. Blanchard-Fillion, B.; Prou, D.; Polydoro, M.; Spielberg, D.; Tsika, E.; Wang, Z.; Hazen, S.L.; Koval, M.; Przedborski, S.; Ischiropoulos, H. Metabolism of 3-Nitrotyrosine Induces Apoptotic Death in Dopaminergic Cells. *J. Neurosci.* **2006**, *26*, 6124–6130. [CrossRef] [PubMed]
8. Zhang, Y.L.; Wei, J.R. 3-Nitrotyrosine, a Biomarker for Cardiomyocyte Apoptosis Induced by Diabetic Cardiomyopathy in a Rat Model. *Mol. Med. Rep.* **2013**, *8*, 989–994. [CrossRef]
9. Díaz-Velasco, S.; González, A.; Peña, F.J.; Estévez, M. Noxious Effects of Selected Food-Occurring Oxidized Amino Acids on Differentiated CACO-2 Intestinal Human Cells. *Food Chem. Toxicol.* **2020**, *144*, 111650. [CrossRef]

10. Villaverde, A.; Morcuende, D.; Estévez, M. Effect of Curing Agents on the Oxidative and Nitrosative Damage to Meat Proteins during Processing of Fermented Sausages. *J. Food Sci.* **2014**, *79*, C1331–C1342. [CrossRef]
11. Vossen, E.; De Smet, S. Protein Oxidation and Protein Nitration Influenced by Sodium Nitrite in Two Different Meat Model Systems. *J. Agric. Food Chem.* **2015**, *63*, 2550–2556. [CrossRef] [PubMed]
12. IARC. Carcinogenicity of Consumption of Red and Processed Meat. *Lancet Oncol.* **2015**, *16*, 1599–1600. [CrossRef] [PubMed]
13. Cheshomi, H.; Bahrami, A.R.; Matin, M.M. Ellagic Acid and Human Cancers: A Systems Pharmacology and Docking Study to Identify Principal Hub Genes and Main Mechanisms of Action. *Mol. Divers.* **2021**, *25*, 333–349. [CrossRef] [PubMed]
14. Zeb, A. Ellagic Acid in Suppressing in Vivo and in Vitro Oxidative Stresses. *Mol. Cell. Biochem.* **2018**, *448*, 27–41. [CrossRef] [PubMed]
15. Díaz-Velasco, S.; Delgado, J.; Peña, F.J.; Estévez, M. Protein Oxidation Marker, α-Amino Adipic Acid, Impairs Proteome of Differentiated Human Enterocytes: Underlying Toxicological Mechanisms. *Biochim. Biophys. Acta Proteins Proteom.* **2022**, *1870*, 140797. [CrossRef]
16. Pinto, M.; Robine Leon, S.; Appay, M.D. Enterocyte-like Differentiation and Polarization of the Human Colon Carcinoma Cell Line Caco-2 in Culture. *Biol. Cell* **1983**, *47*, 323–330.
17. Utrera, M.; Morcuende, D.; Rodríguez-Carpena, J.G.; Estévez, M. Fluorescent HPLC for the Detection of Specific Protein Oxidation Carbonyls—α-Aminoadipic and γ-Glutamic Semialdehydes—In Meat Systems. *Meat Sci.* **2011**, *89*, 500–506. [CrossRef]
18. Akagawa, M.; Sasaki, T.; Suyama, K. Oxidative Deamination of Lysine Residue in Plasma Protein of Diabetic Rats: Novel Mechanism via the Maillard Reaction. *Eur. J. Biochem.* **2002**, *269*, 5451–5458. [CrossRef]
19. Delgado, J.; Núñez, F.; Asensio, M.A.; Owens, R.A. Quantitative Proteomic Profiling of Ochratoxin A Repression in Penicillium Nordicum by Protective Cultures. *Int. J. Food Microbiol.* **2019**, *305*, 108243. [CrossRef]
20. Bindea, G.; Mlecnik, B.; Hackl, H.; Charoentong, P.; Tosolini, M.; Kirilovsky, A.; Fridman, W.-H.; Pagès, F.; Trajanoski, Z.; Galon, J. ClueGO: A Cytoscape Plug-in to Decipher Functionally Grouped Gene Ontology and Pathway Annotation Networks. *Bioinformatics* **2009**, *25*, 1091–1093. [CrossRef]
21. Estévez, M.; Xiong, Y. Intake of Oxidized Proteins and Amino Acids and Causative Oxidative Stress and Disease: Recent Scientific Evidences and Hypotheses. *J. Food Sci.* **2019**, *84*, 387–396. [CrossRef] [PubMed]
22. Vorherr, T.; Knöpfel, L.; Hofmann, F.; Carafoli, E.; Mollner, S.; Pfeuffer, T. The Calmodulin Binding Domain of Nitric Oxide Synthase and Adenylyl Cyclase. *Biochemistry* **1993**, *32*, 6081–6088. [CrossRef] [PubMed]
23. Ribeiro, F.M.; Vieira, L.B.; Pires, R.G.W.; Olmo, R.P.; Ferguson, S.S.G. Metabotropic Glutamate Receptors and Neurodegenerative Diseases. *Pharmacol. Res.* **2017**, *115*, 179–191. [CrossRef] [PubMed]
24. Kammer, G.M. The Adenylate Cyclase-CAMP-Protein Kinase A Pathway and Regulation of the Immune Response. *Immunol. Today* **1988**, *9*, 222–229. [CrossRef]
25. London, E.; Bloyd, M.; Stratakis, C.A. PKA Functions in Metabolism and Resistance to Obesity: Lessons from Mouse and Human Studies. *J. Endocrinol.* **2020**, *246*, R51–R64. [CrossRef] [PubMed]
26. Lanner, J.T.; Georgiou, D.K.; Joshi, A.D.; Hamilton, S.L. Ryanodine Receptors: Structure, Expression, Molecular Details, and Function in Calcium Release. *Cold Spring Harb. Perspect. Biol.* **2010**, *2*, a003996. [CrossRef]
27. Santulli, G.; Nakashima, R.; Yuan, Q.; Marks, A.R. Intracellular Calcium Release Channels: An Update. *J. Physiol.* **2017**, *595*, 3041. [CrossRef]
28. Cunningham, K.E.; Novak, E.A.; Vincent, G.; Siow, V.S.; Griffith, B.D.; Ranganathan, S.; Rosengart, M.R.; Piganelli, J.D.; Mollen, K.P. Calcium/Calmodulin–Dependent Protein Kinase IV (CaMKIV) Activation Contributes to the Pathogenesis of Experimental Colitis via Inhibition of Intestinal Epithelial Cell Proliferation. *FASEB J.* **2019**, *33*, 1330–1346. [CrossRef]
29. Dubey, R.K.; Gillespie, D.G.; Jackson, E.K. Cyclic AMP-Adenosine Pathway Induces Nitric Oxide Synthesis in Aortic Smooth Muscle Cells. *Hypertension* **1998**, *31*, 296–302. [CrossRef]
30. Pacher, P.; Beckman, J.S.; Liaudet, L. Nitric Oxide and Peroxynitrite in Health and Disease. *Physiol. Rev.* **2007**, *87*, 315–424. [CrossRef]
31. Brito, C.; Naviliat, M.; Tiscornia, A.C.; Vuillier, F.; Gualco, G.; Dighiero, G.; Radi, R.; Cayota, A.M. Peroxynitrite Inhibits T Lymphocyte Activation and Proliferation by Promoting Impairment of Tyrosine Phosphorylation and Peroxynitrite-Driven Apoptotic Death. *Am. Assoc. Immnol.* **1999**, *162*, 3356–3366.
32. Birnboim, H.C.; Lemay, A.-M.; Lam, D.K.Y.; Goldstein, R.; Webb, J.R. Cutting Edge: MHC Class II-Restricted Peptides Containing the Inflammation-Associated Marker 3-Nitrotyrosine Evade Central Tolerance and Elicit a Robust Cell-Mediated Immune Response. *J. Immunol.* **2003**, *171*, 528–532. [CrossRef] [PubMed]
33. Udenwobele, D.I.; Su, R.C.; Good, S.V.; Ball, T.B.; Shrivastav, S.V.; Shrivastav, A. Myristoylation: An Important Protein Modification in the Immune Response. *Front. Immunol.* **2017**, *8*, 751. [CrossRef] [PubMed]
34. Mohammadinejad, A.; Mohajeri, T.; Aleyaghoob, G.; Heidarian, F.; Kazemi Oskuee, R. Ellagic Acid as a Potent Anticancer Drug: A Comprehensive Review on in Vitro, in Vivo, in Silico, and Drug Delivery Studies. *Biotechnol. Appl. Biochem.* **2021**. [CrossRef] [PubMed]
35. Roche, P.A.; Furuta, K. The Ins and Outs of MHC Class II-Mediated Antigen Processing and Presentation. *Nat. Rev. Immunol.* **2015**, *15*, 203–216. [CrossRef]
36. Wosen, J.E.; Mukhopadhyay, D.; MacAubas, C.; Mellins, E.D. Epithelial MHC Class II Expression and Its Role in Antigen Presentation in the Gastrointestinal and Respiratory Tracts. *Front. Immunol.* **2018**, *9*, 2144. [CrossRef]

37. Betapudi, V. Myosin II Motor Proteins with Different Functions Determine the Fate of Lamellipodia Extension during Cell Spreading. *PLoS ONE* **2010**, *5*, e8560. [CrossRef]
38. Sebbagh, M.; Hamelin, J.; Bertoglio, J.; Solary, E.; Bréard, J. Direct Cleavage of ROCK II by Granzyme B Induces Target Cell Membrane Blebbing in a Caspase-Independent Manner. *J. Exp. Med.* **2005**, *201*, 465–471. [CrossRef]
39. Ma, M.P.C.; Chircop, M. SNX9, SNX18 and SNX33 Are Required for Progression through and Completion of Mitosis. *J. Cell Sci.* **2012**, *125 Pt 18*, 4372–4382. [CrossRef]
40. Lee, A.S.Y.; Kranzusch, P.J.; Doudna, J.A.; Cate, J.H.D. EIF3d Is an MRNA Cap-Binding Protein That Is Required for Specialized Translation Initiation. *Nature* **2016**, *536*, 96–99. [CrossRef]
41. Ayloo, S.; Lazarus, J.E.; Dodda, A.; Tokito, M.; Ostap, E.M.; Holzbaur, E.L.F. Dynactin Functions as Both a Dynamic Tether and Brake during Dynein-Driven Motility. *Nat. Commun.* **2014**, *5*, 4807. [CrossRef] [PubMed]
42. Zhao, B.; Shu, C.; Gao, X.; Sankaran, B.; Du, F.; Shelton, C.L.; Herr, A.B.; Ji, J.Y.; Li, P. Structural Basis for Concerted Recruitment and Activation of IRF-3 by Innate Immune Adaptor Proteins. *Proc. Natl. Acad. Sci. USA* **2016**, *113*, E3403–E3412. [CrossRef] [PubMed]
43. Moreno-Corona, N.C.; Lopez-Ortega, O.; Flores Hermenegildo, J.M.; Berron-Ruiz, L.; Rodriguez-Alba, J.C.; Santos-Argumedo, L.; Lopez-Herrera, G. Lipopolysaccharide-Responsive Beige-like Anchor Acts as a CAMP-Dependent Protein Kinase Anchoring Protein in B Cells. *Scand. J. Immunol.* **2020**, *92*, e12922. [CrossRef] [PubMed]
44. Ahsan, H. 3-Nitrotyrosine: A Biomarker of Nitrogen Free Radical Species Modified Proteins in Systemic Autoimmunogenic Conditions. *Hum. Immunol.* **2013**, *74*, 1392–1399. [CrossRef] [PubMed]
45. Teixeira, D.; Fernandes, R.; Prudêncio, C.; Vieira, M. 3-Nitrotyrosine Quantification Methods: Current Concepts and Future Challenges. *Biochimie* **2016**, *125*, 1–11. [CrossRef]
46. Lachance, Y.; Luu-the, V.; Verreault, H.; Dumont, M.; Rhéaume, E.; Leblanc, G.; Labrie, F. Structure of the Human Type II 3 Beta-Hydroxysteroid Dehydrogenase/Delta 5-Delta 4 Isomerase (3 Beta-HSD) Gene: Adrenal and Gonadal Specificity. *DNA Cell Biol.* **1991**, *10*, 701–711. [CrossRef]
47. Whirledge, S.; Cidlowski, J.A. Steroid Hormone Action. *Yen Jaffes Reprod. Endocrinol. Physiol. Pathophysiol. Clin. Manag. Eighth Ed.* **2019**, 115–131. [CrossRef]
48. Atanassova, N.; Koeva, Y. Hydrohysteroid Dehydrogenases—Biological Role and Clinical Importance—Review. *Dehydrogenases* **2012**. [CrossRef]
49. Requena, J.R.; Chao, C.C.; Levine, R.L.; Stadtman, E.R. Glutamic and Aminoadipic Semialdehydes Are the Main Carbonyl Products of Metal-Catalyzed Oxidation of Proteins. *Proc. Natl. Acad. Sci. USA* **2001**, *98*, 69–74. [CrossRef]
50. Kausar, S.; Wang, F.; Cui, H. The Role of Mitochondria in Reactive Oxygen Species Generation and Its Implications for Neurodegenerative Diseases. *Cells* **2018**, *7*, 274. [CrossRef]
51. Khosravi, S.; Harner, M.E. The MICOS Complex, a Structural Element of Mitochondria with Versatile Functions. *Biol. Chem.* **2020**, *401*, 765–778. [CrossRef] [PubMed]
52. Duan, J.; Li, Y.; Gao, H.; Yang, D.; He, X.; Fang, Y.; Zhou, G. Phenolic Compound Ellagic Acid Inhibits Mitochondrial Respiration and Tumor Growth in Lung Cancer. *Food Funct.* **2020**, *11*, 6332–6339. [CrossRef] [PubMed]
53. Shafie, B.; Pourahmad, J.; Rezaei, M. N-Acetylcysteine Is More Effective than Ellagic Acid in Preventing Acrolein Induced Dysfunction in Mitochondria Isolated from Rat Liver. *J. Food Biochem.* **2021**, *45*, e13775. [CrossRef] [PubMed]
54. Alfei, S.; Marengo, B.; Zuccari, G. Oxidative Stress, Antioxidant Capabilities, and Bioavailability: Ellagic Acid or Urolithins? *Antioxidants* **2020**, *9*, 707. [CrossRef]
55. Llavanera, M.; Delgado-Bermúdez, A.; Mateo-Otero, Y.; Padilla, L.; Romeu, X.; Roca, J.; Barranco, I.; Yeste, M. Exploring Seminal Plasma GSTM3 as a Quality and In Vivo Fertility Biomarker in Pigs—Relationship with Sperm Morphology. *Antioxidants* **2020**, *9*, 741. [CrossRef] [PubMed]
56. Schieber, M.; Chandel, N.S. ROS Function in Redox Signaling and Oxidative Stress. *Curr. Biol.* **2014**, *24*, R453–R462. [CrossRef]
57. Schaich, K.M. Toxicity of Lipid Oxidation Products Consumed in the Diet. *Baileys Ind. Oil Fat Prod.* **2020**, 1–88. [CrossRef]
58. Davis, C.W.; Hawkins, B.J.; Ramasamy, S.; Irrinki, K.M.; Cameron, B.A.; Islam, K.; Daswani, V.P.; Doonan, P.J.; Manevich, Y.; Madesh, M. Nitration of the Mitochondrial Complex I Subunit NDUFB8 Elicits RIP1- and RIP3-Mediated Necrosis. *Free Radic. Biol. Med.* **2010**, *48*, 306–317. [CrossRef]
59. Ott, C.; Dorsch, E.; Fraunholz, M.; Straub, S.; Kozjak-Pavlovic, V. Detailed Analysis of the Human Mitochondrial Contact Site Complex Indicate a Hierarchy of Subunits. *PLoS ONE* **2015**, *10*, e0120213. [CrossRef]
60. Bragança, C.E.; Kraut, D.A. Mode of Targeting to the Proteasome Determines GFP Fate. *J. Biol. Chem.* **2020**, *295*, 15892–15901. [CrossRef]
61. Hass, C.S.; Lam, K.; Wold, M.S. Repair-Specific Functions of Replication Protein A. *J. Biol. Chem.* **2012**, *287*, 3908–3918. [CrossRef] [PubMed]

Capítulo 4.4. α-Amino Adipic Acid, Marker of Protein Oxidation and Analogue of Neurotransmitter Glutamic Acid, Causes Mitochondrial Disturbance, Oxidative Stress and Apoptosis on Differentiated Human Neuronal SH-SY5Y Cells

El ácido α-Amino adípico, marcador de la oxidación de proteínas y análogo del neurotransmisor ácido glutámico, causa perturbación mitocondrial, estrés oxidativo y apoptosis en células neuronales humanas diferenciadas SH-SY5Y

Autores: Silvia Díaz-Velasco, Josué Delgado, Fernando J. Peña, Mario Estévez

α-Amino Adipic Acid, Marker of Protein Oxidation and Analogue of Neurotransmitter Glutamic Acid, Causes Mitochondrial Disturbance, Oxidative Stress and Apoptosis on Differentiated Human Neuronal SH-SY5Y Cells

S. Díaz-Velasco[1], J. Delgado[2], F.J. Peña[3], M. Estévez[1*]

[1] Food Technology and Quality (TECAL), Institute of Meat and Meat Products (IPROCAR), University of Extremadura, Cáceres, Spain.

[2] Food Hygiene and Safety (HISEALI), Institute of Meat and Meat Products (IPROCAR), University of Extremadura, Cáceres, Spain.

[3] Spermatology Laboratory, University of Extremadura, Cáceres, Spain.

Short title: "oxidative stress on differentiated human neuronal cells caused by α-amino adipic acid and glutamic acid"

*Corresponding author: Mario Estévez, Institute of Meat and Meat Products (IPROCAR), University of Extremadura, Avda. de las Ciencias, s/n. 10003, Cáceres, Spain. Phone number: +34 927251390. Email: mariovet@unex.es

Abstract

The α-amino adipic acid (α-AA), a six-carbon analog of glutamic acid (GLU), is an oxidized amino acid present in ultra-processed foods and other biological systems, which is involved in oxidative stress and chronic diseases. The aim of the present study was to unveil the molecular mechanisms of the cytotoxicity of 4mM α-AA when compared to the same concentration of GLU on differentiated human neuronal SH-SY5Y cells for 24h. Their effects and potential functional analogy were assessed by means of a MS-based platform (Orbitrap) for proteomics analyses, flow cytometry and protein oxidation markers. Results revealed that only the neurotransmitter GLU was able to induce activation of mitochondrial activity, which is consistent with its bioactivity on neuronal cells. Yet, such activation occurred along with a higher abundance of mitochondrial superoxide dismutase [Mn] enzyme (SOD2), which is a protective mechanism against formation of reactive oxygen species and oxidative stress. The analog α-AA did not seem to display the same protective effects and the lack of a proper mitochondrial activity, led to increased accretion of protein carbonyls and apoptotic proteins. In conclusion, α-AA may lead to oxidation-driven toxicological effects on neurons. The analogy with GLU may have facilitated these noxious mechanisms by using similar entrance mechanisms or initially activating similar biological processes. The clinical consequences on enduring exposure to this oxidized amino acid are being analyzed in *in vivo* studies.

Keywords: α-Amino adipic Acid; Glutamic acid; Flow cytometry; Proteomics; Protein oxidation; Superoxide dismutase

1. INTRODUCTION

The onset of enduring oxidative stress is a major factor involved in neurodegenerative disorders, such as Alzheimer's disease [1], Parkinson's syndrome [2], depression and amyotrophic lateral sclerosis [3], among others. In addition, oxidative stress is the underlying molecular mechanism in other number of diseases, such as diabetes and metabolic syndrome [4], chronic inflammation [5,6] or colorectal carcinogenesis [7]. Glutamic acid (GLU) is the main excitatory neurotransmitter in human brain and is essential for the normal functioning of the body [8]. However, when GLU is present in excess outside of protein as a single amino acid, turns into excitotoxic leading to neuronal damage or death [9]. In this regard, Sun et al. [10] reported that a positive correlation took place between a significant decrease in cell viability on differentiated human neuronal SH-SY5Y cells and the outside increase concentration of GLU from 0 to 100 mM in 24 h.

The α-amino adipic acid (α-AA), a final oxidation product of the amino acid lysine, is structurally similar to GLU and is considered a six-carbon structural analogue of this neurotransmitter [11,12]. da Silva et al. [13] claimed that α-AA induced oxidative stress and disturbance of glutamatergic neurotransmission in cerebral cortex slices of adolescent rats at 4mM. In a previous *in vitro* study by Díaz-Velasco et al. [14], α-AA was found to cause a significant decrease in cell viability on differentiated human colon CACO-2 cells at 200 μM, and Estaras et al. [15] reported the deleterious actions of α-AA on mouse pancreatic acinar cells. In brain, α-AA is considered a gliotoxin affecting astrocytes and glial cells [16–18], but neurons did not appear to accumulate α-AA [19]. At present, the underlying mechanisms involved in the possible molecular analogy between α-AA and GLU and their possible toxicity or neuroprotection in neurons are in study. The α-AA and its potential toxicity has gained particular attention given that this oxidized amino acid is accumulated in ultra-processed foods as a result of the oxidation of dietary proteins [20]. Given the attributed role of ultra-processed foods on the onset of

chronic diseases, including neurodegenerative disorders [21] and that such foods are a dietary source of α-AA, gaining further insight into the potential neurotoxicity of this oxidized amino acid seems of indisputable scientific interest.

Therefore, the aim of the present study was to decipher the molecular basis of the possible toxicological effects of α-AA when exposed at 4mM to differentiated human neuronal SH-SY5Y cells for 24h. The effect on these cells was compared to that displayed by GLU for their potential role as molecular analogue of the latter. To fulfil this objective an MS-based untargeted proteomic approach was planned together with flow cytometry analysis and carbonyls measurements as protein oxidation biomarkers.

2. MATERIAL AND METHODS

2.1 Chemicals and cells

α-AA (CAS number 542-32-5) and glutamic acid (CAS number 6106-04-3) were purchased from Sigma-Aldrich (Sigma-Aldrich, Steinheim, Germany). The other reagents were acquired from Fisher (Fisher Scientific S.L., Madrid, Spain) and Panreac (Panreac Química, S. A., Barcelona, Spain). Water used was purified by passage through a Milli-Q system (Millipore Corp., Bedford, MA). Human neuroblastoma SH-SY5Y cell line was obtained from ECACC (European Collection of Authenticated Cell Cultures, Salisbury, UK).

2.2. Cell culture

SH-SY5Y cells, which had been widely used in the study of neurodegenerative diseases, were cultured in Dulbecco's modified eagle medium (DMEM), fetal bovine serum (FBS) (15% v/v), L-glutamine (1% v/v) and non-essential amino acids (1% v/v) in T-75 flasks at 37 ºC in a humidified atmosphere and 5% CO_2. Reaching confluence, SH-SY5Y cells were differentiated with retinoic acid (RA) at 10 μM for 7 days to obtain neuron-like properties such as neurite growth and morphological changes to mimic neuron response [22].

2.3. Experimental setting

Both α-AA and GLU were used at presumably toxicological doses of GLU (4mM) [10,13] and dissolved in 10 mL of supplemented DMEM. α-AA and GLU were then added and exposed to differentiated human neuronal SH-SY5Y cells for 24h in T-75 flasks at 37 ºC in a humidified incubator 95%air/5%CO_2. For comparison purposes, CONTROL cells were incubated in standard DMEM in the same conditions. Preliminary analysis of the culture media revealed GLU concentrations at negligible levels (<0.1 mm) while α-AA was not found (below detection/quantification limit). The experiment was replicated five times in independent flasks for α-AA, GLU and CONTROL cells. At 24 h, cells were harvested using 0.25% trypsin in 1 mM EDTA, centrifuged at 126 g for 5 min and suspended in 1 mL of phosphate-buffered saline (PBS) solution for further analysis.

2.4. Flow cytometry analysis

Samples were diluted in PBS to a final concentration 5 x 10^6 cells/mL and analyses were conducted using a Cytoflex® LX flow cytometer (Beckman Coulter, Brea, CA, USA) and a MYV flow cytometer (Miltenyi Biotec, Bergisch Gladbach, Germany,) equipped with red, blue, violet, ultraviolet, yellow and infrared lasers. The instruments were calibrated daily employing specific calibration beads provided by the manufacturer. A compensation overlap was performed before each experiment. Files were exported as FCS files and loaded and analyzed using Cytobank Software (Beckman Coulter, Brea, CA, USA). Harvested cells were divided into two groups for differentiated staining prior to cell cytometry analysis. On one hand, suspended cells were stained with 1 µL of Hoechst 33342 (16.2 mM stock solution) and 1 µL of CellEvent Caspase-3/7 Green Detection Reagent (2 mM stock solution) to measure cell viability and apoptosis, respectively. After thorough mixing, the cell suspension was incubated at room temperature in the dark for 20 min; then cells were loaded with 1 µL of ethidium homodimer (1.167 mM in DMSO) to measure necrosis and were incubated for further 10 min. These samples were filtered through MACS® smart trainer 30 µm filters and

immediately run on the Cytoflex® LX flow cytometer. Another batch of cells from the same experiment was stained with 0.3 µL of JC-1 (1µM) to measure mitochondrial activity and were incubated in the dark at room temperature for 20 min. Later, cells were loaded with 0.3 µL of MCB-1 (10 µM) to measure the reduced form of glutathione (GSH) concentration. After thorough mixing, samples were incubated for further 10 min and finally were filtered and immediately run on the MYV flow cytometer. Hoechst 33342 was excited with the violet laser (355nm) and fluorescence recorded at 450/50nm band pass filter. JC-1 was excited with the yellow laser (561nm) the aggregates and blue laser (488nm) the monomers and fluorescence collected at 525/50 and 610/20 nm bandpass filters respectively. MCB-1 was excited with the violet laser (405nm) and fluorescence recorded at 405/30 bandpass filter. The controls consisted of unstained and single-stained controls to properly set gates and compensations. Positive controls for high mitochondrial membrane potential (JC-1) consisted in high-quality stallion spermatozoa, as these cells have been found to display a high mitochondrial activity [23].

2.5. Sample preparation for LC-MS/MS Based Proteomics

Samples were processed as described by Díaz-Velasco et al. [14]. Briefly, samples were added 0.5 mL of lysis buffer pH 7,5 (100 mM Tris-HCl, 50 mM NaCl, 10% glycerol, 0.5 M EDTA pH 8,5). Immediately before use, lysis buffer was added 100 mM PMSF (Phenylmethansulfonylfluorid) and 100 µg/mL Pepstatin in a 1:100 proportion. Samples were shaken and sonicated (Branson Ultrasonics, Danbury, USA). Lysates were incubated on ice for 1h and were centrifuged in a 5427 R (Eppendorf, Hamburg, Germany) at 17562 g at 4 ºC for 10 min. All the clean supernatant was passed into new screw-capped Eppendorf tubes and protein concentration was measured, being an appropriate value ≥ 1µg/µL. Aliquots containing 50 µg of proteins were partially run in SDS-PAGE (4% stacking and 12% separating), just stopped when they reached the separating part of the gel. The gel was stained, and each lane was cut into 1 mm^3 pieces, distained, and subjected to in-gel digestion. Samples were incubated with 0.5 M DTT in

50 mM ammonium bicarbonate for 20 min at 56 °C for protein reduction. The resulting free thiol (-SH) groups were alkylated by incubating the samples with 0.55 M iodoacetamide in 50 mM ammonium bicarbonate at room temperature for 15 min in the dark. Later, a mix of 50 mM ammonium bicarbonate, ProteaseMAX (Promega, USA) and trypsin (Promega, USA) was added to the samples and incubated at 37 ºC for 8 h. After, acid formic was added to stop the proteolysis and the supernatant was removed of each sample and placed it into new Eppendorf tubes for drying in a vacuum concentrator. Finally, samples were added loading buffer (98% milli-Q water, 2% acetonitrile and 0.05% trifluoroacetic acid) and analyzed by an Orbitrap LC-MS/MS.

2.6. Label-free quantitative proteomic analyses

A Q-Exactive Plus mass spectrometer coupled to a Dionex Ultimate 3000 RSLCnano (Thermo Scientific) analyzed 5 µg from each digest. Data was collected using a Top15 method for MS/MS scans [24]. Comparative proteome abundance and data analysis were carried out using MaxQuant software (version 1.6.0.15.0; https://www.maxquant.org/download_asset/maxquant/latest) and Perseus (v 1.6.14.0) to organize the data and perform statistical analysis. Carbamidomethylation of cysteines was set as a fixed modification; oxidation of methionines and acetylation of N-terminals were set as variable modifications. Database searching was performed against Homo sapiens protein database (www.uniprot.org). The maximum peptide/protein false discovery rates (FDR) were set to 1% based on comparison to a reverse database. The MaxLFQ algorithm was used to generate normalized spectral intensities and infer relative protein abundance. Among all the identified proteins, only those detected in at least two replicates (from five replicates in each treatment) from at least one treatment (CONTROL, GLU or α-AA), were retained for analysis. In other words, proteins found only in one replicate from just one treatment were not considered for further analysis. Additionally, proteins that matched to a contaminant database or the reverse database were removed from further analysis. When proteins fulfilled the aforementioned

requirements and occurred in at least 2 treatments, quantitative analysis was performed using a T-test to compare such treatments in paired analysis (GLU vs CONTROL; α-AA vs CONTROL and GLU vs. α-AA). Significant fold changes were calculated for each protein to assess the relative abundance (increase or decrease) of such protein in a treatment as compared to the counterpart. This fold change was expressed as Log_2. A qualitative analysis was also performed when proteins were found in at least three replicates of a given group in study but were undetectable in the counterpart group. Proteins satisfying one of these two aforementioned criteria and hence, subjected to quantitative or qualitative analysis were identified as discriminating proteins, and their corresponding genes were grouped by biological processes and molecular functions through ClueGO (v. 2.5.6) [25]. To define term-term interrelations and functional groups based on shared genes between the terms, the Kappa score was stablished at 0.4. Three GO terms and 4% of genes covered were set as the minimum required to be retained in the final result. The *p-value* was corrected by Bonferroni step down and set as $p \leq 0.05$.

2.6. Quantification of reduced and oxidized glutathione

The reduced (GSH) form of glutathione was analyzed in cells by UHPLC-MS/MS according to the method reported by Ortega-Ferrusola et al. [26]. Analytes were extracted from lysed cells upon sonication (1 min) and ultracentrifugation (4000 g/5 min). The supernatant was filtered through 0.22 µL nylon filters and diluted for LC analysis. Chromatographic and spectrometer conditions were published elsewhere [26]. Quantification was performed injecting standard curves of the original compounds in the same conditions. Results were expressed as nmol GSH/mg protein.

2.7. Analysis of protein oxidation markers

Early protein carbonyls, α-aminoadipic semialdehyde (α-AS) and γ-glutamic semialdehyde (γ-GS), and an advanced oxidation protein product (AOPP, pentosidine), were analyzed as oxidation biomarkers in differentiated human neuronal cells. The

procedure was followed as described by Utrera et al. [27] with minor modifications. One hundred µL of the cell lysates were treated with 1 mL of cold 10% trichloroacetic acid (TCA) solution, then proteins were precipitated with centrifugation at 2240 g for 5 min at 4 °C. The supernatant was removed, and the pellet was added 1 mL of cold 5% TCA solution. A new centrifugation was performed at 2240 g for 5 min at 4 °C for protein precipitation. The supernatant was removed again, and the pellets were derivatized with p-amino-benzoic acid (ABA), purified and hydrolyzed following the procedure described by Utrera et al. [27]. The hydrolysates were evaporated at 40 °C in a vacuum concentrator and the generated residues were reconstituted with 200 µL of Milli-Q water and then filtered through hydrophilic polypropylene GH Polypro (GHP) syringe filters (0.45 µm pore size, Pall Corporation, NJ, USA) for HPLC analysis. Details on the chromatograph apparatus as well as on the separation, elution and identification of the compounds of interest were published elsewhere [27]. ABA and γ-GS-ABA were synthesized and purified following the procedure of Akagawa et al. [28] and injected in the same conditions than samples. Both semialdehydes and pentosidine were identified in samples by comparing their retention times with those of the reference pure compounds. Standard solutions of ABA (ranging from 0.1 to 0.5 mM) were also injected in the same chromatographic conditions to create a standard curve. The peaks corresponding to both semialdehydes and pentosidine were manually integrated and the resulting areas plotted against the aforementioned standard curve. Results are expressed as nmol of protein carbonyl per mg of protein.

2.8. Statistical Analysis

All experiments were performed five times and each individual sample was analyzed twice for flow cytometry. Data was analyzed for normality and homoscedasticity. The effect of the exposure to α-AA and GLU 4mM was assessed by Analysis of Variance (ANOVA). Tukey's test was used for multiple comparisons of the means. The

significance level was set at $p<0.05$. SPSS (version 27) was used for statistical analysis of the data.

3. RESULTS

3.1. Flow Cytometry and Protein Oxidation Markers

Regarding flow cytometry analyses, the parameters assessed were cell viability, apoptosis, necrosis, mitochondrial activity and reduced form of glutathione (GSH) concentration. No significant differences were found for cell viability (Fig.1A), which is in accordance with the lack of significant differences observed for late apoptosis and necrosis (Fig.1C and D, respectively), among the three groups. Yet, significant differences were found for apoptosis with neurons challenged with α-AA having higher percentage of apoptotic cells than control cells ($p<0.05$) while those exposed to GLU had an intermediate position. Irrespective of the statistical significance of these results, we may emphasize that differences between control and α-AA cells accounted for less than 6 percent points. Significant differences were also found between treated cells and control cells in regard to the population of cells producing ROS (Fig. 1E). Neurons exposed to α-AA had the significantly highest values, followed by GLU and control cells ($p<0.05$). Yet, a lack of significant differences was found when the concentration of ROS was calculated in subpopulations of apoptotic cells (Fig. 1F). No significant differences were found for GSH concentration among any of the treatments (Fig. 1G). This is in disagreement with the concentration of both reduced (GSH) and oxidized (GSSH) forms of glutathione as quantified by GC-MS. Table 1 shows that neurons challenged with α-AA had significantly lower concentration of GSH and higher of GSSH than the other two groups of cells. Finally, a significant increase was observed in mitochondrial activity in GLU treated cells ($p<0.01$) (Fig. 1H), compared to cells exposed to α-AA, and also to control cells. Fig. 2 illustrates two cytograms as obtained from the equipment and used for data processing.

The analysis of protein oxidation biomarkers was evaluated by the detection of early protein carbonyls (α-AS and γ-GS) and advanced oxidation protein products (AOPPs, pentosidine). The results showed a significant increase of both protein semialdehydes α-AS and γ-GS in cells exposed to the oxidized amino acid α-AA (3.11±0.72 nmol/mg protein and 0.29±0.04 nmol/mg protein, respectively) in comparison GLU counterparts (1.40±0.31 nmol/mg protein and 0.11±0.04 nmol/mg protein, respectively) (p<0.001). CONTROL cells had basal levels of protein carbonyls, which is compatible with cell homeostasis (1.05±0.36 nmol/mg protein and 0.08±0.02 nmol/mg protein). On the contrary, no significant differences were observed between treatment for the advanced oxidation protein product pentosidine (C: 3.72±0.61 nmol/mg protein; α-AA: 3.69±0.36 nmol/mg protein; GLU: 3.90±0.40 nmol/mg protein; p>0.05).

3.2. Proteomic Analyses

The MS-based proteomic platform enabled the identification of 2355 proteins in total. All these proteins were identified with at least two peptides and a FDR<1%. Quantitative (p<0.05) and qualitative (only detected in one condition) changes in protein abundance were evaluated (Tables S1-S2-S3).

On the one hand, the study between the proteomes from control cells *versus* α-AA - treated cells was performed, in which 186 proteins were significantly influenced by α-AA, among those, 63 proteins were detected in lower quantity in α-AA treatment and 24 were only found in non-treated control samples. On the other hand, 49 proteins were found in higher abundance in α-AA treated cells and 50 were only found in cells treated with α-AA.

Regarding the comparison of the proteomes control samples and GLU-treated cells, 433 proteins were significantly influenced by GLU. In this case, 179 were found in lower abundance in GLU-treated cells and 76 proteins were only found in non-treated control

samples, whereas 107 proteins were detected in higher quantity in GLU-treated cells and 71 were only found in GLU treatment.

To study the differences in the proteomes from α-AA-treated cells and GLU-treated cells, an additional comparison was performed between these two treatment groups. In this case, 361 proteins were significantly influenced by α-AA compared with GLU, among those, 153 were detected in lower quantity in GLU samples compared to α-AA-treated cells and 64 were only found in α-AA treated cells. Conversely, 115 proteins were found in higher abundance in GLU treatment compared to α-AA treatment and 29 were only found in GLU treated cells.

For a comprehensible and organized description and discussion of results, discriminating proteins were grouped by biological processes and molecular functions. The comparison between control cells *versus* α-AA-treated cells is shown in Fig. 3A-B; the comparison between non-treated control cells *versus* GLU-treated cells is shown in Fig. 4A-B; and finally, the comparison between α-AA- *versus* GLU-treated cells corresponds to Fig. 5A-B. Specific terms for each of these processes and full details of discriminating proteins and associated genes are provided in Supplementary material Tables S4-S9. Tables 2, 3 and 4 show a selection of representative proteins from each relevant biological process or molecular function affected by the presence of α-AA, GLU and the comparison between α-AA *versus* GLU, respectively. Only discriminating proteins having a defined biological significance to decipher the role of α-AA and GLU, are presented in the following sections.

3.2.1. Proteins found in lower relative abundance in cells exposed to α-AA compared to control counterparts

3.2.1.1. Cell cycle DNA replication

Among all the biological processes and molecular functions affected in differentiated human neuronal SH-SY5Y cells by the exposure of 4mM α-AA, the proteins involved in

cell cycle DNA replication were the most affected, leading to a disturbance in these cells. Almost one half of proteins found in lower concentration in α-AA-challenged neuron cells were related to this biological mechanism (42.86%, $p<0.01$) (Fig. 3A). We found low abundance of the proteins related to the MCM complex (Minichromosome maintenance complex), such as different DNA replication licensing factors (MCM2, fold change: 0.80; MCM3, fold change: 0.75; MCM4, fold change: 0.82; MCM6, fold change: 0.78) (Tables 2 and S1). These proteins are relevant in the pre-replicative complex assembly and the nuclear cell cycle DNA replication initiation (Supplementary Table S4).

3.2.1.2. Endothelial cell development

The exposure of α-AA induced a significant decrease in proteins related to the endothelial cell development (14.29%, $p<0.01$) (Fig. 3A). Among these proteins we may highlight actin filament capping and actin filament polymerization and depolymerization processes, such as alpha-adducin (ADD1, fold change: 0.88), radixin (RADI, fold change: 0.79), and tropomodulin 2 (TMOD2, only in control). Moreover, the vesicle-mediated transport between endosomal compartments was also impaired in proteins Coronin-1A (COR1A, only in control), and ezrin (EZRI fold change: 0.85) (Tables 2 and S1-S4).

3.2.1.3. COPI vesicle coat

The process of COPI formation (Coat Protein Complex I) was also influenced by α-AA exposure to differentiated human neuronal SH-SY5Y cells (8.93%, $p<0.01$) (Fig. 3A). The proteins implicated in the assembly of COPI were found in lower abundance in comparison with non-treated control cells, namely the subunits delta (COPD), beta (COPB2) and epsilon (COPE) of the coatomer (fold changes: 0.90; 0.89 and 0.78, respectively) (Tables 2 and S1-S4).

3.2.1.4. Other proteins of biological significance found in lower relative quantity in cells exposed to α-AA

Other biologically relevant proteins that have not been included in previous paragraphs, and were found in lower abundance in cells exposed to α-AA compared to control counterparts are tropomyosin alpha-1 (TPM1, fold change: 0.48), insulin-degrading enzyme (IDE, fold change: 0.89), amine oxidase (flavin-containing) A (AOFA, only in control), plexin-A4 (PLXA4, only in control), cytochrome b-c1 complex subunit (QCR7, only in control) and N-chimaerin (CHIN, only in control) (Tables 2 and S1).

3.2.2. Proteins found in higher relative quantity in cells exposed to α-AA compared to control counterparts

3.2.2.1. Establishment of protein localization to mitochondrion

The exposure to α-AA had, as most remarkable effect, a positive regulation of protein insertion into mitochondrial membrane involved in apoptotic signaling pathway (40.48%, $p<0.01$) (Fig. 3B). Proteins implicated in this process were BH3-interacting domain death agonist (BID, fold change: 1.33), glycylpeptide N-tetradecanoyltransferase 1 (NMT1, fold change: 1.15) and subunit theta of 14-3-3 protein (YWHAQ, fold change: 1.07) (Tables 2 and S1-S5).

3.2.2.2. Nuclear localization sequence binding

The nuclear localization sequence binding was also affected by α-AA exposure (28.57%, $p<0.01$) (Fig. 3B). In this process, the proteins found in higher quantity were related with the nuclear pore complex, such as, NUP214 (only in α-AA), NUP85 (fold change: 1.25), NUP98 (NUP98, fold change: 1.18) and Transportin-2 (TNPO2, only in α-AA) (Tables 2 and S1-S5).

3.2.3. Proteins found in lower relative abundance in cells exposed to GLU compared to control counterparts

3.2.3.1.DNA replication

Four mM GLU for 24 h had a similar effect on SH-SY5Y cells to that exerted by 4mM α-AA on the same cells in regard to the DNA replication. This process was affected by 26.24% (p<0.01) (Fig. 4A), and the proteins found in lower abundance were related to the MCM complex, as in the case of α-AA. The subunit 2 (MCM2, fold change: 0.74); subunit 3 (MCM3, fold change: 0.80) subunit 4 (MCM4, fold change: 0.85), subunit 5 (MCM5, fold change: 0.79) and subunit 6 (MCM6, fold change: 0.75) were relevant in lower quantity in comparison with control counterparts (Tables 3 and S2-S6).

3.2.3.2. mRNA metabolic process

mRNA metabolic process was influence by GLU exposure by 24.11% (p<0.01) (Fig. 4A). All the proteins found in lower quantity as compared to control counterparts were related to different steps of mRNA formation, namely, members of the cleavage and polyadenylation specificity factors of mRNA (CPFS1, fold change: 0.78; NUDT21, fold change: 0.85), the subunits 1 (ELAVL1) and 4 (ELAVL4) of the ELAVL-like protein family (fold changes: 0.89 and 0.83 respectively), heterogeneous nuclear ribonucleoprotein D0 (HNRNPD, fold change: 0.87), DAZ-associated protein 1 (DAZAP1, fold change: 0.74), heterogeneous nuclear ribonucleoprotein L-like (HNRNPLL, fold change: 0.76) (SNRNP70, fold change: 0.81) and zinc finger protein ZPR1 (ZRP1, fold change: 0.81) (Tables 3 and S2-S6).

3.2.3.3. Other proteins of biological significance found in lower relative quantity in GLU treated cells

Other biologically relevant proteins found in significantly lower abundance in GLU treated cells compared to control counterparts were serine/threonine-protein kinase Nek9 (NEK9, fold change: 0.53), cell division cycle and apoptosis regulator protein 1 (CCAR1, fold change: 0.68), torsin-1A (TOR1A, fold change: 0.76) and IDE (fold change: 0.75). On the other hand, proteins of biological significance only found in non-treated control cells were serine/threonine-protein kinase VRK1 (VRK1), programmed cell death protein

10 (PDCD10), tropomodulin-2 (TMOD2), coronin-1A (COR1A) and caspase-3 (CASP3) (Tables 3 and S2).

3.2.4. Proteins found in higher relative quantity in cells exposed to GLU compared to control counterparts

3.2.4.1. Mitochondrial inner membrane

Among the molecular processes and biological functions upregulated by GLU the mitochondrial inner membrane was the most affected (35.59%, $p<0.01$) (Fig. 4B). Certain proteins found in higher relative quantity compared to control counterparts, such as the subunits alpha (ATPF1A, fold change: 1.11), delta (ATP5F1D, only in GLU), e (ATP5ME, only in GLU) and K (ATP5MD, fold change: 1.54) were related to the mitochondrial proton-transporting ATP synthase activity (Supplementary table S7). Moreover, the subunit B1 of the mitochondrial ATP synthase F (0) complex (ATP5PB, fold change: 1.16) and the catalytic subunit A of the V-type proton ATPase (ATP6V1A, fold change: 1.11) were also present in higher abundance (Tables 2 and S2-S7). On the other hand, the subunits of the MICOS complex MIC19 (CHCHD3) and MIC60 (IMMT) (fold changes: 1.26 and 1.15 respectively), along with the mitochondrial stress-70 protein (HSPA9, fold change: 1.12) were relevant in higher relative abundance in comparison with non-treated control cells (Tables 3 and S2-S7).

3.2.4.2. Protein localization to endoplasmic reticulum

Within the protein localization to endoplasmic reticulum, the process ubiquitin ligase inhibitor activity was one of the most influenced by the exposure to GLU 4mM (31.36 %, $p<0.01$) (Fig. 4B). All the proteins found in higher abundance in this process, compared to non-treated control cells, were a ubiquitin-conjugating enzyme E2 L3 (UBE2L3, fold change: 1.13) and proteins of the rough endoplasmic reticulum (RER), such as protein RER1 (RER1, fold change: 1.37), reticulon-4 (RTN4, fold change: 1.22) and signal recognition particles, subunits SRP68 and SRP72 (fold changes: 1.26 and 1.21,

407 respectively). Furthermore, different ribosomal proteins were found (RPS7, RPS15,
408 RPS19, RPS20 and RPS23) (Table S7), among others (see fold changes in Tables 3
409 and S2).

410 *3.2.4.3. Other proteins of biological significance found in higher relative quantity*

411 Some relevant proteins that have not been included in previous paragraphs, and have a
412 significant biological relevance in GLU treated cells compared to control counterparts
413 were, mitochondrial manganese superoxide dismutase (SOD2, fold change: 4.49),
414 cytoplasmic cooper-zinc superoxide dismutase (SOD 1, only in GLU), the isoform 1 of
415 the subunit 4 of the cytochrome c oxidase (COX4I1, fold change: 1.80), mitochondrial
416 dihydrolipoyl dehydrogenase (DLD, fold change 2.14) and mitochondrial pyrroline-5-
417 carboxylate reductase 1 (PYCR1, fold change: 1.38) (Tables 3 and S2).

418 *3.2.5. Proteins found in lower relative abundance in cells exposed to GLU compared to*
419 *α-AA counterparts*

420 *3.2.5.1. RNA export from nucleus*

421 When comparing cells exposed to GLU compared to α-AA treated cells, the molecular
422 function most impaired by the exposure to GLU (33.68%, p<0.01) was RNA export from
423 nucleus (Fig. 5A). The tRNA export from nucleus and the structural constituent of nuclear
424 pore processes were the most affected (Table S8) in different nuclear pore complex
425 proteins, such as NUP205, NUP62, NUP88, NUP93 (fold changes: 0.90, only in α-AA,
426 0.84 and 0.75, respectively) and E3 SUMO-protein ligase RanBP2 (RANBP2, fold
427 change: 0.83) (Table 4 and S3-S8).

428 *3.2.5.2. Endopeptidase complex*

429 The endopeptidase complex was influenced in GLU treated cells compared to α-AA
430 counterparts (15.79%, p<0.01) (Fig 4A). In particular, the cytosolic proteasome complex
431 was the most remarkable process (Table S8) affected by GLU compared to α-AA

treatment. Noticeable proteins found in lower quantity in this process were IDE (fold change: 0.84) and different proteasome regulatory subunits, such as PSMC5, PSMC1, PSMA6, PSMB7 and ADRM1 (see fold changes in Table 4). Moreover, isozyme L5 of ubiquitin carboxyl-terminal hydrolase (UCHL5, fold change: 0.89), the homolog A of UV excision repair protein RAD23 (RD23A, fold change: 0.84), and proteins involved in anchoring in the endoplasmic reticulum, PIGK (fold change: 0.80) and PIGU (only in α-AA), were also found in lower abundance (Table 4 and S3-S8).

3.2.5.3. Regulation of mRNA metabolic process

Other process influenced to GLU 4mM exposure compared to α-AA treatment, was the regulation of mRNA metabolic process (9.47%, $p<0.01$) (Fig. 5A). Proteins found in lower quantity in this process were related to the constitutive and alternative splicing (Table S8), namely, SNRNP70 (fold change: 0.78), SRPK2 (only in α-AA), SMU1 (fold change: 0.89), LARP7 (fold change: 0.88), KHDRBS1 (fold change: 0.83) and DDX17 (fold change: 0.90) (see complete protein names in Table 4).

3.2.5.4. Other proteins of biological significance found in lower relative abundance

Some proteins that have not been included previously and have a significant relevant in cells exposed to GLU compared to α-AA counterparts are NEK9 (fold change:0.48), CCAR1 (fold change: 0.72), TOR1A (fold change: 0.74), VRK1 (fold change: only in AAA), TNPO2 (only in α-AA), NMT1 (fold change: 0.85) and the subunits theta, beta/alpha and epsilon of 14-3-3 protein, namely YWHAQ, YWHAB and YWHAE (fold changes: 0.88, 0.76 and 0.87, respectively) (Table 4 and S3).

3.2.6. Proteins found in higher relative quantity in cells exposed to GLU compared to α-AA counterparts

3.2.6.1. Protein targeting to ER

The most affected process in cells exposed to GLU compared to α-AA treatment, was protein targeting to ER (endoplasmic reticulum) (35.25%, p<0.01) (Fig. 5B). In this case, the proteins found in higher abundance were different components of the large and small ribosomal subunits involved in SRP-dependent cotranslational protein targeting to membrane process (Table S9), namely, PIN4, LMS1, RPS14, RPS15, RPS27, RPS5, RPSA, RPS26, RPL31 and RPL35 (see complete names and fold changes in Tables 4 and S3), among many others.

3.2.6.2. Vacuolar transport

Other biological process influenced in GLU treated cells compared to α-AA counterparts, was vacuolar transport (10.79%, p<0.01) (Fig. 5B), in which the proteins found in higher quantity were vacuolar proteins, such as, the protein 4b of charged multivesicular body (CHMP4B, only in GLU), protein 25 of vacuolar protein-sorting-associated (VPS25, fold change: 1.13), and homolog protein VTA1 of vacuolar protein sorting-associated (VTA1, fold change: 1.22). In addition, proteins hepatocyte growth factor-regulated tyrosine kinase substrate (HGS, fold change: 1.22), and heterogeneous nuclear ribonucleoprotein U (HNRNPU, fold change: 1.10) were also found in higher abundance (Table 4 and S3-S9).

3.2.6.3. Branched-chain amino acid catabolic process

Branched-chain amino acid catabolic process was also affected in GLU treated cells (10.07%, p< 0.01) (Fig. 5B). Proteins involved in this process and found in higher quantity compared to α-AA treatment were the mitochondrial acetyl-CoA acetyltransferase (ACAT1, fold change: 1.11), branched-chain-amino-acid aminotransferase (BCAT2, only in GLU), hydroxymethylglutaryl-CoA lyase (HMGCL, only in GLU), the subunit alpha of the methylcrotonoyl-CoA carboxylase (MCCC1, only in GLU) and DLD (fold change: 1.70). (Table 4 and S3). These enzymes are related to the catabolism of the essential branched chain amino acids leucine, isoleucine and valine (Table S9).

3.2.6.4. Other proteins of biological significance found in higher relative abundance

Proteins of biological significance that have not been included previously and have found in higher abundance compared to α-AA counterparts are AOFA (only in GLU), SOD2 (fold change: 2.60), TPM1 (fold change: 2.01), microsomal glutathione S-transferase 3 (MGST3, fold change: 1.44) and alpha-synuclein (SNCA, fold change: 1.34) (Table 4 and S3).

4. DISCUSSION

Oxidative stress is a condition involved in neurodegenerative disorders such as Alzheimer's disease [29] and Parkinson's syndrome [30], among many others. α-AA, a six-carbon homologue of GLU, is an oxidized amino acid associated with pathological disorders where oxidative stress has a critical role [31,32]. α-AA has been studied previously on differentiated human enterocytes CACO-2 cells, verifying an impact in cytoskeletal dynamics, mitochondrial function, depletion of antioxidant defenses and the accretion of protein carbonyls Díaz-Velasco et al. [14]. GLU, as a main excitatory neurotransmitter, is essential for the normal functioning of the brain [8], but also can exert a neuronal damage or even cell death [9]. The structural homology between α-AA and GLU could explain the involvement of both species on the same biological processes and molecular functions in these cells, but the results revealed that α-AA and GLU share similarities in increasing or decreasing concentrations of certain proteins comparing with non-treated control cells, but the altered molecular mechanisms are not the same. The most relevant biological impairments caused by a-AA and GLU in differentiated human neuronal SH-SY5Y cells are discussed below. Fig. 6 illustrates the biological processes and molecular functions affected in these cells by the exposure to a-AA and GLU.

4.1. Impact of α-AA and GLU in DNA replication, cytoskeletal dynamics and vesicle transport

In the presence of either α-AA or GLU at 4mM, a significant decrease in MCM complex proteins was observed, when compared to control counterparts. MCM complex is related to the pre-replicative complex assembly involved in cell cycle DNA replication (Tables 1, 2, S4 and S6). MCM complex is a DNA helicase which consists in a 2-7 protein complex required for the initiation and elongation of DNA replication [33]. MCM complex is targeted by several checkpoints, such as S-phase entry and S-phase arrest [34]. Overexpression in MCM2-7 complex is involved in several types of cancer in humans, but its role in neurons is not clear [35]. Thus, in this regard, both α-AA and GLU, could be considered as analogues exerting a positive effect on neurons, preventing their aberrant entry into the cell cycle, which is involved in many types of neurodegenerative diseases [36]. These proteomics results are compatible with those obtained by flow cytometry, in which cell viability is not affected by any of the compounds.

Yet, some differences were found between GLU and α-AA in regards to physiology of cell cycle. The exposure to GLU caused a downward trend in proteins implicated in aberrant cell cycle progression as compared to cells exposed to α-AA and also to CONTROL cells. Proteins involved in G1/S transition and S phase progression, and in cell cycle progression and proliferation were found in lower abundance in GLU-treated cells. In neurons, TOR1A protein can link the cytoskeleton to the nuclear envelope, a mechanism that appears to be crucial for the control of nuclear polarity, cell movement and nuclear envelope integrity [37]. Furthermore, CCAR1 protein, involved in cell division cycle and apoptosis regulator [38], and NEK9 protein, implicated in centrosome separation and mitotic spindle assembly, were found in lower quantity in GLU-treated cells. Particularly, NEK9 is also involved in nuclear pore complex disassembly [39], a biological process that was also decreased in cells exposed to GLU. Taken together, these effects could indicate that GLU avoid, at the tested dose (4mM) an aberrant reentry

of neuronal cells into the cell cycle. Conversely, proteins of the proteasome complex, from the ubiquitin system, and proteins from the nuclear pore complex and constitutive and alternative splicing proteins were found in higher abundance in cells exposed to the GLU analogue, α-AA, corroborating that this oxidized amino acid would significantly affect core biological processes in neurons, such as those related to protein turnover and a potential DNA damage.

On the other hand, processes involved in cytoskeletal dynamics, such as actin filament polymerization and depolymerization and the stabilization of cytoskeleton actin filaments in cells were influence by α-AA (Table 2). The proteins involved in these biological processes were found in lower quantity in cells exposed to α-AA compared to non-treated CONTROL cells (Table S4). Moreover, the stabilization of cytoskeleton actin filaments was also decreased in α-AA treated cells when we compared to GLU treatment at the same dose (Table 4). The lower abundance found in proteins involved in these processes, and more specifically, tropomyosin (TPM1), could lead to a disturbance in the normal organization of cytoskeleton and in the formation of neurites, contributing to the onset of neurological diseases [40]. The vesicle-mediated transport between endosomal compartments was also impaired in similar proteins (Table S4). In fact, vesicle transport and multivesicular body (MVB) formation and sorting of endosomal cargo proteins into MVBs, were also found in lower quantity in α-AA-treated cells compared to those exposed to GLU (Table 4). Proteins implicated in the assembly of the coat protein complex I (COPI), also related to vesicle transport, were found in lower abundance in α-AA treated cells compared to control counterparts. The COPI, which is involved in the sorting of proteins and lipids between Golgi cisternae and retrieval from the Golgi to the ER, was significantly affected by α-AA in different protein subunits of this complex. This pathway plays an important role on key cellular processes, such as protein quality control [41]. Therefore, α-AA impaired vacuolar transport and protein targeting to ER, potentially leading to a negative impact in the formation of blebs implicated in Golgi-

562 ER transport. The sequestration of α-AA in vacuoles is considered as a safety
563 mechanism to avoid the toxicity of the oxidized amino acid in cells [42]. Interestingly, the
564 present results indicate that α-AA could facilitate the execution of cytotoxic effects by
565 decreasing the cellular mechanisms of protection against it.

566 While it could be discussed that all the aforementioned biological processes affected by
567 α-AA and GLU, were mildly impaired according to the fold changes obtained in proteomic
568 analyses (Tables 1, 2 and 3), even subtle changes in key proteome components may
569 have physiological and/or clinical consequences. Hence the chronic exposure to α-AA
570 and/or GLU at 4mM on neurons biology may be an interesting topic of study.

571 **4.2. Influence of α-AA and GLU in mitochondrial activity, oxidative stress, and**
572 **antioxidant defenses**

573 Mitochondrial activity was the only flow cytometry condition that was found to significantly
574 increase in GLU-treated cells, compared to α-AA and the CONTROL counterparts (Fig.
575 1F). This finding is reasonable since GLU is a recognized neurotransmitter, and the
576 activation of mitochondrial activity is a common and typical feature of cellular
577 functionality, including neurons [43]. These results agree with proteomic analyses (Table
578 3), in which proteins related to ATP synthase and MICOS complex (mitochondrial contact
579 site and cristae organizing system) are found in higher quantity in GLU-treated cells, in
580 comparison with non-treated CONTROL cells and α-AA-treated counterparts (Tables 1
581 and 3). In particular, two main mitochondrial complex, MIB complex (mitochondrial
582 intermembrane space bridging complex), and SAM complex (sorting and assembly
583 machinery complex) [44,45], were influenced in several proteins found in higher
584 abundance in GLU-treated cells. Specifically, IMMT protein plays a crucial role in the
585 maintenance of the MICOS complex stability and the mitochondrial cristae morphology,
586 essential for the normal functioning of the mitochondria [46]. A correct morphology and
587 functionality of mitochondria in central nervous system is essential to guarantee
588 membrane excitability and to execute the complex processes of neurotransmission and

589 plasticity [47]. Otherwise, an inefficient mitochondrial activity and impaired ATP synthesis
590 leads to potential neurological disorders [48]. At this point, it seems reasonable to
591 hypothesize that while GLU analogue, α-AA, may be able to utilize certain cell resources
592 in cells, including GLU channels for mitochondrial transportation [49], the functional
593 outcome of its intracellular excursion is different. α-AA may not be able to activate
594 mitochondrial activity and conversely, leads to biological impairments as described as
595 follows.

596 The generation of ROS is an expected outcome of oxidative metabolism in mitochondria
597 from cells, including neurons [50]. Yet, the formation of reactive species is under tight
598 control by endogenous antioxidant defenses in these cells, given the role of oxidative
599 stress in neurological disorders [50]. The analysis of early protein oxidation markers in
600 in the cells studied, revealed that α-AA and GLU at 4mM promoted the onset of a pro-
601 oxidative environment as compared to CONTROL cells, yet the severity of the protein
602 damage was significantly higher in cells exposed to α-AA than in cells exposed to GLU.
603 The latter cells contained protein carbonyls within a physiological range [51]. According
604 to the proteome of neurons exposed to GLU, these cells were able to alleviate the
605 oxidative threat by strengthening some components of the endogenous antioxidant
606 defenses. Two main antioxidant defenses, SOD1 and SOD2, that scavenge superoxide
607 anion ($O_2^{\cdot-}$) in mitochondria [52], and which exert a protecting effect on neurons from
608 oxidative stress [53], were found in higher abundance in GLU- treated cells compared to
609 the CONTROL and α-AA counterparts. According to Vincent et al. [54], the abundance
610 of the mitochondrial SOD2 decreases $O_2^{\cdot-}$, and prevents subsequent cellular injury and
611 the activation of caspase-3-mediated mechanisms of apoptosis [54]. It is known that the
612 formation of SOD1 and SOD2 is into the mitochondria [55]. Thus, it is therefore
613 reasonable to consider that the increase in higher quantity of these two antioxidant
614 defenses are strongly related to the significant increase in mitochondrial activity, fact that
615 links with the reduction of oxidative stress conditions reflected in the decreasing of early

carbonyls. This situation takes place in our study, in which an increase in mitochondrial activity in neurons exposed to GLU is found, and it is not accompanied by a significant apoptosis or necrosis, corroborated by both flow cytometry analyses (Fig.1B-D) and proteomics results (Table 3).

On the contrary, cells exposed to α-AA did not seem to be able to respond effectively to the oxidative stress, which in fact, led to significantly elevated protein oxidation markers and to a significantly higher quantity in several proteins involved in apoptosis (Table 2). It is worth highlighting that the increase in apoptotic proteins in neurons exposed to α-AA was significant and was in fact manifested in higher extent of apoptotic events as analyzed by flow cytometry (Fig. 1B). The onset of oxidative stress in α-AA-treated cells as a result of an imbalance between the generation of ROS and SOD2 proteins may have biological consequences given that a shortage of SOD2 in neurons has been reported to be involved in decrease neurite outgrowth under basal conditions [54]. Thus, the results of the accretion of oxidized proteins, and lack of SOD2 in cells exposed to α-AA could be related to the decrease in proteins related to the cytoskeletal organization and DNA replication and elongation (previously reported), as long as these processes are involved in the formation of neurites. The impairment of the endogenous antioxidant defenses has been already proposed as a toxicological mechanism of α-AA. A study by da Silva et al. [13] found a significant depletion of GSH in the cerebral cortex of rats exposed to 4 mM of a-AA, but in our case, neither α-AA, nor GLU, had a significant effect on the concentration of intracellular GSH as measured by flow cytometry. Conversely the quantification of GSH and its oxidized form (GSSH) by GC-MS revealed the depletion of GSH and increase in GSSH in α-AA-treated cells which in line with results from Silva et al. [13] and compatible with cells suffering oxidative stress. Therefore, the differences between α-AA and GLU in the activation of routes involved in the elimination of oxidative stress through the activation of the antioxidant defenses SOD1 and SOD2 and the

differences in concentration of GSH, described for the first time in this study, may be critical to explain the oxidation-driven noxious effects of α-AA on neurons.

4.3. Impact of α-AA and GLU in apoptosis and necrosis

According to the proteomic analyses, α-AA treated-cells displayed, compared to CONTROL counterparts, a positive regulation of protein insertion into mitochondrial membrane involved in apoptotic signaling pathway. In particular, cells exposed to α-AA had increased concentration of proteins related to apoptotic mechanisms, such as BID, NMT1 and YWHAQ (Table 2 and S1). The amplified activation of apoptosis mechanisms in α-AA treatment was corroborated when GLU treated-cells were compared with α-AA counterparts, where NMT1 protein and more isoforms of 14-3-3 protein apart from YWHAQ (YWHAB and YWHAE) were found in higher quantity in neurons exposed to α-AA (Table 4 and S3). BID protein plays a crucial role in apoptosis [56], and the NMT1 enzyme is implicated in protein N-myristoylation, a post-translational modification that has been implicated in the onset and progression of a number of human diseases, such as cancer or Alzheimer's disease [57]. On the other hand, 14-3-3 proteins are a family of essential components in signaling pathways involved in apoptosis and cell proliferation [58]. Consistently, the implication of α-AA in the occurrence of apoptosis is probed through the significant increase in these apoptotic proteins.

The concentration of α-AA used in this study increases the concentration of proteins involved in apoptosis and this was in fact reflected in significant apoptosis events as shown by flow cytometry results (Fig. 1B). In the human brain, the concentration of α-AA is around 18 μM [12] and is found mostly in astrocytes and glial cells [19]. Even if the α-AA dose used in the present study (4mM) is higher than physiological concentrations in certain brain cells, α-AA did not affect the viability of neurons, showing the large plasticity and ability of neuronal cells to handle and detoxify potentially toxic species. Yet, as this compound is found at high quantities (from 200 to 800 μM) in certain ultra-processed foods [20], a sustained exposure of these cells to high concentrations of α-AA and other

669 oxidized amino acids could, in fact, contribute to explain neuronal physiological
670 impairments and hence, explain the connection between the intake of ultra-processed
671 foods and neurodegenerative disorders [59]. In fact, proteins related to the nuclear pore
672 complex (NPC) were also found in higher quantity in α-AA-treated cells (Table 2). NPC
673 is involved in the bidirectional transport of macromolecules between the nucleus and
674 cytoplasm [60], and its control is related to the onset and progression of pathological
675 diseases [61]. In particular, both NUP98 and NUP214 (both cytoplasmic filament NUPs),
676 have been found as a part of aberrant fusion proteins in cancers [62]. In contrast, cells
677 treated with GLU compared to CONTROL counterparts, showed no trend towards
678 apoptosis using a dose of 4mM. In flow cytometry analyses, apoptosis and necrosis in
679 GLU treated cells was not significant, nor was there a significant decrease in cell viability
680 compared to CONTROL cells. In addition, in proteomic analyses, the regulation of
681 intrinsic apoptotic signaling pathway process was only influenced a 0.85% (p<0.01) in
682 GLU treatment (Fig. 3B). Interestingly, proteins found in higher quantity in this process
683 were, unlike cells treated with α-AA, the antioxidant defenses SOD1 and SOD2, among
684 others (Table S7). Furthermore, SOD1 and SOD2, together with PYCR1, another
685 enzyme involved in cell protection against oxidative stress [63], were also found in higher
686 abundance in regulation of oxidative stress-induced cell death process. This explains the
687 basal levels of protein carbonyls in cells exposed to GLU (Table 1). The intracellular
688 concentration of GLU in neuronal cells is about 10 mM in the cytoplasm [64], therefore,
689 it is a normal situation that an exposure to GLU 4mM does not cause any tendency
690 towards oxidative stress or apoptosis.

691 **5. CONCLUSION**

692 α-AA, an oxidized amino acid present in severely processed foods, is a six-carbon
693 analogue of GLU involved in oxidative stress. We can confirm that these two compounds,
694 despite their structural analogy, are not functionally analogues, since α-AA leads, in most
695 of the biological processes under study, to diverge effects to those exhibited by the

neurotransmitter GLU. On the other hand, α-AA is implicated in boosting oxidative stress and apoptotic mechanisms in differentiated human neuronal SH-SY5Y cells, with this condition not being induced by GLU. The occurrence of antioxidant defenses linked to the increasing of mitochondrial activity in GLU-treated cells prevents the emergence of apoptotic proteins. In summary, an activation of harmful conditions is taking place in neurons exposed to 4mM α-AA while the eventual biological and clinical consequences of such molecular effects are unknown and required further elucidation.

Credit authorship contribution statement

S. Díaz-Velasco: data curation, methodology, formal analysis, writing - original draft.

J. Delgado: data curation, methodology, funding acquisition, supervision, formal analysis, validation, writing – review & editing.

F.J. Peña: data curation, methodology, funding acquisition, supervision, formal analysis, validation, writing – review & editing.

Mario Estévez: conceptualization, funding acquisition, project administration, resources, supervision, validation, writing – review & editing. All authors have read and agreed to the published version of the manuscript.

Declaration of competing interest

The authors declare that they have no known competing financial interests or personal relationships that could have appeared to influence the work reported in this paper.

Funding

This research was funded by the Spanish Ministry of Economics and Competitiveness (SMEC) (project number: AGL2017-84586-R), “Junta de Extremadura/FEDER” (project number: GR18104) and the Ministry of Science and Innovation (project number: PID2021-126193OB-I00). S. Díaz-Velasco is recipient of a fellowship from the Spanish Ministry of Science, Innovation and Universities (grant number PRE2018-084001). Q-

Exactive Orbitrap equipment was acquired by a grant from the Spanish Ministry of Science and Innovation (MCIN/AEI/ 10.13039/501100011033) (grant number: UNEX-AE-3394).

Data Availability Statement

All data is contained within the article or supplementary material, including raw data from Proteomics.

References

[1] F. Cioffi, R.H.I. Adam, K. Broersen, Molecular Mechanisms and Genetics of Oxidative Stress in Alzheimer's Disease, J. Alzheimer's Dis. 72 (2019) 981–1017. https://doi.org/10.3233/JAD-190863.

[2] J. Blesa, I. Trigo-Damas, A. Quiroga-Varela, V.R. Jackson-Lewis, Oxidative stress and Parkinson's disease, Front. Neuroanat. 9 (2015) 91. https://doi.org/10.3389/FNANA.2015.00091/BIBTEX.

[3] M. Yusuf, M. Khan, M.A. Robaian, R.A. Khan, Biomechanistic insights into the roles of oxidative stress in generating complex neurological disorders, Biol. Chem. 399 (2018) 305–319. https://doi.org/10.1515/HSZ-2017-0250/ASSET/GRAPHIC/J_HSZ-2017-0250_FIG_004.JPG.

[4] J.M. Dos Santos, S. Tewari, R.H. Mendes, The role of oxidative stress in the development of diabetes mellitus and its complications, J. Diabetes Res. 2019 (2019). https://doi.org/10.1155/2019/4189813.

[5] A. Federico, F. Morgillo, C. Tuccillo, F. Ciardiello, C. Loguercio, Chronic inflammation and oxidative stress in human carcinogenesis, Int. J. Cancer. 121 (2007) 2381–2386. https://doi.org/10.1002/IJC.23192.

[6] F.U. Vaidya, A.S. Chhipa, N. Sagar, C. Pathak, Oxidative stress and inflammation can fuel cancer, Role Oxidative Stress Pathophysiol. Dis. (2020)

746 229–258. https://doi.org/10.1007/978-981-15-1568-2_14/COVER.

747 [7] F. Carini, M. Mazzola, F. Rappa, A. Jurjus, A.G. Geagea, S. Al Kattar, T. Bou-
748 Assi, R. Jurjus, P. Damiani, A. Leone, G. Tomasello, Colorectal Carcinogenesis:
749 Role of Oxidative Stress and Antioxidants, Anticancer Res. 37 (2017) 4759–
750 4766. https://doi.org/10.21873/ANTICANRES.11882.

751 [8] A. Samuels, Dose dependent toxicity of glutamic acid: a review, Int. J. Food
752 Prop. 23 (2020) 412–419. https://doi.org/10.1080/10942912.2020.1733016.

753 [9] S. Magi, S. Piccirillo, S. Amoroso, The dual face of glutamate: from a neurotoxin
754 to a potential survival factor-metabolic implications in health and disease, Cell.
755 Mol. Life Sci. 76 (2019) 1473–1488. https://doi.org/10.1007/S00018-018-3002-X.

756 [10] J.F. Sun, M.Y. Zhao, Y.J. Xu, Y. Su, X.H. Kong, Z.Y. Wang, Fenamates Inhibit
757 Human Sodium Channel Nav1.2 and Protect Glutamate-Induced Injury in SH-
758 SY5Y Cells, Cell. Mol. Neurobiol. 40 (2020) 1405–1416.
759 https://doi.org/10.1007/S10571-020-00826-1/FIGURES/8.

760 [11] S. Huck, F. Grass, H. Hortnagl, The glutamate analogue alpha-aminoadipic acid
761 is taken up by astrocytes before exerting its gliotoxic effect in vitro, J. Neurosci. 4
762 (1984) 2650–2657. https://doi.org/10.1523/JNEUROSCI.04-10-02650.1984.

763 [12] P. Guidetti, R. Schwarcz, Determination of α-aminoadipic acid in brain,
764 peripheral tissues, and body fluids using GC/MS with negative chemical
765 ionization, Mol. Brain Res. 118 (2003) 132–139.
766 https://doi.org/10.1016/J.MOLBRAINRES.2003.08.004.

767 [13] J.C. da Silva, A.U. Amaral, C. Cecatto, A. Wajner, K. dos Santos Godoy, R.T.
768 Ribeiro, A. de Mello Gonçalves, Â. Zanatta, M.S. da Rosa, S.O. Loureiro, C.R.
769 Vargas, G. Leipnitz, D.O.G. de Souza, M. Wajner, α-Ketoadipic Acid and α-
770 Aminoadipic Acid Cause Disturbance of Glutamatergic Neurotransmission and

Induction of Oxidative Stress In Vitro in Brain of Adolescent Rats, Neurotox. Res. 32 (2017) 276–290. https://doi.org/10.1007/s12640-017-9735-8.

[14] S. Díaz-Velasco, J. Delgado, F.J. Peña, M. Estévez, Protein oxidation marker, α-amino adipic acid, impairs proteome of differentiated human enterocytes: Underlying toxicological mechanisms, Biochim. Biophys. Acta. Proteins Proteomics. 1870 (2022) 140797. https://doi.org/10.1016/J.BBAPAP.2022.140797.

[15] M. Estaras, F.Z. Ameur, M. Estévez, S. Díaz-Velasco, A. Gonzalez, The lysine derivative aminoadipic acid, a biomarker of protein oxidation and diabetes-risk, induces production of reactive oxygen species and impairs trypsin secretion in mouse pancreatic acinar cells, Food Chem Toxicol. 145 (2020) 111594. https://doi.org/10.1016/j.fct.2020.111594.

[16] D.R. Brown, H.A. Kretzschmar, The glio-toxic mechanism of α-aminoadipic acid on cultured astrocytes, J. Neurocytol. 27 (1998) 109–118. https://doi.org/10.1023/A:1006947322342.

[17] M. Pereira, I. Amaral, C. Lopes, C. Leitão, D. Madeira, P. Agosthino, T. FASEB, l-α-aminoadipate causes astrocyte pathology with negative impact on mouse hippocampal synaptic plasticity and memory, Wiley Online Libr. 35 (2021). https://doi.org/10.1096/fj.202100336R.

[18] A.D. Sherpa, P. van de Nes, F. Xiao, J. Weedon, S. Hrabetova, Gliotoxin-induced swelling of astrocytes hinders diffusion in brain extracellular space via formation of dead-space microdomains, Glia. 62 (2014) 1053–1065. https://doi.org/10.1002/GLIA.22661.

[19] D. V. Pow, Visualising the activity of the cystine-glutamate antiporter in glial cells using antibodies to aminoadipic acid, a selectively transported substrate, Glia. 34 (2001) 27–38. https://doi.org/10.1002/GLIA.1037.

[20] M. Estévez, S. Díaz-Velasco, R. Martínez, Protein carbonylation in food and nutrition: a concise update, Amin. Acids 2021 544. 54 (2021) 559–573. https://doi.org/10.1007/S00726-021-03085-6.

[21] B. Cardoso, P. Machado, E.M. Steele, Association between ultra-processed food consumption and cognitive performance in US older adults: a cross-sectional analysis of the NHANES 2011–2014, Eur. J. Nutr. 61 (2022) 3975–3985. https://doi.org/10.1007/S00394-022-02911-1/TABLES/3.

[22] S. Påhlman, A.I. Ruusala, L. Abrahamsson, M.E.K. Mattsson, T. Esscher, Retinoic acid-induced differentiation of cultured human neuroblastoma cells: a comparison with phorbolester-induced differentiation, Cell Differ. 14 (1984) 135–144. https://doi.org/10.1016/0045-6039(84)90038-1.

[23] J.M. Ortiz-Rodríguez, F.E. Martín-Cano, G.L. Gaitskell-Phillips, A. Silva, C. Ortega-Ferrusola, M.C. Gil, F.J. Peña, Low glucose and high pyruvate reduce the production of 2-oxoaldehydes, improving mitochondrial efficiency, redox regulation, and stallion sperm function†, Biol. Reprod. 105 (2021) 519–532. https://doi.org/10.1093/BIOLRE/IOAB073.

[24] J. Delgado, F. Núñez, M.A. Asensio, R.A. Owens, Quantitative proteomic profiling of ochratoxin A repression in Penicillium nordicum by protective cultures, Int. J.Food Microbiol. 305 (2019) 108243. https://doi.org/10.1016/j.ijfoodmicro.2019.108243.

[25] G. Bindea, B. Mlecnik, H. Hackl, P. Charoentong, M. Tosolini, A. Kirilovsky, W.-H. Fridman, F. Pagès, Z. Trajanoski, J. Galon, ClueGO: a Cytoscape plug-in to decipher functionally grouped gene ontology and pathway annotation networks, Bioinformatics. 25 (2009) 1091–1093. https://doi.org/10.1093/bioinformatics/btp101.

[26] C. Ortega Ferrusola, L. Anel-López, J.M. Ortiz-Rodriguez, P. Martin Muñoz, M.

Alvarez, P. de Paz, J. Masot, E. Redondo, C. Balao da Silva, J.M. Morrell, H. Rodriguez Martinez, J.A. Tapia, M.C. Gil, L. Anel, F.J. Peña, Stallion spermatozoa surviving freezing and thawing experience membrane depolarization and increased intracellular Na+, Andrology. 5 (2017) 1174–1182. https://doi.org/10.1111/ANDR.12419.

[27] M. Utrera, D. Morcuende, J.G. Rodríguez-Carpena, M. Estévez, Fluorescent HPLC for the detection of specific protein oxidation carbonyls - α-aminoadipic and γ-glutamic semialdehydes - in meat systems, Meat Sci. 89 (2011) 500–506. https://doi.org/10.1016/j.meatsci.2011.05.017.

[28] M. Akagawa, T. Sasaki, K. Suyama, Oxidative deamination of lysine residue in plasma protein of diabetic rats: Novel mechanism via the Maillard reaction, Eur. J. Biochem. 269 (2002) 5451–5458. https://doi.org/10.1046/j.1432-1033.2002.03243.x.

[29] J. Tchekalarova, R. Tzoneva, Oxidative Stress and Aging as Risk Factors for Alzheimer's Disease and Parkinson's Disease: The Role of the Antioxidant Melatonin, Int. J. Mol. Sci. (2023). https://doi.org/10.3390/ijms24033022.

[30] T. Sohrabi, B. Mirzaei-Behbahani, R. Zadali, M. Pirhaghi, L.A. Morozova-Roche, A.A. Meratan, Common Mechanisms Underlying α-Synuclein-Induced Mitochondrial Dysfunction in Parkinson's Disease, J. Mol. Biol. (2023) 167992. https://doi.org/10.1016/J.JMB.2023.167992.

[31] T.J. Wang, D. Ngo, N. Psychogios, A. Dejam, M.G. Larson, R.S. Vasan, A. Ghorbani, J. O'Sullivan, S. Cheng, E.P. Rhee, S. Sinha, E. McCabe, C.S. Fox, C.J. O'Donnell, J.E. Ho, J.C. Florez, M. Magnusson, K.A. Pierce, A.L. Souza, Y. Yu, C. Carter, P.E. Light, O. Melander, C.B. Clish, R.E. Gerszten, 2-Aminoadipic acid is a biomarker for diabetes risk, J. Clin. Invest. 123 (2013) 4309–4317. https://doi.org/10.1172/JCI64801.

[32] H.J. Lee, H.B. Jang, W.H. Kim, K.J. Park, K.Y. Kim, S.I. Park, H.J. Lee, 2-Aminoadipic acid (2-AAA) as a potential biomarker for insulin resistance in childhood obesity, Sci. Rep. 9 (2019) 1–10. https://doi.org/10.1038/s41598-019-49578-z.

[33] N.J. Rzechorzek, S.W. Hardwick, V.A. Jatikusumo, D.Y. Chirgadze, L. Pellegrini, CryoEM structures of human CMG–ATPγS–DNA and CMG–AND-1 complexes, Nucleic Acids Res. 48 (2020) 6980–6995. https://doi.org/10.1093/NAR/GKAA429.

[34] M.L. Bochman, A. Schwacha, The Mcm Complex: Unwinding the Mechanism of a Replicative Helicase, Microbiol. Mol. Biol. Rev. 73 (2009) 652. https://doi.org/10.1128/MMBR.00019-09.

[35] I. Rubio-Ferrera, P. Baladrón-De-Juan, L. Clarembaux-Badell, M. Truchado-Garcia, S. Jordán-Álvarez, S. Thor, J. Benito-Sipos, I.M. Cobeta, Selective role of the DNA helicase Mcm5 in BMP retrograde signaling during Drosophila neuronal differentiation, PLoS Genet. 18 (2022). https://doi.org/10.1371/JOURNAL.PGEN.1010255.

[36] S. Nandakumar, E. Rozich, L. Buttitta, Cell Cycle Re-entry in the Nervous System: From Polyploidy to Neurodegeneration, Front. Cell Dev. Biol. 9 (2021). https://doi.org/10.3389/FCELL.2021.698661/FULL.

[37] J. Hettich, S.D. Ryan, O.N. de Souza, L.F. Saraiva Macedo Timmers, S. Tsai, N.A. Atai, C.C. da Hora, X. Zhang, R. Kothary, E. Snapp, M. Ericsson, K. Grundmann, X.O. Breakefield, F.C. Nery, Biochemical and Cellular Analysis of Human Variants of the DYT1 Dystonia Protein, TorsinA/TOR1A, Hum. Mutat. 35 (2014) 1101–1113. https://doi.org/10.1002/HUMU.22602.

[38] K. Promthep, C. Nopparat, S. Mukda, S. Pannengpetch, P. Wisomka, V. Chantadul, M. Phanchana, J. Panmanee, Proteomic profiling reveals neuronal

ion channel dysregulation and cellular responses to DNA damage-induced cell cycle arrest and senescence in human neuroblastoma SH-SY5Y cells exposed to cypermethrin, Neurotoxicology. 93 (2022) 71–83. https://doi.org/10.1016/J.NEURO.2022.08.015.

[39] A. Fry, L. O'Regan, S. Sabir, R.J. of cell science Bayliss, 2012, Cell cycle regulation by the NEK family of protein kinases, Journals.Biologists.Com. (2012). https://doi.org/10.1242/jcs.111195.

[40] G. Schevzov, N.M. Curthoys, P.W. Gunning, T. Fath, Functional Diversity of Actin Cytoskeleton in Neurons and its Regulation by Tropomyosin, Int. Rev. Cell Mol. Biol. 298 (2012) 33–94. https://doi.org/10.1016/B978-0-12-394309-5.00002-X.

[41] E.C. Arakel, B. Schwappach, Formation of COPI-coated vesicles at a glance, J. Cell Sci. 131 (2018). https://doi.org/10.1242/JCS.209890.

[42] J.F. Martín, Transport systems, intracellular traffic of intermediates and secretion of β-lactam antibiotics in fungi, Fungal Biol. Biotechnol. 7 (2020). https://doi.org/10.1186/S40694-020-00096-Y.

[43] S.C. Rosenkranz, A.A. Shaposhnykov, S. Träger, J.B. Engler, M.E. Witte, V. Roth, V. Vieira, N. Paauw, S. Bauer, C. Schwencke-Westphal, C. Schubert, L.C. Bal, B. Schattling, O. Pless, J. van Horssen, M. Freichel, M.A. Friese, Enhancing mitochondrial activity in neurons protects against neurodegeneration in a mouse model of multiple sclerosis, Elife. 10 (2021) 1–60. https://doi.org/10.7554/ELIFE.61798.

[44] M.A. Huynen, M. Mühlmeister, K. Gotthardt, S. Guerrero-Castillo, U. Brandt, Evolution and structural organization of the mitochondrial contact site (MICOS) complex and the mitochondrial intermembrane space bridging (MIB) complex, Biochim. Biophys. Acta - Mol. Cell Res. 1863 (2016) 91–101.

https://doi.org/10.1016/J.BBAMCR.2015.10.009.

[45] K.A. Diederichs, X. Ni, S.E. Rollauer, I. Botos, X. Tan, M.S. King, E.R.S. Kunji, J. Jiang, S.K. Buchanan, Structural insight into mitochondrial β-barrel outer membrane protein biogenesis, Nat. Commun. 2020 111. 11 (2020) 1–13. https://doi.org/10.1038/s41467-020-17144-1.

[46] C. Ott, E. Dorsch, M. Fraunholz, S. Straub, V. Kozjak-Pavlovic, Detailed analysis of the human mitochondrial contact site complex indicate a hierarchy of subunits, PLoS One. 10 (2015). https://doi.org/10.1371/JOURNAL.PONE.0120213.

[47] O. Kann, R. Kovács, Mitochondria and neuronal activity, Am. J. Physiol. - Cell Physiol. 292 (2007) 641–657. https://doi.org/10.1152/AJPCELL.00222.2006/ASSET/IMAGES/LARGE/ZH00020750970002.JPEG.

[48] Z.H. Sheng, Q. Cai, Mitochondrial transport in neurons: impact on synaptic homeostasis and neurodegeneration, Nat. Rev. Neurosci. 13 (2012) 77. https://doi.org/10.1038/NRN3156.

[49] M. Monné, A. Vozza, F.M. Lasorsa, V. Porcelli, F. Palmieri, Mitochondrial Carriers for Aspartate, Glutamate and Other Amino Acids: A Review, Int. J.Mol. Sci. 20 (2019) 4456. https://doi.org/10.3390/ijms20184456.

[50] A. Singh, R. Kukreti, L. Saso, S. Kukreti, Oxidative Stress: A Key Modulator in Neurodegenerative Diseases, Mol. 2019, Vol. 24, Page 1583. 24 (2019) 1583. https://doi.org/10.3390/MOLECULES24081583.

[51] M.J. Davies, The oxidative environment and protein damage, Biochim. Biophys. Acta - Proteins Proteomics. 1703 (2005) 93–109. https://doi.org/10.1016/j.bbapap.2004.08.007.

[52] E.C.A. Eleutherio, R.S. Silva Magalhães, A. de Araújo Brasil, J.R. Monteiro

926 Neto, L. de Holanda Paranhos, SOD1, more than just an antioxidant, Arch.
927 Biochem. Biophys. 697 (2021) 108701.
928 https://doi.org/10.1016/J.ABB.2020.108701.

929 [53] A.G. Miranda-Díaz, A. García-Sánchez, E.G. Cardona-Muñoz, F.J.B. Mendonça
930 Junior, Foods with Potential Prooxidant and Antioxidant Effects Involved in
931 Parkinson's Disease, Oxid. Med. Cell. Longev. 2020 (2020).
932 https://doi.org/10.1155/2020/6281454.

933 [54] A.M. Vincent, J.W. Russell, K.A. Sullivan, C. Backus, J.M. Hayes, L.L. McLean,
934 E.L. Feldman, SOD2 protects neurons from injury in cell culture and animal
935 models of diabetic neuropathy, Exp. Neurol. 208 (2007) 216–227.
936 https://doi.org/10.1016/J.EXPNEUROL.2007.07.017.

937 [55] F.R. Palma, C. He, J.M. Danes, V. Paviani, D.R. Coelho, B.N. Gantner, M.G.
938 Bonini, Mitochondrial Superoxide Dismutase: What the Established, the
939 Intriguing, and the Novel Reveal About a Key Cellular Redox Switch, Antioxid.
940 Redox Signal. 32 (2020) 701. https://doi.org/10.1089/ARS.2019.7962.

941 [56] P. Selvakumar, A. Lakshmikuttyamma, A. Shrivastav, S.B. Das, J.R. Dimmock,
942 R.K. Sharma, Potential role of N-myristoyltransferase in cancer, Prog. Lipid Res.
943 46 (2007) 1–36. https://doi.org/10.1016/j.plipres.2006.05.002.

944 [57] E. Thinon, R.A. Serwa, M. Broncel, J.A. Brannigan, U. Brassat, M.H. Wright,
945 W.P. Heal, A.J. Wilkinson, D.J. Mann, E.W. Tate, Global profiling of co- and
946 post-translationally N-myristoylated proteomes in human cells, Nat. Commun.
947 2014 51. 5 (2014) 1–13. https://doi.org/10.1038/ncomms5919.

948 [58] A. Malaspina, N. Kaushik, J. Belleroche, A 14-3-3 mRNA is up-regulated in
949 amyotrophic lateral sclerosis spinal cord, J. Neurochem. 75 (2000) 2511–2520.
950 https://doi.org/10.1046/J.1471-4159.2000.0752511.X.

[59] H. Li, S. Li, H. Yang, Y. Zhang, S. Zhang, Y. Ma, Y. Hou, X. Zhang, K. Niu, Y. Borné, Y. Wang, Association of Ultraprocessed Food Consumption With Risk of Dementia, Neurology. 99 (2022) e1056–e1066. https://doi.org/10.1212/WNL.0000000000200871.

[60] M. Gomar-Alba, M. Mendoza, Modulation of Cell Identity by Modification of Nuclear Pore Complexes, Front. Genet. 10 (2020) 1301. https://doi.org/10.3389/FGENE.2019.01301/BIBTEX.

[61] S. Sakuma, M.A. D'Angelo, The roles of the nuclear pore complex in cellular dysfunction, aging and disease, Semin. Cell Dev. Biol. 68 (2017) 72. https://doi.org/10.1016/J.SEMCDB.2017.05.006.

[62] V. Nofrini, D. DI Giacomo, C. Mecucci, Nucleoporin genes in human diseases, Eur. J. Hum. Genet. 24 (2016) 1388–1395. https://doi.org/10.1038/EJHG.2016.25.

[63] S. Xiao, S. Li, Z. Yuan, L. Zhou, Pyrroline-5-carboxylate reductase 1 (PYCR1) upregulation contributes to gastric cancer progression and indicates poor survival outcome, Ann. Transl. Med. 8 (2020) 937–937. https://doi.org/10.21037/ATM-19-4402.

[64] C. Giménez, F. Zafra, C. Aragón, Pathophysiology of the glutamate and the glycine transporters: New therapeutic targets, Rev. Neurol. 67 (2018) 491–504. https://doi.org/10.33588/rn.6712.2018067.

FIGURE CAPTION

Figure 1. Flow cytometry analysis of cells for cell viability, apoptosis, necrosis, reduced form of glutathione (GSH) concentration, reactive oxygen species (ROS) and mitochondrial activity. On one hand, half of the cells were washed and stained with CellEvent® for detection of active Caspases 3 and 7 Ethidium homodimer (Eth-1) to identify necrotic cells, and CellRox Deep Red® to identify ROS. Five populations were identified, A) corresponding with viable cells, negative for Eth-1 and CellEvent®, B) apoptotic cells expressing Caspase 3 and 7 activities, C) late apoptotic cells, positive for both CellEvent®, Eth-1, and D) depicting necrotic cells, only positive for Eth-1; then the amount of ROS production (relative fluorescence units RFU) were studied in the late apoptotic population of cells (E) and apoptotic cells (F). On the other hand, the other half of the cells were stained with monochlorobimane (MCB) to detect reduced thiols and with JC-1 to investigate mitochondrial membrane potential, G) Percentage of live cells with more reduced thiols (Live high GSH) and H) changes in mitochondrial membrane potential in live cells representing active mitochondria. Results are derived from five independent experiments (n=5) and given as means ± standard error of the mean.

Figure 2. Representative cytograms of the flow cytometry assays. Graphical representation of the distribution of neuronal cells in various subpopulations as affected by (A) their biological state (live, necrotic and early/late apoptotic); and (B) their concentration of glutathione (GSH) in live and dead cells.

Figure 3. Percentages of proteins annotated by Gene Ontology (* $p<0.05$, ** $p<0.01$) found in lower relative quantity in biological processes and molecular functions (A), and percentages of proteins found in higher relative abundance in biological processes and molecular functions (B) on differentiated human neuronal SH-SY5Y cells as affected by exposure to 4mM α-AA for 24 h compared to control counterparts.

Figure 4. Percentages of proteins annotated by Gene Ontology (* p<0.05, ** p<0.01) found in lower relative abundance in biological processes and molecular functions (A), and percentages of proteins found in higher relative quantity in biological processes and molecular functions (B) on differentiated human neuronal SH-SY5Y cells as affected by exposure to 4mM GLU for 24 h compared to control counterparts.

Figure 5. Percentages of proteins annotated by Gene Ontology (* p<0.05, ** p<0.01) found in lower relative abundance in biological processes and molecular functions (A), and percentages of proteins found in higher relative quantity in biological processes and molecular functions (B) on differentiated human neuronal SH-SY5Y cells in 4mM GLU treated cells compared to 4mM α-AA treatment for 24 h.

Figure 6. Proposal of underlying molecular mechanisms of the effects of α-AA and GLU at 4mM for 24 h on differentiated human neuronal SH-SY5Y cells. Upstream head green arrows indicate higher concentration of proteins in GLU treated cells. Up- and Downstream head red arrows indicate higher and lower concentration of proteins, respectively, in α-AA treated cells. Blunt head red arrows indicate an inhibited biological process or metabolic pathway.

SUPPLEMENTARY MATERIAL

Table S1. Proteins identified on differentiated neuronal cells in the presence of α-AA along with Log_2 fold change (Student's T-test Difference) and significance values (p). Proteins identified in lower abundance in α-AA treated cells in comparison to the non-treated control cells; proteins identified in higher quantity in α-AA treated cells in comparison to the non-treated control cells; proteins identified only in control samples in comparison to α-AA treated cells and proteins identified only in the presence of α-AA in comparison to the non-treated control cells. Control samples are marked in blue, α-AA treated cells in grey and statistical differences in green.

Table S2. Proteins identified on differentiated neuronal cells in the presence of GLU along with Log_2 fold change (Student's T-test Difference) and significance values (*p*). Proteins identified in lower quantity in GLU treated cells in comparison to the non-treated control cells; proteins identified in higher abundance in GLU treated cells in comparison to the non-treated control cells; proteins identified only in control samples in comparison to GLU treated cells and proteins identified only in the presence of GLU in comparison to the non-treated control cells. Control samples are marked in blue, GLU treated cells in grey and statistical differences in green.

Table S3. Proteins identified on differentiated neuronal cells in α-AA treated cells *vs* GLU treated cells along with Log_2 fold change (Student's T-test Difference) and significance values (*p*). Proteins identified in lower quantity in GLU treated cells in comparison to α-AA treated cells; proteins identified in higher abundance in GLU treated cells in comparison to α-AA cells; proteins identified only in GLU samples in compared to α-AA treated cells and proteins identified only in α-AA samples in comparison to GLU treated cells. α-AA samples are marked in blue, GLU treated cells in grey and statistical differences in green.

Table S4. Terms and associated genes by Gene Ontology among proteins found in lower quantity in the presence of α-AA.

Table S5. Terms and associated genes by Gene Ontology among proteins found in higher quantity in the presence of α-AA.

Table S6. Terms and associated genes by Gene Ontology among proteins found in lower quantity in the presence of GLU.

Table S7. Terms and associated genes by Gene Ontology among proteins found in higher quantity in the presence of GLU.

Table S8. Terms and associated genes by Gene Ontology among proteins found in lower quantity in the comparison α-AA treated cells *vs* GLU treated cells.

Table S9. Terms and associated genes by Gene Ontology among proteins found in higher quantity in the comparison α-AA treated cells *vs* GLU treated cells.

FIGURE 1

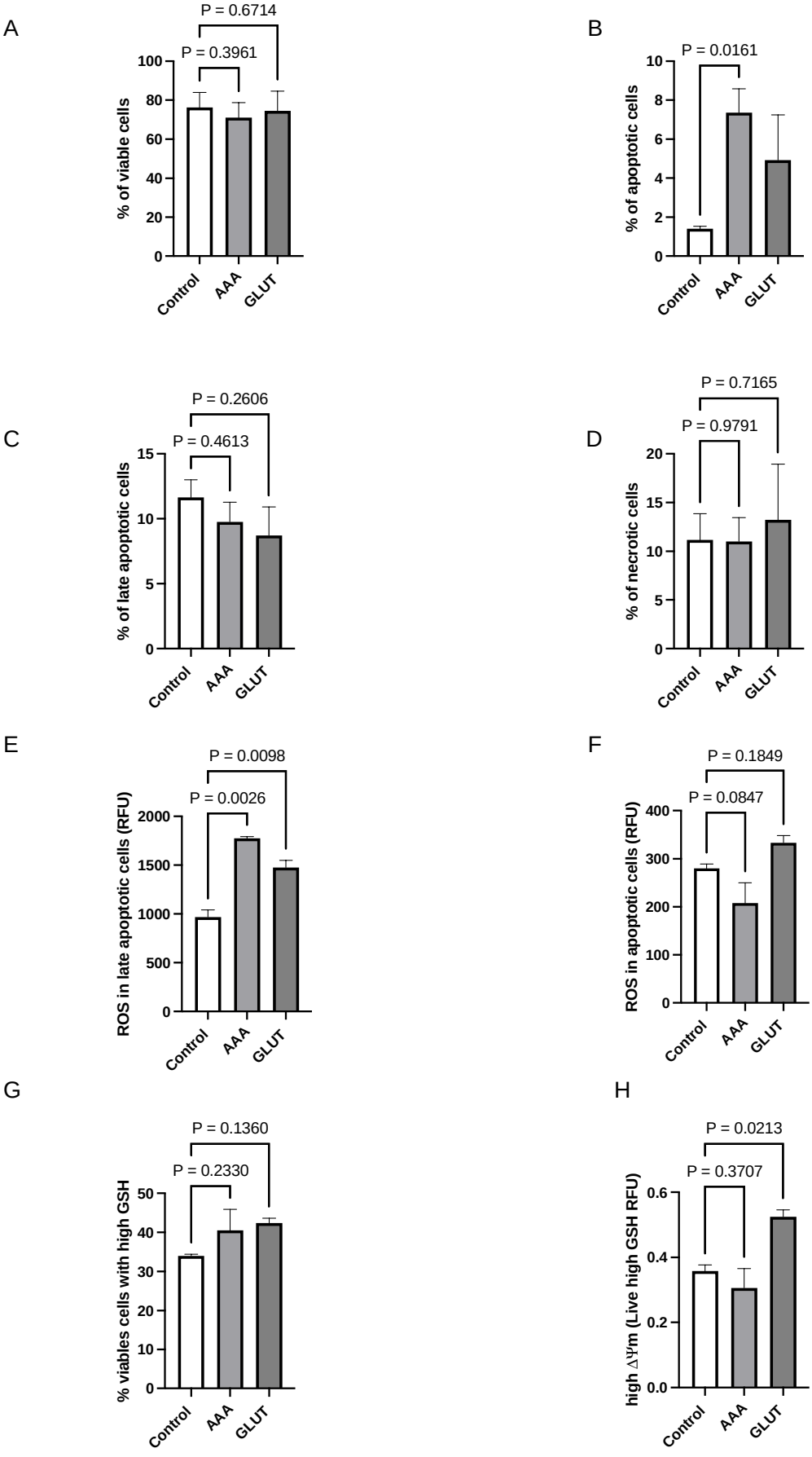
A
P = 0.6714
P = 0.3961
% of viable cells
100
80
60
40
20
0
Control
AAA
GLUT
B
P = 0.0161
% of apoptotic cells
10
8
6
4
2
0
Control
AAA
GLUT
C
P = 0.2606
P = 0.4613
% of late apoptotic cells
15
10
5
0
Control
AAA
GLUT
D
P = 0.7165
P = 0.9791
% of necrotic cells
20
15
10
5
0
Control
AAA
GLUT
E
P = 0.0098
P = 0.0026
ROS in late apoptotic cells (RFU)
2000
1500
1000
500
0
Control
AAA
GLUT
F
P = 0.1849
P = 0.0847
ROS in apoptotic cells (RFU)
400
300
200
100
0
Control
AAA
GLUT
G
P = 0.1360
P = 0.2330
% viables cells with high GSH
50
40
30
20
10
0
Control
AAA
GLUT
H
P = 0.0213
P = 0.3707
high ΔΨm (Live high GSH RFU)
0.6
0.4
0.2
0.0
Control
AAA
GLUT

FIGURE 2

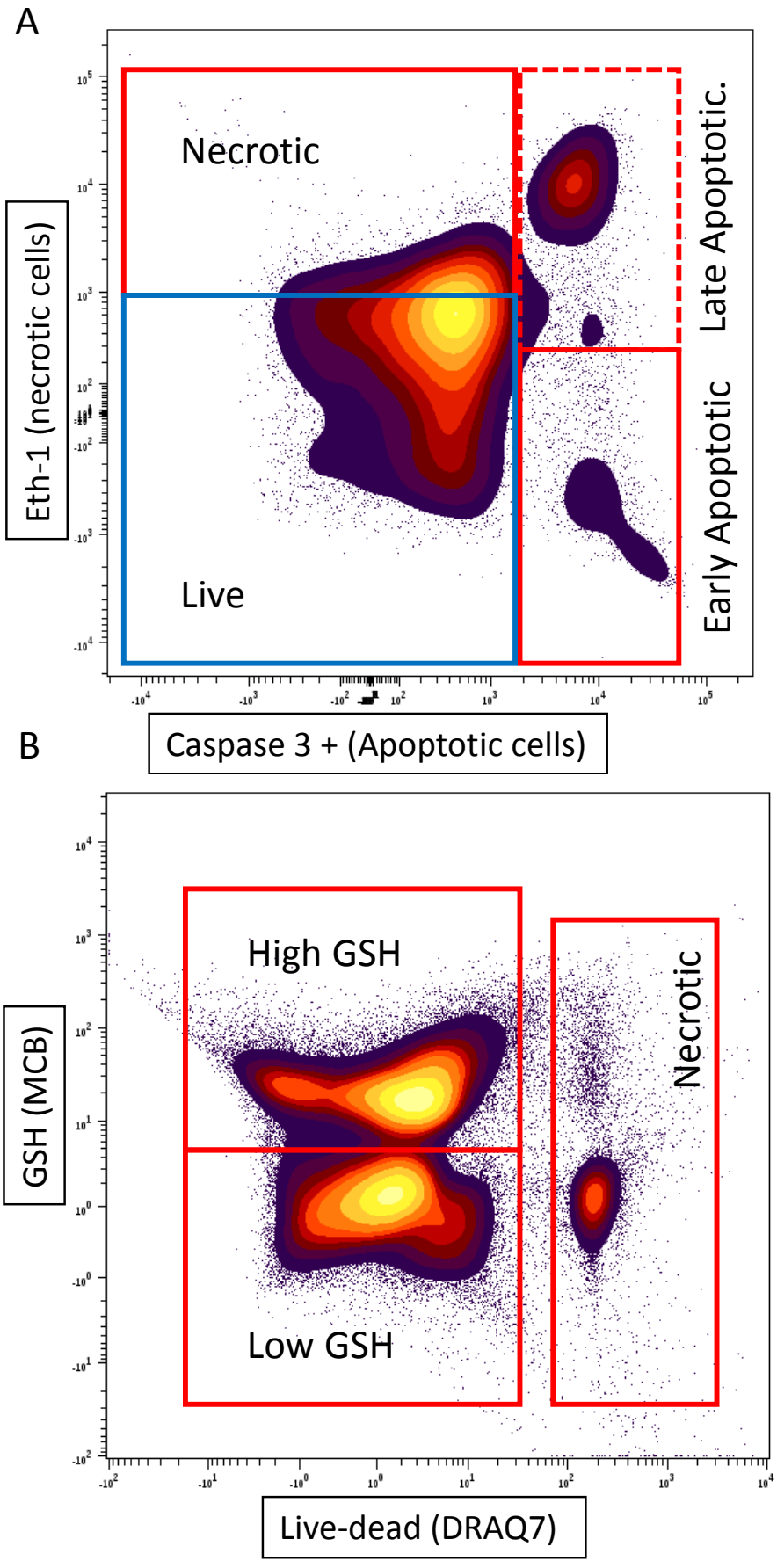
A
Necrotic
Late Apoptotic.
Early Apoptotic
Live
Eth-1 (necrotic cells)
Caspase 3 + (Apoptotic cells)
B
High GSH
Necrotic
Low GSH
GSH (MCB)
Live-dead (DRAQ7)

FIGURE 3

A

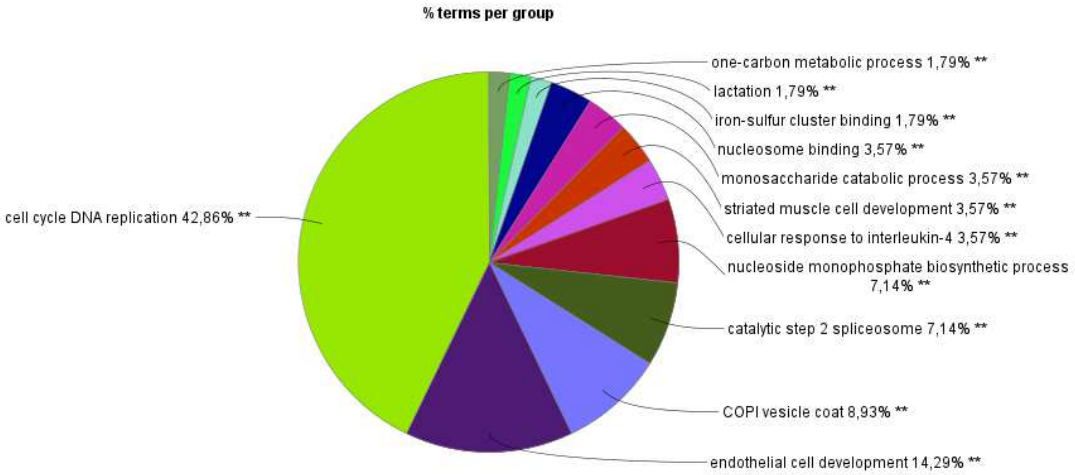
% terms per group
one-carbon metabolic process 1,79% **
lactation 1,79% **
iron-sulfur cluster binding 1,79% **
nucleosome binding 3,57% **
monosaccharide catabolic process 3,57% **
striated muscle cell development 3,57% **
cellular response to interleukin-4 3,57% **
nucleoside monophosphate biosynthetic process 7,14% **
catalytic step 2 spliceosome 7,14% **
COPI vesicle coat 8,93% **
endothelial cell development 14,29% **
cell cycle DNA replication 42,86% **

B

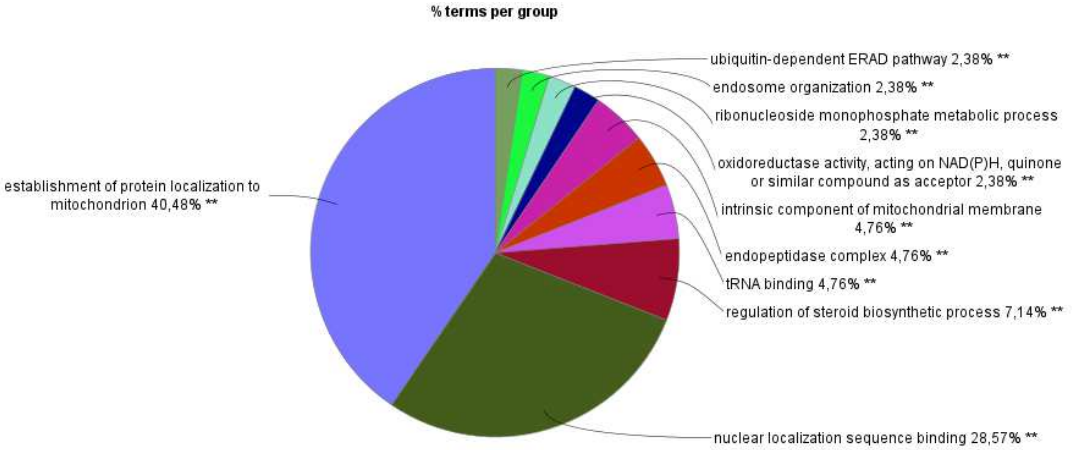
% terms per group
ubiquitin-dependent ERAD pathway 2,38% **
endosome organization 2,38% **
ribonucleoside monophosphate metabolic process 2,38% **
oxidoreductase activity, acting on NAD(P)H, quinone or similar compound as acceptor 2,38% **
intrinsic component of mitochondrial membrane 4,76% **
endopeptidase complex 4,76% **
tRNA binding 4,76% **
regulation of steroid biosynthetic process 7,14% **
nuclear localization sequence binding 28,57% **
establishment of protein localization to mitochondrion 40,48% **

FIGURE 4

A

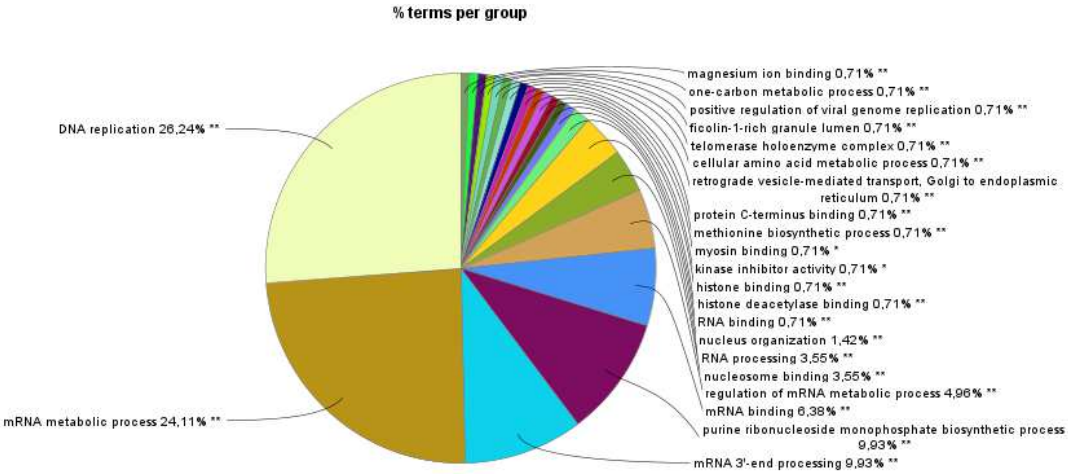
% terms per group
magnesium ion binding 0,71% **
one-carbon metabolic process 0,71% **
positive regulation of viral genome replication 0,71% **
ficolin-1-rich granule lumen 0,71% **
telomerase holoenzyme complex 0,71% **
cellular amino acid metabolic process 0,71% **
retrograde vesicle-mediated transport, Golgi to endoplasmic reticulum 0,71% **
protein C-terminus binding 0,71% **
methionine biosynthetic process 0,71% **
myosin binding 0,71% *
kinase inhibitor activity 0,71% *
histone binding 0,71% **
histone deacetylase binding 0,71% **
RNA binding 0,71% **
nucleus organization 1,42% **
RNA processing 3,55% **
nucleosome binding 3,55% **
regulation of mRNA metabolic process 4,96% **
mRNA binding 6,38% **
purine ribonucleoside monophosphate biosynthetic process 9,93% **
mRNA 3'-end processing 9,93% **
DNA replication 26,24% **
mRNA metabolic process 24,11% **

B

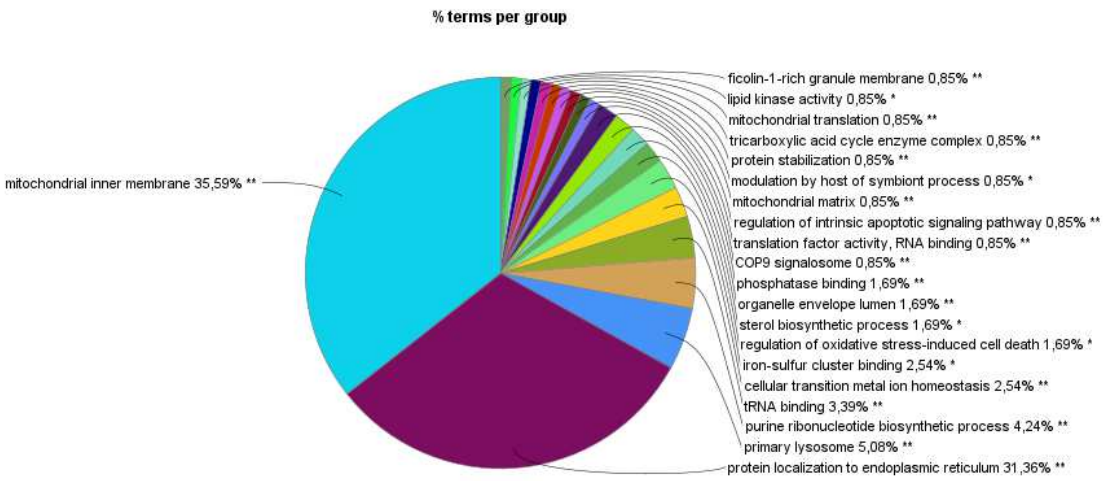
% terms per group
ficolin-1-rich granule membrane 0,85% **
lipid kinase activity 0,85% *
mitochondrial translation 0,85% **
tricarboxylic acid cycle enzyme complex 0,85% **
protein stabilization 0,85% **
modulation by host of symbiont process 0,85% *
mitochondrial matrix 0,85% **
regulation of intrinsic apoptotic signaling pathway 0,85% **
translation factor activity, RNA binding 0,85% **
COP9 signalosome 0,85% **
phosphatase binding 1,69% **
organelle envelope lumen 1,69% **
sterol biosynthetic process 1,69% *
regulation of oxidative stress-induced cell death 1,69% *
iron-sulfur cluster binding 2,54% *
cellular transition metal ion homeostasis 2,54% **
tRNA binding 3,39% **
purine ribonucleotide biosynthetic process 4,24% **
primary lysosome 5,08% **
protein localization to endoplasmic reticulum 31,36% **
mitochondrial inner membrane 35,59% **

FIGURE 5

A

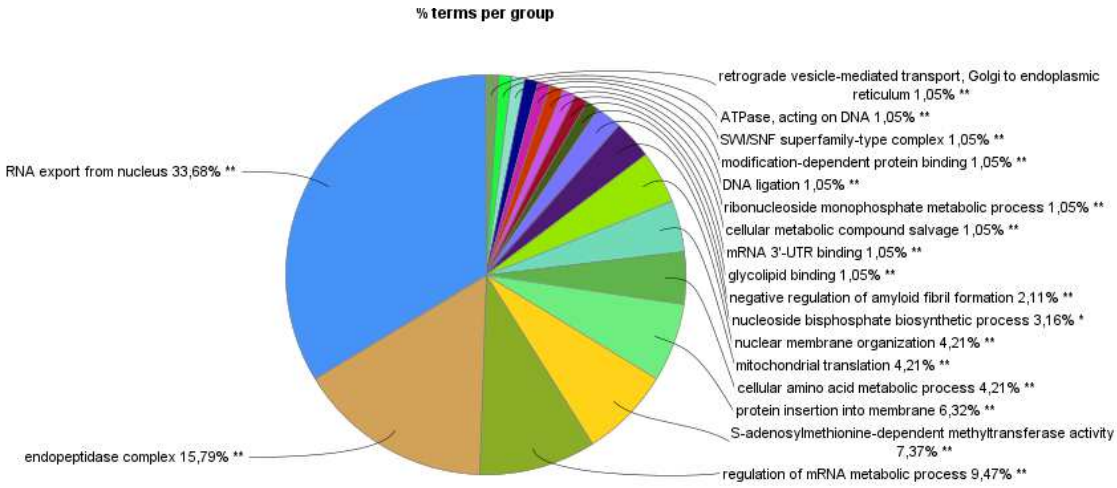
% terms per group
retrograde vesicle-mediated transport, Golgi to endoplasmic reticulum 1,05% **
ATPase, acting on DNA 1,05% **
SWI/SNF superfamily-type complex 1,05% **
modification-dependent protein binding 1,05% **
DNA ligation 1,05% **
ribonucleoside monophosphate metabolic process 1,05% **
cellular metabolic compound salvage 1,05% **
mRNA 3'-UTR binding 1,05% **
glycolipid binding 1,05% **
negative regulation of amyloid fibril formation 2,11% **
nucleoside bisphosphate biosynthetic process 3,16% *
nuclear membrane organization 4,21% **
mitochondrial translation 4,21% **
cellular amino acid metabolic process 4,21% **
protein insertion into membrane 6,32% **
S-adenosylmethionine-dependent methyltransferase activity 7,37% **
regulation of mRNA metabolic process 9,47% **
endopeptidase complex 15,79% **
RNA export from nucleus 33,68% **

B

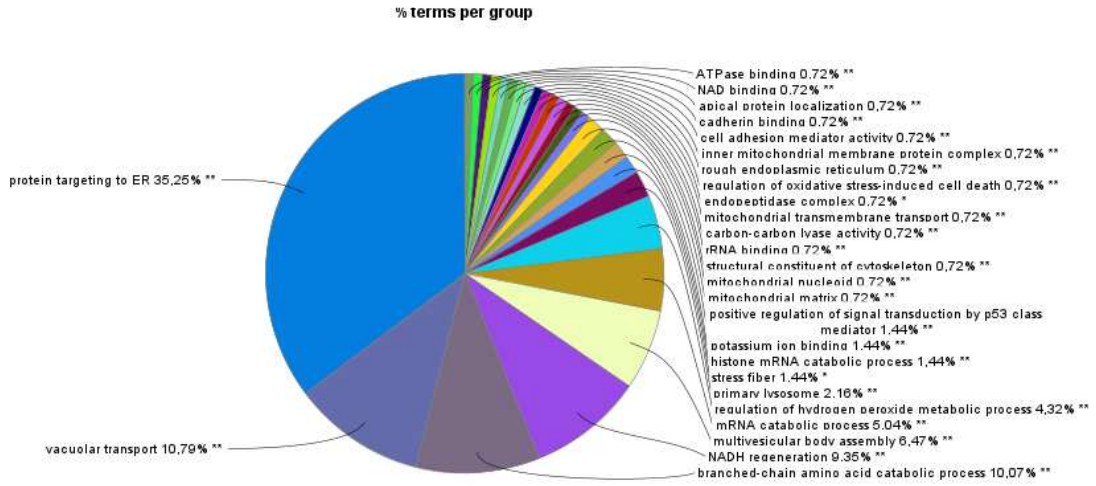
% terms per group
ATPase binding 0,72% **
NAD binding 0,72% **
apical protein localization 0,72% **
cadherin binding 0,72% **
cell adhesion mediator activity 0,72% **
inner mitochondrial membrane protein complex 0,72% **
rough endoplasmic reticulum 0,72% **
regulation of oxidative stress-induced cell death 0,72% **
endopeptidase complex 0,72% *
mitochondrial transmembrane transport 0,72% **
carbon-carbon lyase activity 0,72% **
rRNA binding 0,72% **
structural constituent of cytoskeleton 0,72% **
mitochondrial nucleoid 0,72% **
mitochondrial matrix 0,72% **
positive regulation of signal transduction by p53 class mediator 1,44% **
potassium ion binding 1,44% **
histone mRNA catabolic process 1,44% **
stress fiber 1,44% *
primary lysosome 2,16% **
regulation of hydrogen peroxide metabolic process 4,32% **
mRNA catabolic process 5,04% **
multivesicular body assembly 6,47% **
NADH regeneration 9,35% **
branched-chain amino acid catabolic process 10,07% **
vacuolar transport 10,79% **
protein targeting to ER 35,25% **

1173 **FIGURE 6**

1174

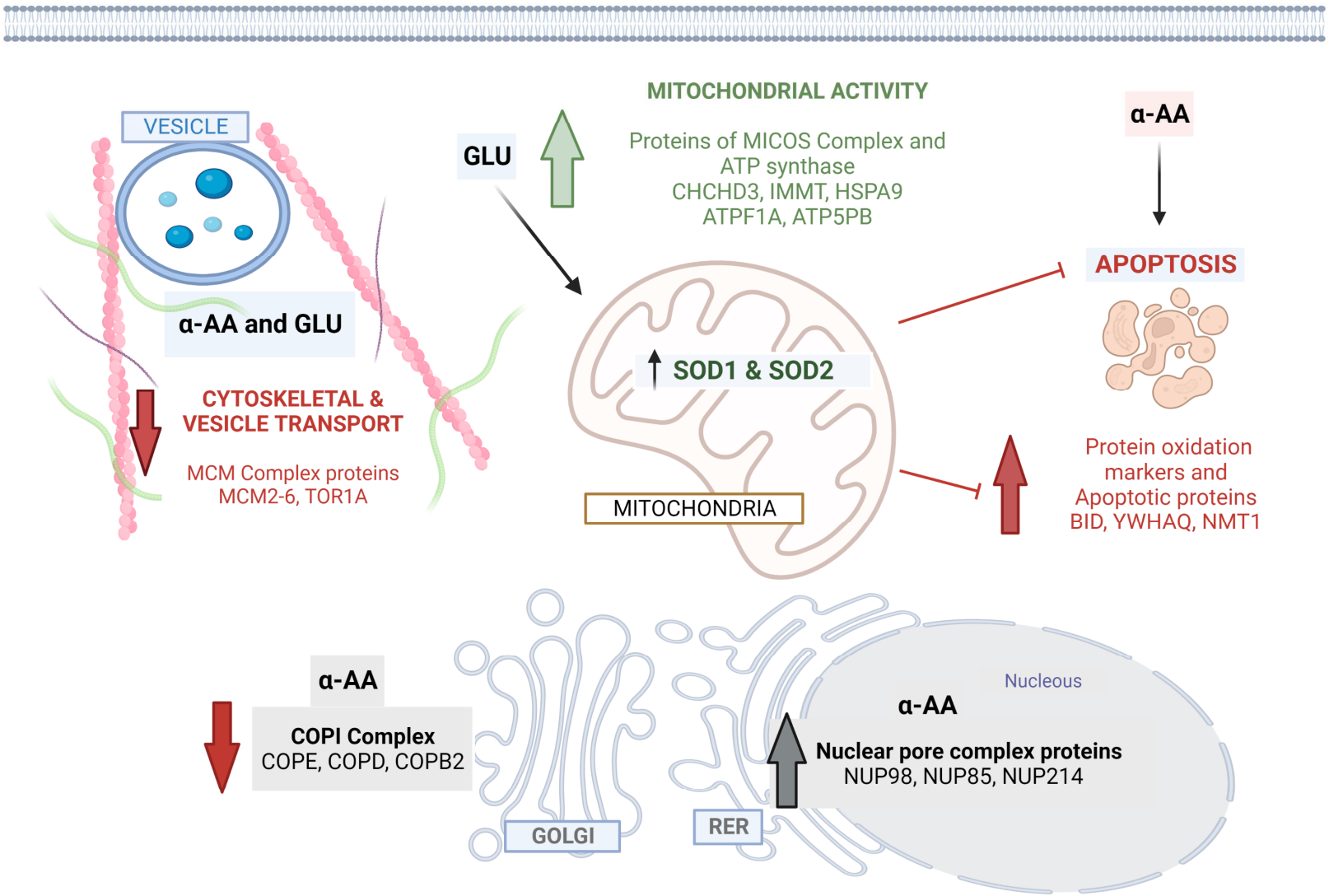

Table 1. Cell redox parameters (markers of oxidative stress and reduced and oxidized glutathione) in differentiated human neuronal SH-SY5Y cells affected by the exposure to whether 4 mM of glutamate (GLU) or 4mM α-Aminoadipic acid (α-AA) for 24 h in comparison to the non-treated control (C).

	C	α-AA	GLU	*p*-Value
α-AS[1]	1.05[b]±0.36	3.11[a]±0.72	1.40[b]±0.31	0.004
γ-GS[1]	0.08[b]±0.02	0.29[a]±0.04	0.11[b]±0.04	0.019
Total protein carbonyls[1]	1.12[b]±0.42	3.44[a]±1.05	1.55[b]±0.51	0.008
Pentosidine[1]	3.72±0.61	3.69±0.36	3.90±0.41	ns
Reduced glutathione (GSH)[1]	0.35±0.06	0.20±0.08	0.36±0.06	0.007
Oxidized glutathione (GSSH)[1]	1.38±0.15	1.93±0.27	1.35±0.14	0.039

[1] Results expressed as nmol per mg of protein

α-AS: α-aminoadipic semialdehyde

γ-GS: γ-glutamic semialdehyde

p-Value: significance value in an analysis of variance; Means with different letter were significantly different at a post-hoc Tukey test ($p<0.05$). ns: no significant.

Table 2. Proteins from differentiated human neuronal SH-SY5Y cells affected by the exposure to 4mM α-Aminoadipic acid for 24 h in comparison to the non-treated control (C).

PROTEIN NAME	GENE NAME	*p*-Value	FOLD CHANGE[1]	BIOLOGICAL FUNCTION	FASTA accession number
Coronin-1A	*COR1A*	-	C	Component of the cytoskeleton	P31146
Tropomodulin 2	*TMOD2*	-	C	Caps the pointed end of actin filaments preventing both elongation and depolymerization	Q9NZR1
Amine oxidase	*AOFA*	-	C	Involved in metabolism of neuroactive amines	P21397
Plexin-A4	*PLXA4*	-	C	Plays a role in axon guidance in the developing nervous system	Q9HCM2
Cytochrome b-c1 complex subunit 7	*QCR7*	-	C	Component of the mitochondrial electron transport chain in oxidative phosphorylation	P14927
N-chimaerin	*CHIN*	-	C	Involved in the assembly of neuronal locomotor circuits	P15882
Tropomyosin alpha-1	*TPM1*	0.034	0.48	Implicated in stabilizing cytoskeleton actin filaments	P09493
DNA replication licensing factor MCM3	*MCM3*	0.004	0.75	Component of the MCM complex, DNA replication initiation and elongation	P25205
DNA replication licensing factor MCM6	*MCM6*	0.006	0.78	Component of the MCM complex, DNA replication initiation and elongation	Q14566
Coatomer subunit epsilon	*COPE*	0.045	0.78	Formation of COPI. Protein transport from the ER via the Golgi up to the trans Golgi network	O14579
Radixin	*RADI*	0.004	0.79	Membrane-cytoskeletal crosslinkers in actin-rich cell surface structures	P35241
DNA replication licensing factor MCM2	*MCM2*	0.005	0.80	Component of the MCM complex, DNA replication initiation and elongation	P49736
DNA replication licensing factor MCM4	*MCM4*	0.002	0.83	Component of the MCM complex, DNA replication initiation and elongation	P33991
Ezrin	*EZRI*	0.003	0.85	Involved in connections of cytoskeletal structures	P15311
Alpha-adducin	*ADD1*	0.018	0.88	Promotes the assembly of the spectrin-actin network	P35611

Insulin-degrading enzyme	*IDE*	0.034	0.89	Breakdown of insulin. Elimination of APP-derived amyloidogenic peptides involved in Alzheimer	P14735
Coatomer subunit beta	*COPB2*	0.039	0.89	Formation of COPI. Protein transport from the ER via the Golgi up to the trans Golgi network	P35606
Coatomer subunit delta	*COPD*	0.036	0.90	Formation of COPI. Protein transport from the ER via the Golgi up to the trans Golgi network	P48444
14-3-3 protein theta	*YWHAQ*	0.018	1.07	Essential component of key signalling pathways involved in apoptosis and cell proliferation	P27348
Glycylpeptide N-tetradecanoyltransferase 1	*NMT1*	0.024	1.15	Adds a myristoyl group to the N-terminal glycine residue of proteins, involved in apoptosis	P30419
Nuclear pore complex protein Nup98	*NUP98*	0.047	1.18	Bidirectional transport across the nuclear pore complex	P52948
Nuclear pore complex protein Nup85	*NUP85*	0.033	1.25	Essential component in assembly and maintenance of the nuclear pore complex	Q9BW27
BH3-interacting domain death agonist	*BID*	0.006	1.33	Induces caspases and apoptosis	P55957
Nuclear pore complex protein Nup214	*NUP214*	-	α-AA	Nucleocytoplasmic transport in nuclear pore complex	P35658
Transportin-2	*TNPO2*	-	α-AA	Involved in nuclear protein import as nuclear transport receptor	O14787

[1]Fold change indicates the degree of quantity change for a particular protein between cells (control *vs*. α-AA); FC <1 denotes a decrease in the concentration of protein in the treated sample (*vs*. control); FC >1 indicates a significant increase in the concentration of the protein in treated sample (*vs*. control). When a given protein is only present in one of the groups, fold change cannot be measured, and such condition is denoted as “C” (if protein is only present in C cells) or α-AA (if protein is only present in α-AA -exposed cells).

Table 3. Proteins from differentiated human neuronal SH-SY5Y cells affected by the exposure to 4mM glutamic acid for 24 h in comparison to the non-treated control (C).

PROTEIN NAME	GENE NAME	*p*-Value	FOLD-CHANGE[1]	BIOLOGICAL FUNCTION	FASTA accession number
Serine/threonine-protein kinase VRK1	*VRK1*	-	C	Serine/threonine kinase involved in cell cycle	Q99986
Programmed cell death protein 10	*PDCD10*	-	C	Promotes cell proliferation and modulates apoptotic pathways	Q9BUL8
Tropomodulin-2	*TMOD2*	-	C	Caps the pointed end of actin filaments preventing both elongation and depolymerization	Q9NZR1
Coronin-1A	*COR1A*	-	C	Component of the cytoskeleton	P31146
Caspase-3	*CASP3*	-	C	Involved in apoptosis	P42574
Serine/threonine-protein kinase Nek9	*NEK9*	0.014	0.53	Involved in G1/S transition and S phase progression	Q8TD19
Cell division cycle and apoptosis regulator protein 1	*CCAR1*	0.001	0.68	Cell cycle progression and/or cell proliferation	Q8IX12
Torsin-1A	*TOR1A*	0.010	0.76	Link cytoskeleton to the nuclear envelope	O14656
DNA replication licensing factor MCM2	*MCM2*	4×10^{-4}	0.74	Component of MCM complex, DNA replication initiation and elongation	P49736
DAZ-associated protein 1	*DAZAP1*	0.024	0.74	RNA-binding protein	Q96EP5
Insulin-degrading enzyme	*IDE*	0.002	0.75	Breakdown of insulin. Elimination of APP-derived amyloidogenic peptides involved in Alzheimer	P14735
DNA replication licensing factor MCM6	*MCM6*	3×10^{-4}	0.75	Component of MCM complex, DNA replication initiation and elongation	Q14566
Heterogeneous nuclear ribonucleoprotein L-like	*HNRNPLL*	0.016	0.76	Regulator of splicing for multiple target mRNAs	Q8WVV9
Cleavage and polyadenylation specificity factor 1	*CPFS1*	0.028	0.78	Cleavage and polyadenylation processing for the maturation of pre-mRNA	Q10570
DNA replication licensing factor MCM5	*MCM5*	0.014	0.79	Component of MCM complex, DNA replication initiation and elongation	P33992

DNA replication licensing factor MCM3	*MCM3*	0.010	0.80	Component of MCM complex, DNA replication initiation and elongation	P25205
Zinc finger protein ZPR1	*ZPR1*	1.8×10^{-4}	0.80	Involved in the positive regulation of cell cycle progression	O75312
U1 small nuclear ribonucleoprotein 70 kDa	*SNRNP70*	0.007	0.81	Component of the spliceosomal U1 snRNP, recognition of the pre-mRNA 5'	P08621
ELAV-like protein 4	*ELAVL4*	9×10^{-5}	0.83	Binds to the 3'-UTR region of mRNA increasing stability	P26378
Heterogeneous nuclear ribonucleoprotein D0	*HNRNPD*	0.024	0.87	Binds to RNA molecules with AU-rich elements	Q14103
DNA replication licensing factor MCM4	*MCM4*	4×10^{-4}	0.85	Component of MCM complex, DNA replication initiation and elongation	P33991
Cleavage and polyadenylation specificity factor subunit 5	*NUTD21*	0.034	0.85	Cleavage and polyadenylation processing for the maturation of pre-mRNA	O43809
ELAV-like protein 1	*ELAVL1*	0.032	0.89	Binds to the 3'-UTR region of mRNA increasing stability	Q15717
ATP synthase subunit alpha, mitochondrial	*ATPF1A*	0.031	1.11	Component of the ATP synthase	P25705
V-type proton ATPase catalytic subunit A	*ATP6V1A*	0.036	1.11	Catalytic subunit of the V1 complex of vacuolar(H+)-ATPase	P38606
Stress-70 protein, mitochondrial	*HSPA9*	0.027	1.12	Chaperone protein involved in MIB and SAM complex	P38646
Ubiquitin-conjugating enzyme E2 L3	*UBE2L3*	0.009	1.13	Involved in the selective degradation of short-lived and abnormal proteins	P68036
MICOS complex subunit MIC60	*IMMT*	0.048	1.15	Component of the MICOS complex	Q16891
ATP synthase F(0) complex subunit B1, mitochondrial	*ATP5PB*	0.018	1.16	Component of the ATP synthase	P24539
Signal recognition particle subunit SRP72	*SRP72*	0.033	1.21	Component of the signal recognition particle complex	O76094
Reticulon-4	*RTN4*	0.016	1.22	Formation and stabilization of endoplasmic reticulum tubules	Q9NQC3

Signal recognition particle subunit SRP68	*SRP68*	0.029	1.26	Component of the signal recognition particle complex	Q9UHB9
MICOS complex subunit MIC19	*CHCHD3*	1.4×10^{-4}	1.26	Component of the MICOS complex	Q9NX63
40S ribosomal protein S20	*RPS20*	3.1×10^{-4}	1.31	Component of the ribosome	P60866
Protein RER1	*RER1*	0.006	1.37	Involved in the retrieval of RER proteins from the early Golgi compartment	O15258
Pyrroline-5-carboxylate reductase 1, mitochondrial	*PYCR1*	2.14×10^{-5}	1.38	involved in cell protection against oxidative stress	P32322
40S ribosomal protein S7	*RPS7*	0.024	1.50	Component of the ribosome	P62081
40S ribosomal protein S15	*RPS15*	0.049	1.52	Component of the ribosome	62841
ATP synthase membrane subunit K, mitochondrial	*ATP5MD*	1.3×10^{-3}	1.54	Component of the ATP synthase	Q96IX5
40S ribosomal protein S19	*RPS19*	0.034	1.55	Component of the ribosome	P39019
40S ribosomal protein S23	*RPS23*	0.004	1.55	Component of the ribosome	P62266
Cytochrome c oxidase subunit 4 isoform 1, mitochondrial	*COX41*	0.038	1.80	Component of the cytochrome c oxidase, mitochondrial electron transport chain	P13073
Dihydrolipoyl dehydrogenase, mitochondrial	*DLD*	2.3×10^{-4}	2.14	Component of 2-oxoglutarate dehydrogenase multienzyme complex	P09622
Superoxide dismutase [Mn], mitochondrial	*SOD2*	1.7×10^{-3}	4.49	Destroy radicals in biological systems	P04179
Superoxide dismutase [Cu-Zn], cytosolic	*SOD1*	-	GLU	Destroy radicals in biological systems	P00441
ATP synthase subunit delta, mitochondrial	*ATP5F1D*	-	GLU	Component of the ATP synthase	P30049
ATP synthase subunit e, mitochondrial	*ATP5ME*	-	GLU	Component of the ATP synthase	P56385

[1]Fold change indicates the degree of quantity change for a particular protein between cells (control *vs*. GLU); FC <1 denotes a decrease in the concentration of protein in the treated sample (*vs*. control); FC >1 indicates a significant increase in the concentration of the protein in treated

sample (*vs*. control). When a given protein is only present in one of the groups, fold change cannot be measured, and such condition is denoted as “C” (if protein is only present in C cells) or GLU (if protein is only present in GLU-exposed cells).

Table 4. Proteins from differentiated human neuronal SH-SY5Y cells affected by the exposure to 4mM glutamic acid for 24 h in comparison to the those exposed to 4mM α-Aminoadipic acid for 24 h.

PROTEIN NAME	GENE NAME	*p*-Value	FOLD CHANGE[1]	BIOLOGICAL FUNCTION	FASTA accession number
Serine/threonine-protein kinase VRK1	*VRK1*	-	α-AA	Serine/threonine kinase involved in cell cycle	Q99986
Transportin-2	*TNPO2*	-	α-AA	Involved in nuclear protein import as nuclear transport receptor	O14787
Nuclear pore glycoprotein p62	*NUP62*	-	α-AA	Role in mitotic cell cycle progression by regulating centrosome homeostasis	P37198
Phosphatidylinositol glycan anchor biosynthesis class U protein	*PIGU*	-	α-AA	Anchoring in the endoplasmic reticulum	Q9H490
Proteasomal ubiquitin receptor ADRM1	*ADRM1*	-	α-AA	Component of proteasome complex	Q16186
SRSF protein kinase 2	*SRPK2*	-	α-AA	Involved in constitutive and alternative splicing	78362
Serine/threonine-protein kinase Nek9	*NEK9*	0.012	0.48	Involved in G1/S transition and S phase progression	Q8TD19
Cell division cycle and apoptosis regulator protein 1	*CCAR1*	5.6×10^{-4}	0.72	Cell cycle progression and/or cell proliferation	Q8IX12
Torsin-1A	*TOR1A*	8.5×10^{-5}	0.74	Link cytoskeleton to the nuclear envelope	O14656
Nuclear pore complex protein Nup93	*NUP93*	0.015	0.75	Assembly and/or maintenance of nuclear pore complex	Q8N1F7
14-3-3 protein beta/alpha	*YWHAB*	0.012	0.76	Essential component of key signalling pathways involved in apoptosis and cell proliferation	P31946
U1 small nuclear ribonucleoprotein 70 kDa	*SNRNP70*	7.6×10^{-4}	0.78	Involved in constitutive and alternative splicing	P08621
GPI-anchor transamidase	*PIGK*	0.012	0.80	Anchoring in the endoplasmic reticulum	Q92643
Proteasome subunit beta type-7	*PSMB7*	0.012	0.80	Component of proteasome complex	Q99436
Proteasome subunit alpha type-6	*PSMA6*	0.006	0.81	Component of proteasome complex	P60900

E3 SUMO-protein ligase RanBP2	*RANBP2*	0.028	0.83	Component of the nuclear export pathway	P49792
KH domain-containing, RNA-binding, signal transduction-associated protein 1	*KHDRBS1*	0.042	0.83	Involved in constitutive and alternative splicing	Q07666
Insulin-degrading enzyme	*IDE*	0.021	0.84	Breakdown of insulin. Elimination of APP-derived amyloidogenic peptides involved in Alzheimer	P14735
UV excision repair protein RAD23 homolog A	*RD23A*	0.004	0.84	Multiubiquitin chain receptor involved in modulation of proteasomal degradation	P54725
Glycylpeptide N-tetradecanoyltransferase 1	*NMT1*	0.017	0.85	Adds a myristoyl group to the N-terminal glycine residue of proteins, involved in apoptosis	P30419
Nuclear pore complex protein Nup88	*NUP88*	0.018	0.85	Component of nuclear pore complex	Q99567
26S proteasome regulatory subunit 4	*PSMC1*	0.031	0.85	Component of proteasome complex	P62191
14-3-3 protein epsilon	*YWHAE*	0.025	0.87	Essential component of key signalling pathways involved in apoptosis and cell proliferation	P62258
26S proteasome regulatory subunit 8	*PSMC5*	0.012	0.88	Component of proteasome complex	P62195
La-related protein 7	*LARP7*	0.022	0.88	Involved in constitutive and alternative splicing	Q4G0J3
14-3-3 protein theta	*YWHAQ*	0.030	0.88	Essential component of key signalling pathways involved in apoptosis and cell proliferation	P27348
Ubiquitin carboxyl-terminal hydrolase isozyme L5	*UCHL5*	0.038	0.89	Constituent of the ubiquitin system	Q9Y5K5
WD40 repeat-containing protein SMU1	*SMU1*	0.007	0.89	Involved in constitutive and alternative splicing	Q2TAY7
Nuclear pore complex protein Nup205	*NUP205*	0.035	0.90	Assembly and/or maintenance of nuclear pore complex	Q92621
Probable ATP-dependent RNA helicase DDX17	*DDX17*	0.002	0.90	Involved in constitutive and alternative splicing	Q92841

Heterogeneous nuclear ribonucleoprotein U	*HNRNPU*	0.040	1.10	mRNA alternative splicing and stability	Q00839
Acetyl-CoA acetyltransferase, mitochondrial	*ACAT1*	0.012	1.11	Breaks down fatty acids into acetyl-CoA	P24752
40S ribosomal protein SA	*RPSA*	4×10^{-4}	1.12	Component of small ribosome subunit	P08865
Vacuolar protein-sorting-associated protein 25	*VPS25*	0.039	1.13	Multivesicular body (MVB) formation and sorting of endosomal cargo proteins into MVBs	Q9BRG1
Vacuolar protein sorting-associated protein VTA1 homolog	*VTA1*	0.014	1.22	Involved in the endosomal multivesicular bodies pathway	Q9NP79
Hepatocyte growth factor-regulated tyrosine kinase substrate	*HGS*	0.039	1.22	Multivesicular body (MVB) formation and sorting of endosomal cargo proteins into MVBs	O14964
40S ribosomal protein S14	*RPS14*	0.031	1.32	Component of small ribosome subunit	P62263
Alpha-synuclein	*SNCA*	0.028	1.34	Regulation of synaptic vesicle trafficking and neurotransmitter release	P37840
60S ribosomal protein L35	*RPL35*	0.005	1.36	Component of large ribosome subunit	P42766
40S ribosomal protein S5	*RPS5*	0.013	1.37	Component of small ribosome subunit	P46782
40S ribosomal protein S27	*RPS27*	0.043	1.37	Component of small ribosome subunit	P42677
60S ribosomal protein L31	*RPL31*	0.009	1.40	Component of large ribosome subunit	P62899
Microsomal glutathione S-transferase 3	*MGST3*	0.011	1.44	Involved in lipid metabolism oxidizing hydroxy-fatty acids	O14880
40S ribosomal protein S26	*RPS26*	1.5×10^{-3}	1.52	Component of small ribosome subunit	P62854
40S ribosomal protein S15	*RPS15*	0.024	1.57	Component of small ribosome subunit	P62841
Dihydrolipoyl dehydrogenase, mitochondrial	*DLD*	2.2×10^{-5}	1.70	Component of 2-oxoglutarate dehydrogenase multienzyme complex	P09622
U6 snRNA-associated Sm-like protein LSm1	*LMS1*	0.040	1.90	Involved in mRNA processing	O15116
Tropomyosin alpha-1 chain	*TPM1*	0.004	2.02	Stabilizing cytoskeleton actin filaments	P09493

Peptidyl-prolyl cis-trans isomerase NIMA-interacting 4	*PIN4*	6.0×10^{-4}	2.20	Ribosomal RNA processing factor in ribosome biogenesis	Q9Y237
Superoxide dismutase [Mn], mitochondrial	*SOD2*	1.5×10^{-5}	2.60	Destroy radicals in biological systems	P04179
Amine oxidase	*AOFA*	-	GLU	Involved in metabolism of neuroactive amines	P21397
Charged multivesicular body protein 4b	*CHMP4B*	-	GLU	Involved in multivesicular bodies formation	Q9H444
Branched-chain-amino-acid aminotransferase, mitochondrial	*BCAT2*	-	GLU	Catalyzes the catabolism of the essential branched chain amino acids	O15382
Hydroxymethylglutaryl-CoA lyase, mitochondrial	*HMGCL*	-	GLU	Essential in leucine catabolism	P35914
Methylcrotonoyl-CoA carboxylase subunit alpha, mitochondrial	*MCCC1*	-	GLU	Essential in leucine catabolism	Q96RQ3

[1]Fold change (FC) indicates the degree of quantity change for a particular protein between cells (α-AA *vs*. GLU). FC <1 denotes a decrease in the concentration of protein in GLU-treated cells as compared to α-AA counterparts; FC >1 indicates a significant increase in the concentration of the protein in GLU-treated cells as compared to α-AA counterparts. When a given protein is only present in one of the groups, fold change cannot be measured, and such condition is denoted as α-AA (if protein is only present in α-AA-exposed cells) or GLU (if protein is only present in GLU-exposed cells).

Capítulo 4.5. The intake of ellagic acid decreases the oxidative stress caused by α-amino adipic acid in the brain of C57BL/6 mice: underlying molecular mechanisms via proteomic approach

La ingesta de ácido elágico disminuye el estrés oxidativo causado por el ácido α-amino adípico en el cerebro de ratones C57BL/6: mecanismos moleculares subyacentes a través de un enfoque proteómico

Autores: Silvia Díaz-Velasco, Remigio Martínez, Josué Delgado, Mario Estévez

The Intake of Ellagic Acid Decreases the Oxidative Stress Caused by α-Amino Adipic Acid in the Brain of C57BL/6 Mice: Underlying Molecular Mechanisms via Proteomic Approach

S. Díaz-Velasco[1], R. Martínez[1], J. Delgado[2], Mario Estévez[1*]

[1] Food Technology and Quality (TECAL), Institute of Meat and Meat Products (IPROCAR), University of Extremadura, Cáceres, Spain.

[2] Food Hygiene and Safety (HISEALI), Institute of Meat and Meat Products (IPROCAR), University of Extremadura, Cáceres, Spain.

Short title: "Effects of α-amino adipic acid and ellagic acid in C57BL/6 mice"

*Corresponding author: Mario Estévez, Institute of Meat and Meat Products (IPROCAR), University of Extremadura, Avda. de las Ciencias, s/n. 10003, Cáceres, Spain. Phone number: +34 927251390. Email: mariovet@unex.es

Abstract

The consumption of ultraprocessed food is related to the onset and progression of neurological disorders and cognitive impairment. The oxidized amino acid, α-amino adipic acid (α-AA), is present in a variety of foods, including meat and dairy processed products and processed food in general. On the other hand, the ellagic acid (EA), a well-documented phytochemical with therapeutic applications, could be used in the mitigation of the harmful effects produced by α-AA in brain. For this purpose, C57BL/6 mice were exposed to α-AA and the combination of α-AA+EA at food-compatible doses for 6 weeks. The possible loss of spatial memory was studied by Morris Water Maze (MWM) test, in addition to a proteomic approach and measurements of oxidation biomarkers in the brain of C57BL/6 mice. The results displayed a significant increase both in oxidative stress and antioxidant defenses in mice exposed to α-AA, indicating the correct functioning of these latter against a harmful compound. This situation was accompanied by a lower abundance of proteins involved in actin cytoskeleton of neurons and oligodendrocytes. On other hand, mice treated with α-AA+EA showed a significant decrease both in oxidative stress and antioxidant enzymes corroborating the alleviating effects of EA. In addition, the compromised situation of actin-rich structures was reverted. In conclusion, in none of the treatments, the changes observed in a proteomic approach had an impact on the behaviour of the mice that indicated loss of spatial memory.

Keywords: α-amino adipic acid; ellagic acid; Morris Water Maze, proteomics; brain; oxidative stress; C57BL/6 mice.

1. INTRODUCTION

The oxidative stress is associated with multiple health disorders such as inflammatory bowel disease (IBD) (D'Haens et al., 2022; Van Hecke et al., 2017), cardiovascular diseases (Forman and Zhang, 2021) and aging (Maldonado et al., 2023), among many others. Regarding neurological pathologies, Parkinson syndrome (Puspita et al., 2017), Alzheimer's disease (Bai et al., 2022) and depression (Correia et al., 2023), they all display a robust correlation with oxidative stress. The consumption of ultraprocessed and severely oxidized foods has been found to increase post-prandial oxidative stress (Estévez, 2021). Furthermore, the sustained intake of such foods may facilitate the onset and progression of neurological disorders, such as Alzheimer's disease, dementia (Li et al., 2022) and cognitive performance (Cardoso et al., 2022). Under a pro-oxidative environment, where reactive oxygen species (ROS) are in imbalance with antioxidant defenses, amino acids and proteins are susceptible to oxidation. This is the case of the amino acid lysine, that is oxidized by ROS into α-amino adipic semialdehyde or allysine (α-AS), an abundant protein carbonyl present in processed foods (de La Pomélie et al., 2018; Estévez et al., 2021). In a further degradation stage, via carboxylation, α-AS is oxidized into α-amino adipic acid (α-AA) (Hellwig, 2019). α-AA is considered a biomarker of protein oxidation and is related to diabetes, obesity (Lee et al., 2019; Wang et al., 2013), renal failure, sepsis (Sell et al., 2007) and impaired endocrine and exocrine pancreatic function (Estaras et al., 2020; Wang et al., 2013). α-AA, at 200 μM, led to a significant decrease in cell viability and oxidative stress on differentiated human CACO-2 cells (Díaz-Velasco et al., 2022, 2020). This oxidized amino acid has also been studied on differentiated human neuronal SH-SY5Y cells at 4mM. The results showed that α-AA at this dose resulted in oxidative stress leading to impaired physiological functions in neurons (Díaz-Velasco et al., 2023; *submitted*). Likewise, da Silva et al. (2017) reported that oxidative stress was induced by α-AA in cerebral cortex slices of adolescent rats at 4mM. Other studies link neurological disorders with α-AA, in which this oxidized product

is involved in the pathogenesis of neurodegenerative disorders, anxiety and depression (David et al., 2019; Ni et al., 2014; Voronkov et al., 2021; Wu et al., 1995). In this study, C57BL/6 mice were used, with this particular mouse strain being the most widely employed in the investigation of diseases such as, diabetes, obesity (Goodarzi et al., 2019; Pearson et al., 2022), and in neurobehavioral investigations (Sloin et al., 2022), among many others. On the other hand, ellagic acid (EA) is a phytochemical with assorted anti-inflammatory, anti-proliferative and antioxidant properties, both *in vivo* and *in vitro* studies (Sharifi-Rad et al., 2022). This compound is abundant in the fruit of *Punica granatum L*. (García-Villalba et al., 2015) and its alleviating effects against oxidative stress has been documented in numerous studies (Rosillo et al., 2012; Zeb, 2018). The aim of the present investigation was to analyze whether the results obtained on differentiated human neuronal SH-SY5Y cells (Díaz-Velasco et al., 2023; *submitted*) are confirmed *in vivo* and the impairment at cellular level is manifested at a clinical level. To achieve this purpose, the possible noxious effect of the oral administration of α-AA on the brain and spatial memory of C57BL/6 mice was studied. The possible protective effect of the phytochemical EA was analyzed in the same conditions. To perform this investigation, a Morris water maze test was employed, together with an MS-based untargeted proteomic analysis of the mice brain cells and protein oxidation measurements.

2. MATERIAL AND METHODS

2.1. Animals and chemicals

Eight-weeks old C57BL/6 mice were supplied from the animal experimentation laboratory of the University of Extremadura (Cáceres, Spain). Handling, euthanasia, and the experimental protocols were approved by the institutional Bioethical Committee (reference 57/2016). α-AA (CAS Number 542-32-5) and EA (CAS Number 476-66-4) were obtained from Sigma-Aldrich (Sigma-Aldrich, Steinheim, Germany). Other reagents were purchased in Panreac (Panreac Química, S. A., Barcelona, Spain), Sigma-Aldrich

(Sigma-Aldrich, Steinheim, Germany) and Fisher (Fisher Scientific S.L., Madrid, Spain). Water used was purified by passage through a Milli-Q system (Millipore Corp., Bedford, MA).

2.2. Experimental procedure

During an adaptation period of one week, the mice were individually identified by means of a perforation code in the auditory pavilion and maintained in ventilated cages, with water and feed ad libitum. Mice were housed at room temperature (21±2 ºC), with humidity control (55% ± 10%) and with a 12-h light/12-h dark cycle. During the assay, C57BL/6 mice had free access to feed and water *ad libitum* for 6 weeks. Once the adaptation period finished, mice were randomly allocated into one of these three experimental groups depending on the oral administration of α-AA and EA (n=5, per group): α-AA (challenged with dietary α-AA), α-AA+EA (challenged with dietary α-AA and EA) and a control group. Dietary components under study were dissolved in drinking water at concentrations of 2.5 mg/L (α-AA) and 30 mg/L (EA) with these doses being food-compatible according to the data available in the literature (De et al., 2018; Kang et al., 2016; Wang et al., 2013). In the control group, the aforementioned solutions were replaced by basal drinking water. During the assay (6 weeks), mice were daily checked to warrant safety and well-being. During the treatment, food and water/solutions consumption were gravimetrically monitored every time they were filled in order to calculate the energy intake and effective doses of both compounds. This procedure was performed depending on the demand of the animals (every two or three days, approximately). Body weights were register weekly. The addition of dietary supplements (α-AA and EA) did not affect the volume of drinking water which was similar irrespective of the treatments.

2.3. Morris Water Maze Test

Morris water maze (MWM) test was carried out to study the possible loss of spatial memory caused by α-AA and the hypothetical protective effect of EA. The training of C57BL/6 mice before experiment and acquisition phases were conducted according to Patil et al. (2009). Briefly, mice (n=5 per group) were located in a circular pool (120 cm diameter, walls 20 cm depth), in which a 1.5 cm diameter platform was hidden beneath water surface. The location of the platform could be only identified by a distal reference platform attached to the pool wall. The pool was divided in two zones, as shown in Fig. 1A-B, matching zone 1 with the area where the platform was. Water temperature was maintained at 21±1ºC. The experiment was divided into two phases to study short-term (3 weeks) and long-term (6 weeks) spatial memory. The parameters analyzed were total distance (mm), average speed (mm/s), average acceleration (mm/s^2), exploration rate (%), inside time zone 1 (seconds) and inside rate zone 1 (%). Videos were recorded using a video camera (Sony, HDR-CX240E, Tokio, Japan) and analyzed by ToxTrac program (Rodriguez et al., 2018).

2.4. Euthanasia and sample collection

After the last MWM assay, mice were euthanized by exsanguination via cardiac puncture. Previously, the animals were anaesthetized using 5% inhaled isoflurane. Brains were collected and cryopreserved at -80ºC.

2.5. Assessment of protein oxidation

Two early protein oxidation biomarkers, α-aminoadipic semialdehyde (α-AS) and γ-glutamic semialdehyde (γ-GS), and an advanced one (pentosidine) were measured in mice brain. The procedure described by Utrera et al. (2011) was followed with some modifications. Firstly, 50 mg of brain were homogenized in 0.5 mL of PBS adding magnetized metal balls. Later, 100 µL of brain lysates were treated with 1 mL of cold 10% trichloroacetic acid (TCA) solution. Then, proteins were precipitated with centrifugation at 2240 g for 5 min at 4 °C. The supernatant was removed, and the pellet

was treated with 1 mL of cold 5% TCA. Proteins were precipitated again with centrifugation at 2240g for 5 min at 4 ºC. After removing supernatant, the pellet obtained were derivatized with p-amino-benzoic acid (ABA), purified and hydrolyzed as described elsewhere (Utrera et al., 2011). The hydrolysates were evaporated at 40 °C *in vacuo* and the generated residues were reconstituted with 200 µL of Milli-Q water and then filtered through hydrophilic polypropylene GH Polypro (GHP) syringe filters (0.45 µm pore size, Pall Corporation, NJ, USA) for HPLC analysis. Details on the chromatograph apparatus as well as on the separation, elution and identification of the compounds of interest were published (Utrera et al., 2011). α-AS-ABA and γ-GS-ABA were synthesized and purified following the procedure of (Akagawa et al., 2002) and injected in the same conditions than samples. α-AS and γ-GS were identified in samples by comparing their retention times with those of the reference pure compounds. Standard solutions of ABA (ranging from 0.1 to 0.5 mM) were also injected in the same chromatographic conditions to create a standard curve. The peaks corresponding to both semialdehydes were manually integrated and the resulting areas plotted against the aforementioned standard curve. Results are expressed as nmol of protein carbonyl per mg of protein.

2.5. Sample preparation for LC-MS/MS Based Proteomics

At first, 50 mg of brain were added in 0.5 mL of lysis buffer pH 7,5 (100 mM Tris-HCl, 50 mM NaCl, 10% glycerol, 0.5 M EDTA pH 8,5, 100 mM of PMSF (Phenylmethansulfonylfluorid) and 100 µg/mL Pepstatin A in a 1:100 proportion), adding magnetized metal balls. Samples were homogenized and sonicated 3 times in batches of 10 pulses (Branson Ultrasonics, Danbury, USA). Lysates were incubated on ice for 1 hour and the tissue debris was removed by centrifugation at 14452 g for 10 min at 4 ºC, then supernatants were passed into new Eppendorf tubes. Protein concentration was measured with a Coomasie Protein Assay Reagent Ready to Use using a Nanodrop 2000c Spectophotometer and a Nanodrop 2000 software (USA). A protein concentration of 1µg/µL is appropriate. Aliquots containing 50 µg of proteins were partially run in SDS-

PAGE (4% stacking and 12% separating), just stopped when they reached the separating part of the gel to be in gel digested according to Shevchenko et al. (2007), with some modifications. The gel was stained with Coomassie blue R250 and each lane was cut into 1 mm3 pieces and subjected to in-gel digestion. For protein reduction, samples were incubated with 0.5 M DTT in 50 mM ammonium bicarbonate for 20 min at 56 °C. The resulting free thiol (-SH) groups were alkylated by incubating the samples with 0.55 M iodoacetamide in 50 mM ammonium bicarbonate for 15 min in the dark at room temperature. Later, samples were treated with a mix of 50 mM ammonium bicarbonate, ProteaseMAX (Promega, USA) and trypsin (Promega, USA), and incubated for 2 h at 37 ºC carrying out the proteolysis. After, acid formic was added to stop the proteolysis. Supernatant was removed of each sample and placed it into new Eppendorf tubes for drying in a vacuum concentrator (Gyrozen, Daejeon, Korea). Samples were added loading buffer (98% milli-Q water, 2% acetonitrile and 0.05% trifluoroacetic acid) and analyzed on the Orbitrap LC-MS/MS.

2.6. Label-free quantitative proteomic analyses

A Q-Exactive Plus mass spectrometer coupled to a Dionex Ultimate 3000 RSLCnano (Thermo Scientific) analyzed 5 µg from each digest. Data was collected using a Top15 method for MS/MS scans following the procedure described by Delgado et al. (2019), with some modifications as described in Díaz-Velasco et al. (2022). Comparative proteome abundance and data analysis were conducted using MaxQuant software (version 1.6.0.15.0; https://www.maxquant.org/download_asset/maxquant/latest)) and Perseus (v 1.6.14.0) to organize the data and perform statistical analysis. Carbamidomethylation of cysteines was set as a fixed modification; oxidation of methionines and acetylation of N-terminals were set as variable modifications. Database searching was carried out against Homo sapiens protein database (www.uniprot.org). The maximum peptide / protein false discovery rates (FDR) were set to 1% based on comparison to a reverse database. The MaxLFQ algorithm was used to generate

normalized spectral intensities and infer relative protein abundance. Proteins were only retained in final analysis if they were detected in at least two replicates from at least one treatment, and the proteins that matched to a contaminant database or the reverse database were removed. Quantitative analysis was performed using a T-test to compare treatments with the control. Fold change is expressed as Log2.The qualitative analysis was also performed to detect proteins that were found in at least three replicates of a given treated group but were undetectable in the comparison control group. Proteins satisfying one of these two aforementioned criteria were identified as discriminating proteins, and their corresponding genes were grouped by biological processes and molecular functions through ClueGO (v. 2.5.6) (Bindea et al., 2009). To define term-term interrelations and functional groups based on shared genes between the terms, the Kappa score was established at 0.4. Three GO terms and 4 % of genes covered were set as the minimum required to be retained in the final result. The p-value was corrected by Bonferroni step down and set as $p<0.05$.

2.7. Statistical Analysis

Data was analyzed for normality and homoscedasticity and the effect of the exposure to α-AA and α-AA+EA was evaluated by Analysis of Variance (ANOVA). The effect of time on the same measurements was assessed by Student's t-test. The Tukey's test was performed for multiple comparisons of the means. SPSS (version 27.0) was used for statistical analysis of the data and the significance level was set at $p<0.05$.

3. RESULTS & DISCUSSION

Dietary oxidized amino acids, present in processed food, are involved in oxidative stress (Estévez and Xiong, 2019). When such oxidative stress takes place in brain cells, the occurrence of certain neurological diseases such as Alzheimer's disease (Bai et al., 2022), Parkinson's syndrome (Puspita et al., 2017) and cognitive impairment (Li et al.,

2022) is facilitated. Previous *in vitro* studies on differentiated human enterocytes CACO-2 cells (Díaz-Velasco et al., 2022, 2020) and on differentiated human neuronal SH-SY5Y cells (Díaz-Velasco et al., 2023, *submitted*), found that α-AA caused oxidative stress, mitochondrial disturbance and apoptosis. α-AA is not only an intermediate metabolite in the *in vivo* degradation of lysine, but also a common oxidation product of lysine in ultraprocessed foods which has been found to cause deleterious effects *in vitro* and *in vivo* upon oral administration. The sustained intake of ultraprocessed foods has been found to be linked to mental impairments including cognitive problems (Henney et al., 2023). It is, hence, reasonable to hypothesize that this little-known dietary component of ultraprocessed foods, could contribute to such impairments while the molecular mechanisms are ignored. *In vivo*, C57BL/6 mice were exposed to food-compatible doses of α-AA and the combination of α-AA+EA to study the possible benefit effect of the phytochemical in the harmful consequences of the oxidized amino acid.

3.1. Morris Water Maze test

The Morris Water Maze test showed a significant decrease ($p<0.05$) in the parameter 'exploration rate' in control mice at the 6th week of the assay as compared to the 3rd week (Table 1). No significant differences were found in any of the other parameters and comparisons ($p>0.05$) (Table 1).

3.2. Protein Oxidation Markers

The analysis of protein oxidation markers was evaluated by the detection of early protein carbonyls (α-AS and γ-GS) and advanced oxidation protein products (pentosidine). The results showed significant elevated concentration of protein carbonyls in the brain of animals exposed to α-AA (1.78±0.36 nmol/mg protein) as compared to control group of mice (0.88±0.22 nmol/mg protein; $p<0.05$). Similar results were obtained for pentosidine as the levels of this metabolite was significantly higher in α-AA-treated mice (2.18±0.28 area units) than the control counterparts (1.09±0.19 area units). The supplementation

with EA led to a significant decrease (α-AA vs. α-AA+EA; $p<0.05$) of both protein carbonyls (0.97±0.29 nmol/mg protein) and pentosidine (1.15±0.23 area units) with the levels of both species being similar to the control group of animals (α-AA+EA vs control; $p>0.05$).

3.3. Proteomic Analyses

The MS-based proteomic platform enabled the identification of 1763 proteins in total. All these proteins were identified with at least two peptides and an FDR<1%. Quantitative ($p<0.05$) and qualitative (only detected in one group of animals) changes in protein abundance were evaluated (Supplementary tables S1-S2).

A first comparison was made between the proteomes of the brains from α-AA-treated mice versus brains of the control counterparts. In this case, 168 proteins were significantly influenced by α-AA, among which, 68 were found in lower abundance in the brain of mice exposed to a-AA while 5 were only found in control samples. Conversely, 75 proteins were detected in higher quantity in the brain of animals treated with α-AA and 25 were only found in α-AA treated mice (Table S1).

To study the hypothetical protective role of EA against α-AA, an additional comparison was made between the proteomes of brains from α-AA-treated mice *versus* α-AA+EA-challenged animals. In this case, 350 proteins were significantly influence by α-AA+EA; among which, 118 were detected in lower abundance in mice exposed to α-AA+EA, 194 were found in higher quantity in α-AA+EA-treated animals, 20 were only detected in the presence of α-AA+EA and 18 were only found in α-AA treated mice (Table S2).

For a logical and hierarchical description of results, discriminating proteins were grouped by biological processes and molecular functions. The comparison between control animals *versus* α-AA-treated mice is shown in Fig. 2A-B. The comparison between α-AA treated mice and α-AA+EA is displayed in Fig. 3A-B. Specific terms for each of these processes and full details of discriminating proteins and associated genes are provided

in Supplementary material Tables S3-S6. Tables 2 and 3 show a selection of representative proteins from each relevant biological process or molecular function affected by the presence of α-AA (vs. control) and the comparison between α-AA *vs.* α-α-AA+EA, respectively. Only discriminating proteins having a defined biological significance are presented in the following sections.

3.3.1 Impact of dietary α-AA on the brain proteome of C57BL/6 brain mice

The most relevant findings caused by α-AA (vs. control) in the brain of C57BL/6 mice are discussed considering the most affected biological processes/metabolic routes for a more comprehensive understanding of the massive proteomic data obtained.

3.3.1.1. Impairment of cytoskeleton and synaptic/myelinating function of neurons/oligodendrocytes

Among all the biological processes and molecular functions affected in the brain of mice exposed to α-AA, positive regulation of the actin filament polymerization process was the most affected (25%) along with linked biological functions of neuronal cells such as the filopodium assembly (15%) and the oligodendrocyte differentiation (10%) (p<0.01; vs. control). All together, these processes account for almost 50% of the total modification of proteome caused by the intake of α-AA. The oral administration of this oxidized amino acid to mice led to a significant depletion of proteins involved in the normal formation of dendritic spines, neurons and oligodendrocytes as compared to the brains of the control counterparts. Other related such as the actin-related protein 2/3 complex and septin ring formation, were also impaired in the presence of the final oxidation product of lysine.

Firstly, the actin-related protein Arp2/3 complex is an essential component of the actin cytoskeleton and actin polymerization in eukaryotic cells. In our study, the subunits 2 and 5 of the actin-related protein 2/3 complex (ARPC2, fold change: 0.70; ARPC5, fold change: 0.82), related to this complex, were found in lower abundance in α-AA treated mice in comparison with control counterparts. Actin polymerization is involved in

morphological changes in cells such as division, phagocytosis and migration (Swaney and Li, 2016). In the nervous system, the Arp2/3 complex is responsible to the growth cone motility, axon guidance and development of dendritic spines and synapses (Wang et al., 2016). In mature dendritic spines, the Arp2/3 complex plays a critical role in actin remodeling, fact that is essential for spine structural plasticity *in vivo* (Kim et al., 2013). Its disruption is associated with asymmetric structural plasticity of dendritic spines that can leads into complex psychiatric disorders (Kim et al., 2013). Other studies have claimed that the inhibition of the Arp2/3 complex significantly affected the ability of glioma cells to migrate and invade other tissues (Liu et al., 2013). On the other hand, dendritic filopodia are actin-rich structures that are involved into the early spine synapse formation (Spence et al., 2016). As anticipated, proteins implicated in the positive regulation of filopodium assembly were found in lower abundance in α-AA-treated mice. Proteins such as fascin (FSCN1, fold change: 0.74) and Ras-related protein Ral-A (RALA, fold change: 0.83) (Tables 2 and S1) were also found in lower quantity in the brain of mice challenged with α-AA in contrast to control counterparts (Table S3). RALA is a molecular switch that can alternate between inactive states bound to GDP and active states bound to GTP to regulate a number of functions, such as vesicle traffic and filopodium formation (Richardson et al., 2022). Alongside this protein, fascin protein (Hu et al., 2021) and ARPC2 were also found in lower quantity in this process. Very much related to actin polymerization and filopodium assembly, some neuronal-specific protein such as septin, were found in lower abundance in their subunits 3, 6 and 11 (SEPT3, fold change: 0.73; SEPT6, fold change:0.81; SEPT11, fold change: 0.77) (Tables 2 and S1). Septins are considered the fourth component of the cytoskeleton. This is a group of proteins that contain a conserved GTP-binding region and are located at the base of dendritic spines in neurons (Mostowy and Cossart, 2012). In particular, SEPT3 is highly expressed in presynaptic terminals of neurons and associated with synaptic vesicles, being a crucial protein for synapse formation, maturation and synaptic vesicle traffic (Tsang et al., 2008). Thus, it is reasonable to consider that the lower abundance of septins would lead to

functional impairment in neurons. Septins have also been associated with actin and microtubule filaments (Mostowy and Cossart, 2012). Proteins implicated in the regulation of microtubule polymerization (Fu et al., 2019) were also found in lower abundance in the proteome of brains of mice exposed to α-AA, such as the factor β of glia maturation (GMFB, fold change: 0.77), guanine deaminase (GDA, fold change: 0.76), protein 2 of the growth factor receptor-bound (GRB2, fold change: 0.65), profilin-2 (PFN2, fold change: 0.83) and tubulin polymerization-promoting protein (TPPP, fold change: 0.82) (Tables 2 and S1). Other proteins implicated in synaptic structures and functions (Yoshida and Goedert, 2012) such as protein canopy homolog 2 (CNPY2, fold change:0.37) and microtubule-associated protein (MAPT, fold change: 0.56) were among the most depleted in the brain cells of mice exposed to α-AA.

On the same line, proteins linked to oligodendrocyte differentiation such as CD9 antigen (Cd9, fold change: 0.68) and myelin proteolipid protein (PLP1, fold change: 0.61) (Tables 2 and S1) were also lowered in brains from mice challenged with α-AA. Oligodendrocytes, a type of neuroglia cells, are responsible for myelinating neuronal axons, through a complex process that requires multiple cellular interactions (García-Montes and Crespo, 2023). In our investigation, proteins such as PLP1, the main myelin protein of the central nervous system, was found in lower quantity, together with CD9 and TPPP. The crucial role played by PLP1 in the formation and maintenance of the myelin structure, requires a continuous high-level expression in oligodendrocytes (Kim et al., 2021). Thus, the lower amount of this protein in brains, as induced by dietary α-AA, could be related with alterations in the nervous system. It is well known that α-AA acts as a gliotoxin (Brown and Kretzschmar, 1998; Pereira et al., 2021; Sherpa et al., 2014), and the underlying molecular mechanism could be, among many others, the lower abundance of this protein.

Finally, it is worth mentioning other biologically relevant proteins which concentration was significantly lowered in brain cells from mice exposed to α-AA, such as cystatin-C

(CST3, fold change: 0.45) and alpha-amylase (AMY2, fold change: 0.56) (Tables 2 and S1). Various studies reported that low levels of CST3 (cystatin-C) were found in cerebrospinal fluid of Alzheimer's patients (Zhong et al., 2013), compared to individuals without dementia, and also is associated with an anticipation of the onset of dementia (Maetzler et al., 2010).

Recently, α-amylase (AMY2), a glycogen degradation enzyme, has been reported to be present in the human brain (Chen et al., 2022). The aforementioned authors found that the increase in AMY2 was linked to the onset of Alzheimer's disease. On the contrary, other studies claimed that neuronal AMY2 was absent in patients with Alzheimer's disease and this situation induced a worsening condition of this disease (Byman et al., 2021). AMY2 is known to play a crucial role in glycogenolysis at the synapse, potentially being important in memory formation. Therefore, the significant depletion of AMY2 by dietary α-AA could have been manifested in symptoms related to memory loss. Yet, the lack of impact of dietary α-AA as observed in the MWM assay could respond to dose and/or length of consumption. While the depletion of AMY2 was close to 50% in mice treated with α-AA, maybe more severe depletions (alone or along with other key proteins) are required to observe clinical manifestations.

3.3.1.2 Increase of chaperones, cellular amino acid metabolic processes and antioxidant defenses

Further to the impairment of biological processes by the significant depletion of key proteins, dietary α-AA also caused an increase of other proteins in brain of treated mice that would respond to cellular responses to some of the chemical threats caused by this oxidized amino acid. Among all proteins upregulated by dietary α-AA, those targeting to mitochondrion were among the most affected as compared to control mice (16.13%, $p<0.01$) (Fig. 2B). In this process, chaperone proteins such as the α-heat shock protein

90 (HSP90, fold change: 1.48), endoplasmin (fold change: 1.46), nucleophosmin (NPM1, fold change: 1.55), IMPACT protein (IMPACT, fold change: 1.37), DnaJ homolog subfamily C protein (DNAJC3, fold change: 1.25) and 78 kDa glucose-regulated protein (HSPA5, fold change: 1.16), among others, were found in higher quantities in brain cells from mice exposed to α-AA (see Tables 2 and S1). Subunits α and β of the mitochondrial-processing peptidase (PMPCA, fold change: 1.40; PMPCB, fold change: only in α-AA) and high mobility group protein B2 (HMGB2, fold change: 1.35) were also altered in this process (Tables 2 and S1-S4).

Chaperones or heat shock proteins are involved in the folding of new formed proteins, prevent inappropriate folding and restore the three-dimensional structure of proteins. Their occurrence and bioactivity is essential after a cytotoxic cellular stress (Den and Lu, 2012) which seems to be the case of the present study. Proteins NPM1 (Liu et al., 2012), IMPACT and DNAJC3 (Cambiaghi et al., 2014), involved in response to stress, were increased in the regulation of initiation in response to translational stress process (Table S4). Moreover, the proteins PMPCA and PMPCB, related to the mitochondrial processing peptidase (MPP) (Kunová et al., 2022) were also increased in the brains of α-AA-treated mice. These proteins are responsible for the cleavage of protein presequences, which target is specifically the mitochondria (Kunová et al., 2022) and their malfunction is related to neurodegenerative diseases. Mitochondria, in addition to providing energy to cells, maintain calcium homeostasis and biosynthesize heme and steroid molecules (Kunová et al., 2022), processes that are all increased in the brain of mice challenged with α-AA (Table S4).

On the other hand, overexpression of the IMPACT protein contributes to block the activation of certain protein kinases, which would lead to a lack of certain amino acids (Roffé et al., 2013). This may explain why cellular amino acid metabolic processes were found to be increased in the brain of mice treated with α-AA. In this biological samples, proteins related to tRNA, implicated in the biosynthesis of proteins, are upregulated such

414 as mitochondrial cysteine--tRNA ligase (CARS2, fold change: 1.39), the subunit β of
415 phenylalanine--tRNA ligase (FARSB, fold change: 1.31), the cytoplasmic isoleucine--
416 tRNA ligase (IARS, fold change: 1.23) and tryptophan--tRNA ligase (WARS, fold change:
417 1.18) (Tables 2 and S1) (Table S4). Consistently, proteins involved in the smooth
418 endoplasmic reticulum functions such as correct folding of proteins and the inhibition of
419 the misfolded ones such as DnaJ homolog subfamily C (DNAJC3, fold change: 1.25),
420 HSPA5 (Ni and Lee, 2007) and protein disulfide-isomerase A6 (PDIA6, fold change:
421 1.90) (Eletto et al., 2014), were all increased in α-AA mice.

422 Mammalian cells acquire tolerance against multiple stress situations through increased
423 expression of stress-related genes. The PDI protein along with ubiquilin-1 (UBQLN1, fold
424 change: 1.61) have been found to be positively regulated in response to hypoxia/cerebral
425 ischemia (Ko et al., 2004). According to our results, these proteins may also be positively
426 regulated in brain cells in response to a chemical threat such as dietary α-AA (Table 2
427 and S1). It is interesting to emphasize that both, hypoxia and α-AA exposure, seems to
428 promote, by different mechanisms, oxidative stress and hence, the similar cellular
429 response to both situations is reasonable. In fact, in mice exposed to α-AA (*vs*. control),
430 an increase in different subunits of hemoglobin (HBA-A1, fold change: 1.55; HBB-B1,
431 fold change: 1.59) was found, alongside with an increase in the major structural element
432 of the erythrocyte membrane skeleton protein (EPB41, fold change: 2.43). An increase
433 in hemoglobin is known to be related to episodes of acute hypoxia (Yalcin and Cabrales,
434 2012), suggesting that in the cell brains of mice exposed to α-AA, a microenvironment
435 similar to that of hypoxia is created. Ubiquilin acts as an adaptive protein that interacts
436 with PDI and mediates the delivery of ubiquitylated proteins to the proteosome in the
437 cytosol close to the endoplasmic reticulum membrane (Ko et al., 2004), a fact that occurs
438 under severe oxidative stressful conditions such as those observed in our biological
439 samples. Therefore, the occurrence of cumulative oxidative damage to proteins such as

shown in the protein oxidation markers, would explain the increasing concentration of chaperones and other proteins related to the increase of toxic cellular stresses.

In line with the aforementioned results, the brain of mice treated with α-AA (*vs*. control), had a higher concentration of antioxidant enzymes such as catalase (CAT, fold change: 1.34) and glutathione peroxidase (GPX4, fold change: 1.26), which are implicated in detoxifying reactive oxygen species (Flohé et al., 2022). In view of these results, we can hypothesize that brain cells from mice exposed to α-AA suffered oxidative stress and responded by various defensive mechanisms including the strengthening of the endogenous antioxidant defenses. This fact is also corroborated by the occurrence of the GMFB protein, that is implicated in the modulation of the antioxidant enzyme superoxide dismutase (SOD1) (Fan et al., 2018).

In summary, our results demonstrate that the intake of food-compatible doses of α-AA cause a disturbance in the normal formation and function of neurons and oligodendrocyte cells, which is partly alleviated by increasing protein synthesis and proper folding mechanisms, as well as a raise of antioxidant enzymes. Changes in mice exposed to α-AA are observable at the molecular level, but not noticeable in studies of spatial memory loss.

3.3.2. Impact of dietary EA on the brain proteome of C57BL/6 brain mice challenged with α-AA

The expected situation of the combination of α-AA together with the phytochemical EA, was an alleviation of the harmful effects produced (and already described) by the oxidized amino acid in the brain of mice. The comparison of the proteome of mice treated with α-AA with that of mice treated with α-AA+EA revealed the ability of the dietary phytochemical to counteract some of the negative effects of the intake of the oxidized amino acid. Conversely, the effects of EA on certain biological processes of the proteome can be interpreted as harmful while the clinical significance of these changes is ignored.

3.3.2.1. Impact on synaptic and neurotransmission processes

The supplementation of EA decreased the concentration of proteins associated with the synaptic vesicle fusion to presynaptic active zone membrane, with this biological process being the most affected in the brain of mice exposed to α-AA+EA (*vs*. α-AA) (17.08%, $p<0.01$) (Fig. 3A). In this biological process, proteins found in lower abundance were involved in the release of neurotransmitters through calcium signaling, such as complexin-1 (CPLX1, fold change: 0.60), complexin-2 (CPLX2, fold change: 0.65), proline-rich transmembrane protein 2 (PRRT2, fold change: 0.55), synaptotagmin-2 (SYT2, fold change: 0.61), synaptosomal-associated protein 25 (SNAP25, fold change: 0.61), clathrin heavy chain 1 (CLTC, fold change: 0.083), kinesin-1 heavy chain (KIF5B, fold change: 0.62), subunit alpha-1 of sodium/potassium-transporting ATPase (ATP1A1, fold change: 0.59) and spectrin beta chain, non-erythrocytic 1 (SPTBN1, fold change: 0.72). (Tables 3 and S2).

Complexins, which are essential for the activation of multiple types of exocytosis induced by calcium. CPLX1 positively regulates synaptic vesicle exocytosis (Cao et al., 2013), while CPLX2 is involved in the negative regulation of the formation of synaptic vesicle clusters in the active area of the presynaptic membrane in postmitotic neurons (Reim et al., 2001). These proteins are regulated by SYT proteins, with SYT2 being identified as another discriminating protein between brains from α-AA and α-AA+EA-treated mice. SYT proteins accumulate in the nerve terminals and works in calcium triggering of neurotransmitter release (Pang et al., 2006). Another key protein in the release machinery of calcium-dependent neurotransmitters is the protein PRRT2 (Valente et al., 2016). PRRT2 is most abundant in presynaptic terminals and its silencing decreases the number of synapses and increases the number of synaptic vesicles docked at rest. The decrease in all these key proteins may be interpreted as a negative effect of EA supplementation in mice. In fact, in experiments using MWM test in CPLX2 knockout mice, deficits in mouse learning were found at 8 weeks, increasing their severity by the

493 year of age (Glynn et al., 2003). In humans, the decrease in this protein is associated
494 with schizophrenia and Huntington's disease (Glynn et al., 2003). According to other
495 authors, PRRT2 silenced-neurons exhibit a severe deterioration of synchronous release
496 of neurotransmitters due to a decrease in calcium sensitivity, a situation that is related to
497 epilepsy and migraine (Valente et al., 2016). While the supplementation of EA along with
498 α-AA did not lead to any clinical sign of mental disorder, including no effect on spatial
499 memory in MWM assay, this effect may be attributed to the ability of α-AA to act as
500 analogue of neurotransmitter glutamate (Díaz-Velasco et al., *submitted*). α-AA enhances
501 neuronal excitation by blocking the biosynthesis of kynurenic acid, an endogenous
502 inhibitor of glutamatergic and cholinergic neurotransmission (Hilmas et al., 2001).
503 Studies with experimental animals confirmed the ability of α-AA to strongly reduce the
504 extracellular levels of kynurenic acid in the rat brain, which would cause neuronal
505 excitation problems (Wu et al., 1995). These physiological impairments, if happened in
506 our study, may have not affected the proteome and hence, would have passed
507 unnoticed. The effect of dietary EA in decreasing proteins implicated in synaptic function
508 may be a response to a potential neuronal excitation cause by α-AA. Yet, the
509 confirmation of the physiological and clinical consequences of these proteomic effects of
510 EA requires further elucidation.

511 Other biological processes affected in mice brain by the exposure of α-AA+EA were the
512 growth cone (13.33%, $p<0.01$) and the postsynaptic intermediate filament cytoskeleton
513 (7.08%, $p<0.01$) (Fig. 3A). In this function, proteins related to the postsynaptic
514 intermediate filament cytoskeleton and the neurofilament cytoskeleton organization
515 (Table S5), such as KIF5B (fold change: 0.62), neurofilament light polypeptide (NEFL,
516 fold change: 0.44), superoxide dismutase [Cu-Zn] (SOD1, fold change: 0.38), alpha-
517 internexin (INA, fold change: 0.51), neurofilament medium polypeptide (NEFM, fold
518 change: 0.39), microtubule-associated protein 6 (MAP6, fold change: 0.82) and
519 microtubule-associated protein tau (MAPT, fold change: 0.72) (Tables 3 and S2) were

the most affected. These proteins are involved in binding activity of actin filaments, maintenance of neuronal caliber or microtubule stabilization and regulation of the axonal growth.

Other relevant process involved in neurotransmission and influenced by the dietary intake of α-AA+EA was the clathrin binding process (7.5%, $p<0.01$) (Fig. 3A). Proteins such as clathrin light chain B (CLTB, fold change: 0.53), clathrin heavy chain C (CLTC, fold change, 0.083), epsin-1 (EPN1, fold change: 0.81) and synergin gamma (SYNRG, fold change: 0.80) (Tables 3 and S2), were found in lower abundance in this process (Table S5) as compared to α-AA treated mice. Particularly relevant is the significant decrease in clathrin heavy chain (CLTC), the main component of the vesicle coat and the protein with the lowest fold change of all those found in the experiment. Clathrin is involved in neurotransmission, as well as directing neurotoxic aggregates to lysosomes for degradation. In addition, clathrin is part of the vesicles formed by endocytosis in neurons, which function is to maintain the balance of the membrane at the synapse (Camblor-Perujo and Kononenko, 2022).

Hence, it can be stated that, at the proteomic level, the proteins that are interconnected in the formation of neurofilaments in neurons are affected to a greater extent by the combination of α-AA+EA than by the mere presence of the oxidized amino acid alone, but at the behavioral level these changes are not observed in the alteration of the spatial memory of mice.

3.3.2.2. Counteraction of EA to the biological processes impaired by α-AA

Unlike the aforementioned effect of dietary α-AA, the Arp2/3 protein complex was positively influenced by the exposure of α-AA+EA in brain of mice (16,56%, $p<0.01$) (Fig. 3B). Various units of actin-related protein 2/3 complex (see fold changes in Tables 3 and S2) alongside the actin-related protein 2 (ACTR2, fold change: 1.29) and the actin alpha cardiac muscle 1 (ACTC1, fold change: 2.04), were found in higher abundance in this

546 complex. In addition, proteins such as FSCN1 (fold change: 1.53) and WD repeat-
547 containing protein 1 (WDR1, fold change: 1.19) were also found in higher quantity in
548 positive regulation of the podosome assembly (Table S6), As aforementioned, Arp2/3
549 protein complex, an essential component in the formation of actin cytoskeleton, was
550 decreased in mice exposed to α-AA, affecting the normal formation of actin-rich
551 structures in cells of the nervous system. Therefore, it is reasonable to hypothesize that
552 the presence of EA alleviates the harmful effects of α-AA in mice brain at this respect. In
553 addition to the Arp2/3 complex, proteins involved in other actin-rich structures, such as
554 podosomes (Rottiers et al., 2009), were also increased upon intake of the phytochemical.
555 The strengthening of Arp2/3 protein complex and other proteins involved in actin
556 polymerization, are also related to the increase in both nucleobase-containing small
557 molecule metabolic process and the energy metabolism. In fact, the supplementation
558 with EA to mice exposed to α-AA severely modulated the nucleobase-containing small
559 molecule metabolic process (39.38%, $p<0.01$) (Fig. 3B). Proteins such as ribose-
560 phosphate pyrophosphokinase 1 (PRPS1, fold change: 1.26), phosphoribosyl
561 pyrophosphate synthase-associated protein 1 and 2 (PRPSAP2, fold change: 1.19;
562 PRPSAP1, fold change: 1.14), guanine deaminase (GAD, fold change: 1.48), GMP
563 reductase 2 (GMPR2, fold change: 1.40) and cytosolic type of the 5(3)-
564 deoxyribonucleotidase, (NT5C, fold change: 1.19) (Tables 2 and S2) among many
565 others, were found in higher abundance in the brain cells of mice treated with α-AA+EA
566 than in mice challenged with the oxidized amino acid, alone (Table S6). This enzymatic
567 complex catalyzes the synthesis of phosphoribosylpyrophosphate (PRPP), which is
568 essential for nucleotide synthesis, NAD and NADP (Santos et al., 2020). PRPP plays a
569 crucial role in *de novo* synthesis and purine recovery. EA and microbial metabolites of
570 this phenolic acid, namely, urolithins, have been found to positively modulate purine
571 metabolism and reduce the onset of related health disorders (Adachi et al., 2020). The
572 necessity to synthesize new nucleotides for the formation of DNA and RNA in order to
573 produce new proteins to counteract the depletion produced by the presence of α-AA in

574 brain cells, would explain the increase of deoxyribonucleotide and ribonucleotide
575 metabolic processes by dietary EA. Proteins such as the cytoplasmic isocitrate
576 dehydrogenase [NADP] (IDH1, fold change: 1.55), and the mitochondrial proteins
577 isocitrate dehydrogenase [NADP] IDH2, (fold change: 1.37), IDH3B (fold change: 1.30)
578 and IDH3G (fold change: 1.30) (Tables 3 and S2) were found in higher abundance in
579 isocitrate metabolic and dehydrogenase activity (Table S6). Moreover, the proteins ATP-
580 citrate synthase (ACLY, fold change: 1.33), the mitochondrial citrate synthase (CS, fold
581 change: 1.33) and the cytoplasmic hydroxymethylglutaryl-CoA synthase (HMGCS1, fold
582 change: 1.25), among many others (Table S6), were also found in higher quantity related
583 to the energy metabolism. The positive modulation in energy metabolism is consistent
584 with the upregulation of nucleotide synthesis which is a costly anabolic process.

585 In addition, protein GDA, involved in the deamination of guanine to xanthine, which is an
586 essential part of the guanine degradation pathway, was also found in higher quantity.
587 GDA-deficient cells cannot effectively eliminate guanine and this excess alters the
588 metabolism of adenine, cytosine and thymine-based nucleotides, inhibiting DNA
589 synthesis and cell growth that eventually results in cell apoptosis (Wang et al., 2019).
590 Therefore, the effect of the combination of the oxidized amino acid and the
591 phytochemical, influences, in a positive manner the mouse brain increasing the
592 degradation of guanine to avoid an imbalance in the formation of the other nucleotides,
593 which can lead to fatal consequences for cells.

594 Other relevant counteracting mechanism of EA is the regulation of redox metabolism and
595 the modulation of the synthesis of proteins implicated in antioxidant defense. α-AA led to
596 a significant increase of antioxidant enzymes such as CAT and GPX4 and this was
597 attributed to the severe oxidative stress induced by α-AA and manifested in increased
598 carbonylated proteins. The supplementation with EA reversed this situation by
599 decreasing the abundance of these proteins in the brain of mice (CAT, fold change: 0.77;
600 GPX4, fold change: 0.91) (Tables 2 and S2). These results indicate that EA may

counteract the oxidative stress caused by α-AA and hence, inhibit the necessity of upregulate the synthesis of antioxidant enzymes. In good agreement with this hypothesis, the extent of protein carbonylation in brain of cells supplemented with EA was significantly lower as compared to the degree of carbonylation in brain of mice exposed to α-AA. The antioxidant activity of EA is well documented in studies of chronic inflammation of the colon (Rosillo et al., 2012) and chronic colitis in rats (Marín et al., 2013), in which EA caused an alleviating effect on the symptoms of the disease. In brain, the effect of EA in neurological disorders has been studied with promising results (Gupta et al., 2021; Zhu et al., 2022). In addition to the decrease in abundance of antioxidant enzymes, other processes increased by the intake of α-AA were inverted in mice exposed to α-AA+EA, such as aminoacyl-tRNA synthetase multienzyme complex (Table S5), smooth endoplasmic reticulum with the protein HSPA5 found in lower quantity, alongside with protein 4.1 (EPB41, fold change: 0.62) and hypoxia up-regulated protein 1 (HYOU1, fold change: 0.22), which emphasizes the positive effects of EA in mice exposed to α-AA.

4. CONCLUSIONS

The intake of oxidized amino acids, especially in processed foods, is related to the onset and progression of neurological disorders and cognitive impairment. In this study the oral administration of lysine oxidation product α-AA up to 6 weeks led to severe oxidative stress along with significant modification in the proteome of brain cells in mice. Yet, these modifications did not affect the spatial memory of mice as assessed by the Morris Maze. The use of plant phenolics as dietary supplements to mitigate harmful effects of oxidized amino acids should be made with caution as EA led to certain modifications in the brain proteome of mice that could be interpreted as potentially harmful.

Credit authorship contribution statement

S. Díaz-Velasco: data curation, methodology, formal analysis, writing - original draft.

R. Martínez: data curation, methodology, funding acquisition, supervision, formal analysis, validation, writing – review & editing.

J. Delgado: data curation, methodology, funding acquisition, supervision, formal analysis, validation, writing – review & editing.

Mario Estévez: conceptualization, funding acquisition, project administration, resources, supervision, validation, writing – review & editing. All authors have read and agreed to the published version of the manuscript.

Declaration of competing interest

The authors declare that they have no known competing financial interests or personal relationships that could have appeared to influence the work reported in this paper.

Funding

This research was funded by Grant PID2021-126193OB-I00 funded by MCIN/AEI/ 10.13039/501100011033 and by "ERDF: A way of making Europe". S. Díaz-Velasco is recipient of a fellowship from the Spanish Ministry of Science and Innovation (grant number PRE2018-084001) Q-Exactive Orbitrap equipment was acquired by a grant from the Spanish Ministry of Science and Innovation (MCIN/AEI/ 10.13039/501100011033) (grant number UNEX-AE-3394).

Data Availability Statement

All data is contained within the article or supplementary material, including raw data from proteomics.

References

Adachi, S.I., Sasaki, K., Kondo, S., Komatsu, W., Yoshizawa, F., Isoda, H., Yagasaki, K., 2020. Antihyperuricemic Effect of Urolithin A in Cultured Hepatocytes and Model Mice. Mol. 2020, Vol. 25, Page 5136 25, 5136. https://doi.org/10.3390/MOLECULES25215136

652 Akagawa, M., Sasaki, T., Suyama, K., 2002. Oxidative deamination of lysine residue in
653 plasma protein of diabetic rats: Novel mechanism via the Maillard reaction. Eur. J.
654 Biochem. 269, 5451–5458. https://doi.org/10.1046/j.1432-1033.2002.03243.x

655 Bai, R., Guo, J., Ye, X., Xie, Y., Reviews, T.X.-A. research, 2022, U., 2022. Oxidative
656 stress: The core pathogenesis and mechanism of Alzheimer's disease. Ageing
657 Res. Rev. 77, 101699.

658 Bindea, G., Mlecnik, B., Hackl, H., Charoentong, P., Tosolini, M., Kirilovsky, A.,
659 Fridman, W.-H., Pagès, F., Trajanoski, Z., Galon, J., 2009. ClueGO: a Cytoscape
660 plug-in to decipher functionally grouped gene ontology and pathway annotation
661 networks. Bioinformatics 25, 1091–1093.
662 https://doi.org/10.1093/bioinformatics/btp101

663 Brown, D.R., Kretzschmar, H.A., 1998. The glio-toxic mechanism of α-aminoadipic acid
664 on cultured astrocytes. J. Neurocytol. 27, 109–118.
665 https://doi.org/10.1023/A:1006947322342

666 Byman, E., Martinsson, I., Haukedal, H., Gouras, G., Freude, K.K., Wennström, M.,
667 2021. Neuronal α-amylase is important for neuronal activity and glycogenolysis
668 and reduces in presence of amyloid beta pathology. Aging Cell 20.
669 https://doi.org/10.1111/ACEL.13433

670 Cambiaghi, T.D., Pereira, C.M., Shanmugam, R., Bolech, M., Wek, R.C., Sattlegger,
671 E., Castilho, B.A., 2014. Evolutionarily conserved IMPACT impairs various stress
672 responses that require GCN1 for activating the eIF2 kinase GCN2. Biochem.
673 Biophys. Res. Commun. 443, 592–597.
674 https://doi.org/10.1016/J.BBRC.2013.12.021

675 Camblor-Perujo, S., Kononenko, N.L., 2022. Brain-specific functions of the endocytic
676 machinery. FEBS J. 289, 2219–2246. https://doi.org/10.1111/FEBS.15897

Cao, P., Yang, X., Südhof, T.C., 2013. Complexin activates exocytosis of distinct secretory vesicles controlled by different synaptotagmins. J. Neurosci. 33, 1714–1727. https://doi.org/10.1523/JNEUROSCI.4087-12.2013

Cardoso, B., Machado, P., Steele, E.M., 2022. Association between ultra-processed food consumption and cognitive performance in US older adults: a cross-sectional analysis of the NHANES 2011–2014. Eur. J. Nutr. 61, 3975–3985. https://doi.org/10.1007/S00394-022-02911-1/TABLES/3

Chen, W.N., Tang, K.S., Yeong, K.Y., 2022. Potential Roles of α-amylase in Alzheimer's Disease: Biomarker and Drug Target. Curr. Neuropharmacol. 20, 1554. https://doi.org/10.2174/1570159X20666211223124715

Correia, A.S., Cardoso, A., Vale, N., 2023. Oxidative Stress in Depression: The Link with the Stress Response, Neuroinflammation, Serotonin, Neurogenesis and Synaptic Plasticity. Antioxidants 2023, Vol. 12, Page 470 12, 470. https://doi.org/10.3390/ANTIOX12020470

D'Haens, G., Rieder, F., Feagan, B.G., Higgins, P.D.R., Panés, J., Maaser, C., Rogler, G., Löwenberg, M., van der Voort, R., Pinzani, M., Peyrin-Biroulet, L., Danese, S., Allocca, M., De Hertogh, G., Denton, C., Distler, J., McCarrier, K., McGovern, D., Radstake, T., Serrano, D., Stoker, J., 2022. Challenges in the Pathophysiology, Diagnosis, and Management of Intestinal Fibrosis in Inflammatory Bowel Disease. Gastroenterology 162, 26–31. https://doi.org/10.1053/j.gastro.2019.05.072

da Silva, J.C., Amaral, A.U., Cecatto, C., Wajner, A., dos Santos Godoy, K., Ribeiro, R.T., de Mello Gonçalves, A., Zanatta, Â., da Rosa, M.S., Loureiro, S.O., Vargas, C.R., Leipnitz, G., de Souza, D.O.G., Wajner, M., 2017. α-Ketoadipic Acid and α-Aminoadipic Acid Cause Disturbance of Glutamatergic Neurotransmission and Induction of Oxidative Stress In Vitro in Brain of Adolescent Rats. Neurotox. Res. 32, 276–290. https://doi.org/10.1007/s12640-017-9735-8

David, J., Gormley, S., McIntosh, A.L., Kebede, V., Thuery, G., Varidaki, A., Coffey, E.T., Harkin, A., 2019. L-alpha-amino adipic acid provokes depression-like behaviour and a stress related increase in dendritic spine density in the pre-limbic cortex and hippocampus in rodents. Behav. Brain Res. 362, 90–102. https://doi.org/10.1016/j.bbr.2019.01.015

de La Pomélie, D., Santé-Lhoutellier, V., Sayd, T., Gatellier, P., 2018. Oxidation and nitrosation of meat proteins under gastro-intestinal conditions: Consequences in terms of nutritional and health values of meat. Food Chem. 243, 295–304. https://doi.org/10.1016/j.foodchem.2017.09.135

De, R., Sarkar, A., Ghosh, P., Ganguly, M., Karmakar, B.C., Saha, D.R., Halder, A., Chowdhury, A., Mukhopadhyay, A.K., 2018. Antimicrobial activity of ellagic acid against Helicobacter pylori isolates from India and during infections in mice. J. Antimicrob. Chemother. 73, 1595–1603. https://doi.org/10.1093/JAC/DKY079

Delgado, J., Núñez, F., Asensio, M.A., Owens, R.A., 2019. Quantitative proteomic profiling of ochratoxin A repression in Penicillium nordicum by protective cultures. Int. J.Food Microbiol. 305, 108243. https://doi.org/10.1016/j.ijfoodmicro.2019.108243

Den, R.B., Lu, B., 2012. Heat shock protein 90 inhibition: Rationale and clinical potential. Ther. Adv. Med. Oncol. 4, 211–218. https://doi.org/10.1177/1758834012445574

Díaz-Velasco, S., Delgado, J., Peña, F.J., Estévez, M., 2022. Protein oxidation marker, α-amino adipic acid, impairs proteome of differentiated human enterocytes: Underlying toxicological mechanisms. Biochim. Biophys. acta. Proteins proteomics 1870, 140797. https://doi.org/10.1016/J.BBAPAP.2022.140797

Díaz-Velasco, S., González, A., Peña, F.J., Estévez, M., 2020. Noxious effects of selected food-occurring oxidized amino acids on differentiated CACO-2 intestinal

human cells. Food Chem. Toxicol. 144, 1–8. https://doi.org/10.1016/j.fct.2020.111650

Eletto, Davide, Eletto, Daniela, Dersh, D., Gidalevitz, T., Argon, Y., 2014. Protein Disulfide Isomerase A6 Controls the Decay of IRE1α Signaling via Disulfide-Dependent Association. Mol. Cell 53, 562–576. https://doi.org/10.1016/J.MOLCEL.2014.01.004

Estaras, M., Ameur, F.Z., Estévez, M., Díaz-Velasco, S., Gonzalez, A., 2020. The lysine derivative aminoadipic acid, a biomarker of protein oxidation and diabetes-risk, induces production of reactive oxygen species and impairs trypsin secretion in mouse pancreatic acinar cells. Food Chem Toxicol. 145, 111594. https://doi.org/10.1016/j.fct.2020.111594

Estévez, M., 2021. Critical overview of the use of plant antioxidants in the meat industry: Opportunities, innovative applications and future perspectives. Meat Sci. 181, 108610. https://doi.org/10.1016/J.MEATSCI.2021.108610

Estévez, M., Díaz-Velasco, S., Martínez, R., 2021. Protein carbonylation in food and nutrition: a concise update. Amin. Acids 2021 544 54, 559–573. https://doi.org/10.1007/S00726-021-03085-6

Estévez, M., Xiong, Y., 2019. Intake of Oxidized Proteins and Amino Acids and Causative Oxidative Stress and Disease: Recent Scientific Evidences and Hypotheses. J. Food Sci. 84, 387–396. https://doi.org/10.1111/1750-3841.14460

Fan, J., Fong, T., Chen, X., Chen, C., Luo, P., Xie, H., 2018. Glia maturation factor-β: a potential therapeutic target in neurodegeneration and neuroinflammation. Neuropsychiatr. Dis. Treat. 14, 495. https://doi.org/10.2147/NDT.S157099

Flohé, L., Toppo, S., Orian, L., 2022. The glutathione peroxidase family: Discoveries and mechanism. Free Radic. Biol. Med. 187, 113–122.

https://doi.org/10.1016/J.FREERADBIOMED.2022.05.003

Forman, H.J., Zhang, H., 2021. Targeting oxidative stress in disease: promise and limitations of antioxidant therapy. Nat. Rev. Drug Discov. 2021 209 20, 689–709. https://doi.org/10.1038/s41573-021-00233-1

Fu, M. meng, McAlear, T.S., Nguyen, H., Oses-Prieto, J.A., Valenzuela, A., Shi, R.D., Perrino, J.J., Huang, T.T., Burlingame, A.L., Bechstedt, S., Barres, B.A., 2019. The Golgi Outpost Protein TPPP Nucleates Microtubules and Is Critical for Myelination. Cell 179, 132-146.e14. https://doi.org/10.1016/J.CELL.2019.08.025

García-Montes, M., Crespo, I., 2023. La mielinización como un factor modulador de los circuitos de memoria. Rev. Neurol. 76, 101. https://doi.org/10.33588/RN.7603.2022325

García-Villalba, R., Espín, J.C., Aaby, K., Alasalvar, C., Heinonen, M., Jacobs, G., Voorspoels, S., Koivumäki, T., Kroon, P.A., Pelvan, E., Saha, S., Tomás-Barberán, F.A., 2015. Validated Method for the Characterization and Quantification of Extractable and Nonextractable Ellagitannins after Acid Hydrolysis in Pomegranate Fruits, Juices, and Extracts. J. Agric. Food Chem. 63, 6555–6566. https://doi.org/10.1021/ACS.JAFC.5B02062

Glynn, D., Bortnick, R.A., Morton, A.J., 2003. Complexin II is essential for normal neurological function in mice. Hum. Mol. Genet. 12, 2431–2448. https://doi.org/10.1093/HMG/DDG249

Goodarzi, G., Shirgir, A., Alavi, S., Khoshi, A., 2019. Effect of insulin-glucose metabolism compared with obesity on adipose omentin gene expression in different models of diabetic C57BL/6 mice. Diabetol. Metab. Syndr. 11. https://doi.org/10.1186/S13098-019-0460-8

Gupta, A., Singh, A.K., Kumar, R., Jamieson, S., Pandey, A.K., Bishayee, A., 2021.

779 Neuroprotective Potential of Ellagic Acid: A Critical Review. Adv. Nutr. 12, 1211.
780 https://doi.org/10.1093/ADVANCES/NMAB007

781 Hellwig, M., 2019. The Chemistry of Protein Oxidation in Food. Angew.Chemie - Int.
782 Ed. 58, 16742–16763. https://doi.org/10.1002/anie.201814144

783 Henney, A.E., Gillespie, C.S., Alam, U., Hydes, T.J., Mackay, C.E., Cuthbertson, D.J.,
784 2023. High intake of ultra-processed food is associated with dementia in adults: a
785 systematic review and meta-analysis of observational studies. J. Neurol. 1, 1–13.
786 https://doi.org/10.1007/S00415-023-12033-1/FIGURES/4

787 Hilmas, C., Pereira, E.F.R., Alkondon, M., Rassoulpour, A., Schwarcz, R.,
788 Albuquerque, E.X., 2001. The Brain Metabolite Kynurenic Acid Inhibits α7
789 Nicotinic Receptor Activity and Increases Non-α7 Nicotinic Receptor Expression:
790 Physiopathological Implications. J. Neurosci. 21, 7463–7473.
791 https://doi.org/10.1523/JNEUROSCI.21-19-07463.2001

792 Hu, L.L., Pan, M.H., Yang, F.L., Zong, Z.A., Tang, F., Pan, Z.N., Lu, X., Ren, Y.P.,
793 Wang, J.L., Sun, S.C., 2021. FASCIN regulates actin assembly for spindle
794 movement and polar body extrusion in mouse oocyte meiosis. J. Cell. Physiol.
795 236, 7725–7733. https://doi.org/10.1002/JCP.30443

796 Kang, I., Buckner, T., Shay, N.F., Gu, L., Chung, S., 2016. Improvements in Metabolic
797 Health with Consumption of Ellagic Acid and Subsequent Conversion into
798 Urolithins: Evidence and Mechanisms. Adv. Nutr. 7, 961–972.
799 https://doi.org/10.3945/AN.116.012575

800 Kim, D., An, H., Fan, C., Park, Y., 2021. Identifying oligodendrocyte enhancers
801 governing Plp1 expression. Hum. Mol. Genet. 30, 2225.
802 https://doi.org/10.1093/HMG/DDAB184

803 Kim, I.H., Racz, B., Wang, H., Burianek, L., Weinberg, R., Yasuda, R., Wetsel, W.C.,

804 Soderling, S.H., 2013. Disruption of Arp2/3 Results in Asymmetric Structural
805 Plasticity of Dendritic Spines and Progressive Synaptic and Behavioral
806 Abnormalities. J. Neurosci. 33, 6081–6092.
807 https://doi.org/10.1523/JNEUROSCI.0035-13.2013

808 Ko, H.S., Uehara, T., Tsuruma, K., Nomura, Y., 2004. Ubiquilin interacts with
809 ubiquitylated proteins and proteasome through its ubiquitin-associated and
810 ubiquitin-like domains. FEBS Lett. 566, 110–114.
811 https://doi.org/10.1016/J.FEBSLET.2004.04.031

812 Kunová, N., Havalová, H., Ondrovičová, G., Stojkovičová, B., Bauerová-Hlinková, V.,
813 Pevala, V., Kutejová, E., Bauer, J.A., 2022. Mitochondrial Processing
814 Peptidases—Structure, Function and the Role in Human Diseases. Int. J. Mol. Sci.
815 23, 23. https://doi.org/10.3390/IJMS23031297

816 Lee, Hyo Jung, Jang, H.B., Kim, W.H., Park, K.J., Kim, K.Y., Park, S.I., Lee, Hye Ja,
817 2019. 2-Aminoadipic acid (2-AAA) as a potential biomarker for insulin resistance in
818 childhood obesity. Sci. Rep. 9, 1–10. https://doi.org/10.1038/s41598-019-49578-z

819 Li, H., Li, S., Yang, H., Zhang, Y., Zhang, S., Ma, Y., Hou, Y., Zhang, X., Niu, K.,
820 Borné, Y., Wang, Y., 2022. Association of Ultraprocessed Food Consumption With
821 Risk of Dementia. Neurology 99, e1056–e1066.
822 https://doi.org/10.1212/WNL.0000000000200871

823 Liu, Xijun, Liu, D., Qian, D., Dai, J., An, Y., Jiang, S., Stanley, B., Yang, J., Wang, B.,
824 Liu, Xinyuan, Liu, D.X., 2012. Nucleophosmin (NPM1/B23) interacts with
825 activating transcription factor 5 (ATF5) protein and promotes proteasome- and
826 caspase-dependent ATF5 degradation in hepatocellular carcinoma cells. J. Biol.
827 Chem. 287, 19599–19609. https://doi.org/10.1074/JBC.M112.363622

828 Liu, Z., Yang, X., Chen, C., Liu, B., Ren, B., Wang, L., Zhao, K., Yu, S., Ming, H., 2013.
829 Expression of the Arp2/3 complex in human gliomas and its role in the migration

and invasion of glioma cells. Oncol. Rep. 30, 2127–2136. https://doi.org/10.3892/OR.2013.2669

Maetzler, W., Schmid, B., Synofzik, M., Schulte, C., Riester, K., Huber, H., Brockmann, K., Gasser, T., Berg, D., Melms, A., 2010. The CST3 BB genotype and low cystatin C cerebrospinal fluid levels are associated with dementia in Lewy body disease. J. Alzheimers. Dis. 19, 937–942. https://doi.org/10.3233/JAD-2010-1289

Maldonado, E., Morales-Pison, S., Urbina, F., Solari, A., 2023. Aging Hallmarks and the Role of Oxidative Stress. Antioxidants 2023, Vol. 12, Page 651 12, 651. https://doi.org/10.3390/ANTIOX12030651

Marín, M., María Giner, R., Ríos, J.L., Carmen Recio, M., 2013. Intestinal anti-inflammatory activity of ellagic acid in the acute and chronic dextrane sulfate sodium models of mice colitis. J. Ethnopharmacol. 150, 925–934. https://doi.org/10.1016/J.JEP.2013.09.030

Mostowy, S., Cossart, P., 2012. Septins: the fourth component of the cytoskeleton. Nat. Rev. Mol. Cell Biol. 2012 133 13, 183–194. https://doi.org/10.1038/nrm3284

Ni, J., Yang, P., Li, X., Tian, J., Jing, F., Qu, C., Lin, L., Zhang, H., 2014. Alterations of Amino Acid Level in Depressed Rat Brain. Korean J Physiol Pharmacol 18, 371–376. https://doi.org/10.4196/kjpp.2014.18.5.371

Ni, M., Lee, A.S., 2007. ER chaperones in mammalian development and human diseases. FEBS Lett. 581, 3641. https://doi.org/10.1016/J.FEBSLET.2007.04.045

Pang, Z.P., Melicoff, E., Padgett, D., Liu, Y., Teich, A.F., Dickey, B.F., Lin, W., Adachi, R., Südhof, T.C., 2006. Synaptotagmin-2 is essential for survival and contributes to Ca2+ triggering of neurotransmitter release in central and neuromuscular synapses. J. Neurosci. 26, 13493–13504. https://doi.org/10.1523/JNEUROSCI.3519-06.2006

Patil, S.S., Sunyer, B., Höger, H., Lubec, G., 2009. Evaluation of spatial memory of C57BL/6J and CD1 mice in the Barnes maze, the Multiple T-maze and in the Morris water maze. Behav. Brain Res. 198, 58–68. https://doi.org/10.1016/j.bbr.2008.10.029

Pearson, J.A., Ding, H., Hu, C., Peng, J., Galuppo, B., Wong, F.S., Caprio, S., Santoro, N., Wen, L., 2022. IgM-associated gut bacteria in obesity and type 2 diabetes in C57BL/6 mice and humans. Diabetologia 65, 1398–1411. https://doi.org/10.1007/S00125-022-05711-8

Pereira, M., Amaral, I., Lopes, C., Leitão, C., Madeira, D., Agosthino, P., FASEB, T., 2021. l-α-aminoadipate causes astrocyte pathology with negative impact on mouse hippocampal synaptic plasticity and memory. Wiley Online Libr. 35. https://doi.org/10.1096/fj.202100336R

Puspita, L., Chung, S.Y., Shim, J.W., 2017. Oxidative stress and cellular pathologies in Parkinson's disease. Mol. Brain 2017 101 10, 1–12. https://doi.org/10.1186/S13041-017-0340-9

Reim, K., Mansour, M., Varoqueaux, F., McMahon, H.T., Südhof, T.C., Brose, N., Rosenmund, C., 2001. Complexins regulate a late step in Ca2+-dependent neurotransmitter release. Cell 104, 71–81. https://doi.org/10.1016/S0092-8674(01)00192-1

Richardson, D.S., Spehar, J.M., Han, D.T., Chakravarthy, P.A., Sizemore, S.T., 2022. The RAL Enigma: Distinct Roles of RALA and RALB in Cancer. Cells 11. https://doi.org/10.3390/CELLS11101645

Rodriguez, A., Zhang, H., Klaminder, J., Brodin, T., Andersson, P.L., Andersson, M., 2018. ToxTrac: A fast and robust software for tracking organisms. Methods Ecol. Evol. 9, 460–464. https://doi.org/10.1111/2041-210X.12874

880 Roffé, M., Hajj, G.N.M., Azevedo, H.F., Alves, V.S., Castilho, B.A., 2013. IMPACT is a
881 developmentally regulated protein in neurons that opposes the eukaryotic initiation
882 factor 2βkinase GCN2 in the modulation of neurite outgrowth. J. Biol. Chem. 288,
883 10860–10869. https://doi.org/10.1074/JBC.M113.461970

884 Rosillo, M.A., Sánchez-Hidalgo, M., Cárdeno, A., Aparicio-Soto, M., Sánchez-Fidalgo,
885 S., Villegas, I., De La Lastra, C.A., 2012. Dietary supplementation of an ellagic
886 acid-enriched pomegranate extract attenuates chronic colonic inflammation in
887 rats. Pharmacol. Res. 66, 235–242. https://doi.org/10.1016/J.PHRS.2012.05.006

888 Rottiers, P., Saltel, F., Daubon, T., Chaigne-Delalande, B., Tridon, V., Billottet, C.,
889 Reuzeau, E., Génot, E., 2009. TGFβ-induced endothelial podosomes mediate
890 basement membrane collagen degradation in arterial vessels. J. Cell Sci. 122,
891 4311–4318. https://doi.org/10.1242/JCS.057448

892 Santos, K.D., Kwon, E., Moon, N.S., 2020. PRPS-Associated Disorders and the
893 Drosophila Model of Arts Syndrome. Int. J. Mol. Sci. 21, 4824.
894 https://doi.org/10.3390/IJMS21144824

895 Sell, D.R., Strauch, C.M., Shen, W., Monnier, V.M., 2007. 2-Aminoadipic acid is a
896 marker of protein carbonyl oxidation in the aging human skin: Effects of diabetes,
897 renal failure and sepsis. Biochem J. 404, 269–277.
898 https://doi.org/10.1042/BJ20061645

899 Sharifi-Rad, J., Quispe, C., Castillo, C.M.S., Caroca, R., Lazo-Vélez, M.A., Antonyak,
900 H., Polishchuk, A., Lysiuk, R., Oliinyk, P., De Masi, L., Bontempo, P., Martorell,
901 M., Daştan, S.D., Rigano, D., Wink, M., Cho, W.C., 2022. Ellagic Acid: A Review
902 on Its Natural Sources, Chemical Stability, and Therapeutic Potential. Oxid. Med.
903 Cell. Longev. 2022, 24. https://doi.org/10.1155/2022/3848084

904 Sherpa, A.D., van de Nes, P., Xiao, F., Weedon, J., Hrabetova, S., 2014. Gliotoxin-
905 induced swelling of astrocytes hinders diffusion in brain extracellular space via

formation of dead-space microdomains. Glia 62, 1053–1065. https://doi.org/10.1002/GLIA.22661

Shevchenko, A., Tomas, H., Havliš, J., Olsen, J. V., Mann, M., 2007. In-gel digestion for mass spectrometric characterization of proteins and proteomes. Nat. Protoc. 1, 2856–2860. https://doi.org/10.1038/nprot.2006.468

Sloin, H.E., Bikovski, L., Levi, A., Amber-Vitos, O., Katz, T., Spivak, L., Someck, S., Gattegno, R., Sivroni, S., Sjulson, L., Stark, E., 2022. Hybrid Offspring of C57BL/6J Mice Exhibit Improved Properties for Neurobehavioral Research. eNeuro 9, 1–16. https://doi.org/10.1523/ENEURO.0221-22.2022

Spence, E.F., Kanak, D.J., Carlson, B.R., Soderling, S.H., 2016. The Arp2/3 Complex Is Essential for Distinct Stages of Spine Synapse Maturation, Including Synapse Unsilencing. J. Neurosci. 36, 9696–9709. https://doi.org/10.1523/JNEUROSCI.0876-16.2016

Swaney, K.F., Li, R., 2016. Function and regulation of the Arp2/3 complex during cell migration in diverse environments. Curr. Opin. Cell Biol. 42, 63. https://doi.org/10.1016/J.CEB.2016.04.005

Tsang, C.W., Fedchyshyn, M., Harrison, J., Xie, H., Xue, J., Robinson, P.J., Wang, L.-Y., Trimble, W.S., 2008. Superfluous role of mammalian septins 3 and 5 in neuronal development and synaptic transmission. Mol. Cell. Biol. 28, 7012–7029. https://doi.org/10.1128/MCB.00035-08

Utrera, M., Morcuende, D., Rodríguez-Carpena, J.G., Estévez, M., 2011. Fluorescent HPLC for the detection of specific protein oxidation carbonyls - α-aminoadipic and γ-glutamic semialdehydes - in meat systems. Meat Sci. 89, 500–506. https://doi.org/10.1016/j.meatsci.2011.05.017

Valente, P., Castroflorio, E., Rossi, P., Fadda, M., Sterlini, B., Cervigni, R.I., Prestigio,

C., Giovedì, S., Onofri, F., Mura, E., Guarnieri, F.C., Marte, A., Orlando, M., Zara, F., Fassio, A., Valtorta, F., Baldelli, P., Corradi, A., Benfenati, F., 2016. PRRT2 Is a Key Component of the Ca2+-Dependent Neurotransmitter Release Machinery. Cell Rep. 15, 117–131. https://doi.org/10.1016/J.CELREP.2016.03.005

Van Hecke, T., Van Camp, J., De Smet, S., 2017. Oxidation During Digestion of Meat: Interactions with the Diet and Helicobacter pylori Gastritis, and Implications on Human Health. Compr. Rev. Food Sci. Food Saf. 16, 214–233. https://doi.org/10.1111/1541-4337.12248

Voronkov, D.N., Lyzhin, A.A., Dikalova, Y. V., Stavrovskaya, A. V., Khudoerkov, R.M., Khaspekov, L.G., 2021. Features of Brain Astrocyte Damage under the Influence of L-Aminoadipic Acid In Vitro and In Vivo. Cell tissue biol. 15, 347–355. https://doi.org/10.1134/S1990519X21040106/FIGURES/3

Wang, J., Bing, T., Zhang, N., Shen, L., He, J., Liu, X., Wang, L., Shangguan, D., 2019. The Mechanism of the Selective Antiproliferation Effect of Guanine-Based Biomolecules and Its Compensation. ACS Chem. Biol. 14, 1164–1173. https://doi.org/10.1021/ACSCHEMBIO.9B00062/ASSET/IMAGES/LARGE/CB-2019-00062R_0005.JPEG

Wang, P.S., Chou, F.S., Ramachandran, S., Xia, S., Chen, H.Y., Guo, F., Suraneni, P., Maher, B.J., Li, R., 2016. Crucial roles of the Arp2/3 complex during mammalian corticogenesis. Development 143, 2741–2752. https://doi.org/10.1242/DEV.130542

Wang, T.J., Ngo, D., Psychogios, N., Dejam, A., Larson, M.G., Vasan, R.S., Ghorbani, A., O'Sullivan, J., Cheng, S., Rhee, E.P., Sinha, S., McCabe, E., Fox, C.S., O'Donnell, C.J., Ho, J.E., Florez, J.C., Magnusson, M., Pierce, K.A., Souza, A.L., Yu, Y., Carter, C., Light, P.E., Melander, O., Clish, C.B., Gerszten, R.E., 2013. 2-Aminoadipic acid is a biomarker for diabetes risk. J. Clin. Invest. 123, 4309–4317.

https://doi.org/10.1172/JCI64801

Wu, H.Q., Ungerstedt, U., Schwarcz, R., 1995. l-α-Aminoadipic acid as a regulator of kynurenic acid production in the hippocampus: a microdialysis study in freely moving rats. Eur. J. Pharmacol. 281, 55–61. https://doi.org/10.1016/0014-2999(95)00224-9

Yalcin, O., Cabrales, P., 2012. Increased hemoglobin O2 affinity protects during acute hypoxia. Am. J. Physiol. - Hear. Circ. Physiol. 303, H271. https://doi.org/10.1152/AJPHEART.00078.2012

Yoshida, H., Goedert, M., 2012. Phosphorylation of microtubule-associated protein tau by AMPK-related kinases. J. Neurochem. 120, 165–176. https://doi.org/10.1111/J.1471-4159.2011.07523.X

Zeb, A., 2018. Ellagic acid in suppressing in vivo and in vitro oxidative stresses. Mol. Cell. Biochem. 448, 27–41. https://doi.org/10.1007/S11010-018-3310-3

Zhong, X.M., Hou, L., Luo, X.N., Shi, H.S., Hu, G.Y., He, H.B., Chen, X.R., Zheng, D., Zhang, Y.F., Tan, Y., Liu, X.J., Mu, N., Chen, J.P., Ning, Y.P., 2013. Alterations of CSF cystatin C levels and their correlations with CSF Aβ40 and Aβ42 levels in patients with Alzheimer's disease, dementia with lewy bodies and the atrophic form of general paresis. PLoS One 8. https://doi.org/10.1371/JOURNAL.PONE.0055328

Zhu, H., Yan, Y., Jiang, Y., Meng, X., 2022. Ellagic Acid and Its Anti-Aging Effects on Central Nervous System. Int. J. Mol. Sci. 2022, Vol. 23, Page 10937 23, 10937. https://doi.org/10.3390/IJMS231810937

FIGURE CAPTION

Figure 1. (A) Circular pool with a hidden a platform 1.5 cm beneath water surface. The location of the platform was identified by a distal reference platform attached to the pool wall. (B) Division of pool in zone 1 and 2, matching zone 1 with the area where the platform was.

Figure 2. Percentages of proteins annotated by Gene Ontology (* p<0.05, ** p<0.01) found in lower relative abundance in biological processes and molecular functions (A), and percentages of proteins found in higher relative quantity in biological processes and molecular functions (B) in mice brain affected by the exposure to α-AA compared to control counterparts. For a visual improvement of the pie chart, biological processes y molecular functions with an influence <6% in B were grouped.

Figure 3. Percentages of proteins annotated by Gene Ontology (* p<0.05, ** p<0.01) found in lower relative abundance in biological processes and molecular functions (A), and percentages of proteins found in higher relative quantity in biological processes and molecular functions (B) in mice brain affected by the exposure to α-AA+EA compared to α-AA counterparts. For a visual improvement of the pie chart, biological processes y molecular functions with an influence <6% (A) and <3% (B) were grouped.

SUPPLEMENTARY MATERIAL

Table S1. Proteins identified in C57BL/6 mice brain in the presence of α-AA along with Log2 fold change (Student's T-test Difference) and significance values (p). Proteins identified in lower abundance in α-AA-treated mice in comparison to the non-treated control animals; proteins identified in higher quantity in α-AA-treated mice in comparison to the non-treated control mice; proteins identified only in control mice in comparison to α-AA-treated animals and proteins identified only in the presence of α-AA in comparison

to the non-treated control mice. Control mice are marked in yellow, α-AA-treated mice in green and statistical differences in blue.

Table S2. Proteins identified in C57BL/6 mice brain in the presence of α-AA+EA along with Log2 fold change (Student's T-test Difference) and significance values (*p*). Proteins identified in lower quantity in α-AA+EA-treated mice in comparison to α-AA counterparts; proteins identified in higher abundance in α-AA+EA-treated animals in comparison to α-AA-challenged mice; proteins identified only in α-AA mice in comparison to α-AA+EA-treated mice and proteins identified only in the presence of α-AA+EA in comparison to α-AA counterparts. α-AA-treated mice are marked in yellow, α-AA+EA-treated animals in green and statistical differences in blue.

Table S3. Terms and associated genes found in lower quantity in the presence of α-AA compared to control counterparts.

Table S4. Terms and associated genes found in higher abundance in the presence of α-AA compared to control counterparts.

Table S5. Terms and associated genes found in lower quantity in the presence of α-AA+EA compared to α-AA treated cells.

Table S6. Terms and associated genes found in higher abundance in the presence of α-AA+EA compared to α-AA treated cells.

FIGURE 1

(A)

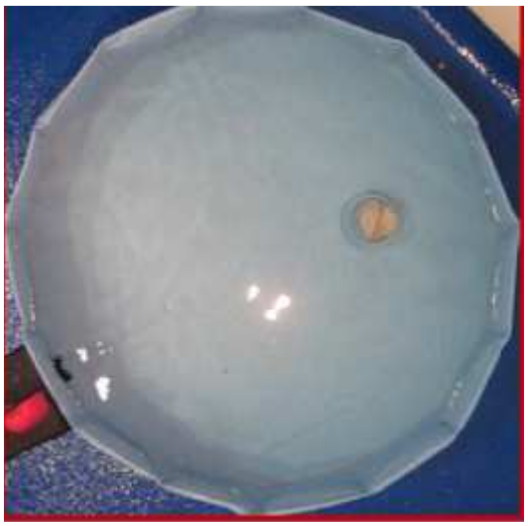

(B)

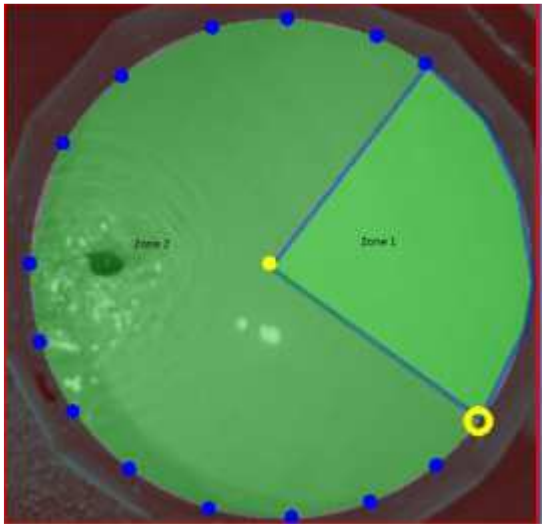

FIGURE 2

(A)

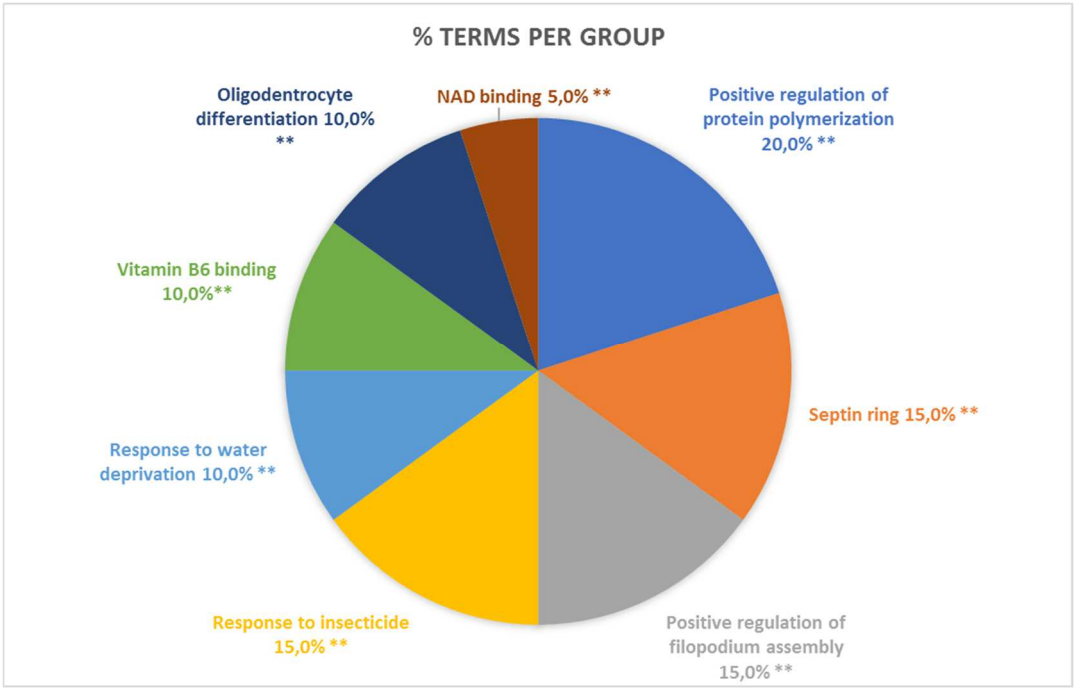
% TERMS PER GROUP
Oligodentrocyte differentiation 10,0% **
NAD binding 5,0% **
Positive regulation of protein polymerization 20,0% **
Vitamin B6 binding 10,0%**
Septin ring 15,0% **
Response to water deprivation 10,0% **
Response to insecticide 15,0% **
Positive regulation of filopodium assembly 15,0% **

(B)

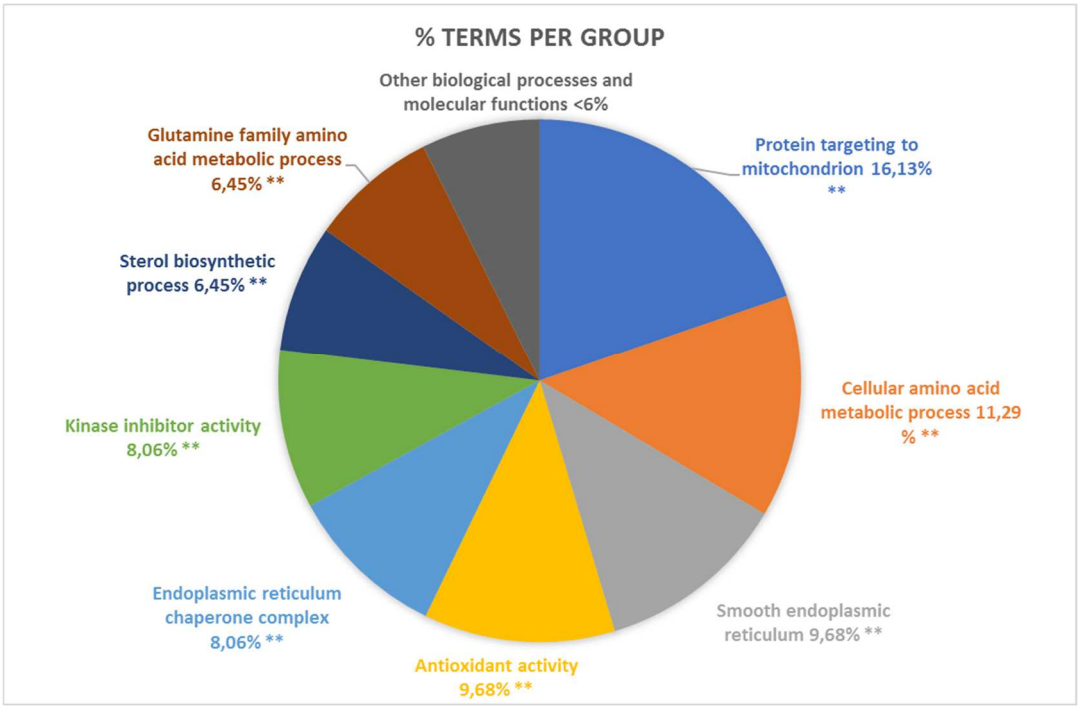
% TERMS PER GROUP
Other biological processes and molecular functions <6%
Glutamine family amino acid metabolic process 6,45% **
Protein targeting to mitochondrion 16,13% **
Sterol biosynthetic process 6,45% **
Cellular amino acid metabolic process 11,29 % **
Kinase inhibitor activity 8,06% **
Endoplasmic reticulum chaperone complex 8,06% **
Smooth endoplasmic reticulum 9,68% **
Antioxidant activity 9,68% **

FIGURE 3

(A)

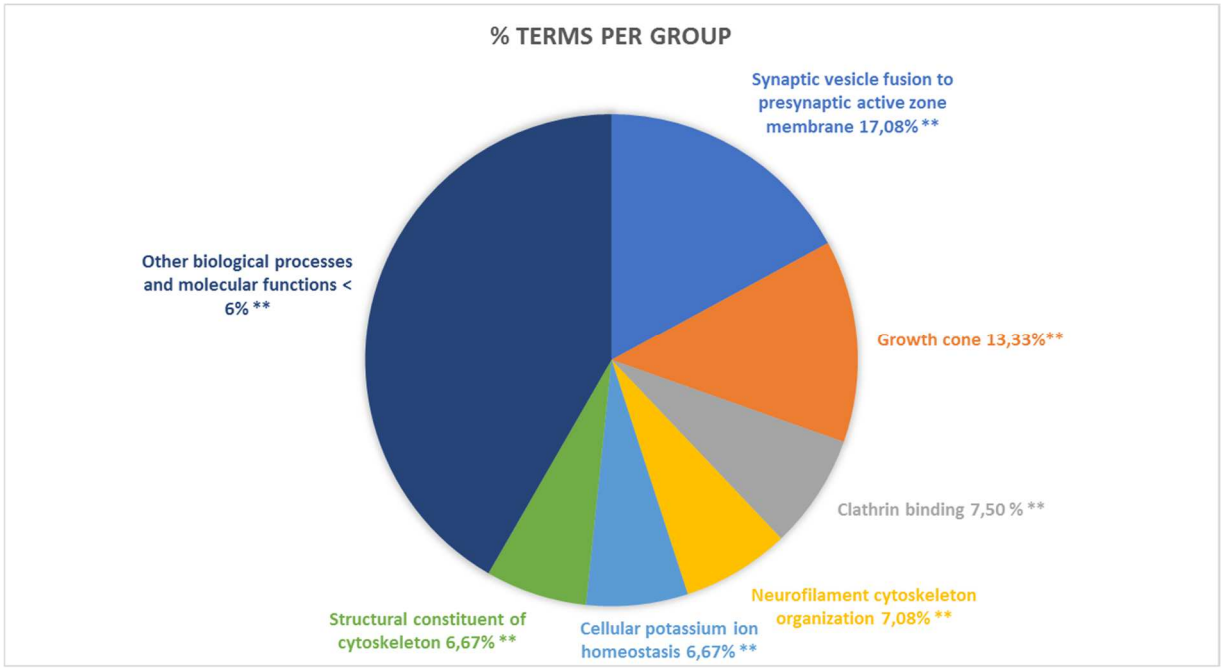
% TERMS PER GROUP
Synaptic vesicle fusion to presynaptic active zone membrane 17,08% **
Growth cone 13,33%**
Clathrin binding 7,50 % **
Neurofilament cytoskeleton organization 7,08% **
Cellular potassium ion homeostasis 6,67% **
Structural constituent of cytoskeleton 6,67% **
Other biological processes and molecular functions < 6% **

(B)

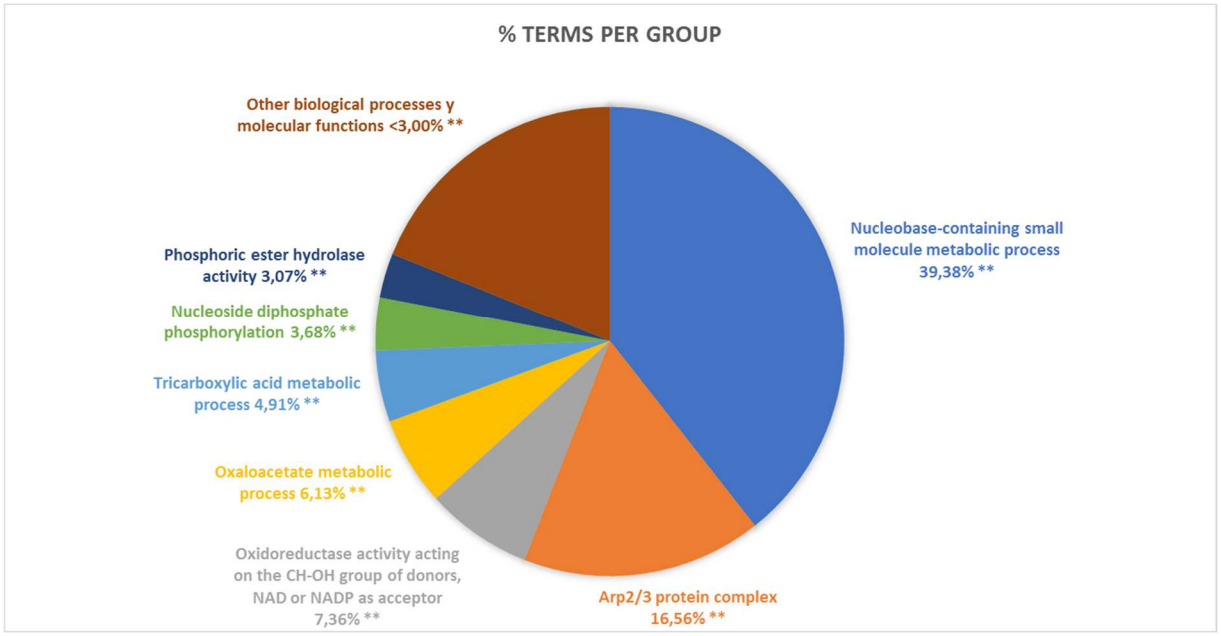
% TERMS PER GROUP
Other biological processes y molecular functions <3,00% **
Nucleobase-containing small molecule metabolic process 39,38% **
Phosphoric ester hydrolase activity 3,07% **
Nucleoside diphosphate phosphorylation 3,68% **
Tricarboxylic acid metabolic process 4,91% **
Oxaloacetate metabolic process 6,13% **
Oxidoreductase activity acting on the CH-OH group of donors, NAD or NADP as acceptor 7,36% **
Arp2/3 protein complex 16,56% **

Table 1. Results of Morris Maze behavioral parameters (mean± standard deviation) of C57BL/6 black mice under various experimental conditions. Control, α-Amino adipic acid (α-AA) and α-Amino adipic acid (α-AA) + Ellagic acid (EA) for 3 and 6 weeks.

WEEK 3 CONTROL vs. α-AA vs. α-AA+EA						
	Total distance (mm)	Av. Speed (mm/s)	Av. Acceleration (mm/s^2)	Inside time zone 1 (seconds)	Inside rate zone 1 (%)	Exploration rate (%)
CONTROL	4955,44±952,72	94,5±17,10	436,07±69,95	12,09±4,97	23,71 ±8,56	52,67±5,46
α-AA	5647,42±2022,99	107,17±38,94	483,81±166,00	11,49±6,80	2 2,21±14,06	51,45±11,71
α-AA+EA	5533,24±1551,79	101,30±22,11	465,22±97,37	10,24±6,87	18 ,48±10,21	45,84±5,01
p -VALUE	>0,05	>0,05	>0,05	>0,05	>0,05	>0,05
WEEK 6 CONTROL vs. α-AA vs. α-AA+EA						
	Total distance (mm)	Av. Speed (mm/s)	Av. Acceleration (mm/s^2)	Inside time zone 1 (seconds)	Inside rate zone 1 (%)	Exploration rate (%)
CONTROL	4569,84±706,11	89,53±15,95	418,98±71,89	17,02±7,01	33,2 3±12,02	41,11±3,34
α-AA	5568,4±1832,42	108,70±35,45	505,45±154,04	15,14±4,51	30 ,05±9,30	42,63±10,00
α-AA+EA	5335,62±1977,49	90,43±26,91	412,73±109,51	11,54±3,05	20 ,35±7,06	43,05±13,47
p -VALUE	>0,05	>0,05	>0,05	>0,05	>0,05	>0,05
CONTROL WEEK 3 vs. WEEK 6						
	Total distance (mm)	Av. Speed (mm/s)	Av. Acceleration (mm/s^2)	Inside time zone 1 (seconds)	Inside rate zone 1 (%)	Exploration rate (%)
CONTROL WEEK 3	4955,43±952,72	94,49±17,10	436,07±69,95	12,09±4,97	23,7 1±8,56	52,67±5,45
CONTROL WEEK 6	4569,84±706,11	89,53±15,95	418,98±71,89	17,02±7,01	33,2 2±12,02	41,11±3,34
p -VALUE	>0,05	>0,05	>0,05	>0,05	>0,05	**<0,05**
α-AA WEEK 3 vs. WEEK 6						
	Total distance (mm)	Av. Speed (mm/s)	Av. Acceleration (mm/s^2)	Inside time zone 1 (seconds)	Inside rate zone 1 (%)	Exploration rate (%)
α-AA WEEK 3	5647,41±2022,99	107,57±39,03	483,81±166,00	11,49±6,80	2 2,21±14,06	51,45±11,71
α-AA WEEK 6	5568,40±1832,42	108,70±35,44	505,45±154,04	15,14±4,51	3 0,05±9,30	42,63±10,00
p -VALUE	>0,05	>0,05	>0,05	>0,05	>0,05	>0,05
		α-AA+EA WEEK 3 vs. WEEK 6				
	Total distance (mm)	Av. Speed (mm/s)	Av. Acceleration (mm/s^2)	Inside time zone 1 (seconds)	Inside rate zone 1 (%)	Exploration rate (%)
α-AA+EA WEEK 3	5533,24±1551,79	101,30±22,11	465,22±97,37	10,24±6,87	18 ,48±10,21	45,84±5,01
α-AA+EA WEEK 6	5335,62±1977,49	90,43±26,91	412,73±109,51	11,54±3,05	20 ,35±7,06	43,05±13,47
p -VALUE	>0,05	>0,05	>0,05	>0,05	>0,05	>0,05

Table 2. Proteins from C57BL/6 brain mice affected by the exposure to α-Amino adipic acid (α-AA) in comparison to the non-treated control (C).

PROTEIN NAME	GENE NAME	p-VALUE	FOLD CHANGE1	BIOLOGICAL FUNCTION	FASTA Accession Number
Protein canopy homolog 2	*CNPY2*	0.019	0.37	Positive regulator of neurite outgrowth	Q9QXT0
Cystatin-C	*CST3*	0.006	0.45	Involved in dementia and Alzheimer's disease	P21460
Microtubule-associated protein	*MAPT*	0.017	0.56	Promotes microtubule assembly and stability and the establishment and maintenance of neuronal polarity	P10637
Alpha-amylase	*AMY2*	0.040	0.56	Glycogen degradation enzyme	P00688
Mitogen-activated protein kinase 10	*MAPK10*	0.015	0.56	Serine/threonine-protein kinase activated by pro-inflammatory cytokines or physical stress	Q3TQZ7
Myelin proteolipid protein	*PLP1*	0.003	0.61	Formation and maintenance of the multilamellar structure of myelin	P60202
Tyrosine 3-monooxygenase	*TH*	0.015	0.64	Catalyzes the conversion of L-tyrosine to L-dihydroxyphenylalanine (L-Dopa)	P24529
Growth factor receptor-bound protein 2	*GRB2*	0.032	0.65	Tyrosine kinase implicated in signal transduction	Q60631

CD9 antigen	*CD9*	0.040	0.68	Myelin protein involved in the formation of paranodal junctions	P40240
Actin-related protein 2/3 complex subunit 2	*ARPC2*	0.026	0.70	Component of Arp2/3 protein complex involved in actin polymerization	Q9CVB6
Neuronal-specific septin-3	*SEPT3.*	0.022	0.73	Associated with actin filaments and microtubules, located at the base of dendritic spines	A0A571BE69
Fascin	*FSCN1*	0.013	0.74	Actin-binding and bundling protein	Q61553
Guanine deaminase	*GDA*	0.031	0.76	Positive regulation of microtubule polymerization	Q9R111
Neuronal-specific Septin-11	*SEPT11.*	0.026	0.77	Associated with actin filaments and microtubules, located at the base of dendritic spines	A0A0J9YTY0
Glia maturation factor beta	*GMFB*	0.014	0.77	Stimulation of neural regeneration, differentiation of brain cells and inhibition of proliferation of tumor cells	Q9CQI3
Neuronal-specific Septin-6	*SEPT6.*	0.022	0.81	Associated with actin filaments and microtubules, located at the base of dendritic spines	Q9R1T4
Actin-related protein 2/3 complex subunit 5	*ARPC5*	0.032	0.82	Component of Arp2/3 protein complex involved in actin polymerization	Q9CPW4

Tubulin polymerization-promoting protein	*TPPP*	0.009	0.82	Regulator of microtubule dynamics	Q7TQD2
Profilin2	*PFN2*	0.014	0.83	Regulation of actin polymerization	Q9JJV2
Ras-related protein Ral-A	*RALA*	0.022	0.83	Involved in gene expression, vesicle trafficking, filopodia formation	P63321
78 kDa glucose-regulated protein	*HSPA5*	0.046	1.16	Chaperones in response to endoplasmic reticulum (ER) stress	P20029
Tryptophan--tRNA ligase, cytoplasmic	*WARS*	0.014	1.18	Catalyze the aminoacylation of tRNA by their cognate amino acid, tryptophan	P32921
TOM1-like protein 2	*TOM1l2*	0.003	1.21	Adapter protein involved in signaling pathways	Q5SRX1
Alpha-aminoadipic semialdehyde synthase	*AASS*	0.026	1.23	Bifunctional enzyme that catalyzes the first two steps in lysine degradation	Q9SMZ4
Isoleucine--tRNA ligase, cytoplasmic	*IARS*	0.037	1.23	Catalyze the aminoacylation of tRNA by their cognate amino acid, isoleucine	Q8BU30
60 kDa heat shock protein, mitochondrial	*HSPD1*	0.004	1.25	Unfolding polypeptides	P63038
DnaJ homolog subfamily C member 3	*DNAJC3*	0.003	1.25	Involved in the unfolded protein response (UPR) during endoplasmic reticulum (ER) stress	Q91YW3

Glutathione peroxidase	*GPX4*	0.006	1.26	Key role in protecting cells from oxidative damage by preventing membrane lipid peroxidation	S4R1E5
Phenylalanine--tRNA ligase beta subunit	*FARSB*	0.014	1.31	Responsible for attaching L-phenylalanine to the terminal adenosine of the appropriate tRNA	Q9WUA2
Catalase	*CAT*	0.018	1.34	Antioxidant enzyme in response to oxidative stress in response to H_2O_2	P24270
High mobility group protein B2	*HMGB2*	0.005	1.35	Involved in transcription, chromatin remodeling and recombination	P30681
Protein IMPACT	*IMPACT*	0.021	1.37	Translational regulator of translation in stress conditions	O55091
Probable cysteine--tRNA ligase, mitochondrial	*CARS2*	0.036	1.39	Play a critical role in protein biosynthesis by charging tRNAs with their cognate amino acids	Q8BYM8
Mitochondrial-processing peptidase subunit alpha	*PMPCA*	0.008	1.40	Binding subunit of the essential mitochondrial processing protease (MPP)	Q9DC61
T-complex protein 1 subunit gamma	*CCT3*	0.022	1.42	Component of the chaperonin-containing T-complex	Q3U0I3
Endoplasmin	*HSP90B1*	0.038	1.46	Chaperone related to the processing and transport of secreted proteins	P08113

Heat shock protein HSP 90-alpha	*HSP90AA1*	0.047	1.48	Promote proper protein folding and prevent misfolding	P07901
Apolipoprotein E	*APOE*	0.017	1.51	Lipid transport between organs via the plasma and interstitial fluids	P08226
Hemoglobin subunit alpha	*HBA-A1*	0.012	1.55	Involved in oxygen transport	Q91VB8
Nucleophosmin	*NPM1*	0.033	1.55	Involved in protein chaperoning	Q5SQB0
D-amino-acid oxidase	*DAO*	0.011	1.57	Acts as a detoxifying agent which removes D-amino acids accumulated during aging	P18894
Hemoglobin subunit beta-1	*HBB-B1*	0.008	1.59	Involved in oxygen transport	A8DUK4
Ubiquilin-1	*UBQLN1*	0.032	1.61	Plays an important role in the regulation of different protein degradation mechanisms	Q8R317
Calcium-dependent secretion activator 1	*CADPS*	0.042	1.74	Calcium-binding protein involved in exocytosis of neurotransmitters	Q80TJ1
Protein disulfide-isomerase A6	*PDIA6*	0.032	1.90	Involved in the unfolded protein response (UPR) during endoplasmic reticulum (ER) stress	Q3TML0
Complement C3	*C3*	0.027	2.08	Mediator of local inflammatory process	P01027
Alpha-2-HS-glycoprotein	*AHSG*	0.004	2.18	Promotes endocytosis, possesses opsonic properties, affinity for calcium	A0A338P703

Homer protein homolog 3	*HOMER3*	0.043	2.30	Postsynaptic density scaffolding protein, related to calcium release and immune response	Q99JP6
Protein 4.1	*EPB41*	0.016	2.54	Major structural element of the erythrocyte membrane skeleton	A2A842
Mitochondrial-processing peptidase subunit beta	*PMPCB*	-	α-AA	Binding subunit of the essential mitochondrial processing protease (MPP)	Q9CXT8

[1]Fold change indicates the degree of quantity change for a particular protein between animals (control vs. α-AA); FC <1 denotes a decrease in the concentration of protein in the treated mice (vs. control); FC >1 indicates a significant increase in the concentration of the protein in treated mice (vs. control). When a given protein is only present in one of the groups, fold change cannot be measured, and such condition is denoted as "α-AA" (if protein is only present in α-AA -exposed animals).

1068 **Table 3.** Proteins from C57BL/6 brain mice affected by the exposure to α-Amino adipic acid (α-AA) + Ellagic acid (EA) in comparison to α-Amino
1069 adipic acid treated animals (α-AA).

PROTEIN NAME	GENE NAME	p-VALUE	FOLD CHANGE[1]	BIOLOGICAL FUNCTION	FASTA accession number
Clathrin heavy chain 1	*CLTC*	$1.2x10^{-3}$	0.083	Main component of clathrin-coated vesicles	Q68FD5
Hypoxia up-regulated protein 1	*HYOU1*	$7.8x10^{-3}$	0.22	Crucial role in cytoprotective cellular mechanisms triggered by oxygen deprivation	Q9JKR6
SPARC-like protein 1	*SPARCL1*	$3.79x10^{-5}$	0.31	Present in the extracellular matrix of synaptic cleft	P70663
Spectrin alpha chain, non-erythrocytic 1	*SPTAN1*	0.031	0.32	Binding activity of actin filaments	A3KGU7
Superoxide dismutase [Cu-Zn]	*SOD1*	$4.8x10^{-3}$	0.38	Antioxidant enzyme involved in detoxifying radical superoxide	P08228
Neurofilament medium polypeptide	*NEFM*	0.004	0.39	Component of neurofilaments involved in maintenance of neuronal caliber	A0A0R4J036
Complement C3	*C3*	0.013	0.43	Mediator of local inflammatory process	P01027

Neurofilament light polypeptide	*NEFL*	0.021	0.44	Component of neurofilaments involved in maintenance of neuronal caliber	P08551
Alpha-internexin	*INA*	0.027	0.51	Cooperates with NEFL and NEFM to form the filamentous backbone in neurons	P46660
Clathrin light chain B	*CLTB*	0.005	0.53	Main component of vesicle coat	Q6IRU5
Proline-rich transmembrane protein 2	*PRRT2*	0.016	0.55	In presynaptic terminals, involved in the release of calcium	E9PUL5
Sodium/potassium-transporting ATPase subunit alpha-1	*ATP1A1*	0.049	0.59	Component of sodium/potassium ATPase	Q8VDN2
Complexin-1	*CPLX1*	0.014	0.60	Positively regulates a late step in exocytosis in synaptic vesicles	P63040
Synaptotagmin-2	*SYT2*	0.039	0.61	In presynaptic terminals, involved in the release of calcium	P46097
Kinesin-1 heavy chain	*KIF5B*	8.3×10^{-3}	0.61	Microtubule-dependent motor involved in the normal distribution of mitochondria and lysosomes	Q61768
Synaptosomal-associated protein 25	*SNAP25*	0.031	0.61	Modulates different voltage-dependent calcium channels in neurons	P60879

Protein 4.1	*EPB41*	0.038	0.62	Major structural element of the erythrocyte membrane skeleton	A2A839
Complexin-2	*CPLX2*	$1.5x10^{-3}$	0.65	Positively regulates a late step in exocytosis in synaptic vesicles	P84086
Microtubule-associated protein tau	*MAPT*	$2.5x10^{-3}$	0.72	Promotes microtubule assembly and stability, maintenance of neuronal polarity	P10637
Spectrin beta chain, non-erythrocytic 1	*SPTBN1*	0.044	0.72	Binding activity of actin filaments	Q62261
Catalase	*CAT*	0.020	0.77	Antioxidant enzyme involved in detoxifying hydrogen peroxide	P24270
Synergin gamma	*SYNRG*	0.008	0.80	Component of clathrin-coated vesicles	Q5SV85
Epsin-1	*EPN1*	0.043	0.81	Facilitates the formation of clathrin-coated invaginations	Q80VP1
Microtubule-associated protein 6	*MAP6*	0.030	0.82	Involved in microtubule stabilization and regulates axonal growth during neuron polarization	Q7TSJ2
78 kDa glucose-regulated protein	*HSPA5*	0.012	0.87	Chaperones in response to endoplasmic reticulum (ER) stress	P20029
Glutathione peroxidase	*GPX4*	0.042	0.91	Antioxidant enzyme with peroxidase activity	S4R1E5

Actin-related protein 2/3 complex subunit 5	*ARPC5*	0.025	1.18	Component of Arp2/3 protein complex involved in actin polimerization	Q9CPW4
Phosphoribosyl pyrophosphate synthase-associated protein 2	*PRPSAP2*	0.005	1.19	Part of ribose phosphate diphosphokinase complex, essential in nucleotide synthesis	Q8R574
5(3)-deoxyribonucleotidase, cytosolic type	*NT5C*	0.036	1.19	Involved in deoxyribonucleotide catabolic process.	Q9JM14
WD repeat-containing protein 1	*WDR1*	0.015	1.19	Implicated in cytokinesis	O88342
Hydroxymethylglutaryl-CoA synthase, cytoplasmic	*HMGCS1*	0.018	1.25	Catalyzes acetyl-CoA	Q8JZK9
Ribose-phosphate pyrophosphokinase 1	*PRPS1*	0.003	1.26	Catalyzes the synthesis of phosphoribosylpyrophosphate (PRPP)	Q9D7G0
Actin-related protein 2/3 complex subunit 1A	*ARPC1A*	0.018	1.28	Component of Arp2/3 protein complex involved in actin polimerization	Q9R0Q6
Actin-related protein 2	*ACTR2*	0.031	1.29	ATP-binding component of the Arp2/3 complex, mediates actin polymerization	P61161
Isocitrate dehydrogenase [NAD] subunit, mitochondrial	*IDH3B*	0.049	1.30	Component of tricarboxylic acid cycle	Q91VA7

Isocitrate dehydrogenase [NAD] subunit gamma 1, mitochondrial	*IDH3G*	0.011	1.30	Component of tricarboxylic acid cycle	P70404
ATP-citrate synthase	*ACLY*	0.046	1.33	Catalyzes the cleavage of citrate into oxaloacetate and acetyl-CoA	Q91V92
Citrate synthase, mitochondria	*CS*	0.030	1.33	Component of tricarboxylic acid cycle	Q9CZU6
Actin-related protein 2/3 complex subunit 3	*ARPC3*	0.003	1.37	Component of Arp2/3 protein complex involved in actin polimerization	H7BWZ3
Isocitrate dehydrogenase [NADP], mitochondrial	*IDH2*	0.001	1.37	Component of tricarboxylic acid cycle	P54071
GMP reductase 2	*GMPR2*	0.016	1.40	Maintenance of intracellular balance of nucleotides A and G	Q99L27
Actin-related protein 2/3 complex subunit 2	*ARPC2*	1.6×10^{-3}	1.43	Component of Arp2/3 protein complex involved in actin polimerization	Q9CVB6
Guanine deaminase	*GDA*	0.005	1.48	Essential in the guanine degradation pathway	Q9R111
Fascin	FSCN1	4.8×10^{-4}	1.53	Actin-binding and bundling protein	Q61553
Isocitrate dehydrogenase [NADP] cytoplasmic	*IDH1*	0.006	1.55	Component of tricarboxylic acid cycle	O88844

Actin, alpha cardiac muscle 1	*ACTC1*	1.6×10^{-3}	2.04	Invasion and prognosis marker in glioma	P68033

[1]Fold change indicates the degree of abundance change for a particular protein between animals (α-AA vs. α-AA+EA); FC <1 denotes a decrease in the concentration of protein in α-AA+EA treated mice (vs. α-AA); FC >1 indicates a significant increase in the concentration of the protein in α-AA+EA treated mice (vs. α-AA).

Capítulo 4.6. Food-compatible doses of 3-nitrotyrosine causes loss of spatial memory in C57BL/6 mice: investigation of molecular mechanisms by brain proteomics

Dosis compatibles con alimentos de 3-nitrotirosina causa pérdida de memoria espacial en ratones C57BL/6: investigación de mecanismos moleculares mediante proteómica en cerebro

Autores: Silvia Díaz-Velasco, Remigio Martínez, Josué Delgado, Mario Estévez

Food-Compatible Doses of 3-Nitrotyrosine Causes Loss of Spatial Memory in C57BL/6 Mice: Investigation of Molecular Mechanisms by Brain Proteomics

S. Díaz-Velasco[1], R. Martínez[1], J. Delgado[2], Mario Estévez[1*]

[1] Food Technology and Quality (TECAL), Institute of Meat and Meat Products (IPROCAR), University of Extremadura, Cáceres, Spain.

[2] Food Hygiene and Safety (HISEALI), Institute of Meat and Meat Products (IPROCAR), University of Extremadura, Cáceres, Spain.

Short title: “Effects of 3-nitrotyrosine and ellagic acid in C57BL/6 mice”

*Corresponding author: Mario Estévez, Institute of Meat and Meat Products (IPROCAR), University of Extremadura, Avda de las Ciencias, s/n. 10003, Cáceres, Spain. Phone number: +34 927251390. Email: mariovet@unex.es

Abstract

The nitrosation of the tyrosine amino acid by reactive nitrogen species (RNS) in a pro-oxidant environment leads to the formation of 3-nitrotyrosine (3NT), which is found in nitrite-added foods, such as cured meats, sausages and other ultraprocessed foods. The sustained consumption of the latter is linked to neurological disorders such as memory loss. The aim of this study was to analyze the possible toxicological impact of 3NT (320 µg 3NT/ kg live weight) in the brain of C57BL/6 mice and its possible mitigation with ellagic acid (EA) supplementation (1.9 mg/ kg live weight). The intake of 3NT at food-compatible doses caused severe oxidative stress in brain of mice and a temporary loss of spatial memory in a Morris Maze at week 3 of the assay. Yet, the plausible activation of plasticity mechanisms including strengthening of antioxidant defenses led to recovery of spatial memory at week 6 of the assay. 3NT induced changes in brain proteome which involved impairment of cytoskeletal proteins and synaptic functions. Dietary EA seemed to counteract the oxidative stress and cognitive impairments caused by 3NT. The proteome changes induced by supplemented EA includes the increase concentration of proteins with proven neurological benefits.

Keywords: 3-nitrotyrosine; ellagic acid; proteomics; brain; oxidative stress; C57BL/6 mice; spatial memory.

1. INTRODUCTION

The nitrosation of proteins is a phenomenon caused by reactive nitrogen species (RNS) in pro-oxidative conditions (Estévez et al., 2017). The imbalance between antioxidant defenses and reactive oxygen species (ROS) in an organism, leads to a redox environment that affects biological molecules. The superoxide radical ($O_2^{\bullet}$) reacts with nitrogen-derived compounds, such as nitric oxide (NO), an important cell signalling molecule, resulting in a powerful RNS named peroxinitrite ($ONOO^-$) (Pacher et al., 2007). The reaction between $O_2^{\bullet-}$ and NO is fast and spontaneous, making the peroxinitrite formation inevitable. In this manner, peroxinitrite and other RNS affect contiguous molecules such as proteins, which suffer a phenomenon of nitrosation that is irreversible, affecting the activity of metabolic enzymes and the regulation of cell signalling (Griswold-Prenner et al., 2023; Mallozzi et al., 1997). Thus, RNS cause the nitrosation of amino acids, specially of aromatic amino acids such as tryptophan and tyrosine, leading this latter to the formation of 3-nitrotyrosine (3NT) (Ceriello, 2002; Estévez et al., 2017). 3NT is formed during processing of nitrite-added foods such as sausages and cured meats (Ozyurt and Otles, 2020, 2017; Villaverde et al., 2014a, 2014b), being, in this regard, one of the main nitro compounds in processed foods and a biological marker of nitrosation. RNS and nitrosated amino acids are involved in a number of diseases, particularly with a strong correlation in inflammatory bowel disease (IBD) (Zhu and Li, 2012), and the formation of genotoxic compounds during digestion (Van Hecke et al., 2015). 3NT may be involved in the harmful effects that ultra-processed foods cause in the long-term, such as the increase of cognitive impairment in older and middle-aged adults after an 8-year follow-up (Gomes Gonçalves et al., 2023). This nitrosated amino acid can be considered as a reliable biomarker in the early diagnosis of diseases such as Alzheimer's, Huntington's and Parkinson's diseases, among others, since the increase of 3NT occurs long before any symptoms of disease appear (Bandookwala and Sengupta, 2020). Curiously, in 2015, the International Agency for Research on Cancer, included processed meat products in group 1 of carcinogens based on epidemiological

studies (IARC, 2015). Currently, the underlying molecular mechanisms of the causal connection between the intake of such foods and the health disorders are under study. In previous investigations, 3NT has been analyzed on differentiated human enterocytes CACO-2 cells (Díaz-Velasco et al., 2020), finding a cytotoxic effect and a significant increase in necrosis in these cells. In a study with a proteomic approach (Díaz-Velasco et al., 2022b), an increased binding to metabotropic type 3 glutamate receptors was found, affecting the regulation of calcium release channels and nitric oxide synthase regulation through increased protein calmodulin, leading to a significant increase in necrosis and in protein oxidation markers. Likewise, it was also involved in a significant decrease of the processing and presentation of antigens through the major histocompatibility complex. Ellagic acid (EA) is a phenolic acid with multiple benefits found both *in vitro* and *in vivo* studies, such as antioxidant and anti-inflammatory effects (Ascacio-Valdés et al., 2014; Cerda-Cejudo et al., 2022). Díaz-Velasco et al. (2022b) reported that the combination of this phytochemical with 3NT caused a decrease in proteins involved in the formation of mitochondrial crests, leading to a massive cell necrosis and a wide increase in protein oxidation biomarkers and antioxidant defenses. The aim of this investigation was to study by means of a Morris water maze assay, the effect of 3NT and its combination with EA on the loss of spatial memory in C57BL/6 mice for 3 and 6 weeks. Further to this, a MS-based untargeted proteomic approach and the analysis of biomarkers of protein oxidation in the brain of the same animals were applied to comprehend the molecular mechanisms behind the hypothetical brain injury and neuropathic disorder. Ellagic acid was evaluated for its ability to counteract the potential noxious effects of 3NT.

2. MATERIAL AND METHODS

2.1. Animals and chemicals

Eight-weeks old C57BL/6 mice were supplied from the animal experimentation laboratory of the University of Extremadura (Cáceres, Spain). Handling, euthanasia, and

the experimental protocols were approved by the institutional Bioethical Committee (reference 57/2016). 3-NT (CAS Number 621-44-3) and EA (CAS Number 476-66-4) were obtained from Sigma-Aldrich (Sigma-Aldrich, Steinheim, Germany). Other reagents were purchased in Panreac (Panreac Química, S. A., Barcelona, Spain), Sigma-Aldrich (Sigma-Aldrich, Steinheim, Germany) and Fisher (Fisher Scientific S.L., Madrid, Spain). Water used was purified by passage through a Milli-Q system (Millipore Corp., Bedford, MA).

2.2. Experimental procedure

During an adaptation period of one week, the mice were individually identified by means of a perforation code in the auditory pavilion. During adaptation, mice were maintained in ventilated cages, with water and feed *ad libitum* and housed at room temperature (21±2 ºC), with humidity control (55% ± 10%) and with a 12-h light/12-h dark cycle. During the assay, C57BL/6 mice had free access to feed and water *ad libitum* for 6 weeks. Once the adaptation period finished, mice were randomly allocated into one of these three experimental groups depending on the oral administration of 3NT and EA (n=5, per group): 3NT (challenged with dietary 3NT), 3NT+EA (challenged with dietary 3NT and EA) and a control group. Dietary components under study were dissolved in drinking water at concentrations of 5 mg/L (3NT) and 30 mg/L (EA) with these doses being food-compatible according to the data available in the literature (De et al., 2018; Kang et al., 2016; Lu et al., 2020; Tang et al., 2023). In the control group, the aforementioned solutions were replaced by basal drinking water. During the assay (6 weeks), mice were daily checked to warrant safety and well-being. During the treatment, food and water/solutions consumption were gravimetrically monitored every time they were filled in order to calculate the energy intake and effective doses of both compounds. This procedure was performed depending on the demand of the animals (every two or three days, approximately). Body weights were register weekly. The addition of dietary supplements (α-AA and EA) did not affect the volume of drinking water, which was similar

irrespective of the treatments. Considering the water intake and the weight of animals, the effective doses of each dietary compound were 320 µg 3NT/ kg live weight and 1.9 mg EA/kg live weight.

2.3. Morris Water Maze Test

Morris water maze (MWM) test was carried out to study the possible alterations in spatial memory caused by 3NT and 3NT+EA. The training of C57BL/6 mice before experiment and acquisition phases were conducted according to Patil et al. (2009). Briefly, mice (n=5, each group) were located in a circular pool (120 cm diameter, walls 20 cm depth), in which a platform 1.5 cm was hidden beneath water surface. The location of the platform could be only identified by a distal reference platform attached to the pool wall. During 2 weeks, the mice were trained to identify the location of the platform and scape from the maze. The effectiveness of the training was assessed by observing a significant reduction in the time spent by the mice in scaping from the maze. During the spatial memory assay, the platform was removed from the maze. The pool was divided in two zones, as shown in Fig. 1A-B, in which zone 1 (zone of interest) matched with the area where the platform was. Water temperature was maintained at 21±1ºC. The experiment was divided into two phases to study short-term (3 weeks) and long-term (6 weeks) spatial memory. The parameters analyzed were total distance (mm), average speed (mm/s), average acceleration (mm/s^2), exploration rate (%), inside time zone 1 (seconds) and inside rate zone 1 (%). Videos were recorded using a video camera (Sony, Tokio, Japan) and analyzed by ToxTrac program (Rodriguez et al., 2018).

2.4. Euthanasia and sample collection

After the last MWM assay, mice were euthanized by exsanguination via cardiac puncture. Previously, the animals were anaesthetized using 5% inhaled isoflurane. Brains were collected and cryopreserved at -80ºC.

2.5. Assessment of protein oxidation

Two main protein oxidation biomarkers, α-aminoadipic semialdehyde (α-AS) and γ-glutamic semialdehyde (γ-GS), and an additional marker of advanced protein oxidation (pentosidine), were measured in mice brain. The procedure described by Utrera et al. (2011) was followed. Firstly, 50 mg of brain were homogenized in 0.5 mL of PBS adding magnetized metal balls. Later, 100 µL of brain lysates were treated with 1 mL of cold 10% trichloroacetic acid (TCA) solution. Then, proteins were precipitated with centrifugation at 2240 g for 5 min at 4 °C. The supernatant was removed, and the pellet was treated with 1 mL of cold 5% TCA. Proteins were precipitated again with centrifugation at 2240g for 5 min at 4 ºC. After removing supernatant, the pellet obtained were derivatized with p-amino-benzoic acid (ABA), purified and hydrolyzed as described elsewhere (Utrera et al., 2011). The hydrolysates were evaporated at 40 °C in vacuo and the generated residues were reconstituted with 200 µL of Milli-Q water and then filtered through hydrophilic polypropylene GH Polypro (GHP) syringe filters (0.45 µm pore size, Pall Corporation, NJ, USA) for HPLC analysis. Details on the chromatograph apparatus as well as on the separation, elution and identification of the compounds of interest were published (Utrera et al., 2011). α-AS-ABA and γ-GS-ABA were synthesized and purified following the procedure of Akagawa et al. (2002) and injected in the same conditions than samples. α-AS and γ-GS were identified in samples by comparing their retention times with those of the reference pure compounds. Standard solutions of ABA (ranging from 0.1 to 0.5 mM) were also injected in the same chromatographic conditions to create a standard curve. The peaks corresponding to both semialdehydes were manually integrated and the resulting areas plotted against the aforementioned standard curve. Results are expressed as nmol of protein carbonyl per mg of protein.

2.6. Sample preparation for LC-MS/MS Based Proteomics

At first, 50 mg of brain were added in 0.5 mL of lysis buffer pH 7,5 (100 mM Tris-HCl, 50 mM NaCl, 10% glycerol, 0.5 M EDTA pH 8,5, 100 mM of PMSF (Phenylmethansulfonylfluorid) and 100 µg/mL Pepstatin A in a 1:100 proportion), adding

magnetized metal balls. Samples were homogenized and sonicated 3 times in batches of 10 pulses (Branson Ultrasonics, Danbury, USA). Lysates were incubated on ice for 1 hour and the tissue debris was removed by centrifugation at 14452 g for 10 min at 4 ºC, then supernatants were passed into new Eppendorf tubes. Protein concentration was measured with a Coomasie Protein Assay Reagent Ready to Use using a Nanodrop 2000c Spectophotometer and a Nanodrop 2000 software (USA). A protein concentration of 1µg/µL is appropriate. Aliquots containing 50 µg of proteins were partially run in SDS-PAGE (4% stacking and 12% separating), just stopped when they reached the separating part of the gel to be in gel digested according to Shevchenko et al. (2007), with some modifications. The gel was stained with Coomassie blue R250 and each lane was cut into 1 mm3 pieces and subjected to in-gel digestion. For protein reduction, samples were incubated with 0.5 M DTT in 50 mM ammonium bicarbonate for 20 min at 56 °C. The resulting free thiol (-SH) groups were alkylated by incubating the samples with 0.55 M iodoacetamide in 50 mM ammonium bicarbonate for 15 min in the dark at room temperature. Later, samples were treated with a mix of 50 mM ammonium bicarbonate, ProteaseMAX (Promega, USA) and trypsin (Promega, USA), and incubated for 2 h at 37 ºC carrying out the proteolysis. After, acid formic was added to stop the proteolysis. Supernatant was removed of each sample and placed it into new Eppendorf tubes for drying in a vacuum concentrator (Gyrozen, Daejeon, Korea). Samples were added loading buffer (98% milli-Q water, 2% acetonitrile and 0.05% trifluoroacetic acid) and analyzed on the Orbitrap LC-MS/MS.

2.7. Label-free quantitative proteomic analyses

A Q-Exactive Plus mass spectrometer coupled to a Dionex Ultimate 3000 RSLCnano (Thermo Scientific) analyzed 5 µg from each digest. Data was collected using a Top15 method for MS/MS scans following the procedure described by Delgado et al. (2019), with some modifications as described in Díaz-Velasco et al. (2022a). Comparative proteome abundance and data analysis were conducted using MaxQuant software

(version 1.6.0.15.0; https://www.maxquant.org/download_asset/maxquant/latest)) and Perseus (v 1.6.14.0) to organize the data and perform statistical analysis. Carbamidomethylation of cysteines was set as a fixed modification; oxidation of methionines and acetylation of N-terminals were set as variable modifications. Database searching was carried out against Homo sapiens protein database (www.uniprot.org). The maximum peptide / protein false discovery rates (FDR) were set to 1% based on comparison to a reverse database. The MaxLFQ algorithm was used to generate normalized spectral intensities and infer relative protein abundance. Proteins were only retained in final analysis if they were detected in at least two replicates from at least one treatment, and the proteins that matched to a contaminant database or the reverse database were removed. Quantitative analysis was performed using a T-test to compare treatments with the control. Fold change is expressed as Log2.The qualitative analysis was also performed to detect proteins that were found in at least three replicates of a given treated group but were undetectable in the comparison control group. Proteins satisfying one of these two aforementioned criteria were identified as discriminating proteins, and their corresponding genes were grouped by biological processes and molecular functions through ClueGO (v. 2.5.6) (Bindea et al., 2009). To define term-term interrelations and functional groups based on shared genes between the terms, the Kappa score was established at 0.4. Three GO terms and 4 % of genes covered were set as the minimum required to be retained in the final result. The p-value was corrected by Bonferroni step down and set as $p<0.05$.

2.8. Statistical Analysis

Data was analyzed for normality and homoscedasticity and the effect of the exposure to 3NT and 3NT+ EA was evaluated by Analysis of Variance (ANOVA). The effect of time on the same measurements was assessed by Student's t-test. The Tukey's test was performed for multiple comparisons of the means. SPSS (version 27.0) was used for statistical analysis of the data and the significance level was set at $p<0.05$.

3. RESULTS & DISCUSSION

The formation of 3NT in nitrite-added foods may be involved in harmful effects in brain in the long-term, such as the increase of cognitive impairment in older and middle-aged adults, attributed to ultraprocessed foods (Gomes Gonçalves et al., 2023). Multiple pathologies are linked to nitrosative and oxidative stress (Liguori et al., 2018), and 3NT could be used as a reliable oxidative stress biomarker by its implication in different neurological diseases long before any symptoms of disease appear (Bandookwala and Sengupta, 2020). In previous *in vitro* studies, the onset of oxidative stress induced by 3NT was reported in intestinal CACO cells (Díaz-Velasco et al., 2022b, 2020). Since no information is available in regards to the impact of dietary 3NT on brain cells, this study focus on unraveling the changes in the proteome, the occurrence of oxidative stress in the brain of C57BL/6 mice and their consequences in possible loss of spatial memory.

3.1. Morris Water Maze test

The Morris Water Maze test showed that dietary 3NT led to a significant increase ($p<0.05$) of parameters related to the ability of mice to identify the zone of interest inside the maze (increased 'inside time' and 'inside rate') at week 6 as compared to week 3 (Table 1). These parameters remained unchanged in control mice over time. No significant differences ($p>0.05$) of interest were found in the other parameters analyzed in the rest of comparisons (Table 1). These results indicate that the dietary exposure to 3NT led to a partial loss of memory in the short term (3 weeks) that was reversed at longer exposure (6 weeks) to the nitrosated metabolite. To similar conclusions came Li et al. (2019) when testing the ability of oxidized tyrosine (dityrosine) at levels of 420 µg/kg body weight, to impair the spatial memory of C57BL/6J mice using several assays including the Morris Maze employed in the current study. To our knowledge, this is the first time that food-compatible doses of 3NT is found to be able to induce temporal neurological disorders in experimental animals. This is also suggesting that brain from challenged mice would have triggered protection mechanisms to counteract the effect of

3NT. The supplementation with EA did not seem to have any impact on the harmful effect of 3NT.

3.2. Protein Oxidation Markers

The analysis of protein oxidation markers was evaluated by the detection of early protein carbonyls (α-AS and γ-GS) and advanced oxidation protein products (pentosidine). The results showed that the intake of 3NT led to a quantitatively remarkable and significant increase of protein carbonyls in the brain of mice (2.39±0.41 nmol/mg protein) as compared to control group of mice (0.88±0.22 nmol/mg protein; $p<0.05$). Results for pentosidine are consistent as the levels of this species was significantly higher in brain from mice exposed to 3NT (3.09±0.35 area units) than the control counterparts (1.09±0.19 area units). The supplementation with EA led to a significant decrease (3NT *vs*. 3NT+EA; $p<0.05$) of both protein carbonyls (1.86±0.39 nmol/mg protein) and pentosidine (1.69±0.33 area units) with the levels of both species being still higher to those found in the brains from the control group of animals (3NT+EA *vs* control; $p<0.05$).

These results are in agreement with previous *in vitro* studies performed by ourselves in differentiated human enterocytes CACO-2 cells (Díaz-Velasco et al., 2022b, 2020). A proteomic and flow cytometric analysis carried out on the same samples revealed disturbances at the mitochondrial level and the generation of ROS, which led to elevated concentration of carbonylated proteins.

3.3. Proteomic Analyses

The MS-based proteomic platform enabled the identification of 1679 proteins in total. All these proteins were identified with at least two peptides and a FDR<1%. Quantitative ($p<0.05$) and qualitative (only detected in one condition) changes in protein abundance were evaluated (Tables S1-S2).

A first comparison was made between the proteomes of the brains from 3NT-treated mice *versus* brains of the control counterparts. In this case, the dietary administration of

3NT significantly influenced the concentration of 476 proteins in the brain of challenged mice, among which, 134 were found in lower abundance in animals treated with 3NT while 20 were only found in control samples. On the other hand, 253 proteins were detected in higher quantity in samples from mice exposed to 3NT and 69 were only found in 3NT-treated mice (Table S1).

To explore the potential benefits of dietary EA against 3NT, another comparison was made between the proteomes of brains from 3NT-treated mice *versus* those provided with 3NT+EA. In this case, 171 proteins were significantly influence by 3NT+EA; among which, 147 were detected in lower abundance in mice exposed to 3NT+EA, 6 were only detected in the presence of 3NT+EA and 18 were only found in 3NT-treated mice (Table S2).

For a comprehensible and organized description of results, discriminating proteins were grouped by biological processes and molecular functions. The comparison between control animals *versus* 3NT-treated mice is shown in Fig. 2A-B. The comparison between 3NT-treated mice and 3NT+EA is displayed in Fig. 3. Specific terms for each of these processes and full details of discriminating proteins and associated genes are provided in Supplementary material Tables S3-S6. Tables 2 and 3 show a selection of representative proteins from each relevant biological process or molecular function affected by the presence of 3NT (*vs*. control) and the comparison between 3NT *vs.* 3NT+EA, respectively. Only discriminating proteins having a relevant biological function are discussed in the following sections.

3.3.1 Impact of dietary 3NT on the brain proteome of C57BL/6 mice

The most relevant effects caused by 3NT (*vs*. control) on the proteome of the brain of C57BL/6 mice are discussed considering the most affected biological processes/metabolic routes for a more comprehensive understanding of the massive proteomic data obtained.

3.3.1.1. Impairment of synaptic function

From a proteomic approach, a severe impact of 3NT in the brain of mice was found and reflected in a number of proteins found in lower abundance in relevant biological processes related to the normal functioning of neurons, such as regulation of calcium channel activity, adequate formation of microtubules and synaptic vesicles and the regulation of signal transduction in synapse. The endopolyphosphatase activity was the molecular function most affected by the intake of 3NT (25.47%, $p<0.01$), followed the synaptic vesicle fusion to presynaptic active zone membrane (24.75%, $p<0.01$) and protein localization to synapse (13.86%, $p<0.01$) (Fig. 2A).

Firstly, the proteins found in lower abundance in endopolyphosphatase activity were subunits 2, 3-α and 3-β of diphosphoinositol polyphosphate phosphohydrolase (NUDT4, NUDT10 and NUDT11, fold change: 0.73), the mitochondrial ADP-ribose pyrophosphatase (NUDT9, fold change: 0.78) and the cytosolic purine 5-nucleotidase (NT5C2, fold change: 0.79) (Table 2 and S1). These proteins are part of the diphosphoinositol polyphosphate phosphohydrolase (DIPP) system (Carreras-Puigvert et al., 2017), which mediates the hydrolysis of some nucleoside diphosphate derivatives. This mechanism is implicated in the reversible phosphorylation of downstream effector molecules involved in signal transduction in brain (Ballif et al., 2004).

Proteins involved in the synaptic vesicle fusion to presynaptic membrane were also reduced in quantity in the brain of mice treated with 3NT such as complexin-1 (CPLX1, fold change: 0.50), complexin-2 (CPLX2, fold change: 0.42), synaptosomal-associated protein 25 (SNAP25, fold change: 0.76) and the protein 1 of vesicle-associated membrane (VAMP1, fold change: 0.81) (Tables 2, S1 and S3). While CPLX1 is involved in synaptic vesicle exocytosis (Cao et al., 2013), CPLX2 is implicated in the negative regulation of the formation of synaptic vesicle clusters in presynaptic membrane (Reim et al., 2001). Complexins are essential for the activation of multiple types of exocytosis induced by calcium. The depletion of complexins is consistent with the decreased

concentration of proteins involved in the regulation of calcium channel activity, such as striatin-4 (STRN4, fold change: 0.27), the subunit alpha-2/delta-1 voltage-dependent calcium channel (CACNA2D1, fold change: 0.29) (Dahimene et al., 2022). It is worth mentioning that these two latter proteins showed some of the most decreased fold changes in the comparison of 3NT *vs*. control mice. In line with the aforementioned results, proteins involved in protein localization to synapse were also altered. Amyloid beta A4 protein (APP, fold change: 0.89), tau microtubule-associated protein (MAPT, fold change: 0.21), superoxide dismutase [Cu-Zn] (SOD1, fold change: 0.46) and growth factor receptor-bound protein 2 (GRB2, fold change: 0.64) are some relevant examples (Tables 2 and S1). Some of these proteins are also related to the positive regulation of reactive oxygen species metabolic process (Table S3). In this function, MAPT protein, which is involved in the regulation of microtubule polymerization (Yoshida and Goedert, 2012), displayed the lowest fold change from the entire experiment (3NT *vs*. control).

The impairment of the synaptic function in brains from mice exposed to dietary 3NT may be responsible for some of altered parameters that would display impaired spatial memory in the experimental animals. In fact, some of the key discriminating proteins have been identified to play a crucial role in the onset of cognitive disorders in experimental animals and humans. The impairment of the concentration of both complexins, 1 and 2, are involved in the disruption synaptic terminals that may trigger to cognitive impairments in deceased humans diagnosed from Alzheimer's disease (Ramos-Miguel et al., 2017). On the same line, Ablinger et al. (2020) reported mutations in *CACNA2D1-4* genes which would lead to synaptic disturbances that would, in turn, lead to autism, schizophrenia and epilepsy among other disorders of the central nervous system. It is worth emphasizing that in the present study, the concentration of CACNA2D1 was almost 4 times lower in the brain of mice treated with 3NT than in the control counterparts. On the other hand, perilipins are conserved proteins located at intracellular lipid droplets and they seem to modulate lipid metabolism. To our

knowledge, there is limited information on their expression in human brain or their implication in neuronal functions. A recent study by Conte et al. (2022) proposed that accumulation of perilipin-2 in central nervous system could be an early sign of brain inflammation and neurodegeneration and affected mainly neurons. According to our results, perilipin-3 (PLIN3, fold change: 0.23) was in between 4- and 5-fold times lower concentration in the brain of mice exposed to 3NT than in brains from control counterparts. The PLIN3 is expressed more in astrocytes (Conte et al., 2022) and could play a relevant role in brain homeostasis and be implicated in the loss of spatial memory observed in 3NT-challenged mice.

Interestingly, the most affected molecular function according to the proteomic analysis of the brain of mice treated with 3NT, the endopolyphosphatase activity, is barely mentioned in studies aimed to unveil the molecular mechanisms of memory loss. The present untargeted proteomic approach indicates that discriminating proteins belonging to this function deserve more detailed examination for the potential role that may play in brain function.

Yet, it is worth noting that there is a time-lapse between such cognitive issues (week 3) and the proteomic analysis (week 6). The latter was made right after the animals seemed to have recovered from the temporary brain disturbance. Therefore, the impaired proteome in the brain of 3NT-treated cells may be a reflection of some of the impaired biological processes responsible for the cognitive alterations that the animals had started to restore. On this line, Rosenberg et al. (2014) reported on the plasticity of the expression of proteins involved in synaptic function in neurons and the consolidation of memory. While the authors related the relevance of turning-over dysfunctional proteins and the role of an impaired proteasome on the onset of cognitive disorders, the depletion of such proteins as a result of a dietary component with neurotoxic ability, such as 3NT, may have similar consequences to the inability to create new functional proteins implicated in neural synapsis.

3.3.1.2. Increase of metabolic processes, mitochondrial activity and strengthening of antioxidant defenses

The metabolic processes of nucleotides and carboxylic acids in brain of mice were the two most upregulated metabolic routes by the intake of 3NT (13.97 % and 12.23 % of the total proteins affected, respectively, $p<0.01$) (Fig. 2B). Enzymes such as trifunctional purine biosynthetic protein adenosine-3 (GART, fold change: 1.37), multifunctional protein ADE2 (PAICS, fold change: 1.23), ribose-phosphate pyrophosphokinase 1 (PRPS1, fold change: 1.42) and inosine-5-monophosphate dehydrogenase 2 (IMPDH2, fold change: 1.38) (Table 2 and S1) are all implicated in purine nucleoside and ribonucleoside monophosphate biosynthetic process (Table S4). In regards to the metabolism of carboxylic acids, some of the proteins found in higher quantities in the brain of challenged mice were N(G),N(G)-dimethylarginine dimethylaminohydrolase 2 (DDAH2, fold change: 1.46), glutamate decarboxylase 2 (GAD2, fold change: 1.70), the mitochondrial kidney isoform of glutaminase, aspartate aminotransferase and ornithine aminotransferase (GLS, fold change: 1.34; GOT2, fold change: 1.21; OAT, fold change: 1.26, respectively), branched-chain-amino-acid aminotransferase 1 (BCAT1, fold change: 1.30), kynurenine--oxoglutarate transaminase 3 (KYAT3, fold change: 1.53) and diphosphoinositol-polyphosphate diphosphatase (NUDT3, fold change: 1.33) (Tables 2 and S1). Most of these enzymes are involved in transaminase activity and transferase activity transferring nitrogenous groups (Table S4).

The upregulation of these two processes along with the increase in the concentration of proteins responsible for generation of precursor metabolites and energy (6.99 %, $p<0.01$) (Fig. 2B), such as adenylosuccinate lyase (ADSL, fold change: 1.33), the cytoplasmic (IDH1) and the mitochondrial (IDH2) isocitrate dehydrogenase [NADP] (fold changes: 1.36 and 1.39, respectively), and citrate synthase (CS, fold change: 1.25) (Tables 2 and S1), indicates cellular efforts in counteracting the noxious effects of 3NT exposure by promoting RNA and protein synthesis. The hypothesis that upregulation mechanisms

may be intended to improve brain function against the impairments caused by the intake of the nitrosated amino acid gains strength by observing that the metabolism of sulphur-containing species (11.35%, $p<0.01$) (Fig. 2B) is also reinforced in 3NT-challenged mice. Most of these discriminating enzymes (3NT *vs*. control) are directly implicated in the endogenous antioxidant defenses of brain cells such as components of the thioredoxin peroxidase activity, and the glutathione metabolic and transferase activities (Table S4). Among the former we identified several subunits of peroxiredoxin (PRDX1 and PRDX5, fold changes: 1.46 and 1.17, respectively), the mitochondrial thioredoxin-dependent peroxide reductase and the mitochondrial superoxide dismutase [Mn] (PRDX3, fold change: 1.35; SOD2, fold change: 1.39, respectively). Among the latter, we underline glutathione peroxidase (GPX4, fold change: 1.33), glutathione S-transferase omega-1 (GSTO, fold change: 1.28) and glutathione S-transferase kappa 1 (GSTK1, fold change: 1.37), among others. PRDXs are members of a family of cysteine-dependent peroxidase enzymes that play a crucial role catalyzing the reduction of hydrogen peroxide and organic hydroperoxides (Perkins et al., 2015), as the same manner of GPX4 (Pei et al., 2023) in oxidative stress. PRDXs are not only scavenging enzymes of hydrogen peroxide, but also reactive nitrogen species such as peroxinitrite (Perkins et al., 2015), involved in the formation of 3NT. Alongside PRDX and GPX4, SOD2, another antioxidant defense that neutralizes superoxide radical in mitochondria (Eleutherio et al., 2021), was found in higher abundance, exerting a protecting effect on neurons under oxidative stress conditions (Miranda-Díaz et al., 2020).

The strengthening of the enzymatic antioxidant defenses as a response to the intake of 3NT confirms that the nitrosated amino acid was able to induce a pro-oxidative environment leading to oxidative stress as confirmed by the significant and remarkable increase in carbonylated proteins in brains of challenged mice. Furthermore, the fact that SOD2 (and not SOD1) was found in higher quantity, contributes to considering that oxidative stress was caused by mitochondrial disturbance, which is in line with previous

findings (Díaz-Velasco et al., 2022a, 2020). The increased metabolism and energy supply is consistent with the boosting antioxidant defenses in response to ROS production as such metabolic processes are required to support anti-oxidation and immunity systems (Yang and Lian, 2020). In brain tissues, ROS are typically generated from mitochondrial disorders, which is associated with inflammatory processed and neurodegenerative diseases (Kausar et al., 2018). Along with the already described increase in antioxidant defenses, the brain from mice exposed to 3NT had remarkable higher amounts of septin-5 (SEPT5, fold change: 2.90) which is known to be elevated in human and mice brains in neurological disorders with underlying inflammatory processes (Honorat et al., 2018). Interestingly, 3NT has been recently proposed as a reliable biomarker of neurological disorders (Bandookwala and Sengupta, 2020).

Thus, the present results suggest that the nitrosated amino acid may not only indicate but also contribute to the onset of brain disorders such as temporary loss of spatial memory by promoting oxidative stress and impairing a number of key neurological functions. In particular, this study shows that the intake of food-compatible doses of 3NT, delivered to humans by the intake of nitrite-added processed foods, causes disturbances in normal formation of the cytoskeleton and synapse in mice brain.

3.3.2. Impact of dietary EA on the proteome of brain of C57BL/6 mice challenged with 3NT

The expected situation of the combination of 3NT together with the phytochemical EA, was an alleviation of the harmful effects produced (and already described) by the nitrosated amino acid in the brain of mice. In fact, the reduction of the extent of protein carbonylation in the brain of mice treated with 3NT+EA as compared that in the brain of 3NT-challenged mice anticipated a protective effect of the dietary phytochemical against oxidative stress. Furthermore, the MWM results indicate, as well, that supplementation

with EA to mice challenged with 3NT alleviated the loss of spatial memory observed in the latter. Yet, the comparison of the proteome of mice treated with 3NT with that of mice treated with 3NT+EA revealed that, unlike we expected, the effects of EA on certain biological processes of the proteome of the mice brains may be interpreted as harmful while the clinical significance of these changes were not perceived and remain, currently, ignored.

Proteins involved in presynapse and glutamatergic synapse (21.28% and 10.87% of the total proteins affected, respectively, $p<0.01$) (Fig. 3A), alongside those affected in protein polymerization (6.15%, $p<0.01$; Fig. 3A) were found in lower abundance in the brains of mice treated with 3NT+EA as compared to brains from mice exposed to 3NT only. These changes produced in the proteome of the mice brain were not reflected in the MWM test, in which no significant differences were found in any of the comparisons, either with control counterparts or mice exposed to 3NT (Table 1). Important proteins involved in the coating of synaptic vesicles that bind to the cytoskeleton were found in lower quantity, such as synaptin 1 and 2 (SYN1 and SYN2, fold changes: 0.86 and 0.84, respectively) (Table 3 and S2), included in the synaptins family. Synaptins are phosphoproteins that play an important role in neuronal development and neurotransmitter release (Longhena et al., 2021). The interaction of these proteins with others that participate in membranes and cytoskeletal components, is essential for the suitable functioning of neuronal cells, including the formation and growth of the synapse, the maturation and renewal of neurons and the fusion and recycling of synaptic vesicles. Interestingly, the lack of SYN1 and SYN2 can trigger epileptic seizures and learning deficits (Longhena et al., 2021) and an increased age-dependent cognitive impairment (Corradi et al., 2008).

On the other hand, subunits 1 and 3 of calmodulin (CALM1 and CALM3, fold change: 0.57), an important Ca^{2+}-binding protein involved in the neuronal response in brain, among many other processes, were found in lower quantity in the brain of mice exposed to 3NT+EA in comparison with the 3NT counterparts. CALM action is mediated by its

Ca^{2+} binding ability and, consequently, is sensitive to changes in the intracellular Ca^{2+} concentration (Solà et al., 2001). CALM may bind to a great variety of Ca^{2+}-dependent enzymes, including the calcium/calmodulin-dependent protein kinase, a relevant protein in the participation in glutamatergic synapses (Mohanan et al., 2022), which also found in lower quantity in our study (CAMK2A, fold change: 0.71). Many other proteins, such as adenylyl cyclases (CAP1, fold change: 0.76; CAP2, fold change: 0.70), dynamin proteins (DNM1l, fold change: 0.44; OPA1, fold change: 0.77), mitogen-activated protein kinases (MAP2K1 and 1MAPK1, fold changes: 0.63 and 0.80, respectively) and neuronal proteins acting as a calcium sensor (NCS1, fold change: 0.81), ATPase 2 of sarcoplasmic/endoplasmic reticulum (ATP2A2, fold change: 0.73), protein kinase C (PRKCA, fold change: 0.76), all of them interconnected with CALM, were found in lower abundance. In a previous *in vitro* study, CALM was found in lower abundance in intestinal human cells exposed to 3NT+EA as compared to 3NT treated cells (Díaz-Velasco et al., 2022b). In the present study, this effect is only attributable to the combination of the nitrosated amino acid and the phytochemical as no differences were found between 3NT and control mice. In addition to the aforementioned proteins, the isoforms 1 and 3 of Wiskott-Aldrich syndrome protein family (WASF1 and 3, fold changes: 0.56 and 0.77, respectively; Tables 3 and S2) were also found in lower abundance in brains from mice challenged with 3NT. In particular, WASF1 is located in the outer mitochondrial membrane, where is involved in the trafficking of mitochondria to the dendritic spines (Sung et al., 2008) regulating mitochondrial dynamics (Ito et al., 2018) and fission (Li et al., 2004) and initiating actin polymerization (Ito et al., 2018).

In our study, the depletion of these proteins had no impact on any clinical sign. Otherwise, we found a benefit in terms of spatial memory which implies that the extent of depletion could have led to regulation of neuronal functions that would have led to certain benefits. The available literature hinders a straightforward match between the measured protein oxidation markers and the MWM assay with the proteomics. While

some of the cited literature links certain pathological conditions with the complete lack, or severe depletion of a particular protein, the present results seem to indicate that calculated changes in proteome caused by a dietary phytochemical may lead to clinical benefits such as counteracting the cognitive impairments caused by a dietary nitrosated amino acid. Certain proteins, identified only in the brain of mice exposed to the combination of 3NT and EA and hence, absent in the brain of mice exposed to 3NT alone, may contribute to explaining the potential benefits of supplementing with the phytochemical. Among these proteins, we underline cerebellin-1 (CBLN1), a synaptic organizer essential in glutamatergic synapse (Elegheert et al., 2016). This finding suggests that the impairment caused by 3NT by depleting proteins involved in particular synaptic processes could have been compensated with the increased in abundance of other proteins activating alternative glutamatergic synapse mechanisms. The α-N-acetylgalactosaminidase (NAGA), only found in 3NT+EA mice brain, could have also been involved in restoring the imbalanced caused by 3NT in synapses and actin polymerization in brain cells. Clinical studies with NAGA have detected an improvement in diseases with a global neurological manifestation using this essential lysosomal enzyme in the gradual metabolic degradation of glycosaminoglycan in lysosomes (Fu et al., 2010). Lastly, supplementation with EA also activated the synthesis of cathepsin L1 (CTSL, only found in 3NT+EA mice brain) which is one of the most abundant lysosomal proteases in brain. This protein is involved in degrading crucial neuronal substrates that induce a variety of neurodegenerative disorders (Drobny et al., 2023). Thus, it is reasonable to hypothesize that the occurrence of this protein in mice brain exposed to 3NT and supplemented with EA may contribute to keep mice brain homeostasis and hence, its functionality.

5. CONCLUSION

Food-compatible doses of 3NT (320 µg 3NT/ kg live weight) induces temporary loss of spatial memory in C57BL/6 mice in the short term (3 weeks) owing to the onset of severe

oxidative stress and impairment of the concentration of proteins implicated in protein polymerization and synaptic functionality. The activation of antioxidant mechanisms could have plausibly contributed to recover from this physiological impairment in the long term (6 weeks). The supplementation with 1.9 mg EA/kg live weight led to benefits in terms of antioxidant protection and maintenance of spatial memory. While the analysis of the proteomic changes induced by EA supplementation leads to intricated modulation of neurological functions, the increase of certain enzymes with documented beneficial effects in brain tissue could have contributed to counteract the harmful effects of 3NT.

Credit authorship contribution statement

S. Díaz-Velasco: data curation, methodology, formal analysis, writing - original draft.

R. Martínez: data curation, methodology, funding acquisition, supervision, formal analysis, validation, writing – review & editing.

J. Delgado: data curation, methodology, funding acquisition, supervision, formal analysis, validation, writing – review & editing.

Mario Estévez: conceptualization, funding acquisition, project administration, resources, supervision, validation, writing – review & editing. All authors have read and agreed to the published version of the manuscript.

Declaration of competing interest

The authors declare that they have no known competing financial interests or personal relationships that could have appeared to influence the work reported in this paper.

Funding

This research was funded by the Grant PID2021-126193OB-I00 funded by MCIN/AEI/ 10.13039/501100011033 and by “ERDF A way of making Europe”. S. Díaz-Velasco is recipient of a fellowship from the Spanish Ministry of Science and Innovation (grant number PRE2018-084001). Q-Exactive Orbitrap equipment was acquired by a grant

from the Spanish Ministry of Science and Innovation (MCIN/AEI/ 10.13039/501100011033) (grant number UNEX-AE-3394).

Data Availability Statement

All data is contained within the article or supplementary material, including raw data from proteomics.

References

Ablinger, C., Geisler, S.M., Stanika, R.I., Klein, C.T., Obermair, G.J., 2020. Neuronal α2δ proteins and brain disorders. Pflügers Arch. - Eur. J. Physiol. 2020 4727 472, 845–863. https://doi.org/10.1007/S00424-020-02420-2

Akagawa, M., Sasaki, T., Suyama, K., 2002. Oxidative deamination of lysine residue in plasma protein of diabetic rats: Novel mechanism via the Maillard reaction. Eur. J. Biochem. 269, 5451–5458. https://doi.org/10.1046/j.1432-1033.2002.03243.x

Ascacio-Valdés, J.A., Buenrostro, J.J., De La Cruz, R., Sepúlveda, L., Aguilera, A.F., Prado, A., Contreras, J.C., Rodríguez, R., Aguilar, C.N., 2014. Fungal biodegradation of pomegranate ellagitannins. Wiley Online Libr. Ascacio-Valdés, JJ Buenrostro, R la Cruz, L Sepúlveda, AF Aguilera, A PradoJournal Basic Microbiol. 2014•Wiley Online Libr. 54, 28–34. https://doi.org/10.1002/jobm.201200278

Ballif, B.A., Villén, J., Beausoleil, S.A., Schwartz, D., Gygi, S.P., 2004. Phosphoproteomic analysis of the developing mouse brain. Mol. Cell. Proteomics 3, 1093–1101. https://doi.org/10.1074/MCP.M400085-MCP200

Bandookwala, M., Sengupta, P., 2020. 3-Nitrotyrosine: a versatile oxidative stress biomarker for major neurodegenerative diseases. Int. J. Neurosci. 130, 1047–1062. https://doi.org/10.1080/00207454.2020.1713776

Bindea, G., Mlecnik, B., Hackl, H., Charoentong, P., Tosolini, M., Kirilovsky, A.,

Fridman, W.-H., Pagès, F., Trajanoski, Z., Galon, J., 2009. ClueGO: a Cytoscape plug-in to decipher functionally grouped gene ontology and pathway annotation networks. Bioinformatics 25, 1091–1093. https://doi.org/10.1093/bioinformatics/btp101

Cao, P., Yang, X., Südhof, T.C., 2013. Complexin activates exocytosis of distinct secretory vesicles controlled by different synaptotagmins. J. Neurosci. 33, 1714–1727. https://doi.org/10.1523/JNEUROSCI.4087-12.2013

Carreras-Puigvert, J., Zitnik, M., Jemth, A.S., Carter, M., Unterlass, J.E., Hallström, B., Loseva, O., Karem, Z., Calderón-Montanõ, J.M., Lindskog, C., Edqvist, P.H., Matuszewski, D.J., Ait Blal, H., Berntsson, R.P.A., Häggblad, M., Martens, U., Studham, M., Lundgren, B., Wählby, C., Sonnhammer, E.L.L., Lundberg, E., Stenmark, P., Zupan, B., Helleday, T., 2017. A comprehensive structural, biochemical and biological profiling of the human NUDIX hydrolase family. Nat. Commun. 8. https://doi.org/10.1038/S41467-017-01642-W

Cerda-Cejudo, N.D., Buenrostro-Figueroa, J.J., Sepúlveda, L., Torres-León, C., Chávez-González, M.L., Aguilar, C.N., Ascacio-Valdés, J.A., 2022. Advances in the Biotechnological Process for Obtaining Ellagic Acid from Rambutan. Quant. Methods Anal. Tech. Food Microbiol. 165–187. https://doi.org/10.1201/9781003277453-11

Ceriello, A., 2002. Nitrotyrosine: new findings as a marker of postprandial oxidative stress. Int. J. Clin. Pract. Suppl. 51–58.

Conte, M., Medici, V., Malagoli, D., Chiariello, A., Cirrincione, A., Davin, A., Chikhladze, M., Vasuri, F., Legname, G., Ferrer, I., Vanni, S., Marcon, G., Poloni, T.E., Guaita, A., Franceschi, C., Salvioli, S., 2022. Expression pattern of perilipins in human brain during aging and in Alzheimer's disease. Neuropathol. Appl. Neurobiol. 48, e12756. https://doi.org/10.1111/NAN.12756

Corradi, A., Zanardi, A., Giacomini, C., Onofri, F., Valtorta, F., Zoli, M., Benfenati, F., 2008. Synapsin-I- and synapsin-II-null mice display an increased age-dependent cognitive impairment. J. Cell Sci. 121, 3042–3051. https://doi.org/10.1242/JCS.035063

Dahimene, S., Von Elsner, L., Holling, T., Mattas, L.S., Pickard, J., Lessel, D., Pilch, K.S., Kadurin, I., Pratt, W.S., Zhulin, I.B., Dai, H., Hempel, M., Ruzhnikov, M.R.Z., Kutsche, K., Dolphin, A.C., 2022. Biallelic CACNA2D1 loss-of-function variants cause early-onset developmental epileptic encephalopathy. Brain 145, 2721–2729. https://doi.org/10.1093/BRAIN/AWAC081

De, R., Sarkar, A., Ghosh, P., Ganguly, M., Karmakar, B.C., Saha, D.R., Halder, A., Chowdhury, A., Mukhopadhyay, A.K., 2018. Antimicrobial activity of ellagic acid against Helicobacter pylori isolates from India and during infections in mice. J. Antimicrob. Chemother. 73, 1595–1603. https://doi.org/10.1093/JAC/DKY079

Delgado, J., Núñez, F., Asensio, M.A., Owens, R.A., 2019. Quantitative proteomic profiling of ochratoxin A repression in Penicillium nordicum by protective cultures. Int. J.Food Microbiol. 305, 108243. https://doi.org/10.1016/j.ijfoodmicro.2019.108243

Díaz-Velasco, S., Delgado, J., Peña, F.J., Estévez, M., 2022a. Ellagic Acid Triggers the Necrosis of Differentiated Human Enterocytes Exposed to 3-Nitro-Tyrosine: An MS-Based Proteomic Study. Antioxidants (Basel, Switzerland) 11. https://doi.org/10.3390/ANTIOX11122485

Díaz-Velasco, S., Delgado, J., Peña, F.J., Estévez, M., 2022b. Protein oxidation marker, α-amino adipic acid, impairs proteome of differentiated human enterocytes: Underlying toxicological mechanisms. Biochim. Biophys. acta. Proteins proteomics 1870, 140797. https://doi.org/10.1016/J.BBAPAP.2022.140797

Díaz-Velasco, S., González, A., Peña, F.J., Estévez, M., 2020. Noxious effects of selected food-occurring oxidized amino acids on differentiated CACO-2 intestinal human cells. Food Chem. Toxicol. 144, 1–8. https://doi.org/10.1016/j.fct.2020.111650

Drobny, A., Boros, F.A., Balta, D., Prieto Huarcaya, S., Caylioglu, D., Qazi, N., Vandrey, J., Schneider, Y., Dobert, J.P., Pitcairn, C., Mazzulli, J.R., Zunke, F., 2023. Reciprocal effects of alpha-synuclein aggregation and lysosomal homeostasis in synucleinopathy models. Transl. Neurodegener. 12, 1–21. https://doi.org/10.1186/S40035-023-00363-Z/FIGURES/5

Elegheert, J., Kakegawa, W., Clay, J.E., Shanks, N.F., Behiels, E., Matsuda, K., Kohda, K., Miura, E., Rossmann, M., Mitakidis, N., Motohashi, J., Chang, V.T., Siebold, C., Greger, I.H., Nakagawa, T., Yuzaki, M., Aricescu, A.R., 2016. Structural basis for integration of GluD receptors within synaptic organizer complexes. Science (80-.). 353, 295–300. https://doi.org/10.1126/SCIENCE.AAE0104/SUPPL_FILE/AAE0104_ELEGHEERT_SM.PDF

Eleutherio, E.C.A., Silva Magalhães, R.S., de Araújo Brasil, A., Monteiro Neto, J.R., de Holanda Paranhos, L., 2021. SOD1, more than just an antioxidant. Arch. Biochem. Biophys. 697, 108701. https://doi.org/10.1016/J.ABB.2020.108701

Estévez, M., Li, Z., Soladoye, O.P., Van-Hecke, T., 2017. Health Risks of Food Oxidation. Adv. Food Nutr. Res. 82, 45–81. https://doi.org/10.1016/bs.afnr.2016.12.005

Fu, H., DiRosario, J., Kang, L., Muenzer, J., McCarty, D.M., 2010. Restoration of central nervous system α-N-acetylglucosaminidase activity and therapeutic benefits in mucopolysaccharidosis IIIB mice by a single intracisternal recombinant adeno-associated viral type 2 vector delivery. J. Gene Med. 12, 624–633.

https://doi.org/10.1002/JGM.1480

Gomes Gonçalves, N., Vidal Ferreira, N., Khandpur, N., Martinez Steele, E., Bertazzi Levy, R., Andrade Lotufo, P., Bensenor, I.M., Caramelli, P., Alvim De Matos, S.M., Marchioni, D.M., Suemoto, C.K., 2023. Association Between Consumption of Ultraprocessed Foods and Cognitive Decline. JAMA Neurol. 80, 142–150. https://doi.org/10.1001/JAMANEUROL.2022.4397

Griswold-Prenner, I., Kashyap, A.K., Mazhar, S., Hall, Z.W., Fazelinia, H., Ischiropoulos, H., 2023. Unveiling the human nitroproteome: Protein tyrosine nitration in cell signaling and cancer. J. Biol. Chem. 299. https://doi.org/10.1016/J.JBC.2023.105038/ATTACHMENT/12464E56-973F-4F0A-A50E-A8A1F1808B52/MMC1.XLSX

Honorat, J.A., Sebastian Lopez-Chiriboga, A., Kryzer, T.J., Fryer, J.P., Devine, M., Flores, A., Lennon, V.A., Pittock, S.J., McKeon, A., 2018. Autoimmune septin-5 cerebellar ataxia. Neurol. Neuroimmunol. neuroinflammation 5. https://doi.org/10.1212/NXI.0000000000000474

IARC, 2015. Carcinogenicity of consumption of red and processed meat. Lancet Oncol. https://doi.org/10.1016/S1470-2045(15)00444-1

Ito, Y., Carss, K.J., Duarte, S.T., Hartley, T. et al., 2018. De Novo Truncating Mutations in WASF1 Cause Intellectual Disability with Seizures. Am. J. Hum. Genet. 103, 144–153. https://doi.org/10.1016/j.ajhg.2018.06.001

Kang, I., Buckner, T., Shay, N.F., Gu, L., Chung, S., 2016. Improvements in Metabolic Health with Consumption of Ellagic Acid and Subsequent Conversion into Urolithins: Evidence and Mechanisms. Adv. Nutr. 7, 961–972. https://doi.org/10.3945/AN.116.012575

Kausar, S., Wang, F., Cui, H., 2018. The Role of Mitochondria in Reactive Oxygen

Species Generation and Its Implications for Neurodegenerative Diseases. Cells 7, 274. https://doi.org/10.3390/cells7120274

Li, B., Ge, Y., Xu, Y., Lu, Y., Yang, Y., Han, L., Jiang, Y., Shi, Y., Le, G., 2019. Spatial Learning and Memory Impairment in Growing Mice Induced by Major Oxidized Tyrosine Product Dityrosine. J. Agric. Food Chem. 67, 9039–9049. https://doi.org/10.1021/ACS.JAFC.9B04253/ASSET/IMAGES/LARGE/JF9B04253_0011.JPEG

Li, Z., Okamoto, K.I., Hayashi, Y., Sheng, M., 2004. The importance of dendritic mitochondria in the morphogenesis and plasticity of spines and synapses. Cell 119, 873–887. https://doi.org/10.1016/j.cell.2004.11.003

Liguori, I., Russo, G., Curcio, F., Bulli, G., Aran, L., Della-Morte, D., Gargiulo, G., Testa, G., Cacciatore, F., Bonaduce, D., Abete, P., 2018. Oxidative stress, aging, and diseases. Clin. Interv. Aging 13, 757. https://doi.org/10.2147/CIA.S158513

Longhena, F., Faustini, G., Brembati, V., Pizzi, M., Benfenati, F., Bellucci, A., 2021. An updated reappraisal of synapsins: structure, function and role in neurological and psychiatric disorders. Neurosci. Biobehav. Rev. 130, 33–60. https://doi.org/10.1016/J.NEUBIOREV.2021.08.011

Lu, Y., Ma, S., Tang, X., Li, B., Ge, Y., Zhang, K., Yang, S., Zhao, Q., Xu, Y., Ren, H., 2020. Dietary Dityrosine Induces Mitochondrial Dysfunction by Diminished Thyroid Hormone Function in Mouse Myocardia. J. Agric. Food Chem. 68, 9223–9234. https://doi.org/10.1021/ACS.JAFC.0C03926/ASSET/IMAGES/LARGE/JF0C03926_0009.JPEG

Mallozzi, C., Di Stasi, A.M.M., Minetti, M., 1997. Peroxynitrite modulates tyrosine-dependent signal transduction pathway of human erythrocyte band 3. FASEB J. 11, 1281–1290. https://doi.org/10.1096/FASEBJ.11.14.9409547

Miranda-Díaz, A.G., García-Sánchez, A., Cardona-Muñoz, E.G., Mendonça Junior, F.J.B., 2020. Foods with Potential Prooxidant and Antioxidant Effects Involved in Parkinson's Disease. Oxid. Med. Cell. Longev. 2020. https://doi.org/10.1155/2020/6281454

Mohanan, A.G., Gunasekaran, S., Jacob, R.S., Omkumar, R. V., 2022. Role of Ca2+/Calmodulin-Dependent Protein Kinase Type II in Mediating Function and Dysfunction at Glutamatergic Synapses. Front. Mol. Neurosci. 15, 855752. https://doi.org/10.3389/FNMOL.2022.855752/BIBTEX

Ozyurt, V.H., Otles, S., 2020. Investigation of the effect of sodium nitrite on protein oxidation markers in food protein suspensions. J. Food Biochem. 44, e13152. https://doi.org/10.1111/JFBC.13152

Ozyurt, V.H., Otles, S., 2017. Determination of 3-nitrotyrosine in food protein suspensions. Talanta 171, 81–89. https://doi.org/10.1016/J.TALANTA.2017.04.059

Pacher, P., Beckman, J.S., Liaudet, L., 2007. Nitric oxide and peroxynitrite in health and disease. Physiol. Rev. 87, 315–424. https://doi.org/10.1152/PHYSREV.00029.2006

Patil, S.S., Sunyer, B., Höger, H., Lubec, G., 2009. Evaluation of spatial memory of C57BL/6J and CD1 mice in the Barnes maze, the Multiple T-maze and in the Morris water maze. Behav. Brain Res. 198, 58–68. https://doi.org/10.1016/j.bbr.2008.10.029

Pei, J., Pan, X., Wei, G., Hua, Y., 2023. Research progress of glutathione peroxidase family (GPX) in redoxidation. Front. Pharmacol. 14, 1147414. https://doi.org/10.3389/FPHAR.2023.1147414/BIBTEX

Perkins, A., Nelson, K.J., Parsonage, D., Poole, L.B., Karplus, P.A., 2015.

Peroxiredoxins: Guardians Against Oxidative Stress and Modulators of Peroxide Signaling. Trends Biochem. Sci. 40, 435. https://doi.org/10.1016/J.TIBS.2015.05.001

Ramos-Miguel, A., Sawada, K., Jones, A.A., Thornton, A.E., Barr, A.M., Leurgans, S.E., Schneider, J.A., Bennett, D.A., Honer, W.G., 2017. Presynaptic proteins complexin-I and complexin-II differentially influence cognitive function in early and late stages of Alzheimer's disease. Acta Neuropathol. 133, 395–407. https://doi.org/10.1007/S00401-016-1647-9/FIGURES/3

Reim, K., Mansour, M., Varoqueaux, F., McMahon, H.T., Südhof, T.C., Brose, N., Rosenmund, C., 2001. Complexins regulate a late step in Ca2+-dependent neurotransmitter release. Cell 104, 71–81. https://doi.org/10.1016/S0092-8674(01)00192-1

Rodriguez, A., Zhang, H., Klaminder, J., Brodin, T., Andersson, P.L., Andersson, M., 2018. ToxTrac: A fast and robust software for tracking organisms. Methods Ecol. Evol. 9, 460–464. https://doi.org/10.1111/2041-210X.12874

Rosenberg, T., Gal-Ben-Ari, S., Dieterich, D.C., Kreutz, M.R., Ziv, N.E., Gundelfinger, E.D., Rosenblum, K., 2014. The roles of protein expression in synaptic plasticity and memory consolidation. Front. Mol. Neurosci. 7, 118027. https://doi.org/10.3389/FNMOL.2014.00086/BIBTEX

Shevchenko, A., Tomas, H., Havliš, J., Olsen, J. V., Mann, M., 2007. In-gel digestion for mass spectrometric characterization of proteins and proteomes. Nat. Protoc. 1, 2856–2860. https://doi.org/10.1038/nprot.2006.468

Solà, C., Barrón, S., Tusell, J.M., Serratosa, J., 2001. The Ca2+/calmodulin system in neuronal hyperexcitability. Int. J. Biochem. Cell Biol. 33, 439–455. https://doi.org/10.1016/S1357-2725(01)00030-9

Sung, J.Y., Engmann, O., Teylan, M.A., Nairn, A.C., Greengard, P., Kim, Y., 2008. WAVE1 controls neuronal activity-induced mitochondrial distribution in dendritic spines. Proc. Natl. Acad. Sci. U. S. A. 105, 3112–3116. https://doi.org/10.1073/PNAS.0712180105

Tang, X., Zeng, F., Wang, J., Lyu, Y., Yu, R., Lu, N., Zhou, Z., Chen, A., 2023. Dietary Dityrosine Induces Oxidative Stress and Mitochondrial-Lipid Imbalance in Mouse Liver via MiR-144-3p-Mediated Downregulation of Nrf2. Mol. Nutr. Food Res. 67, 2200674. https://doi.org/10.1002/MNFR.202200674

Utrera, M., Morcuende, D., Rodríguez-Carpena, J.G., Estévez, M., 2011. Fluorescent HPLC for the detection of specific protein oxidation carbonyls - α-aminoadipic and γ-glutamic semialdehydes - in meat systems. Meat Sci. 89, 500–506. https://doi.org/10.1016/j.meatsci.2011.05.017

Van Hecke, T., Vossen, E., Hemeryck, L.Y., Vanden Bussche, J., Vanhaecke, L., De Smet, S., 2015. Increased oxidative and nitrosative reactions during digestion could contribute to the association between well-done red meat consumption and colorectal cancer. Food Chem. 187, 29–36. https://doi.org/10.1016/J.FOODCHEM.2015.04.029

Villaverde, A., Morcuende, D., Estévez, M., 2014a. Effect of Curing Agents on the Oxidative and Nitrosative Damage to Meat Proteins during Processing of Fermented Sausages. J. Food Sci. 79, C1331–C1342.

Villaverde, A., Ventanas, J., Estévez, M., 2014b. Nitrite promotes protein carbonylation and Strecker aldehyde formation in experimental fermented sausages: Are both events connected? Meat Sci. 98, 665–672. https://doi.org/10.1016/j.meatsci.2014.06.017

Yang, S., Lian, G., 2020. ROS and diseases: role in metabolism and energy supply. Mol. Cell. Biochem. 467, 1. https://doi.org/10.1007/S11010-019-03667-9

Yoshida, H., Goedert, M., 2012. Phosphorylation of microtubule-associated protein tau by AMPK-related kinases. J. Neurochem. 120, 165–176. https://doi.org/10.1111/J.1471-4159.2011.07523.X

Zhu, H., Li, Y.R., 2012. Oxidative stress and redox signaling mechanisms of inflammatory bowel disease: Updated experimental and clinical evidence. Exp. Biol. Med. 237, 474–480. https://doi.org/10.1258/ebm.2011.011358

FIGURE CAPTION

Figure 1. (A) Circular pool with a hidden a platform 1.5 cm beneath water surface. The location of the platform was identified by a distal reference platform attached to the pool wall. (B) Division of pool in zone 1 and 2, matching zone 1 with the area where the platform was.

Figure 2. Percentages of proteins annotated by Gene Ontology (* p<0.05, ** p<0.01) found in lower relative abundance in biological processes and molecular functions (A), and percentages of proteins found in higher relative quantity in biological processes and molecular functions (B) in mice brain affected by the exposure to 3NT compared to control counterparts. For a visual improvement of the pie chart, biological processes y molecular functions with an influence <3% (A) and <5% (B) were grouped.

Figure 3. Percentages of proteins annotated by Gene Ontology (* p<0.05, ** p<0.01) found in lower relative abundance in biological processes and molecular functions, in mice brain affected by the exposure to 3NT+EA compared to 3NT counterparts. For a visual improvement of the pie charts, biological processes y molecular functions with an influence <4% were grouped. Percentages of higher relative abundance in biological processes and molecular functions in mice brain affected by the exposure to 3NT+EA compared to 3NT counterparts are not shown due to non-detection by equipment.

SUPPLEMENTARY MATERIAL

Table S1. Proteins identified in C57BL/6 mice brain in the presence of 3NT along with Log2 fold change (Student's T-test Difference) and significance values (p). Proteins identified in lower abundance in 3NT-treated mice in comparison to the non-treated control mice; proteins identified in higher quantity in 3NT-treated mice in comparison to the non-treated control mice; proteins identified only in control mice in comparison to 3NT-treated mice and proteins identified only in the presence of 3NT in comparison to

the non-treated control mice. Control mice are marked in yellow, 3NT-treated cells in green and statistical differences in blue.

Table S2. Proteins identified in C57BL/6 mice brain in the presence of 3NT+EA along with Log2 fold change (Student's T-test Difference) and significance values (*p*). Proteins identified in lower quantity in 3NT+EA-treated mice in comparison to 3NT counterparts; proteins identified in higher abundance in 3NT+EA-treated mice in comparison to 3NT-treated mice; proteins identified only in 3NT-treated mice in comparison to 3NT+EA-challenged mice and proteins identified only in the presence of 3NT+EA in comparison to 3NT counterparts. 3NT-treated mice are marked in yellow, 3NT+EA- challenged mice in green and statistical differences in blue.

Table S3. Terms and associated genes found in lower quantity in the presence of 3NT compared to control counterparts.

Table S4. Terms and associated genes found in higher abundance in the presence of 3NT compared to control counterparts.

Table S5. Terms and associated genes found in lower quantity in the presence of 3NT+EA compared to 3NT-treated mice.

FIGURE 1

(A)

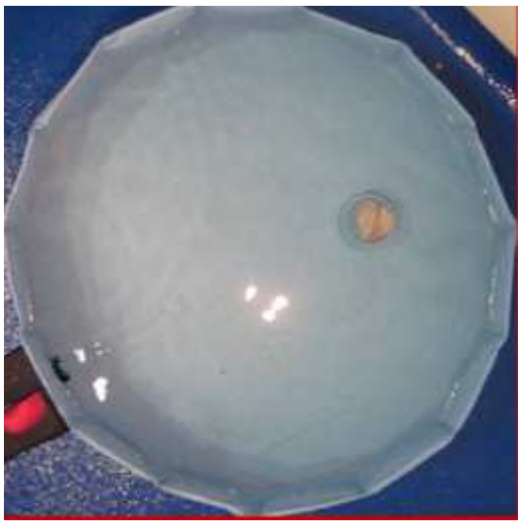

(B)

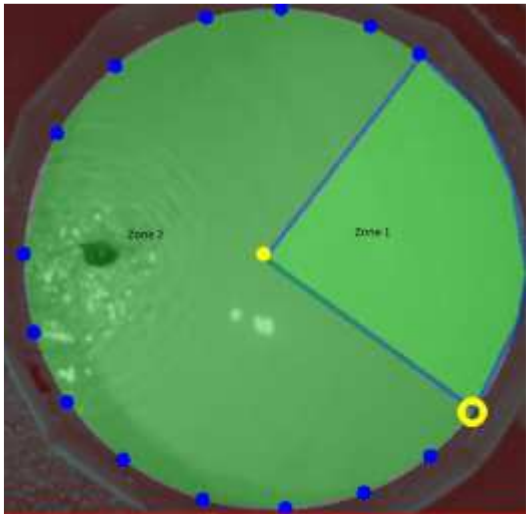

FIGURE 2

(A)

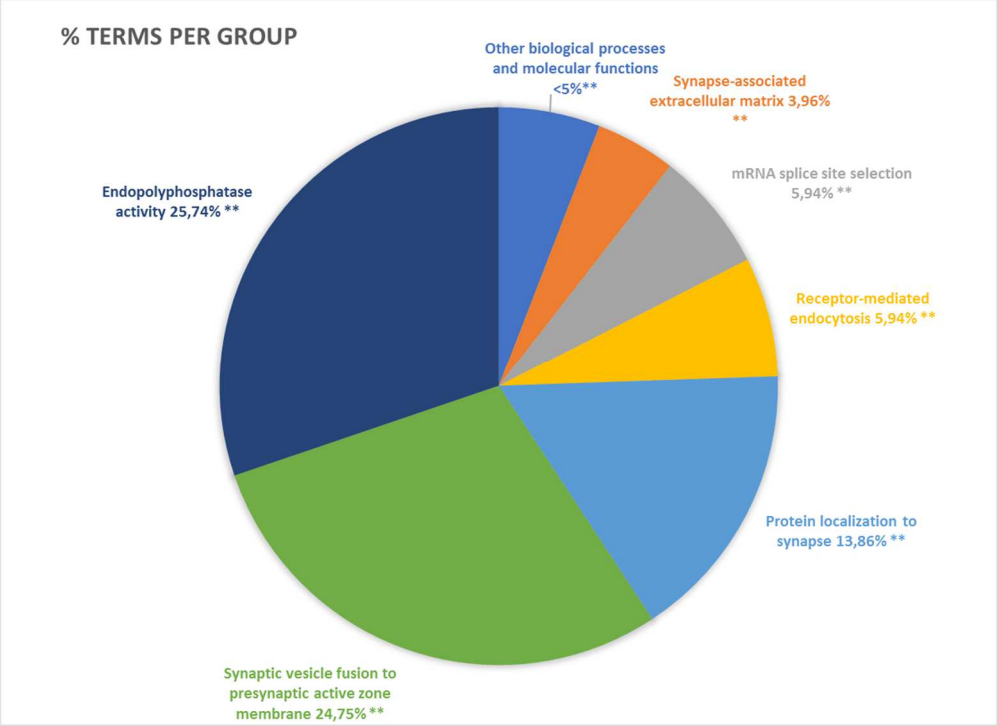
% TERMS PER GROUP
Other biological processes and molecular functions <5%**
Synapse-associated extracellular matrix 3,96% **
mRNA splice site selection 5,94% **
Receptor-mediated endocytosis 5,94% **
Protein localization to synapse 13,86% **
Synaptic vesicle fusion to presynaptic active zone membrane 24,75% **
Endopolyphosphatase activity 25,74% **

(B)

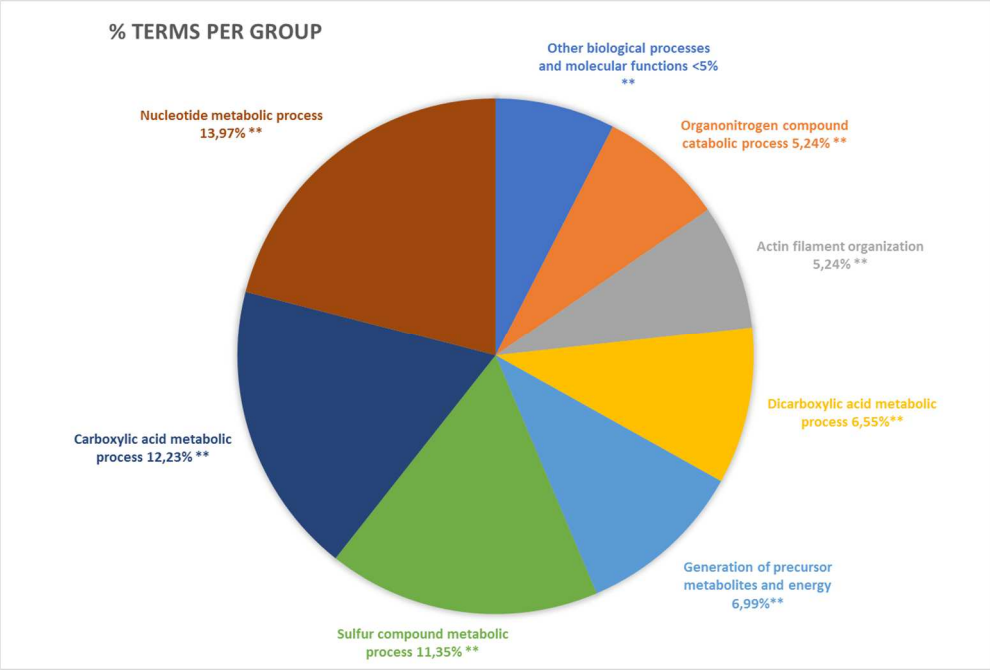
% TERMS PER GROUP
Other biological processes and molecular functions <5% **
Organonitrogen compound catabolic process 5,24% **
Actin filament organization 5,24% **
Dicarboxylic acid metabolic process 6,55%**
Generation of precursor metabolites and energy 6,99%**
Sulfur compound metabolic process 11,35% **
Carboxylic acid metabolic process 12,23% **
Nucleotide metabolic process 13,97% **

FIGURE 3

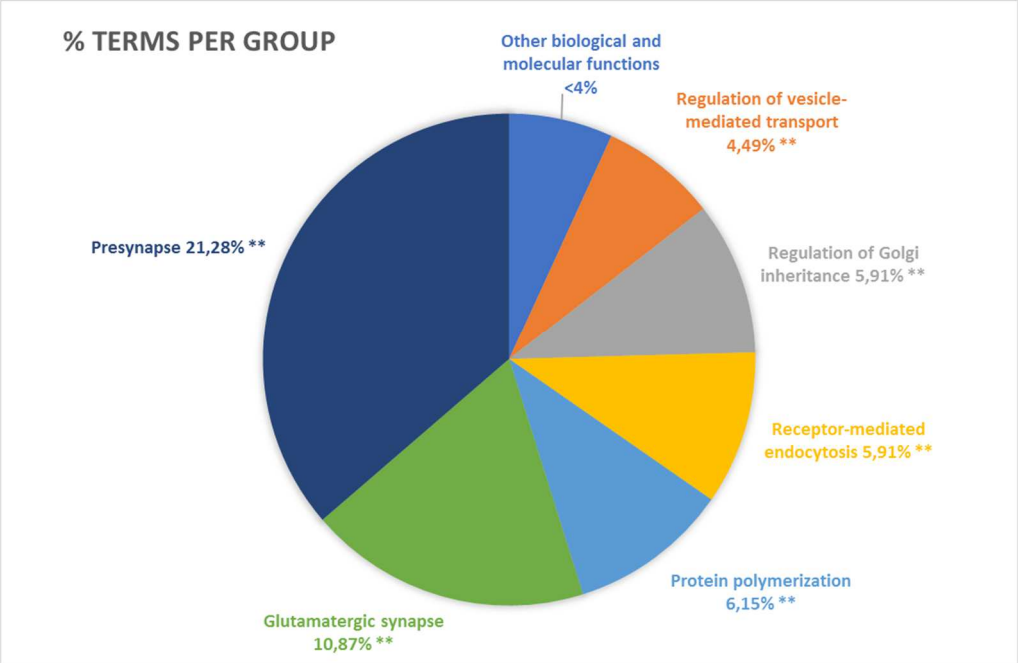
% TERMS PER GROUP
Other biological and molecular functions <4%
Regulation of vesicle-mediated transport 4,49% **
Regulation of Golgi inheritance 5,91% **
Receptor-mediated endocytosis 5,91% **
Protein polymerization 6,15% **
Glutamatergic synapse 10,87% **
Presynapse 21,28% **

Table 1. Results of Morris Maze behavioral parameters (mean± standard deviation) of C57BL/6 black mice under various experimental conditions. Control, 3-Nitrotyrosine (3NT) and 3-Nitrotyrosine (3NT) + Ellagic acid (EA) for 3 and 6 weeks.

WEEK 3 CONTROL vs. 3NT vs. 3NT+EA						
	Total distance (mm)	Av. Speed (mm/s)	Av. Acceleration (mm/s^2)	Inside time zone 1 (seconds)	Inside rate zone 1 (%)	Exploration rate (%)
CONTROL	4955,44±952,72	94,5±17,10	436,07±69,95	12,09±4,97	23,71 ±8,56	52,67±5,46
3NT	5974,37±1417,69	106,32±23,43	495,18±108,66	8,99±3,61	16 ,25±5,19	47,71±6,74
3NT+EA	6097,53±1916,55	107,05±32,63	498,72±137,59	14,29±5,39	2 5,54±9,66	50,09±7,81
p -VALUE	>0,05	>0,05	>0,05	>0,05	>0,05	>0,05
WEEK 6 CONTROL vs. 3NT vs. 3NT+EA						
	Total distance (mm)	Av. Speed (mm/s)	Av. Acceleration (mm/s^2)	Inside time zone 1 (seconds)	Inside rate zone 1 (%)	Exploration rate (%)
CONTROL	4569,84±706,11	89,45±16,05	418,98±71,89	17,02±7,01	33,2 3±12,02	41,11±3,34
3NT	7157,35±1757,42	119,28±11,90	557,11±47,86	17,30±6,72	29 ,37±11,80	45,13±7,79
3NT+EA	6523±2977,38	96,66±34,16	444,54±151,87	18±12,04	26,02±1 2,62	47,92±12,53
p -VALUE	>0,05	>0,05	>0,05	>0,05	>0,05	>0,05
CONTROL WEEK 3 vs. WEEK 6						
	Total distance (mm)	Av. Speed (mm/s)	Av. Acceleration (mm/s^2)	Inside time zone 1 (seconds)	Inside rate zone 1 (%)	Exploration rate (%)
CONTROL WEEK 3	4955,43±952,72	94,49±17,10	436,07±69,95	12,09±4,97	23,7 1±8,56	52,67±5,46
CONTROL WEEK 6	4569,84±706,11	89,45±16,05	418,98±71,89	17,02±7,01	33,2 2±12,02	41,11±3,34
p -VALUE	>0,05	>0,05	>0,05	>0,05	>0,05	**0,008**
3NT WEEK 3 vs. WEEK 6						
	Total distance (mm)	Av. Speed (mm/s)	Av. Acceleration (mm/s^2)	Inside time zone 1 (seconds)	Inside rate zone 1 (%)	Exploration rate (%)
3NT WEEK 3	5974,37±1417,69	106,32±23,43	495,18±108,66	8,99±3,61	16 ,25±5,19	47,71±6,74
3NT WEEK 6	7157,35±1757,42	119,28±11,90	557,11±47,86	17,30±6,72	29 ,37±11,80	45,13±7,79
p -VALUE	>0,05	>0,05	>0,05	**0,026**	**0,041**	>0,05
		3NT+EA WEEK 3 vs. WEEK 6				
	Total distance (mm)	Av. Speed (mm/s)	Av. Acceleration (mm/s^2)	Inside time zone 1 (seconds)	Inside rate zone 1 (%)	Exploration rate (%)
3NT+EA WEEK 3	6097,53±1916,55	107,05±32,63	498,72±137,59	14,29±5,39	2 5,54±9,66	50,09±7,81
3NT+EA WEEK 6	6523±2977,38	96,66±34,16	444,54±151,87	18±12,04	26,02±1 2,62	47,92±12,53
p -VALUE	>0,05	>0,05	>0,05	>0,05	>0,05	>0,05

Table 2. Proteins from C57BL/6 mice brain affected by the exposure to 3-Nitrotyrosine (3NT) in comparison to the non-treated control (C).

PROTEIN NAME	GENE NAME	*p*-VALUE	FOLD CHANGE[1]	BIOLOGICAL FUNCTION	FASTA Accession number
Microtubule-associated protein	*MAPT*	1.97×10^{-8}	0.21	Promotes microtubule assembly and stability on neurons	B1AQW2
Perilipin-3	*PLIN3*	2.95×10^{-4}	0.26	Structural component of lipid droplets, important for the growth and survival of cancer cells	Q9DBG5
Striatin-4	*STRN4*	1.2×10^{-3}	0.27	It binds calcium-dependent calmodulin, signaling protein	P58404
Voltage-dependent calcium channel subunit alpha-2/delta-1	*CACNA2D1*	0.026	0.29	Regulates calcium current density and calcium channel activation/inactivation kinetics	O08532

Neural cell adhesion molecule L1-like protein	*CHL1*	0.028	0.30	Involved in synaptic plasticity	P70232
Clathrin light chain B	*CTLB*	$1x10^{-4}$	0.37	Main component of vesicle coat	Q6IRU5
Complexin-2	*CPLX2*	0.002	0.42	Regulates exocytosis in synaptic vesicles	P84086
Protein canopy homolog 2	*CNPY2*	0.025	0.42	Positive regulator of neurite outgrowth	A0A1W2P729
Superoxide dismutase [Cu-Zn], cytosolic	*SOD1*	$3.7x10^{-3}$	0.46	Antioxidant enzyme involved in detoxifying radical superoxide	P08228
Complexin-1	*CPLX1*	0.031	0.50	Regulates exocytosis in synaptic vesicles	P63040
Growth factor receptor-bound protein 2	*GRB2*	0.013	0.64	Tyrosine kinase implicated in signal transduction	Q60631
Diphosphoinositol polyphosphate phosphohydrolases 3-alpha, 3-beta and 2	*NUDT10* *NUDT11* *NUDT4*	0.044	0.73	Regulates the replacement of diphosphoinositol polyphosphate	P0C027
Synaptosomal-associated protein 25	*SNAP25*	0.002	0.76	Modulates different voltage-dependent calcium channels in neurons	P60879

ADP-ribose pyrophosphatase, mitochondrial	*NUDT9*	0.018	0.78	Involved in purine ribonucleotide catabolic process	Q8BVU5
Cytosolic purine 5-nucleotidase	*NT5C2*	0.032	0.79	Involved in purine ribonucleotide catabolic process	A0A494BBP6
Vesicle-associated membrane protein 1	*VAMP1*	0.035	0.81	Regulates exocytosis	A0A0N4SUV3
Amyloid beta A4 protein	*APP*	0.033	0.89	Implicated in neurite growth, neuronal adhesion and axonogenesis	A0A2I3BQZ9
Cytochrome c, somatic	*CYCS*	0.028	1.16	Final protein carrier in the mitochondrial electron-transport chain	P62897
Peroxiredoxin-5, mitochondrial	*PRDX5*	0.026	1.17	Thiol-specific peroxidase involved in reduction of hydrogen peroxide and organic hydroperoxides	P99029
5(3)-deoxyribonucleotidase, cytosolic type	*NT5C*	0.005	1.18	Involved in deoxiribonucleotide catabolic process	Q9JM14

Aspartate aminotransferase, mitochondrial	*GOT2*	0.017	1.21	Catalyzes the irreversible transamination of the L-tryptophan into kynurenic acid	P05202
Multifunctional protein ADE2	*PAICS*	0.036	1.23	Catalyzes de novo purine biosynthetic pathway	Q9DCL9
Citrate synthase, mitochondrial	*CS*	0.049	1.25	Component of tricarboxylic acid cycle	Q9CZU6
Ornithine aminotransferase, mitochondrial	*OAT*	0.016	1.26	Catalyzes interconversion of L-ornithine and 2-oxoglutarate to L-glutamate semialdehyde and L-glutamate	P29758
Glutathione S-transferase omega-1	*GSTO1*	0.019	1.28	Glutathione-dependent thiol transferase activity	O09131
Adenylosuccinate synthetase isozyme 1	*ADSSL1*	0.030	1.29	Component of the purine nucleotide cycle	P28650
Branched-chain-amino-acid aminotransferase	*BCAT1*	0.013	1.30	Catalyzes the first reaction in the catabolism of the essential branched chain amino acids	Q8CBC8
Diphosphoinositol-polyphosphate diphosphatase	*NUDT3*	0.040	1.31	Regulates the replacement of diphosphoinositol polyphosphate	A0A3B2W864

Glutathione peroxidase	*GPX4*	0.025	1.33	Protects cells from oxidative damage by preventing membrane lipid peroxidation	S4R1E5
Adenylosuccinate lyase	*ADSL*	0.001	1.33	Contributes to de novo AMP synthesis	P54822
Glutaminase kidney isoform, mitochondrial	*GLS*	0.008	1.34	Regulates the levels of the neurotransmitter glutamate	D3Z7P3
Thioredoxin-dependent peroxide reductase, mitochondrial	*PRDX3*	0.010	1.35	Thiol-specific peroxidase involvd in reduction of hydrogen peroxide and organic hydroperoxides	P20108
Isocitrate dehydrogenase [NADP] cytoplasmic	*IDH1*	0.005	1.36	Component of tricarboxylic acid cycle	O88844
Trifunctional purine biosynthetic protein adenosine-3	*GART*	0.020	1.37	Catalyzes the de novo IMP	Q64737
Glutathione S-transferase kappa 1	*GSTK1*	0.008	1.37	Catalyzes the conjugation of glutathione to exogenous and endogenous compounds	Q9DCM2
Inosine-5-monophosphate dehydrogenase 2	*IMPDH2*	0.024	1.38	Involved in the de novo synthesis of guanine nucleotides	P24547

Isocitrate dehydrogenase [NADP], mitochondrial	*IDH2*	0.002	1.39	Component of tricarboxylic acid cycle	P54071
Superoxide dismutase [Mn], mitochondrial	*SOD2*	$5.8x10^{-4}$	1.39	Antioxidant enzyme involved in detoxifying radical superoxide	P09671
Isocitrate dehydrogenase [NAD] subunit gamma 1, mitochondrial	*IDH3G*	0.002	1.41	Component of tricarboxylic acid cycle	P70404
Ribose-phosphate pyrophosphokinase 1	*PRPS1*	$4.61x10^{-5}$	1.42	Catalyzes PRPP, essential for nucleotide synthesis	G3UXL2
N(G),N(G)-dimethylarginine dimethylaminohydrolase 2	*DDAH2*	0.025	1.46	Regulator of nitric oxide generation	Q99LD8
Peroxiredoxin-1	*PRDX1*	$1x10^{-4}$	1.46	Implicated in cell protection against oxidative stress by detoxifying peroxides	P35700
Kynurenine--oxoglutarate transaminase 3	*KYAT3*	0.026	1.53	Catalyzes the irreversible transamination of the L-tryptophan to kynurenic acid	Q71RI9
Glutamate decarboxylase 2	*GAD2*	$6.4x10^{-3}$	1.70	Catalyzes the production of GABA	P48320

Mitochondrial carrier homolog 2	*MTCH2*	0.044	2.30	Mediates insertion of transmembrane proteins into the mitochondrial outer membrane	A2AFW6
Actin, alpha cardiac muscle 1	*ACTC1*	$6.7x10^{-6}$	2.57	Implicated in cell motility	P68033
Proteasome subunit beta type-7	*PSMB7*	$5.21x10^{-5}$	2.65	Involved in the proteolytic degradation	P70195
Septin-5	*SEPT5*	0.005	2.90	Filament-forming cytoskeletal GTPase	Q9Z2Q6

[1]Fold change indicates the degree of quantity change for a particular protein between animals (control vs. 3NT); FC <1 denotes a decrease in the concentration of protein in the treated mice (vs. control); FC >1 indicates a significant increase in the concentration of the protein in treated mice (vs. control).

Table 3. Proteins from C57BL/6 mice brain affected by the exposure to 3-Nitrotyrosine (3NT) + Ellagic acid (EA) in comparison to 3-Nitrotyrosine treated animals (3NT).

PROTEIN NAME	GENE NAME	*p*-VALUE	FOLD CHANGE[1]	BIOLOGICAL FUNCTION	FASTA Accesion number
Brain acid soluble protein 1	*BASP1*	0.014	0.32	Involved in neurite outgrowth and plasticity	Q91XV3
cAMP-regulated phosphoprotein 19	*ARPP19*	$5.3x10^{-4}$	0.34	Implicated in presynapse	E9Q827
Dynamin-1-like protein	*DNM1l*	0.025	0.44	Acts in mitochondrial and peroxisomal division	Q8K1M6
Kinesin-1 heavy chain	*KIF5B*	$3.6x10^{-4}$	0.50	Microtubule-dependent motor required for normal distribution of mitochondria and lysosomes	Q61768
Cytoplasmic FMR1-interacting protein 2	*CYFIP2*	0.010	0.56	Implicated in endocytic trafficking and signaling from early endosomes	F6QD74
Wiskott-Aldrich syndrome protein family member 1	*WASF1*	0.004	0.56	Regulates actin filament reorganization via its interaction with the Arp2/3 complex	Q8R5H6

Calmodulin-1; Calmodulin-3	*CALM1* *CALM3*	$1.4x10^{-4}$	0.57	Ca2+-binding proteins involved in the neuronal response	P0DP28
Neuron-specific calcium-binding protein hippocalcin	*HPCA*	0.003	0.62	Calcium-binding protein implicated in regulation of voltage-dependent calcium channels	P84075
Dual specificity mitogen-activated protein kinase kinase 1	*MAP2K1*	0.044	0.63	Essential component of the MAP kinase signal transduction pathway	P31938
Superoxide dismutase [Cu-Zn], cytoplasmic	*SOD1*	0.001	0.65	Antioxidant enzyme involved in detoxifying radical superoxide	P08228
Complexin-1	*CPLX1*	$1.9x10^{-3}$	0.65	Regulates exocytosis in synaptic vesicles	P63040
Nck-associated protein 1	*NCKAP1*	0.002	0.69	Involved in neuronal cytoskeletal dynamics	A2AS98
Adenylyl cyclase-associated protein 2	*CAP2*	0.049	0.70	Implicated on actin pointed end dynamics	Q9CYT6
Calcium/calmodulin-dependent protein kinase type II subunit alpha	*CAMK2A*	0.041	0.71	Involved in synaptic plasticity, neurotransmitter release and long-term potentiation	F8WIS9

Sarcoplasmic/endoplasmic reticulum calcium ATPase 2	*ATP2A2*	0.045	0.73	Catalyzes the hydrolysis of ATP coupled with the translocation of calcium to the sarcoplasmic reticulum lumen	O55143
Synaptic vesicle membrane protein VAT-1 homolog	*VAT1*	0.005	0.75	Implicated in the regulation of vesicular transport, mitochondrial fusion, phospholipid transport and cell migration	Q62465
Adenylyl cyclase-associated protein 1	*CAP1*	0.014	0.76	Directly regulates filament dynamics	P40124
Protein kinase C alpha type	*PRKCA*	0.028	0.76	Calcium-activated, involved in processes related to presynapse	Q4VA93
Dynamin-like 120 kDa protein, mitochondrial	*OPA1*	0.013	0.77	Density regulator of functional presynaptic terminals	H7BX01
Wiskott-Aldrich syndrome protein family member 3	*WASF3*	0.023	0.77	Regulates actin filament reorganization via its interaction with the Arp2/3 complex	Q8VHI6
Microtubule-associated protein	*MAPT*	7.3×10^{-4}	0.78	Promotes microtubule assembly and stability on neurons	A2A5Y6

Mitogen-activated protein kinase 1	*MAPK1*	0.042	0.80	Essential component of the MAP kinase signal transduction pathway	P63085
Neuronal calcium sensor 1	*NCS1*	0.007	0.81	Neuronal calcium sensor, regulator of G protein-coupled receptor phosphorylation in a calcium dependent manner	Q8BNY6
Synapsin-2	*SYN2*	0.017	0.84	Regulator of synaptic vesicles trafficking, control of neurotransmitter release at the pre-synaptic terminal	Q64332
Synapsin-1	*SYN1*	$1.6x10^{-3}$	0.86	Regulator of synaptic vesicles trafficking, control of neurotransmitter release at the pre-synaptic terminal	O88935
15 kDa selenoprotein	*SEP15.*	-	3NT+EA	Thioredoxin-like, endoplasmic reticulum-resident protein	Q9ERR7
Alpha-N-acetylgalactosaminidase	*NAGA*	-	3NT+EA	Involved in degradation of glycosaminoglycan in lysosomes	A0A2R8VHC0
Cathepsin L1	*CTSL*	-	3NT+EA	Lysosomal proteases	P06797
U6 snRNA-associated Sm-like protein LSm8	*LSM8*	-	3NT+EA	Involved in spliceosome assembly	Q6ZWM4

Transcription factor BTF3 homolog 4	*BTF3L4*	-	3NT+EA	Transcription factor	Q9CQH7
Cerebellin-1	*CBLN1*	-	3NT+EA	Synaptic organizer essential in glutamatergic synapse	Q9R171

[1]Fold change indicates the degree of abundance change for a particular protein between animals (3NT vs. 3NT+EA); FC <1 denotes a decrease in the concentration of protein in 3NT+EA treated mice (vs. 3NT). When a given protein is only present in one of the groups, fold change cannot be measured, and such condition is denoted as “3NT+EA” (if protein is only present in 3NT+EA -exposed mice).

5. DISCUSIÓN CONJUNTA

5. DISCUSIÓN CONJUNTA

En la presente Tesis Doctoral, en una primera aproximación, se decidió estudiar el efecto de diversos aminoácidos oxidados y nitrosados, tales como α-AA, ditirosina, 3NT, quinurenina y ácido quinurénico, sobre células diferenciadas de adenocarcinoma de colon humano CACO-2. Las dosis empleadas fueron compatibles con las encontradas en alimentos. Los análisis se llevaron a cabo mediante citometría de flujo, UHPLC-MS/MS y HPLC-FLD, para determinar cambios en la viabilidad celular asociada a apoptosis/necrosis, ROS, GSH y productos de oxidación proteica (carbonilos) (Capítulo 4.1). Este primer estudio puso de manifiesto que los efectos causados en las células eran específicos de cada aminoácido empleado, lo que indicaba mecanismos de acción diferente según la naturaleza de los mismos.

En vista de los hallazgos obtenidos de cada uno de los compuestos y en base a la literatura científica existente, se decidió dirigir la tesis hacia el estudio más pormenorizado de dos aminoácidos en concreto, α-AA y 3NT, utilizando técnicas moleculares avanzadas como la proteómica. Para contrarrestar los efectos toxicológicos encontrados a priori en el primer estudio, se decidió emplear un compuesto fenólico ampliamente conocido por su capacidad antioxidante como el EA, para analizar los posibles efectos beneficiosos que pudiese tener sobre la toxicidad de los aminoácidos seleccionados.

Seguidamente se van a discutir los efectos más relevantes inducidos tanto por el α-AA como por el 3NT a dosis encontradas en alimentos, tanto en dos modelos *in vitro* como en un modelo *in vivo,* para posteriormente analizar su combinación con el EA.

5.1. Efecto del ácido α-AA en cultivos celulares y modelos animales

Uno de los objetivos de esta Tesis Doctoral es estudiar el efecto potencialmente pernicioso para la salud causado por el α-AA, producto final de la oxidación del aminoácido lisina, tanto *in vitro* como *in vivo*, empleando dosis presentes en los alimentos. Para cumplir con este objetivo se emplearon dos líneas celulares, CACO-2, procedente de adenocarcinoma de colon humano y, SH-SY5Y, derivada de neuroblastoma humano. Previamente a la incubación con el α-AA, ambos cultivos celulares fueron sometidos a diferenciación, para la adquisición por parte de las células de características morfológicas

y bioquímicas similares a los enterocitos y a las neuronas, respectivamente. Posteriormente, se realizaron estudios sobre el efecto del aminoácido oxidado en cerebro del modelo animal C57BL/6, cepa de ratón empleada comúnmente en laboratorio.

En este caso, además de realizar los mismos estudios que en los cultivos celulares, se empleó la prueba del laberinto de Morris para detectar si la ingesta de este aminoácido oxidado producía pérdida de memoria espacial. La incubación de α-AA a una dosis de 200 µM con los cultivos diferenciados de CACO-2 (Capítulos 4.1 y 4.2) y a 4mM con las células diferenciadas de SH-SY5Y (Capítulo 4.4), obtuvieron, como se esperaba, resultados diferentes en el aumento y disminución de proteínas implicadas en procesos biológicos y moleculares debido al diferente origen celular, pero con similitudes en la aparición de estrés oxidativo y marcadores de oxidación proteica. En el caso del estudio del impacto del α-AA en el cerebro de ratón (Capítulo 4.5), la dosis empleada de α-AA de 2.5 mg/L (135 µg α-AA/kg peso vivo), compartió ciertas similitudes con los resultados obtenidos en el cultivo de células neuronales. A continuación, se comparan más en profundidad los efectos causados por el α-AA tanto *in vitro* como *in vivo*.

5.1.1. Impacto del α-AA sobre el estrés oxidativo, apoptosis, homeostasis celular y metabolismo energético

Mediante las determinaciones realizadas en esta Tesis Doctoral por citometría de flujo, proteómica, y mediciones de marcadores de oxidación proteica, se pone de manifiesto, de manera original, que el α-AA, a las dosis empleadas presentes en alimentos, produce estrés oxidativo tanto en cultivos celulares como en animales.

El aumento de estrés oxidativo en las células diferenciadas procedentes de adenocarcinoma de colon humano observado por primera vez en el Capítulo 4.1., se confirma en el Capítulo 4.2, manifestándose en un aumento de los marcadores de oxidación proteica α-AS y γ-GS, acompañado de un agotamiento de la defensa antioxidante GSH y un aumento de la apoptosis. Gracias a los ensayos realizados mediante proteómica, se observa que la disminución significativa de la viabilidad y la aparición de apoptosis encontrada en las células intestinales no se manifiesta en una elevación de la cantidad de proteínas implicadas en este proceso, sino en una menor abundancia de proteínas involucradas en un adecuado mantenimiento del ciclo celular, tal y como se observa en el Capítulo 4.2. En cambio, en las

células neuronales diferenciadas, se observó un aumento significativo de los marcadores primarios de oxidación proteica (Capítulo 4.4), acompañado de un incremento de apoptosis en los ensayos de citometría de flujo y un aumento de proteínas relacionadas con la misma mediante proteómica. Adicionalmente, se encontró una disminución del ratio GSH/GSSH, lo cual se encuentra asociado a enfermedades neurodegenerativas (Owen & Butterfiel, 2010).

En el experimento llevado a cabo *in vivo*, las defensas antioxidantes se encuentran aumentadas significativamente en el cerebro de los ratones en presencia de dosis de α-AA compatibles con alimentos. En estudios llevados a cabo en cultivos de astrocitos y en animales, el α-AA es considerado una gliotoxina (Brown & Kretzschmar, 1998; Pereira *et al*., 2021), es decir, un compuesto que tiene efectos tóxicos sobre las células gliales, dentro de las cuales se encuentran los astrocitos y los oligodendrocitos. Por lo tanto, el aumento de las defensas antioxidantes *in vivo* parece estar desencadenado por la amenaza del estrés oxidativo causado por el α-AA sobre los astrocitos del cerebro de los ratones en estudio. Este hecho también se corresponde con la disminución de proteínas pertenecientes a la diferenciación de oligodendrocitos en los ratones, resultado hallado mediante análisis de proteómica.

El establecimiento de condiciones de estrés oxidativo se encuentra respaldado por el aumento de los productos de oxidación proteica causado por el aminoácido oxidado. En estudios realizados por da Silva *et al*. (2017), se afirmó de que el α-AA inducía estrés oxidativo en estudios *in vitro* de cerebro de ratón adolescente. Este hecho es compatible con la toxicidad encontrada tanto *in vitro* como *in vivo* de este aminoácido oxidado, ya que, al tratarse de cortes de tejido, formado por los diferentes tipos de células que conforman el cerebro, el aumento del estrés oxidativo se produce a nivel global de todo el órgano, pero afectando más en concreto a las células gliales.

Los resultados obtenidos mediante proteómica demuestran que las células intestinales diferenciadas se encuentran significativamente afectadas, principalmente, en la disminución de proteínas relacionadas con la actividad ATPasa de la célula, en el ciclo de los ácidos tricarboxílicos y en proteínas chaperonas implicadas en el adecuado plegamiento de proteínas para su correcto funcionamiento (Saibil, 2013) (Capítulo 4.2). De esta manera, el aminoácido oxidado, α-AA, a dosis encontradas en alimentos, disminuye de modo general, el correcto funcionamiento de la homeostasis celular y el

metabolismo energético de las células *in vitro*, entre otros procesos. La generación de ROS se encuentra vinculada a una actividad mitocondrial alterada (Kausar *et al*., 2018) y el control de la homeostasis intestinal se encuentra regulado por diferentes factores, entre ellos el correcto funcionamiento de las mitocondrias. Cuando las mitocondrias se encuentran desreguladas pueden aparecer problemas a nivel de intestino tanto delgado como grueso (Guerbette *et al*., 2022). Adicionalmente, la inhibición de la actividad ATPasa se encuentra relacionada con la mala absorción de nutrientes esenciales en la enteritis crónica (Nepal *et al*., 2021). Por otra parte, las proteínas aumentadas en procesos biológicos implicados en reparación post-replicación, acompañado del aumento de la síntesis de nucleótidos y nucleósidos, proteínas ribosómicas y procesos de splicing (empalme de ARN mediante la eliminación de intrones) (Chao *et al*., 2021), entre otros, corroboran el aumento de los procesos de reparación, como consecuencia del efecto toxicológico causado por el aminoácido oxidado.

5.1.2. Consecuencias de la exposición e ingesta del α-AA en proteínas estructurales

El α-AA afecta a procesos biológicos y moleculares distintos y de manera diferente, tanto a células intestinales y neuronales diferenciadas, como en el cerebro de ratón. Puede ser que este hecho sea muy probablemente a causa de que el aminoácido oxidado afecte a cada tipo celular en proteínas diferentes, además de las diferencias en la dosis empleadas y el tiempo de exposición dentro de cada uno de los experimentos.

Aun así, hay ciertas similitudes entre ellos, como, por ejemplo, la disminución de la cantidad de proteínas estructurales tanto en las células *in vitro* como en ratones. Estas proteínas estructurales ejercen una función de “carreteras”, por donde las proteínas viajan para alcanzar su destino y ejercer su función. Esta afectación en proteínas como la tubulina, en el caso de las células intestinales, influye en el desplazamiento de proteínas hacia la zona apical de las células (Gilbert *et al*., 1991). Por su parte, tanto en las células neuronales cultivadas *in vitro* como en el cerebro de ratón, esta afectación en proteínas estructurales como la actina, proteína esencial en la formación del citoesqueleto, puede desembocar en una inadecuada o insuficiente formación del mismo, pudiendo provocar una alteración

en la organización normal del citoesqueleto y en la formación de neuritas, lo que conduce a la aparición de enfermedades neurológicas (Schevzov *et al*., 2012).

En particular, el complejo proteico Arp2/3, implicado de manera importante con la remodelación de actina, es considerado un factor esencial en la plasticidad neuronal *in vivo* (Kim *et al*., 2013). Su alteración se asocia con una plasticidad estructural asimétrica de las espinas dendríticas que puede conducir a trastornos psiquiátricos como esquizofrenia o trastornos del espectro autista (Kim *et al*., 2013). Aunque, por otro lado, estudios llevados a cabo por Liu *et al*. (2013) afirman que la inhibición del complejo Arp2/3 reduce la migración y alteración de la morfología de las células de glioma, un tipo de tumor muy común en el cerebro que se origina en las células gliales. Curiosamente, en las células intestinales, las proteínas relacionadas con la polimerización de actina se encuentran aumentadas (Capítulo 4.2). De esta manera, se confirma nuevamente que el mismo compuesto puede afectar de manera diferente según el tipo celular.

Adicionalmente, el estudio proteómico en ratones reveló que el α-AA, además de afectar a los procesos relacionados con la actina, también está involucrado en la disminución de otros componentes estructurales del citoesqueleto como septinas (Mostowy & Cossart, 2012) (consideradas el cuarto componente del citoesqueleto), tubulina y mielina, ésta última relacionada con la adecuada transmisión de impulsos eléctricos a lo largo de las neuronas (Kim *et al*., 2021), donde una desmielinización de los axones se encuentra involucrada en la esclerosis múltiple (Lemus *et al*., 2018).

Otros procesos comunes afectados por el α-AA tanto en ambos cultivos celulares como en animales son los relacionados con los procesos de reparación post-replicación. Estos procesos se encuentran aumentados en la presencia del aminoácido oxidado, determinando que las células y el organismo están detectando situaciones anómalas, intentando devolver a la célula a su correcto funcionamiento.

De esta manera, se puede confirmar en esta Tesis Doctoral que, parte de los efectos causados por el aminoácido oxidado α-AA a dosis compatibles con alimentos, son comunes en el modelo *in vitro* y en el modelo *in vivo*, siempre que se trate del mismo tipo celular, pero es necesario continuar complementando el modelo *in vitro* con los resultados obtenidos en experimentación animal, para tener una visión global de los mecanismos que se encuentran afectados *in vivo* y por tanto poder ser extrapolables al ser humano.

5.1.3. Influencia del α-AA sobre la memoria espacial

En base a los resultados obtenidos mediante la prueba de laberinto de Morris (Patil *et al*., 2009), se puede afirmar que, a las dosis presentes en alimentos, el aminoácido oxidado α-AA, en el modelo *in vivo* de ratón C57BL/6, no causa pérdida de memoria espacial, ni a corto ni a largo plazo. El aumento de la respuesta antioxidante, comprobado por el aumento de las enzimas CAT y GPX4, junto con el aumento de subunidades pertenecientes a la hemoglobina y procesos de reparación, evitan la aparición de síntomas relacionados con la pérdida de memoria espacial debido a la ingesta del α-AA, el cual se ha comprobado que está relacionado con diversas patologías.

El efecto acumulativo en el tiempo de aminoácidos oxidados en el organismo podría estar detrás de enfermedades relacionas con el estrés oxidativo. Si la acumulación excesiva, en este caso del α-AA, no pudiera ser paliada por los mecanismos de defensa y reparación, podría derivar en la aparición de daños en astrocitos (Pereira *et al*., 2021; Voronkov *et al*., 2021), en la alteración de la regulación de neurotransmisores (Wu *et al*., 1995), en desórdenes neurológicos como ansiedad y depresión (David *et al*., 2019; Ni *et al*., 2014), y además en obesidad y diabetes (Lee *et al*., 2019; Wang *et al*., 2013).

Gran cantidad de alimentos, sobre todo procesados, contienen cantidades significativas de α-AA. El consumo abusivo de este tipo de alimentos está relacionado con el aumento del deterioro cognitivo (Cardoso *et al*., 2022), y enfermedades como Alzheimer y demencia (Li *et al*., 2022). Existen trabajos donde se ha estudiado el efecto de los alimentos ultraprocesados a largo plazo, observándose un aumento del deterioro cognitivo en adultos de mediana-avanzada edad después de un seguimiento de 8 años (Gomes Gonçalves *et al*., 2023).

Por lo tanto, en esta Tesis Doctoral se confirma, de manera original, la aparición de estrés oxidativo tanto en cultivos celulares como en ratones por el consumo del α-AA a dosis encontradas en alimentos. La activación de enzimas antioxidantes y otros mecanismos de reparación son capaces de actuar revirtiendo esta situación, impidiendo que se produzcan, *a priori*, efectos negativos sobre la memoria espacial *in vivo*, aunque sí se observan cambios en el proteoma relacionados con la disminución de proteínas estructurales. Como recomendación, podrían realizarse en el futuro estudios a más largo plazo para comprobar si, efectivamente, el consumo de este aminoácido oxidado causa

comportamientos derivados de la pérdida de deterioro cognitivo, ya que en humanos estos síntomas suelen aparecer en personas de mediana-avanzada edad.

5.2. Efecto de la 3-nitrotirosina en cultivos celulares y modelos animales

Una vez estudiado el efecto del aminoácido oxidado α-AA tanto en cultivos celulares como en animales, se planteó como nuevo objetivo analizar el efecto del aminoácido nitrosado, 3NT, sobre el cultivo de células intestinales CACO-2 (Capítulo 4.3) y el modelo animal de ratón C57BL/6 (Capítulo 4.6), ya que como se puso de manifiesto en el primer estudio, los efectos sobre las células fueron diferentes según la exposición a un aminoácido o a otro (Capítulo 4.1). Como en el caso del α-AA, se procedió a la diferenciación de las células CACO-2 antes de exponerlas a la 3NT a una concentración compatible con las encontradas en alimentos (320 μg/Kg de peso vivo) (Lu *et al*., 2020; Tang *et al*., 2023) y se llevaron a cabo análisis de citometría de flujo, medición de marcadores de oxidación proteica y ensayos de proteómica. Posteriormente, se realizó un estudio *in vivo* en la cepa C57BL/6 de ratón, donde además de analizar las diferencias en el proteoma entre los ratones control y los expuestos a 3NT, se empleó la prueba del laberinto de Morris, para detectar si se producían pérdidas de memoria espacial atribuidas al consumo de 3NT. Contrariamente a la hipótesis inicial, no se encontraron diferencias significativas con respecto a la pérdida de memoria espacial entre el grupo control y el grupo que consumía 3NT, aunque sí se encontraron diferencias significativas entre los ratones tratados con 3NT durante 3 semanas y los ratones tratados al final del experimento.

A continuación, se van a discutir las similitudes y diferencias obtenidas en el estudio de 3NT tanto en las células intestinales diferenciadas como en el modelo animal.

5.2.1. Consecuencias de la 3NT sobre el estrés oxidativo

Tras la exposición a 3NT en el cultivo celular diferenciado de CACO-2 y el modelo animal C57BL/6, se pone de manifiesto de manera original en esta Tesis Doctoral que, en los dos casos, la 3NT es capaz de causar estrés oxidativo, a dosis encontradas en alimentos.

En los dos modelos experimentales se produce, en primer lugar, un aumento significativo de los productos de oxidación proteica α-AS y γ-GS, como consecuencia directa de la aparición de estrés oxidativo. En el caso de la cepa de ratón C57BL/6, además, tiene lugar un incremento significativo de enzimas antioxidantes, tales como peroxirredoxina, CAT y SOD2, detectadas mediante ensayos de proteómica. Es importante destacar que, aunque el origen de las células sea diferente, uno proveniente de células intestinales *in vitro*, y el otro de células de cerebro *in vivo*, se observa, en ambos casos, un incremento de estrés oxidativo, aunque no acompañado en el modelo *in vitro* por un aumento en las defensas antioxidantes. El aumento del estrés oxidativo/nitrosativo generalmente se describe como una circunstancia en la que las defensas antioxidantes no son capaces de neutralizar completamente las ROS/RNS producidas a causa de una superproducción de las mismas, agotamiento de las defensas antioxidantes o ambas (Kurutas, 2016). Es razonable pensar que, por uno de estos motivos, no se observa un incremento de defensas antioxidantes en el modelo *in vitro* en nuestro estudio.

El aumento de estrés oxidativo en las células diferenciadas CACO-2 tiene como consecuencia una disminución significativa de la viabilidad celular ligada a un aumento de la necrosis, hecho que puede estar relacionado directamente con el agotamiento de las defensas antioxidantes CAT y SOD (análisis llevados a cabo mediante ensayos espectrofotométricos). El incremento de la muerte celular en nuestro estudio concuerda con los resultados obtenidos por Blanchard-Fillion *et al*. (2006) en ratas, en los cuales la exposición a la 3NT producía apoptosis en células dopaminérgicas, implicadas en la enfermedad de Parkinson. En los ratones C57BL/6 no existen resultados a nivel comportamental que corroboren que se están produciendo fenómenos de necrosis en las células cerebrales, pero sí es cierto que muchas proteínas involucradas en la plasticidad neuronal se encuentran afectadas, tal y como se discutirá a continuación.

5.2.2. Influencia de la exposición a 3NT sobre la plasticidad neuronal

Gracias a técnicas moleculares avanzadas como la proteómica, aplicada en esta Tesis Doctoral, se puede confirmar que la ingesta de 3NT a dosis compatibles con alimentos, por parte de ratones C57BL/6, se encuentra involucrada en la disminución de proteínas implicadas en procesos biológicos y moleculares relacionados con la plasticidad sináptica.

La plasticidad sináptica es la capacidad que tienen las células neuronales para cambiar su morfología y/o funcionalidad a través del desarrollo, siendo la potenciación a largo plazo el mecanismo principal de plasticidad que permite la generación de la memoria (Bassi *et al*., 2019). En el caso de los ratones C57BL/6, el proteoma se encuentra alterado principalmente en la disminución de proteínas implicadas en procesos de polimerización de microtúbulos (Yoshida & Goedert, 2012), liberación de neurotransmisores u hormonas mediante exocitosis de vesículas sinápticas (Cao *et al*., 2013; Corradini *et al*., 2009), regulación de la señalización por calcio (Dahimene et al., 2022) y componentes del recubrimiento de vesículas sinápticas (Camblor-Perujo & Kononenko, 2022), entre otros, todos ellos relacionados con la plasticidad sináptica (Xue *et al*., 2021).

En las células diferenciadas de CACO-2, los procesos biológicos afectados por la 3NT a dosis encontradas en alimentos no son los mismos que los encontrados en los ensayos proteómicos llevados a cabo *in vivo*. En este caso, la 3NT afectó en gran medida, a la disminución del procesamiento y presentación de antígenos a través del complejo mayor de histocompatilidad (CMH) clase II. De esta manera, se comprueba que el aminoácido nitrosado compromete el sistema inmune, sobre todo a través de la disminución de proteínas involucradas en la formación de vesículas portadoras de antígenos. En diversos estudios se han puesto de manifiesto la influencia de la 3NT en el sistema inmune, sobre todo en los trastornos autoinmunes (Birnboim *et al*., 2003).

Adicionalmente, y de manera importante, se produce en las células CACO-2 expuestas a la 3NT un aumento de proteínas implicadas en la unión a receptores metabotrópicos de glutamato tipo 3, en concreto al aumento de la proteína calmodulina (CALM). CALM es una proteína que tiene múltiples implicaciones fisiológicas, formando con el calcio el complejo Ca^{2+}-CALM (Vorherr *et al*., 1993). La enzima óxido nítrico sintasa se encuentra regulada también por este complejo (Dubey *et al*., 1998), hallándose precisamente un incremento significativo en la proteína CALM ligada a este proceso. Es sabido que una alta concentración de NO en presencia de radicales libres puede dar lugar a la formación de peroxinitrito, un potente agente oxidante, provocando episodios de necrosis en las células (Pacher *et al*., 2007), situación que se podría estar produciendo en este estudio. Es cierto que *in vivo*, a la vista de los resultados obtenidos mediante las distintas técnicas empleadas, no parece que se estén produciendo situaciones de necrosis celular en el cerebro de ratón, pero si cabe mencionar que en los ensayos de proteómica se detectó el aumento de una proteína reguladora de la generación

de NO, que, aunque se detectara en concentraciones poco más elevadas que en el grupo control, dicho incremento podría indicar el comienzo de la formación de manera anómala de concentraciones de NO más elevada de lo fisiológicamente deseable.

5.2.3. Repercusión de la exposición a la 3NT en la memoria espacial

En los ratones C57BL/6 expuestos a la 3NT, se observó un aumento significativo de pérdida de memoria espacial en los ratones que habían consumido 3NT durante 3 semanas en comparación con los resultados obtenidos al final del experimento, donde se observa una restauración de la memoria espacial. Esta pérdida transitoria de memoria espacial se encuentra reflejada en la disminución del tiempo y el ratio (%) que se encontraban los ratones dentro del área de estudio buscando la plataforma. Aun así, no se encontraron diferencias significativas comparando este grupo de ratones tratados con 3NT con el grupo de ratones control, ni a mitad ni al final del experimento, muy probablemente a las (esperadas) elevadas desviaciones de las medidas realizadas del comportamiento de los ratones dentro del laberinto de Morris. Los datos muestran sin embargo una clara tendencia de los animales expuestos a 3NT en la semana 3 a presentar valores distintos a los animales del grupo control.

Esta pérdida transitoria de memoria espacial a las 3 semanas de ingesta con 3NT podría estar relacionada con la disminución de todas las funciones comentadas anteriormente relacionadas con la plasticidad sináptica. Adicionalmente, el probable incremento de NO en el cerebro de los ratones, dentro del ambiente pro-oxidante que se está formando por el aumento de estrés oxidativo, podría dar lugar a la formación de peroxinitrito (no medido en la presente Tesis) causando daños que se reflejan en la prueba del laberinto de Morris. El aumento de las defensas antioxidantes, a la vista de los resultados obtenidos mediante ensayos de proteómica, al final del experimento (semana 6), refuerzan la hipótesis de que la restauración de la memoria espacial se debe al aumento de estas defensas contrarrestando los efectos nocivos causados por este aminoácido nitrosado en los ratones a mitad del experimento (semana 3).

Comparando los estudios desarrollados en α-AA y 3NT *in vivo*, se observa que la 3NT es más nociva para el cerebro a corto plazo en términos de pérdida de memoria espacial que el α-AA. Puede ser que, en experimentos con un mayor tiempo de consumo de esta sustancia por parte de los ratones, dé como resultado un aumento de la pérdida de memoria espacial, pero a la vista de los resultados obtenidos en esta Tesis Doctoral, a corto plazo es más nociva la 3NT que el aminoácido oxidado, aunque en ambos estén aumentando los niveles de defensas antioxidantes en respuesta a la amenaza de estrés oxidativo.

De manera interesante, en base a la literatura científica existente, la 3NT ya es considerada como un marcador de estrés nitrosativo en muchos estudios (Ahsan, 2013; Bandookwala & Sengupta, 2020). Ciertos trabajos han confirmado el aumento de la 3NT a nivel plasmático y en el hipocampo de ratones expuestos a este aminoácido nitrosado a través de administración intragástrica, encontrándose en este caso con pérdidas de memoria espacial en la prueba del laberinto de Morris entre el grupo control y el grupo tratado durante 35 días, vinculadas a la instauración de situaciones de estrés oxidativo (Li *et al*., 2019b). Otros trabajos también confirman la neurotoxicidad en células dopaminérgicas en relación con la 3NT cuando se dan circunstancias de estrés oxidativo. Iravani *et al*. (2006) confirmaron que un aumento de NO en el cerebro no está vinculado directamente a un daño en el mismo, sino que tiene lugar a través de la conjunción entre la presencia de NO y estrés oxidativo, dando lugar a peroxinitrito y, en consecuencia, a neurotoxicidad. Curiosamente, la presencia de aductos de 3NT es común en los cuerpos de Lewy presente en la enfermedad de Parkinson (Iravani *et al*., 2006). En este sentido, la ingesta de este aminoácido nitrosado a través del consumo de alimentos que lo contengan, podrían estar contribuyendo a un aumento de la concentración de esta especie u otras RNS en tejido nervioso central, contribuyendo a alteraciones cognitivas como las observadas en este y otros trabajos.

5.3. Efecto de la suplementación de α-AA y 3NT con el compuesto fenólico EA en modelos *in vitro* e *in vivo*

Como último objetivo de la tesis, se planteó el estudio de la utilización del compuesto fenólico EA, en su posible aplicación terapéutica frente a los efectos nocivos causados tanto por el aminoácido oxidado α-AA como por el aminoácido nitrosado 3NT. La dosis empleada de EA fue de 1.9 mg/Kg de peso vivo en base a estudios previos (De *et al*., 2018; Kang *et al*., 2016). Esta dosis es perfectamente compatible

con la cantidad ingerida por un humano a través del consumo habitual de frutas y otros vegetales que de forma natural presenten este tipo de compuesto fenólico como, por ejemplo, la granada. Los estudios se realizaron tanto en las células intestinales diferenciadas como en la cepa de ratón C57BL/6 en el caso de la suplementación de 3NT con EA (Capítulos 4.3 y 4.6). En cambio, el estudio en el caso de la combinación del α-AA con el fitoquímico solamente se llevó a cabo *in vivo* (Capítulo 4.5).

Contrariamente a la hipótesis inicial, en las células intestinales se obtuvieron resultados más nocivos con la combinación del aminoácido nitrosado y el compuesto antioxidante que frente al aminoácido solo. Por el contrario, en los ratones tratados con la combinación de α-AA+EA, sí se observaron resultados positivos con respecto a la utilización del compuesto fenólico como agente paliativo frente a los efectos toxicológicos causados por el aminoácido oxidado en cerebro.

Seguidamente, se van a discutir los resultados obtenidos más relevantes de la suplementación del aminoácido oxidado y el aminoácido nitrosado con el compuesto fenólico EA.

5.3.1. Efectos beneficiosos de la suplementación de α-AA con EA

Los efectos antioxidantes atribuidos al compuesto fenólico EA en la literatura científica (Ascacio-Valdés *et al*., 2013; Sharifi-Rad *et al*., 2022), se observan positivamente en los ratones expuestos a la combinación de este polifenol junto con el aminoácido oxidado a dosis compatibles con alimentos. No se han encontrado efectos contraproducentes sobre la memoria espacial en la prueba del laberinto de Morris, ni a corto ni a largo plazo, aunque tampoco se detectaron en los estudios realizados tanto en los ratones control como en los ratones que ingirieron solamente al α-AA.

El estrés oxidativo, acompañado del aumento de los marcadores de oxidación proteica, observado en el cerebro de los ratones tratados con el aminoácido oxidado, se encuentra disminuido cuando se emplea en combinación con el compuesto fenólico. La disminución significativa de las enzimas antioxidantes frente al incremento significativo encontrado en las mismas enzimas en la presencia en solitario del α-AA, corrobora la mitigación del estrés oxidativo por parte de este compuesto

antioxidante, tal y como evidencian diversos estudios en la verificación del efecto neuroprotector del EA (Gupta *et al*., 2021; Zhu *et al*., 2022).

A pesar de la disminución del estrés oxidativo observado en el cerebro de los ratones suplementados con EA, la combinación del aminoácido oxidado y el fitoquímico repercute de manera negativa en proteínas implicadas en procesos neurológicos. Los ensayos realizados mediante proteómica destacan la disminución de proteínas implicadas en el proceso de fusión de vesículas sinápticas con la membrana de la zona presináptica, situación que ocurría curiosamente, en el mismo proceso y en casi las mismas proteínas que en los ratones expuestos al aminoácido nitrosado 3NT. Proteínas moduladoras de la liberación de vesículas sinápticas y controladas por sinaptotagminas (Cao *et al*., 2013), se encontraron en menor abundancia en ratones expuesto a la combinación de α-AA y EA, en comparación con los ratones tratados solamente con el aminoácido oxidado. También dentro de este proceso de fusión de vesículas sinápticas, tuvo lugar una disminución significativa concomitante de proteínas pertenecientes a la envoltura de dichas vesículas y proteínas asociadas al mantenimiento y regulación del calibre axonal. Proteínas pertenecientes al complejo SNARE, involucrado en la regulación de la exocitosis, también se encontraron en menor abundancia, lo que se ha relacionado con desequilibrios neuronales y trastornos de déficit de atención/hiperactividad, epilepsia y esquizofrenia (Corradini *et al*., 2009). En general, la combinación de α-AA junto con el compuesto fenólico EA, provoca perturbaciones en la fusión de vesículas sinápticas en la zona presináptica, necesario en el normal funcionamiento de la sinapsis.

A pesar de estos efectos negativos atribuidos al EA *in vivo*, en combinación con el α-AA, sí que se han observado ciertos efectos positivos en los mecanismos moleculares del cerebro de ratón, como, por ejemplo, el aumento en abundancia de proteínas pertenecientes al complejo Arp2/3, componente importante en la plasticidad neuronal (Kim *et al*., 2013), encontrado disminuido en la exposición *in vivo* al aminoácido oxidado en solitario. Adicionalmente, proteínas involucradas en el metabolismo energético de las mitocondrias, se encuentran aumentadas con la exposición a este antioxidante en comparación con la disminución que se producía en el cultivo celular CACO-2. Esta mejora en ciertos procesos moleculares relacionados con el funcionamiento neuronal, unido al alivio de las condiciones de estrés oxidativo, podría ser la causante de la ausencia de pérdida de memoria espacial en los ratones evaluados mediante la prueba del laberinto de Morris.

5.3.2. Efectos positivo y nocivos derivados de la combinación de 3NT y EA

La combinación del aminoácido nitrosado 3NT junto con el compuesto fenólico, de manera contraria a la hipótesis inicial, no solo no mejora los efectos nocivos causados por el 3NT, sino que los exacerba en células diferenciadas CACO-2. Afortunadamente, tiene lugar de manera contraria en los estudios *in vivo*, donde sí se produce una mejora de los efectos nocivos observados en ratones expuestos a 3NT.

En la exposición del modelo *in vitro* frente a este aminoácido nitrosado junto con EA, se observa una disminución significativa de la viabilidad celular ligada a una necrosis celular masiva y a un aumento muy notable tanto de los carbonilos primarios como del producto avanzado de oxidación pentosidina. Todo esto sucede a pesar del aumento significativo de las defensas antioxidantes, lo que indica un intento fallido de neutralizar efectos nocivos del estrés oxidativo sobre proteínas. Enzimas como CAT y glutatión sintetasa, involucradas en la detoxificación en ambientes pro-oxidantes (Schieber & Chandel, 2014), se encuentran aumentadas en abundancia, junto al incremento de la actividad enzimática de CAT y SOD en presencia de 3NT+EA. A pesar de estos hallazgos, las defensas antioxidantes no son capaces, como ya se ha comentado, de paliar la ingente necrosis celular que está teniendo lugar en el cultivo celular.

Mediante ensayos de proteómica, se comprueba que la mezcla del aminoácido nitrosado y el compuesto fenólico provoca una disminución generalizada de proteínas implicadas en la formación de crestas mitocondriales y componentes de la cadena transportadora de electrones, esenciales para la correcta producción de energía en las células del cerebro. En particular, el complejo multiproteico de sitio de contacto mitocondrial y sistema de organización de crestas mitocondriales (en inglés, *mitochondrial contact site and cristae organizing system*, MICOS) (Khosravi & Harner, 2020), presente en la membrana mitocondrial interna, se encuentra profundamente afectado en la disminución en abundancia de gran cantidad de proteínas.

Se sabe que una disfunción de las mitocondrias se encuentra relacionada con una arquitectura anómala de las mismas (Khosravi & Harner, 2020). Estudios llevados a cabo por Duan *et al*. (2020) confirman que el EA tiene efectos adversos sobre la respiración mitocondrial en células tumorales, disminuyendo notablemente los niveles de ATP, el potencial de la membrana mitocondrial interna y el consumo de oxígeno *in vitro*. En nuestro estudio, las células del cultivo celular se encuentran

diferenciadas, adquiriendo características morfológicas y bioquímicas parecidas a los enterocitos (Ding *et al*., 2021), pero también se encuentran afectadas en la membrana mitocondrial interna.

En base a estos resultados, se puede afirmar que, la combinación de 3NT junto con EA es tan agresiva para las células neuronales cultivadas *in vitro*, que las mitocondrias se alteran gravemente en su conformación, afectando evidentemente a su funcionalidad, desembocando en un vasto estrés oxidativo y una necrosis celular masiva a pesar del aumento de mecanismos antioxidantes y de reparación, observados también mediante proteómica. De manera interesante, la óxido nítrico sintasa, incrementada en las células expuestas solamente al aminoácido nitrosado, se encuentra disminuida en presencia de la combinación de 3NT con EA en comparación con las células expuestas solamente a la 3NT, también relacionado con la disminución de la proteína CALM. Contrariamente, no se observan resultados en consonancia con la mejora del CMH II.

Con respecto a los estudios realizados *in vivo*, se observa que la suplementación con EA conduce a una disminución de estrés oxidativo causado por el consumo de 3NT. Sin embargo, dicha disminución no hace que los niveles de marcadores de oxidación proteicos lleguen a los niveles basales encontrados en los ratones control. El aumento y disminución de ciertas enzimas antioxidantes encontradas mediante ensayos de proteómica corroboran que las condiciones pro-oxidantes que están teniendo lugar en el cerebro de los animales que consumieron 3NT+EA no son tan severas como las encontradas en los cerebros de los ratones que consumieron solo 3NT.

A pesar de estos efectos protectores frente al estrés oxidativo atribuidos al compuesto fenólico, diversos procesos importantes implicados en la sinapsis se encuentran alterados a la vista de los resultados obtenidos en los ensayos de proteómica, comparando los ratones tratados con la combinación de 3NT+EA frente a los ratones que ingirieron solamente el aminoácido nitrosado. Gran cantidad de proteínas relacionadas con el proceso de presinapsis se encontraron significativamente disminuidas, en funciones tales como la regulación del tráfico de vesículas sinápticas hacia la zona presináptica, la estabilización de microtúbulos y actina y proteínas relacionadas con el calcio.

En primer lugar, el complejo proteico Arp2/3, relacionado con la actina e importante en la plasticidad neuronal, mencionado ya anteriormente, se encuentra disminuido por la mezcla de ambas sustancias, a diferencia del incremento que se producía en este complejo en la presencia de α-AA+EA *in vivo*,

hecho que confirma de nuevo que los efectos causados en las células son específicos de cada aminoácido. El proceso de exocitosis es sumamente importante en el adecuado funcionamiento de la sinapsis (Xue *et al*., 2021). Las vesículas sinápticas, cargadas de neurotransmisores, son transportadas desde el citosol de la célula hasta la membrana presináptica a través de microtúbulos y vías de actina. A continuación, en un proceso denominado acoplamiento, se unen a la membrana plasmática presináptica, donde de manera dependiente de ATP, quedan listas para ser liberadas. Finalmente, cuando las células se excitan, a través del aumento de la concentración de calcio intracelular, se desencadena la fusión de las vesículas y la membrana plasmática presináptica provocando la liberación de las cargas secretoras (Xue *et al*., 2021). A la vista de los resultados obtenidos, se puede afirmar que la mezcla de 3NT+EA afecta, inequívocamente, a todos estos procesos involucrados en la exocitosis de vesículas sinápticas, y, por ende, a la regulación de la presinapsis. La afectación en los mismos procesos y prácticamente en las mismas proteínas ocurre también en los ratones expuestos solamente a 3NT, por lo que se confirma que tanto en presencia del aminoácido nitrosado, como en su combinación con EA, provocan perturbaciones en la membrana presináptica, siendo incluso más acuciantes aún en la presencia de los dos compuestos juntos.

En concreto, la sinapsis glutamatérgica, sinapsis en la que se encuentra involucrada el neurotransmisor glutamato (Giménez *et al*., 2018), es la que se halla alterada por el consumo de 3NT junto al EA. Por una parte, diversas proteínas implicadas en este proceso se encontraron en una cantidad significativamente menor, aunque cualitativamente otras proteínas se encontraron aumentadas, lo que puede indicar que la combinación de estos dos compuestos puede estar ejerciendo tanto efectos beneficiosos como perjudiciales en la sinapsis glutamatérgica. Alteraciones en este tipo de sinapsis puede derivar en trastornos como la enfermedad de Alzheimer (Rudy *et al*., 2015; Zott & Konnerth, 2023), aunque se encuentra asociada más en particular a un aumento del glutamato en el espacio perisináptico que no a una disminución en sí de este tipo de sinapsis.

La sinapsis glutamatérgica no solamente tiene lugar en las neuronas, sino también en las células gliales (Giménez *et al*., 2018). En el caso de los astrocitos, el aumento de la concentración de calcio desencadena la liberación de gliotransmisores (equivalente a los neurotransmisores, pero secretados por las células gliales), que modulan la fuerza sináptica mediante la unión a los receptores pre y post-sinápticos de las neuronas, ya que ambas forman el modelo de la sinapsis tripartita (Nedergaard &

Verkhratsky, 2012). De esta manera, al existir una sinapsis glutamatérgica también en los astrocitos, es razonable deducir que la combinación de 3NT+EA afecta en su conjunto a todos los tipos de células implicadas en la sinapsis de este tipo. El aminoácido oxidado α-AA, como se ha comentado previamente, también parece estar afectando a las células gliales, por lo que los dos aminoácidos estudiados tendrían en común la afectación a este tipo de células cerebrales.

La alteración de la sinapsis glutamatérgica, tanto en neuronas como en células gliales, podría inducir, a más largo plazo, desequilibrios palpables a nivel comportamental en la fina regulación que requiere la sinapsis para una adecuada función cerebral. Por lo tanto, como se ha recomendado también para el caso del α-AA, sería apropiado desarrollar futuros estudios en los que se evaluara más a largo plazo este tipo de aminoácidos oxidados/nitrosados, en presencia/ausencia de compuestos antioxidantes mediante el laberinto de Morris u otro tipo de pruebas que indiquen una pérdida de memoria espacial o desequilibrios neurológicos en los animales, para poder extrapolar las conclusiones y futuras recomendaciones a seres humanos.

Para finalizar, en la Tabla 5.1 se muestran los resultados más relevantes atribuidos al efecto del aminoácido oxidado y nitrosado tanto *in vivo* como *in vitro* y a la repercusión de su suplementación con el compuesto fenólico EA en esta Tesis Doctoral.

Tabla 5.1. Efecto de los distintos aminoácidos oxidados/nitrosados en modelos experimentales *in vitro* e *in vivo*

Modelo de experimentación	**Compuestos empleados**	**Efecto**
Células diferenciadas CACO-2	α-AA	Aumento de estrés oxidativo Incremento de carbonilos Disminución de viabilidad celular ligada a aumento de apoptosis Agotamiento defensas antioxidantes Disminución de proteínas implicadas en homeostasis celular y metabolismo energético Disminución de procesos estructurales relacionados con tubulina Aumento de proteínas implicadas en mecanismos de reparación
Células diferenciadas SH-SY5Y	α-AA	Aumento de estrés oxidativo Incremento de carbonilos y productos avanzados de oxidación Aumento ratio GSH/GSSH Incremento de proteínas implicadas en la apoptosis Disminución procesos estructurales relacionados con la actina Aumento de proteínas implicadas en mecanismos de reparación

Ratones CB57L/6	α-AA	Incremento de estrés oxidativo Aumento de carbonilos y pentosidina Aumento de las defensas antioxidantes Disminución de proteínas y complejos proteicos relacionados con citoesqueleto Disminución de proteínas implicadas en la diferenciación de oligodendrocitos Incremento de proteínas involucradas en mecanismos de reparación Ausencia de pérdida de memoria espacial
Células diferenciadas CACO-2	3NT	Aumento de estrés oxidativo Incremento de carbonilos Disminución de viabilidad celular ligada a necrosis No aumento de actividad antioxidante Disminución de proteínas involucradas en el procesamiento y presentación de antígenos a través del complejo mayor de histocompatilidad (CMH) clase II Aumento de proteínas implicadas en la unión a receptores metabotrópicos de glutamato tipo 3 Aumento de la enzima óxido nítrico sintasa a través de la proteínas CALM

Ratones CB57L/6	3NT	Incremento de estrés oxidativo Aumento de carbonilos y pentosidina Incremento de enzimas antioxidantes Disminución de proteínas implicadas en la plasticidad neuronal y presinapsis Pérdida transitoria de memoria espacial a corto plazo, restaurándose a largo plazo
Ratones CB57L/6	α-AA+EA	Disminución de estrés oxidativo Disminución de carbonilos y pentosidina Agotamiento de enzimas antioxidantes Incremento de proteínas y complejos proteicos relacionados con citoesqueleto Disminución de proteínas implicadas en la fusión de vesículas sinápticas con la membrana presináptica Ausencia de pérdida de memoria espacial
Células diferenciadas CACO-2	3NT+EA	Incremento exacerbado de estrés oxidativo Aumento muy notable de carbonilos y pentosidina Disminución de viabilidad celular ligado a una necrosis masiva Incremento en abundancia y actividad de defensas antioxidantes

		Disminución de proteínas implicadas en la conformación mitocondrial Aumento de mecanismos de reparación
Ratones CB57L/6	3NT+EA	Disminución de estrés oxidativo Disminución de carbonilos y pentosidina Falta de resultados concluyentes relativo a enzimas antioxidantes Disminución de proteínas implicadas en procesos de exocitosis presináptica Disminución de sinapsis glutamatérgica Ausencia de pérdida de memoria espacial

6. CONCLUSIONES

6. CONCLUSIONES

1. Los efectos producidos por aminoácidos oxidados/nitrosados en células intestinales cultivadas *in vitro* son específicos para cada uno de ellos, indicando mecanismos de acción diferentes según la naturaleza de los mismos.

2. El aminoácido oxidado α-AA y el aminoácido nitrosado 3NT, estudiados en dosis compatibles con alimentos, provocan estrés oxidativo generalizado tanto *in vitro* como *in vivo.*

3. La exposición a α-AA a dosis encontradas en alimentos, tanto en el modelo *in vitro* como en el modelo *in vivo*, provoca una disminución de proteínas estructurales de células tanto intestinales como en el cerebro de ratón.

4. La exposición *in vitro* y la ingesta *in vivo* de 3NT a dosis encontradas en alimentos, es más nociva en el modelo celular que en los ratones debido al aumento de las defensas antioxidantes en estos últimos.

5. La suplementación de α-AA y 3NT con el compuesto fenólico en el modelo *in vivo*, reduce los marcadores de estrés oxidativo, aunque induce alteraciones en el proceso normal de la formación del citoesqueleto neuronal y la sinapsis, pudiendo establecerse a más largo tiempo condiciones favorables para la instauración de neuropatologías.

6. La ingesta de ambos productos de oxidación/nitrosación provocan un aumento de procesos de reparación post-replicación en células de cerebro de ratón, lo que denota una detección por parte de estas células de un daño o amenaza que intenta ser compensando mediante mecanismos de reparación y de fortalecimiento de las defensas antioxidantes.

7. La ingesta del α-AA y la 3NT, tanto solos, como en combinación con el compuesto fenólico, no causan, *a priori*, pérdida de memoria espacial en ratones a largo plazo. A corto plazo, la 3NT causa pérdida transitoria de memoria espacial, restaurándose a largo plazo gracias al aumento de las defensas antioxidantes.

8. Los resultados observados *in vitro* e *in vivo*, relativos al mismo tipo celular, comparten ciertas similitudes en respuesta a la exposición a los mismos compuestos, lo que confirma que los cultivos celulares son una alternativa interesante al uso de animales de experimentación en fases iniciales de

estudios toxicológicos de alimentos o componentes de los mismos. Sin embargo, los modelos animales resultan imprescindibles en estudios más pormenorizados que busquen trasladar los efectos y mecanismos fisiopatológicos al ser humano.

9. Las técnicas moleculares avanzadas, como la proteómica, son de enorme interés para elucidar los mecanismos moleculares y las proteínas implicadas en las alteraciones de los procesos biológicos que tienen lugar en las células tanto *in vitro* como *in vivo*, como consecuencia de su exposición a productos potencialmente nocivos presentes en alimentos.

7. BIBLIOGRAFÍA

Ahmed, I., Leach, D.N., Wohlmuth, H., De Voss, J.J., Blanchfield, J.T., 2020. Caco-2 Cell Permeability of Flavonoids and Saponins from Gynostemma pentaphyllum: The Immortal Herb. ACS Omega 5, 21561–21569. https://doi.org/10.1021/ACSOMEGA.0C02180/SUPPL_FILE/AO0C02180_SI_001.PDF

Ahsan, H., 2013. 3-Nitrotyrosine: A biomarker of nitrogen free radical species modified proteins in systemic autoimmunogenic conditions. Hum. Immunol. 74, 1392–1399. https://doi.org/10.1016/J.HUMIMM.2013.06.009

Akagawa, M., Sasaki, T., Suyama, K., 2002. Oxidative deamination of lysine residue in plasma protein of diabetic rats: Novel mechanism via the Maillard reaction. Eur. J. Biochem. 269, 5451–5458. https://doi.org/10.1046/j.1432-1033.2002.03243.x

Al-Amrani, S., Al-Jabri, Z., Al-Zaabi, A., Alshekaili, J., Al-Khabori, M., 2021. Proteomics: Concepts and applications in human medicine. World J. Biol. Chem. 12, 57. https://doi.org/10.4331/WJBC.V12.I5.57

Alfei, S., Marengo, B., Zuccari, G., 2020. Oxidative Stress, Antioxidant Capabilities, and Bioavailability: Ellagic Acid or Urolithins? Antioxidants 2020, Vol. 9, Page 707 9, 707. https://doi.org/10.3390/ANTIOX9080707

Andrade, N., Araújo, J.R., Correia-Branco, A., Carletti, J. V., Martel, F., 2017. Effect of dietary polyphenols on fructose uptake by human intestinal epithelial (Caco-2) cells. J. Funct. Foods 36, 429–439. https://doi.org/10.1016/J.JFF.2017.07.032

Arfin, S., Jha, N.K., Jha, S.K., Kesari, K.K., Ruokolainen, J., Roychoudhury, S., Rathi, B., Kumar, D., 2021. Oxidative Stress in Cancer Cell Metabolism. Antioxidants 2021, Vol. 10, Page 642 10, 642. https://doi.org/10.3390/ANTIOX10050642

Armenteros, M., Morcuende, D., Ventanas, J., Estévez, M., 2016. The application of natural antioxidants via brine injection protects Iberian cooked hams against lipid and protein oxidation. Meat Sci. 116, 253–259. https://doi.org/10.1016/J.MEATSCI.2016.02.027

Ascacio-Valdés, J., Burboa, E., Aguilera-Carbo, A.F., Aparicio, M., Pérez-Schmidt, R., Rodríguez, R., Aguilar, C.N., 2013. Antifungal ellagitannin isolated from Euphorbia antisyphilitica Zucc. Asian Pac. J. Trop. Biomed. 3, 41. https://doi.org/10.1016/S2221-1691(13)60021-0

Aune, D., Chan, D.S.M., Vieira, A.R., Navarro Rosenblatt, D.A., Vieira, R., Greenwood, D.C., Kampman,

E., Norat, T., 2013. Red and processed meat intake and risk of colorectal adenomas: a systematic review and meta-analysis of epidemiological studies. Cancer Causes Control 24, 611–627. https://doi.org/10.1007/S10552-012-0139-Z

Awada, M., Soulage, C.O., Meynier, A., Debard, C., Plaisancié, P., Benoit, B., Picard, G., Loizon, E., Chauvin, M.A., Estienne, M., Peretti, N., Guichardant, M., Lagarde, M., Genot, C., Michalski, M.C., 2012. Dietary oxidized n-3 PUFA induce oxidative stress and inflammation: role of intestinal absorption of 4-HHE and reactivity in intestinal cells. J. Lipid Res. 53, 2069–2080. https://doi.org/10.1194/JLR.M026179

Bai, R., Guo, J., Ye, X., Xie, Y., Reviews, T.X.-A. research, 2022, U., 2022. Oxidative stress: The core pathogenesis and mechanism of Alzheimer's disease. Ageing Res. Rev. 77, 101699.

Bandookwala, M., Sengupta, P., 2020. 3-Nitrotyrosine: a versatile oxidative stress biomarker for major neurodegenerative diseases. Int. J. Neurosci. 130, 1047–1062. https://doi.org/10.1080/00207454.2020.1713776

Baraibar, M.A., Liu, L., Ahmed, E.K., Friguet, B., 2012. Protein oxidative damage at the crossroads of cellular senescence, aging, and age-related diseases. Oxid. Med. Cell. Longev. 2012. https://doi.org/10.1155/2012/919832

Bassi, M.S., Iezzi, E., Gilio, L., Centonze, D., Buttari, F., 2019. Synaptic Plasticity Shapes Brain Connectivity: Implications for Network Topology. Int. J. Mol. Sci. 20. https://doi.org/10.3390/IJMS20246193

Bastide, N.M., Chenni, F., Audebert, M., Santarelli, R.L., Taché, S., Naud, N., Baradat, M., Jouanin, I., Surya, R., Hobbs, D.A., Kuhnle, G.G., Raymond-Letron, I., Gueraud, F., Corpet, D.E., Pierre, F.H.F., 2015. A central role for heme iron in colon carcinogenesis associated with red meat intake. Cancer Res. 75, 870–879. https://doi.org/10.1158/0008-5472.CAN-14-2554

Beckman, J.S., 1996. Oxidative damage and tyrosine nitration from peroxynitrite. Chem. Res. Toxicol. 9, 836–844. https://doi.org/10.1021/TX9501445/ASSET/IMAGES/LARGE/TX9501445F00004.JPEG

Biasi, F., Leonarduzzi, G., Oteiza, P.I., Poli, G., 2013. Inflammatory Bowel Disease: Mechanisms, Redox Considerations, and Therapeutic Targets. Antioxid. Redox Signal. 19, 1711. https://doi.org/10.1089/ARS.2012.4530

Biernacki, T., Sandi, D., Bencsik, K., Vécsei, L., 2020. Kynurenines in the Pathogenesis of Multiple Sclerosis: Therapeutic Perspectives. Cells 2020, Vol. 9, Page 1564 9, 1564. https://doi.org/10.3390/CELLS9061564

Birnboim, H.C., Lemay, A.-M., Lam, D.K.Y., Goldstein, R., Webb, J.R., 2003. Cutting Edge: MHC Class II-Restricted Peptides Containing the Inflammation-Associated Marker 3-Nitrotyrosine Evade Central Tolerance and Elicit a Robust Cell-Mediated Immune Response. J. Immunol. 171, 528–532. https://doi.org/10.4049/JIMMUNOL.171.2.528

Bitalebi, S., Nikoo, M., Rahmanifarah, K., Noori, F., Ahmadi Gavlighi, H., 2019. Effect of apple peel extract as natural antioxidant on lipid and protein oxidation of rainbow trout (Oncorhynchus mykiss) mince. Int. Aquat. Res. 11, 135–146. https://doi.org/10.1007/S40071-019-0224-Y/TABLES/2

Blanchard-Fillion, B., Prou, D., Polydoro, M., Spielberg, D., Tsika, E., Wang, Z., Hazen, S.L., Koval, M., Przedborski, S., Ischiropoulos, H., 2006. Metabolism of 3-nitrotyrosine induces apoptotic death in dopaminergic cells. J. Neurosci. 26, 6124–6130. https://doi.org/10.1523/JNEUROSCI.1038-06.2006

Bouaziz, C., Sharaf el dein, O., El Golli, E., Abid-Essefi, S., Brenner, C., Lemaire, C., Bacha, H., 2008. Different apoptotic pathways induced by zearalenone, T-2 toxin and ochratoxin A in human hepatoma cells. Toxicology 254, 19–28. https://doi.org/10.1016/J.TOX.2008.08.020

Boye, J., Wijesinha-Bettoni, R., Burlingame, B., 2012. Protein quality evaluation twenty years after the introduction of the protein digestibility corrected amino acid score method. Br. J. Nutr. 108 Suppl 2. https://doi.org/10.1017/S0007114512002309

Braidy, N., Grant, R., 2017. Kynurenine pathway metabolism and neuroinflammatory disease. Neural Regen Res 12, 39–42.

Brown, D.R., Kretzschmar, H.A., 1998. The glio-toxic mechanism of α-aminoadipic acid on cultured astrocytes. J. Neurocytol. 27, 109–118. https://doi.org/10.1023/A:1006947322342

Camblor-Perujo, S., Kononenko, N.L., 2022. Brain-specific functions of the endocytic machinery. FEBS J. 289, 2219–2246. https://doi.org/10.1111/FEBS.15897

Cao, P., Yang, X., Südhof, T.C., 2013. Complexin activates exocytosis of distinct secretory vesicles controlled by different synaptotagmins. J. Neurosci. 33, 1714–1727.

https://doi.org/10.1523/JNEUROSCI.4087-12.2013

Cardoso, B., Machado, P., Steele, E.M., 2022. Association between ultra-processed food consumption and cognitive performance in US older adults: a cross-sectional analysis of the NHANES 2011–2014. Eur. J. Nutr. 61, 3975–3985. https://doi.org/10.1007/S00394-022-02911-1/TABLES/3

Carvalho, L.M., Rocha, T.C., Delgado, J., Díaz-Velasco, S., Madruga, M.S., Estévez, M., 2023. Deciphering the underlying mechanisms of the oxidative perturbations and impaired meat quality in Wooden breast myopathy by label-free quantitative MS-based proteomics. Food Chem. 423, 136314. https://doi.org/10.1016/J.FOODCHEM.2023.136314

Ceriello, A., 2002. Nitrotyrosine: new findings as a marker of postprandial oxidative stress. Int. J. Clin. Pract. Suppl. 51–58.

Chan, D.S.M., Lau, R., Aune, D., Vieira, R., Greenwood, D.C., Kampman, E., Norat, T., 2011. Red and processed meat and colorectal cancer incidence: meta-analysis of prospective studies. PLoS One 6. https://doi.org/10.1371/JOURNAL.PONE.0020456

Chang, D., Wang, F., Zhao, Y.S., Pan, H.Z., 2008. Evaluation of oxidative stress in colorectal cancer patients. Biomed. Environ. Sci. 21, 286–289. https://doi.org/10.1016/S0895-3988(08)60043-4

Chao, Y., Jiang, Y., Zhong, M., Wei, K., Hu, C., Qin, Y., Zuo, Y., Yang, L., Shen, Z., Zou, C., 2021. Regulatory roles and mechanisms of alternative RNA splicing in adipogenesis and human metabolic health. Cell Biosci. 11. https://doi.org/10.1186/S13578-021-00581-W

Chen, Z., Leinisch, F., Greco, I., Zhang, W., Shu, N., Chuang, C.Y., Lund, M.N., Davies, M.J., 2019. Characterisation and quantification of protein oxidative modifications and amino acid racemisation in powdered infant milk formula. Free Radic. Res. 53, 68–81. https://doi.org/10.1080/10715762.2018.1554250

Choi, J.S., Chin, K.B., 2021. Structural changes of meat protein of chicken sausages with various levels of salt and phosphate and their effects on in vitro digestion. Int. J. Food Sci. Technol. 56, 5250–5258. https://doi.org/10.1111/IJFS.15181

Christi, W.W., Harwoo, J.L., 2020. Oxidation of polyunsaturated fatty acids to produce lipid mediators. Essays Biochem. 64, 401. https://doi.org/10.1042/EBC20190082

Cilla, A., Rodrigo, M.J., Zacarías, L., De Ancos, B., Sánchez-Moreno, C., Barberá, R., Alegría, A., 2018. Protective effect of bioaccessible fractions of citrus fruit pulps against H2O2-induced oxidative

stress in Caco-2 cells. Food Res. Int. 103, 335–344. https://doi.org/10.1016/j.foodres.2017.10.066

Circu, M., Aw, T.Y., 2012. Intestinal redox biology and oxidative stress. Semin. Cell Dev. Biol. 23, 729–737.

Collins, A.R., 2014. Measuring oxidative damage to DNA and its repair with the comet assay. Biochim. Biophys. Acta 1840, 794–800. https://doi.org/10.1016/J.BBAGEN.2013.04.022

Condello, M., Meschini, S., 2021. Role of Natural Antioxidant Products in Colorectal Cancer Disease: A Focus on a Natural Compound Derived from Prunus spinosa, Trigno Ecotype. Cells 10. https://doi.org/10.3390/CELLS10123326

Corradini, I., Verderio, C., Sala, M., Wilson, M.C., Matteoli, M., 2009. SNAP-25 IN NEUROPSYCHIATRIC DISORDERS. Ann. N. Y. Acad. Sci. 1152, 93. https://doi.org/10.1111/J.1749-6632.2008.03995.X

Correia, A.S., Cardoso, A., Vale, N., 2023. Oxidative Stress in Depression: The Link with the Stress Response, Neuroinflammation, Serotonin, Neurogenesis and Synaptic Plasticity. Antioxidants 2023, Vol. 12, Page 470 12, 470. https://doi.org/10.3390/ANTIOX12020470

Cossarizza, A., Chang, H.D., Radbruch, A., 2019. Guidelines for the use of flow cytometry and cell sorting in immunological studies (second edition). Eur. J. Immunol. 49, 1457–1973. https://doi.org/10.1002/EJI.201970107

D'Haens, G., Rieder, F., Feagan, B.G., Higgins, P.D.R., Panés, J., Maaser, C., Rogler, G., Löwenberg, M., van der Voort, R., Pinzani, M., Peyrin-Biroulet, L., Danese, S., Allocca, M., De Hertogh, G., Denton, C., Distler, J., McCarrier, K., McGovern, D., Radstake, T., Serrano, D., Stoker, J., 2022. Challenges in the Pathophysiology, Diagnosis, and Management of Intestinal Fibrosis in Inflammatory Bowel Disease. Gastroenterology 162, 26–31. https://doi.org/10.1053/j.gastro.2019.05.072

da Silva, J.C., Amaral, A.U., Cecatto, C., Wajner, A., dos Santos Godoy, K., Ribeiro, R.T., de Mello Gonçalves, A., Zanatta, Â., da Rosa, M.S., Loureiro, S.O., Vargas, C.R., Leipnitz, G., de Souza, D.O.G., Wajner, M., 2017. α-Ketoadipic Acid and α-Aminoadipic Acid Cause Disturbance of Glutamatergic Neurotransmission and Induction of Oxidative Stress In Vitro in Brain of Adolescent Rats. Neurotox. Res. 32, 276–290. https://doi.org/10.1007/s12640-017-9735-8

Dahimene, S., Von Elsner, L., Holling, T., Mattas, L.S., Pickard, J., Lessel, D., Pilch, K.S., Kadurin, I., Pratt, W.S., Zhulin, I.B., Dai, H., Hempel, M., Ruzhnikov, M.R.Z., Kutsche, K., Dolphin, A.C., 2022. Biallelic

CACNA2D1 loss-of-function variants cause early-onset developmental epileptic encephalopathy. Brain 145, 2721–2729. https://doi.org/10.1093/BRAIN/AWAC081

David, J., Gormley, S., McIntosh, A.L., Kebede, V., Thuery, G., Varidaki, A., Coffey, E.T., Harkin, A., 2019. L-alpha-amino adipic acid provokes depression-like behaviour and a stress related increase in dendritic spine density in the pre-limbic cortex and hippocampus in rodents. Behav. Brain Res. 362, 90–102. https://doi.org/10.1016/J.BBR.2019.01.015

Davies, M.J., 2016. Protein oxidation and peroxidation. Biochem. J. 473, 805–825. https://doi.org/10.1042/BJ20151227

De Bruijn, K.M.J., Arends, L.R., Hansen, B.E., Leeflang, S., Ruiter, R., Van Eijck, C.H.J., 2013. Systematic review and meta-analysis of the association between diabetes mellitus and incidence and mortality in breast and colorectal cancer. Br. J. Surg. 100, 1421–1429. https://doi.org/10.1002/BJS.9229

De Palo, P., Maggiolino, A., Centoducati, P., Tateo, A., 2013. Effects of two different packaging materials on veal calf meat quality and shelf life. J. Anim. Sci. 91, 2920–2930. https://doi.org/10.2527/JAS.2012-5292

De, R., Sarkar, A., Ghosh, P., Ganguly, M., Karmakar, B.C., Saha, D.R., Halder, A., Chowdhury, A., Mukhopadhyay, A.K., 2018. Antimicrobial activity of ellagic acid against Helicobacter pylori isolates from India and during infections in mice. J. Antimicrob. Chemother. 73, 1595–1603. https://doi.org/10.1093/JAC/DKY079

Delgado, J., Núñez, F., Asensio, M.A., Owens, R.A., 2019. Quantitative proteomic profiling of ochratoxin A repression in Penicillium nordicum by protective cultures. Int. J.Food Microbiol. 305, 108243. https://doi.org/10.1016/j.ijfoodmicro.2019.108243

Deng, L., Gui, Z., Zhao, L., Wang, J., Shen, L., 2012. Diabetes mellitus and the incidence of colorectal cancer: an updated systematic review and meta-analysis. Dig. Dis. Sci. 57, 1576–1585. https://doi.org/10.1007/S10620-012-2055-1

Dewanjee, S., Chakraborty, P., Bhattacharya, H., Chacko, L., Singh, B., Chaudhary, A., Javvaji, K., Pradhan, S.R., Vallamkondu, J., Dey, A., Kalra, R.S., Jha, N.K., Jha, S.K., Reddy, P.H., Kandimalla, R., 2022. Altered glucose metabolism in Alzheimer's disease: Role of mitochondrial dysfunction and oxidative stress. Free Radic. Biol. Med. 193, 134–157.

https://doi.org/10.1016/J.FREERADBIOMED.2022.09.032

Ding, X., Hu, X., Chen, Y., Xie, J., Ying, M., Wang, Y., Yu, Q., 2021. Differentiated Caco-2 cell models in food-intestine interaction study: Current applications and future trends. Trends Food Sci. Technol. 107, 455–465. https://doi.org/10.1016/J.TIFS.2020.11.015

Ding, Y.Y., Li, Z.Q., Cheng, X.R., Ran, Y.M., Wu, S.J., Shi, Y., Le, G., 2017. Dityrosine administration induces dysfunction of insulin secretion accompanied by diminished thyroid hormones T3 function in pancreas of mice. Amino Acids 49, 1401–1414. https://doi.org/10.1007/s00726-017-2442-1

Domínguez, R., Pateiro, M., Munekata, P.E.S., Zhang, W., Garcia-Oliveira, P., Carpena, M., Prieto, M.A., Bohrer, B., Lorenzo, J.M., 2022. Protein Oxidation in Muscle Foods: A Comprehensive Review. Antioxidants 11. https://doi.org/10.3390/ANTIOX11010060

Donzelli, E., Carfì, M., Miloso, M., Strada, A., Galbiati, S., Bayssas, M., Griffon-Etienne, G., Cavaletti, G., Petruccioli, M.G., Tredici, G., 2004. Neurotoxicity of platinum compounds: Comparison of the effects of cisplatin and oxaliplatin on the human neuroblastoma cell line SH-SY5Y. J. Neurooncol. 67, 65–73. https://doi.org/10.1023/B:NEON.0000021787.70029.CE/METRICS

dos Santos, L.M., da Silva, T.M., Azambuja, J.H., Ramos, P.T., Oliveira, P.S., da Silveira, E.F., Pedra, N.S., Galdino, K., do Couto, C.A.T., Soares, M.S.P., Tavares, R.G., Spanevello, R.M., Stefanello, F.M., Braganhol, E., 2017. Methionine and methionine sulfoxide treatment induces M1/classical macrophage polarization and modulates oxidative stress and purinergic signaling parameters. Mol. Cell. Biochem. 424, 69–78. https://doi.org/10.1007/S11010-016-2843-6/FIGURES/4

Duan, J., Li, Y., Gao, H., Yang, D., He, X., Fang, Y., Zhou, G., 2020. Phenolic compound ellagic acid inhibits mitochondrial respiration and tumor growth in lung cancer. Food Funct. 11, 6332–6339. https://doi.org/10.1039/D0FO01177K

Dubey, R.K., Gillespie, D.G., Jackson, E.K., 1998. Cyclic AMP-Adenosine Pathway Induces Nitric Oxide Synthesis in Aortic Smooth Muscle Cells. Hypertension 31, 296–302. https://doi.org/10.1161/01.HYP.31.1.296

Duda-Chodak, A., Markiewicz, D., Pierzchalski, P., 2009. The effect of quercetin, chlorogenic acid and epigallocatechin on proliferation of Caco-2 cells. Acta Sci. Pol. Technol. Aliment. 8, 63–69.

Estévez, M., 2021. Critical overview of the use of plant antioxidants in the meat industry:

Opportunities, innovative applications and future perspectives. Meat Sci. 181, 108610. https://doi.org/10.1016/J.MEATSCI.2021.108610

Estévez, M., 2015. Oxidative damage to poultry: From farm to fork. Poult. Sci. 94, 1368–1378. https://doi.org/10.3382/ps/pev094

Estévez, M., 2011. Protein carbonyls in meat systems: A review. Meat Sci. 89, 259–279. https://doi.org/10.1016/J.MEATSCI.2011.04.025

Estévez, M., Díaz-Velasco, S., Martínez, R., 2021. Protein carbonylation in food and nutrition: a concise update. Amin. Acids 2021 544 54, 559–573. https://doi.org/10.1007/S00726-021-03085-6

Estévez, M., Li, Z., Soladoye, O.P., Van-Hecke, T., 2017. Health Risks of Food Oxidation. Adv. Food Nutr. Res. 82, 45–81. https://doi.org/10.1016/bs.afnr.2016.12.005

Estévez, M., Luna, C., 2017. Dietary protein oxidation: A silent threat to human health? Crit. Rev. Food Sci. Nutr. 57, 3781–3793. https://doi.org/10.1080/10408398.2016.1165182

Estévez, M., Xiong, Y., 2019. Intake of Oxidized Proteins and Amino Acids and Causative Oxidative Stress and Disease: Recent Scientific Evidences and Hypotheses. J. Food Sci. 84, 387–396. https://doi.org/10.1111/1750-3841.14460

Falowo, A.B., Fayemi, P.O., Muchenje, V., 2014. Natural antioxidants against lipid-protein oxidative deterioration in meat and meat products: A review. Food Res. Int. 64, 171–181. https://doi.org/10.1016/J.FOODRES.2014.06.022

Faria, J., Barbosa, J., Queirós, O., Moreira, R., Carvalho, F., Dinis-Oliveira, R.J., 2016. Comparative study of the neurotoxicological effects of tramadol and tapentadol in SH-SY5Y cells. Toxicology 359–360, 1–10. https://doi.org/10.1016/J.TOX.2016.06.010

Forman, H.J., Zhang, H., 2021. Targeting oxidative stress in disease: promise and limitations of antioxidant therapy. Nat. Rev. Drug Discov. 2021 209 20, 689–709. https://doi.org/10.1038/s41573-021-00233-1

Frame, C.A., Huff-Lonergan, E.J., Rossoni Serao, M.C., 2020. Impact of storage conditions on protein oxidation of rendered by-product meals. Transl. Anim. Sci. 4. https://doi.org/10.1093/TAS/TXAA205

Frijhoff, J., Winyard, P.G., Zarkovic, N., Davies, S.S., Stocker, R., Cheng, D., Knight, A.R., Taylor, E.L.,

Oettrich, J., Ruskovska, T., Gasparovic, A.C., Cuadrado, A., Weber, D., Poulsen, H.E., Grune, T., Schmidt, H.H.H.W., Ghezzi, P., 2015. Clinical Relevance of Biomarkers of Oxidative Stress. Antioxid. Redox Signal. 23, 1144–1170. https://doi.org/10.1089/ARS.2015.6317

García-Villalba, R., Espín, J.C., Aaby, K., Alasalvar, C., Heinonen, M., Jacobs, G., Voorspoels, S., Koivumäki, T., Kroon, P.A., Pelvan, E., Saha, S., Tomás-Barberán, F.A., 2015. Validated Method for the Characterization and Quantification of Extractable and Nonextractable Ellagitannins after Acid Hydrolysis in Pomegranate Fruits, Juices, and Extracts. J. Agric. Food Chem. 63, 6555–6566. https://doi.org/10.1021/ACS.JAFC.5B02062

Gilbert, T., Le Bivic, A., Quaroni, A., Rodriguez-Boulan, E., 1991. Microtubular organization and its involvement in the biogenetic pathways of plasma membrane proteins in Caco-2 intestinal epithelial cells. J. Cell Biol. 113, 275–288. https://doi.org/10.1083/jcb.113.2.275

Giménez, C., Zafra, F., Aragón, C., 2018. Pathophysiology of the glutamate and the glycine transporters: New therapeutic targets. Rev. Neurol. 67, 491–504. https://doi.org/10.33588/rn.6712.2018067

Givan, A.L., 2011. Flow cytometry: an introduction. Methods Mol. Biol. 699, 1–29. https://doi.org/10.1007/978-1-61737-950-5_1

Gomes Gonçalves, N., Vidal Ferreira, N., Khandpur, N., Martinez Steele, E., Bertazzi Levy, R., Andrade Lotufo, P., Bensenor, I.M., Caramelli, P., Alvim De Matos, S.M., Marchioni, D.M., Suemoto, C.K., 2023. Association Between Consumption of Ultraprocessed Foods and Cognitive Decline. JAMA Neurol. 80, 142–150. https://doi.org/10.1001/JAMANEUROL.2022.4397

Gómez, L.J., Gómez, N.A., Zapata, J.E., López-García, G., Cilla, A., Alegría, A., 2019. In-vitro antioxidant capacity and cytoprotective/cytotoxic effects upon Caco-2 cells of red tilapia (Oreochromis spp.) viscera hydrolysates. Food Res. Int. 120, 52–61. https://doi.org/10.1016/J.FOODRES.2019.02.029

González Esquivel, D., Ramírez-Ortega, D., Pineda, B., Castro, N., Ríos, C., Pérez de la Cruz, V., 2017. Kynurenine pathway metabolites and enzymes involved in redox reactions. Neuropharmacology 112, 331–345. https://doi.org/10.1016/j.neuropharm.2016.03.013

Graves, P., Haystead, T., 2002. Molecular biologist's guide to proteomics. Microbiol Mol Biol Rev. 66, 39–63. https://doi.org/10.1128/MMBR.66.1.39-63.2002

Griswold-Prenner, I., Kashyap, A.K., Mazhar, S., Hall, Z.W., Fazelinia, H., Ischiropoulos, H., 2023. Unveiling the human nitroproteome: Protein tyrosine nitration in cell signaling and cancer. J. Biol.

Chem. 299. https://doi.org/10.1016/J.JBC.2023.105038/ATTACHMENT/12464E56-973F-4F0A-A50E-A8A1F1808B52/MMC1.XLSX

Guéraud, F., Taché, S., Steghens, J.P., Milkovic, L., Borovic-Sunjic, S., Zarkovic, N., Gaultier, E., Naud, N., Héliès-Toussaint, C., Pierre, F., Priymenko, N., 2015. Dietary polyunsaturated fatty acids and heme iron induce oxidative stress biomarkers and a cancer promoting environment in the colon of rats. Free Radic. Biol. Med. 83, 192–200. https://doi.org/10.1016/J.FREERADBIOMED.2015.02.023

Guerbette, T., Boudry, G., Lan, A., 2022. Mitochondrial function in intestinal epithelium homeostasis and modulation in diet-induced obesity. Mol. Metab. 63. https://doi.org/10.1016/J.MOLMET.2022.101546

Guibourdenche, M., Haug, J., Chevalier, N., Spatz, M., Barbezier, N., Gay-Quéheillard, J., Anton, P.M., 2021. Food Contaminants Effects on an In Vitro Model of Human Intestinal Epithelium. Toxics 9. https://doi.org/10.3390/TOXICS9060135

Gupta, A., Singh, A.K., Kumar, R., Jamieson, S., Pandey, A.K., Bishayee, A., 2021. Neuroprotective Potential of Ellagic Acid: A Critical Review. Adv. Nutr. 12, 1211. https://doi.org/10.1093/ADVANCES/NMAB007

Hayes, J., Dinkova-Kostova, A., cell, K.T.-C., 2020, undefined, 2020. Oxidative stress in cancer. cell.com. https://doi.org/10.1016/j.ccell.2020.06.001

He, J., Zhang, X., Lian, C., Wu, J., Fang, Y., Ye, X., 2019. KEAP1/NRF2 axis regulates H 2 O 2 -induced apoptosis of pancreatic β-cells, Gene. Elsevier B.V. https://doi.org/10.1016/j.gene.2018.11.100

Hellwig, M., 2019. The Chemistry of Protein Oxidation in Food. Angew.Chemie - Int. Ed. 58, 16742–16763. https://doi.org/10.1002/anie.201814144

Hernández-López, S.H., Rodríguez-Carpena, J.G., Lemus-Flores, C., Grageola-Nuñez, F., Estévez, M., 2016. Avocado waste for finishing pigs: Impact on muscle composition and oxidative stability during chilled storage. Meat Sci. 116, 186–192. https://doi.org/10.1016/J.MEATSCI.2016.02.018

Höhn, A., Weber, D., Jung, T., Ott, C., Hugo, M., Kochlik, B., Kehm, R., König, J., Grune, T., Castro, J.P., 2017. Happily (n)ever after: Aging in the context of oxidative stress, proteostasis loss and cellular senescence. Redox Biol. 11, 482–501. https://doi.org/10.1016/j.redox.2016.12.001

Holman, J.D., Dasari, S., Tabb, D.L., 2013. Informatics of protein and posttranslational modification

detection via shotgun proteomics. Methods Mol. Biol. 1002, 167–179. https://doi.org/10.1007/978-1-62703-360-2_14

Hu, X., Liang, Y., Zhao, B., Wang, Y., 2019. Oxyresveratrol protects human lens epithelial cells against hydrogen peroxide-induced oxidative stress and apoptosis by activation of Akt/HO-1 pathway. J. Pharmacol. Sci. 139, 166–173. https://doi.org/10.1016/J.JPHS.2019.01.003

IARC, 2015. Carcinogenicity of consumption of red and processed meat. Lancet Oncol. https://doi.org/10.1016/S1470-2045(15)00444-1

Iravani, M.M., Haddon, C.O., Rose, S., Jenner, P., 2006. 3-Nitrotyrosine-dependent dopaminergic neurotoxicity following direct nigral administration of a peroxynitrite but not a nitric oxide donor. Brain Res. 1067, 256–262. https://doi.org/10.1016/J.BRAINRES.2005.10.086

Jakobsen, L.M.A., Yde, C.C., Van Hecke, T., Jessen, R., Young, J.F., De Smet, S., Bertram, H.C., 2017. Impact of red meat consumption on the metabolome of rats. Wiley Online Libr. Jakobsen, CC Yde, T Van Hecke, R Jessen, JF Young, S Smet, HC BertramMolecular Nutr. food Res. 2017•Wiley Online Libr. 61, 1600387. https://doi.org/10.1002/mnfr.201600387

Johnson, S.L., Park, H.Y., Vattem, D.A., Grammas, P., Ma, H., Seeram, N.P., 2020. Equol, a Blood–Brain Barrier Permeable Gut Microbial Metabolite of Dietary Isoflavone Daidzein, Exhibits Neuroprotective Effects against Neurotoxins Induced Toxicity in Human Neuroblastoma SH-SY5Y Cells and Caenorhabditis elegans. Plant Foods Hum. Nutr. 75, 512–517. https://doi.org/10.1007/S11130-020-00840-0/TABLES/1

Juan-García, A., Manyes, L., Ruiz, M.J., Font, G., 2013. Applications of flow cytometry to toxicological mycotoxin effects in cultured mammalian cells: A review. Food Chem. Toxicol. 56, 40–59. https://doi.org/10.1016/j.fct.2013.02.005

Kalaitsidis, K., Sidiropoulou, E., Tsiftsoglou, O., Mourtzinos, I., Moschakis, T., Basdagianni, Z., Vasilopoulos, S., Chatzigavriel, S., Lazari, D., Giannenas, I., 2021. Effects of Cornus and Its Mixture with Oregano and Thyme Essential Oils on Dairy Sheep Performance and Milk, Yoghurt and Cheese Quality under Heat Stress. Anim. 2021, Vol. 11, Page 1063 11, 1063. https://doi.org/10.3390/ANI11041063

Kamat, Pradip K, Kalani, Anuradha, Rai, Shivika, Swarnkar, Supriya, Tota, Santoshkumar, Nath, Chandishwar, Tyagi, Neetu, Kamat is Senior Author P K Kamat, P.K., Kalani, A, Tyagi, N, Kamat, P

K, Rai, S, Tota, S, Nath, C, Swarnkar, S, 2014. Mechanism of Oxidative Stress and Synapse Dysfunction in the Pathogenesis of Alzheimer's Disease: Understanding the Therapeutics Strategies. Mol. Neurobiol. 2014 531 53, 648–661. https://doi.org/10.1007/S12035-014-9053-6

Kang, I., Buckner, T., Shay, N.F., Gu, L., Chung, S., 2016. Improvements in Metabolic Health with Consumption of Ellagic Acid and Subsequent Conversion into Urolithins: Evidence and Mechanisms. Adv. Nutr. 7, 961–972. https://doi.org/10.3945/AN.116.012575

Kanner, J., Selhub, J., Shpaizer, A., Rabkin, B., Shacham, I., Tirosh, O., 2017. Redox homeostasis in stomach medium by foods: The Postprandial Oxidative Stress Index (POSI) for balancing nutrition and human health. Redox Biol. 12, 929–936. https://doi.org/10.1016/j.redox.2017.04.029

Kausar, S., Wang, F., Cui, H., 2018. The Role of Mitochondria in Reactive Oxygen Species Generation and Its Implications for Neurodegenerative Diseases. Cells 7, 274. https://doi.org/10.3390/cells7120274

Khosravi, S., Harner, M.E., 2020. The MICOS complex, a structural element of mitochondria with versatile functions. Biol. Chem. 401, 765–778. https://doi.org/10.1515/HSZ-2020-0103/XML

Kim, D., An, H., Fan, C., Park, Y., 2021. Identifying oligodendrocyte enhancers governing Plp1 expression. Hum. Mol. Genet. 30, 2225. https://doi.org/10.1093/HMG/DDAB184

Kim, I.H., Racz, B., Wang, H., Burianek, L., Weinberg, R., Yasuda, R., Wetsel, W.C., Soderling, S.H., 2013. Disruption of Arp2/3 Results in Asymmetric Structural Plasticity of Dendritic Spines and Progressive Synaptic and Behavioral Abnormalities. J. Neurosci. 33, 6081–6092. https://doi.org/10.1523/JNEUROSCI.0035-13.2013

Klran, T.R., Otlu, O., Karabulut, A.B., 2023. Oxidative stress and antioxidants in health and disease. J. Lab. Med. 47, 1–11. https://doi.org/10.1515/LABMED-2022-0108/ASSET/GRAPHIC/J_LABMED-2022-0108_FIG_003.JPG

Kotha, R.R., Tareq, F.S., Yildiz, E., Luthria, D.L., 2022. Oxidative Stress and Antioxidants—A Critical Review on In Vitro Antioxidant Assays. Antioxidants 2022, Vol. 11, Page 2388 11, 2388. https://doi.org/10.3390/ANTIOX11122388

Kurutas, E.B., 2016. The importance of antioxidants which play the role in cellular response against oxidative/nitrosative stress: current state. Nutr. J. 15. https://doi.org/10.1186/S12937-016-0186-5

Lee, Hyo Jung, Jang, H.B., Kim, W.H., Park, K.J., Kim, K.Y., Park, S.I., Lee, Hye Ja, 2019. 2-Aminoadipic acid (2-AAA) as a potential biomarker for insulin resistance in childhood obesity. Sci. Rep. 9, 1–10. https://doi.org/10.1038/s41598-019-49578-z

Lee, J.Y., Hong, S.N., Kim, J.H., Choe, W.H., Lee, S.Y., Sung, I.K., Park, H.S., Shim, C.S., 2013. Risk for coronary heart disease increases risk for colorectal neoplasm. Clin. Gastroenterol. Hepatol. 11, 695–702. https://doi.org/10.1016/J.CGH.2012.10.017

Lefaki, M., Papaevgeniou, N., Chondrogianni, N., 2017. Redox regulation of proteasome function. Redox Biol. 13, 452. https://doi.org/10.1016/J.REDOX.2017.07.005

Lemus, H.N., Warrington, A.E., Rodriguez, M., 2018. Multiple Sclerosis: Mechanisms of Disease and Strategies for Myelin and Axonal Repair. Neurol. Clin. 36, 1–11. https://doi.org/10.1016/J.NCL.2017.08.002

Li, B., Ge, Y., Xu, Y., Lu, Y., Yang, Y., Han, L., Jiang, Y., Shi, Y., Le, G., 2019a. Spatial Learning and Memory Impairment in Growing Mice Induced by Major Oxidized Tyrosine Product Dityrosine. J. Agric. Food Chem. 67, 9039–9049. https://doi.org/10.1021/ACS.JAFC.9B04253/ASSET/IMAGES/LARGE/JF9B04253_0011.JPEG

Li, B., Ge, Y., Xu, Y., Lu, Y., Yang, Y., Han, L., Jiang, Y., Shi, Y., Le, G., 2019b. Spatial Learning and Memory Impairment in Growing Mice Induced by Major Oxidized Tyrosine Product Dityrosine. J. Agric. Food Chem. 67, 9039–9049. https://doi.org/10.1021/acs.jafc.9b04253

Li, B., Mo, L., Yang, Y., Zhang, S., Xu, J., Ge, Y., Xu, Y., Shi, Y., Le, G., 2019c. Processing milk causes the formation of protein oxidation products which impair spatial learning and memory in rats. RSC Adv. 9, 22161–22175. https://doi.org/10.1039/C9RA03223A

Li, H., Li, S., Yang, H., Zhang, Y., Zhang, S., Ma, Y., Hou, Y., Zhang, X., Niu, K., Borné, Y., Wang, Y., 2022. Association of Ultraprocessed Food Consumption With Risk of Dementia. Neurology 99, e1056–e1066. https://doi.org/10.1212/WNL.0000000000200871

Li, Z.L., Mo, L., Le, G., Shi, Y., 2014. Oxidized casein impairs antioxidant defense system and induces hepatic and renal injury in mice. Food Chem. Toxicol. 64, 86–93. https://doi.org/10.1016/J.FCT.2013.10.039

Liguori, I., Russo, G., Curcio, F., Bulli, G., Aran, L., Della-Morte, D., Gargiulo, G., Testa, G., Cacciatore, F., Bonaduce, D., Abete, P., 2018. Oxidative stress, aging, and diseases. Clin. Interv. Aging 13, 757.

https://doi.org/10.2147/CIA.S158513

Liochev, S.I., 2013. Reactive oxygen species and the free radical theory of aging. Free Radic. Biol. Med. 60, 1–4. https://doi.org/10.1016/J.FREERADBIOMED.2013.02.011

Liu, Z., Yang, X., Chen, C., Liu, B., Ren, B., Wang, L., Zhao, K., Yu, S., Ming, H., 2013. Expression of the Arp2/3 complex in human gliomas and its role in the migration and invasion of glioma cells. Oncol. Rep. 30, 2127–2136. https://doi.org/10.3892/OR.2013.2669

Lopez-Suarez, L., Awabdh, S. Al, Coumoul, X., Chauvet, C., 2022. The SH-SY5Y human neuroblastoma cell line, a relevant in vitro cell model for investigating neurotoxicology in human: Focus on organic pollutants. Neurotoxicology 92, 131–155. https://doi.org/10.1016/J.NEURO.2022.07.008

Lu, Y., Ma, S., Tang, X., Li, B., Ge, Y., Zhang, K., Yang, S., Zhao, Q., Xu, Y., Ren, H., 2020. Dietary Dityrosine Induces Mitochondrial Dysfunction by Diminished Thyroid Hormone Function in Mouse Myocardia. J. Agric. Food Chem. 68, 9223–9234. https://doi.org/10.1021/ACS.JAFC.0C03926/ASSET/IMAGES/LARGE/JF0C03926_0009.JPEG

Luna, C., Estévez, M., 2019. Formation of allysine in β-lactoglobulin and myofibrillar proteins by glyoxal and methylglyoxal: Impact on water-holding capacity and in vitro digestibility. Food Chem. 271, 87–93. https://doi.org/10.1016/j.foodchem.2018.07.167

Maina, M.B., Al-Hilaly, Y.K., Oakley, S., Burra, G., Khanom, T., Biasetti, L., Mengham, K., Marshall, K., Harrington, C.R., Wischik, C.M., Serpell, L.C., 2022. Dityrosine Cross-links are Present in Alzheimer's Disease-derived Tau Oligomers and Paired Helical Filaments (PHF) which Promotes the Stability of the PHF-core Tau (297-391) In Vitro. J. Mol. Biol. 434. https://doi.org/10.1016/J.JMB.2022.167785

Maldonado, E., Morales-Pison, S., Urbina, F., Solari, A., 2023. Aging Hallmarks and the Role of Oxidative Stress. Antioxidants 2023, Vol. 12, Page 651 12, 651. https://doi.org/10.3390/ANTIOX12030651

Malheiros, J., Braga, C., Grove, R., Science, F.R.-M., 2019, U., 2019. Influence of oxidative damage to proteins on meat tenderness using a proteomics approach. Meat Sci. 148, 64–71.

Mallozzi, C., Di Stasi, A.M.M., Minetti, M., 1997. Peroxynitrite modulates tyrosine-dependent signal transduction pathway of human erythrocyte band 3. FASEB J. 11, 1281–1290. https://doi.org/10.1096/FASEBJ.11.14.9409547

McGovern, D.P.B., Kugathasan, S., Cho, J.H., 2015. Genetics of Inflammatory Bowel Diseases.

Gastroenterology 149, 1163-1176.e2. https://doi.org/10.1053/J.GASTRO.2015.08.001

McKinnon, K.M., 2018. Flow Cytometry: An Overview. Curr. Protoc. Immunol. 120, 5.1.1. https://doi.org/10.1002/CPIM.40

Micha, R., Michas, G., Mozaffarian, D., 2012. Unprocessed red and processed meats and risk of coronary artery disease and type 2 diabetes--an updated review of the evidence. Curr. Atheroscler. Rep. 14, 515–524. https://doi.org/10.1007/S11883-012-0282-8

Micha, R., Wallace, S.K., Mozaffarian, D., 2010. Red and processed meat consumption and risk of incident coronary heart disease, stroke, and diabetes mellitus: a systematic review and meta-analysis. Circulation 121, 2271–2283. https://doi.org/10.1161/CIRCULATIONAHA.109.924977

Mitra, B., Lametsch, R., Akcan, T., Ruiz-Carrascal, J., 2018. Pork proteins oxidative modifications under the influence of varied time-temperature thermal treatments: A chemical and redox proteomics assessment. Meat Sci. 140, 134–144. https://doi.org/10.1016/J.MEATSCI.2018.03.011

Moloney, J.N., Cotter, T.G., 2018. ROS signalling in the biology of cancer. Semin. Cell Dev. Biol. 80, 50–64. https://doi.org/10.1016/J.SEMCDB.2017.05.023

Morén, C., deSouza, R.M., Giraldo, D.M., Uff, C., 2022. Antioxidant Therapeutic Strategies in Neurodegenerative Diseases. Int. J. Mol. Sci. 23. https://doi.org/10.3390/IJMS23169328

Mostowy, S., Cossart, P., 2012. Septins: the fourth component of the cytoskeleton. Nat. Rev. Mol. Cell Biol. 2012 133 13, 183–194. https://doi.org/10.1038/nrm3284

Nedergaard, M., Verkhratsky, A., 2012. Artifact versus reality--how astrocytes contribute to synaptic events. Glia 60, 1013–1023. https://doi.org/10.1002/GLIA.22288

Nepal, N., Arthur, S., Haynes, J., Palaniappan, B., Sundaram, U., 2021. Mechanism of Na-K-ATPase inhibition by PGE2 in intestinal epithelial cells. Cells 10. https://doi.org/10.3390/CELLS10040752/S1

Neto, D.C. d. S., Cordeiro, Â.M.T.M., Meireles, B.R.L.A., Araújo, Í.B.S., Estévez, M., Ferreira, V.C.S., Silva, F.A.P., 2021. Inhibition of Protein and Lipid Oxidation in Ready-to-Eat Chicken Patties by a Spondias mombin L. Bagasse Phenolic-Rich Extract. Foods (Basel, Switzerland) 10. https://doi.org/10.3390/FOODS10061338

Ni, J., Yang, P., Li, X., Tian, J., Jing, F., Qu, C., Lin, L., Zhang, H., 2014. Alterations of Amino Acid Level in

Depressed Rat Brain. Korean J Physiol Pharmacol 18, 371–376. https://doi.org/10.4196/kjpp.2014.18.5.371

Nicolini, G., Miloso, M., Zoia, C., Di Silvestro, A., Cavaletti, G., Tredici, G., 1998. Retinoic acid differentiated SH-SY5Y human neuroblastoma cells: an in vitro model to assess drug neurotoxicity. Anticancer Res. 18, 2477–2481.

Oguntibeju, O.., 2019. Type 2 diabetes mellitus, oxidative stress and inflammation: examining the links. Int J Physiol Pathophysiol Pharmacol 11, 45–63.

Ortega Ferrusola, C., Anel-López, L., Ortiz-Rodriguez, J.M., Martin Muñoz, P., Alvarez, M., de Paz, P., Masot, J., Redondo, E., Balao da Silva, C., Morrell, J.M., Rodriguez Martinez, H., Tapia, J.A., Gil, M.C., Anel, L., Peña, F.J., 2017. Stallion spermatozoa surviving freezing and thawing experience membrane depolarization and increased intracellular Na+. Andrology 5, 1174–1182. https://doi.org/10.1111/ANDR.12419

Owen, J.B., Butterfiel, D., 2010. Measurement of oxidized/reduced glutathione ratio. Methods Mol. Biol. 648, 269–277. https://doi.org/10.1007/978-1-60761-756-3_18

Ozyurt, V.H., Otles, S., 2020. Investigation of the effect of sodium nitrite on protein oxidation markers in food protein suspensions. J. Food Biochem. 44, e13152. https://doi.org/10.1111/JFBC.13152

Pacher, P., Beckman, J.S., Liaudet, L., 2007. Nitric oxide and peroxynitrite in health and disease. Physiol. Rev. 87, 315–424. https://doi.org/10.1152/PHYSREV.00029.2006

Påhlman, S., Ruusala, A.I., Abrahamsson, L., Mattsson, M.E.K., Esscher, T., 1984. Retinoic acid-induced differentiation of cultured human neuroblastoma cells: a comparison with phorbolester-induced differentiation. Cell Differ. 14, 135–144. https://doi.org/10.1016/0045-6039(84)90038-1

Pamplona, R., Costantini, D., 2011. Molecular and structural antioxidant defenses against oxidative stress in animals. Am. J. Physiol. - Regul. Integr. Comp. Physiol. 301, 843–863. https://doi.org/10.1152/AJPREGU.00034.2011/ASSET/IMAGES/LARGE/ZH60101177060004.JPEG

Pan, A., Sun, Q., Bernstein, A.M., Schulze, M.B., Manson, J.A.E., Willett, W.C., Hu, F.B., 2011. Red meat consumption and risk of type 2 diabetes: 3 cohorts of US adults and an updated meta-analysis. Am. J. Clin. Nutr. 94, 1088. https://doi.org/10.3945/AJCN.111.018978

Panche, A., Diwan, A., science, S.C.-J. of nutritional, 2016, undefined, 2016. Flavonoids: an overview.

cambridge.orgAN Panche, AD Diwan, SR ChandraJournal Nutr. Sci. 2016•cambridge.org 5, 1–15. https://doi.org/10.1017/jns.2016.41

Pandey, A., Chakraborty, S., Chakraborty, N., 2018. Nuclear Proteome: Isolation of Intact Nuclei, Extraction of Nuclear Proteins, and 2-DE Analysis. Methods Mol. Biol. 1696, 41–55. https://doi.org/10.1007/978-1-4939-7411-5_3

Papuc, C., Goran, G. V, Predescu, C.N., Nicorescu, V., 2017. Mechanisms of oxidative processes in meat and toxicity induced by postprandial degradation products: A review. Wiley Online Libr. 16, 96–123. https://doi.org/10.1111/1541-4337.12241

Passos, R.A., Costa, P.R.F., da Maia Lima, C.F., Santana, G.M.S., David, V., de Jesus Santos, G., Zaltman, C., Soares-Mota, M., Rocha, R., 2023. Thiols as a marker of inflammatory bowel disease activity: a systematic review. BMC Gastroenterol. 23. https://doi.org/10.1186/S12876-023-02711-9

Patil, S.S., Sunyer, B., Höger, H., Lubec, G., 2009. Evaluation of spatial memory of C57BL/6J and CD1 mice in the Barnes maze, the Multiple T-maze and in the Morris water maze. Behav. Brain Res. 198, 58–68. https://doi.org/10.1016/j.bbr.2008.10.029

Patti, G.J., Yanes, O., Siuzdak, G., 2012. Metabolomics: the apogee of the omic triology. Nat. Rev. Mol. Cell Biol. 13, 263. https://doi.org/10.1038/NRM3314

Pena, I.A., Marques, L.A., Laranjeira, Â.B.A., Yunes, J.A., Eberlin, M.N., MacKenzie, A., Arruda, P., 2017. Mouse lysine catabolism to aminoadipate occurs primarily through the saccharopine pathway; implications for pyridoxine dependent epilepsy (PDE). Biochim. Biophys. Acta - Mol. Basis Dis. 1863, 121–128. https://doi.org/10.1016/J.BBADIS.2016.09.006

Peng, L., He, Z., Chen, W., Holzman, I.R., Lin, J., 2007. Effects of Butyrate on Intestinal Barrier Function in a Caco-2 Cell Monolayer Model of Intestinal Barrier. Pediatr. Res. 2007 611 61, 37–41. https://doi.org/10.1203/01.pdr.0000250014.92242.f3

Pereira, M., Amaral, I., Lopes, C., Leitão, C., Madeira, D., Agosthino, P., FASEB, T., 2021. l-α-aminoadipate causes astrocyte pathology with negative impact on mouse hippocampal synaptic plasticity and memory. Wiley Online Libr. 35. https://doi.org/10.1096/fj.202100336R

Perfetto, S.P., Chattopadhyay, P.K., Roederer, M., 2004. Seventeen-colour flow cytometry: unravelling the immune system. Nat. Rev. Immunol. 2004 48 4, 648–655. https://doi.org/10.1038/nri1416

Peskin, A. V., Turner, R., Maghzal, G.J., Winterbourn, C.C., Kettle, A.J., 2009. Oxidation of methionine

to dehydromethionine by reactive halogen species generated by neutrophils. Biochemistry 48, 10175–10182. https://doi.org/10.1021/BI901266W/ASSET/IMAGES/MEDIUM/BI-2009-01266W_0006.GIF

Picot, J., Guerin, C.L., Le Van Kim, C., Boulanger, C.M., 2012. Flow cytometry: retrospective, fundamentals and recent instrumentation. Cytotechnology 64, 109–130. https://doi.org/10.1007/S10616-011-9415-0

Pinto, M., Robine Leon, S., Appay, M.D., 1983. Enterocyte-like differentiation and polarization of the human colon carcinoma cell line Caco-2 in culture. Biol. Cell 47, 323–330.

Puspita, L., Chung, S.Y., Shim, J.W., 2017. Oxidative stress and cellular pathologies in Parkinson's disease. Mol. Brain 2017 101 10, 1–12. https://doi.org/10.1186/S13041-017-0340-9

Qiao, Y., Sun, J., Ding, Y., Le, G., Shi, Y., 2013. Alterations of the gut microbiota in high-fat diet mice is strongly linked to oxidative stress. Appl. Microbiol. Biotechnol. 97, 1689–1697. https://doi.org/10.1007/S00253-012-4323-6

Qiu, J., Zhang, J., Li, A., 2023. Cytotoxicity and intestinal permeability of phycotoxins assessed by the human Caco-2 cell model. Ecotoxicol. Environ. Saf. 249, 114447. https://doi.org/10.1016/J.ECOENV.2022.114447

Rabilloud, T., Lelong, C., 2011. Two-dimensional gel electrophoresis in proteomics: a tutorial. J. Proteomics 74, 1829–1841.

Ranjbar, L., Foley, J.P., Breadmore, M.C., 2017. Multidimensional liquid-phase separations combining both chromatography and electrophoresis – A review. Anal. Chim. Acta 950, 7–31. https://doi.org/10.1016/J.ACA.2016.10.025

Rodríguez-Viso, P., Domene, A., Vélez, D., Devesa, V., Monedero, V., Zúñiga, M., 2022. Mercury toxic effects on the intestinal mucosa assayed on a bicameral in vitro model: Possible role of inflammatory response and oxidative stress. Food Chem. Toxicol. 166, 113224. https://doi.org/10.1016/J.FCT.2022.113224

Rombouts, C., Hemeryck, L.Y., Van Hecke, T., De Smet, S., De Vos, W.H., Vanhaecke, L., 2017. Untargeted metabolomics of colonic digests reveals kynurenine pathway metabolites, dityrosine and 3-dehydroxycarnitine as red versus white meat discriminating metabolites. Sci. Rep. 7, 1–13. https://doi.org/10.1038/srep42514

Rudy, C.C., Hunsberger, H.C., Weitzner, D.S., Reed, M.N., 2015. The Role of the Tripartite Glutamatergic Synapse in the Pathophysiology of Alzheimer's Disease. Aging Dis. 6, 131. https://doi.org/10.14336/AD.2014.0423

Ruvalcaba-Márquez, J.C., Álvarez-Ruíz, P., Zenteno-Savín, T., Martínez-Antonio, E., Goytortúa-Bores, E., Casillas-Hernández, R., Mejía-Ruíz, H., Magallón-Barajas, F.J., 2021. Performance, immune response, and oxidative stress parameters of Litopenaeus vannamei fed diets containing varying carbohydrate/protein, lipid/protein, and energy/protein ratios. Aquac. Reports 21, 100771. https://doi.org/10.1016/J.AQREP.2021.100771

Sahoo, D.K., Heilmann, R.M., Paital, B., Patel, A., Yadav, V.K., Wong, D., Jergens, A.E., 2023. Oxidative stress, hormones, and effects of natural antioxidants on intestinal inflammation in inflammatory bowel disease. Front. Endocrinol. (Lausanne). 14. https://doi.org/10.3389/FENDO.2023.1217165

Saibil, H., 2013. Chaperone machines for protein folding, unfolding and disaggregation. Nat. Rev. Mol. Cell Biol. 14, 630–642. https://doi.org/10.1038/nrm3658

Samuels, A., 2020. Dose dependent toxicity of glutamic acid: a review. Int. J. Food Prop. 23, 412–419. https://doi.org/10.1080/10942912.2020.1733016

Santé-Lhoutellier, V., Astruc, T., Marinova, P., Greve, E., Gatellier, P., 2008. Effect of meat cooking on physicochemical state and in vitro digestibility of myofibrillar proteins. J. Agric. Food Chem. 56, 1488–1494. https://doi.org/10.1021/JF072999G/ASSET/IMAGES/LARGE/JF-2007-02999G_0007.JPEG

Schevzov, G., Curthoys, N.M., Gunning, P.W., Fath, T., 2012. Functional Diversity of Actin Cytoskeleton in Neurons and its Regulation by Tropomyosin. Int. Rev. Cell Mol. Biol. 298, 33–94. https://doi.org/10.1016/B978-0-12-394309-5.00002-X

Schieber, M., Chandel, N.S., 2014. ROS function in redox signaling and oxidative stress. Curr. Biol. 24, R453–R462. https://doi.org/10.1016/j.cub.2014.03.034

Šebeková, K., Klenovicsová, K., Ferenczová, J., Hedvig, J., Podracká, L., Heidland, A., 2012. Advanced Oxidation Protein Products and Advanced Glycation End Products in Children and Adolescents With Chronic Renal Insufficiency. J. Ren. Nutr. 22, 143–148. https://doi.org/10.1053/J.JRN.2011.10.022

Sell, D.R., Strauch, C.M., Shen, W., Monnier, V.M., 2007. 2-Aminoadipic acid is a marker of protein

carbonyl oxidation in the aging human skin: Effects of diabetes, renal failure and sepsis. Biochem J. 404, 269–277. https://doi.org/10.1042/BJ20061645

Sharifi-Rad, J., Quispe, C., Castillo, C.M.S., Caroca, R., Lazo-Vélez, M.A., Antonyak, H., Polishchuk, A., Lysiuk, R., Oliinyk, P., De Masi, L., Bontempo, P., Martorell, M., Daştan, S.D., Rigano, D., Wink, M., Cho, W.C., 2022. Ellagic Acid: A Review on Its Natural Sources, Chemical Stability, and Therapeutic Potential. Oxid. Med. Cell. Longev. 2022, 24. https://doi.org/10.1155/2022/3848084

Sharifi-Rad, M., Anil Kumar, N. V., Zucca, P., Varoni, E.M., Dini, L., Panzarini, E., Rajkovic, J., Tsouh Fokou, P.V., Azzini, E., Peluso, I., Prakash Mishra, A., Nigam, M., El Rayess, Y., Beyrouthy, M. El, Polito, L., Iriti, M., Martins, N., Martorell, M., Docea, A.O., Setzer, W.N., Calina, D., Cho, W.C., Sharifi-Rad, J., 2020. Lifestyle, Oxidative Stress, and Antioxidants: Back and Forth in the Pathophysiology of Chronic Diseases. Front. Physiol. 11, 552535. https://doi.org/10.3389/FPHYS.2020.00694/BIBTEX

Sharma, A., Weber, D., Raupbach, J., Dakal, T.C., Fließbach, K., Ramirez, A., Grune, T., Wüllner, U., 2020. Advanced glycation end products and protein carbonyl levels in plasma reveal sex-specific differences in Parkinson's and Alzheimer's disease. Redox Biol. 34, 101546. https://doi.org/10.1016/J.REDOX.2020.101546

Silva, F.A.P., Ferreira, V.C.S., Madruga, M.S., Estévez, M., 2016. Effect of the cooking method (grilling, roasting, frying and sous-vide) on the oxidation of thiols, tryptophan, alkaline amino acids and protein cross-linking in jerky chicken. J. Food Sci. Technol. 53, 3137–3146. https://doi.org/10.1007/S13197-016-2287-8

Skaff, O., Jolliffe, K.A., Hutton, C.A., 2005. Synthesis of the side chain cross-linked tyrosine oligomers dityrosine, trityrosine, and pulcherosine. J. Org. Chem. 70, 7353–7363. https://doi.org/10.1021/JO051076M/SUPPL_FILE/JO051076MSI20050629_074759.PDF

Soladoye, O.P., Juárez, M.L., Aalhus, J.L., Shand, P., Estévez, M., 2015. Protein oxidation in processed meat: Mechanisms and potential implications on human health. Compr. Rev. Food Sci. Food Saf. 14, 106–122. https://doi.org/10.1111/1541-4337.12127

Soladoye, O.P., Shand, P., Dugan, M.E.R., Gariépy, C., Aalhus, J.L., Estévez, M., Juárez, M., 2017. Influence of cooking methods and storage time on lipid and protein oxidation and heterocyclic aromatic amines production in bacon. Food Res. Int. 99, 660–669. https://doi.org/10.1016/J.FOODRES.2017.06.029

Sosa, V., Moliné, T., Somoza, R., Paciucci, R., Kondoh, H., LLeonart, M.E., 2013. Oxidative stress and cancer: An overview. Ageing Res. Rev. 12, 376–390. https://doi.org/10.1016/J.ARR.2012.10.004

Stadtman, E.R., Levine, R.L., 2003. Free radical-mediated oxidation of free amino acids and amino acid residues in proteins. Amino Acids 25, 207–218. https://doi.org/10.1007/S00726-003-0011-2/METRICS

Tang, X., Zeng, F., Wang, J., Lyu, Y., Yu, R., Lu, N., Zhou, Z., Chen, A., 2023. Dietary Dityrosine Induces Oxidative Stress and Mitochondrial-Lipid Imbalance in Mouse Liver via MiR-144-3p-Mediated Downregulation of Nrf2. Mol. Nutr. Food Res. 67, 2200674. https://doi.org/10.1002/MNFR.202200674

Tauffenberger, A., Magistretti, P.J., 2021. Reactive Oxygen Species: Beyond Their Reactive Behavior. Neurochem. Res. 46, 77–87. https://doi.org/10.1007/S11064-020-03208-7

Tomasello, G., Mazzola, M., … A.L.-B.P.M.F., 2016, U., 2016. Nutrition, oxidative stress and intestinal dysbiosis: Influence of diet on gut microbiota in inflammatory bowel diseases. Biomed Pap Med Fac 160, 461–466.

Traore, S., Aubry, L., Gatellier, P., Przybylski, W., Jaworska, D., Kajak-Siemaszko, K., Santé-Lhoutellier, V., 2012. Effect of heat treatment on protein oxidation in pig meat. Meat Sci. 91, 14–21. https://doi.org/10.1016/j.meatsci.2011.11.037

Tsuji, A., Ikeda, Y., Yoshikawa, S., Taniguchi, K., Sawamura, H., Morikawa, S., Nakashima, M., Asai, T., Matsuda, S., 2023. The Tryptophan and Kynurenine Pathway Involved in the Development of Immune-Related Diseases. Int. J. Mol. Sci. 24. https://doi.org/10.3390/IJMS24065742

Unno, K., Pervin, M., Nakagawa, A., Iguchi, K., Hara, A., Takagaki, A., Nanjo, F., Minami, A., Nakamura, Y., 2017. Blood-Brain Barrier Permeability of Green Tea Catechin Metabolites and their Neuritogenic Activity in Human Neuroblastoma SH-SY5Y Cells. Mol. Nutr. Food Res. 61. https://doi.org/10.1002/MNFR.201700294

Utrera, M., Estévez, M., 2013. Oxidative damage to poultry, pork, and beef during frozen storage through the analysis of novel protein oxidation markers. J. Agric. Food Chem. 61, 7987–7993. https://doi.org/10.1021/jf402220q

Utrera, M., Morcuende, D., Rodríguez-Carpena, J.G., Estévez, M., 2011. Fluorescent HPLC for the detection of specific protein oxidation carbonyls - α-aminoadipic and γ-glutamic semialdehydes -

in meat systems. Meat Sci. 89, 500–506. https://doi.org/10.1016/j.meatsci.2011.05.017

Uttara, B., Singh, A. V., Zamboni, P., Mahajan, R.., 2009. Oxidative Stress and Neurodegenerative Diseases: A Review of Upstream and Downstream Antioxidant Therapeutic Options. Curr. Neuropharmacol. 7, 65. https://doi.org/10.2174/157015909787602823

Valdés, A., Artemenko, K.A., Bergquist, J., García-Cañas, V., Cifuentes, A., 2016. Comprehensive proteomic study of the antiproliferative activity of a polyphenol-enriched rosemary extract on colon cancer cells using nanoliquid chromatography-Orbitrap MS/MS. J. Proteome Res. 15, 1971–1985. https://doi.org/10.1021/acs.jproteome.6b00154

Valko, M., Leibfritz, D., Moncol, J., Cronin, M.T.D., Mazur, M., Telser, J., 2007. Free radicals and antioxidants in normal physiological functions and human disease. Int. J. Biochem. Cell Biol. 39, 44–84. https://doi.org/10.1016/j.biocel.2006.07.001

Vallejo, M.J., Salazar, L., Grijalva, M., 2017. Oxidative stress modulation and ROS-mediated toxicity in cancer: A review on in vitro models for plant-derived compounds. Oxid. Med. Cell. Longev. 2017. https://doi.org/10.1155/2017/4586068

Van Hecke, T., De Vrieze, J., Boon, N., De Vos, W.H., Vossen, E., De Smet, S., 2019. Combined Consumption of Beef-Based Cooked Mince and Sucrose Stimulates Oxidative Stress, Cardiac Hypertrophy, and Colonic Outgrowth of Desulfovibrionaceae in Rats. Mol. Nutr. Food Res. 63. https://doi.org/10.1002/MNFR.201800962

Van Hecke, T., Jakobsen, L.M.A., Vossen, E., Guéraud, F., De Vos, F., Pierre, F., Bertram, H.C.S., De Smet, S., 2016. Short-term beef consumption promotes systemic oxidative stress, TMAO formation and inflammation in rats, and dietary fat content modulates these effects. Food Funct. 7, 3760–3771. https://doi.org/10.1039/C6FO00462H

Van Hecke, T., Van Camp, J., De Smet, S., 2017. Oxidation During Digestion of Meat: Interactions with the Diet and Helicobacter pylori Gastritis, and Implications on Human Health. Compr. Rev. Food Sci. Food Saf. 16, 214–233. https://doi.org/10.1111/1541-4337.12248

Van Hecke, T., Vossen, E., Hemeryck, L.Y., Vanden Bussche, J., Vanhaecke, L., De Smet, S., 2015. Increased oxidative and nitrosative reactions during digestion could contribute to the association between well-done red meat consumption and colorectal cancer. Food Chem. 187, 29–36. https://doi.org/10.1016/J.FOODCHEM.2015.04.029

Vanek, T., Kohli, A., 2023. Biochemistry, Myoglobin. StatPearls.

Ventanas, S., Ventanas, J., Tovar, J., García, C., Estévez, M., 2007. Extensive feeding versus oleic acid and tocopherol enriched mixed diets for the production of Iberian dry-cured hams: Effect on chemical composition, oxidative status and sensory traits. Meat Sci. 77, 246–256. https://doi.org/10.1016/J.MEATSCI.2007.03.010

Vercauteren, F., Bergeron, J., Vandesande, F., Arckens, L., Quirion, R., 2004. Proteomic approaches in brain research and neuropharmacology. Eur. J. Pharmacol. 500, 385–398. https://doi.org/10.1016/j.ejphar.2004.07.039

Villaverde, A., Morcuende, D., Estévez, M., 2014a. Effect of Curing Agents on the Oxidative and Nitrosative Damage to Meat Proteins during Processing of Fermented Sausages. J. Food Sci. 79, C1331–C1342. https://doi.org/10.1111/1750-3841.12481

Villaverde, A., Ventanas, J., Estévez, M., 2014b. Nitrite promotes protein carbonylation and Strecker aldehyde formation in experimental fermented sausages: Are both events connected? Meat Sci. 98, 665–672. https://doi.org/10.1016/j.meatsci.2014.06.017

Vorherr, T., Knöpfel, L., Hofmann, F., Carafoli, E., Mollner, S., Pfeuffer, T., 1993. The calmodulin binding domain of nitric oxide synthase and adenylyl cyclase. Biochemistry 32, 6081–6088. https://doi.org/10.1021/BI00074A020

Voronkov, D.N., Lyzhin, A.A., Dikalova, Y. V., Stavrovskaya, A. V., Khudoerkov, R.M., Khaspekov, L.G., 2021. Features of Brain Astrocyte Damage under the Influence of L-Aminoadipic Acid In Vitro and In Vivo. Cell tissue biol. 15, 347–355. https://doi.org/10.1134/S1990519X21040106/FIGURES/3

Wang, T.J., Ngo, D., Psychogios, N., Dejam, A., Larson, M.G., Vasan, R.S., Ghorbani, A., O'Sullivan, J., Cheng, S., Rhee, E.P., Sinha, S., McCabe, E., Fox, C.S., O'Donnell, C.J., Ho, J.E., Florez, J.C., Magnusson, M., Pierce, K.A., Souza, A.L., Yu, Y., Carter, C., Light, P.E., Melander, O., Clish, C.B., Gerszten, R.E., 2013. 2-Aminoadipic acid is a biomarker for diabetes risk. J. Clin. Invest. 123, 4309–4317. https://doi.org/10.1172/JCI64801

Wang, Z., He, Z., Gan, X., Li, H., 2018. Interrelationship among ferrous myoglobin, lipid and protein oxidations in rabbit meat during refrigerated and superchilled storage. Meat Sci. 146, 131–139. https://doi.org/10.1016/J.MEATSCI.2018.08.006

Washburn, M., Wolters, D., Biotechnology, J.Y.-N., 2001, U., 2001. Large-scale analysis of the yeast

proteome by multidimensional protein identification technology. Nat. Biotech 19, 242–247. https://doi.org/10.1038/85686

Wehkamp, J., Götz, M., Herrlinger, K., Steurer, W., Stange, E.F., 2016. Inflammatory Bowel Disease: Crohn's disease and ulcerative colitis. Dtsch. Arztebl. Int. 113, 72. https://doi.org/10.3238/ARZTEBL.2016.0072

Wilkins, M.R., Sanchez, J.C., Gooley, A.A., Appel, R.D., Humphery-Smith, I., Hochstrasser, D.F., Williams, K.L., 1996. Progress with proteome projects: Why all proteins expressed by a genome should be identified and how to do it. Biotechnol. Genet. Eng. Rev. 13, 19–50. https://doi.org/10.1080/02648725.1996.10647923

Wiseman, H., Halliwell, B., 1996. Damage to DNA by reactive oxygen and nitrogen species: Role in inflammatory disease and progression to cancer. Biochem. J. 313, 17–29. https://doi.org/10.1042/bj3130017

Wolters, D., Washburn, M., Chemistry, J.Y.-A., 2001, U., 2001. An automated multidimensional protein identification technology for shotgun proteomics. Anal Chem 73, 5683–5690. https://doi.org/10.1021/ac010617e

Wu, H.Q., Ungerstedt, U., Schwarcz, R., 1995. l-α-Aminoadipic acid as a regulator of kynurenic acid production in the hippocampus: a microdialysis study in freely moving rats. Eur. J. Pharmacol. 281, 55–61. https://doi.org/10.1016/0014-2999(95)00224-9

Xie, F., Sun, S., Xu, A., Zheng, S., Xue, M., Wu, P., Zeng, J.H., Bai, L., 2014. Advanced oxidation protein products induce intestine epithelial cell death through a redox-dependent, c-jun N-terminal kinase and poly (ADP-ribose) polymerase-1-mediated pathway. Cell Death Dis. 5. https://doi.org/10.1038/CDDIS.2013.542

Xu, X., Yu, E., Gao, X., Song, N., Liu, L., Wei, X., Zhang, W., Fu, C., 2013. Red and processed meat intake and risk of colorectal adenomas: a meta-analysis of observational studies. Int. J. cancer 132, 437–448. https://doi.org/10.1002/IJC.27625

Xue, R., Meng, H., Yin, J., Xia, J., Hu, Z., Liu, H., 2021. The Role of Calmodulin vs. Synaptotagmin in Exocytosis. Front. Mol. Neurosci. 14, 691363. https://doi.org/10.3389/FNMOL.2021.691363/BIBTEX

Yang, S.Y., Kim, Y.S., Chung, S.J., Song, J.H., Choi, S.Y., Park, M.J., Yim, J.Y., Lim, S.H., Kim, D., Kim, C.H.,

Kim, J.S., Song, I.S., 2010. Association between colorectal adenoma and coronary atherosclerosis detected by CT coronary angiography in Korean men; a cross-sectional study. J. Gastroenterol. Hepatol. 25, 1795–1799. https://doi.org/10.1111/J.1440-1746.2010.06330.X

Yang, Y., Zhang, H., Yan, B., Zhang, T., Gao, Y., Shi, Y., Le, G., 2017. Health Effects of Dietary Oxidized Tyrosine and Dityrosine Administration in Mice with Nutrimetabolomic Strategies. J. Agric. Food Chem. 65, 6957–6971. https://doi.org/10.1021/acs.jafc.7b02003

Yeh, C.C., Lai, C.Y., Hsieh, L.L., Tang, R., Wu, F.Y., Sung, F.C., 2010. Protein carbonyl levels, glutathione S-transferase polymorphisms and risk of colorectal cancer. Carcinogenesis 31, 228–233. https://doi.org/10.1093/CARCIN/BGP286

Yoshida, H., Goedert, M., 2012. Phosphorylation of microtubule-associated protein tau by AMPK-related kinases. J. Neurochem. 120, 165–176. https://doi.org/10.1111/J.1471-4159.2011.07523.X

Yruela, I., Sebastián, Á., 2014. 7 - Macromoléculas biológicas: proteínas, DNA y RNA. https://doi.org/10.5281/ZENODO.1067867

Yu, D., Zhao, Y., Li, T., Li, D., Chen, S., Wu, N., Jiang, L., Wang, L., 2018. Effect of electrochemical modification on the structural characteristics and emulsion storage stability of soy protein isolate. Process Biochem. 75, 166–172. https://doi.org/10.1016/J.PROCBIO.2018.10.001

Zhang, X., Lu, P., Xue, W., Wu, D., Wen, C., Zhou, Y., 2017. An evaluation of heat on protein oxidation of soy protein isolate or soy protein isolate mixed with soybean oil in vitro and its consequences on redox status of broilers at early age. Asian-Australasian J. Anim. Sci. 30, 1135–1142. https://doi.org/10.5713/AJAS.16.0683

Zhao, Y., Kong, H., Zhang, X., Hu, X., Wang, M., 2019. The effect of Perilla (Perilla frutescens) leaf extracts on the quality of surimi fish balls. Food Sci. Nutr. 7, 2083. https://doi.org/10.1002/FSN3.1049

Zhu, H., Yan, Y., Jiang, Y., Meng, X., 2022. Ellagic Acid and Its Anti-Aging Effects on Central Nervous System. Int. J. Mol. Sci. 2022, Vol. 23, Page 10937 23, 10937. https://doi.org/10.3390/IJMS231810937

Zott, B., Konnerth, A., 2023. Impairments of glutamatergic synaptic transmission in Alzheimer's disease. Semin. Cell Dev. Biol. 139, 24–34. https://doi.org/10.1016/J.SEMCDB.2022.03.013

8. ANEXOS

OTRAS PUBLICACIONES

Food and Chemical Toxicology 145 (2020) 111594

Contents lists available at ScienceDirect

Food and Chemical Toxicology

journal homepage: www.elsevier.com/locate/foodchemtox

The lysine derivative aminoadipic acid, a biomarker of protein oxidation and diabetes-risk, induces production of reactive oxygen species and impairs trypsin secretion in mouse pancreatic acinar cells

Matias Estaras [a], Fatma Z. Ameur [b], Mario Estévez [c], Silvia Díaz-Velasco [c], Antonio Gonzalez [a,*]

[a] Institute of Molecular Pathology Biomarkers, University of Extremadura, Cáceres, Spain
[b] Laboratoire de Physiologie de la Nutrition et de Sécurité Alimentaire, Université d'Oran1 Ahmed BenBella, Algeria
[c] IPROCAR Research Institute, TECAL Research Group, University of Extremadura, 10003, Cáceres, Spain

ARTICLE INFO

Keywords:
α-aminoadipic acid
Calcium
Reactive oxygen species
Trypsin secretion
Exocrine pancreas

ABSTRACT

We have examined the effects of α-aminoadipic acid, an oxidized derivative from the amino acid lysine, on the physiology of mouse pancreatic acinar cells. Changes in intracellular free-Ca^{2+} concentration, the generation of reactive oxygen species, the levels of carbonyls and thiobarbituric-reactive substances, cellular metabolic activity and trypsin secretion were studied. Stimulation of mouse pancreatic cells with cholecystokinin (1 nM) evoked a transient increase in $[Ca^{2+}]_i$. In the presence of α-amoniadipic acid increases in $[Ca^{2+}]_i$ were observed. In the presence of the compound, cholecystokinin induced a Ca^{2+} response that was smaller compared with that observed when cholecystokinin was applied alone. Stimulation of cells with cholecystokinin in the absence of Ca^{2+} in the extracellular medium abolished further mobilization of Ca^{2+} by α-aminoadipic acid. In addition, potential pro-oxidant conditions, reflected as increases in ROS generation, oxidation of proteins and lipids, were noted in the presence of α-aminoadipic acid. Finally, the compound impaired trypsin secretion induced by the secretagogue cholecystokinin. We conclude that the oxidized derivative from the amino acid lysine induces pro-oxidative conditions and the impairment of enzyme secretion in pancreatic acinar cells. α-aminoadipic acid thus creates a situation that could potentially lead to disorders in the physiology of the pancreas.

1. Introduction

The oxidative damage to cellular proteins is a consequence of the imbalance between the generation of reactive-oxygen species (ROS) and the endogenous antioxidant defences (Davies, 2005). The formation of protein carbonyls has been emphasized as one of the most remarkable chemical changes occurred in proteins as a result of a radical-mediated oxidation (Stadtman and Levine, 2003). As other post-translational modifications, protein carbonylation has been found to play a role in cellular signalling and regulates biological processes such as protein turnover and apoptosis (Wong et al., 2010). However, under severe and/or enduring oxidative stress, severely oxidized proteins accumulate in cells leading to impaired biological functions (Rudzińska et al., 2020). In fact, the accretion of oxidized proteins is recognized as a biochemical hallmark of aging and age-related health disorders such as cataractogenesis and Alzheimer's and Parkinson's diseases (Stadtman, 2001; Rudzińska et al., 2020).

The α-aminoadipic semialdehyde (α-AS), a major protein carbonyl and intermediate oxidation product from lysine, undergoes further oxidation in the presence of peroxides to yield the α-aminoadipic acid (α-AA). The α-AA has been highlighted as a reliable indicator of *in vivo* protein oxidation, aging and disease in humans. Particularly, Sell et al. (2007, 2008), Fan et al. (2009) and Lee et al. (2019), among others, reported that α-AA is a more reliable marker for protein oxidation than

Abbreviations: α-AA, α-aminoadipic acid; BAPNA, Nα-Benzoyl-DL-arginine 4-nitroanilide hydrochloride; BAPTA, 1,2-Bis(2-aminophenoxy)ethane-N,N,N′,N′-tetraacetic acid tetrakis(acetoxymethyl ester); CCK-8, cholecystokinin octapeptide; $[Ca^{2+}]_i$, intracellular free Ca^{2+} concentration; CM-H_2DCFDA, 5-(and-6)-chloromethyl-2′,7′-dichlorodihydrofluorescein diacetate acetyl ester; EGTA, ethylene glycol-bis(2-aminoethylether)-N,N,N'N'-tetraacetic acid; Fura-2/AM, fura-2 acetoxymethyl ester; H_2O_2, hydrogen peroxide; ROS, reactive oxygen species; SERCA, sarcoendoplasmic reticulum Ca^{2+}-ATPase; TBARS, thiobarbituric-reactive substances.

* Corresponding author. Institute of Molecular Pathology Biomarkers, Department of Physiology, University of Extremadura, Avenida Universidad s/n, E-10003, Caceres, Spain.
E-mail address: agmateos@unex.es (A. Gonzalez).

https://doi.org/10.1016/j.fct.2020.111594
Received 14 May 2020; Received in revised form 6 July 2020; Accepted 8 July 2020
Available online 30 July 2020
0278-6915/© 2020 Elsevier Ltd. All rights reserved.

its precursor, AAS, in diverse pathological conditions such as skin aging, crystalline sclerosis, diabetes and renal failure.

Beyond its role as indicators of oxidative stress and physiological impairment, α-AA may actually play a role in the pathogenesis of disorders in brain and pancreatic tissues (Brown & Kretzschmar, 1998; Kiss et al., 2003).

The pancreas is especially sensitive to oxidative stress. Overstimulation of the gland (Saluja et al., 2007) or noxious substances, as for example ethanol (Gonzalez et al., 2006; Tapia et al., 2010), may induce the generation of reactive oxygen species (ROS) that, if not resolved, may lead to diseases of the gland. Pancreatic disorders include majorly pancreatitis (McClave, 2019) and, in long term, pancreatic cancer (Palanissami and Paul, 2018). It is noteworthy to highlight that the proximity of the pancreas to the gut might render the gland as a primary site of action of products entering the body with food (Verma et al., 2014).

The pancreas has also been identified as a target tissue for α-AA accumulation and bioactivity upon oral administration (Wang et al., 2013). α-AA was found to modulate glucose metabolism in mice by increasing circulating insulin levels without shifting peripheral insulin resistance (Wang et al., 2013). The results recently reported by Lee et al. (2019) indicated that α-AA was increased in plasma from children affected by insulin-resistant obesity. It was reported that an elevated α-AA concentration caused impaired insulin signalling in liver, adipose cells and skeletal muscle and induced abnormal gluconeo- and adipogenesis.

In view of these remarkable biological effects, and taking into account that, in addition to endogenous formation of α-AA, processed foods are dietary sources of this oxidized amino acid (Estévez and Xiong, 2019), the potential toxicity of α-AA deserves further consideration.

The present study aims to evaluate the biological effects of α-AA in mouse pancreatic acinar cells with special interest on the induction of oxidative stress and its ability to impair functionality.

2. Materials and methods

2.1. Animals and chemicals

Freshly isolated pancreatic acinar cells were prepared from pancreas obtained from adult (25–30 g) male *Swiss* mice. Animals were obtained from the animal house of the University of Extremadura (Caceres, Spain). Handling, sacrifice and the experimental protocols were approved by the institutional Bioethical Committee (reference 57/2016). Collagenase was obtained from Worthington Biochemical Corporation (Lakewood, NJ, U.S.A.). DL-2-aminoadipic acid, 1,2-Bis(2-aminophenoxy)ethane-N,N,N',N'-tetraacetic acid tetrakis(acetoxymethyl ester) (BAPTA/AM), benzoyl-DL-arginine 4-nitroanilide hydrochloride (BAPNA), (Tyr[SO_3H]^{27}) cholecystokinin fragment 26–33 amide (CCK-8), enterokinase from porcine intestine, ethylene glycol-bis (2-aminoethylether)-N,N,N'N'-tetraacetic acid (EGTA), melatonin, thapsigargin and trypsin were obtained from Sigma-Aldrich (Merck, Madrid, Spain). Fura-2-AM, 5-(and-6)-chloromethyl-2′,7′-dichlorodihydrofluorescein diacetate acetyl ester (CM-H_2DCFDA), hydrogen peroxide (H_2O_2) and MitoSOX™ Red were obtained from Life Technologies (Invitrogen, Barcelona, Spain). All other analytical grade chemicals used were obtained from Sigma Chemicals Co. (Madrid, Spain).

2.2. Preparation of isolated pancreatic acinar cells

A suspension of isolated and small clusters of mouse pancreatic acinar cells was prepared following previously described techniques (Gonzalez et al., 1997). Briefly, after sacrifice of animals the pancreas was removed and rapidly placed in a physiological buffer 1 (NaCl 130 mM; KCl 4.7 mM; $CaCl_2$ 1.3 mM; $MgCl_2$ 1 mM; KH_2PO_4 1.2 mM; glucose 10 mM; HEPES 10 mM; 0.01% trypsin inhibitor (soybean) and 0.2% bovine serum albumin, pH adjusted to 7.4 with NaOH). The tissue was injected with a solution of collagenase (30 units/mL) prepared in this buffer 1. Next, tissues were incubated for 10 min at 37 °C in a shaking bath (100 cycles/min). The enzymatic treatment was followed by mechanical dissociation using tips of decreasing diameter. After centrifugation at 30×*g* for 5 min at 4 °C, cells were resuspended in buffer 1 without collagenase. With this procedure a preparation of dispersed cells and small acini was obtained. No contamination of other cell types was noted, as assessed by microscopic observation (Williams, 2010b).

2.3. Determination of changes in intracellular free-Ca^{2+} concentration ($[Ca^{2+}]_i$)

Changes in $[Ca^{2+}]_i$ were detected following methods described previously (Santofimia-Castaño et al., 2014a). For this purpose, cells were loaded with the fluorescent ratiometric Ca^{2+} indicator fura-2 prepared in buffer 1. After the incubation the cell suspension was centrifuged (30×*g*), the supernatant was discarded and the pellet was resuspended with a buffer 2 (140 mM NaCl, 4.7 mM KCl, 1 mM $CaCl_2$, 1.1 mM $MgCl_2$, 10 mM Hepes, 10 mM glucose; pH adjusted to 7.4 with NaOH) to remove the dye remaining in the extracellular solution.

Small aliquots of dye-loaded cells were transferred to a coverslip mounted on an experimental perfusion chamber, which was placed on the stage of an epifluorescence inverted microscope (Nikon Diaphot T200, Melville, NY, USA). An image acquisition system was employed to monitor fura-2-derived fluorescence (Hamamatsu Photonics, Hamamatsu, Japan). Cells were alternatively excited at 340/380 nm using a high-speed monochromator (Polychrome IV, Photonics, Hamamatsu, Japan). An ORCA Flash 4.0 V2 digital CMOS camera (Hamamatsu Photonics-France, Barcelona, Spain) was used to detect fluorescence emitted at 505 nm, and was recorded using dedicated software (HCImage from Hamamatsu Corp. Sewickley, PA, USA).

When Ca^{2+}-free medium was used, the buffer 2 was prepared without Ca^{2+} and 0.5 mM EGTA was added. All stimuli were dissolved in buffer 2, with or without Ca^{2+}, and were applied directly to the cells in the perfusion chamber.

Results are expressed as the ratio of fluorescence emitted at 340 nm and 380 nm excitation wavelengths, normalized to the basal fluorescence. For comparisons, the mean peak of $[Ca^{2+}]_i$ response, estimated as the maximal value achieved after stimulation of cells with α-AA, was calculated. In addition, the total Ca^{2+} mobilization was calculated as the integral of the rise in $[Ca^{2+}]_i$ over the basal values for 5 min after stimulation of cells with α-AA. All fluorescence measurements were made from areas considered individual cells. The experiments were carried out employing different batches of cells.

2.4. Determination of reactive oxygen species (ROS) generation

Determination of ROS generation was carried out using methods described previously (Gonzalez and Salido, 2016). For this purpose, cells were loaded with CM-H_2DCFDA or MitoSOX™ Red. Loading of cells with the dyes was performed in buffer 1, using a final concentration of 10 μM for CM-H_2DCFDA and 2.5 μM for MitoSOX™ Red. After incubation, cells were centrifuged (30×*g* for 5 min) and resuspended in buffer 2. Red-ox state of cells was determined by measuring cellular fluorescence at 530 nm/590 nm (excitation/emission) for CM-H_2DCFDA and 510 nm/580 nm (excitation/emission) for MitoSOX™ Red.

Detection of fluorescence was performed using a plate reader (Tecan Infinite M200, Grödig, Austria). Data are expressed as the mean increase of fluorescence in percentage ± SEM (n) with respect to non-stimulated cells; n is the number of independent experiments.

2.5. Study of metabolic activity

The effect of treatment on metabolic activity was performed by using the oxidation-reduction sensitive dye Alamar Blue® (Springer et al.,

1998). The basis of the process is the generation of a fluorometric/colorimetric indicator that is related with the metabolic activity of the cell and serves as a valuable tool for examining mitochondrial function. The determinations were carried out following the manufacturer's directions.

2.6. Protein carbonyls (allysine)

Detection of protein carbonyls was performed following the methods described by Villaverde et al. (2014). In brief, after stimulation, cells were lysed. Next, five hundred μL of each sample were treated with cold 10% trichloroacetic acid (TCA) solution. After centrifugation (600×*g* for 5 min at 4 °C) the supernatants were removed and the pellets were incubated with the following solutions: 0.5 mL 250 mM 2-(N-morpholino) ethanesulfonic acid (MES) buffer pH 6.0 containing 1 mM diethylenetriaminepentaacetic acid (DTPA), 0.5 mL 50 mM ABA in 250 mM MES buffer pH 6.0 and 0.25 mL 100 mM $NaBH_3CN$ in 250 mM MES buffer pH 6.0. Afterwards, the samples were treated with a cold 50% TCA solution and centrifuged (1200×*g* for 10 min). The pellets were then washed twice with 10% TCA and diethyl ether-ethanol (1:1). Thereafter, the pellet was treated with 6 M HCl and kept in an oven at 110 °C for 18 h until completion of hydrolysis. Finally, the samples were dried and the residue was reconstituted with 200 μL of milliQ water.

The samples were subjected to HPLC analysis using a Shimadzu 'Prominence' HPLC apparatus (Shimadzu Corporation, Japan). The elutes were monitored with excitation/emission wavelengths set at 283/350 nm, respectively. Results are shown as the mean in nmol of allysine per mg of protein ±SEM (n) (n is the number of independent experiments).

2.7. Analysis of thiobarbituric-reactive substances

Lysates were prepared after treatment of the cells. Two hundred μL of each sample were used to detect the content of malondialdehyde (MDA) and other thiobarbituric-reactive substances (TBARS). For this purpose, 500 μL of thiobarbituric acid (0.02 M) and of 500 μL trichloroacetic acid (10%) were added to the samples, followed by incubation at 90 °C for 20 min. After cooling, samples were centrifuged (5 min, at 600×*g*). Next, the absorbance of supernatant was measured at 532 nm employing a plate reader (VariosKan Lux 3020–205, Thermo Sci. Vantaa, Finland). The amount of TBARS was calculated. Results are shown as the mean of TBARS detected in each sample (in μg/L) ± SEM (n) (n is the number of independent experiments).

2.8. Determination of trypsin secretion

Trypsin secretion was monitored employing previously described methods (Ameur et al., 2018). After stimulation of cells, 150 μL of the supernatant were incubated with 50 μL of a solution containing enterokinase (4 units/mL) and BAPNA (1 mg/mL). The mixture was then incubated at 37 °C during 10 min to allow the release of coloured 4-nitroaniline. Next, the absorbance (at 405 nm) of each sample was measured employing a plate reader (Tecan Infinite M200, Grödig, Austria). Trypsin secretion was calculated employing a calibration curve with known trypsin concentrations. Results are expressed as units of trypsin (UT) secreted by the cells ± SEM (n), were n is the number of independent preparations.

2.9. Statistical analysis

Data were checked for normal distribution. Statistical analysis of data was performed by one-way analysis of variance (ANOVA) followed by Tukey *post hoc* test, and only p values < 0.05 were considered statistically significant. Comparisons and statistics between individual treatments were carried out using Student's t-test and only P values < 0.05 were considered statistically significant.

3. Results

3.1. Changes in $[Ca^{2+}]_i$ evoked by α-AA

Ca^{2+}-signalling plays a pivotal role in pancreatic physiology (Williams, 2010a). Taking this into account, a key point for analysis in our study was to study whether α-AA exerts any effect on $[Ca^{2+}]_i$. Stimulation of cells with the secretagogue cholecystokinin-octapeptide (CCK-8) 1 nM induced a rapid increase in $[Ca^{2+}]_i$ followed by a decrease towards a value over the prestimulation level (Fig. 1A).

Next, pancreatic acinar cells were incubated with different concentrations of α-AA (1 μM, 10 μM, 100 μM or 1 mM). α-AA induced an increase in $[Ca^{2+}]_i$ that consisted of single transient increases or of a progressive increase towards an elevated plateau. These patterns of response were observed at all concentrations tested; however, it was less frequent at the concentration of 1 mM α-AA (Fig. 1B–I). The mean peak of $[Ca^{2+}]_i$ observed after incubation of cells with 1 μM, 10 μM, 100 μM or 1 mM α-AA was 1.52 ± 0.03 u.f. (n = 86 cells), 1.95 ± 0.04u.f. (n = 65 cells), 1.93 ± 0.05 u.f. (n = 91 cells) and 2.09 ± 0.04 u.f. (n = 64 cells), respectively. The mean peak of $[Ca^{2+}]_i$, measured in arbitrary units of fluorescence (u.f.), achieved in the presence of 1 μM α-AA was significantly lower in comparison with the values observed with the other three concentrations of α-AA ($P < 0.001$). However, no statistically significant differences were noted between the mean peak values of $[Ca^{2+}]_i$ achieved with 10 μM, 100 μM or 1 mM α-AA (Fig. 2A). The total Ca^{2+} mobilization that was observed in cells incubated in the presence of α-AA was 54.47 ± 4.12 u.f. (n = 86 cells), 102.20 ± 5.56 u.f. (n = 65 cells), 101.30 ± 6.20 u.f. (n = 91 cells) and 98.33 ± 3.93 u.f. (n = 64 cells) respectively for 1 μM, 10 μM, 100 μM and 1 mM. The total Ca^{2+} mobilization evoked by 1 μM α-AA was significantly smaller in comparison with that detected in cells incubated with the other concentrations of α-AA ($P < 0.001$). On the contrary, no statistically significant differences were observed between the values of total Ca^{2+} mobilization evoked by 100 μM, 100 μM and 1 mM α-AA (Fig. 2B).

In the presence of α-AA, addition of CCK-8 to the cells further induced an additional transient increase in $[Ca^{2+}]_i$ that decreased towards a value that, in most cases, remained elevated with respect to the prestimulation level. However, the response induced by CCK-8 was smaller in comparison with that evoked by CCK-8 alone. In occasions the response evoked by CCK-8 was nearly negligible, but this did not seem to depend on the concentration of α-AA used before the secretagogue (Fig. 1B–I).

In the next set of experiments, we tested whether the effect of α-AA was reversible. The concentration of α-AA used for this purpose was 1 μM, with this being the lowest concentration used in the studies. The effect of incubating the cells with 1 μM α-AA was the above described. Upon removal of α-AA, $[Ca^{2+}]_i$ remained at an elevated value and did not return towards the prestimulation level. Next, 1 nM CCK-8 was included in the extracellular solution and evoked a small and transient change in $[Ca^{2+}]_i$. Again, the response induced by CCK-8 was smaller than that evoked when the secretagogue was applied alone (Fig. 3A).

It was of interest now to examine the source for Ca^{2+} mobilization in response to α-AA. Therefore, cells were first incubated with 1 nM CCK-8 in the absence of Ca^{2+} in the extracellular solution (medium containing 0.5 mM EGTA). The secretagogue induced its typical response. In the presence of CCK-8, addition of α-AA (1 mM) to the cells failed to induce additional changes in $[Ca^{2+}]_i$ (Fig. 3B). These results suggest that α-AA evokes mobilization of Ca^{2+} from CCK-8-sensitive stores.

3.2. Effect of α-AA on reactive oxygen species (ROS) production

At this stage we studied whether α-AA induces ROS generation in pancreatic acinar cells. In a first set of experiments, pancreatic acinar cells were loaded with the ROS-sensitive fluorescent dye CM-H_2DCFDA. Next, cells were incubated during 1 h with different concentrations of α-AA (1 μM, 10 μM, 100 μM or 1 mM). CCK-8 (1 mM) was tested as a

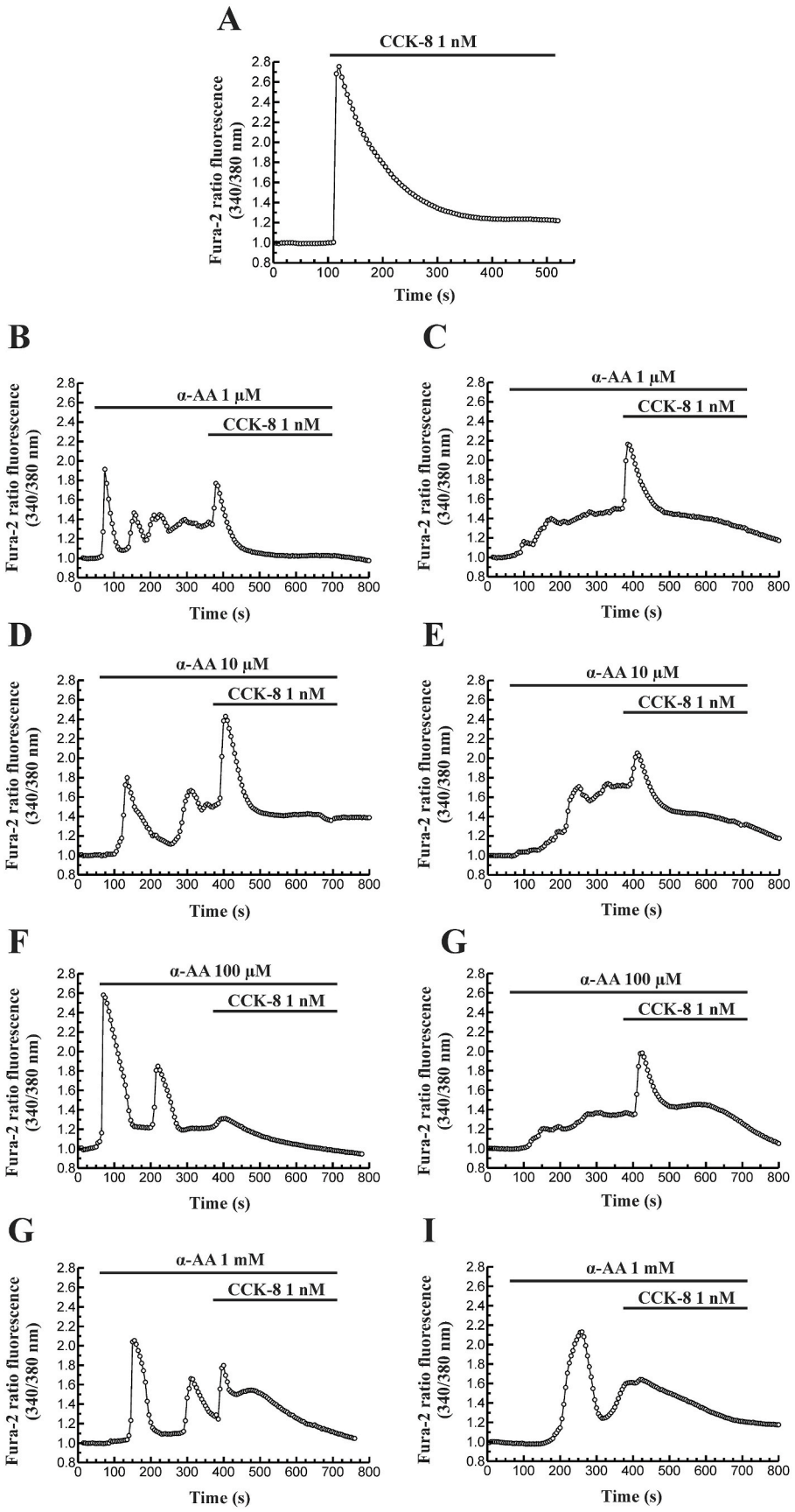

Fig. 1. Changes in $[Ca^{2+}]_i$ in response to cholecystokinin (CCK)-8 and to α-AA. Time-course of changes in $[Ca^{2+}]_i$ in fura-2-loaded mouse pancreatic acinar cells stimulated with 1 nM CCK-8 (A) or with different concentrations of α-AA (B–I). The horizontal bars indicate the time during which the stimuli were applied to the cells. The traces show the typical response of one cell taken from those studied in four to seven independent experiments (more than 100 cells for each treatment).

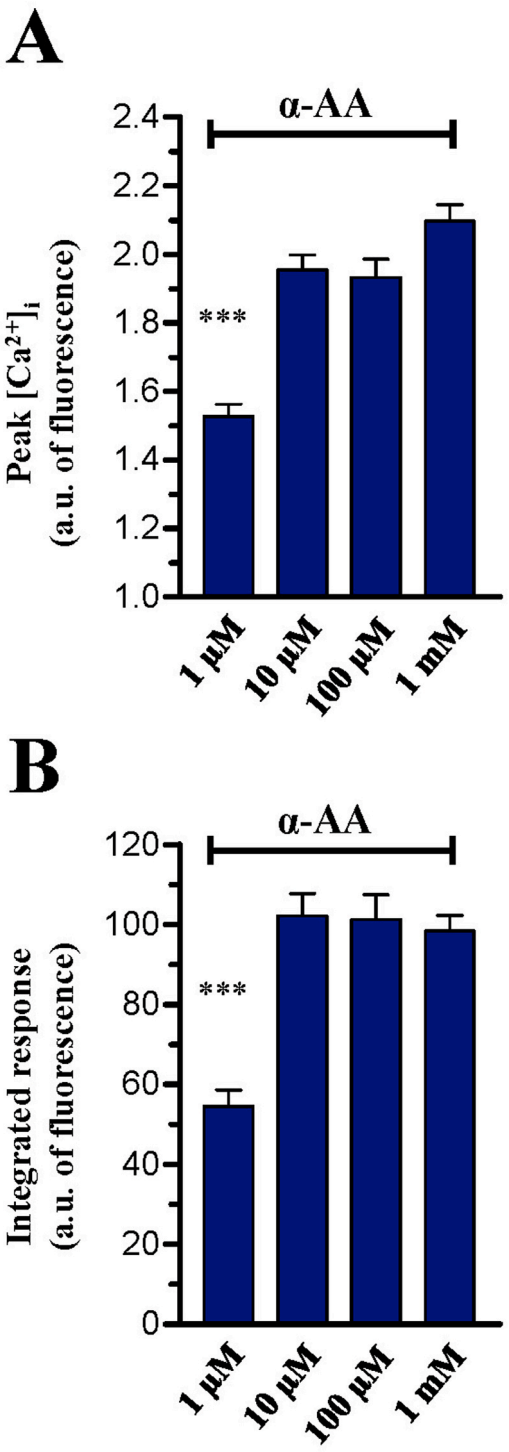

Fig. 2. Mean peak of $[Ca^{2+}]_i$ mobilization and integrated response after incubation of cells in the presence of α-AA. (A) The bars show the mean peak of $[Ca^{2+}]_i$ response reached after stimulation of cells with different concentrations of α-AA. (B) The bars show the total Ca^{2+} mobilization (integrated response) achieved after incubation of cells for 5 min in the presence of different concentrations of α-AA (***, $P < 0.001$ of 1 μM α-AA *vs* the other concentrations of α-AA tested). The analysis was carried out in cells from four to seven independent experiments.

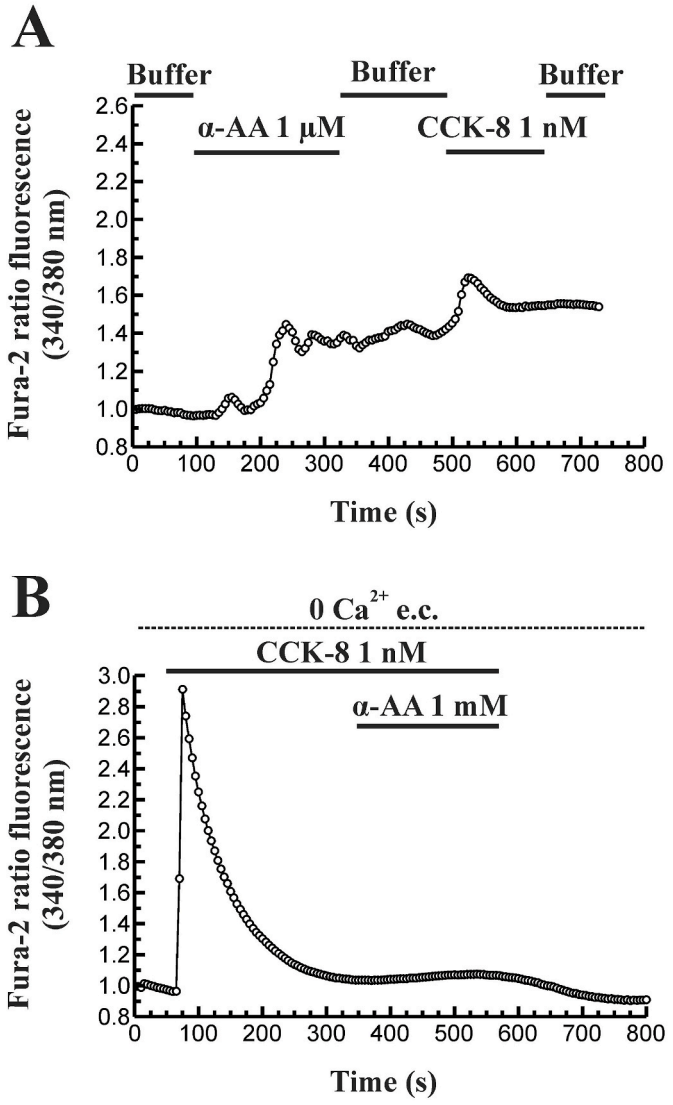

Fig. 3. Study of the reversibility of the effect of αAA and search of the source for Ca^{2+} mobilization in response to αAA. (A) Time-course of changes in $[Ca^{2+}]_i$ in fura-2-loaded mouse pancreatic acinar cells incubated sequentially in the presence of 1 μM α-AA, physiological buffer solution without stimulus and 1 nM CCK-8.
(B) Time-course of changes in $[Ca^{2+}]_i$ in cells incubated with CCK-8 (1 nM), in the absence of Ca^{2+} in the extracellular medium (medium containing 0.5 mM EGTA). The additional incubation of cells with α-AA (1 mM) failed to induce further mobilization of Ca^{2+}. The horizontal bars indicate the time during which the stimuli were applied to the cells. The traces show the typical response of one cell taken from 40 to 61 cells studied in five to seven independent experiments for each treatment.

control for ROS generation. The effect was compared with the level of ROS found in cells incubated in the absence of stimulus. α-AA induced a concentration-dependent increase in CM-H_2DCFDA-derived fluorescence compared with that detected in non-stimulated cells (Fig. 4A). In cells incubated in the presence of CCK-8 (1 nM) an increase in the oxidation of the dye was noted (Fig. 4A).

In order to check whether ROS generation in response to α-AA was dependent on Ca^{2+} mobilization, cells, loaded with the intracellular Ca^{2+}-chelator BAPTA (10 μM), were stimulated during 1 h in the absence of extracellular Ca^{2+} (medium containing 0.5 mM EGTA). Under these conditions, an increase in the fluorescence of CM-H_2DCFDA was detected. Although the increase was slightly smaller than that observed in the presence of extracellular Ca^{2+}, the differences were not statistically significant (Fig. 4C).

We were also interested in testing whether α-AA induced ROS generation in the mitochondria. It is well known that mitochondria are the major intracellular point for ROS generation (Granados et al., 2004).

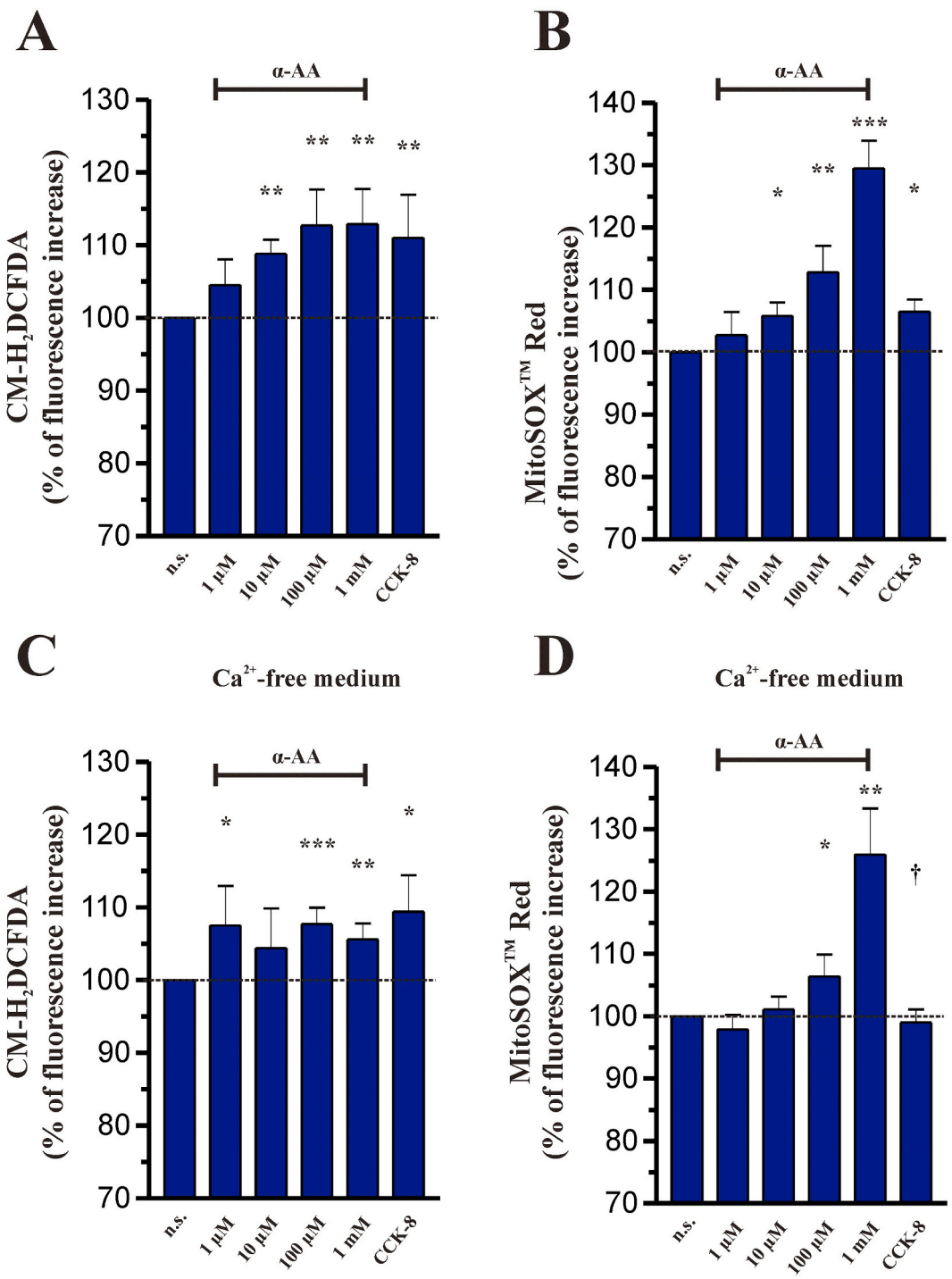

Fig. 4. Effect of α-AA on ROS production in pancreatic acinar cells. Cells were loaded with the red-ox-sensitive dyes CM-H_2DCFDA or MitoSOX™ Red and were challenged with different concentrations of α-AA (1 μM, 10 μM, 100 μM or 1 mM) or with CCK-8 (1 nM) in the presence (A and B) or in the absence of Ca^{2+} in the extracellular solution (medium containing 0.5 mM EGTA). In this case cells were additionally loaded with the intracellular Ca^{2+}-chelator BAPTA (10 μM) (C and D). The bars show the oxidative state of treated cells compared with that of non-stimulated cells. A horizontal dashed line represents the level of ROS detected in non-stimulated cells. Data are representative of four independent experiments (n.s. non-stimulated cells; *, $P < 0.05$; **, $P < 0.01$; and ***, $P < 0.001$ *vs* non-stimulated cells; †, $P < 0.05$ *vs* respective concentration of stimulus in the presence of Ca^{2+}). (For interpretation of the references to color in this figure legend, the reader is referred to the Web version of this article.)

Cells, loaded with the ROS-sensitive fluorescent dye MitoSOX™ Red, were incubated for 1 h in the absence of stimulus or in the presence of α-AA (1 μM, 10 μM, 100 μM or 1 mM). Some cells were incubated in the presence of CCK-8 (1 mM). α-AA induced a concentration-dependent increase in MitoSOX™ Red-derived fluorescence compared with that detected in non-stimulated cells (Fig. 4B). CCK-8 (1 nM) also evoked an increase in the oxidation of the dye (Fig. 4B).

We also studied the contribution of Ca^{2+} to ROS generation in the mitochondria in response to α-AA. Cells were loaded with the intracellular Ca^{2+}-chelator BAPTA (10 μM) and were incubated during 1 h with α-AA (1 μM, 10 μM, 100 μM or 1 mM) in the absence of extracellular Ca^{2+} (medium containing 0.5 mM EGTA). We only detected statistically

significant increases in MitoSox™ Red-derived fluorescence in the presence of 100 μM and 1 mM α-AA (Fig. 4D), with respect to non-stimulated cells. The production of ROS in the absence of Ca^{2+} was lower with respect to that detected in cells stimulated in the presence of Ca^{2+}, although the differences were not statistically significant. Mitochondrial ROS production in response to CCK-8 (1 nM) was significantly reduced in comparison with the value detected in the presence of Ca^{2+} (Fig. 4D).

3.3. Effect of α-AA on metabolic activity

Mitochondria remain at the centre of metabolic activity of the cell. At this point it was of interest to analyse whether α-AA treatment induced changes in mitochondrial metabolism. Alamar Blue® has been successfully used as a tool for examining mitochondrial function (Springer et al., 1998). Therefore, pancreatic acinar cells were incubated during 1 h in the presence of α-AA (1 μM, 10 μM, 100 μM or 1 mM) or in the presence of CCK-8 (1 nM). The results obtained are shown in Fig. 4 α-AA evoked a concentration-dependent increase in metabolic activity, compared with the value noted in non-stimulated cells. Incubation of cells in the presence of the secretagogue CCK-8 also evoked an increase in metabolic activity (Fig. 5).

3.4. Effect of α-AA on protein carbonyls and lipid peroxidation

As a consequence of the increase in ROS production, the oxidative status of cellular proteins and lipids could be affected. Therefore, we decided to study the influence of α-AA on protein carbonyls and on the level of TBARS. For this purpose, cells were incubated during 1 h in the presence of α-AA (1 μM, 10 μM, 100 μM or 1 mM) or in the presence of the oxidant hydrogen peroxide (H_2O_2, 100 μM). α-AA induced a concentration-dependent increase in the level of protein carbonyls over

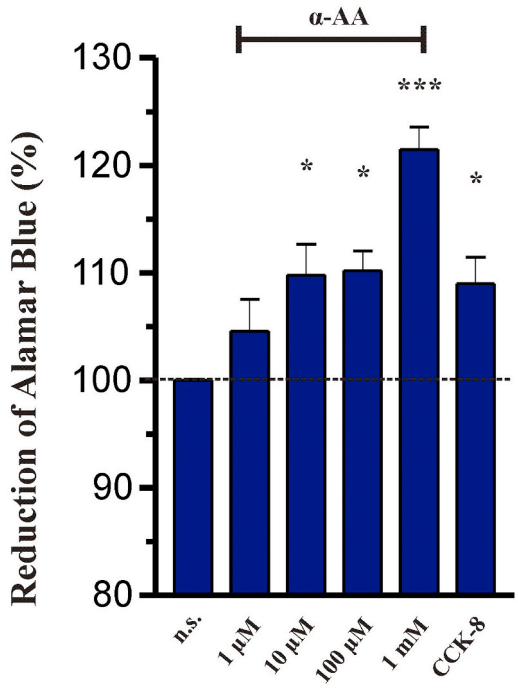

Fig. 5. Effect of α-AA on metabolic activity in pancreatic acinar cells. Cells were incubated in the presence of α-AA (1 μM, 10 μM, 100 μM or 1 mM) or in the presence of CCK-8 (1 nM). The bars show effect of the treatments on metabolic activity, which was analysed as described in Materials and methods section. A horizontal dashed line represents the value observed in non-stimulated cells. Data are representative of three independent experiments (n. s. non-stimulated cells; *, $P < 0.05$; **, $P < 0.001$ *vs* non-stimulated cells).

that noted in non-stimulated cells, although the increase was not statistically significant at the concentrations of 1 and 10 μM H_2O_2 evoked a statistically significant increase in the level of protein carbonyls (Fig. 6A). In the case of lipid peroxidation, we only detected increases in TBARS in cells treated with 100 μM or 1 mM α-AA in comparison with the level noted in non-stimulated cells. Again, incubation of cells with H_2O_2 (100 μM) evoked a statistically significant increase of TBARS (Fig. 6B).

3.5. Effect of α-AA on CCK-8-induced trypsin secretion

Thus, the next step was to evaluate whether α-AA could affect enzyme secretion evoked by CCK-8 in pancreatic acinar cells. In this part of the study, we analysed the secretion of trypsin evoked by a CCK-8 (applied in a concentration-response curve) alone or in the presence of α-AA (added 5 min prior to CCK-8). We decided to use the concentration of 10 μM α-AA, because it was the lowest concentration that induced a statistically significant increase in ROS production.

Incubation of pancreatic acinar cells during 1 h with CCK-8 (10^{-12} to 10^{-8} M) led to a concentration-dependent release of trypsin, reaching a maximum at 10^{-10} M (Fig. 6, open circles - continuous line). In the presence of 10 μM α-AA alone, an increase in trypsin secretion was noted, compared with non-stimulated cells (Fig. 5; full circles-dashed line). In the presence of α-AA (10 μM), CCK-8 failed to induce its typical concentration-dependent effect on trypsin secretion; in other words, trypsin secretion in response to CCK-8 was impaired by α-AA pretreatment (Fig. 7; full circles - dashed line).

4. Discussion

Under uncontrolled oxidative stress, oxidative damage to cellular components occurs with the accumulation of oxidized proteins, in particular, being recognized for inducing impairment of cellular function (Rudzińska et al., 2020). Oxidative stress is a common hallmark among conditions that are majorly involved in disorders such as obesity, pancreatitis or cancer (Forte et al., 2012). Under oxidative stress conditions, proteins in body tissues and fluids undergo reactions that lead to their oxidation and glycation. Moreover, exposure to oxidation and glycation adducts can be potentially harmful to the body due to probable inactivation of signalling molecules, and/or modification of cellular structures, which occurs in ageing and in certain diseases (Thornalley and Rabbani, 2014). In this line, the formation of specific protein oxidation products like α-AA has been signalled as a marker of risk for pancreatic diseases, insulin resistance, diabetes risk and obesity (Arcanjo et al., 2018; Lee et al., 2019; Wang et al., 2013). α-AA forms part of a chain reaction that starts with the oxidation of the amino acid lysine to form α-AS which yields, upon further oxidation, α-AA (Bhattacharjee, 1985). As mentioned in the introduction, α-AS might play a role in the pathogenesis of disorders that affect different tissues like brain and pancreas, which could have an oxidative stress basis. Despite prominent research exists on the effects of α-AA on the endocrine pancreas and its relationships with diabetes (Koska et al., 2018; Lee et al., 2019; Lees et al., 2017; Lin et al., 2017), studies on the effects of this compound on the exocrine pancreas are currently lacking. Here we provide evidences for potentially damaging actions of α-AA on the exocrine pancreas function.

Our results show increases in $[Ca^{2+}]_i$ following treatment of pancreatic acinar cells with α-AA. The smaller effect was noted with 1 μM α-AA in comparison with the responses induced by the other concentrations of α-AA tested; however, the differences for Ca^{2+} mobilization evoked by 10 μM, 100 μM or 1 mM were not statistically significant among them. The compound releases Ca^{2+} from the stores from which the secretagogue CCK-8 majorly elicits its responses, which is the endoplasmic reticulum. This is a key concern in pancreatic physiology, because this ion is pivotal for the regulation of pancreatic function (Williams, 2010a). Moreover, impairment of Ca^{2+} signals can induce

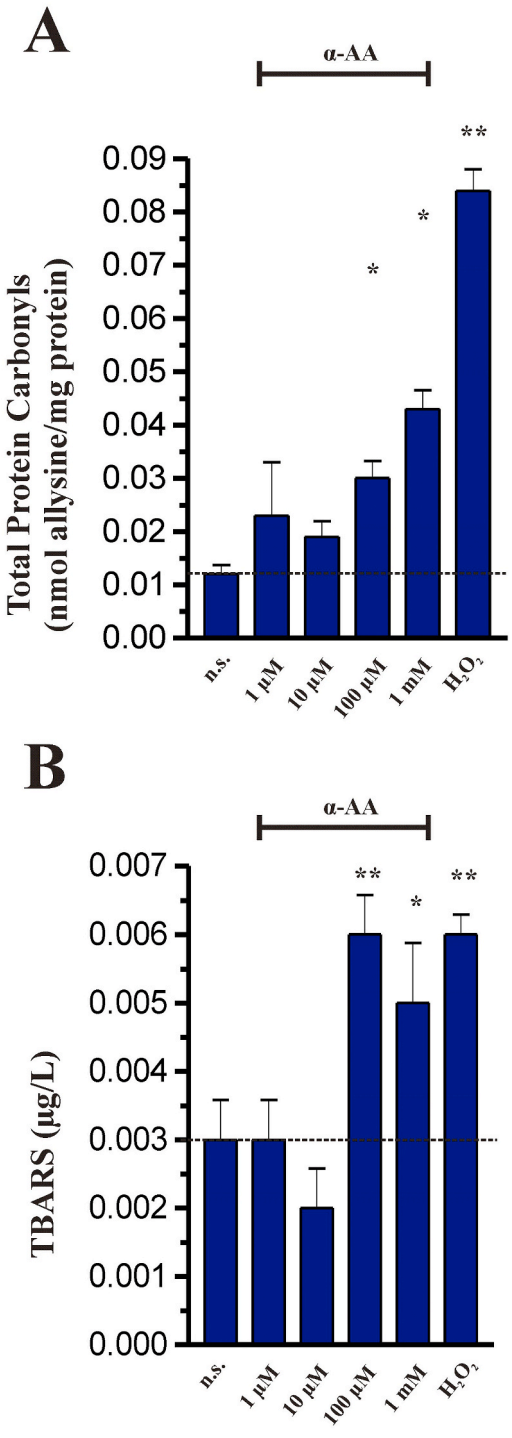

Fig. 6. Effect of α-AA on protein carbonyls and lipid peroxidation. Cells were incubated in the presence of α-AA (1 μM, 10 μM, 100 μM or 1 mM) or in the presence of the oxidant hydrogen peroxide (H_2O_2 100 μM). The bars show effect of the treatments on protein (A) and lipid (B) oxidation. A horizontal dashed line represents the value detected in non-stimulated cells. Data are representative of three independent experiments (n.s. non-stimulated cells; *, $P < 0.05$; **, $P < 0.001$ *vs* non-stimulated cells).

disorders of the cells' function that can lead to the development of pancreatic diseases (Petersen, 2004). To our knowledge, this is the first study that reports effects of α-AA on Ca^{2+} in the pancreas. A former work by Wakakura and Yamamoto (1992) reported effects of the oxidized amino acid on Ca^{2+} in retinal Müller cells and neurons.

We also detected ROS generation in the presence of α-AA, both in the

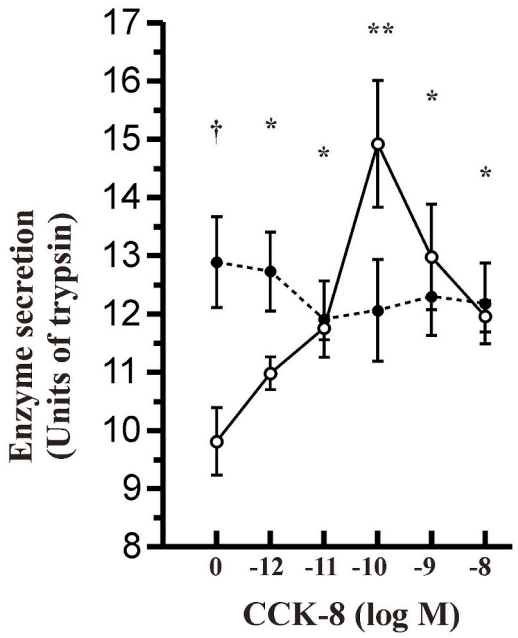

Fig. 7. Effect of α-AA on CCK-8-evoked trypsin secretion. CCK-8 induced a concentration-dependent increase in trypsin secretion in pancreatic acinar cells (open circles - continuous line). Enzyme secretion in response to CCK-8 was impaired by pretreatment of cells with 10 μM α-AA (full circles - dashed line). Data show the units of trypsin secreted to the extracellular medium expressed as the mean ± SEM (*, $P < 0.05$; **, $P < 0.01$ of CCK-8 alone *vs* non-stimulated cells; †, $P < 0.05$ of α-AA *vs* non-stimulated cells; n = four independent experiments).

cytosol and in the mitochondria. ROS production was decreased, although it was not statistically significant, in the absence of Ca^{2+}. This suggests that, at least in part, Ca^{2+} mobilization is involved in ROS generation by α-AA treatment. However, we cannot discard direct oxidative actions of α-AA. Generation of ROS in response to α-AA has been previously reported in brain, where the oxidized amino acid impaired glutamatergic neurotransmission (da Silva et al., 2017). In a recent report, Diaz-Velasco et al. (2019) observed a pro-oxidative effect of 200 μM α-AA on human intestinal CACO-2 cells via ROS formation. Overproduction of ROS within the cells can induce damage that can impair cellular function. We have previously shown that mobilization of Ca^{2+} by exogenous substances (Ameur et al., 2018), as well as by high doses of pancreatic secretagogues (Granados et al., 2004), can lead to ROS production. Our findings are in agreement with these previously reported observations.

In addition, two compartments, cytosol and mitochondria, are sites of accumulation of ROS generated in response to α-AA. Among them, mitochondria appear as critical organelles that can be affected by the compound, provided that α-AA increased metabolic activity, as supported by the experiments in which Alamar Blue® reduction was tested. This colorimetric/fluorimetric compound has been successfully used to examine mitochondrial function (Springer et al., 1998). The increase in the reduction of Alamar Blue® in cells treated with α-AA supports this hypothesis. Moreover, stimulation of pancreatic acinar cells with secretagogues induces changes in the physiology of these organelles (Gonzalez et al., 2003; Gonzalez and Salido, 2001). In this regard, oxidized forms of lysine have been shown to be responsible for ROS generation in mitochondrial hepatocytes. Complex I activity of the electron transport chain appeared to be involved (Ying et al., 2015). Moreover, it has been shown that aberrant amino acid metabolism causes mitochondrial damage by disrupting mitochondrial dynamics (Zhou et al., 2019). In relation with this observation, lysine-metabolizing enzymes are localized majorly in mitochondria and less in the cytosol (Bhattacharjee, 1985). As a consequence,

mitochondrial could be a primary site of action of α-AA. This observation could also account for ROS production in the mitochondria in cells challenged with α-AA. Thereafter, mitochondrial ROS could be transferred to the cytosol. Nevertheless, direct actions of α-AA on cytosolic structures cannot be ruled out. Thus, our results signal that mitochondrial metabolism could be affected by α-AA, which could lead to ROS production via Ca^{2+} mobilization.

Moreover, the induction of a pro-oxidative condition in the presence of α-AA is suggested by the increase in the presence of protein carbonyls and of TBARS (Utrera and Estévez, 2012). Potentially, the ingestion of α-AA with food (dietary oxidative stress) and/or the generation of α-AA from oxidized lysine in the cell in response to ROS generation could actually worsen the pro-oxidative environment in the cell with consequences in terms of oxidative damage and functionality. Interestingly, we observed that α-AA induced an increase in the generation of its precursor α-AS, which we measured as protein carbonyls. This could be regarded to as the establishing of a putative vicious circle that could amplify the injurious actions of α-AA, which could contribute to uncontrolled oxidative stress conditions. Our findings agree with these previous observations and highlight the potential impact of oxidation on the functional properties of the cell. Altogether, our results point out a potential pro-oxidant effect of α-AA that could impair cell physiology. In fact, it is generally accepted that oxidative stress is a major contributor to pancreatic pathophysiology (Binker et al., 2014; Tandon and Garg, 2011).

The synthesis and release of digestive enzymes is the major role of exocrine pancreas. Moreover, the release of digestive enzymes in response to secretagogues like cholecystokinin can be impaired by oxidative stress (Gonzalez et al., 2012). In relation with the information given above, and as expected, our results show that trypsin secretion stimulated by CCK-8 was impaired by pretreatment of cells with α-AA. Indeed, it has been demonstrated that impairment of Ca^{2+} homeostasis and excessive accumulation of ROS, induced by different substances, alter enzyme secretion in the exocrine pancreas (Ameur et al., 2018; Estaras et al., 2019; Gerasimenko and Gerasimenko, 2012; Gonzalez et al., 2006, 2012, 2016). As a consequence, α-AA might create conditions that could lead to the development of diseases within the gland.

The concentrations of α-AA used in these *in vitro* experiments fall within the range which may occur *in vivo* from dietary sources and/or endogenous protein oxidation. Wang et al. (2013) reported concentrations between 20 and 120 μM in different tissues, being the highest levels detected in the pancreas. Lee et al. (2019) reported levels for α-AA in the low micro-molar range (1–2 μM). On its side, Utrera et al. (2014) quantified high levels of α-AA per mg of protein in beef. The lowest concentration corresponded to 200 mM. In another study, the concentrations of α-AA in processed beef, pork and poultry fell within the same range (Utrera and Estévez, 2013).

In conclusion, here we provide evidences that support that the oxidized derivative from the amino acid lysine, α-AA, exerts deleterious actions on pancreatic acinar cells. Its actions are based on the release of Ca^{2+} stored in the pools sensitive to secretagogues and on the generation of ROS. As a consequence, trypsin secretion is impaired. Altogether, the actions of α-AA on pancreatic cell physiology might create a situation that could potentially lead to the development of diseases in the exocrine pancreas.

CRediT authorship contribution statement

Matias Estaras: Funding acquisition, Formal analysis. **Fatma Z. Ameur:** Funding acquisition, Formal analysis. **Mario Estévez:** Writing - original draft. **Silvia Díaz-Velasco:** Funding acquisition, Formal analysis. **Antonio Gonzalez:** Writing - original draft.

Declaration of competing interest

The authors declare that they have no known competing financial interests or personal relationships that could have appeared to influence the work reported in this paper.

Acknowledgements

This study was partly funded by Ministerio de Economía y Competitividad (BFU2016-79259-R and AGL2017-84586R) and Junta de Extremadura-FEDER (IB16006; GR18070). The funding sources had no role in the study design, in the collection, analysis and interpretation of data, in the writing of the report, or in the decision to submit the paper for publication.

References

Ameur, F.Z., Mehedi, N., Kheroua, O., Saïdi, D., Salido, G.M., Gonzalez, A., 2018. Sulfanilic acid increases intracellular free-calcium concentration, induces reactive oxygen species production and impairs trypsin secretion in pancreatic AR42J cells. Food Chem. Toxicol. 120, 71–80. https://doi.org/10.1016/j.fct.2018.07.001.

Arcanjo, N.M.O., Luna, C., Madruga, M.S., Estévez, M., 2018. Antioxidant and pro-oxidant actions of resveratrol on human serum albumin in the presence of toxic diabetes metabolites: glyoxal and methyl-glyoxal. Biochim. Biophys. Acta Gen. Subj. 1862, 1938–1947. https://doi.org/10.1016/j.bbagen.2018.06.007.

Bhattacharjee, J.K., 1985. alpha-Aminoadipate pathway for the biosynthesis of lysine in lower eukaryotes. Crit. Rev. Microbiol. 12, 131–151. https://doi.org/10.3109/10408418509104427.

Binker, M.G., Cosen-Binker, L.I., 2014. Acute pancreatitis: the stress factor. World J. Gastroenterol. 20, 5801–5807. https://doi.org/10.3748/wjg.v20.i19.5801.

Brown, D.R., Kretzschmar, H.A., 1998. The glio-toxic mechanism of alpha-aminoadipic acid on cultured astrocytes. J. Neurocytol. 27, 109–118. https://doi.org/10.1023/a:1006947322342.

da Silva, J.C., Amaral, A.U., Cecatto, C., Wajner, A., Dos Santos Godoy, K., Ribeiro, R.T., de Mello Gonçalves, A., Zanatta, Â., da Rosa, M.S., Loureiro, S.O., Vargas, C.R., Leipnitz, G., de Souza, D.O.G., Wajner, M., 2017. α-Ketoadipic acid and α-aminoadipic acid cause disturbance of glutamatergic neurotransmission and induction of oxidative stress in vitro in brain of adolescent rats. Neurotox. Res. 32, 276–290. https://doi.org/10.1007/s12640-017-9735-8.

Davies, M.J., 2005. The oxidative environment and protein damage. Biochim. Biophys. Acta 1703, 93–109. https://doi.org/10.1016/j.bbapap.2004.08.007.

Díaz-Velasco, S., González, A., Peña, F.J., Estévez, M., 2019. Oxidized amino acids induce apoptosis and necrosis in CACO-2 cells by promoting oxidative stress and depleting the endogenous antioxidant defenses. In: 2nd Food Chemistry Conference. https://www.elsevier.com/events/conferences/food-chemistry-conference.

Estaras, M., Ameur, F.Z., Roncero, V., Fernandez-Bermejo, M., Blanco, G., Lopez, D., Mateos, J.M., Salido, G.M., Gonzalez, A., 2019. The melatonin receptor antagonist luzindole induces Ca2+ mobilization, reactive oxygen species generation and impairs trypsin secretion in mouse pancreatic acinar cells. Biochim. Biophys. Acta Gen. Subj. 1863, 129407. https://doi.org/10.1016/j.bbagen.2019.07.016.

Estevez, M., Xiong, Y., 2019. Intake of oxidized proteins and amino acids and causative oxidative stress and disease: recent scientific evidences and hypotheses. J. Food Sci. 84, 387–396. https://doi.org/10.1111/1750-3841.14460.

Fan, X., Zhang, J., Theves, M., Strauch, C., Nemet, I., Liu, X., Qian, J., Giblin, F.J., Monnier, V.M., 2009. Mechanism of lysine oxidation in human lens crystallins during aging and in diabetes. J. Biol. Chem. 284, 34618–34627. https://doi.org/10.1074/jbc.M109.032094.

Forte, V., Pandey, A., Abdelmessih, R., Forte, G., Whaley-Connell, A., Sowers, J.R., McFarlane, S.I., 2012. Obesity, diabetes, the cardiorenal syndrome, and risk for cancer. Cardiorenal Med 2, 143–162. https://doi.org/10.1159/000337314.

Gerasimenko, O.V., Gerasimenko, J.V., 2012. Mitochondrial function and malfunction in the pathophysiology of pancreatitis. Pflügers Archiv 464, 89–99. https://doi.org/10.1007/s00424-012-1117-8.

González, A., Camello, P.J., Pariente, J.A., Salido, G.M., 1997. Free cytosolic calcium levels modify intracellular pH in rat pancreatic acini. Biochem. Biophys. Res. Commun. 230, 652–656. https://doi.org/10.1006/bbrc.1996.6026.

González, A., Granados, M.P., Salido, G.M., Pariente, J.A., 2003. Changes in mitochondrial activity evoked by cholecystokinin in isolated mouse pancreatic acinar cells. Cell. Signal. 15, 1039–1048. https://doi.org/10.1016/s0898-6568(03)00067-6.

González, A., Núñez, A.M., Granados, M.P., Pariente, J.A., Salido, G.M., 2006. Ethanol impairs CCK-8-evoked amylase secretion through Ca2+-mediated ROS generation in mouse pancreatic acinar cells. Alcohol 38, 51–57. https://doi.org/10.1016/j.alcohol.2006.03.002.

González, A., Salido, G.M., 2001. Participation of mitochondria in calcium signalling in the exocrine pancreas. J. Physiol. Biochem. 57, 331–339. https://doi.org/10.1007/bf03179827.

Gonzalez, A., Salido, G.M., 2016. Determination of reactive oxygen species production in pancreatic acinar cells. Pancreapedia: Exocrine Pancreas Knowledge Base. https://doi.org/10.3998/panc.2016.32.

Gonzalez, A., Santofimia-Castaño, P., Rivera-Barreno, R., Salido, G.M., 2012. Cinnamtannin B-1, a natural antioxidant that reduces the effects of H2O2 on CCK-8-evoked responses in mouse pancreatic acinar cells. J. Physiol. Biochem. 68, 181–191. https://doi.org/10.1007/s13105-011-0130-2.

Granados, M.P., Salido, G.M., Pariente, J.A., Gonzalez, A., 2004. Generation of ROS in response to CCK-8 stimulation in mouse pancreatic acinar cells. Mitochondrion 3, 285–296. https://doi.org/10.1016/j.mito.2004.02.003.

Kiss, C., Ceresoli-Borroni, G., Guidetti, P., Zielke, C.L., Zielke, H.R., Schwarcz, R., 2003. Kynurenate production by cultured human astrocytes. J. Neural. Transm. 110, 1–14. https://doi.org/10.1007/s00702-002-0770-z.

Koska, J., Saremi, A., Howell, S., Bahn, G., De Courten, B., Ginsberg, H., Beisswenger, P. J., Reaven, P.D., Investigators, V.A.D.T., 2018. Advanced glycation end products, oxidation products, and incident cardiovascular events in patients with type 2 diabetes. Diabetes Care 41, 570–576. https://doi.org/10.2337/dc17-1740.

Lee, H.J., Jang, H.B., Kim, W.H., Park, K.J., Kim, K.Y., Park, S.I., Lee, H.J., 2019. 2-Aminoadipic acid (2-AAA) as a potential biomarker for insulin resistance in childhood obesity. Sci. Rep. 9, 13610. https://doi.org/10.1038/s41598-019-49578-z.

Lees, T., Nassif, N., Simpson, A., Shad-Kaneez, F., Martiniello-Wilks, R., Lin, Y., Jones, A., Qu, X., Lal, S., 2017. Recent advances in molecular biomarkers for diabetes mellitus: a systematic review. Biomarkers 22, 604–613. https://doi.org/10.1080/1354750X.2017.1279216.

Lin, H., Levison, B.S., Buffa, J.A., Huang, Y., Fu, X., Wang, Z., Gogonea, V., DiDonato, J. A., Hazen, S.L., 2017. Myeloperoxidase-mediated protein lysine oxidation generates 2-aminoadipic acid and lysine nitrile in vivo. Free Radic. Biol. Med. 104, 20–31. https://doi.org/10.1016/j.freeradbiomed.2017.01.006.

McClave, S.A., 2019. Factors that worsen disease severity in acute pancreatitis: implications for more innovative nutrition therapy. Nutr. Clin. Pract. 1, S43–S48. https://doi.org/10.1002/ncp.10371.

Palanissami, G., Paul, S.F.D., 2018. RAGE and its ligands: molecular interplay between glycation, inflammation, and hallmarks of cancer-a review. Horm. Cancer 9, 295–325. https://doi.org/10.1007/s12672-018-0342-9.

Petersen, O.H., 2007. Local and global Ca2+ signals: physiology and pathophysiology. Biol. Res. 37, 661–664. https://doi.org/10.4067/s0716-97602004000400023.

Rudzińska, M., Parodi, A., Balakireva, A.V., Chepikova, O.E., Venanzi, F.M., Zamyatnin Jr., A.A., 2020. Cellular aging characteristics and their association with age-related disorders. Antioxidants 9, 94. https://doi.org/10.3390/antiox9020094.

Saluja, A.K., Lerch, M.M., Phillips, P.A., Dudeja, V., 2007. Why does pancreatic overstimulation cause pancreatitis? Annu. Rev. Physiol. 69, 249–269. https://doi.org/10.1146/annurev.physiol.69.031905.161253.

Santofimia-Castaño, P., Garcia-Sanchez, L., Ruy, D.C., Fernandez-Bermejo, M., Salido, G. M., Gonzalez, A., 2014. The seleno-organic compound ebselen impairs mitochondrial physiology and induces cell death in AR42J cells. Toxicol. Lett. 229, 465–473. https://doi.org/10.1016/j.toxlet.2014.07.025.

Sell, D.R., Strauch, C.M., Shen, W., Monnier, V.M., 2007. 2-aminoadipic acid is a marker of protein carbonyl oxidation in the aging human skin: effects of diabetes, renal failure and sepsis. Biochem. J. 404, 269–277. https://doi.org/10.1042/BJ20061645.

Sell, D.R., Strauch, C.M., Shen, W., Monnier, V.M., 2008. Aging, diabetes, and renal failure catalyze the oxidation of lysyl residues to 2-aminoadipic acid in human skin collagen: evidence for metal-catalyzed oxidation mediated by alpha-dicarbonyls. Ann. N. Y. Acad. Sci. 1126, 205–209. https://doi.org/10.1196/annals.1433.065.

Springer, J.E., Azbill, R.D., Carlson, S.L., 1998. A rapid and sensitive assay for measuring mitochondrial metabolic activity in isolated neural tissue. Brain Res. Brain Res. Protoc. 4, 259–263. https://doi.org/10.1016/s1385-299x(97)00045-7.

Stadtman, E.R., 2001. Protein oxidation in aging and age-related diseases. Ann. N. Y. Acad. Sci. 928, 22–38. https://doi.org/10.1111/j.1749-6632.2001.tb05632.x.

Stadtman, E.R., Levine, R.L., 2003. Free radical-mediated oxidation of free amino acids and amino acid residues in proteins. Amino Acids 25, 207–218. https://doi.org/10.1007/s00726-003-0011-2.

Tandon, R.K., Garg, P.K., 2011. Oxidative stress in chronic pancreatitis: pathophysiological relevance and management. Antioxidants Redox Signal. 15, 2757–2766. https://doi.org/10.1089/ars.2011.4115.

Tapia, J.A., Salido, G.M., González, A., 2010. Ethanol consumption as inductor of pancreatitis. World J. Gastrointest. Pharmacol. Therapeut 1, 3–8. https://doi.org/10.4292/wjgpt.v1.i1.3.

Thornalley, P.J., Rabbani, N., 2014. Detection of oxidized and glycated proteins in clinical samples using mass spectrometry–a user's perspective. Biochim. Biophys. Acta 1840, 818–829. https://doi.org/10.1016/j.bbagen.2013.03.025.

Utrera, M., Estevez, M., 2012. Oxidation of myofibrillar proteins and impaired functionality: underlying mechanisms of the carbonylation pathway. J. Agric. Food Chem. 60, 8002–8011. https://doi.org/10.1021/jf302111j.

Utrera, M., Estevez, M., 2013. Oxidative damage to poultry, pork, and beef during frozen storage through the analysis of novel protein oxidation markers. J. Agric. Food Chem. 61, 7987–7993. https://doi.org/10.1021/jf402220q.

Utrera, M., Morcuende, D., Estevez, M., 2014. Temperature of frozen storage affects the nature and consequences of protein oxidation in beef patties. Meat Sci. 96 https://doi.org/10.1016/j.meatsci.2013.10.032, 1250-127.

Verma, S., Kesh, K., Ganguly, N., Jana, S., Swarnakar, S., 2014. Matrix metalloproteinases and gastrointestinal cancers: impacts of dietary antioxidants. World J. Biol. Chem. 5, 355–376. https://doi.org/10.4331/wjbc.v5.i3.355.

Villaverde, A., Parra, V., Estévez, M., 2014. Oxidative and nitrosative stress induced in myofibrillar proteins by a hydroxyl-radical-generating system: impact of nitrite and ascorbate. J. Agric. Food Chem. 62, 2158–2164. https://doi.org/10.1021/jf405705t.

Wakakura, M., Yamamoto, N., 1992. Rapid increase of intracellular Ca2+ concentration caused by aminoadipic acid enantiomers in retinal Müller cells and neurons in vitro. Doc. Ophthalmol. 80, 385–395. https://doi.org/10.1007/bf00154389.

Wang, T.J., Ngo, D., Psychogios, N., Dejam, A., Larson, M.G., Vasan, R.S., Ghorbani, A., O'Sullivan, J., Cheng, S., Rhee, E.P., Sinha, S., McCabe, E., Fox, C.S., O'Donnell, C.J., Ho, J.E., Florez, J.C., Magnusson, M., Pierce, K.A., Souza, A.L., Yu, Y., Carter, C., Light, P.E., Melander, O., Clish, C.B., Gerszten, R.E., 2013. 2-Aminoadipic acid is a biomarker for diabetes risk. J. Clin. Invest. 123, 4309–4317. https://doi.org/10.1172/JCI64801.

Williams, J.A., 2010a. Regulation of acinar cell function in the pancreas. Curr. Opin. Gastroenterol. 26, 478–483. https://doi.org/10.1097/MOG.0b013e32833d11c6.

Williams, J.A., 2010b. Isolation of rodent pancreatic acinar cells and acini by collagenase digestion. Pancreapedia: Exocrine Pancreas Knowledge Base. https://doi.org/10.3998/panc.2010.18.

Wong, C.M., Marcocci, L., Liu, L., Suzuki, Y.J., 2010. Cell signaling by protein carbonylation and decarbonylation. Antioxidants Redox Signal. 12, 393–404. https://doi.org/10.1089/ars.2009.2805.

Ying, Y., Yun, J., Guoyao, W., Kaiji, S., Zhaolai, D., Zhenlong, W., 2015. Dietary L-methionine restriction decreases oxidative stress in porcine liver mitochondria. Exp. Gerontol. 65, 35–41. https://doi.org/10.1016/j.exger.2015.03.004.

Zhou, J., Wang, X., Wang, M., Chang, Y., Zhang, F., Ban, Z., Tang, R., Gan, Q., Wu, S., Guo, Y., Zhang, Q., Wang, F., Zhao, L., Jing, Y., Qian, W., Wang, G., Guo, W., Yang, C., 2019. The lysine catabolite saccharopine impairs development by disrupting mitochondrial homeostasis. J. Cell Biol. 218, 580–597. https://doi.org/10.1083/jcb.201807204.

Amino Acids
https://doi.org/10.1007/s00726-021-03085-6

ORIGINAL ARTICLE

Protein carbonylation in food and nutrition: a concise update

Mario Estévez[1] · **Silvia Díaz-Velasco**[1] · **Remigio Martínez**[1]

Received: 30 June 2021 / Accepted: 28 September 2021
© The Author(s) 2021

Abstract

Protein oxidation is a topic of indisputable scientific interest given the impact of oxidized proteins on food quality and safety. Carbonylation is regarded as one of the most notable post-translational modifications in proteins and yet, this reaction and its consequences are poorly understood. From a mechanistic perspective, primary protein carbonyls (i.e. α-aminoadipic and γ-glutamic semialdehydes) have been linked to radical-mediated oxidative stress, but recent studies emphasize the role alternative carbonylation pathways linked to the Maillard reaction. Secondary protein carbonyls are introduced in proteins via covalent linkage of lipid carbonyls (i.e. protein-bound malondialdehyde). The high reactivity of protein carbonyls in foods and other biological systems indicates the intricate chemistry of these species and urges further research to provide insight into these molecular mechanisms and pathways. In particular, protein carbonyls are involved in the formation of aberrant and dysfunctional protein aggregates, undergo further oxidation to yield carboxylic acids of biological relevance and establish interactions with other biomolecules such as oxidizing lipids and phytochemicals. From a methodological perspective, the routine dinitrophenylhydrazine (DNPH) method is criticized not only for the lack of accuracy and consistency but also authors typically perform a poor interpretation of DNPH results, which leads to misleading conclusions. From a practical perspective, the biological relevance of protein carbonyls in the field of food science and nutrition is still a topic of debate. Though the implication of carbonylation on impaired protein functionality and poor protein digestibility is generally recognized, the underlying mechanism of such connections requires further clarification. From a medical perspective, protein carbonyls are highlighted as markers of protein oxidation, oxidative stress and disease. Yet, the specific role of specific protein carbonyls in the onset of particular biological impairments needs further investigations. Recent studies indicates that regardless of the origin (in vivo or dietary) protein carbonyls may act as signalling molecules which activate not only the endogenous antioxidant defences but also implicate the immune system. The present paper concisely reviews the most recent advances in this topic to identify, when applicable, potential fields of interest for future studies.

Keywords Protein carbonylation · α-Aminoadipic semialdehyde · α-Aminoadipic acid · Oxidative stress · Maillard reaction · Protein oxidation · Nutrition · Safety · Disease

Abbreviations

4-HNE	4-Hydroxynonenal
α-AA	α-Aminoadipic acid
α-AS	α-Aminoadipic semialdehyde
γ-GS	γ-Glutamic semialdehyde
AA	Acetaldehyde
DNPH	Dinitrophenylhydrazine
$FINH_2$	Fluoresceinamine
GC	Gas chromatography
GIT	Gastrointestinal tract
GO	Glyoxal
HAVA	Hydroxyaminovaleric acid
HACA	Hydroxyaminocaproic acid
HPLC	High-performance liquid chromatography
HSA	Human serum albumin
MCO	Metal-catalysed oxidation
MDA	Malondialdehyde
MGO	Methyl glyoxal
MR	Maillard reaction
MS	Mass spectrometry
p-ABA	P-aminobenzoic acid
ROS	Reactive oxygen species
WHC	Water-holding capacity

Handling editor: D. Tsikas.

✉ Mario Estévez
mariovet@unex.es

[1] Food Technology, IPROCAR Research Institute, Universidad de Extremadura, 10003 Cáceres, Spain

Published online: 20 October 2021

Introduction

Oxidative stress is a major cause of post-translational changes in proteins and includes severe chemical modifications such as aggregation via protein crosslinks and fragmentations via peptide scission (Davies 2016; Kehm et al. 2021). The oxidation of the aminoacids' side chain leads to the formation of derivatives of assorted nature including sulphur compounds (i.e. methionine sulphoxide; from methionine), aromatic species (i.e. kynurenines; from tryptophan) and carboxylic acids (α-aminoadipic acid; α-AA; from lysine) (Estévez et al. 2020; Davies 2016). In food systems, these chemical changes are manifested in loss of protein functionality and digestibility with relevant consequences in terms of food protein quality and nutritional value (Soladoye et al. 2015; Xiong and Guo 2021). In cells and living organisms, protein oxidation is linked to biological impairments, aging and the onset of various pathological conditions (Akagawa 2020).

The formation of protein carbonyls typically responds to the oxidative deamination of alkaline amino acids such as lysine, arginine and proline (Estévez 2011; Davies 2016). The α-aminoadipic semialdehyde (α-AS) is a specific oxidation product from lysine and account for up to the 70% of total protein carbonyls in cells (Requena et al. 2001) and food systems (Estévez 2011). Owing to their ubiquity in oxidized proteins and their simple detection and quantification by the routine dinitrophenylhydrazine (DNPH) method, protein carbonyls have been emphasized as general markers of protein oxidation in foods, cells and tissues (Estévez 2011; Hellwig 2020). Yet, limitations in both, accuracy of the technique, and the interpretation of the data, makes the DNPH method unsuitable to gain knowledge of scientific in-depth and mechanistic nature (Estévez et al. 2019; Hellwig 2020; Estévez 2021). The understanding of the intricate chemistry behind protein carbonylation is essential to comprehend its biological meaning. More accurate and advanced methodologies have been proposed to gain further insight into the molecular basis of the formation and biological effects of protein carbonyls (Fedorova et al. 2014; Hellwig 2020). Owing to the application of spectroscopic and mass spectrometric methodologies, recent relevant advances have been made in regards to the role of the Maillard reaction and the glyco-oxidation as alternative routes for protein carbonylation in biological samples (Trnková et al. 2015; Arcanjo et al. 2018; Luna et al. 2021). On the same line, recent studies have reported innovative evidence on the toxicological effects of dietary protein carbonyls and other oxidized amino acids (Estévez and Xiong 2019) and the role of these compounds in cell signalling mechanisms (Wong et al. 2012; Kehm et al. 2021). This review concisely collects and analyses the most recent advances in this topic and aims to elucidate future challenges.

Concise update on carbonylation chemistry

Carbonylation is an irreversible post-translational modification through which carbonyl moieties are formed and/or introduced in proteins. This reaction takes place under various mechanisms of diverse nature though it is generally accepted that carbonylation typically takes place in a pro-oxidative environment and as a result of oxidative stress (Fedorova et al. 2014; Akagawa 2020). Notable exceptions should be denoted such as the carbonylation that occurs in certain cells and tissues under physiological conditions such as the formation of α-AS from lysine prior to condensation reactions in connective tissue (Xu and Shi 2014). This reaction, is yet, enzymatically controlled (e.g. lysyl oxidase) and does not respond to the non-enzymatic oxidative stress-induced conditions in which uncontrolled protein carbonylation commonly occurs. Depending on whether carbonyls are formed in proteins or introduced in proteins subsequent to its formation, two types of protein carbonylation can be clearly discriminated. "Primary carbonyls" are formed on-site consequently to an oxidative damage to the protein structure while "secondary protein carbonyls" are formed from lipid oxidation and subsequently introduced in proteins via covalent linkages (Estévez et al. 2019; Akagawa 2020). In turn, the former can be generated via three mechanisms, namely, (i) oxidative deamination of alkaline amino acids (lysine, threonine, arginine and proline) by a radical-mediated mechanism; (ii) oxidative deamination of alkaline amino acids by dicarbonyls from the Maillard reaction (MR); and (iii) by oxidative cleavage of the peptide backbone via the α-amidation pathway or via oxidation of glutamyl side chains (Berlett and Stadtman 1997; Estévez 2011; Akagawa 2020). Quantitatively, it is generally assumed that the latter among these three mechanisms is of negligible importance, and it is unusually reported as a source of protein carbonyls in biological samples. Among the relevant primary carbonylation mechanisms, the radical-mediated, known as 'Stadtman' pathway (Fig. 1A), normally involves a metal-catalysed oxidation (MCO) mechanism with the Fenton reaction being source of hydroxyl radicals and other reactive oxygen species (ROS) (Stadtman and Levine 2003). The reactive species would attack the ε-amino moiety from the alkaline amino acid by abstracting a hydrogen atom from the neighbouring carbon, leading to the formation, in a first step, of an imino group. This intermediate and unstable product is readily hydrolysed to form the corresponding protein carbonyl. According to this reaction pathway, the α-AS, also known as allysine, is formed from the oxidative deamination of lysine while the γ-glutamic semialdehyde

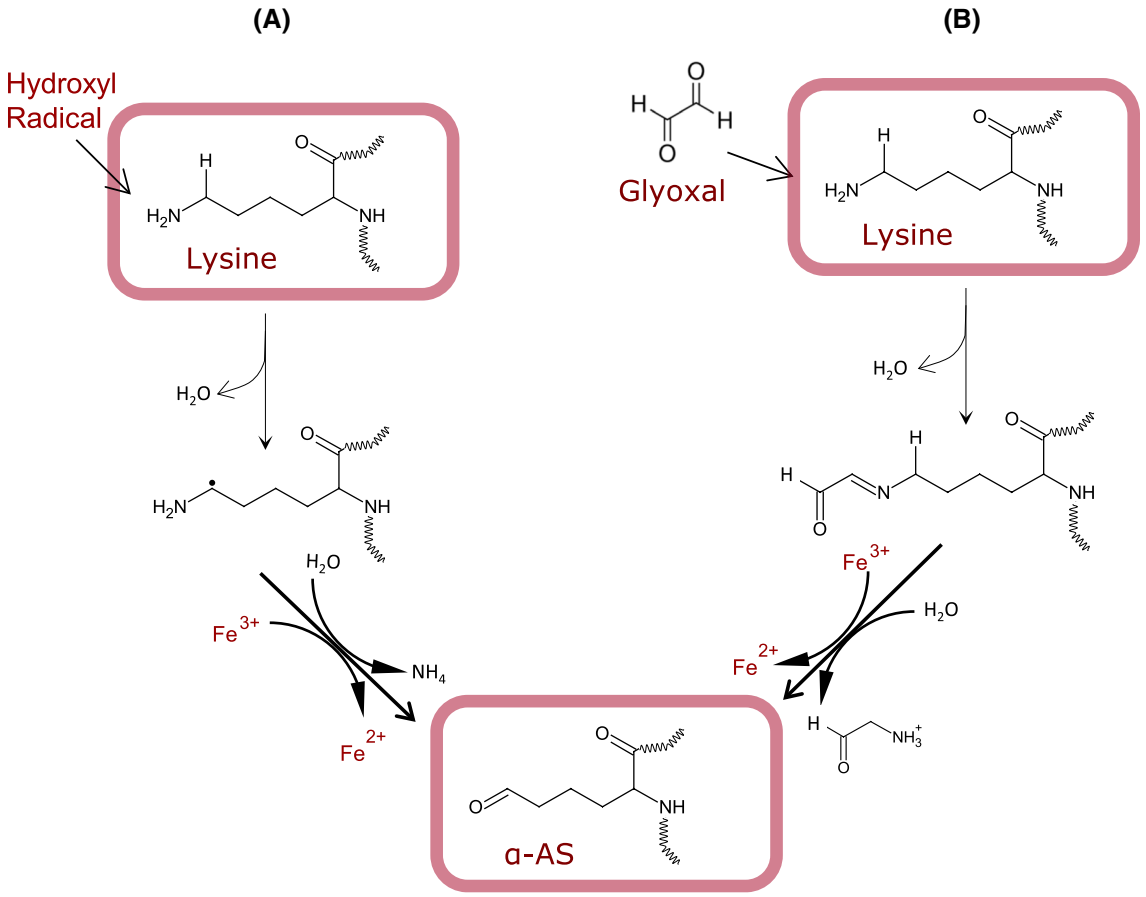

Fig. 1 Mechanisms of primary carbonylation: formation of α-aminoadipic acid (*α*-AS). **A** Radical-mediated oxidative deamination of protein-bound lysine; **B** Maillard-mediated oxidative deamination of protein-bound lysine

(*γ*-GS) is formed from arginine and proline (Stadtman and Levine 2003; Estévez 2011). The alternative MR mediated mechanism, known as the 'Suyama' pathway (Fig. 1B), and also described as glyco-oxidation, implies the degradation of reducing sugars and the formation of reactive *α*-dicarbonyls such as glyoxal (GO) and methylglyoxal (MGO) (Akagawa et al. 2005). These highly reactive dicarbonyls react with *ε*-amino groups in proteins causing the oxidative deamination of the alkaline amino acids and the formation of the same aforementioned protein carbonyls. Hence, both mechanisms lead to the same oxidation products and depending on the experimental approach and detection method, the relative contribution of each pathway to the carbonylation of proteins is indefinite. In food systems, most authors assume that protein oxidation, typically assessed as protein carbonylation, is the result of a radical-mediated mechanism (Estévez 2011; Hellwig 2020). Yet, recent results indicate that the glyco-oxidation of proteins leading to the formation of primary carbonyls is not only applicable. Under favourable conditions (e.g. occurrence of reducing sugars), this mechanism may be even most relevant than ROS-mediated carbonylation (Luna and Estévez 2019; Luna et al. 2021). Villaverde and Estévez (2013) originally reported the occurrence of Maillard-mediated protein carbonylation in myofibrillar proteins at as low concentrations of glucose as those found in post-mortem muscle (~0.02 M). Luna and Estévez (2018) subsequently observed that glucose (0.05 M) was more efficient than hydrogen peroxide (0.6 mM) in reacting with metal ions to create the required pro-glyco-oxidative environment to induce protein carbonylation in a variety of food proteins, including meat proteins, ovalbumin, *β*-lactoglobulin and soy proteins. In a following study, the same authors confirmed the involvement of GO and MGO in the "Suyama pathway" and found that glyco-oxidized meat and dairy proteins displayed impaired functionality and digestibility (Luna and Estévez 2019). Recent studies performed in a variety of food proteins such as glutenin (Wang et al. 2019a) and *α*-lactalbumin (Wu et al. 2021), have confirmed severe chemical changes induced by reactive Maillard dicarbonyls. While this mechanism may be highly relevant in food systems with high protein and sugar concentration (i.e. fermented meat products or certain dairy foods), the carbonylation of proteins in such foods is rarely attributed to this pathway by food scientists. The carbonylation of proteins

during digestion has also been hypothesized to be affected by sugar concentration (Duque-Estrada et al. 2019). In a recent study, we observed that 10 mg/mL of glucose and GO strikingly promoted the carbonylation of meat proteins during simulated gastric digestion (unpublished data). The concentration of total protein carbonyls in the glyco-oxidized proteins increased ~ 20-fold times in meat proteins digested in the presence of glucose vs the control counterparts.

In living systems, the "Suyama pathway" was originally described to occur in plasma proteins from diabetic rats (Akagawa et al. 2006). The authors precisely described the underlying mechanisms and the role of GO and MGO in such carbonylation process (Akagawa et al. 2006). In the last five years, subsequent studies have contributed to identify the routes and mechanisms of protein carbonylation in proteins from plasma and other tissues under pathological hyperglycemic conditions. Given the connection between protein carbonylation in diabetic patients and the onset of oxidative stress and the metabolic syndrome (Hecker and Wagner 2018), strategies of carbonylation inhibition have been proposed to alleviate the associated biological impairments. Özyurt et al. (2016) reported fourfold increases of specific semialdehydes in human hemoglobin and human serum albumin (HSA) upon exposure to simulated hyperglycemic conditions (12 mM glucose/0.2 mM Fe^{3+}) for 10 days. Epicatechin, epigallocatechin and epigallocatechin-3-gallate at 0.7 µM, were found to keep protein carbonyls at basal levels through anti-glycation mechanisms. Arcanjo et al. (2018) was able to double the concentration of α-AS and γ-GS in HSA upon incubation with pathological concentrations of GO and MGO (0.4 mM; Lapolla et al. 2003) for 48 h. The same authors found that resveratrol (2.5 µM) effectively inhibited the carbonylation of HSA by forming adducts with the aforementioned Maillard dicarbonyls. More recently, Luna et al. (2021) reported that glucose induces dose-dependent carbonylation of HSA at relevant pathophysiological concentrations (4–12 mM) and observed that the main protein carbonyl (α-AS) suffered a further oxidation step to yield the lysine oxidation end product, the α-amino adipic acid (α-AA). Interestingly, this oxidized form of lysine has been recently emphasized as an early and reliable marker of insulin resistance and diabetes in humans (Lee et al. 2019).

Finally, considerable progresses have also been made in relation to the understanding of the chemistry involved in the formation of secondary protein carbonyls. Malondialdehyde (MDA), 4-hydroxynonenal (4-HNE) and other lipid-derived carbonyls have been found to react with protein-bound amino groups and form complexes with food proteins (Zhou et al. 2015; Gürbüz and Heinonen 2015; Wang et al. 2019b). Unlike the aforementioned dicarbonyls from MR (GO and MGO), MDA and other lipid carbonyls are unable to induce the oxidative deamination of lysine residues to yield primary protein carbonyls such as α-AS from lysine. Instead, MDA and 4-HNE remain bound to proteins as secondary protein carbonyls via a Michael addition-type reaction (Fig. 2). This reaction occurs between MDA [and its degradation products, acetaldehyde (AA) and formaldehyde (FA) and other carbonyls], and lysine and other alkaline amino acids to form adducts of assorted stability. It is worth noting that a second aldehyde moiety from the added MDA remains free and available to react with DNPH or other derivatization agents, which enables its detection as (secondary) protein carbonyls. Alternatively, the free aldehyde from a protein-bound MDA could react with another lysine residue, which leads to the formation of intra- and/or intermolecular covalent crosslinks. In a recent study, Estévez et al. (2019) observed that the accretion of protein hydrazones (DNPH-derivatized

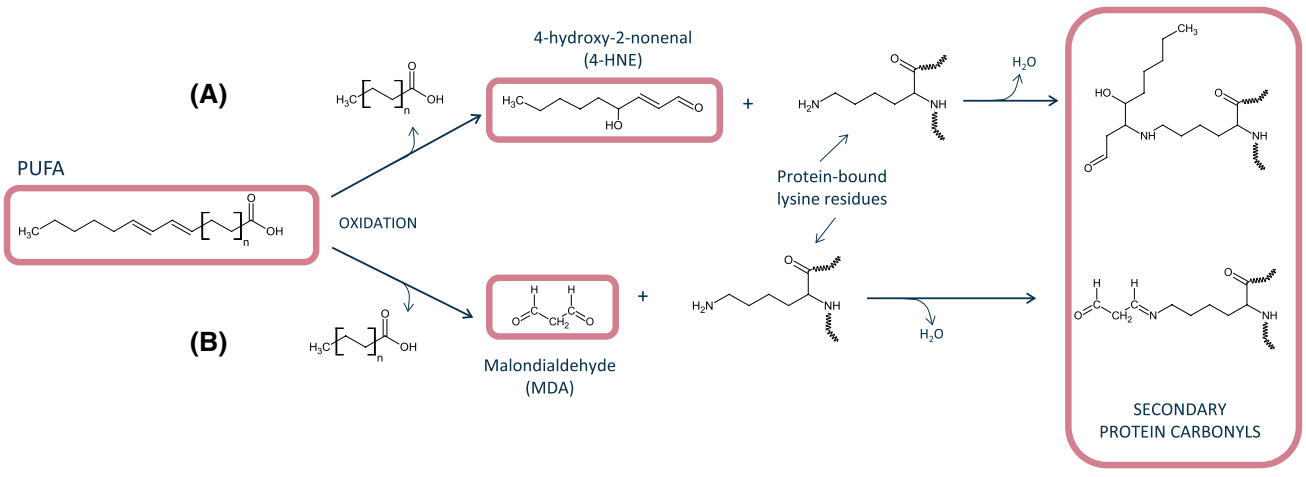

Fig. 2 Mechanisms of secondary carbonylation. **A** Michael addition of 4-hydroxynonenal to protein-bound lysine; **B** Michael addition of malondialdehyde to protein-bound lysine

carbonyls) in HSA was affected by the exposure to a broad concentration range of MDA (0.05–5 mM). The authors concluded that the concentration of secondary protein carbonyls, corresponding to protein-bound MDA, increased with the concentration of MDA. The extent of carbonylation in HSA exposed to 5 mM peaked at around 22 nmol per mg of protein. At such experimental concentrations, the addition of MDA molecules to lysine residues occurs at so high levels, that the formation of primary protein carbonyls from such alkaline amino acid is completely inhibited. The authors report that in foods or biological systems subjected from moderate to severe lipid oxidation (concentrations of MDA between 0.05 and 1 mM), between 50 and 80% of protein carbonyls detected by the DNPH method would be secondary carbonyls. According to the recent and interesting results reported by Wang et al. (2019b), MDA may not only be responsible of secondary carbonylation of myoglobin and myofibrillar proteins from rabbit skeletal muscle. This lipid-derived carbonyl may be able to induce the formation of hypervalent myoglobin species, which promotes the creation of a pro-oxidative environment in the muscle tissue, and worsen, in turn, the oxidative stress. The comprehensive review by Tsikas (2017) provides further details on the formation, reactivity and analytical methods of MDA. Other reactive carbonyls such as acrolein and crotonaldehyde have been found to induce carbonylation stress in cells and other biological systems (Mello et al. 2007). Their implication in the secondary carbonylation of food proteins requires further elucidation.

Concise update on methodological approaches

The DNPH method is the most common procedure for the routine quantification of total protein carbonyls from a biological sample and the results are broadly used as a general index of protein oxidation (Estévez 2011; Hellwig 2020). The technique involves a concurrent spectrophotometric determination of DNPH-derivatized protein-bound carbonyls [as 2,4-dinitrophenyl (DNP) hydrazones] and the total protein content of the sample (Oliver et al. 1987). Eventually, the results are expressed as nmol protein hydrazones per mg of protein. It is worth emphasizing that (i) the original procedure was set to evaluate protein oxidation in plasma samples (Oliver et al. 1987) and that (ii) the DNPH reacts with carbonyl moieties regardless of the origin or formation pathway. Because of this, the method has been modified to facilitate the analysis of proteins from solid samples and low solubility (i.e. myofibrillar proteins) and to avoid interferences caused by lipid carbonyls and assorted chromophores. These modifications include the homogenization of solid samples with high ionic strength buffers and treating the samples with acid and organic solvents to eliminate interfering chromophores such as haemoglobin, retinoids or unreacted DNPH [reviewed by Estevez et al. (2008) and Hellwig (2020)]. Besides the in-solution procedure, in-gel techniques based on western blotting and ELISA-type immunodetection by DNPH-tagged protein antibodies, can also be applied (Meyer et al. 2012; Augustyniak et al. 2015). Despite of recent optimization of the DNPH method for the assessment of protein carbonylation in food systems (Soglia et al. 2016) and other biological samples (Colombo et al. 2016; Bayarsaikhan et al. 2019), this procedure suffers from lack of specificity and has been recurrently criticized for providing an unreliable estimation of the real extent of the protein oxidative damage.

In regards to the specificity, it is generally recognized that the DNPH method provides limited information on the nature and or formation pathway of the quantified carbonyls (Hellwig 2020). Further to that, the overestimation of protein carbonyls by accounting lipid carbonyls introduced into proteins has been recently reported as a major flaw of the DNPH method (Estévez et al. 2019). The authors found that MDA readily reacts with ε-amino groups from protein-bound lysine residues and as a result, the DNP hydrazones quantified correspond to a major extent (up to 80% of total protein carbonyls) to protein-bound MDA carbonyl moieties. Therefore, at a certain range of MDA concentrations (0.05–1 mM), both the formation of primary protein carbonyls by either MCO or MR pathways, and their subsequent detection, is partially blocked by MDA and likely, other lipid-derived carbonyls. It is hence, worth taking into consideration that under severe lipid oxidative environment and MDA production, protein carbonyls quantified by DNPH may mostly reflect a secondary carbonylation process (Fig. 3).

To gain specificity and information of mechanistic nature, the analysis of specific protein carbonyls by chromatographic techniques, such as α-AS and γ-GS, is the election technique. These carbonyl compounds can be tagged by several derivatization procedures, eventually separated, and detected by HPLC or GC attached to fluorescence or MS detectors (Utrera et al. 2011; Estévez 2011; Hellwig 2020). *p*-Amino benzoic acid (*p*-ABA) has been used to tag and stabilize protein carbonyls prior to the hydrolysis procedure. The subsequent detection and quantification of *p*-ABA-derivatized carbonyls has been performed using MS (Estévez et al. 2009) and fluorescence detectors (Akagawa et al. 2009; Utrera et al. 2011). Alternative means of detection involves derivatization with fluoresceinamine ($FINH_2$) prior to separation and identification using HPLC–MS (Climent et al. 1989). The analysis of protein carbonyls by GC involves the prior preparation of volatile hydroxyl derivatives from α-AS (hydroxyaminovaleric acid; HAVA) and γ-GS (hydroxyaminocaproic acid; HACA) and subsequent

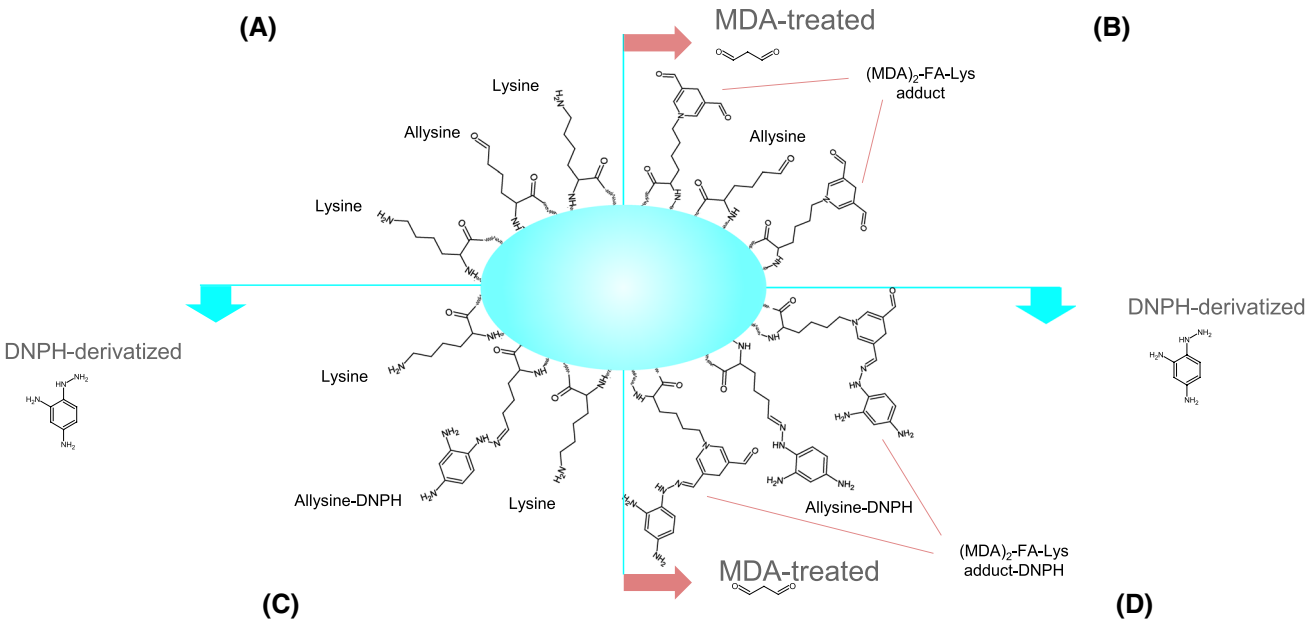

Fig. 3 Illustration of the overestimation of primary carbonylation in malondialdehyde-exposed proteins by the dinitrophenylhydrazine method as reported by Estévez et al. (2019). *A-quadrant* occurrence of protein-bound lysine and α-AS residues, *B-quadrant* addition of malondialdehyde to protein-bound lysine residues, *C-quandrant* derivatization of protein-bound α-AS residues by the dinitrophenylhydrazine, *D-quadrant* derivatization of protein-bound α-AS and malondialdehyde residues by the dinitrophenylhydrazine

reduction with sodium borohydride ($NaBH_4$) (Requena et al. 2001). Table 1 shows the concentration of protein carbonyls in various food products as analysed by the DNPH method or chromatographic techniques. Other innovative approaches include hydrazine-based derivatization prior to a 2D-electrophoresis gel analysis of redox proteomics (Malheiros 2019) and the cellular localization of protein carbonyls using mass spectrometry imaging (Flinders et al. 2015). The description of these and other methods for assessing protein oxidation in meat samples have been reviewed by Fedorova et al. (2014), Alomari et al. (2018), Hawkins and Davies (2019) and Hellwig (2020). Recent redox-proteomic approaches have contributed to understanding the occurrence of protein carbonylation and its underlying mechanisms in post-mortem muscle from mammals (Sayd et al. 2012), seafood (Lin et al. 2021), processed meat (Malheiros 2019; Mitra et al. 2018) and various biological samples (Verrastro et al. 2015; Driessen et al. 2015).

Concise update on the biological consequences of protein carbonylation

Beyond their role as indicators of the extent of the oxidative damage to proteins, protein carbonyls may be directly implicated in the onset of processes leading to food quality deterioration, nutritional impairments, and pathophysiological conditions. The oxidation of lysine residues may have consequences on protein functionality and on the susceptibility of proteins to hydrolytic degradation. Further, protein carbonyls formed from lysine oxidation are reactive compounds, which are involved in the formation of crosslinks and carboxylic acids, with all of these having consequences of biological relevance. In this section, recent advances in the understanding of the impact of protein carbonylation on food quality, nutrition and health are concisely reported.

Protein carbonylation and food protein functionality and digestibility

Proteins are major components of foods from animal origin, and, therefore, play an indisputable role in the technological, nutritional, and sensory properties of muscle, dairy and egg foods. Soon after the discovery that muscle proteins were susceptible to oxidation and protein carbonyls were quantified in food samples, this oxidative damage was linked to loss of protein functionality including impairments of the ability to form gels, emulsions and hold water (Xiong 2000). In subsequent studies, carbonylation was also associated to decreased susceptibility of oxidized proteins to proteases, which had consequences on meat tenderization during aging (Rowe et al. 2004) and on protein degradation during digestion of severely oxidized foods (Sante-Lhoutellier et al. 2007; Soladoye et al. 2015). In a previous comprehensive review about protein carbonylation in meat systems, Estévez (2011) already warned that most causative connections

Table 1 Concentration of protein carbonyls in various food products reported in recent literature

Food system	Method	Protein carbonyls[A]	References
Raw lamb cutlets	DNPH	9	Lahmar et al. (2018)
Ready-to-eat chicken patties	DNPH	15	de Santana Neto et al. (2021)
Soy protein isolate	DNPH	13.6	Yu et al. (2018)
Soy protein isolate	DNPH	10.4	Zhang et al. (2017)
Milk	DNPH	23.6[B]	Kalaitsidis et al. (2021)
Yogurt	DNPH	11.8[B]	Kalaitsidis et al. (2021)
Feta cheese	DNPH	30.9[B]	Kalaitsidis et al. (2021)
Cooked ham	DNPH	8	Armenteros et al. (2016)
Rainbow trout mince	DNPH	3.6	Bitalebi et al. (2019)
Surimi fishballs	DNPH	4.2	Zhao et al. (2019)
Powdered infant milk	DNPH	3.1	Chen et al. (2019)
Silver carp fillets	DNPH	4	Zhang et al. (2021)
Raw shrimp	DNPH	11.9	Ruvalcaba-Márquez et al. (2021)
Blood meal	DNPH	127	Frame et al. (2020)
Raw rabbit meat	DNPH	7	Wang et al. (2018)
Air-dried yak meat	DNPH	8.5	Ma et al. (2021)
Fresh pork	DNPH	4.5	Hernández-López et al. (2016)
Cooked beef patties	HPLC[C]	1.3	Rysman et al. (2016)
Frozen rainbow trout fillet	HPLC[C]	4.5	Timm-Heinrich et al. (2013)
Fermented sausages	HPLC[C]	0.9	Öztürk-Kerimoğlu et al. (2019)
Fermented sausages	HPLC[C]	0.9	Villaverde et al. (2014)
Jerky chicken	HPLC[C]	85	Silva et al. (2016)
Cooked bacon	HPLC[C]	80	Soladoye et al. (2017)
Sous vide-cooked lamb loin	HPLC[C]	0.42	Roldán et al. (2014)
Raw wooden chicken breast	HPLC[C]	3.2	de Carvalho et al. (2021)

DNPH quantification of protein carbonyls as hydrazones according to the dinitrophenylhydrazine method, *HPLC* quantification of specific protein carbonyls, α-AS and γ-GS, by high-performance liquid chromatography

[A]Results expressed as nmol of protein carbonyls/mg protein, unless otherwise noted

[B]Results expressed as ng of protein carbonyls/mL sample

[C]Results refer to the sum of α-AS and γ-GS

between protein carbonyls and the alleged effects on protein functionality were based on the calculations of positive and significant correlations. Since correlation does not involve causation, only by defining the underlying molecular mechanisms of the deleterious effects of protein carbonylation on protein functionality and food quality, the causative connection between both events can be rationally supported. In this regard, great efforts have been made in the last years to comprehend such connections. Utrera and Estévez (2012) thoroughly reported the occurrence of the "carbonylation pathway" in myofibrillar proteins subjected to a radical generating system. The formation of α-AS, as an early product from lysine oxidation, was followed by the formation of its oxidative degradation product (α-AA) and the formation of Schiff bases upon reaction of α-AS with protein-bound amino groups. These chemical changes were proposed to contribute to the impaired water functionality of meat proteins. Namely, the authors indicated that protein carbonylation could likely alter protein-water molecular interactions by (i) modification of the isoelectric point in oxidized proteins and (ii) by formation of protein aggregates; with both processes explaining an impaired protein functionality. Conversely, Bao et al. (2018) observed that protein carbonylation and protein crosslinks affected protein net charges though protein functionality was eventually improved. Yet, the authors induced oxidation by hypochlorous acid, and the results seemed to diverge from those reported by Utrera and Estévez (2012) who employed a hydroxyl radical oxidation system. Using a similar in vitro radical-induced oxidation system, Zhang et al. (2020) recently confirmed that protein crosslinking, aggregation and other severe structural changes in oxidized proteins compromise their water solubility and functionality. As recently reviewed by Zhao et al. (2021), the functionality of muscle proteins, including their ability to hold water and form gels, can be modulated by an appropriate management of the nature and extent of protein

oxidation. Xiong (2000) already reported that mild and progressive protein oxidation may facilitate protein functionality and leads to stable gels, while severe oxidation leads to decreased protein functionality and impaired rheological properties. Numerous scientific evidences support this hypothesis and interestingly, phytochemicals (polyphenols, phenolic acids) may contribute to modify the functional and rheological properties of gels from mild to moderately oxidized proteins (Guo and Xiong 2021). The carbonylation of proteins via the "Suyama" pathway (Maillard-mediated mechanism) has also been found to affect the functionality of meat, dairy and soy proteins (Luna and Estévez 2019; Feng et al. 2021). Luna and Estévez (2019) observed that incubation of β-lactoglobulin and myofibrillar proteins with GO and MGO (2 M) at 80 °C cause severe carbonylation (> 20 nmo/mg protein) and reduced ability of the carbonylated proteins to hold water (90% loss of functionality). Glucose-treated soy proteins have also been reported to undergo extremely severe carbonylation and impaired surface properties when heated at 60 °C for 24 h (Feng et al. 2021). The occurrence of secondary carbonylation has also been found to affect protein functionality though the effect depends on the nature of the lipid-derived carbonyl and its concentration. Cheng et al. (2021a, b) recently observed that 5–20 mM MDA improved the WHC and rheological properties of gels from myofibrillar proteins while at even higher MDA concentrations (40 mM), the emulsion gel was completely lost. It is worth clarifying that these experimental MDA concentrations are out of the range found in processed or digested food products (Steppeler et al. 2016). Table 2 shows recent data on the concentration of protein carbonyls, MDA and 4-HNE in food digests. Wang et al. (2021) reported deleterious effects of 5 mM MDA on the functionality of myofibrillar proteins while these effects were found to be counteracted by phenolic terpenes such as linalool or limonene. The MDA-induced oxidative stress and consequent impaired functionality in myofibrillar proteins can also be modulated by the ionic strength of the media, which is dependent, in turn, on NaCl concentration (Zhou et al. 2015). In a recent paper, Keller et al. (2020) reported the heme–iron-induced production of 4-HNE in the intestinal lumen and the role of this reactive carbonyl in the formation of protein-adducts in heart, liver and skeletal muscle of rats.

The impact of protein carbonylation on protein digestibility has also been a topic of recurring debate. As for the impact on the functional properties, the effect of the carbonylation of the susceptibility of proteins to undergo hydrolytic degradation depends on the severity of the oxidative damage. In this regard, mild protein oxidation may favour partial unfolding which facilitates enzymatic approach, recognition and action on the substrate. Conversely, the formation of irreversible protein aggregates owing to a severe and enduring oxidative damage may lead to a decreased proteolytic susceptibility (Soladoye et al. 2015). Morzel et al. (2006) ascribed the decreased susceptibility of oxidized myofibrillar proteins to papain, to the carbonylation of arginine and lysine as this enzyme hydrolyses at bonds involving such amino acids. In this regard, similar effects could be expected

Table 2 Concentration of protein carbonyls (PC), malondialdehyde (MDA) and 4-hydroxynonenal (4-HNE) in various food digests

Food system	GID[A]	PC[B]	MDA	4-HNE	References
Processed pork	Simulated static system (i)	8	30[C]	–	Van Hecke et al. (2018)
Mackerel	Simulated static system (i)	13	0.88[D]	34[E]	Van Hecke et al. (2019)
Salmon	Simulated static system (i)	9.5	0.53[D]	19[E]	Van Hecke et al. (2019)
Tuna	Simulated static system (i)	5.5	0.55[D]	13[E]	Van Hecke et al. (2019)
Parma ham	Simulated static system (g)	9	65[F]	8[F]	Goethals et al (2020)
Cooked chicken patties	Simulated static system (i)	10	124[F]	200[F]	Sobral et al. (2020)
Dry-cured loin	Simulated static system (i)	23	0.8[G]	–	Lavado et al. (2021)
Red cured cooked meat	Simulated static system (g)	8	0.4[D]	140[E]	Van Hecke et al. (2021)
	Sprague–Dawley rats (g)	7	100[F]	–	Van Hecke et al. (2021)
Cooked pork	Simulated static system (g)	5	5[H]	240[I]	Li et al. (2021a, b)

[A]*GID* Gastrointestinal digestion system. (i) data collected at the intestinal digestion phase. (g) data collected at the gastric digestion phase

[B]Results expressed as nmol of protein carbonyls/mg protein

[C]Results expressed as nmol/mL digest

[D]Results expressed as mmol/kg digest

[E]Results expressed as µmol/kg digest

[F]Results expressed as nmol/g digest

[G]Results expressed as µmol/mL digest

[H]Results expressed as µg/mL digest

[I]Results expressed as ng/mL digest

for digestive enzymes with a similar hydrolytic pattern like trypsin. Protein carbonyls could also impair the digestibility of food proteins by contributing to the formation of insoluble aggregates via carbonyl–amine crosslinks. Sante-Lhoutellier et al. (2007) found that the activity of trypsin/α-chymotrypsin on proteins decreased as the carbonylation level in the latter increased, which provides strength to the role of protein carbonylation on the impaired digestibility of oxidized proteins. According to recent literature, the carbonylation of proteins via the Maillard reaction (Luna and Estévez 2019; Wu et al. 2021) or via introduction of secondary lipid carbonyls such as MDA (Niu et al. 2019; Li et al. 2021a, b) have a deleterious impact on the digestibility of meat, dairy and cereal proteins. Recent studies have also established plausible connections between the extent of protein carbonylation and a reduced digestibility of proteins in a variety of foods such as egg white (Cheng et al. 2021a, b), whey isolate (Niu et al. 2019), ready-to-eat chicken patties (Ferreira et al. 2018), fish fillets (Semedo Tavares et al. 2018) and air-dried yak meat (Ma et al. 2021), among many others.

Protein carbonylation and toxicological concerns

The intake of oxidized lipids is known to increase the post-prandial plasma levels of oxidation and inflammation markers (Sies et al. 2005; Estévez et al. 2017). A sustained exposure to dietary lipid oxidation products is associated with an increased risk of suffering certain chronic inflammatory diseases and cancer (Sies et al. 2005). The molecular basis of this pathogenesis is well documented, as lipid-derived carbonyls such as MDA are known to display cytotoxic and mutagenic potential in the gastrointestinal tract (GIT) or in internal organs upon absorption (Esterbauer 1993). In this scenario, it is reasonable to enquiry whether dietary protein carbonyls may also contribute to impair cell homeostasis and induce health disorders. There is, in this regard, a profound lack of knowledge. The high reactivity of α-AS and other protein carbonyls, and the poor commercial availability of purified compounds, hinders the implementation of toxicological studies using such species. Alternatively, experimental animals have been fed with severely oxidized proteins in which carbonyls appeared to be one of the most salient chemical modifications. Using this experimental approach, Li et al. (2014) found that dietary oxidized proteins promoted the collapse of endogenous antioxidant cell defense systems, leading to the onset of oxidative stress and degeneration in kidney and liver of mice. The intake of severely carbonylated beef proteins to Wistar rats has been reported to have a significant impact on gut microbiota (Van-Hecke et al. 2021). To similar conclusions came Ge et al. (2020) who found that the alteration of the gut microbiota in mice by the intake of oxidized pork contributed to the onset of oxidative stress and inflammation processes in this murine model. The same authors reported that dietary oxidized pork induced impaired lipid metabolism by decreasing insulin levels and suppressing of the insulin receptor substrate-1 (IRS-1)/phosphoinositide 3-kinase (PI3K)/protein kinase B (Akt) signaling pathway and its downstream signaling molecules (Ge et al. 2021). Li et al. (2019) observed impaired spatial learning and memory in rats fed with carbonylated proteins from a severely processed milk product. While these studies support the role of dietary protein oxidation on physiological disorders, the identification of specific protein oxidation products as responsible for such effects is unfeasible. To comprehend the impact of particular oxidized amino acids, we recently carried out an experiment (unpublished data) in which Wistar rats were exposed to α-AS/piperideine-6-carboxylate in acute (5 mg/day/kg live weight for 4 weeks) and chronic assays (0.5 mg/day/kg live weight for 20 weeks). Among the most remarkable results, we observed the onset of oxidative stress in several tissues (e.g. small intestine, liver, spleen) and impaired lipid metabolism in treated rats vs. the control counterparts, which agrees with results obtained from some of the aforementioned studies. The most abundant protein carbonyl, α-AS, is oxidized in the presence of peroxides to the lysine oxidation end product, the α-AA. This transformation is readily taking place in pro-oxidative environments such as that created in hyperglycemic conditions (Luna et al. 2021). Unlike its precursor, this oxidized amino acid has been profusely studied in regards to its ability to induce pathological conditions. In a recent study, Díaz-Velasco et al. (2020) documented that the exposure of human CACO-2 cells to a food-relevant α-AA concentration (200 µM) leads to depletion of glutathione, oxidative stress, apoptosis and necrosis (Fig. 4). In a further study using proteomics (unpublished data), the α-AA was found to act as analog of glutamic acid and impair multiple biological processes in human intestinal cells such as the transepithelial transport, mitochondrial activity and protein repair mechanisms. Wang et al. (2013) induced pancreatic malfunction and diabetes in C57BL/6 mice by oral administration of α-AA (500 mg/day/kg live weight). Estaras et al. (2020) challenged mice pancreatic acinar cells with 200 µM α-AA and observed oxidative stress, calcium homeostasis dysfunction and impaired trypsin secretion. More details on the effect of dietary protein oxidation on human health can be found elsewhere (Estévez and Luna 2017; Estévez and Xiong 2019). Likewise, the application of antioxidant strategies to mitigate the negative consequences of the onset of lipid and protein oxidation in foods and in the gastrointestinal tract have been recently reviewed critically and comprehensively

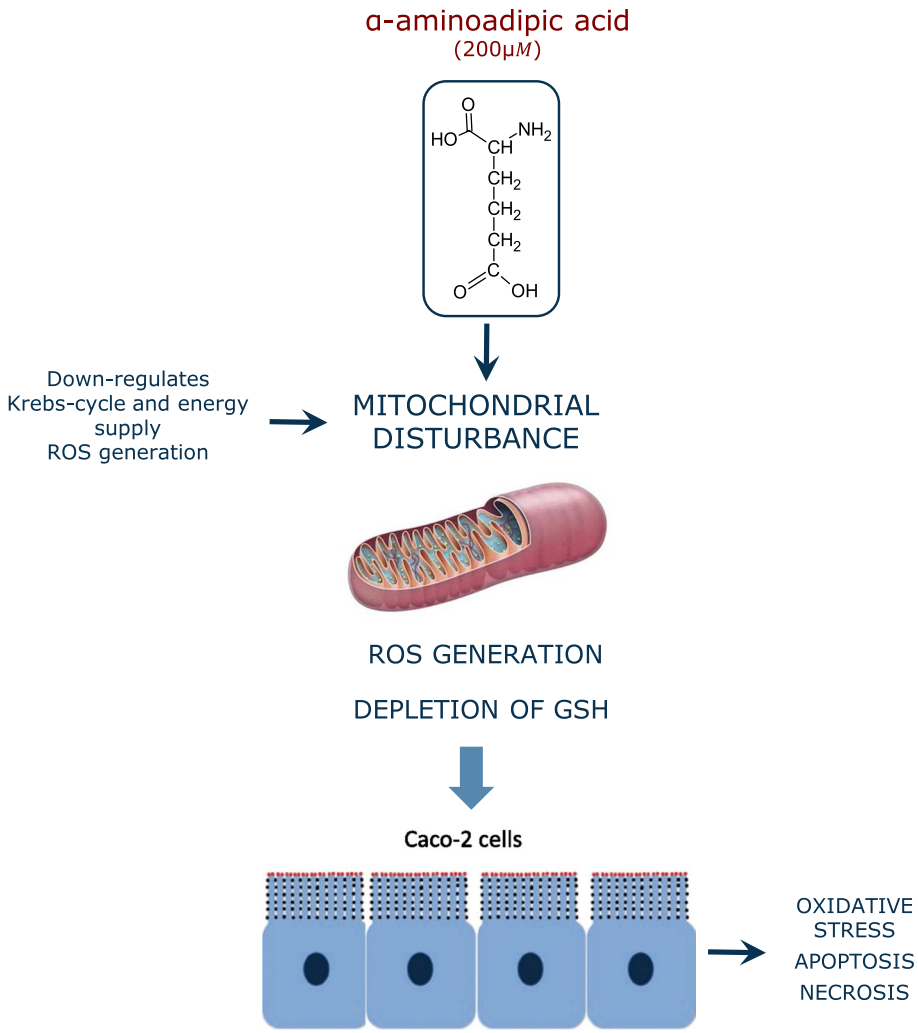

Fig. 4 Mechanisms of the cytotoxic effects of α-AA on CACO-2 cells as reported by Díaz-Velasco et al. (2020)

(Nieva-Echevarría et al. 2020; Lund 2021; Estévez 2021; Xiong and Guo 2021).

Protein carbonylation as mechanism of cell communication

For a long time regarded as markers of protein oxidation, protein carbonyls have been found to participate actively in biological processes and metabolic functions. The understanding of the molecular basis of such bioactivities may be required to identify the role of protein carbonyls in the onset of physiological impairments and pathological conditions. Considering that protein carbonyls are still highly reactive and can be involved in carbonylamine reactions, with this reaction being key in many enzymatic and biological processes, it is plausible to hypothesize that protein carbonyls may act as signalling molecules. The role of protein carbonylation as a reaction of biological consequences is relevant from a food and nutrition perspective, considering the accretion of carbonyls in dietary proteins during processing, storage, culinary preparation and digestion. While the toxicological aspects of *α*-AS, as major protein carbonyl, and its oxidation product *(α*-AA), are still being examined, the dietary exposure to physiological concentrations of these oxidized amino acids may also play a role in the regulation of certain internal physiological processes upon absorption. Unfortunately, these effects are poorly understood. Likewise, the in vivo carbonylation of proteins in cells may also be implicated in mechanisms of cell regulation and control. In the following lines, the most recent discoveries of protein carbonyls as redox signaling molecules are concisely reviewed.

One of the main biological consequences of protein carbonylation is the activation of the protein turnover mechanism. As protein carbonylation is irreversible and cellular enzymes are unable to repair such oxidative damage, carbonylated proteins are degraded by the cell's proteasomal system (Baraibar and Friguet 2012). Otherwise, severely carbonylated proteins may not only be dysfunctional, they tend to form aggregates via increasing intrinsic protein

hydrophobicity and the formation of carbonylamine reactions (Schiff-base structures) between protein carbonyls and ε-amino groups from protein-bound alkaline amino acids (i.e. lysine). The accumulation of aggregates of oxidized proteins in cells and tissues has been highlighted as a pathological hallmark of serious health disorders such as the Alzheimer disease (Levine 2002; Sharma et al. 2020). While cells may degrade aberrant proteins by whether the ATP-ubiquitin dependent 26S proteasome or by the ATP-ubiquitin independent 20S proteasome, carbonylated proteins seem to be preferentially degraded by the 20S proteasome (Jung and Grune 2008; Baraibar and Friguet 2012; Lefaki et al. 2017). It is worth noting that certain proteins may be more susceptible to carbonylation than others but the molecular basis of this specificity still remained unclear though it may respond to mechanisms of protein tagging in turn over or other cellular signaling mechanisms (Maisonneuve et al. 2009). Additionally, severely carbonylated and aggregated proteins are not recognized by the 20S proteasome, which leads to accretion of such oxidized complexes in cell.

Other works indicate the role of protein carbonylation on mitochondrial function and insulin resistance in muscle and adipose tissue (Frohnert and Bernlohr 2013). According to these authors, carbonylation of proteins may display opposite effects depending on the role of the proteins being affected by this post-translational modification. In this regard, certain proteins such as Kelch-like ECH-associated protein 1 (KEAP1) are activated in antioxidant response through carbonylation while insulin receptor substrates 1 and 2 are inactivated when carbonylated, which decreases insulin signaling. Another example is the activation of *c*-Jun N-terminal kinase (JNK) upstream kinase ASK1 by secondary carbonylation via 4-HNE adduction. The activation of this pathway leads to the ultimate expression of pro-inflammatory target genes, linking oxidative stress and inflammation (Curtis et al. 2012; Hecker and Wagner 2018). Proposing a pioneering theory, Wong et al. (2013) reported that primary protein carbonylation could be a physiological mechanism of ROS signaling and that such mechanism is regulated by decarbonylation. Therefore, according to their proposal, the formation of protein carbonyls could be reversed by the involvement of cell reductases, which clearly diverge from the well-established assumption that carbonylation was an irreversible damage to proteins. As a supportive example of their theory, the authors observed that carbonylation of annexin A1, which shows anti-inflammatory, anti-proliferative and pro-apoptotic effects, leads to its degradation by the proteasome. This oxidation-driven degradation of annexin A1 is proposed as a cell signal for cell growth. Though the authors suggest that certain enzymes and redox proteins, such as alcohol dehydrogenases and thioredoxin, may be involved in decarbonylation of proteins, it is currently unclear whether free or protein-bound oxidized amino acids such as α-AS or γ-GS could be reduced under physiological conditions.

Concluding remarks

The recent advances achieved in the field of protein carbonylation facilitate the understanding of the biological significance of this multifaceted reaction. While the carbonylation on food proteins is typically regarded as a reaction of negative consequences owing to the loss of nutritional value, decreased digestibility and impaired functionality, scientific evidences support the benefits of mild and controlled oxidation of proteins in the improvement of their gel abilities and rheological properties. Likewise, the onset of protein carbonylation in cells may play a double role, depending on the severity of the reaction and the protein target of such post-translational modification. On the one hand, severe and enduring oxidative stress leading to massive protein carbonylation and aggregation may block protein turnover and cause pathological conditions related to oxidative stress and inflammation. On the other hand, mild and/or targeted carbonylation in particular proteins may induce physiological responses for the strengthening of the antioxidant defences, the activation of the protein turnover and likely modulation of the immune system. As a truly open topic, further and inspiring discoveries will contribute to consolidate the connections between protein carbonylation, food quality, nutrition and health.

Funding Open Access funding provided thanks to the CRUE-CSIC agreement with Springer Nature. The support from the "FEDER/Ministerio de Ciencia, Innovación y Universidades–Agencia Estatal de Investigación" through the Project: AGL2017-84586-R is acknowledged. Likewise, finantial support was also received from "Gobierno de Extremadura (Consejería de Economía e Infraestructuras)" through the Grant GR18104.

Declarations

Conflict of interest The authors have no conflicts of interest to declare that are relevant to the content of this article.

Open Access This article is licensed under a Creative Commons Attribution 4.0 International License, which permits use, sharing, adaptation, distribution and reproduction in any medium or format, as long as you give appropriate credit to the original author(s) and the source, provide a link to the Creative Commons licence, and indicate if changes were made. The images or other third party material in this article are included in the article's Creative Commons licence, unless indicated otherwise in a credit line to the material. If material is not included in the article's Creative Commons licence and your intended use is not permitted by statutory regulation or exceeds the permitted use, you will need to obtain permission directly from the copyright holder. To view a copy of this licence, visit http://creativecommons.org/licenses/by/4.0/.

References

Akagawa M (2020) Protein carbonylation: molecular mechanisms, biological implications, and analytical approaches. Free Radic Res. https://doi.org/10.1080/10715762.2020.1851027

Akagawa M, Sasaki D, Kurota Y, Suyama K (2005) Formation of α-aminoadipic and γ-glutamic semialdehydes in proteins by the Maillard reaction. Ann NY Acad Sci 1043:129–134. https://doi.org/10.1196/annals.1333.016

Akagawa M, Sasaki D, Ishii Y et al (2006) New method for the quantitative determination of major protein carbonyls, α-aminoadipic and γ-glutamic semialdehydes: Investigation of the formation mechanism and chemical nature in vitro and in vivo. Chem Res Toxicol 19:1059–1065. https://doi.org/10.1021/tx060026p

Akagawa M, Suyama K, Uchida K (2009) Fluorescent detection of α-aminoadipic and γ-glutamic semialdehydes in oxidized proteins. Free Radic Biol Med 46:701–706. https://doi.org/10.1016/j.freeradbiomed.2008.12.014

Alomari E, Bruno S, Ronda L et al (2018) Protein carbonylation detection methods: a comparison. Data Brief 19:2215–2220. https://doi.org/10.1016/j.dib.2018.06.088

Arcanjo NMO, Luna C, Madruga MS, Estévez M (2018) Antioxidant and pro-oxidant actions of resveratrol on human serum albumin in the presence of toxic diabetes metabolites: glyoxal and methylglyoxal. Biochim Biophys Acta 1862:1938–1947. https://doi.org/10.1016/j.bbagen.2018.06.007

Armenteros M, Morcuende D, Ventanas J, Estévez M (2016) The application of natural antioxidants via brine injection protects Iberian cooked hams against lipid and protein oxidation. Meat Sci 116:253–259. https://doi.org/10.1016/j.meatsci.2016.02.027

Augustyniak E, Adam A, Wojdyla K et al (2015) Validation of protein carbonyl measurement: a multi-centre study. Redox Biol 4:149–157. https://doi.org/10.1016/j.redox.2014.12.014

Bao Y, Boeren S, Ertbjerg P (2018) Myofibrillar protein oxidation affects filament charges, aggregation and water-holding. Meat Sci 135:102–108. https://doi.org/10.1016/j.meatsci.2017.09.011

Baraibar MA, Friguet B (2012) Chapter 7—changes of the proteasomal system during the aging process. In: Grune TBT-P in MB, Science T (ed) The Proteasomal system in aging and disease. Academic Press, Cambridge, pp 249–275

Bayarsaikhan G, Avan AN, Çekiç SD, Apak R (2019) Use of modified CUPRAC and dinitrophenylhydrazine colorimetric methods for simultaneous measurement of oxidative protein damage and antioxidant defense against oxidation. Talanta 204:613–625. https://doi.org/10.1016/j.talanta.2019.06.049

Berlett BS, Stadtman ER (1997) Protein oxidation in aging, disease, and oxidative stress. J Biol Chem 272:20313–20316. https://doi.org/10.1074/jbc.272.33.20313

Bitalebi S, Nikoo M, Rahmanifarah K et al (2019) Effect of apple peel extract as natural antioxidant on lipid and protein oxidation of rainbow trout (*Oncorhynchus mykiss*) mince. Int Aquat Res 11:135–146. https://doi.org/10.1007/s40071-019-0224-y

Carvalho LM, Delgado J, Madruga MS, Estévez M (2021) Pinpointing oxidative stress behind the white striping myopathy: depletion of antioxidant defenses, accretion of oxidized proteins and impaired proteostasis. J Sci Food Agric 101:1364–1371. https://doi.org/10.1002/jsfa.10747

Chen Z, Leinisch F, Greco I et al (2019) Characterisation and quantification of protein oxidative modifications and amino acid racemisation in powdered infant milk formula. Free Radic Res 53:68–81. https://doi.org/10.1080/10715762.2018.1554250

Cheng J, Tang D, Yang H et al (2021a) The dose-dependent effects of polyphenols and malondialdehyde on the emulsifying and gel properties of myofibrillar protein-mulberry polyphenol complex. Food Chem 360:130005. https://doi.org/10.1016/j.foodchem.2021.130005

Cheng Y, Chi Y, Geng X, Chi Y (2021b) Effect of 2,2′-azobis(2-amidinopropane) dihydrochloride (AAPH) induced oxidation on the physicochemical properties, in vitro digestibility, and nutritional value of egg white protein. Lwt 143:111103. https://doi.org/10.1016/j.lwt.2021.111103

Climent I, Tsai L, Levine RL (1989) Derivatization of γ-glutamyl semialdehyde residues in oxidized proteins by fluoresceinamine. Anal Biochem 182:226–232. https://doi.org/10.1016/0003-2697(89)90584-8

Colombo G, Clerici M, Garavaglia ME et al (2016) A step-by-step protocol for assaying protein carbonylation in biological samples. J Chromatogr B 1019:178–190. https://doi.org/10.1016/j.jchromb.2015.11.052

Curtis JM, Hahn WS, Long EK et al (2012) Protein carbonylation and metabolic control systems. Trends Endocrinol Metab 23:399–406. https://doi.org/10.1016/j.tem.2012.05.008

Davies MJ (2016) Protein oxidation and peroxidation. Biochem J 473:805–825. https://doi.org/10.1042/BJ20151227

de Santana Neto DC, Cordeiro ÂMTM, Meireles BRLA et al (2021) Inhibition of protein and lipid oxidation in ready-to-eat chicken patties by a spondias mombin *L. Bagasse* Phenolic-Rich Extract. Foods 10:1338. https://doi.org/10.3390/foods10061338

Díaz-Velasco S, González A, Peña FJ, Estévez M (2020) Noxious effects of selected food-occurring oxidized amino acids on differentiated CACO-2 intestinal human cells. Food Chem Toxicol 144:1–8. https://doi.org/10.1016/j.fct.2020.111650

Driessen MD, Mues S, Vennemann A et al (2015) Proteomic analysis of protein carbonylation: a useful tool to unravel nanoparticle toxicity mechanisms. Part Fibre Toxicol 12:1–18. https://doi.org/10.1186/s12989-015-0108-2

Duque-Estrada P, Berton-Carabin CC, Nieuwkoop M et al (2019) Protein oxidation and in vitro gastric digestion of processed soy-based matrices. J Agric Food Chem 67:9591–9600. https://doi.org/10.1021/acs.jafc.9b02423

Estaras M, Ameur FZ, Estévez M et al (2020) The lysine derivative aminoadipic acid, a biomarker of protein oxidation and diabetes-risk, induces production of reactive oxygen species and impairs trypsin secretion in mouse pancreatic acinar cells. Food Chem Toxicol 145:111594. https://doi.org/10.1016/j.fct.2020.111594

Esterbauer H (1993) Cytotoxicity and genotoxicity of lipid-oxidation products. Am J Clin Nutr 57:779S-786S. https://doi.org/10.1093/ajcn/57.5.779S

Estevez M, Morcuende D, Ventanas S (2008) Determination of oxidation. In: Mollet LML, Toldrá F (eds) Handbook of processed meat and poultry analysis. CRC Press, Boca Raton, pp 141–162

Estévez M (2011) Protein carbonyls in meat systems: a review. Meat Sci 89:259–279. https://doi.org/10.1016/j.meatsci.2011.04.025

Estévez M (2021) Critical overview of the use of plant antioxidants in the meat industry: opportunities, innovative applications and future perspectives. Meat Sci 181:108610. https://doi.org/10.1016/j.meatsci.2021.108610

Estévez M, Luna C (2017) Dietary protein oxidation: a Silent threat to human health? Crit Rev Food Sci Nutr 57:3781–3793. https://doi.org/10.1080/10408398.2016.1165182

Estévez M, Xiong Y (2019) Intake of oxidized proteins and amino acids and causative oxidative stress and disease: recent scientific evidences and hypotheses. J Food Sci 84:387–396. https://doi.org/10.1111/1750-3841.14460

Estévez M, Ollilainen V, Heinonen M (2009) Analysis of protein oxidation markers α-Aminoadipic and γ-Glutamic semialdehydes in food proteins using liquid chromatography (LC)-Electrospray ionization (ESI)-Multistage tandem mass spectrometry (MS). J

Agric Food Chem 57:3901–3910. https://doi.org/10.1021/jf804017p
Estévez M, Padilla P, Carvalho L et al (2019) Malondialdehyde interferes with the formation and detection of primary carbonyls in oxidized proteins. Redox Biol 26:101277. https://doi.org/10.1016/j.redox.2019.101277
Estévez M, Geraert PA, Liu R et al (2020) Sulphur amino acids, muscle redox status and meat quality: more than building blocks – Invited review. Meat Sci 163:108087. https://doi.org/10.1016/j.meatsci.2020.108087
Estévez M, Li Z, Soladoye OP, Van-Hecke T (2017) Chapter two - health risks of food oxidation. In: Toldrá F (ed) Advances in Food and Nutrition Research. Academic Press, Cambridge, Massachusetts, USA, pp 45–81
Fedorova M, Bollineni RC, Hoffmann R (2014) Protein carbonylation as a major hallmark of oxidative damage: update of analytical strategies. Mass Spectrom Rev 33:79–97. https://doi.org/10.1002/mas.21381
Feng J, Berton-Carabin CC, Ataç Mogol B et al (2021) Glycation of soy proteins leads to a range of fractions with various supramolecular assemblies and surface activities. Food Chem 343:128556. https://doi.org/10.1016/j.foodchem.2020.128556
Ferreira VCS, Morcuende D, Madruga MS et al (2018) Role of protein oxidation in the nutritional loss and texture changes in ready-to-eat chicken patties. Int J Food Sci Technol 53:1518–1526. https://doi.org/10.1111/ijfs.13733
Flinders B, Morrell J, Marshall PS et al (2015) The use of hydrazine-based derivatization reagents for improved sensitivity and detection of carbonyl containing compounds using MALDI-MSI. Anal Bioanal Chem 407:2085–2094. https://doi.org/10.1007/s00216-014-8223-8
Frame CA, Huff-Lonergan EJ, Rossoni Serao MC (2020) Impact of storage conditions on protein oxidation of rendered by-product meals. Transl Anim Sci 4:1–9. https://doi.org/10.1093/tas/txaa205
Frohnert BI, Bernlohr DA (2013) Protein carbonylation, mitochondrial dysfunction, and insulin resistance. Adv Nutr 4:157–163. https://doi.org/10.3945/an.112.003319
Ge Y, Lin S, Li B et al (2020) Oxidized pork induces oxidative stress and inflammation by altering gut microbiota in mice. Mol Nutr Food Res 64:1901012. https://doi.org/10.1002/mnfr.201901012
Ge Y, Li B, Yang Y et al (2021) Oxidized pork induces disorders of glucose metabolism in mice. Mol Nutr Food Res 65:2000859. https://doi.org/10.1002/mnfr.202000859
Goethals S, Van Hecke T, Vossen E et al (2020) Commercial luncheon meat products and their in vitro gastrointestinal digests contain more protein carbonyl compounds but less lipid oxidation products compared to fresh pork. Food Res Int 136:109585. https://doi.org/10.1016/j.foodres.2020.109585
Guo A, Xiong YL (2021) Myoprotein–phytophenol interaction: Implications for muscle food structure-forming properties. Compr Rev Food Sci Food Saf 20:2801–2824. https://doi.org/10.1111/1541-4337.12733
Gürbüz G, Heinonen M (2015) LC-MS investigations on interactions between isolated β-lactoglobulin peptides and lipid oxidation product malondialdehyde. Food Chem 175:300–305. https://doi.org/10.1016/j.foodchem.2014.11.154
Hawkins CL, Davies MJ (2019) Detection, identification, and quantification of oxidative protein modifications. J Biol Chem 294:19683–19708. https://doi.org/10.1074/jbc.REV119.006217
Hecker M, Wagner AH (2018) Role of protein carbonylation in diabetes. J Inherit Metab Dis 41:29–38. https://doi.org/10.1007/s10545-017-0104-9
Hellwig M (2020) Analysis of protein oxidation in food and feed products. J Agric Food Chem 68:12870–12885. https://doi.org/10.1021/acs.jafc.0c00711
Hernández-López SH, Rodríguez-Carpena JG, Lemus-Flores C et al (2016) Avocado waste for finishing pigs: Impact on muscle composition and oxidative stability during chilled storage. Meat Sci 116:186–192. https://doi.org/10.1016/j.meatsci.2016.02.018
Jung T, Grune T (2008) The proteasome and its role in the degradation of oxidized proteins. IUBMB Life 60:743–752. https://doi.org/10.1002/iub.114
Kalaitsidis K, Sidiropoulou E, Tsiftsoglou O et al (2021) Effects of cornus and its mixture with oregano and thyme essential oils on dairy sheep performance and milk, yoghurt and cheese quality under heat stress. Animals 11:1063. https://doi.org/10.3390/ani11041063
Kehm R, Baldensperger T, Raupbach J, Höhn A (2021) Protein oxidation—formation mechanisms, detection and relevance as biomarkers in human diseases. Redox Biol 42:101901. https://doi.org/10.1016/j.redox.2021.101901
Keller J, Chevolleau S, Noguer-Meireles MH et al (2020) Heme-iron-induced production of 4-hydroxynonenal in intestinal lumen may have extra-intestinal consequences through protein-adduct formation. Antioxidants (basel) 9(12):1293. https://doi.org/10.3390/antiox9121293
Lahmar A, Morcuende D, Andrade MJ et al (2018) Prolonging shelf life of lamb cutlets packed under high-oxygen modified atmosphere by spraying essential oils from North-African plants. Meat Sci 139:56–64. https://doi.org/10.1016/j.meatsci.2018.01.015
Lapolla A, Flamini R, Vedova AD et al (2003) Glyoxal and methylglyoxal levels in diabetic patients: quantitative determination by a new GC/MS method. Clin Chem Lab Med 41:1166–1173. https://doi.org/10.1515/CCLM.2003.180
Lavado G, Higuero N, León-Camacho M, Cava R (2021) Formation of lipid and protein oxidation products during in vitro gastrointestinal digestion of dry-cured loins with different contents of nitrate/nitrite added. Foods 10:1748. https://doi.org/10.3390/foods10081748
Lee HJ, Jang HB, Kim WH et al (2019) 2-Aminoadipic acid (2-AAA) as a potential biomarker for insulin resistance in childhood obesity. Sci Rep 9:1–10. https://doi.org/10.1038/s41598-019-49578-z
Lefaki M, Papaevgeniou N, Chondrogianni N (2017) Redox regulation of proteasome function. Redox Biol 13:452–458. https://doi.org/10.1016/j.redox.2017.07.005
Levine RL (2002) Carbonyl modified proteins in cellular regulation, aging, and disease. Free Radic Biol Med 32:790–796. https://doi.org/10.1016/S0891-5849(02)00765-7
Li ZL, Mo L, Le G, Shi Y (2014) Oxidized casein impairs antioxidant defense system and induces hepatic and renal injury in mice. Food Chem Toxicol 64:86–93. https://doi.org/10.1016/j.fct.2013.10.039
Li B, Mo L, Yang Y et al (2019) Processing milk causes the formation of protein oxidation products which impair spatial learning and memory in rats. RSC Adv 9:22161–22175. https://doi.org/10.1039/c9ra03223a
Li F, Wu X, Wu W (2021a) Effects of oxidative modification by malondialdehyde on the in vitro digestion properties of rice bran protein. J Cereal Sci 97:103158. https://doi.org/10.1016/j.jcs.2020.103158
Li YY, Yaylayan V, Palin M-F et al (2021b) Protective effects of dietary carnosine during in-vitro digestion of pork differing in fat content and cooking conditions. J Food Biochem 45:e13624. https://doi.org/10.1111/jfbc.13624
Lin HM, Qi XE, Shui SS et al (2021) Label-free proteomic analysis revealed the mechanisms of protein oxidation induced by hydroxyl radicals in whiteleg shrimp (*Litopenaeus vannamei*)

muscle. Food Funct 12:4337–4348. https://doi.org/10.1039/d1fo00380a
Luna C, Estévez M (2018) Oxidative damage to food and human serum proteins: radical-mediated oxidation vs. glyco-oxidation. Food Chem 267:111–118. https://doi.org/10.1016/j.foodchem.2017.06.154
Luna C, Estévez M (2019) CEFormation of allysine in β-lactoglobulin and myofibrillar proteins by glyoxal and methylglyoxal: impact on water-holding capacity and in vitro digestibility. Food Chem 271:87–93. https://doi.org/10.1016/j.foodchem.2018.07.167
Luna C, Arjona A, Dueñas C, Estevez M (2021) Allysine and α-aminoadipic acid as markers of the glyco-oxidative damage to human serum albumin under pathological glucose concentrations. Antioxidants 10:1–14. https://doi.org/10.3390/antiox10030474
Lund MN (2021) Reactions of plant polyphenols in foods: Impact of molecular structure. Trends Food Sci Technol 112:241–251. https://doi.org/10.1016/j.tifs.2021.03.056
Ma J, Wang X, Li Q et al (2021) Oxidation of myofibrillar protein and crosslinking behavior during processing of traditional air-dried yak (*Bos grunniens*) meat in relation to digestibility. Lwt 142:110984. https://doi.org/10.1016/j.lwt.2021.110984
Maisonneuve E, Ducret A, Khoueiry P et al (2009) Rules governing selective protein carbonylation. PLoS One 4:e7269. https://doi.org/10.1371/journal.pone.0007269
Malheiros JM (2019) Influence of oxidative damage to proteins on meat tenderness using a proteomics approach. Meat Sci 148:64–71. https://doi.org/10.1016/j.meatsci.2018.08.016
Mello CF, Sultana R, Piroddi M, Cai J, Pierce WMJ, Klein B, Butterfield DA (2007) Acrolein induces selective protein carbonylation in synaptosomes. Neuroscience 147(3):674–679. https://doi.org/10.1016/j.neuroscience.2007.04.003
Meyer B, Baum F, Vollmer G, Pischetsrieder M (2012) Distribution of protein oxidation products in the proteome of thermally processed milk. J Agric Food Chem 60:7306–7311. https://doi.org/10.1021/jf301666r
Mitra B, Lametsch R, Akcan T, Ruiz-Carrascal J (2018) Pork proteins oxidative modifications under the influence of varied time-temperature thermal treatments: a chemical and redox proteomics assessment. Meat Sci 140:134–144. https://doi.org/10.1016/j.meatsci.2018.03.011
Morzel M, Gatellier P, Sayd T et al (2006) Chemical oxidation decreases proteolytic susceptibility of skeletal muscle myofibrillar proteins. Meat Sci 73:536–543. https://doi.org/10.1016/j.meatsci.2006.02.005
Nieva-Echevarría B, Goicoechea E, Guillén MD (2020) Food lipid oxidation under gastrointestinal digestion conditions: a review. Crit Rev Food Sci Nutr 60:461–478. https://doi.org/10.1080/10408398.2018.1538931
Niu X, Wang X, Han Y et al (2019) Influence of malondialdehyde-induced modifications on physicochemical and digestibility characteristics of whey protein isolate. J Food Biochem 43:1–9. https://doi.org/10.1111/jfbc.13041
Oliver CN, Ahn BW, Moerman EJ et al (1987) Age-related changes in oxidized proteins. J Biol Chem 262:5488–5491. https://doi.org/10.1016/s0021-9258(18)45598-6
Öztürk-Kerimoğlu B, Nacak B, Özyurt VH, Serdaroğlu M (2019) Protein oxidation and in vitro digestibility of heat-treated fermented sausages: How do they change with the effect of lipid formulation during processing? J Food Biochem 43:e13007. https://doi.org/10.1111/jfbc.13007
Özyurt H, Luna C, Estévez M (2016) Redox chemistry of the molecular interactions between tea catechins and human serum proteins under simulated hyperglycemic conditions. Food Funct 7:1390–1400. https://doi.org/10.1039/c5fo01525a
Requena JR, Chao CC, Levine RL, Stadtman ER (2001) Glutamic and aminoadipic semialdehydes are the main carbonyl products of metal-catalyzed oxidation of proteins. Proc Natl Acad Sci USA 98:69–74. https://doi.org/10.1073/pnas.98.1.69
Roldan M, Antequera T, Armenteros M, Ruiz J (2014) Effect of different temperature-time combinations on lipid and protein oxidation of sous-vide cooked lamb loins. Food Chem 149:129–136. https://doi.org/10.1016/j.foodchem.2013.10.079
Rowe LJ, Maddock KR, Lonergan SM, Huff-Lonergan E (2004) Influence of early *postmortem* protein oxidation on beef quality. J Anim Sci 82:785–793. https://doi.org/10.1093/ansci/82.3.785
Ruvalcaba-Márquez JC, Álvarez-Ruíz P, Zenteno-Savín T et al (2021) Performance, immune response, and oxidative stress parameters of *Litopenaeus vannamei* fed diets containing varying carbohydrate/protein, lipid/protein, and energy/protein ratios. Aquac Rep 21:100771. https://doi.org/10.1016/j.aqrep.2021.100771
Rysman T, Van Hecke T, Van Poucke C et al (2016) Protein oxidation and proteolysis during storage and in vitro digestion of pork and beef patties. Food Chem 209:177–184. https://doi.org/10.1016/j.foodchem.2016.04.027
Sante-Lhoutellier V, Aubry L, Gatellier P (2007) Effect of oxidation on in vitro digestibility of skeletal muscle myofibrillar proteins. J Agric Food Chem 55:5343–5348. https://doi.org/10.1021/jf070252k
Sayd T, Chambon C, Laville E et al (2012) Early *post-mortem* sarcoplasmic proteome of porcine muscle related to lipid oxidation in aged and cooked meat. Food Chem 135:2238–2244. https://doi.org/10.1016/j.foodchem.2012.07.079
Semedo Tavares WP, Dong S, Yang Y et al (2018) Influence of cooking methods on protein modification and in vitro digestibility of hairtail (*Thichiurus lepturus*) fillets. Lwt 96:476–481. https://doi.org/10.1016/j.lwt.2018.06.006
Sharma A, Weber D, Raupbach J et al (2020) Advanced glycation end products and protein carbonyl levels in plasma reveal sex-specific differences in Parkinson's and Alzheimer's disease. Redox Biol 34:101546. https://doi.org/10.1016/j.redox.2020.101546
Sies H, Stahl W, Sevanian A (2005) Recent advances in nutritional sciences nutritional, dietary and postprandial. J Nutr 135:969–972
Silva FAP, Ferreira VCS, Madruga MS, Estévez M (2016) Effect of the cooking method (grilling, roasting, frying and sous-vide) on the oxidation of thiols, tryptophan, alkaline amino acids and protein cross-linking in jerky chicken. J Food Sci Technol 53:3137–3146. https://doi.org/10.1007/s13197-016-2287-8
Sobral MMC, Casal S, Faria MA et al (2020) Influence of culinary practices on protein and lipid oxidation of chicken meat burgers during cooking and in vitro gastrointestinal digestion. Food Chem Toxicol 141:111401. https://doi.org/10.1016/j.fct.2020.111401
Soglia F, Petracci M, Ertbjerg P (2016) Novel DNPH-based method for determination of protein carbonylation in muscle and meat. Food Chem 197:670–675. https://doi.org/10.1016/j.foodchem.2015.11.038
Soladoye OP, Juárez ML, Aalhus JL et al (2015) Protein oxidation in processed meat: mechanisms and potential implications on human health. Compr Rev Food Sci Food Saf 14:106–122. https://doi.org/10.1111/1541-4337.12127
Soladoye OP, Shand P, Dugan MER et al (2017) Influence of cooking methods and storage time on lipid and protein oxidation and heterocyclic aromatic amines production in bacon. Food Res Int 99:660–669. https://doi.org/10.1016/j.foodres.2017.06.029
Stadtman ER, Levine RL (2003) Free radical-mediated oxidation of free amino acids and amino acid residues in proteins. Amino Acids 25:207–218. https://doi.org/10.1007/s00726-003-0011-2
Steppeler C, Haugen J-E, Rødbotten R, Kirkhus B (2016) Formation of malondialdehyde, 4-hydroxynonenal, and 4-hydroxyhexenal

during in vitro digestion of cooked beef, pork, chicken, and salmon. J Agric Food Chem 64:487–496. https://doi.org/10.1021/acs.jafc.5b04201

Timm-Heinrich M, Eymard S, Baron CP et al (2013) Oxidative changes during ice storage of rainbow trout (*Oncorhynchus mykiss*) fed different ratios of marine and vegetable feed ingredients. Food Chem 136:1220–1230. https://doi.org/10.1016/j.foodchem.2012.09.019

Trnková L, Držata J, Boušová I (2015) Oxidation as an important factor of protein damage: implications for Maillard reaction. J Biosci 40:419–439. https://doi.org/10.1007/s12038-015-9523-7

Tsikas D (2017) Assessment of lipid peroxidation by measuring malondialdehyde (MDA) and relatives in biological samples: analytical and biological challenges. Anal Biochem 524:13–30. https://doi.org/10.1016/j.ab.2016.10.021

Utrera M, Estévez M (2012) Oxidation of myofibrillar proteins and impaired functionality: underlying mechanisms of the carbonylation pathway. J Agric Food Chem 60:8002–8011. https://doi.org/10.1021/jf302111j

Utrera M, Morcuende D, Rodríguez-Carpena JG, Estévez M (2011) Fluorescent HPLC for the detection of specific protein oxidation carbonyls—α-aminoadipic and γ-glutamic semialdehydes—in meat systems. Meat Sci 89:500–506. https://doi.org/10.1016/j.meatsci.2011.05.017

Van Hecke T, Basso V, De Smet S (2018) Lipid and protein oxidation during in vitro gastrointestinal digestion of pork under *Helicobacter pylori* gastritis conditions. J Agric Food Chem 66:13000–13010. https://doi.org/10.1021/acs.jafc.8b04335

Van Hecke T, Goethals S, Vossen E, De Smet S (2019) Long-Chain $n-3$ PUFA content and $n-6/n-3$ PUFA ratio in mammal, poultry, and fish muscles largely explain differential protein and lipid oxidation profiles following in vitro gastrointestinal digestion. Mol Nutr Food Res 63:1–12. https://doi.org/10.1002/mnfr.201900404

Van Hecke T, Vossen E, Goethals S et al (2021) In vitro and in vivo digestion of red cured cooked meat: oxidation, intestinal microbiota and fecal metabolites. Food Res Int 142:110203. https://doi.org/10.1016/j.foodres.2021.110203

Verrastro I, Pasha S, Jensen KT et al (2015) Mass spectrometry-based methods for identifying oxidized proteins in disease: advances and challenges. Biomolecules 5:378–411. https://doi.org/10.3390/biom5020378

Villaverde A, Estévez M (2013) Carbonylation of myofibrillar proteins through the maillard pathway: effect of reducing sugars and reaction temperature. J Agric Food Chem 61:3140–3147. https://doi.org/10.1021/jf305451p

Villaverde A, Morcuende D, Estévez M (2014) Effect of curing agents on the oxidative and nitrosative damage to meat proteins during processing of fermented sausages. J Food Sci 79:C1331–C1342. https://doi.org/10.1111/1750-3841.12481

Wang TJ, Ngo D, Psychogios N et al (2013) 2-Aminoadipic acid is a biomarker for diabetes risk. J Clin Invest 123:4309–4317. https://doi.org/10.1172/JCI64801

Wang Z, He Z, Gan X, Li H (2018) Interrelationship among ferrous myoglobin, lipid and protein oxidations in rabbit meat during refrigerated and superchilled storage. Meat Sci 146:131–139. https://doi.org/10.1016/j.meatsci.2018.08.006

Wang Y, Wang J, Wang S et al (2019a) Modification of glutenin and associated changes in digestibility due to methylglyoxal during heat processing. J Agric Food Chem 67:10734–10743. https://doi.org/10.1021/acs.jafc.9b04337

Wang Z, He Z, Emara AM et al (2019b) Effects of malondialdehyde as a byproduct of lipid oxidation on protein oxidation in rabbit meat. Food Chem 288:405–412. https://doi.org/10.1016/j.foodchem.2019.02.126

Wang Z, He Z, Zhang D et al (2021) The effect of linalool, limonene and sabinene on the thermal stability and structure of rabbit meat myofibrillar protein under malondialdehyde-induced oxidative stress. Lwt 148:111707. https://doi.org/10.1016/j.lwt.2021.111707

Wong CM, Bansal G, Marcocci L, Suzuki YJ (2012) Proposed role of primary protein carbonylation in cell signaling. Redox Rep 17:90–94. https://doi.org/10.1179/1351000212Y.0000000007

Wong CM, Marcocci L, Das D et al (2013) Mechanism of protein decarbonylation. Free Radic Biol Med 65:1126–1133. https://doi.org/10.1016/j.freeradbiomed.2013.09.005

Wu Y, Dong L, Wu Y et al (2021) Effect of methylglyoxal on the alteration in structure and digestibility of α-lactalbumin, and the formation of advanced glycation end products under simulated thermal processing. Food Sci Nutr 9:2299–2307. https://doi.org/10.1002/fsn3.2211

Xiong Y (2000) Protein oxidation and implications for muscle food quality. In: Decker E, Faustman C, López-Bote CJ (eds) Antioxidants in muscle foods: nutritional strategies to improve quality. Jon Wiley and Sons, Hoboken, pp 85–111 (**ref. 63**)

Xiong YL, Guo A (2021) Animal and plant protein oxidation: chemical and functional property significance. Foods 10:40. https://doi.org/10.3390/foods10010040

Xu J, Shi GP (2014) Vascular wall extracellular matrix proteins and vascular diseases. Biochim Biophys Acta 1842:2106–2119. https://doi.org/10.1016/j.bbadis.2014.07.008

Yu D, Zhao Y, Li T et al (2018) Effect of electrochemical modification on the structural characteristics and emulsion storage stability of soy protein isolate. Process Biochem 75:166–172. https://doi.org/10.1016/j.procbio.2018.10.001

Zhang X, Lu P, Xue W et al (2017) An evaluation of heat on protein oxidation of soy protein isolate or soy protein isolate mixed with soybean oil in vitro and its consequences on redox status of broilers at early age. Asian-Australas J Anim Sci 30:1135–1142. https://doi.org/10.5713/ajas.16.0683

Zhang D, Li H, Wang Z et al (2020) Effects of in vitro oxidation on myofibrillar protein charge, aggregation, and structural characteristics. Food Chem 332:127396. https://doi.org/10.1016/j.foodchem.2020.127396

Zhang L, Li Q, Hong H, Luo Y (2021) Tracking structural modifications and oxidative status of myofibrillar proteins from silver carp (*Hypophthalmichthys molitrix*) fillets treated by different stunning methods and in vitro oxidizing conditions. Food Chem 365:130510. https://doi.org/10.1016/j.foodchem.2021.130510

Zhao Y, Kong H, Zhang X et al (2019) The effect of Perilla (*Perilla frutescens*) leaf extracts on the quality of surimi fish balls. Food Sci Nutr 7:2083–2090. https://doi.org/10.1002/fsn3.1049

Zhao X, Xu X, Zhou G (2021) Covalent chemical modification of myofibrillar proteins to improve their gelation properties: a systematic review. Compr Rev Food Sci Food Saf 20:924–959. https://doi.org/10.1111/1541-4337.12684

Zhou F, Sun W, Zhao M (2015) Controlled formation of emulsion gels stabilized by salted myofibrillar protein under malondialdehyde (MDA)-induced oxidative stress. J Agric Food Chem 63:3766–3777. https://doi.org/10.1021/jf505916f

Publisher's Note Springer Nature remains neutral with regard to jurisdictional claims in published maps and institutional affiliations.

Food Chemistry 423 (2023) 136314

Contents lists available at ScienceDirect

Food Chemistry

journal homepage: www.elsevier.com/locate/foodchem

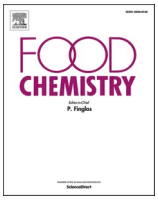

Deciphering the underlying mechanisms of the oxidative perturbations and impaired meat quality in Wooden breast myopathy by label-free quantitative MS-based proteomics

Leila M. Carvalho [a], Thayse C. Rocha [a], Josué Delgado [b], Silvia Díaz-Velasco [c], Marta S. Madruga [a], Mario Estévez [c,*]

[a] Postgraduate Program in Food Science and Technology. Department of Food Engineering, Federal University of Paraiba, João Pessoa, Paraíba, Brazil
[b] Higiene y Seguridad Alimentaria, Instituto Universitario de Investigación de Carne y Productos Cárnicos, Facultad de Veterinaria, Universidad de Extremadura, Avda. de las Ciencias s/n, 10003 Cáceres, Spain
[c] Tecnología de los Alimentos, Instituto Universitario de Investigación de Carne y Productos Cárnicos, Facultad de Veterinaria, Universidad de Extremadura, Avda. de las Ciencias s/n, 10003 Cáceres, Spain

ARTICLE INFO

Keywords:
Wooden-breast
Oxidative stress
Proteomics
Molecular mechanisms

ABSTRACT

The study aimed to investigate biochemical mechanisms occurred in Wooden breast (WB) chicken meat, with attention to the impact on meat quality. Commercial chicken breasts were classified as Normal (N, n = 12), WB-M (moderate degree; focal hardness on cranial region, n = 12) and WB-S (severe degree; extreme and diffused hardness over the entire surface, n = 12). Samples were analyzed for physico-chemical properties, oxidative damage to lipids and proteins, and discriminating sarcoplasmic proteins by using a Q-Exactive mass spectrometer. WB meat presented impaired composition and functionality and higher levels of lipid and protein oxidation markers than N meat. The proteomic profile of WB-S presents a dynamic regulation of the relevant proteins involved in redox homeostasis, carbohydrate, protein and lipid metabolisms. Proteomics results demonstrate that the physiological and metabolic processes of muscles affected by WB myopathy are involved in combating the inflammatory process and in repairing the damaged tissue by oxidative stress.

1. Introduction

Wooden breast (WB) is a disorder that affects the breast muscle of rapidly growing birds. This disorder was provoked by the increased demand and consumption of chicken meat in the last decades, which pressured production systems to maximize meat production through intense genetic selection and improved efficiency of animal feed (Petracci et al. 2019). Excessive muscle hardness and histopathological alterations such as myofibrillar degeneration, lipidosis, fibrosis, and necrosis are inherent features of this myopathy (Sihvo, Immonen & Puolanne, 2014; Sihvo et al., 2017).

Muscles affected by WB myopathy exhibit deterioration in nutritional quality (i.e. protein, essential amino acids, unsaturated fatty acids) (Thanatsang et al. 2020; Liu et al., 2022), technological properties (i.e. water holding capacity) (Zhang et al., 2020), and sensorial properties (texture, appearance, color) (Dalle Zotte et al., 2017). Besides that, the acceptance and purchase intention of these meats by consumers is compromised (Rocha et al., 2022).

Oxidative stress seems to play a central role in the mechanisms behind WB pathology (Petracci et al., 2019). Previous studies focused on metabolomics and RNA-sequencing analyses, established metabolic pathways and some specific genes expression that potentially contribute to oxidative stress in WB muscle (Mutryn, et al., 2015; Abasht et al., 2016). Xing et al. (2021) observed altered levels of reactive oxygen species, oxidative products and antioxidant endogenous defenses in liver of animals affected, with all of these features being typical of mitochondrial dysfunction. On the other hand, Hasegawa et al. (2021) observed accumulation of lipofuscin in WB muscle, which is recognized as one of the indicators of oxidative stress. Several studies found increased lipid and protein markers (i.e. TBARS, protein carbonyls, free thiols) in breast meat of birds affected by WB disorder (Thanatsang et al., 2020; Hasegawa et al., 2021; Li et al., 2022). In addition, altered levels of antioxidant endogenous enzymes, such as catalase, superoxide dismutase, glutathione peroxidase, and glutathione S-transferase, are

* Corresponding author.
E-mail address: mariovet@unex.es (M. Estévez).

https://doi.org/10.1016/j.foodchem.2023.136314
Received 13 February 2023; Received in revised form 25 April 2023; Accepted 3 May 2023
Available online 6 May 2023
0308-8146/© 2023 The Authors. Published by Elsevier Ltd. This is an open access article under the CC BY-NC-ND license (http://creativecommons.org/licenses/by-nc-nd/4.0/).

associated with imbalanced redox in WB meats (Xing et al., 2021). Proteomics has demonstrated to be an efficient tool to unveil physiologic mechanisms beyond breast myopathies such as white striping (Carvalho et al., 2020a). This technique allows the identification and level assessment of multiple protein, directly responsible for the phenotype of the muscle.

Given the remarkable significance of oxidative stress in chicken affected by WB myopathy, this study was designed to provide further insight into the biochemical and pathophysiological mechanisms involved in the onset and severity of the WB myopathy that drives the impairment of the chicken breast quality traits. To fulfil this objective, normal and WB meats were compared in terms quality traits, lipid and protein oxidation markers and proteome of sarcoplasmic proteins using a label-free mass spectromic-based proteomics approach. A better comprehension of the causes of the redox impairment in WB meats would enable the application of targeted prevention and alleviation strategies.

2. Material and methods

2.1. Samples, identification and classification

Thirty-six chicken breasts were collected from a commercial poultry slaughterhouse located in Paraíba, Brazil. The breasts used in the research were from birds slaughtered according to the "Regulation of Industrial and Sanitary Inspection of Products of Animal Origin (RIISPOA)" and "Technical Regulation of Technological and Hygienic-Sanitary Inspection of Poultry Meat" of the National Standards of Brazil. More specifically, the birds (Cobb genetic line), were stunned by electronarcosis prior to slaughter at 42–44 days of age. Samples were allocated to one of the following three groups based on the criteria described by Carvalho et al. (2020b): Normal ([N] *Pectoralis major* muscle without hardened areas on muscle surface), WB-moderate ([WB-M] *P. major* muscle with focal hardness on cranial region with/without petechiae), and WS-severe ([WB-S] *P. major* muscle with extreme and diffused hardness with petechiae). Twelve chicken breasts (n = 12) for each abovementioned group were collected and used for the present study.

2.2. Weight and muscle morphometry

After removing the skin, cartilage and bones that remained after deboning the chicken carcass, the breasts were weighed on a semi analytical balance (CE 2000, Marte Científica, Santa Rita do Sapucaí, Minas Gerais, Brazil) and subjected to geometrical evaluation with a digital caliper (684132, Lee Tools, Santo André, São Paulo, Brazil). Morphometric measurements of *P. major* muscle were determined according to Xing et al. (2020). Length was measured in the longest dimension of the muscle, whereas width was measured from the longest distance from side-to-side in the middle of the muscle. Top height was measured at the highest point in the cranial part, middle height was measured at the midpoint of the breast muscle length, and the bottom height was measured as the vertical distance from the caudal area by 25 mm in the dorsal direction.

2.3. Physical properties

pH was measured 24 h *post-mortem* by direct electrode insertion on the cranial area using a contact pH meter system (Testo 205, Testo do Brasil Instrumentos de Medição Ltda, Campinas, São Paulo, Brazil), according to the methodology proposed by Boulianne & King (1998). Color was measured using a Minolta colorimeter (Chroma Meter CR-400, Minolta Co., Osaka, Japan) in the CIELAB system (L*=lightness; a*=redness, and b*=yellowness) according to Carvalho et al. (2020a). The a*/b* ratio was used to establish the proportion between oxymyoglobin (MbO2) and metmyoglobin (MMb) (Olivo et al, 2001). Cooking loss (CL) was determined as described by Carvalho et al. (2017). Briefly, 5 g of breast meat were weighed, then the meat was cooked in a boiling water bath (100 °C) for 30 min and after cooking it was weighed again. Hardness was performed as described by Carvalho et al. (2020a) using a texturometer (TA.TXplus texturometer, Stable Micro Systems, Godalming, Surrey, UK). Raw samples were cut to size 25 × 25 × 10 mm (length × width × thickness, respectively). The samples were compressed twice to 50% of their original height with a cylindrical probe (5.08 cm diameter) at a test speed of 50 mm min^{-1}.

2.4. Chemical composition

Protein, moisture, ash and collagen contents were analyzed in Normal, WB-M and WB-S meats, according to the Association of Official Analytical Chemists (AOAC, 2000) described in items n° 928.08, 950.46, 920.153 and 920.26, respectively. The fat content was determined according to the methodology described by Folch et al. (1957).

2.5. Oxidative damage

2.5.1. Tbars

Lipid oxidation was determined according to the thiobarbituric acid-reactive substances (TBARS) method described by Ganhão et al. (2011). TBARS were measured at 532 nm using a spectrophotometer (Shimadzu UV-1800, Japan). A blank containing 2 mL of 3.86% perchloric acid and 2 mL of TBA reagent was used. The results from the samples were plotted against a standard curve prepared with concentrations of tetraethoxypropane (TEP) that ranged from 0.0583 to 1.1650 μg TEP mL^{-1}. The results were expressed as mg malondialdehyde (MDA) kg^{-1} breast meat. TBARS measurement was carried out in the raw samples and in the cooked samples after the determination of cooking loss.

2.5.2. Protein carbonyls

Protein oxidation was measured by the reaction of carbonyl groups with 2,4-dinitrophenylhydrazine (DNPH) as described by Ganhão et al. (2010), with minor modifications. Protein concentration was calculated from the absorption at 280 nm using BSA as standard (0.06 to 3 mg/mL). The amount of carbonyls was expressed as nmol of carbonyl per mg of protein (nmol carbonyls mg $protein^{-1}$) using an absorption coefficient of 21.0 nM^{-1} cm^{-1} at 370 nm for protein hydrazones. Total carbonyl content was carried out in the raw samples and in the cooked samples after the determination of cooking loss.

2.5.3. Free thiols and disulphide bonds

Free thiols were analyzed following the methodology of Rysman et al. (2014). The thiol concentration was calculated based on a standard five points curve ranging from 2.5 to 500 μM cysteine in 6 M GuHCl in 1 M citric acid buffer (pH 4.5). Total thiols were determined with 4,4′-dithiodipyridine (4-DPS) as reducing agent. The disulphide content was calculated as the difference between total and free thiols divided by two.

2.6. Proteomic approach

Protein extraction. For the proteomic analysis, only N and WB-S were processed. Sarcoplasmic proteins fractions were extracted according to Zhu et al. (2011) with some modification. A total of 5 breasts from different animals for each condition were used. About 20 g of samples muscle was mixed with 80 mL of buffer containing 10 mM sodium phosphate, 0.1 N NaCl, 2 mM $MgCl_2$, 1 mM EGTA, pH 7.0, at 1200 g for 30 s. The homogenate was centrifuged at 600 g for 15 min at 4 °C, and the supernatant (non-pelleted solution) was decanted and saved. The pellet was resuspended in 80 mL of the same buffer, homogenized in vortex and centrifuged at the same setting. The supernatants were combined after centrifugation to obtain the final extract of sarcoplasmic proteins (SP). Protein content was determined in diluted SP extract (50 μL SP extract to 950 μL buffer) using Bradford method.

Label-free quantitative proteomic analyses. The preparation of chicken samples for proteomic analyses was carried out as follows. Briefly, 50 μg of from the sarcoplasmic fraction were partially run in SDS-PAGE to be picked up and undergone to dithiothreitol reduction and iodoacetamide-mediated alkylation. Subsequently, sequencing-grade trypsin (Promega, USA) and ProteaseMAX surfactant (Promega) were added to the gel pieces and incubated for 1 h at 50 °C, following manufactureŕs instructions. A Q-Exactive Plus mass spectrometer coupled to a Dionex Ultimate 3000 RSLCnano (Thermo Scientific) analyzed around 0.75 μg from each digest. The gradient used ranged from 8 to 30% B (A: 0.1% formic acid (FA), B: acetonitrile, 0.1% FA) for 4 h on an Acclaim PepMap RSLC C18, 2 μm, 100 Å, 75 μm i.d. × 50 cm, nanoViper column (Thermo Scientific), thermostated at 45 °C in the oven compartment. Data were collected using a Top15 method for MS/MS scans (Delgado et al., 2019, 2017; Dolan et al., 2014). Comparative proteome abundance and data analysis was carried out by using MaxQuant software (Version 1.6.15.0; www. maxquant.org/downloads.htm), and Perseus (Version 1.6.14.0) to organize the data and perform statistical analysis. Carbamidomethylation of cysteines was set as a fixed modification; oxidation of methionines and acetylation of *N*-terminals were set as variable modifications. Database searching was performed against *Gallus gallus* protein database (downloaded December 2018, https://www.uniprot.org). The maximum peptide/protein false discovery rates (FDR) were set at 1% based on comparison to a reverse database. The LFQ algorithm was used to generate normalized spectral intensities and infer relative protein abundance. Proteins were identified with at least two peptides, and those proteins that matched to a contaminant database or the reverse database were removed, and proteins were only retained in final analysis if detected in at least three replicates from at least one condition. Quantitative analysis was performed using a *t*-test to compare treatments to the control. All proteins with $p < 0.05$ were included in the quantitative results. The qualitative analysis was also performed to detect proteins that were found in at least three replicates of a given WS level group but undetectable in the comparison group. The enrichment analyses were carried out using ClueGO software (v. 2.5.6). The Kappa score was set at 0.4. value and the *p*-value was analysed by Bonferroni step down and stablished at $p \leq 0.05$.

2.7. Statistical analysis

Data from physical-chemical composition and oxidative damage were analyzed by ANOVA. The means were compared using Tukey's test, using the different breast (Normal, WB-M, WB-S) as main factor. Statistical analyses were performed using XLSTAT software (version 2014.5.03, Addinsoft, New York, USA).

3. Results and discussion

3.1. Morphometry and physico-chemical properties

The results from the morphometric and physico-chemical analyses of chicken breasts are shown in Table 1. The occurrence of WB myopathy influenced weight and all morphometric parameters, mainly in breasts with severe degree, except the width ($p = 0.0628$), The mean weight was significantly higher ($p < 0.0001$) in WB samples (WB-S: 301.19 g, WB-M: 258.19 g) compared to Normal meat (232.25 g). The greatest length and bottom height (caudal area) of the breast was only observed in WB-S compared to Control (means 18.49 and 17.08 cm, respectively). In addition, the increase in the top (17 and 24% for WB-M and WS-S, respectively) and middle (27 and 33% for WB-M and WS-S, respectively) height was observed in both degrees of WB, compared to N. Similar results for weight and morphometric parameters were observed by other authors (Xing et al., 2020; Geronimo, Prudencio & Soares, 2022). Increased *Pectoralis major* muscle weight is result of genetic selection for fast growth and high yields (Petracci et al., 2015). The morphometric changes observed in WB meat can be attributed to the increase and growth of muscle cells. WB myopathy is characterized by histopathological features, including hypertrophy (Hosatani et al., 2020). According to Sihvo et al. (2014) and Sihvo et al. (2017), WB presents greater discrepancy in the muscle fibers, such as variability in shape, size and diameter.

Table 1
Morphometric and physico-chemical properties of chicken breast affected by the WB myopathy in the moderate and severe degrees.

Parameter	N	WB-M	WB-S	P-value
Weight[1]	232.25 ± 25.70^{c}	258.19 ± 14.53^{b}	301.01 ± 19.68 ^{a}	<0.0001
Length[2]	17.49 ± 0.83^{b}	17.45 ± 0.93^{b}	18.49 ± 0.58 ^{a}	0.0098
Width[2]	7.76 ± 0.48	7.72 ± 0.28	7.20 ± 0.80	0.0628
Top height[2]	28.97 ± 4.69^{b}	33.89 ± 3.04 ^{a}	35.98 ± 2.66 ^{a}	0.0007
Middle height[2]	22.40 ± 3.45^{b}	28.39 ± 3.04 ^{a}	29.68 ± 5.12 ^{a}	000,012
Bottom height[2]	12.28 ± 2.54^{b}	12.42 ± 1.65^{b}	17.08 ± 1.38 ^{a}	<0.0001
pH	5.78 ± 0.15	5.86 ± 0.16	5.86 ± 0.11	0.3578
L*	58.75 ± 2.72^{b}	59.35 ± 1.98^{b}	62.04 ± 1.69 ^{a}	0.0018
a*	1.01 ± 0.18^{b}	1.18 ± 0.30 ^{ab}	1.43 ± 0.32 ^{a}	0.0305
b*	2.98 ± 0.70^{c}	4.54 ± 1.00^{b}	6.83 ± 0.77 ^{a}	<0.0001
a*/b*	0.35 ± 0.02 ^{a}	0.27 ± 0.04^{b}	0.21 ± 0.02^{c}	<0.0001
Cooking Loss[3]	30.09 ± 4.72^{b}	34.26 ± 2.95 ^{ab}	36.74 ± 4.45 ^{a}	0.0044
Hardness[4]	35.99 ± 8.18^{b}	67.74 ± 15.57 ^{a}	74.70 ± 20.67 ^{a}	<0.0001
Moisture[5]	75.56 ± 0.78^{b}	76.16 ± 0.73 ^{ab}	76.58 ± 0.81 ^{a}	0.0128
Protein[5]	21.75 ± 0.89 ^{a}	20.50 ± 0.88^{b}	19.51 ± 1.11^{b}	<0.0001
Lipid[5]	2.24 ± 0.26^{b}	2.85 ± 0.64 ^{a}	3.24 ± 0.45 ^{a}	<0.0001
Ash[5]	1.00 ± 0.06^{b}	1.02 ± 0.09 ^{ab}	1.10 ± 0.09 ^{a}	0.0340
Collagen[5]	0.40 ± 0.06^{b}	0.48 ± 0.04 ^{a}	0.48 ± 0.04 ^{a}	0.0018

Lowercase letters on the same line differ significantly by Tukey's test ($p < 0.05$).
[1] Results expressed as g.
[2] Results expressed as cm.
[3] Results expressed as percentage.
[4] Results expressed as Newton.
[5] Results expressed as g 100 g^{-1}.

Physical properties (Fig. 1) were influenced by the presence of the myopathy, except pH ($p = 0.3578$). Higher L* was observed in the severe grade of WB myopathy ($p = 0.0018$) compared to WB-M and N. The a* parameter was higher in WB-S ($p = 0.0305$), while the value in WB-M (1.18) did not differ significantly from WB-S (1.43) and N (1.01) meats. Furthermore, WB-S showed the highest b* (6.83), followed by WB-M (4.54) and N (2.98) ($p < 0.0001$). That is, the more severe the degree of myopathy, the more yellowish the color of the meat. The a*/b* ratio was lower in meat with myopathies, showing values 22.9% and 40% lower for WB-M and WB-S, respectively, compared to N. Cooking loss (CL) was significantly higher in WB-S compared to N, while WB-S showed intermediate levels. An increase of 67.7% and 107.6% was observed in the hardness of WB-M (67.74 Newtons) and WB-S (74.70 Newtons) respectively, compared to the hardness of the N meat (35.99 Newtons). Regarding chemical composition, WB meat differed from N. The protein content was significantly lower ($p < 0.05$) in WB-M and WB-S (20.50 and 19.51 g/100 g, respectively) compared to N (21.75 g/100 g). The opposite effect was observed in relation to the lipid content, since WB-S and WB-M meats had a higher lipid content compared to N (3.24, 2.85 and 2.24 g/100 g, respectively). Collagen content was 20 % higher in chicken meat with myopathy (0.48 g/100 g) than the value observed in N (0.40 g/100 g). In addition, WB-S showed significantly higher values of ash ($p = 0.0340$) and moisture ($p = 0.0128$) contents in relation to N, while WB-M showed intermediate values.

Another well-known feature of meat affected by WB is excessive stiffness as a result of severe fibrosis (Sihvo et al., 2014; Sihvo et al., 2017; Hosatani et al., 2020). This may be explained by increased collagen content on the damaged tissue of WB meats compared to N (Table 1). According to Xing et al. (2020), the increased distributing of

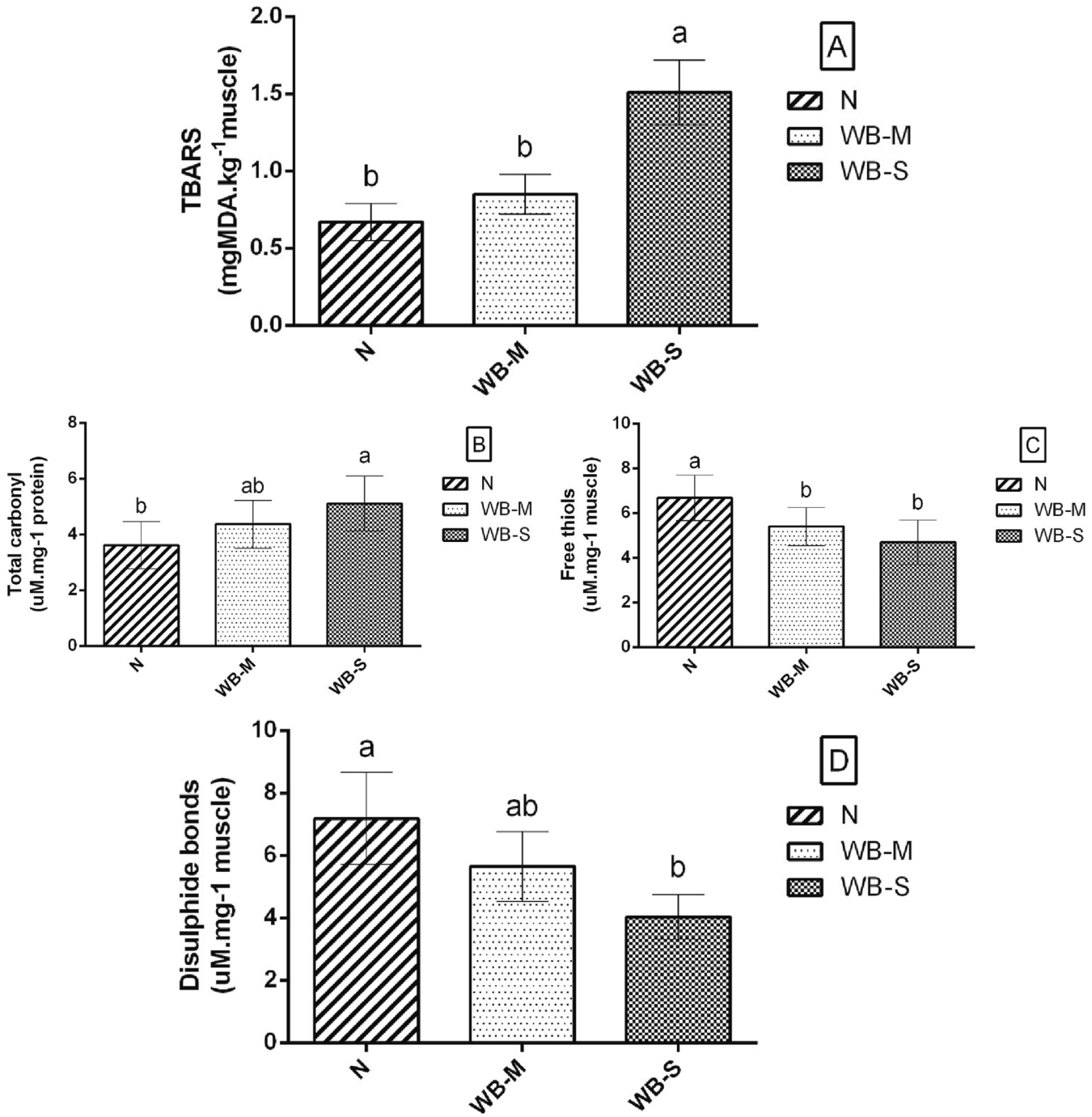

Fig. 1. Markers of oxidative damage in chicken breast affected by the WB myopathy in the moderate and severe degrees. Note: N: Normal breast meat; WB-M: Moderate degree of Wooden Breast myopathy; WB-S: Severe degree of Wooden Breast myopathy. A: Lipid oxidation marker; B-D: Protein oxidation markers. [a,b,c] Different lowercase letters differ significantly by Tukey's test ($p < 0.05$).

fibrotic proteins (collagen-I and fibrinectin) either in perimysium or endomysion is a pathological feature of WB meats. These authors observed a higher mRNA expression of collagen type I alpha 1 chain, collagen type III alpha 1 chain, fibronectin 1, α-smooth muscle actin, and connective tissue growth factor, in WB meats. Furthermore, Sihvo et al. (2014) highlighted that the collagenous structures resulting from fibrosis contributes to increasing the toughness of WB meat. In regards to the color displayed by breast meat, many researchers have reported that raw WB exhibited paler, reddish and yellowish color (Dalle Zotte et al. 2017; Zhuang & Bowker, 2018) than meat from unaffected birds. The most intense redness observed in WB meat may be due to the occurrence of petechiae (hemorrhagic lesion) on the muscle, especially in the more severe condition of this myopathy (Zhuang & Bowker, 2018). The presence of petechial hemorrhages in WB myopathy may be associated with circulatory failure due to muscle hypertrophy caused by the rapid growth rate of these birds (Clark & Velleman, 2016). Furthermore, the more yellowish coloration of WB meat may be related to more intense level of lipid oxidation. Xia et al., (2009) highlighted that the yellow pigments formation in meat are related to reactions between lipid oxidation products and the amine in proteins or in phospholipid head groups. Besides, the reduction in a*/b* ratio (Table 1) observed in affected meat by WB myopathy indicates increased discoloration of these meat, probably caused by myoglobin oxidation to metmyoglobin. According to Carvalho, Shimokomaki & Estévez (2017)

the change in poultry meat color is related to the impairment of redox homeostasis, leading to more intense levels of lipid and protein oxidation, thus promoting changes in pigments state of meat. In addition, WB meat presented poor cooking loss. Similar results were observed by Madruga et al. (2019) and Zhang et al. (2020). The greater susceptibility to protein oxidation (results discussed in the following section) observed in WB meats leads to severe protein modifications that may contribute to intense water loss during cooking. According to Bao and Ertbjerg (2019), changes in structure of muscle and their spatial arrangement resulting from protein oxidation may lead to protein cross-linking and affect protein net charges, influencing the muscle ability to retain water. Other factors that may be associated with greater CL is the reduced protein content and higher water content observed in WB meat (Table 1), both related to muscle degeneration. The increase in water content is linked to the fluid accumulation in muscle tissue due to inflammation process, while the decrease in protein content can be explained by the myofibrillar degeneration (Sihvo et al., 2014). According to Sihvo et al. (2017), the injured tissue due to myofibrillar degeneration is replaced by the deposition of fat and connective tissue, which explains the increase in lipid and collagen content, respectively, observed in this study (Table 1).

3.2. Oxidative damage

Results for the markers of oxidative damage measured in chicken breasts affected by WB myopathy are presented in Fig. 1. Breasts with a severe degree of myopathy had a significantly higher accretion of malondialdehyde and total protein carbonyls levels, which are products of lipid and protein oxidation, respectively (Estévez et al., 2019, 2021). However, in moderate degree of myopathy, it was not possible to observe a significant difference in these levels compared to N. The TBARS values (Fig. 1A) in WB-S (1.51 mg MDA kg^{-1} muscle) was 78% to 125% higher in compared to WS-M (0.85 mg MDA kg^{-1} muscle) and N (0.67 mg MDA kg^{-1} muscle), respectively. The total carbonyl content (Fig. 1B) was 41% higher in WB-S (5.11 μM mg-1 protein) compared to N (3.62 μM mg^{-1} protein). Lower levels of free thiols were observed in affected WB meats (4.70–5.40 μM thiols mg^{-1} muscle) compared to N (6.68 μM thiols mg^{-1} muscle) (Fig. 1C). In addition, there was less formation of disulfide bridges in the WB-S samples (Fig. 1D), with values being 44% lower compared to N (5.65 and 7.19 μM mg^{-1} muscle, respectively).

In general, the increased levels of lipid and protein oxidation in WB meat is directly related to the deterioration of its nutritional value (Thanatsang et al. 2020), formation of toxic products and off-flavor (Li et al., 2022), loss of color (Dalle Zotte, et al., 2017; Zhuang & Bowker, 2018), loss of essential amino acids (Thanatsang et al. 2020), decrease in the muscle's ability to retain water and negative impact on meat texture (Dalle Zotte, et al., 2017; Madruga et al., 2019; Zhang et al., 2020). In addition to compromising the quality and technological properties of WB meats, the highest level of TBARS and total carbonyl content and the lowest content of free thiols observed in this study is indicative of altered redox homeostasis, involving greater exposure of these meats to reactive oxygen species (ROS). Increased level of oxidation products in WB samples were also observed by Pan et al. (2021). Numerous factors can contribute to oxidative stress. Li et al. (2022) underline that high levels of lipid and protein oxidation may be caused by increased metabolic waste, poor blood and oxygen supply in the WB muscles. Furthermore, a potential genetic change can affect redox homeostasis by modifying the antioxidant activity of endogenous enzymes, thereby increasing ROS production in mitochondria (Lake & Abasht, 2020). Papah et al. (2018) observed up-regulation of genes fibromodulin (FMOD), activating transcription factor 3 (ATF3) and ankyrin repeat domain 1 (ANKRD1) related to stress/oxidative stress in WB. In addition, Pan et al. (2021) observed an increase in enzymes antioxidant activities and mitochondrial dysfunction in affected WB meats. Other factors that may explain the higher level of oxidative stress in WB meat could be related to lipidosis and the greater susceptibility to lipid peroxidation of fatty acids. According to Li et al. (2022), the change in lipid composition in affected WB meats is a result of intramuscular fat accumulation. Moreover, the higher content of monounsaturated and polyunsaturated fatty acids and lower content of saturated fatty acids were observed in breasts with WB myopathy (Gratta et al., 2023; Liu et al., 2022), with this modification making these meats more susceptible to lipid oxidation by ROS attack. Although the formation of disulfide bonds (DBs) is also an important marker of protein oxidation, WB meat had a reduced content compared to N meat. DBs are formed by the oxidation of two cysteine residues, and as a reduction in the content of free thiols in WB due to the oxidative protein process was observed, an increase in the formation of these crosslinks was expected. These results may be explained by two reasons: 1) The oxidation of thiols can form many products such as sulfenic, sulfinic and sulfonic acids and not just disulphide bonds (Schilter, 2017), and 2) The level of oxidation in the WB meats was so intense that the DBs could have been oxidized by singlet oxygen forming glutathionylated proteins (Jiang et al., 2021). In a previous study, we observed that most of the increased hardness in chicken breasts affected by breast myopathies was explained by the formation of crosslinking via Schiff base formation while disulphide bonds seemed to play a minor role (Da Rocha et al., 2020). Considering the role that sulphur-containing amino acids have on muscle redox status and meat quality, the depletion of these in chicken breasts affected by WB myopathy shows the sacrificial loss of these biomolecules as described in Estévez et al. (2020). This also suggests that dietary supplementation may be explored for trying to provide the affected muscle with antioxidant elements that seemed to be depleted/consumed in the pro-oxidative scenario caused during the onset of the myopathy.

3.3. Proteomics

Label-free comparative proteomic analyses were carried out for samples from every of the three WB conditions under study in this work. WB-S were compared to N in order to extract differentially abundant proteins (DAPs). Among these DAPs, one hundred and twenty-seven of them were found with differential relative abundance (fold change $\geq$ 1.20 or $\leq$ 0.82 and $p < 0.05$) in chicken breast muscles as affected by the occurrence of the myopathy (Table 2 and 3). Among these, 22 proteins were detected only in chicken breasts affected by severe WB myopathy, and 2 proteins only found in N breast meat. Furthermore, 67 proteins were observed in higher and 36 in lower abundance in WB-S. DAPs at higher amount in WB-S (Table 2) were mainly distributed by gene ontology enrichment in biological process (BP) related to 1) Response to oxidative stress, 2) Impaired myofibrillar protein homeostasis/function, 3) Hypoxia, inflammation and fibrosis, and 4) Apoptosis and necrosis. DEPs found in lower amount in WB-S (Fig. 1) were also distributed in BP related to 1) Failed energetic metabolism cell starvation, 2) Failed antioxidant response/depletion of antioxidant defenses, and 3) Apoptosis.

According to the results found, severe WB myopathy promotes changes in the proteome of chicken muscles. An increased concentration of proteins associated with lipid, protein and carbohydrate metabolism and endogenous antioxidant defense in the breast muscle of affected chickens were observed in this study.

Elevated protein concentration of Glutathione S-transferase (GSH-ST), Thioredoxin domain-containing protein (TXNDC), Glutathione peroxidase (GSH-PX) and peroxiredoxin-1 (PRDX1) was observed in affected birds. All of these proteins act to prevent or delay ROS-mediated oxidative damage to target tissues, playing an important role in maintaining redox homeostasis. GSH-ST enzymes have been previously related to greater susceptibility to oxidative stress-related diseases, including carcinogenesis (Strange, Spiteri, Ramachandran, & Fryer, 2001). According to Singhal et al. (2015), GSH-ST can reduce lipid hydroperoxides and may also detoxify numerous end-products of lipid peroxidation (LPO). TXNDC family proteins have a role in defense

Table 2
Proteins found in higher relative quantity in chicken breasts affected by severe WB myopathy.

Group	Protein	*p*-values	Log_2 Fold-change[1]	Biological function	Accession number
Response to oxidative stress	NTP_transferase domain-containing protein	–	S	GDP-mannose biosynthetic process	F1P574
	NmrA-like family domain-containing protein 1	–	S	Identical protein binding	A0A1D5PPI5
	Peptidase S1 domain-containing protein	–	S	Proteolysis	A0A1L1RUM8
	Non-specific serine/threonine protein kinase	–	S	Intracellular signal transduction, protein phosphorylation, negative regulation of potassium ion transmembrane transporter activity	E1C6W3; A0A3Q2U9U9
	Thioredoxin domain-containing protein	–	S	Protein folding	E1BSL7
	Glutathione S-transferase kappa	–	S	Glutathione metabolic process	F1N9G6
	Heat shock 27 kDa protein	0.0004	3.72	Protein refolding, negative regulation of oxidative stress-induced intrinsic apoptotic signaling pathway	F1P593; Q00649
	Chloride intracellular channel protein	0.0008	2.76	Chloride transport, negative regulation of ryanodine-sensitive calcium-release channel activity	Q5ZKI1
	Glutathione S-transferase	0.0329	2.53	Glutathione metabolic process, xenobiotic metabolic process	Q08392
	Ovotransferrin	0.0008	2.37	Iron ion homeostasis	E1BQC2
	Methanethiol oxidase	0.0101	2.12	Methanethiol oxidase activity, selenium binding	H9KYX6
	Thioredoxin domain-containing protein	0.0119	2.06	Peroxiredoxin activity, cell redox homeostasis	F1NNS8; A0A1D5PLH7
	GTP-binding protein	0.0013	2.03	Actin filament organization, stress fiber assembly	O93467; Q9PSX7
	Apolipoprotein A-I	0.0347	2.00	Cholesterol biosynthetic process, cholesterol homeostasis, lipid storage, lipoprotein biosynthetic/metabolic process, phospholipid homeostasis, positive regulation of stress fiber assembly, protein oxidation	P08250
	Endoplasmin	0.0028	1.93	Intracellular sequestering of iron ion, protein folding, ubiquitin-dependent ERAD pathway, negative regulation of apoptotic process, response to hypoxia	P08110; A0A1D5PPN9
	Protein disulfide-isomerase	0.0012	1.89	Protein disulfide isomerase activity, protein folding, response to endoplasmic reticulum stress	A0A1D5PV06; P09102; A0A1L1RZP5
	Glutathione transferase	0.0136	1.62	Glutathione metabolic process	E1BUB6
	Protein disulfide-isomerase A3	0.0019	1.62	Cellular response to interleukin-7, extrinsic apoptotic signaling pathway, protein folding, response to endoplasmic reticulum stress	Q8JG64
	DNA-(apurinic or apyrimidinic site) lyase	0.0369	1.57	Apoptotic process, DNA repair	F1NPA9
	Protein disulfide-isomerase A4	0.0095	1.57	Protein folding, response to endoplasmic reticulum stress	A0A1D5PWP7
	Aldo_ket_red domain-containing protein	0.0019	1.50	Alditol:NADP + 1-oxidoreductase activity	R4GG24
	Heat shock protein beta-8	0.0048	1.47	Cellular response to unfolded protein, positive regulation of aggrephagy	E1C6V0
	LRRNT domain-containing protein	0.0094	1.46	Extracellular matrix structural constituent	A0A1D5PAN0
	Sulfurtransferase	0.0190	1.35	Transsulfuration	A0A1D5PKN8
	Peptidyl-prolyl cis–trans isomerase	0.0392	1.35	Protein folding, protein peptidyl-prolyl isomerization	D0EKR3; A0A3Q3AT29
	10 kDa heat shock protein, mitochondrial	0.0279	1.33	Chaperone cofactor-dependent protein refolding	O42283; A0A1L1RZ94
	Glutathione peroxidase	0.0004	1.32	Response to oxidative stress	F1NYU4; A0A3Q3AIE0
	AdoHcyase_NAD domain-containing protein	0.0040	1.28	One-carbon metabolic process, S-adenosylmethionine cycle	A0A1D5PPA8; A0A1D5NWI2; A0A1D5PNB8
	Peroxiredoxin-1	0.0132	1.26	Cell redox homeostasis, leukocyte activation, removal of superoxide radicals	P0CB50
	S-formylglutathione hydrolase	0.0071	1.20	Formaldehyde catabolic process	E1BXC2
Impaired myofibrillar protein homeostasis/function	Cytochrome *c* oxidase polypeptide Va	–	S	Mitochondrial electron transport, cytochrome *c* to oxygen	E1C043
	AMP deaminase	–	S	AMP metabolic process, IMP biosynthetic process, IMP salvage	F1NG97
	Arp2/3 complex 34 kDa subunit	–	S	Actin filament polymerization, Arp2/3 complex-mediated actin nucleation, regulation of actin filament polymerization	F1P1K3

(*continued on next page*)

Table 2 (*continued*)

Group	Protein	*p*-values	Log_2 Fold-change[1]	Biological function	Accession number
	Macrophage-capping protein	–	S	Depolymerization, barbed-end actin filament capping, cell projection assembly	A0A1D5P7X3
	Myosin light polypeptide 6	–	S	Actomyosin structure organization, myofibril assembly	A0A3Q2U5H1; A0A1D5PEM4; A0A1L1RLN6; P02607
	Myosin-binding protein C, cardiac-type	–	S	Cell adhesion, positive regulation of ATPase activity, regulation of muscle filament sliding	A0A3Q2U3I8; A0A3Q3ACN5; F1NBZ9; Q90688; A0A3Q2UKP4; A0A1D5PKM9
	Ezrin	–	S	Actin filament bundle assembly, positive regulation of protein localization to early endosome, regulation of cell shape, regulation of organelle assembly	Q9YGW6
	UDP-glucose 6-dehydrogenase	0.0288	4.50	Carbohydrate metabolic process, glycosaminoglycan biosynthetic process, heparan sulfate proteoglycan biosynthetic process, protein hexamerixation	Q5F3T9
	Carbonic anhydrase	0.0088	3.42	One-carbon metabolic process	A0A1D5NTS2
	L-lactate dehydrogenase B chain	0.0011	3.36	Lactate metabolic process, pyruvate metabolic process	P00337
	Actin, cytoplasmic 2	0.0063	2.70	ATP binding	Q5ZMQ2
	Pyruvate kinase	0.0144	2.70	ATP binding	F1NW43
	ADF actin binding protein	0.0037	2.69	Actin filament polymerization	C7G537
	TRANSKETOLASE_1 domain-containing protein	0.0030	2.59	Regulation of growth, ribose phosphate biosynthetic process, glyceraldehyde-3-phosphate biosynthetic process	F1P1A5; A0A1D5NWL4
	Adenylyl cyclase-associated protein	0.0002	2.44	Actin cytoskeleton organization, cell morphogenesis	A0A1D5Q032
	Dystrophin	0.0083	2.28	Actin filament bundle assembly	A0A3Q2U000; A0A3Q2TWR1; A0A3Q2TUU4; A0A3Q2U719; F1NS97; A0A3Q3ABK2; A0A3Q2U0M3; A0A3Q2UJC3; A0A3Q2UPH9; A0A1D5PC47
	Creatine kinase B-type	0.0024	2.22	ATP biosynthetic process, phosphocreatine biosynthetic process	P05122
	Transaldolase	0.0055	2.18	Carbohydrate metabolic process	A0A1D5PC23
	Actin-depolymerizing factor	0.0217	2.14	Actin filament depolymerization, actin filament fragmentation, actin filament severing	Z4YJB8; P18359
	Gelsolin	0.0063	1.82	Actin filament severing	O93510
	Alpha-actinin-1	0.0188	1.76	Sarcomere organization, skeletal muscle fiber development, actin cytoskeleton organization, sarcomere organization	P05094; A0A1D5P9P3; A0A1D5PF13; A0A1D5P522
	Xin actin-binding repeat-containing protein 1	0.0003	1.69	Actin filament organization	Q91957; F1NUI2
	Amidohydro-rel domain-containing protein	0.0220	1.68	Actin crosslink formation, actin filament bundle assembly, response to axon injury	A0A1D5PZ51; A0A3Q2TWY6; F1NS48
	Actin-related protein 2/3 complex subunit 4	0.0031	1.68	Actin filament polymerization, Arp2/3 complex-mediated actin nucleation	F1P010; A0A3Q3ANM5
	Spectrin alpha chain, non-erythrocytic 1	0,0000	1.65	Actin filament capping, actin cytoskeleton organization	A0A1D5PVG1; A0A3Q2TVB7; A0A3Q2U3B7; A0A3Q2U5Z2; A0A3Q2U342; F1NHT3; A0A1D5PQC3; P07751
	Alpha-actinin-2	0,0226	1.52	Microspike assembly	P20111; A0A1D5PNV5; A0A1L1S0L2
	ATP synthase subunit beta	0,0055	1.45	Proton motive force-driven mitochondrial ATP synthesis	A0A1L1RY04
Hypoxia, Inflammation and fibrosis	CAP-Gly domain-containing linker protein 1	–	S	Cytoplasmic microtubule organization, positive regulation of microtubule polymerization	O42184
	Biliverdin reductase A	–	S	Heme catabolic process	A0A1D5NWT1
	Fibrillar collagen NC1 domain-containing protein	–	S	Cell adhesion, collagen fibril organization, extracellular matrix organization	A0A1D5PE74
	Collagen alpha-1(I) chain	–	S	Blood vessel development, cartilage development involved in endochondral bone morphogenesis, cellular response to amino acid stimulus, collagen biosynthetic process, collagen fibril organization	P02457; A0A1D5PYU1
	Ribonuclease homolog	–	S	Angiogenesis, defense response to Gram-negative bacterium, defense response to Gram-positive bacterium	P30374
	Procollagen-lysine 5-dioxygenase	–	S	Peptidyl-lysine hydroxylation	F1NXB0; A0A1D5P079; A0A1L1RSJ4
	Myoglobin	–	S	Oxygen transport, response to hypoxia	P02197
	EF hand-containing protein 1	–	S	Calcium ion binding	Q49B65
	Tenascin	0.0019	14.26	Cell adhesion, regulation of cell population proliferation	P10039; A0A1D5PJ88; A0A3Q2UL32; A0A1D5PZ80; A0A3Q2U5M0; A0A1D5NZY0
	Fibronectin	0.0000	13.82	Cell adhesion, cell migration, regulation of cell shape, acute-phase response, peptide cross-linking	A0A3Q2TW07; P11722; F1NJT4; A0A1D5NU50

(*continued on next page*)

Table 2 (*continued*)

Group	Protein	*p*-values	Log_2 Fold-change[1]	Biological function	Accession number
	Desmin	0.0076	7.52	Intermediate filament organization, intermediate filament polymerization, skeletal muscle organ development	P02542
	Talin-1	0.0025	4.64	Cell adhesion, actin filament organization, endocytosis	P54939; E1C2S1; A0A1D5PTR5
	Vimentin	0.0048	3.60	Intermediate filament organization	F1NJ08; A0A1L1RXL9; P09654
	Protein S100-A6	0.0229	3.44	Cell cycle, positive regulation of cell division	Q98953
	Collagen alpha-3(VI) chain	0.0245	2.91	Cell adhesion	A0A3Q2UD12; F1P2F0; A0A1D5PGD5; A0A3Q3AR07; P15989; A0A3Q2U4U7
	Ferritin heavy chain	0.0019	2.77	Immune response, intracellular sequestering of iron ion, negative regulation of cell population proliferation	P08267
	Transforming growth factor-beta-induced protein ig-h3	0.0194	2.62	Cell adhesion, extracellular matrix organization	A0A1D5PXP9
	Fascin	0.0013	2.56	Actin filament bundle assembly, cell migration, establishment or maintenance of cell polarity	D5LPR1
	Tubulin alpha chain	0.0174	2.35	Microtubule cytoskeleton organization, mitotic cell cycle	A0A1D5P198; A0A1D5NW27; A0A1D5NXV1; P02552; A0A1L1RJP8; F1NWX0; P09644
	SERPIN domain-containing protein	0.0074	1.99	Negative regulation of angiogenesis, negative regulation of endopeptidase activity	E1C7H6
	Annexin A2	0.0007	1.98	Bone mineralization, calcium ion homeostasis, growth plate cartilage development	P17785
	Peptidyl-prolyl cis–trans isomerase B	0.0029	1.91	Negative regulation of collagen fibril organization, protein folding, protein peptidyl-prolyl isomerization	P24367; A0A1L1RRN4
	Alpha-1-acid glycoprotein	0.0431	1.86	Regulation of immune system process	Q8JIG5
	5-aminoimidazole-4-carboxamide ribonucleotide formyltransferase	0.0013	1.71	'de novo' IMP biosynthetic process	Q5XKY5; P31335
	Lumican	0.0448	1.63	Collagen fibril organization, visual perception	P51890
Apoptosis and necrosis	Acidic leucine-rich nuclear phosphoprotein 32 family member E	–	S	Histone exchange, regulation of apoptotic process	Q5F4A3; A0A3Q2UHZ1
	Parvalbumin, thymic	0.0086	4.58	Calcium ion binding	P19753
	Platelet-activating factor acetylhydrolase IB subunit alpha2	0.0020	2.11	Lipid catabolic process	Q5ZMS2; A0A1D5PMU2; A0A3Q2UC12
	Annexin A5	0.0002	1.81	Calcium ion homeostasis, negative regulation of coagulation	P17153
	Albumin	0.0219	1.71	Cellular response to starvation, negative regulation of apoptotic process, response to vitamin A	P19121
	Annexin	0.0303	1.68	Calcium ion binding	F1N9S7
	Cathepsin D	0.0067	1.34	Cell death, positive regulation of apoptotic process, proteolysis	Q05744

S: only found in WB-S chicken breast muscles.

against oxidative stress, and redox control in the plasma membrane, cytosol, endoplasmic reticulum, and nucleus (Cho et al., 2019). TXNDC are essential, among other functions, for reduction of protein disulphide and reduction of hydrogen peroxide (H_2O_2) (Hanschmann et al., 2013). GSH-PXs catalyzes the neutralization of ROS such as the decomposition of H_2O_2 or lipid peroxides by reduced glutathione (GSH) resulting in water or alcohol and oxidized glutathione (GSSG) (Sarıkaya and Doğan, 2020). Peroxiredoxins are cellular redox signaling, acting mainly in response to changes in production of hydrogen peroxide (Ledgerwood, Marshall and Weijman, 2017). The higher concentration of these proteins in WB-S meats is compatible with a pro-oxidative scenario such as that reported by WB muscles (Petracci et al., 2019). Yet, the attempt of the muscle to counteract the oxidation insults seemed to be ineffective looking at the higher levels of lipid (TBARS) and protein oxidation (total carbonyls) in breasts affected by the myopathy. Conversely, the fact that TXNDC is found in higher amount in the severe condition may explain the lower content of disulphide bonds observed in WB-S (Fig. 1D), as this enzyme is implicated in the reduction of disulphide bonds in proteins. Discriminating proteins corroborate that the oxidative stress is a crucial event behind the occurrence of this myopathy. The failed attempt by endogenous antioxidant defenses to maintain redox balance is in agreement with Xing et al. (2021) and Pan et al. (2020) who observed greater activity of antioxidant catalase (CAT), superoxide dismutase (SOD), glutathione peroxidase (GSH-Px) and glutathione S-transferase (GSH-ST) in chicken liver affected by WB myopathies.

Other proteins found in higher relative abundance in WB-S, such as Fibrillar collagen NC1 domain-containing protein, collagen alpha-1(I) chain, procollagen-lysine 5-dioxygenase, fibronectin, collagen alpha-3 (VI) chain, annexin A2, peptidyl-prolyl cis–trans isomerase B and Lumican are indicative of tissue damage and inflammatory process, since their biological function is related to the integrity and stability of collagen and tissue repair. The higher amount of these proteins could be related as an attempt of the muscle fiber to maintain its functionality in the face of fibrosis (Petracci et al., 2019). These proteome results are directly related to the higher collagen content observed in WB meat (Table 1).

The increased quantity of Arp2/3 complex 34 kDa subunit, Macrophage-capping protein, Ezrin, ADF actin binding protein, Adenylyl cyclase-associated protein, Dystrophin, Actin-depolymerizing factor, Gelsolin, Alpha-actinin-1, Xin actin-binding repeat-containing protein 1, Amidohydro-rel domain-containing protein, Actin-related protein 2/3 complex subunit 4, and Spectrin alpha chain, non-erythrocytic 1, are related to the actin structure organization, being directly related to the alteration of myofibrillar proteins function in WB

Table 3
Proteins found in lower relative quantity in chicken breasts affected by severe WB myopathy.

Group	Protein	p-values	Log_2 Fold-change[1]	Biological function	Accession number
Failed energetic metabolism_cell starvation	10-formyltetrahydrofolate dehydrogenase	–	N	10-formyltetrahydrofolate catabolic process, biosynthetic process, one-carbon metabolic process	F1P130
	Alpha-1,4 glucan phosphorylase	0.0033	0.33	Glycogen catabolic process	E1BSN7
	Alpha-1,4 glucan phosphorylase	0.0010	0.33	Carbohydrate metabolic process	A0A3Q3AC33
	Phosphorylase b kinase regulatory subunit	0.0070	0.36	Glycogen metabolic process	A0A1D5P061; A0A1D5PVZ4; E1BQZ7
	Creatine kinase S-type, mitochondrial	0.0018	0.46	Phosphocreatine biosynthetic process, phosphorylation	P11009; F1NAD3
	Glycerol-3-phosphate dehydrogenase 1	0.0030	0.47	Carbohydrate metabolic process, glycerol-3-phosphate metabolic process, NADH oxidation	A0A1D5PA73
	4-alpha-glucanotransferase	0.0031	0.48	Glycogen biosynthetic process, glycogen catabolic process	F1NX83; A0A1D5PF87
	Succinate–CoA ligase [ADP-forming] subunit beta, mitochondrial	0.0443	0.52	Succinyl-CoA metabolic process, tricarboxylic acid cycle	Q5F3B9
	Phosphoglycerate mutase	0.0004	0.53	Glycolytic process	Q5ZHV4
	Phosphoglycerate kinase	0.0001	0.53	Gluconeogenesis, glycolytic process, phosphorylation	F1NU17; P51903
	Succinate–CoA ligase [ADP/GDP-forming] subunit alpha, mitochondrial	0.0131	0.55	Tricarboxylic acid cycle	Q5ZL83
	Glyceraldehyde-3-phosphate dehydrogenase	0.0007	0.56	Gluconeogenesis, glycolytic process, negative regulation of apoptotic process	P00356
	2-phospho-D-glycerate hydro-lyase	0.0408	0.56	Glycolytic process	A0A1D5PSH6
	Guanidinoacetate *N*-methyltransferase	0.0008	0.59	Creatine biosynthetic process, methylation	A0A1D5P3Q3; A0A1L1RRC8; A0A3Q2UE67
	Gal_mutarotas_2 domain-containing protein	0.0056	0.60	Carbohydrate metabolic process, glycan processing	E1BTT7
	Adenylosuccinate lyase	0.0012	0.61	'de novo' AMP biosynthetic process, 'de novo' IMP biosynthetic process	P21265; E1BR00
	Beta-enolase	0.0016	0.61	Glycolytic process	P07322
	Phosphoglycerate mutase 1	0.0009	0.62	Gluconeogenesis, glycolytic process	Q5ZLN1
	Pyruvate kinase PKM	0.0039	0.62	Glycolytic process	P00548; A0A1D5P9V0
	Glucose-6-phosphate isomerase	0.0043	0.63	Gluconeogenesis, glucose 6-phosphate metabolic process, glycolytic process	A0A1L1RQ91; F1NIJ6; A0A1L1RPE8; A0A1D5PRS4
	Fumarate hydratase, mitochondrial	0.0045	0.64	Fumarate metabolic process, malate metabolic process, tricarboxylic acid cycle	Q5ZLD1
	L-lactate dehydrogenase	0.0040	0.65	Lactate metabolic process, pyruvate metabolic process, carboxylic acid metabolic process	E1BTT8; P00340; A0A1D5NZ01
	Triosephosphate isomerase	0.0204	0.66	Gluconeogenesis, glyceraldehyde-3-phosphate biosynthetic process, glycerol catabolic process, glycolytic process, methylglyoxal biosynthetic process	P00940
	Malic enzyme	0.0013	0.67	Malate metabolic process, pyruvate metabolic process	A0A3Q2UB37; F1P0Y6; A0A1D5P779
	Aspartate aminotransferase	0.0253	0.70	Biosynthetic process, cellular amino acid metabolic process, aspartate metabolic process	A0A1L1RPR4; F1P180; P00508
	SGNH_hydro domain-containing protein	0.0126	0.70	Lipid catabolic process	F1NKW4
	Branched-chain-amino-acid aminotransferase	0.0195	0.71	Cellular amino acid biosynthetic process, branched-chain amino acid biosynthetic process, leucine biosynthetic process, valine biosynthetic process	A0A3Q3AF25; A0A3Q2UDM7; E1BSF5; A0A3Q2U4M1
	FIST_C domain-containing protein	0.0300	0.71	Positive regulation of proteasomal ubiquitin-dependent protein catabolic process, protein polyubiquitination, regulation of skeletal muscle fiber development	Q5ZLD9
	Serine/threonine-protein phosphatase	0.0233	0.75	Cell division, glycogen metabolic process	A0A1D5P888; A0A1L1RMC6
	CBM21 domain-containing protein	0.0168	0.75	Regulation of glycogen biosynthetic process	A0A1L1S103; A0A3Q2UB77
Failed antiox response/ depletion of antiox defenses	PDZ domain-containing protein	–	N	Positive regulation of actin filament bundle assembly	F1NH40
	Aldedh domain-containing protein	0.0001	0.56	Aldehyde dehydrogenase (NAD +) activity	E1BT93
	Thioredoxin domain-containing protein 17	0.0216	0.70	Protein-disulfide reductase (NAD(P)) activity	R4GMD9
	Hemoglobin subunit alpha-A	0.0373	0.71	Cellular oxidant detoxification, hydrogen peroxide catabolic process	P01994
	Protein/nucleic acid deglycase DJ-1	0.0024	0.74	Autophagy, cellular response to hydrogen peroxide, cellular response to oxidative stress, DNA repair, hydrogen peroxide metabolic process, inflammatory response	Q8UW59; D5M8S2
	Peroxiredoxin-6	0.0478	0.75	Cell redox homeostasis, lipid catabolic process	F1NBV0; Q5ZJF4
	Dihydrolipoyl dehydrogenase	0.0345	0.82	Cell redox homeostasis	Q5ZM32
Apoptosis	Proteasome inhibitor PI31 subunit	0.0097	0.69	Ubiquitin-dependent protein catabolic process	Q5ZJL3

N: only found in normal chicken breast muscles.

abnormality. In addition, Arp2/3 complex, ezrin, alpha-actin and Xin actin-binding repeat-containing protein 1 are specifically involved in cross-linking actin filaments (May, 2001; Courson & Rock, 2010; Lees, 2015; Kawaguchi, et al. 2017), which contributes to the strengthening of actin filaments making these more mechanically resistant. Thus, their increased quantities may result in the higher hardness observed in WB meat (Table 1). In particular Gelsilin is one of the proteins responsible for assembly and disassembly of actin filaments, its functions include cell motility, proliferation and apoptosis. Furthermore, it plays an important role in localizing inflammation and preventing systemic escape of pro-inflammatory lipids (Gungor et al., 2016). Gelsilin increment may indicate an attempt to combat the inflammatory process resulting from WB myopathy. Infiltration of the muscle tissue and organs (liver) by inflammatory cells has been reported in WB myopathy (Sihvo et al., 2014; Velleman & Clark, 2015, Xing et al., 2021).

The higher abundance of cathepsin D and albumin reveals that WB chicken breasts are more susceptible to apoptosis. In general, Cathepsin D can either induce the programmed cell death in presence of cytotoxic factors, being activated by dysfunction of mitochondria (Minarowska et al., 2007). In addition, the higher amount of albumin could be interpreted as an attempt of the muscle fiber to react to mitochondrial damage induced by reactive oxygen species (Liu et al., 2012).

Lower relative abundance of key proteins in energy and carbohydrate metabolism such as creatine kinase (CK), pyruvate kinase (PK), lactate dehydrogenase (LDH) and aspartate aminotransferase (AST) show the severe perturbation of energetic metabolism and inefficient mitochondrial function and may, in turn, lead to oxidative stress (Carvalho et al., 2020a,b). All of these enzymes are known to be indicators of WB muscle stress and cellular damage (Kawasaki, Yoshida & Watanabe, 2016; Thanatsang, et al. 2020; Carvalho et al., 2020a,b; Kong et al. 2021). Carvalho et al. (2020) observed lower relative abundance of PK, CK, and LDH in meats affected by white striping myopathy, which also originates from intense genetic selection. According to Thanatsang et al. (2020), the expression of LDH gene in WB muscle tissue was lower than the N meat. However, Kawasaki et al. (2016) and Kong et al. (2021) observed greater activity of CK and AST in serum or breast tissue of affected WB compared to N. Other group of DAPs such as Hemoglobin subunit alpha-A, DJ-1, Peroxiredoxin-6 and Dihydrolipoyl dehydrogenase are implicated in cellular response to oxidative stress. The minor abundance of these proteins confirms the failed attempt of the WB muscle to act against oxidative stress and/or the consumption of certain elements of this antioxidant response.

4. Conclusions

Current findings indicate that altered oxidative status is a common feature of WB myopathy in broilers. Oxidative stress involves accretion of malondialdehyde and total protein carbonyls and depletion of sulphur protein components, which seem to have a direct impact on technological characteristics, color and texture of the affected meats. The proteomic analyses suggest: 1) an alteration in redox homeostasis with higher abundance of proteins directly involved in the repair of oxidative damage in tissue, and 2) a failed attempt by the muscle to maintain or recover its functionality with increased amount of proteins related to maintaining muscle structure and combating the inflammatory process. The results from the present study indicates that antioxidant strategies to be applied *in vivo* may help the living muscle in counteracting the oxidative stress and the occurrence of its negative effects on meat quality. Looking at the results, supplementation with sulphur amino acids and other micronutrients with antioxidant potential in muscle is to be explored given the crucial role of oxidative stress in the onset of the myopathy and the impaired quality traits of the meat. Future studies should look into the underlying causes of the oxidative stress in chicken WB and address other means of alleviation such as using lower-growth genetic lines.

CRediT authorship contribution statement

Leila M. Carvalho: Data curation, Methodology, Formal analysis, Supervision, Validation, Writing – original draft. **Thayse C. Rocha:** Data curation, Methodology, Formal analysis, Writing – review & editing. **Josué Delgado:** Data curation, Methodology, Formal analysis, Validation, Writing – review & editing. **Silvia Díaz-Velasco:** Data curation, Methodology, Formal analysis, Writing – review & editing. **Marta S. Madruga:** Funding acquisition, Project administration, Resources, Supervision, Validation, Writing – review & editing. **Mario Estévez:** Conceptualization, Funding acquisition, Project administration, Resources, Supervision, Validation, Writing – review & editing.

Declaration of Competing Interest

The authors declare that they have no known competing financial interests or personal relationships that could have appeared to influence the work reported in this paper.

Data availability

Data will be made available on request.

Acknowledgements

The authors acknowledge the CNPq – Brazilian National Council for Scientific and Technological Development (Process number 430832/2016-8). Q-Exactive mass spectrometer to proteomic research was acquired by the grant UNEX-AE-3394 funded by MCIN/AEI/ 10.13039/501100011033 and by "ERDF A way of making Europe". This study received funding from the European Union's Horizon 2020 research and innovation programme : INTAQT project under grant agreement N°101000250. This study also received funding from the Ministry of Science and Innovation (project code: PID2021-126193OB-I00).

References

Abasht, B., Mutryn, M. F., Michalek, R. D., & Lee, W. R. (2016). Oxidative Stress and Metabolic Perturbations in Wooden Breast Disorder in Chickens. *PLoS ONE, 11*(4), e0153750.

Aoac. (2000). *Official Methods of Analysis*. Gaithersburg, Maryland, USA: Association of Official Analytical Chemists.

Bao, Y., & Ertbjerg, P. (2019). Effects of protein oxidation on the texture and water-holding of meat: A review. *Critical Reviews in Food Science and Nutrition, 59*(22), 3564–3578. https://doi.org/10.1080/10408398.2018.1498444

Carvalho, R. H., Ida, E. I., Madruga, M. S., Martínez, S. L., Shimokomaki, M., & Estévez, M. (2017). Underlying connections between the redox system imbalance, protein oxidation and impaired quality traits in pale, soft and exudative (PSE) poultry meat. *Food Chemistry, 215*, 129–137. https://doi.org/10.1016/j.foodchem.2016.07.182

Carvalho, R., Shimokomaki, M., & Estévez, M. (2017). Poultry Meat Color and Oxidation. *Poultry Quality Evaluation, 133–157*. https://doi.org/10.1016/b978-0-08-100763-1.00006-4

Carvalho, L. M., Delgado, J., Madruga, M. S., & Estévez, M. (2020). Pinpointing oxidative stress behind the white striping myopathy: Depletion of antioxidant defenses, accretion of oxidized proteins and impaired proteostasis. *Journal of the Science of Food and Agriculture, 101*(4), 1364–1371. https://doi.org/10.1002/jsfa.10747

Carvalho, L. M., Madruga, M. S., Estévez, M., Badaró, A. T., & Barbin, D. F. (2020). Occurrence of wooden breast and white striping in Brazilian slaughtering plants and use of near-infrared spectroscopy and multivariate analysis to identify affected chicken breasts. *Journal of Food Science, 85*(10), 3102–3112. https://doi.org/10.1111/1750-3841.15465

Cho, S. Y., Kim, S., Son, M.-J., Rou, W. S., Kim, S. H., & Eun, H. S. (2019). Clinical Signifcance of the Thioredoxin System and Thioredoxin-Domain-Containing Protein Family in Hepatocellular Carcinoma. *Digestive Diseases and Sciences, 64*(1), 123–136. https://doi.org/10.1007/s10620-018-5307-x

Clark, D. L., & Velleman, S. G. (2016). Spatial influence on breast muscle morphological structure, myofiber size, and gene expression associated with the wooden breast myopathy in broilers. *Poultry Science, 95*(12), 2930–2945. https://doi.org/10.3382/ps/pew243

Courson, D. S., & Rock, R. S. (2010). Actin Cross-link Assembly and Disassembly Mechanics for α-Actinin and Fascin. *Molecular Biophysics, 285*(34), 26350–26357. https://doi.org/10.1074/jbc.M110.123117

Dalle Zotte, A., Tasoniero, G., Puolanne, E., Remignon, H., Cecchinato, M., Catelli, E., & Cullere, M. (2017). Effect of "Wooden Breast" Appearance on Poultry Meat Quality,

Histological Traits, and Lesions Characterization. *Czech Journal of Animal Science, 62* (2), 51–57. https://doi.org/10.17221/54/2016-CJAS

Delgado, J., Owens, R. A., Doyle, S., Núñez, F., & Asensio, M. A. (2017). Quantitative proteomics reveals new insights into calcium-mediated resistance mechanisms in Aspergillus flavus against the antifungal protein PgAFP in cheese. *Food Microbiology, 66*, 1–10. https://doi.org/10.1016/j.fm.2017.03.015

Delgado, J., Núñez, F., Asensio, M. A., & Owens, R. A. (2019). Quantitative proteomic profiling of ochratoxin A repression in Penicillium nordicum by protective cultures. *International Journal of Food Microbiology, 305*, Article 108243. https://doi.org/10.1016/j.ijfoodmicro.2019.108243

Da Rocha, T. C., Carvalho, L. M., Soares, A. J., Coutinho, D. G., Olegario, L. S., Galvão, M. S., … Madruga, M. S. (2020). Impact of chicken wooden breast on quality and oxidative stability of raw and cooked sausages subjected to frozen storage. *Journal of the Science of Food and Agriculture, 100*(6), 2630–2637. https://doi.org/10.1002/jsfa.10292

Dolan, S. K., Owens, R. A., O'Keeffe, G., Hammel, S., Fitzpatrick, D. A., Jones, G. W., & Doyle, S. (2014). Regulation of Nonribosomal Peptide Synthesis: Bis-Thiomethylation Attenuates Gliotoxin Biosynthesis in Aspergillus fumigatus. *Chemistry & Biology, 21*(8), 999–1012. https://doi.org/10.1016/j.chembiol.2014.07.006

Estévez, M., Padilla, P., Carvalho, L., Martín, L., Carrapiso, A., & Delgado, J. (2019). Malondialdehyde interferes with the formation and detection of primary carbonyls in oxidized proteins. *Redox Biology, 26*, Article 101277. https://doi.org/10.1016/j.redox.2019.101277

Estévez, M., Geraert, P.-A., Liu, R., Delgado, J., Mercier, Y., & Zhang, W. (2020). Sulphur amino acids, muscle redox status and meat quality: More than building blocks – Invited review. *Meat Science, 163*, Article 108087. https://doi.org/10.1016/j.meatsci.2020.108087

Estévez, M., Díaz-Velasco, S., & Martínez, R. (2021). Protein carbonylation in food and nutrition: A concise update. *Amino Acids, 54*, 559–573. https://doi.org/10.1007/s00726-021-03085-6

Folch, J., Lees, M., & Stanley, G. H. S. (1957). A Simple method for the isolation and purification of total lipids from animal tissues. *Journal of Biological Chemistry, 226* (1), 497–509.

Ganhão, R., Morcuende, D., & Estévez, M. (2010). Protein oxidation in emulsified cooked burger patties with added fruit extracts: Influence on colour and texture deterioration during chill storage. *Meat Science, 85*, 402–409. https://doi.org/10.1016/j.meatsci.2010.02.008

Geronimo, B. C., Prudencio, S. H., & Soares, A. L. (2022). Biochemical and technological characteristics of wooden breast chicken fillets and their consumer acceptance. *Journal of Food Science and Technology, 59*, 1185–1192. https://doi.org/10.1007/s13197-021-05123-3

Gratta, F., Fasolato, L., Birolo, M., Zomeño,C., Novelli, E., Petracci, M., Pascual, A., Xiccato, G., Trocino, A. Effect of breast myopathies on quality and microbial shelf life of broiler meat. *Poultry Science*, 98:2611-2651. https://doi.org/10.3382/ps/pez001.

Gungor, H. E., Sahiner, U. M., Karakukcu, C., Sahiner, N., & Torun, Y. A. (2016). The plasma gelsolin levels in atopic dermatitis: Effect of atopy and disease severity. *Allergologia et Immunopathologia, 44*(3), 221–225. https://doi.org/10.1016/j.aller.2015.05.005

Hanschmann, E. M., Godoy, J. R., Berndt, C., Hudemann, C., & Lillig, C. H. (2013). Thioredoxins, glutaredoxins, and peroxiredoxins – molecular mechanisms and health significance: From cofactors to antioxidants to redox signaling. *Antioxidants & Redox Signaling, 19*(13), 1539–1605. https://doi.org/10.1089/ars.2012.4599

Hasegawa, Y., Kawasaki, T., Maeda, N., Yamada, M., Takahashi, N., Watanabe, T., & Iwasaki, T. (2021). Accumulation of lipofuscin in broiler chicken with wooden breast. *Animal Science Journal, 92*(1), Article e13517. https://doi.org/10.1111/asj.13517

Hosatani, M., Kawasaki, T., Hasegawa, Y., Wakasa, Y., Hoshino, M., Takahashi, N., … Watanabe, T. (2020). Physiological and Pathological Mitochondrial Clearance Is Related to Pectoralis Major Muscle Pathogenesis in Broilers With Wooden Breast Syndrome. *Frontiers in Physiology, 11*, 00579. https://doi.org/10.3389/fphys.2020.00579

Jiang, S., Carroll, L., Rasmussen, L. M., & Davies, M. J. (2021). Oxidation of protein disulfide bonds by singlet oxygen gives rise to glutathionylated proteins. *Redox Biology, 38*, Article 101822. https://doi.org/10.1016/j.redox.2020.101822

Kawasoaki, T., Yoshida, T., & Watanabe, T. (2016). Simple Method for Screening the Affected Birds with Remarkably Hardened Pectoralis Major Muscles among Broiler Chickens. *Japan Poultry Science Association, 53*, 291–297. https://doi.org/10.2141/jpsa.0160036

Kawaguchi, K., Yoshida, S., Hatano, R., & Asano, S. (2017). Pathophysiological Roles of Ezrin/Radixin/Moesin Proteins. *Biological & Pharmaceutical Bulletin, 40*(4), 381–390. https://doi.org/10.1248/bpb.b16-01011

Kong, F., Zhao, G., He, Z., Sun, J., Wang, X., Liu, D., … Wen, J. (2021). Serum Creatine Kinase as a Biomarker to Predict Wooden Breast in vivo for Chicken Breeding. *Frontiers in Physiology, 12*, Article 711711. https://doi.org/10.3389/fphys.2021.711711

Lake, J. A., & Abasht, B. (2020). Glucolipotoxicity: A Proposed Etiology for Wooden Breast and Related Myopathies in Commercial Broiler Chickens. *Frontiers in Physiology, 11*, 169. https://doi.org/10.3389/fphys.2020.00169

Ledgerwood, E. C., Marshall, J. W. A., & Weijman, J. F. (2017). The role of peroxiredoxin 1 in redox sensing and transducing. *Archives of Biochemistry and Biophysics, 617*, 60–67. https://doi.org/10.1016/j.abb.2016.10.009

Lees, S. J. (2015). Novel roles of Xin-repeat protein in skeletal muscle: A new insight into monogenetic myopathies. *Acta Physiologica, 214*(2), 149–151. https://doi.org/10.1111/apha.12495

Li, B., Dong, X., Puolanne, E., & Ertbjerg, P. (2022). Effect of wooden breast degree on lipid and protein oxidation and citrate synthase activity of chicken pectoralis major muscle. *LWT –. Food Science and Technology, 154*(112884). https://doi.org/10.1016/j.lwt.2021.112884

Liu, S.-Y., Chen, C.-L., Yang, T.-T., Huang, W.-C., Hsieh, C.-Y., Shen, W.-J., … Lin, C.-F. (2012). Albumin prevents reactive oxygen species-induced mitochondrial damage, autophagy, and apoptosis during serum starvation. *Apoptosis, 17*, 1156–1169. https://doi.org/10.1007/s10495-012-0758-6

Liu, R., Kong, F., Xing, S., He, Z., Bai, L., Sun, J., … Wen, J. (2022). Dominant changes in the breast muscle lipid profiles of broiler chickens with wooden breast syndrome revealed by lipidomics analyses. *Journal of Animal Science and Biotechnology, 13*, 93. https://doi.org/10.1186/s40104-022-00743-x

Madruga, M.S., Rocha, T.C., Carvalho, L.M., Sousa, A.M.B.L., Sousa Neto, A.C., Coutinho, D.G., Ferreira, A.S.C., Soares, A.J., Galvão, M.S., Ida, E.I., Estévez, M. The impaired quality of chicken affected by the wooden breast myopathy is counteracted in emulsion-type sausages. *Journal of Food Science and Technology*, 56(3):1380-1388. https://doi.org/10.1007/s13197-019-03612-0.

May, R. C. (2001). The Arp2/3 complex: A central regulator of the actin cytoskeleton. *Cellular and Molecular Life Sciences CMLS, 58*, 1607–1626. https://doi.org/10.1007/PL00000800

Minarowska, A., Minarowski, L., Karwowska, A., & Gacko, M. (2007). Regulatory role of cathepsin D in apoptosis. *Folia Histochemica et Cytobiologica, 45*(3), 159–163.

Mutryn, M. F., Brannick, E. M., Fu, W., Lee, W. R., & Abasht, B. (2015). *BMC Genomics, 16*, 399. https://doi.org/10.1186/s12864-015-1623-0

Olivo, R., Soares, A. L., Ida, E. I., & Shimokomaki, M. (2001). Dietary vitamin E inhibits poultry PSE and improves meat functional properties. *Journal of Food Biochemistry, 25*(4), 271–283. https://doi.org/10.1111/j.1745-4514.2001.tb00740.x

Pan, X., Zhang, L., Xing, T., Li, J., & Gao, F. (2020). The impaired redox status and activated nuclear factor-erythroid 2-related factor 2/antioxidant response element pathway in wooden breast myopathy in broiler chickens. *Animal Bioscience, 34*(4), 652–661. https://doi.org/10.5713/ajas.19.0953

Papah, M. B., Brannick, E. M., Schmidt, C. J., & Abasht, B. (2018). Gene expression profiling of the early pathogenesis of wooden breast disease in commercial broiler chickens using RNA-sequencing. *PLoS One, 13*(12), e0207346.

Petracci, M., Mudalal, S., Soglia, F., & Cavani, C. (2015). Meat quality in fast-growing broiler chickens. *World's Poultry Science Journal, 71*(2), 363–374. https://doi.org/10.1017/S0043933915000367

Petracci, M., Soglia, F., Madruga, M., Carvalho, L., Ida, E., & Estévez, M. (2019). Wooden-Breast, White Striping, and Spaghetti Meat: Causes, Consequences and Consumer Perception of Emerging Broiler Meat Abnormalities. *Comprehensive Reviews in Food Science and Food Safety, 18*(2), 565–583. https://doi.org/10.1111/1541-4337.12431

Rysman, T., Jongberg, S., Royen, G. V., Weyenberg, S. V., Smet, S. D., & Lund, M. N. (2014). Protein Thiols Undergo Reversible and Irreversible Oxidation during Chill Storage of Ground Beef as Detected by 4,4′-Dithiodipyridine. *Journal of Agricultural and Food Chemistry, 62*, 12008–12014. https://doi.org/10.1021/jf503408f

Rocha, T. C., Olegario, L. S., Carvalho, L. M., Pereira, D. A., González-Mohino, A., Ventanas, S., … Madruga, M. S. (2022). Consumer behavior towards chicken breasts affected with myopathy (Wooden Breast): Face-to-face vs. online tests. *International Journal of Food Science & Technology, 57*(8), 5514–5522. https://doi.org/10.1111/ijfs.15892

Sarıkaya, E., & Doğan, S. (2020). Glutathione Peroxidase in Health and Diseases. In *Glutathione System and Oxidative Stress in Health and Disease. IntechOpen*. https://doi.org/10.5772/intechopen.91009

Schilter, D. (2017). Thiol oxidation: A slippery slope. *Nature Reviews Chemistry, 1*, 0013. https://doi.org/10.1038/s41570-016-0013

Sihvo, H. K., Immonen, K., & Puolanne, E. (2014). Myodegeneration with fibrosis and regeneration in the pectoralis major muscle of broilers. *Veterinary Pathology, 51*(3), 619–623. https://doi.org/10.1177/0300985813497488

Sihvo, H. K., Linden, J., Airas, N., Immonen, K., Valaja, J., & Puolanne, E. (2017). Wooden breast myodegeneration of pectoralis major muscle over the growth period in broilers. *Veterinary Pathology, 54*(1), 119–128. https://doi.org/10.1177/0300985816658099

Singhal, S. S., Singh, S. P., Singhal, P., Horne, D., Singhal, J., & Awasthi, S. (2015). Antioxidant Role of Glutathione S-Transferases: 4-Hydroxynonenal, a Key Molecule in Stress-Mediated Signaling. *Toxicol Appl Pharmacol., 289*(3), 361–370. https://doi.org/10.1016/j.taap.2015.10.006

Strange, R. C., Spiteri, M. A., Ramachandran, S., & Fryer, A. A. (2001). Glutathione-S-transferase family of enzymes. *Mutation Research, 482*, 21–26. https://doi.org/10.1016/S0027-5107(01)00206-8

Thanatsang, K. V., Malila, Y., Arayamethakorn, S., Srimarut, Y., Tatiyaborworntham, N., Uengwetwanit, T., … Visessanguan, W. (2020). Nutritional Properties and Oxidative Indices of Broiler Breast Meat Affected by Wooden Breast Abnormality. *Animals, 10* (12), 2272. https://doi.org/10.3390/ani10122272

Velleman, S. G., & Clark, D. L. (2015). Histopathologic and myogenic gene expression changes associated with wooden breast in broiler breast muscles. *Avian Diseases, 59* (3), 410–418. https://doi.org/10.1637/11097-042015-Reg.1

Xia, X., Kong, B., Liu, Q., & Liu, J. (2009). Physicochemical change and protein oxidation in porcine longissimus dorsi as influenced by different freeze–thaw cycles. *Meat Science, 83*(2), 239–245. https://doi.org/10.1016/j.meatsci.2009.05.003

Xing, T., Zhao, X., Zhang, L., Li, J. L., Zhou, G. H., Xu, X. L., & Gao, F. (2020). Characteristics and incidence of broiler chicken wooden breast meat under commercial conditions in China. *Poultry Science, 99*(1), 620–628. https://doi.org/10.3382/ps/pez560

Xing, T., Pan, X., Zhang, L., & Gao, F. (2021). Hepatic Oxidative Stress, Apoptosis, and Inflammation in Broiler Chickens With Wooden Breast Myopathy. *Frontiers in Physiology, 12*, Article 659777. https://doi.org/10.3389/fphys.2021.659777

Zhang, Y., Wang, P., Xu, X.-L., Xia, T., Li, Z., & Zhao, T. (2020). Effect of wooden breast myopathy on water-holding capacity, rheological and gelling properties of chicken broiler breast batters. *Poultry Science, 99*(7), 3742–3751. https://doi.org/10.1016/j.psj.2020.03.032

Zhuang, H., & Bowker, B. (2018). The wooden breast condition results in surface discoloration of cooked broiler pectoralis major. *Poultry Science, 12*(1), 4458–4461. https://doi.org/10.3382/ps/pey284

CAPÍTULO DE LIBRO

Chapter 10

Spectrophotometric Analysis of Protein Carbonyls

Francesca Soglia, Giulia Baldi, Alberto González-Mohino, Silvia Díaz-Velasco, Massimiliano Petracci, and Mario Estévez

Abstract

Oxidation of proteins is a major threat to their functionality and to the sensory properties and nutritional value of meat and meat products. Moreover, the intake of protein oxidation products may also involve a potential health risk for consumers. The accurate analysis of food protein oxidation seems to be an issue of scientific and technological relevance. Protein carbonylation is one of the most remarkable modifications in oxidized proteins and protein carbonyls are commonly used as markers of the oxidative damage to meat proteins. Regardless of its documented drawbacks, the dinitrophenylhydrazine (DNPH) method is the most widely used among food scientists for the quantification of protein carbonyls. Therefore, this chapter aims to provide a detailed description of the abovementioned determination which involves a simultaneous quantification of total protein carbonyls and total protein content in a given sample.

Key words Protein oxidation, Carbonyls, Hydrazones, 2,4-Dinitrophenylhydrazine, DNPH, Spectrophotometric method

1 Introduction

Proteins play a crucial role in foods from various perspectives including functionality (i.e., water absorption and retention, gelation, viscosity, emulsification, foam formation, etc.), sensory properties (i.e., texture and rheological properties, flavor-binding properties, enzymatic browning), and nutritional value (e.g., contribution with essential amino acids) [1]. Yet, a number of post-translational modifications in proteins affect their composition and native structure, leading to impairments in their functional properties and nutritional value.

Oxidation is a major threat to protein stability and functionality as the attack of reactive oxygen species (ROS) or reactive Maillard-dicarbonyls such as glyoxal and methylglyoxal, among others, leads to severe chemical changes in proteins, namely, peptide fragmentation, amino acid side chains oxidation, and formation of protein cross-links [2]. These chemical modifications occur all the way from

José Manuel Lorenzo et al. (eds.), *Methods to Assess the Quality of Meat Products*,
Methods and Protocols in Food Science, https://doi.org/10.1007/978-1-0716-2002-1_10,
© The Author(s), under exclusive license to Springer Science+Business Media, LLC, part of Springer Nature 2022

food collection/harvesting until culinary treatment prior to consumption [3]. Yet, protein oxidation is particularly promoted during severe and recurring processing such as the combination of some of the following treatments: mincing, slicing, application of high temperatures, radiation, high-pressure, microwaves, packaging in high-oxygen atmospheres, etc. [1]. The consequences of severe protein oxidation are commonly negative as it is linked to increased toughness in meats, loss of essential amino acids and reduced protein digestibility, among others [4]. Additionally, recent reports emphasized the potential toxicity of oxidized proteins and amino acids and therefore, the intake of protein oxidation products may also involve a potential health risk [5].

In view of the aforementioned statements, the analysis of food protein oxidation seems to be an issue of scientific and technological relevance. The quantification of protein oxidation may be essential to identify the extent to which food proteins have suffered oxidative damage; the effectiveness of a given antioxidant strategy may be assessed by confirming its ability to reduce the amount of protein oxidation products [6]. Since protein oxidation is a complex phenomenon and is manifested as manifold chemical changes, an assortment of analytical procedures has been proposed to evaluate its occurrence in food systems [2]. Among all of them, the quantification of protein carbonyls is, without any doubt, the most common method to assess protein oxidation in biological samples. The occurrence of carbonyls in proteins is an unquestionable indication of an oxidative damage as the oxidative deamination of certain alkaline amino acids, such as lysine, arginine, and proline, leads to the formation of protein-bound carbonyls [7]. While several analytical procedures have been proposed to detect and quantify protein carbonyls, the spectrophotometric method that involves prior derivatization of the protein sample with dinitrophenylhydrazine (DNPH), is, again, the most widely used among food scientists (Fig. 1). The key to this procedure is to facilitate the exposure of protein-bound carbonyls to the DNPH and remove all exceeding reagent so that the numbers from quantification are as accurate as possible. To fulfill this objective, some cleaning steps are required to remove lipids and any other substrate and/or fluorophore that may interfere with the spectrophotometric measurement at 370 nm. The method has been criticized for being time-consuming, poorly accurate and intricate in the way samples have to be handled during the entire method, which facilitates a failed sampling from homogenates, loss of sample during washing steps or a failed derivatization. Even if the method is applied correctly, the nature and origin of the protein carbonyls remains unknown as these can derive from the oxidation of amino acid side chains (primary carbonyls) or from the oxidation of unsaturated lipids (i.e., malondialdehyde, MDA) which appear as protein-bound carbonyls upon reaction and covalent linkage with protein

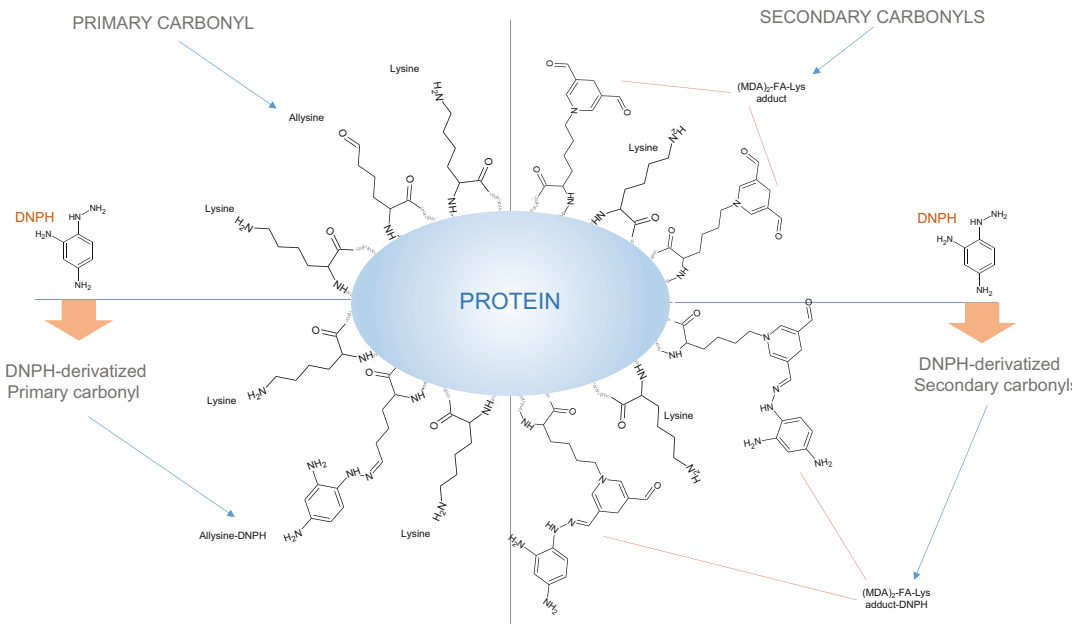

Fig. 1 Schematic representation of the DNPH-derivatization of primary (allysine) and secondary (protein-bound MDA) protein carbonyls (Adapted from Estévez et al. [8])

amines [8]. Figure 1 shows derivatization of DNPH with one primary carbonyl (allysine) and one secondary carbonyl (protein-bound MDA). The method, that involves a simultaneous quantification of total protein carbonyls and total protein content in a given sample, is described in the following sections.

2 Materials

Prepare all solutions using distilled water and/or analytical grade reagents. Prepare and store all the solutions and reagents at 4 ± 1 °C (unless indicated otherwise) with the only exception of Sodium Dodecyl Sulfate (SDS) 5% (w/v) which should be stored at room temperature to avoid crystallization. Diligently follow all waste disposal regulations when disposing waste materials.

2.1 Protein Extraction

1. KCl 0.15 M: Dissolve 11.18 g of potassium chloride (≥98%) in 1 L of distilled water (*see* **Note 1**).
2. TCA 10% (w/v): Dissolve 100.0 g of trichloroacetic acid (≥98%) in 1 L of distilled water (*see* **Note 2**).

2.2 Carbonyl Groups Exposure

1. SDS 5% (w/v): Dissolve 50 g of sodium dodecyl sulfate (≥98%) in 1 L of distilled water (*see* **Note 3**).

2.3 Derivatization

1. HCl 3 M: Mix 248 mL of hydrochloric acid (≥37%) with 752 mL of distilled water (*see* **Notes 2** and **4**).
2. DNPH 0.3% (w/v) in 3 M HCl: Dissolve 6.0 g of 2,4-Dinitrophenylhydrazine (~50%) in 1 L of HCl 3 M (*see* **Notes 2** and **5**).

2.4 Washing

1. TCA 40% (w/v): Dissolve 400.0 g of trichloroacetic acid (≥98%) in 1 L of distilled water (*see* **Note 2**).
2. Ethanol-ethyl acetate (1:1): Mix 500 mL ethanol with 500 mL ethyl acetate (*see* **Note 6**).
3. Guanidine hydrochloride 6 M in NaH_2PO_4 20 mM: Add 573.18 g of guanidine hydrochloride (≥99%) to 1 L of sodium phosphate buffer (*see* the following **item 4**) and adjust the final pH of the solution to 6.5 (*see* **Note 7**).
4. NaH_2PO_4 20 mM: Add 2.40 g of Sodium phosphate monobasic (≥98%) to 1 L of distilled water.

3 Methods

Carry out all procedures at room temperature, unless otherwise specified. Carbonyl content should be measured following the traditional spectrophotometric DNPH-based method described by Levine et al. [9] with the modifications proposed by Soglia et al. [10]. As aforementioned, the spectrophotometric quantification of protein carbonyls at 370 nm is made simultaneously to the spectrophotometric quantification of total protein content at 280 nm since results are commonly expressed as per protein unit. All the steps of protein extraction, carbonyl groups exposure and subsequent quantification are outlined in Fig. 2.

3.1 Protein Extraction

1. Weigh 1.0 g of sample in a 50 mL centrifuge tube and add 10 mL of ice-cold 0.15 M KCl solution (*see* **Notes 1** and **8**).
2. Homogenize the samples by Ultra-Turrax (IKA-WERKE, Labortechnik, Staufen, Germany) or similar apparatus at 9500 rpm for 30 s (*see* **Note 8**).
3. Per each sample, prepare five microcentrifuge tubes of 2 mL in which aliquots of homogenate (100 μL/each) are mixed with 1 mL 10% TCA (*see* **Notes 1** and **9**).
4. Centrifuge the samples at 5000 × *g* for 5 min at room temperature (*see* **Note 10**).

3.2 Carbonyl Groups Exposure

1. After removing and discarding the supernatant, add 400 μL of 5% SDS to the pellet.

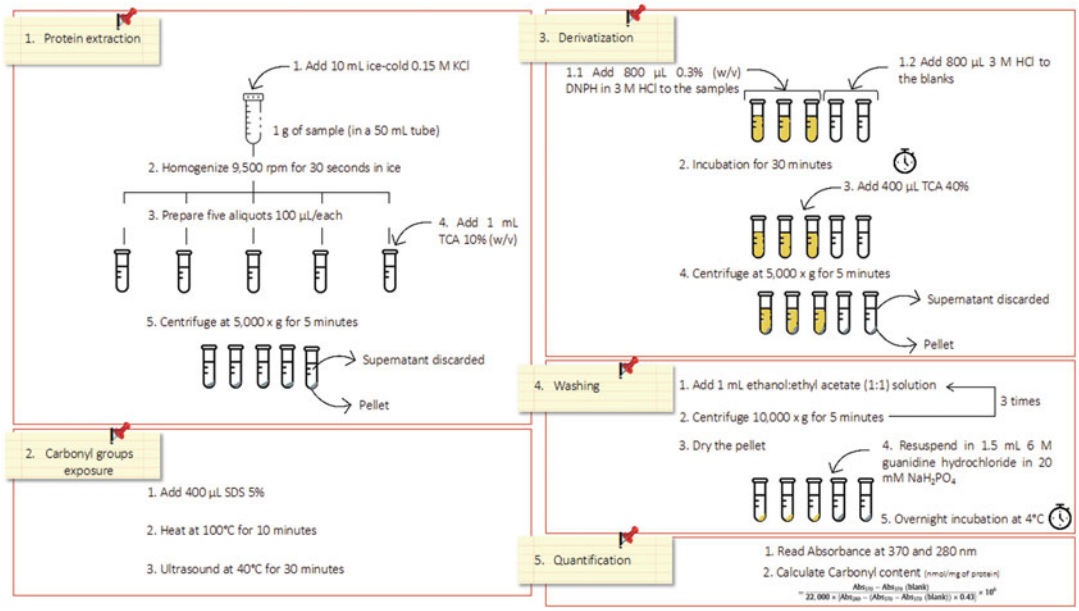

Fig. 2 Schematic and simplified representation of the steps of carbonyls quantification involving protein extraction, carbonyl groups exposure, derivatization, and quantification in the presence of DNPH

2. Heat the samples in a dry bath at 100 °C for 10 min (*see* **Note 11**).
3. Sonicate the samples in an ultrasonic cleaner at 40 °C for 30 min.
4. The implementation of the abovementioned steps has been recently studied and introduced by Soglia et al. [10]. In detail, these steps, inducing protein unfolding, result in the exposure of even the carbonyl groups that being buried in the inner core of the proteins' structure would have not react with DNPH, thus leading to an underestimation of the carbonyls development following protein oxidation.

3.3 Derivatization

1. Add 800 µL of 0.3% DNPH in 3 M HCl to each sample, while the same volume (800 µL) of 3 M HCl is added to the blanks (*see* **Note 2**).
2. Incubate the samples for 30 min at room temperature.
3. Following incubation, add 400 µL 40% TCA to each tube (*see* **Note 2**).

3.4 Washing

1. Centrifuge the samples at 5000 × *g* for 5 min (at room temperature) to precipitate the proteins and separate (and discard) the supernatant (*see* **Note 10**).
2. Add 1 mL of ethanol:ethyl acetate solution (1:1) to each tube (*see* **Note 6**).

3. Centrifuge the samples at 10,000 × *g* for 5 min (at room temperature) and discard the supernatant (*see* **Notes 6** and **10**).
4. Repeat **steps 2** and **3** two more times in order to remove unbound DNPH reagent.
5. After removing the supernatant resulting from the third washing step, evaporate any residual solvent under N_2 flux or allow the pellet to dry under the fume hood (*see* **Note 6**).
6. Resuspend the pellet in 1.5 mL 6 M guanidine hydrochloride in NaH_2PO_4 20 mM (pH 6.5) (*see* **Note 2**).
7. Incubate the samples at 4 ± 1 °C, overnight.

3.5 Quantification

1. Transfer the samples into semi-micro, UV-grade cuvettes (1.5 mL).
2. Read the absorbance of the samples and their respective blanks at 370 nm.
3. Read the absorbance of the samples (only) at 280 nm.
4. Calculate carbonyl content (expressed as nmol/mg of protein) according to the formula:

$$\text{Carbonyl content} = \frac{\text{Abs } 370 - \text{Abs } 370_{\text{blank}}}{22,000 \times [\text{Abs } 280 - (\text{Abs } 370 - \text{Abs } 370_{\text{blank}}) \times 0.43]} \times 10^6$$

4 Notes

1. Depending on the nature of the sample (liquid, solid, semi-solid) and the solubility of the sample's proteins in water, the use of specific buffers and sodium chloride (>2 M) to increase the ionic strength of the solution may be required. In very dry samples (i.e., dry-cured products) and very low protein solubility (i.e., collagen/elastin), the homogenization parameters may be properly modified (e.g., longer time and/or higher speed of homogenization), and the application of urea (>2 M) may be required. The protein extraction should be optimized to guarantee that each sampling aliquot from the homogenate (1) accurately represents the original sample and (2) contains the same protein content.
2. Due to the toxic and/or corrosive nature of the reagents used for protein precipitation, it is necessary for the operator to take the required protective measures (gloves, glasses, etc.) as well as to carry out all the operations in laboratory fume hoods.
3. SDS is an anionic surfactant capable of denaturing proteins' structure. Due to its detergent nature, air bubbles easily develop when the solution is transferred from the beaker, used to dissolve it, to a volumetric flask. To avoid/limit the

formation of air bubbles, gently heat up the solution to a temperature lower than 68 °C while stirring with a magnetic stirrer to assist dissolution.

4. Exothermic reaction. Insert 500 mL of distilled water into a 1 L beaker and slowly add 248 mL of hydrochloric acid (≥37%) while stirring with a magnetic stirrer. Wait for the mixture to cool down to room temperature, then add the remaining 252 mL of distilled water.
5. The eventual water added to moisten and stabilize the reagent should be considered in the calculation. As an example, if about 50% of water is used to moisten DNPH, then 6.0 g (instead of 3.0 g) of reagent should be dissolved in 1 L of HCl 3 M to achieve the final concentration of 0.3%.
6. Due to the irritant nature of the reagents used for washing the pellet, it is necessary for the operator to take all the required protective measures (gloves, glasses, etc.) as well as to carry out all the operations in laboratory fume hoods.
7. Endothermic reaction. The solution should be prepared with constant magnetic stirring and gentle heating (<40 °C) and allowed to equilibrate to room temperature before transferring it to a volumetric flask and fill it up to the mark.
8. Depending on the concentration of protein in the sample as well as on the extent of the oxidative damage, the amount of sample, the sample:dispersing solution ratio, and the homogenization intensity and time may vary.
9. Before pipetting the aliquots in the microcentrifuge tubes, the homogenate should be vortexed (few seconds) to have a homogeneous sample.
10. Depending on the protein nature and concentration, the centrifugation force ($\times g$) as well as the TCA concentration added may be adjusted. The pellet formed upon protein precipitation in these steps should be (1) strong enough to allow the easy removal of supernatant but (2) mild enough to guarantee a complete dissolution in the next step for carbonyl exposure, derivatization, or washing.
11. Once that the microcentrifuge tubes are placed in the dry bath, gently individually raise and shake them to ensure that the pellet is located in the bottom of the tube and submerged with the SDS solution.

References

1. Soladoye OP, Juárez ML, Aalhus JL et al (2015) Protein oxidation in processed meat: mechanisms and potential implications on human health. Compr Rev Food Sci Food Saf 14:106–122

2. Hellwig M (2020) Analysis of protein oxidation in food and feed products. J Agricult Food Chem 68:12870–12885
3. Estévez M (2015) Oxidative damage to poultry: from farm to fork. Poultry Sci 94: 1368–1378
4. Xiong YL, Guo A (2021) Animal and plant protein oxidation: chemical andf property significance. Foods 10:40
5. Estévez M, Xiong Y (2019) Intake of oxidized proteins and amino acids and causative oxidative stress and disease: recent scientific evidences and hypotheses. J Food Sci 84:387–396
6. Estévez M (2021) Critical overview of the use of plant antioxidants in the meat industry: opportunities, innovative applications and future perspectives. Meat Sci 181:108610
7. Estévez M (2011) Protein carbonyls in meat systems: a review. Meat Sci 89:259–279
8. Estévez M, Padilla P, Carvalho L et al (2019) Malondialdehyde interferes with the formation and detection of primary carbonyls in oxidized proteins. Redox Biol 26:101277
9. Levine RL, Garland D, Oliver CN et al (1990) Determination of carbonyl content in oxidatively modified proteins. In: Packer L, Glazer AN (eds) Oxygen radicals in biological systems part B: oxygen radicals and antioxidants, vol 186. Academic, pp 464–478
10. Soglia F, Petracci M, Ertbjerg P (2016) Novel DNPH-based method for determination of protein carbonylation in muscle and meat. Food Chem 197:670–675

COMUNICACIONES ORALES Y POSTERS EN CONGRESOS INTERNACIONALES

2nd FOOD CHEMISTRY Conference

Shaping the Future of Food Quality, Safety, Nutrition and Health

17–19 September 2019 • Seville, Spain

CERTIFICATE OF PRESENTATION

We hereby confirm that

Mario Estévez

presented an oral paper entitled:

Oxidized amino acids induce apoptosis and necrosis in CACO-2 cells by promoting oxidative stress and depleting the endogenous antioxidant defences

S. Díaz-Velasco[1], A. González[2], F.J. Peña[3], M. Estévez*[1], *[1]IPROCAR, University of Extremadura, Spain, [2]Institute of Molecular Pathology Biomarkers, University of Extremadura, Spain, [3]Spermatology Laboratory, University of Extremadura, Spain*

at

2nd *Food Chemistry* Conference

17-19 September, 2019

Signed

K G Russell

For and on behalf of

ELSEVIER

ID: 51794019848

A punicalagin-rich pomegranate supplement counteracts the physiological impairments caused by the intake of ultra-processed beef in Wistar Rats

Remigio Martínez [1,*], Victor Caballero [1], Silvia Díaz-Velasco [1], Alexis Arjona [2], Mario Estévez [1]

[1] IPROCAR Research Institute. University of Extremadura. Avda. Ciencias s/n 10003. Caceres, Spain.

[2] Sistema Extremeño de Salud (SES). Área de Salud de Cáceres, Spain

*Corresponding author: remimar@unex.es

INTRODUCTION & OBJECTIVES

- Punicalagin (PG), a major antioxidant bioactive ingredient in pomegranate juice, has been proven to have anti-oxidative stress properties and protective effects against several chronic diseases (Johanningsmeier and Harris, 2011).
- The intake of highly oxidized ultra-processed red meat and/or fructose-enriched diets are associated with higher incidence of non-communicable diseases (Dekker *et al*., 2010; Händel *et al*., 2019).
- The present study was carried out to analyze the protective effect of a punicalagin-rich pomegranate supplement on the liver function, serum biochemistry and lipid deposition in Wistar rats fed on ultra-processed beef and PG.

MATERIAL & METHODS

All protocols were performed according to Helsinki declaration and all applicable legal texts (approved by Animal Experimentation Ethical panel; process nº EXP-20200904)

21 ♂ WISTAR RATS - 10 WEEKS – FOOD & WATER AD LIBITUM

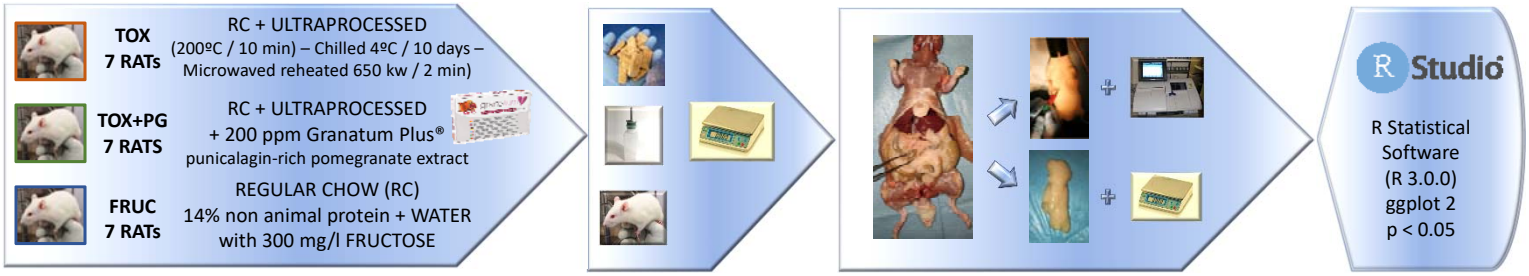

RESULTS & DISCUSSION

- Higher water intake was observed in TOX and TOX+PG groups vs FRUC (33.94 vs 30.98 vs 23.34 g/animal/day) as a likely consequence of the high-protein intake.
- A significant decrease in VAT weights was observed in TOX+PG group vs TOX and FRUC groups. (**Figure 2**). These results are of clinical interest as VAT deposition is related to an enhanced secretion of proinflamatory cytokines and several diseases such as hypertension and dyslipidaemia (Kelley *et al*., 2000).
- Higher values of total protein and albumin were observed in TOX group vs TOX+PG and FRUC groups **(Table).** Moreover, the albumin/globulin ratio value, an indicator of possible impairs in liver, kidneys or intestinal functions was improved in TOX+PG group when comparing to TOX. Likewise, decreased values of creatinine and urea were found in TOX+PG group vs TOX. Similar results have been observed in diabetic mice model orally treated with PG (An *et al*., 2020).
- Moreover, AST (Serum aspartate aminotransferase) values were decreased in TOX+PG group vs TOX, which indicate a liver protective effect of PG. Total cholesterol, LDL-cholesterol were significantly decreased in TOX+PG group compared to the other groups. Those altered serum lipid profiles could be related to an increased VAT deposition in the TOX and FRUC groups.

FIGURE 1

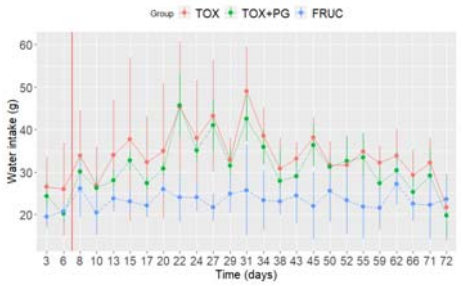

FIGURE 2

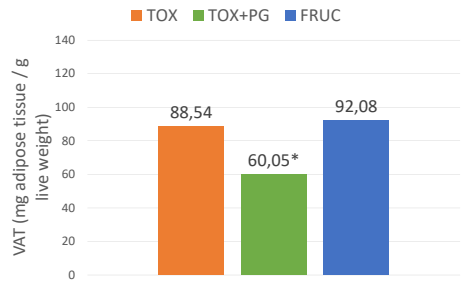

TABLE

SERUM CHEMISTRY	TOX	TOX+PG	FRUC
TOTAL PROTEIN (g/dl)	4.95*	3.50	3.35
ALBUMIN (g/dl)	2.98*	2.51	2.34
ALBUMIN/GLOBULIN RATIO	1.52*	2.28	1.92
UREA (mg/dl)	77.47*	46.33*	18.99*
CREATININE (mg/dl)	0.64*	0.51*	0.42*
AST (U/l)	45.6*	26.83	23.60
TRIGLYCERIDES mg/dl)	176.00*	132.33	143.14
TOTAL CHOLESTEROL (mg/dl)	86.25*	64.40	67.43
LDL-CHOLESTEROL (mg/dl)	10.6*	6.25	9.25*
HDL-CHOLESTEROL (mg/dl)	92.02*	62.18	69.61

Means with asterisc within the same row were significantly different (p<0.05)

Conclusions

The intake of punicalagin as a diet supplement counteracted the physiological impairments caused by ultra-processed beef. These results could contribute to understanding the benefits of this bioactive supplement on humans´ health.

REFERENCES

An, X. *et al.* 2020. Punicalagin protects diabetic nephropathy by inhibiting pyroptosis based on TXNIP/NLRP3 pathway. Nutrients. 12 (5). https://doi.org/10.3390/nu12051516

Dekker, M.J. *et al.* 2010. Fructose: A highly lipogenic nutrient implicated in insulin resistance, hepatic steatosis, and the metabolic syndrome. American Journal of Physiology - Endocrinology and Metabolism. 299 (5). https://doi.org/10.1152/ajpendo.00283.2010

Händel, M.N. *et al.* 2019. Processed meat intake and chronic disease morbidity and mortality: An overview of systematic reviews and meta-analyses. PLoS ONE. 14 (10): 1–20. https://doi.org/10.1371/journal.pone.0223883

Johanningsmeier, S.D., Harris, G.K., 2011. Pomegranate as a Functional Food and Nutraceutical Source. Annual Review of Food Science and Technology. 2 (1): 181–201. https://doi.org/10.1146/annurev-food-030810-153709

ACKNOWLEDGEMENTS AND FINANCIAL SUPPORT STATEMENT

Project AGL2017-84586-R

Project IB20103 & GR18104

ICoMST 2021 KRAKÓW

CERTIFICATE OF PRESENTATION

This is to certify that the following work entitled:

A punicalagin-rich pomegranate supplement counteracts the physiological impairments caused by the intake of ultra-processed beef in Wistar Rats

Remigio Martínez , Victor Caballero , Silvia Díaz-Velasco , Alexis Arjona , Mario Estévez

was presented during poster session
at the 67th International Congress of Meat Science and Technology
which was held in Krakow, Poland, August, 23-27, 2021

Marzena Zając, PhD
Head of the Organizing Commitee

Piotr Kulawik, PhD
Deputy Head of the Organizing Committee

Kraków, August 27, 2021

Euro Fed Lipid
european federation for the science and technology of lipids

Euro Fed Lipid e.V.
PO Box 90 04 40
60444 Frankfurt / Main
Germany
Tel: +49/69/68604846
info@eurofedlipid.org
www.eurofedlipid.org

Vigo, 25 May 2022

Confirmation of Participation and Presentation

Herewith, we confirm that

Silvia Díaz-Velasco Castela, Universidad de Extremadura, Cáceres, SPAIN

presented a poster entitled

"3NT affects type 3 metabotropic glutamate receptor binding through calmodulin on differentiated human enterocytes: A Proteomic-based Study "

in the Session: Lipid Oxidation and Protein and Lipid Co-oxidation

The poster was co-authored by:

J. Delgado, Cáceres/ES, A. Arjona, Cáceres/ES, M. Estévez, Cáceres/ES

during the

4th International Symposium on Lipid Oxidation and Antioxidants

23 - 25 May 2022, Vigo, Spain

European Federation for the Science
and Technology of Lipids e.V.
Euro Fed Lipid

European Federation for the
Science and Technology of Lipids e.V.
P.O. Box 90 04 40
60444 Frankfurt/Main, Germany
www.eurofedlipid.org

Euro Fed Lipid
european federation for the science and technology of lipids

Euro Fed Lipid e.V.
PO Box 90 04 40
60444 Frankfurt / Main
Germany
Tel: +49/69/68604846
info@eurofedlipid.org
www.eurofedlipid.org

Vigo, 25 May 2022

Confirmation of Participation and Presentation

Herewith, we confirm that

Silvia Díaz-Velasco Castela, Universidad de Extremadura, Cáceres, SPAIN
presented a poster entitled

"Cytometry analyses reveal severe cytotoxicity of 3-nitrotyrosine and ellagic acid on differentiated human enterocytes "

in the Session: Lipid Oxidation and Protein and Lipid Co-oxidation

The poster was co-authored by:

C. Dueñas, Cáceres/ES, F.J. Peña, Cáceres/ES, M. Estévez, Cáceres/ES
during the

4th International Symposium on Lipid Oxidation and Antioxidants
23 - 25 May 2022, Vigo, Spain

European Federation for the Science
and Technology of Lipids e.V.
Euro Fed Lipid

European Federation for the
Science and Technology of Lipids e.V.
P.O. Box 90 04 40
60444 Frankfurt/Main, Germany
www.eurofedlipid.org

Ultraprocessed Meat, Protein Oxidation and Oxidative Stress: Recent advances from *in vitro* and *in vivo* Studies

M. Estévez*, S. Díaz-Velasco, G. Sánchez-Terrón, D. Morcuende, R. Martínez
Meat and meat products research institute (IPROCAR). Universidad de Extremadura, 10003, Cáceres, Spain
*Corresponding author, mariovet@unex.es

Epidemiological studies do not seem to agree in the extent to which the acute and or sustained consumption of red and processed meat can be harmful for humans. Whereas some studies indicate that red and processed meat consumption contributes to a higher risk of suffering health disorders such as obesity, type 2 diabetes, cardiovascular diseases and cancer, some others find no connection between reducing the intake of such foods and benefits in terms of health. The main challenge for finding a reliable causality connection between foods and dietary patterns and health/disease conditions is defining the underlying pathophysiological mechanisms of the potentially harmful food components. Recent studies have made progresses in understanding the molecular mechanisms behind the harmful effects of ultraprocessed meats and found that the occurrence of severely oxidized proteins in such foods may play a role. The intake of oxidized proteins has been reported to produce dysbiosis and alter the glucose metabolism in experimental animals. Specific oxidized amino acids seem to display toxic effects on internal organs such as pancreas, thyroid, and liver, leading to oxidative stress, tissue degeneration and impaired physiological functions. Interestingly, some of the negative health effects of attributed to severely oxidized proteins in ultraprocessed meat products could also apply to plant-based meat analogues subjected to ultraprocessing such as commercial tofu or seitan (texturized gluten protein). The present scientific paper aims to collect the most recent information in regards to the health impact of the intake of oxidized proteins and amino acids.

CYTOMETRY ANALYSES REVEAL SEVERE CYTOTOXICITY OF 3-NITROTYROSINE AND ELLAGIC ACID ON DIFFERENTIATED HUMAN ENTEROCYTES

Silvia Díaz-Velasco[1*], Carmen Dueñas[2], Fernando J. Peña[2], Mario Estévez[1*]

[1]Food Technology and Quality (TECAL), Institute of Meat and Meat Products (IPROCAR), University of Extremadura, Cáceres, Spain. [2]Hospital Universitario Cáceres, Servicio Extremeño de Salud, Spain [3]Spermatology Laboratory, University of Extremadura, Cáceres, Spain.

*Corresponding authors: sdiazvel@unex.es; mariovet@unex.es

INTRODUCTION AND OBJECTIVE

- 3-Nitrotyrosine (3NT) is a nitrosated product of tyrosine that is formed during the processing of cured (nitrite-added) foods (Estévez *et al.*, 2017).
- The toxicity of dietary reactive nitrogen species (RNS) and the protective role of phenolic compounds against nitrosative stress is poorly understood.
- The **AIM** of the present study was to analyze the **possible toxicological effect of 3NT** and the **possible protective role** of the phenolic compound **ellagic acid (EA)** against 3NT using **flow cytometry**.

MATERIAL AND METHODS

DIFFERENTIATED HUMAN ENTEROCYTES

200 µM dietary concentrations of 3NT (Ozyurt and Otles, 2020) and 200 µM of EA

37ºC
5% CO_2
72h

CONTROL

3NT

3NT+EA

Cytoflex®

RESULTS AND DISCUSSION

Figure 1

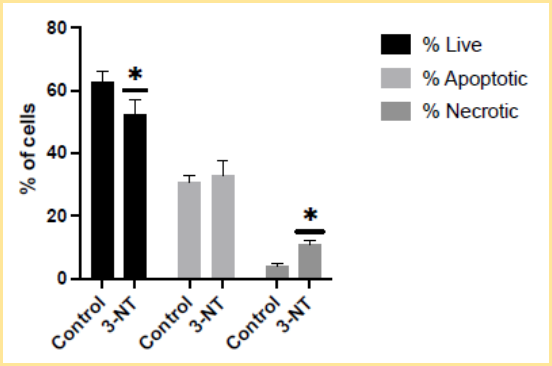

Figure 2

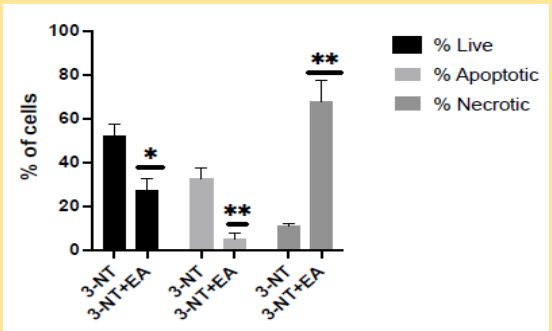

Figure 3

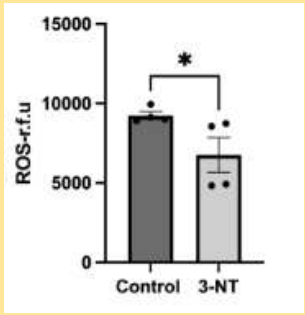

Figure 4

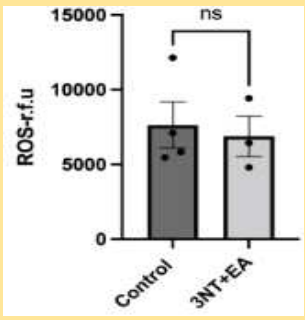

- Both, 3NT and 3NT+EA, caused a significant decrease in percentage of live cells (*p<0.05*) **(Figures 1 and 2)**.
- Decreased viability seemed not to be related to reactive oxygen species **(Figures 3 and 4)**.
- A significant increase in necrosis was found in 3NT treated cells (*p<0.05*), and such event was highly enhanced in 3NT+EA-treated cells as compared to 3NT treated cells (*p<0.01*) **(Figure 1 and 2)**.
- The 3NT results are coherent with a previous study (Díaz-Velasco *et al.*, 2020), while enhanced toxicity caused by EA in 3NT-treated cells has not been documented before.

CONCLUSION

The combination of 3NT and EA leads to remarkable cytotoxicity effects. Further studies may clarify:

- **1) whether the adduct of both species is responsible for these effects**
- **2) the molecular basis of this toxicity**
- **3) potential lessons to learn in relation to food safety and therapeutic application of such cytotoxic combination**

REFERENCES

- Díaz-Velasco, S., González, A., Peña, F.J., Estévez, M., 2020. Noxious effects of selected food-occurring oxidized amino acids on differentiated CACO-2 intestinal human cells. Food Chem. Toxicol. 144, 1–8. https://doi.org/10.1016/j.fct.2020.111650
- Estévez, M., Li, Z., Soladoye, O.P., Van-Hecke, T., 2017. Health Risks of Food Oxidation. Adv. Food Nutr. Res. 82, 45–81. https://doi.org/10.1016/bs.afnr.2016.12.005
- Ozyurt, V.H., Otles, S., 2020. Investigation of the effect of sodium nitrite on protein oxidation markers in food protein suspensions. J. Food Biochem. 44, e13152. https://doi.org/10.1111/JFBC.13152

S. Díaz-Velasco is recipient of a fellowship from the Spanish Ministry of Science, Innovation and Universities (PRE2018-084001)

ACKNOWLEDGEMENTS AND FINANCIAL SUPPORT STATEMENT

Project AGL2017-84586-R

Project IB20103 & GR18104

3NT affects type 3 metabotropic glutamate receptor binding through calmodulin on differentiated human enterocytes: A Proteomic-based Study

Silvia Díaz-Velasco[1*], Josué Delgado[1], Alexis Arjona[2], Mario Estévez[1*]

[1]Institute of Meat and Meat Products (IPROCAR), University of Extremadura, Cáceres, Spain. [2] Servicio Extremeño de Salud, Junta de Extremadura, Spain *Corresponding authors: sdiazvel@unex.es; mariovet@unex.es

INTRODUCTION & OBJECTIVE

- 3-nitrotyrosine (3NT) is a nitrosative stress product of tyrosine commonly formed during the processing of cured (nitrite-added) foods (Estévez *et al*., 2017).
- 3NT has been found to exert cytotoxicity in human enterocytes (Díaz-Velasco *et al*., 2020) but the underlying molecular mechanisms of such effects are unknown
- The **AIM** of present study was to **analyze the underlying molecular mechanisms** involved in the **cytotoxicity** of **3NT** in differentiated human enterocytes by using **proteomic** tools.

MATERIAL & METHODS

DIFFERENTIATED HUMAN ENTEROCYTES

37ºC
5% CO_2
72h

200 µM dietary concentrations of 3NT (Ozyurt and Otles, 2020)

CONTROL

3NT

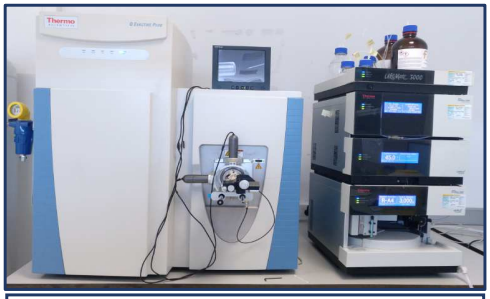

Orbitrap LC-MS/MS

RESULTS & DISCUSSION

FIGURE 1

Biological processes down

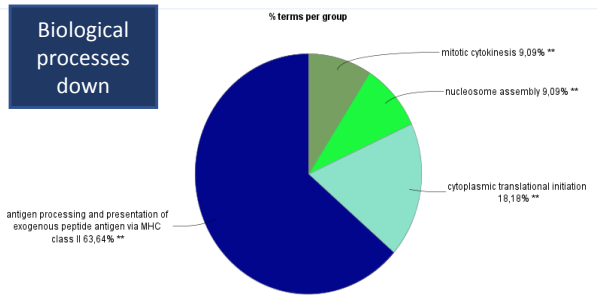

FIGURE 2

Molecular functions up

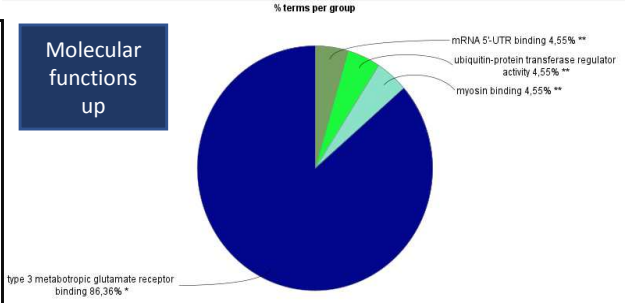

TABLE 1

TERMS AFFECTED BY 3NT	ASSOCIATED PROTEINS FOUND	% ASSOCIATED PROTEINS	ABUNDANCE (FOLD CHANGE)
Type 3 metabotropic glutamate receptor binding	CALM1, CALM2, CALM3	100	1.29
Nitric-oxide synthase activity	CALM1, CALM2, CALM3	25	1.29
Adenylate cyclase activator activity	CALM1, CALM2, CALM3	25	1.29
Regulation of ryanodine-sensitive calcium-release channel activity	CALM1, CALM2, CALM3	23.08	1.29

- 3NT induced a significant decrease in relative quantity of proteins involved in major histocompatibility complex (MHC) class II (63.64%, $p<0.01$) **(Figure 1)**.
- 3NT caused a significant increase in relative abundance of proteins related to type 3 metabotropic glutamate receptor binding (86,36%, $p<0.05$) **(Figure 2)**.
- Calmodulin was found in higher relative abundance in terms related to type 3 metabotropic glutamate receptor binding, such as nitric-oxide synthase activity, adenylate cyclase activator activity and regulation of ryanodine-sensitive calcium-release channel activity **(Table 1)**.
- The increasing of nitric-oxide synthase activity, and hence, higher levels of NO in cells, are related to necrosis (Pacher *et al*., 2007), as has been found in our previous *in vitro* study (Díaz-Velasco *et al*., 2020).

CONCLUSION

The molecular mechanisms affected by 3NT involved important pathways that affects cell viability conducting to necrosis (shown in cytometry analyses, Abstract-ID: 11144-30500), due to the increase of calmodulin through the union of 3NT to type 3 metabotropic glutamate receptors. The molecular basis of this toxicity should be considered in processing of cured (nitrite-added) foods and food safety.

REFERENCES

- Estévez, M., Li, Z., Soladoye, O.P., Van-Hecke, T., 2017. Health Risks of Food Oxidation. Adv. Food Nutr. Res. 82, 45–81. https://doi.org/10.1016/bs.afnr.2016.12.005
- Díaz-Velasco, S., González, A., Peña, F.J., Estévez, M., 2020. Noxious effects of selected food-occurring oxidized amino acids on differentiated CACO-2 intestinal human cells. Food Chem. Toxicol. 144, 1–8. https://doi.org/10.1016/j.fct.2020.111650
- Ozyurt, V.H., Otles, S., 2020. Investigation of the effect of sodium nitrite on protein oxidation markers in food protein suspensions. J. Food Biochem. 44, e13152. https://doi.org/10.1111/JFBC.13152
- Pacher, P., Beckman, J.S., Liaudet, L., 2007. Nitric oxide and peroxynitrite in health and disease. Physiol. Rev. 87, 315–424. https://doi.org/10.1152/PHYSREV.00029.2006

ACKNOWKLEDGEMENTS AND FINANCIAL SUPPORT STATEMENT

Project AGL2017-84586-R Project IB20103 & GR18104

S. Díaz-Velasco is recipient of a fellowship from the Spanish Ministry of Science, Innovation and Universities (PRE2018-084001)

45th ESPEN CONGRESS

EUROPEAN SOCIETY FOR CLINICAL NUTRITION AND METABOLISM

11 - 14 September 2023

CERTIFICATE OF ATTENDANCE

we herewith certify that

Silvia Díaz-Velasco

has participated in the

45th ESPEN Congress

11 - 14 September 2023, Lyon, France

45th ESPEN CONGRESS 2023 France Lyon 11 - 14 SEPTEMBER 2023

Prof. Cécile Chambrier

President of the ESPEN 2023 Congress

Live healthY with Optimal Nutrition

Geneva, 26 September 2023

RE: Presentation certificate

To whom it may concern,

On behalf of the organising committee of the **European Society of Clinical Nutrition and Metabolism Congress** held from 11 to 14 September 2023 in Lyon, France, we hereby certify that **Ms Silvia Díaz-Velasco** has successfully submitted and presented a scientific abstract at the conference as per the details below:

- ID: **P249-T**
- Title: POTENTIAL NEUROTOXICITY OF ALFA-AMINO ADIPIC ACID, A MARKER OF PROTEIN OXIDATION IN ULTRA-PROCESSED FOODS, AND ANALOGUE OF NEUROTRANSMITTER GLUTAMIC ACID
- Type of presentation: Poster Display

This abstract will also be published in a supplement of Clinical Nutrition Journal.

This certificate is issued to serve the purpose it might be required.

Yours sincerely,

ESPEN 2023 Conference – Abstract Management
c/o MCI Suisse
9 Rue du Pré-Bouvier
1242 Satigny
Switzerland

Phone: + 41 22 33 99 524
E-mail: espen.scienti@mci-group.com

Office Opening Hours
Monday to Friday
9:00 to 18:00 Geneva local time (CET)

45th ESPEN Congress
on Clinical Nutrition & Metabolism

Live healthY with Optimal Nutrition
Lyon, France | 11-14 September 2023

Geneva, 26 September 2023

RE: Presentation certificate

To whom it may concern,

On behalf of the organising committee of the **European Society of Clinical Nutrition and Metabolism Congress** held from 11 to 14 September 2023 in Lyon, France, we hereby certify that **Ms Silvia Díaz-Velasco** has successfully submitted and presented a scientific abstract at the conference as per the details below:

- ID: **P315-W**
- Title: ORAL ADMINISTRATION OF OXIDIZED LYSINE (ALFA-AMINO ADIPIC ACID) CAUSES TRANSITORY LOSS OF SPATIAL MEMORY IN C57BL/6 BLACK MICE
- Type of presentation: Poster Display

This abstract will also be published in a supplement of Clinical Nutrition Journal.

This certificate is issued to serve the purpose it might be required.

Yours sincerely,

ESPEN 2023 Conference – Abstract Management
c/o MCI Suisse
9 Rue du Pré-Bouvier
1242 Satigny
Switzerland

Phone: + 41 22 33 99 524
E-mail: espen.scienti@mci-group.com

Office Opening Hours
Monday to Friday
9:00 to 18:00 Geneva local time (CET)

45th ESPEN Congress
on Clinical Nutrition & Metabolism
Live healthY with Optimal Nutrition
Lyon, France | 11-14 September 2023
EUROPEAN SOCIETY FOR CLINICAL NUTRITION AND METABOLISM

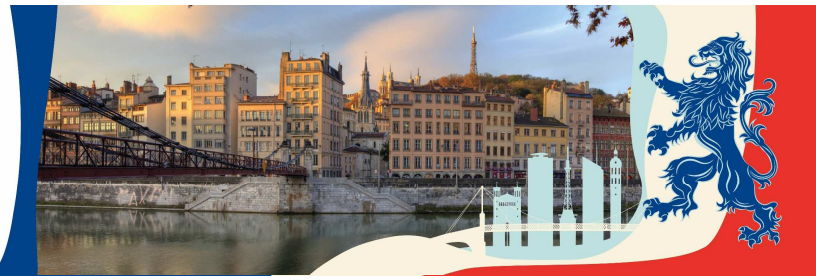

POTENTIAL NEUROTOXICITY OF ALFA-AMINO ADIPIC ACID, A MARKER OF PROTEIN OXIDATION IN ULTRA-PROCESSED FOODS, AND ANALOGUE OF NEUROTRANSMITTER GLUTAMIC ACID

P249-T

S. DÍAZ-VELASCO[1], J. DELGADO[1], A. ARJONA[2], F. J. PEÑA[3] and M. ESTÉVEZ[1]

1 Institute of Meat and Meat Products (IPROCAR), University of Extremadura, Cáceres, Spain. 2 Gobierno de Extremadura, Medicina Familiar y Comunitaria, Servicio Extremeño Salud, Cáceres, Spain.
3 Faculty of Veterinary, Spermatology Laboratory, University of Extremadura, Cáceres, Spain

Background

The **a-amino adipic acid (a-AA),** a six-carbon homologue of neurotransmitter **glutamic acid (GLU),** is an oxidized amino acid **present in ultra-processed food** and involved in **oxidative stress**[1]. Oxidative stress and the accretion of oxidized protein are hallmarks of neurodegenerative diseases[2]. The **AIM** of the present study is to analyze the **possible occurrence of oxidative stress** caused by **a-AA and GLU** at concentrations of 4mM for 24h on differentiated human neuronal **SH-SY5Y cells.**

Results

Figure 1. Changes in mitochondrial membrane potential (PE-A) in live cells representing active mitochondria found by flow cytometry. 4mM GLU for 24 h induced a significant increase (p<0.05) in mitocondrial activity on SH-SY5Y cells

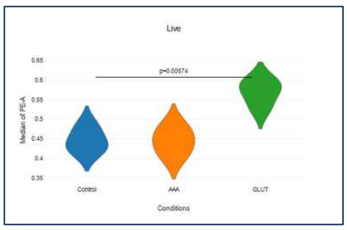

Table 1. Proteins found in a significant increase in relative abundance (FC: Fold change) on SH-SY5Y cells in α-AA and GLU treatment (p<0.05)

PROTEIN NAME	p-VALUE	ABUNDANCE (FC)	FUNCTION	
14-3-3 protein theta	0.018	1,07	Involved in poptosis	
Glycylpeptide N-tetradecanoyltransferase 1	0.024	1.15	Involved in apoptosis	α-AA
BH3-interacting domain death agonist	0.006	1.33	Induces caspases and apoptosis	
ATP synthase membrane subunit K, mitochondrial	1.3 x 10-3	1.54	Component of the ATP synthase	
Cytochrome c oxidase subunit 4 isoform 1, mitochondrial	0.038	1.80	Component of mitochondrial electron transport chain	GLU
Superoxide dismutase [Mn], mitochondrial	1.7 x 10^{-3}	4.49	Destroy radicals in biological systems	

Figure 2. Protein carbonyls (α-AS and γ-GS) and advanced oxidation protein product (Pent) on differentiated human neuronal cells SH-SY5Y upon exposure to 4mM α-AA and 4mM GLU for 24 h

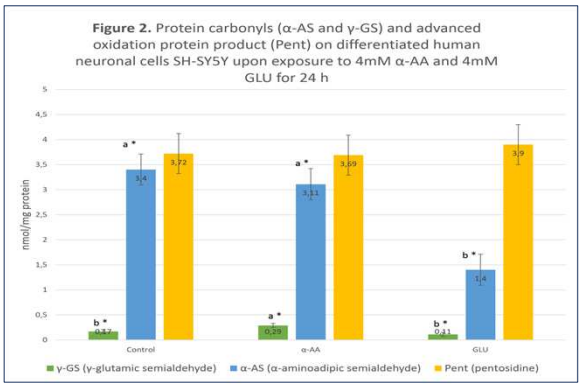

Method

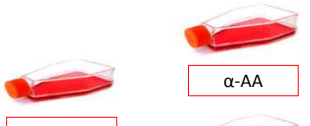

CYTOFLEX®→ FLOW CYTOMETRY

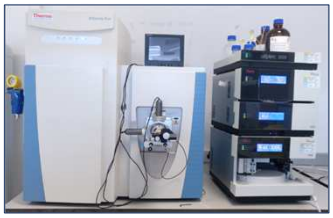

ORBITRAP LC-MS/MS→ PROTEOMICS

FLUORESCENT HPLC→ CARBONYLS

Summary/ Highlights

- α-AA and GLU may act as analogues, but they have a completely different behavior on differentiated human neuronal cells SH-SY5Y
- GLU activates mitochondrial activity keeping redox homeostasis decreasing carbonyls
- α-AA induces oxidative stress through a significant increase in γ-GS and activates proteins involved in apoptosis
- These finding are compatible with previous studies[3] and supports the idea that dietary oxidized amino acids may exert neurotoxicity

SCAN ME!

45th ESPEN Congress
on Clinical Nutrition & Metabolism
Live healthY with Optimal Nutrition
Lyon, France | 11-14 September 2023

References

[1]Díaz-Velasco, S. et al. Noxious effects of selected food-occurring oxidized amino acids on differentiated CACO-2 intestinal human cells. Food Chem. Toxicol. 144 (2020) 1–8
[2]da Silva, J.C. et al. α-Ketoadipic acid and α-aminoadipic acid cause disturbance of glutamatergic neurotransmission and induction of oxidative stress in vitro in brain of adolescent rats, Neurotox. Res. 32 (2017) 276–290
[3]Grimm, S. et al. Protein oxidative modifications in the ageing brain: Consequence for the onset of neurodegenerative disease. Free Radic. Res. 45 (2011) 73-88

Contact information
Silvia Díaz-Velasco
Avda. Universidad s/n 10003
Cáceres, Spain.
sdiazvel@unex.es

ESPEN The European Society for Clinical Nutrition and Metabolism

MINISTERIO DE CIENCIA E INNOVACIÓN
UNIÓN EUROPEA
FONDO EUROPEO DE DESARROLLO REGIONAL "Una manera de hacer Europa"
AGENCIA ESTATAL DE INVESTIGACIÓN

Grant PID2021-126193OB-I00 funded by MCIN/AEI/ 10.13039/501100011033 and by "ERDF A way of making Europe". S. Díaz-Velasco is recipient of a fellowship from the Spanish Ministry of Science and Innovation (grant number PRE2018-084001)

45th ESPEN CONGRESS
EUROPEAN SOCIETY FOR CLINICAL NUTRITION AND METABOLISM

45th ESPEN Congress
on Clinical Nutrition & Metabolism

Live healthY with Optimal Nutrition
Lyon, France | 11-14 September 2023

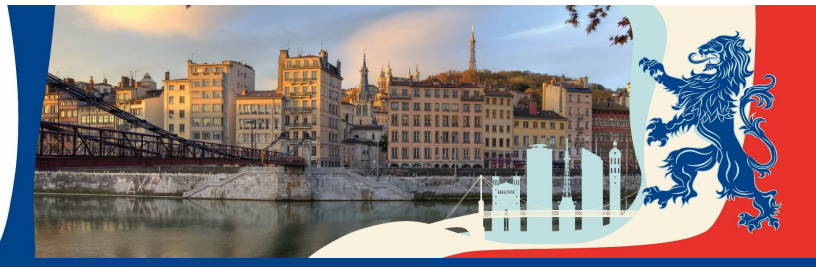

Oral Administration of Oxidized Lysine (α-Amino Adipic Acid) Causes Transitory Loss of Spatial Memory in C57BL/6 Black Mice

P315-W

S. Díaz-Velasco[1], R. Martínez[1], A. Arjona[2], J. Molina[3] and M. Estévez[1]

1 Institute of Meat and Meat Products (IPROCAR), University of Extremadura, Cáceres, Spain. 2 Medicina Familiar y Comunitaria, Servicio Extremeño Salud, Gobierno de Extremadura, Spain. 3 Gastroenterology Unit, University Hospital Cáceres, Servicio Extremeño Salud Gobierno de Extremadura, Spain

INTRODUCTION

- While the intake of ultra-processed meat products has been linked to neurodegenerative disorders[1], the underlying mechanisms remain indefinite.
- We hypothesize that oxidized proteins and amino acids accumulated in ultra-processed foods would display neurotoxicity potential[2].
- Specifically, the lysine oxidation product, α-amino adipic acid (α-AA), is known to cause physiological impairments in differentiated human neuronal SH-SY5Y cells.

AIM

The AIM of this study is to analyze the possible influence of the oxidized amino acid, α-amino adipic acid (α-AA), present in ultra-processed foods, in the the spatial memory of C57BL/6 black mice

METHOD

MORRIZ WATER MAZE TO ANALYZE A POSSIBLE SPATIAL MEMORY LOSS IN C57BL/6 BLACK MICE[3]

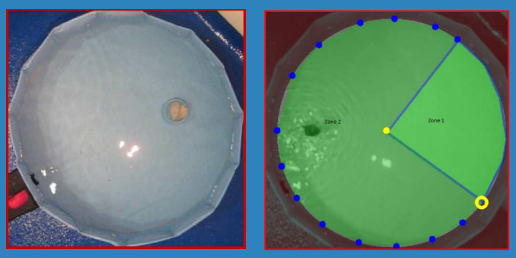

GROUPS	N	α-AA 0.5 mg/day/kg	Properly trained
CONTROL	5	4 and 8 weeks	before experiment[3]
α-AA	5	21ºC	

RESULTS

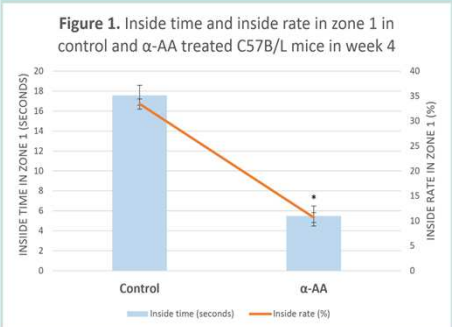

Figure 1. Inside time and inside rate in zone 1 in control and α-AA treated C57B/L mice in week 4

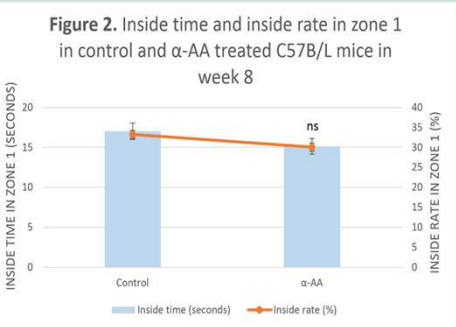

Figure 2. Inside time and inside rate in zone 1 in control and α-AA treated C57B/L mice in week 8

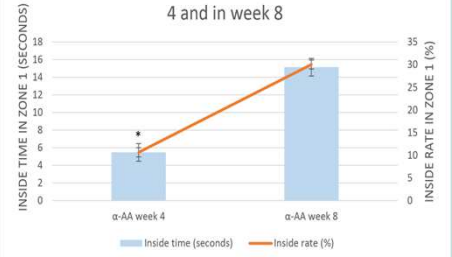

Figure 3. Inside time and inside rate in zone 1 in control and α-AA treated C57B/L mice in week 4 and in week 8

- Unlike controls, which showed clear preference for the quadrant where platform was located, mice exposed to oxidized lysine for 4 weeks had a significant loss of spatial memory (p<0,05), manifested as lack of preference in the maze when platform was absent **(Figure 1).**
- In week 8, all mice, irrespective of treatment, showed no impairment of spatial memory loss (p>0,05) **(Figure 2).**
- Comparing week 4 and week 8 in mice exposed to α-AA, a significant decrease was found in week 4, corroborating the transitory loss of spatial memory (p<0,05) **(Figure 3).**
- In other parameters studied, such as total distance covered, speed, acceleration and exploration rate, no significant differences were found either at week 4 or at week 8, neither in the control nor in the α-AA treated mice.

CONCLUSIONS

- ✓ The oral administration of α-amino adipic acid in C57BL/6 black mice cause transitory loss of spatial memory reflected in week 4.
- ✓ The transitory loss of spatial memory is corroborated by comparing the results obtained in week 4 and in week 8, where no loss of spatial memory was detected in this latter.
- ✓ This transitory loss of spatial memory caused by dietary a-AA may reflect long-term counteracting mechanisms against the neurotoxicity of a-AA while this should be corroborated in further experiments.

SCAN ME!

REFERENCES

1. Mannino, A. et al. Higher consumption of ultra-processed foods and increased likelihood of central nervous system demyelination in a case-control study of Australian adults. Eur. J. Clin. Nutr. (2023). 1-4
2. Díaz-Velasco, S. et al. Noxious effects of selected food-occurring oxidized amino acids on differentiated CACO-2 intestinal human cells. Food Chem. Toxicol. 144 (2020) 1–8
3. Vorhees, C. V. & Williams, M.T. Morris water maze: procedures for assessing spatial and related forms of learning and memory. Nat. Protoc. 1 (2006) 848-858

CONTACT INFORMATION

Silvia Díaz-Velasco
Avda. Universidad s/n 10003 Cáceres, Spain.
sdiazvel@unex.es

ACKNOWLEDGEMENT

MINISTERIO DE CIENCIA E INNOVACIÓN
UNIÓN EUROPEA
FONDO EUROPEO DE DESARROLLO REGIONAL
AGENCIA ESTATAL DE INVESTIGACIÓN

Grant PID2021-126193OB-I00 funded by MCIN/AEI/ 10.13039/501100011033 and by "ERDF A way of making Europe". S. Díaz-Velasco is recipient of a fellowship from the Spanish Ministry of Science and Innovation (grant number PRE2018-084001)